Max-Planck-Institut für
molekulare Physiologie

Technische Universität
Dortmund

Exploiting Modern Catalytic Methods of *C*-glycosylation Using the Vinylogy Concept

Dissertation

For the achievement of academic degree of the

Doctor in Natural Science

(Dr. rer. nat.)

Submitted to

The Faculty of Chemistry and Chemical Biology

Technical University of Dortmund

By

Huei-Ru Wu

from Keelung, Taiwan

Dortmund 2019

1. Gutachter: Prof. Dr. Dr. h.c. Herbert Waldmann

2. Gutachter: Prof. Dr. Carsten Strohmann

Dekan: Prof. Dr. Stefan M. Kast

Datum der ersten Einreichung: 26.09.2019

Datum der zweiten Einreichung: 27.11.2019

Datum der mündlichen Prüfung: 25.11.2019

The present dissertation was written in the period from December 2016 to November 2019 under the supervision and guidance of Dr. Chuanjie Loh (Charles) at the Max-Planck-Institute of Molecular Physiology in Dortmund and the Faculty of Chemistry and Chemical Biology at the Technical University of Dortmund.

Contents

Index of Figures

Index of Schemes

Index of Tables

Abstract

The development of innovative and convenient methods for efficient synthesis of *C*-glycosides could facilitate access to novel potent therapeutics. Distinct carbohydrate donors are useful precursors for direct C-C bond formation. Vinylogous dienolates, as one type of C-C bond formation substrates, can act as enabling chemical tools for introducing the desired motifs in an atom-economical and efficient manner. However, the vinylogous dienolates are underreported in *C*-glycosylation. The development of novel catalytic methods for *C*-glycosylation with vinylogy concept, such as Lewis acid or halogen bond catalysis could open up new ground in carbohydrate chemistry.

In this work, we have demonstrated a number of *C*-glycosylation methods, including a $Zn(OTf)_2$ catalyzed Ferrier rearrangement utilizing vinylogous dienolate nucleophiles achieving α-anomeric selectivity and absolute γ-regioselectivity. Additionally, we have disclosed a $Ca(NTf_2)_2$ catalyzed strain-release pyranosylation displaying high β-anomeric selectivity using various vinylogous dienolates. Further, the influence of different *O*-6 substituents of the carbohydrate as well as protecting groups and α-/γ- substitutions of the dioxinone dienolates were studied. A thorough investigation of the reaction mechanism by *in situ* NMR measurements unveiled the previously unknown significance of water. Finally, we unraveled the first solely halogen bond (XB) catalyzed γ-vinylogous *C*-glycosylation through glycosyl trichloroacetimidate donors. To show also possible applications of the obtained products, the *C*-glycosides were tested in cell-based assays and revealed potential activity in the hedgehog signaling pathway.

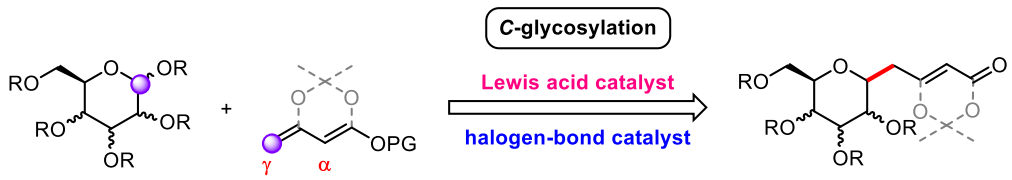

Zusammenfassung

Die Entwicklung von neuen und anwenderfreundlichen Synthesemethoden für *C*-Glykosylierungen könnte zur Entdeckung von neuen und aktiven Wirkstoffen führen. Modifizierte Kohlenhydratdonoren sind nützliche Ausgangsstoffe für die direkte Bildung von neuen C-C Bindungen. Vinyloge Dienolate könnten als Bausteine dienen um die gewünschten Motive auf atomökonomische und effiziente Weise zu synthetisieren. Jedoch sind vinyloge Dienolate im Kontext der *C*-Glykosylierung schlecht erforscht. Die Entwicklung neuer katalytischer Methoden für die *C*-Glykosylierung, zum Beispiel durch Lewis Säure oder Halogen-Bindungs Katalyse, könnten neue Möglichkeiten in der Kohlenhydratchemie eröffnen.

In dieser Arbeit haben wir *C*-Glykosylierungen anhand einer Anzahl verschiedener Reaktionen gezeigt. Diese beinhalten eine $Zn(OTf)_2$-katalysierte Ferrier-Umlagerung mit vinylogen Dienolat-Nukleophilen, welche sich sowohl durch α-Anomerenselektivität als auch durch eine absolute γ-Regioselektivität auszeichnet. Zudem konnten wir eine $Ca(NTf_2)_2$-katalysierte spannungsgetriebene Pyranosylierung mit hoher β-Anomerenselektivität entwickeln, in welcher verschiedenste Dienolate verwendet wurden. Des Weiteren, wurden die Einflüsse verschiedener *O*-6 substituenten am Kohlenhydrat sowie verschiedener Schutzgruppen und α-/γ-Substituenten am Dioxinonedienolaten untersucht. Eine Untersuchung des Mechanismus durch *in situ* NMR-Messungen zeigte eine zuvor unbekannte Beteiligung von Wasser an der Reaktion. Schließlich konnte die erste, nur durch Halogen-Bindungen-katalysierte (XB), γ-vinyloge *C*-Glykosylierung mit Glykosyltrichloroacetimidsäureesterdonoren entwickelt werden. Um potentielle Anwendungen der erhaltenen *C*-Glykoside zu erforschen, wurden diese in Zell-basierten Assays untersucht und zeigten potentielle Aktivität im Hedgehog-Signalweg.

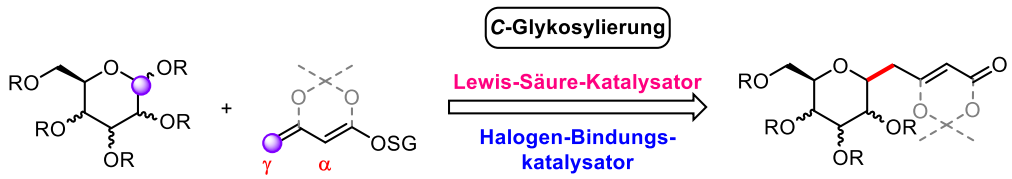

1 Introduction

Efficiently accessing biologically active molecules is a fundamental research area in developing potential candidates or tool compounds in chemical biology, medicinal chemistry and drug discovery. Carbohydrates are considered as one of the most prevalent biomolecules due to their crucial roles in mediating biological processes including cell-cell recognition,[1] inflammation,[2] cellular respiration and post-translational modifications.[3] As a result of this, they can also serve as biological active substances. *C*-glyosidic bonds are enzymatically and chemically stable towards hydrolytic enzymes *in vivo* and therefore *C*-glycosides have become a potential alternative for the naturally labile *O*-glycosides in therapeutic applications.[4]

One successful example is the development of a series of sodium glucose co-transporters (SGLTs) 2 inhibitors to target type II diabetes based on Phlorizin.[5] Phlorizin has played an important role in the investigation of renal glucose reabsorption but was later found to be a non-selective SGLTs inhibitor.[6] The *O*-glycoside Phlorizin has poor metabolic stability due to β-glycosidase degradation *in vivo*. However, the clinically approved *C*-aryl glucoside derivatives, Empagliflozin, Dapagliflozin and Canagliflozin, showed resistance to degradation in the gastrointestinal tract and was confirmed to be a selective SGLT2 inhibitor (Figure 1).[5]

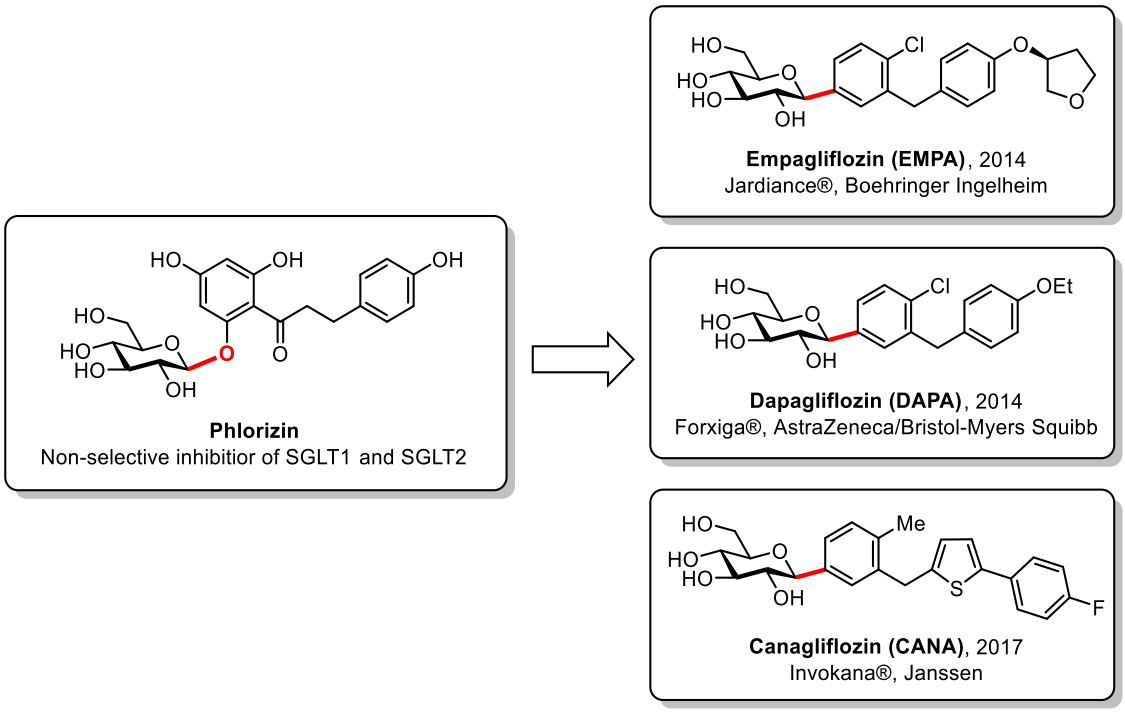

Figure 1. Structure of SGLT2 inhibitors.[5]

1.1 General synthetic methods of *C*-glycosides

Carbohydrate building blocks acting as donor precursors for direct formation of C-C glyosidic linkage are the key substrates in *C*-glycoside synthesis. Examples include *C*-glycosylation via glycals (Figure 2; a),[7] glycosyl halides (Figure 2; b),[8] strain-release reactions from 1,2-cyclopropanated sugars (Figure 2; c),[9] thioglycosides (Figure 2; d)[10] and glycosyl imidates (Figure 2; e).[11]

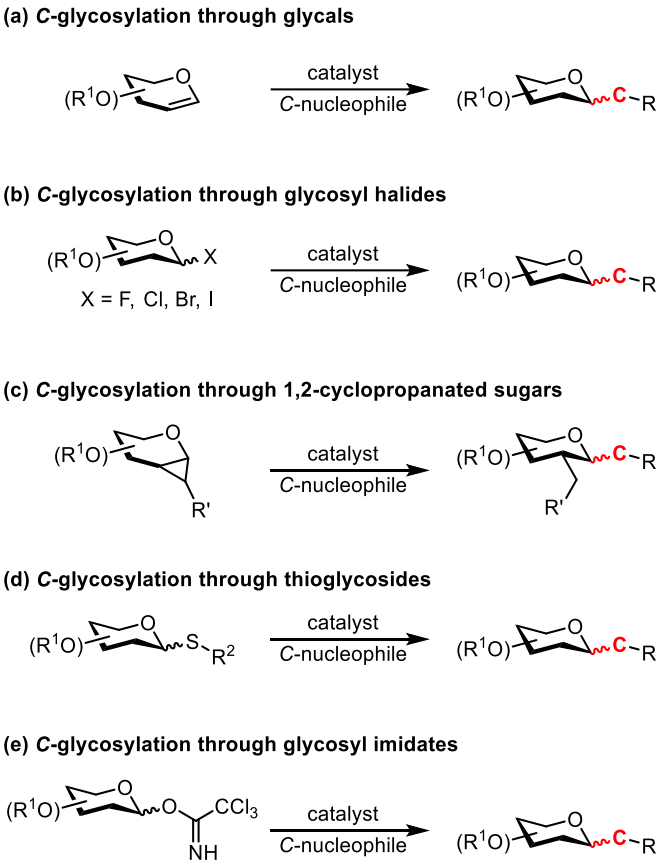

Figure 2. Representative carbohydrate donors and the methods for the synthesis of *C*-glycosides.[4]

1.1.1 *C*-glycosylation via glycals

Reactions in which glycals can undergo nucleophilic substitution at the *C*-1 position followed by allylic rearrangement to convert into 2,3-unsaturated glycosides are commonly referred to as Ferrier rearrangement (FR, Scheme 1).[4,12,13] Lewis acid catalyzed Ferrier rearrangement gets undoubtedly the most attention.[12]

Scheme 1. The Ferrier rearrangement.[12]

The acyl group at *C*-3 is activated by a Lewis acid to form the oxocarbenium ion which is attacked by a nucleophile (Scheme 2).[12] The stereoselectivity is primarily determined by the conformation of the oxocarbenium intermediate at the *C*-3 position. Another factor affecting the stereoselectivity is through nucleophilic attack by the carbon nucleophile of the lower energy conformation **I**. The formation of the favored half-chair conformation (α, ***H***) results from the bottom face attack of **I**; the top face attack of **I** leads to the disfavored boat confirmation (β, ***B***). As a result, the α-anomer is the predominant product but formation of the β-anomer cannot be completely suppressed.

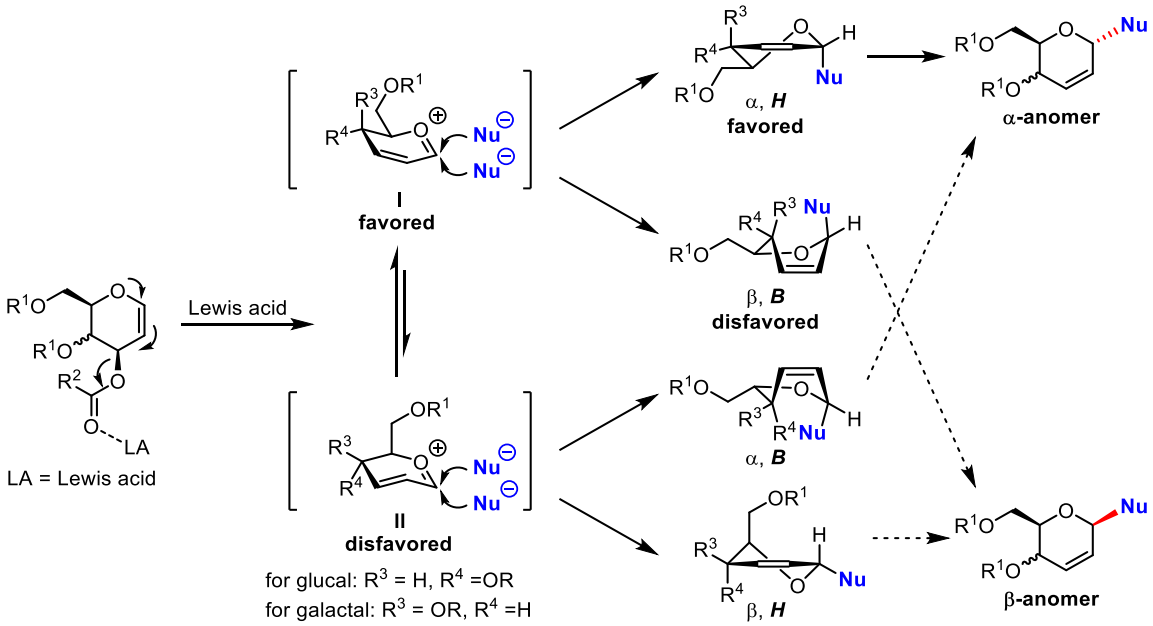

Scheme 2. Stereoselectivity of the Ferrier rearrangement.[12]

Strong Lewis acids such as $BF_3{\cdot}OEt_2$ and $TiCl_4$ were initially employed in the FR reaction, however milder reagents such as $Yb(OTf)_3$ and $Zn(OTf)_2$ were found to be efficient catalysts of these reactions. Schmidt *et al*. reported that $Yb(OTf)_3$ acted as a good catalyst for this reaction with a number of silane nucleophiles **2a** and **2b** on the acetylated glucal **1** (Table 1) with high stereoselectivity and good yields.[7] However, when the optimized condition was applied to the silyl enol ether nucleophiles **2c** and **2d**, the good yields were maintained but the stereoselectivity slightly decreased. Furthermore, it is worth mentioning that enhanced variety was reported by Grée *et al.* who utilized an ionic liquid as solvent under $Yb(OTf)_3$ catalysis to perform the FR reaction with high stereoselectivity for the highly reactive silyl enol ether nucleophiles **2c** and **2d** (Table 1).[14]

Table 1. $Yb(OTf)_3$ catalyzed Ferrier rearrangement with silyl-nucleophiles.[7,14]

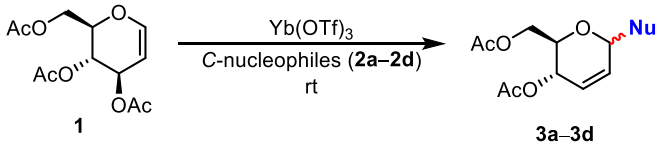

C-nucleophiles	Product	10 mol% $Yb(OTf)_3$		5 % $Yb(OTf)_3$ in $[bmim][NTf_2]$	
		Yield %	α/β	Yield %	α/β
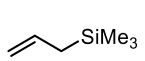 **2a**	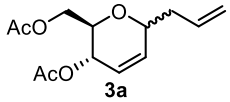 **3a**	94	α	80	> 95:5
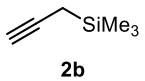 **2b**	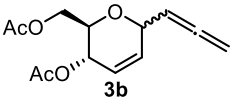 **3b**	92	α	65	> 95:5
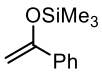 **2c**	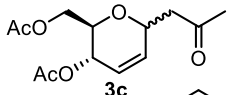 **3c**	90	8:1	65	> 95:5
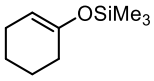 **2d**	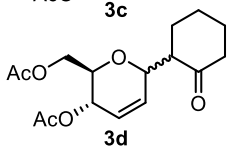 **3d**	89	11:1	65	> 95:5

Kashyap *et al*. developed an efficient and versatile *C*-glycosylation protocol involving non-toxic and mild $Zn(OTf)_2$.[15] The *O*-acetylated glucal **1** (Scheme 3) was converted to the α-anomer as major product in high yields. The silyl enol ether **2d** was successfully incorporated into glucal **1** to generate the desired *C*-glycosylation product **3d** as a stereoisomeric mixture due to the prochirality at α-carbon position. In addition, acetylated galactal **4** was further reacted with

acceptors **2a** and **2d** respectively under Zn-mediated *C*-glycosylation to afford the corresponding galactosides **5a** and **5b** with excellent yields and anomeric selectivity. The stereochemical outcome of the above mentioned reactions commonly favored the α-anomers which were consistent with the mechanism previously discussed.

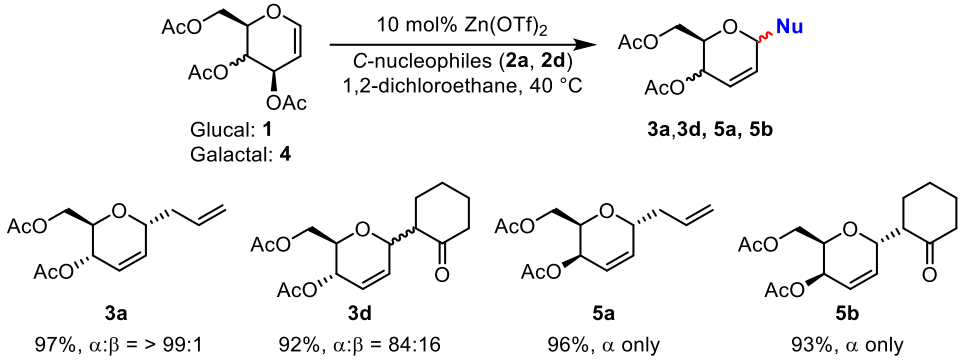

Scheme 3. Zn(OTf)$_2$ catalyzed Ferrier rearrangement with silyl nucleophiles.[15]

1.1.2 *C*-glycosylation via 1,2-cyclopropanated carbohydrates

1,2-cyclopropanated carbohydrates as another sugar substrate class combine the highly reactive cyclopropanes with the diverse functionality and unambiguous stereochemistry of carbohydrate chiral pool. The cyclopropanated carbohydrate ring opening reactions lead to highly stereo- and regioselective products due to the pre-established chiral structures of the cyclopropanes on the carbohydrate. This is aided by the electronic influence of the endocyclic oxygen. For instance, the cleavage of the non-shared 1,1'-cyclopropane bond generates the *C*-2-branched pyranosides (Scheme 4; pathway a). In contrast, the breakage of the fused 1,2-bond results in the ring expanded oxepines (Scheme 4; pathway b).[16]

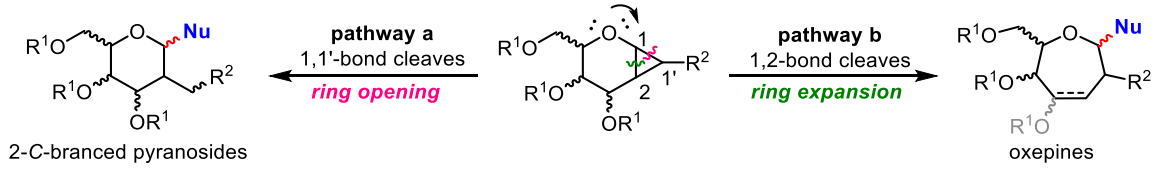

Scheme 4. Possible ring opening pathways of 1,2-cyclopropanated sugars.[16]

The majority of 1,2-cyclopropanated carbohydrates were synthesized by reactions of the glycals under Simmons-Smith conditions, Mąkosza two-phase methods or using diazoesters carbenes (Scheme 5).[16,17,18] The classic Simmons-Smith cyclopropanation utilized diiodomethane in the

presence of a zinc-copper coupling reagent (Zn/Cu) or diethylzinc to convert unfunctionalized alkenes to cyclopropanes.[16] The metal carbenoid was delivered to the same face as the nearest oxygen substituent since the zinc coordinates to the 3-OR^1 group and generated the unsubstituted cyclopropanes. Alternatively, the Mąkosza and diazoester cyclopropanation favored the less sterically hindered face.[17] In the Mąkosza method, glycals were treated with chloroform in the presence of sodium hydroxide which further dehalogenation by $LiAlH_4$. This formed the methylene cyclopropanes. Furthermore, the diazoester cyclopropanation catalyzed by transition metals led to functional donor-acceptor cyclopropanes.

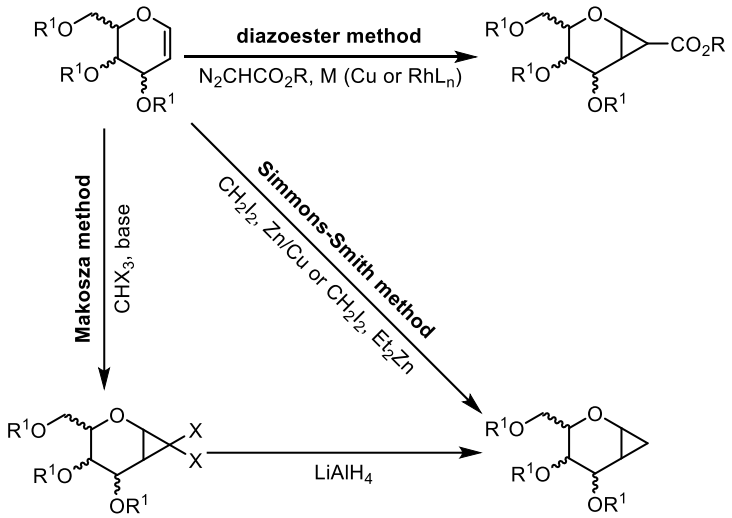

Scheme 5. Synthetic routes to 1,2-cyclopropanated carbohydrates.[16]

The 1,2-cyclopropanated carbohydrates mentioned above typically required relatively harsh conditions for the subsequent ring opening reaction. Shao *et al*. reported a catalytic and stereoselective glycosylation using a newly designed donor-acceptor (D-A) cyclopropanated sugar **6**. It predominantly generated α-anomers with TMSOTf as catalyst, whereas the major β-anomer products were obtained using $BF_3{\cdot}OEt_2$ as catalyst (Scheme 6).[19]

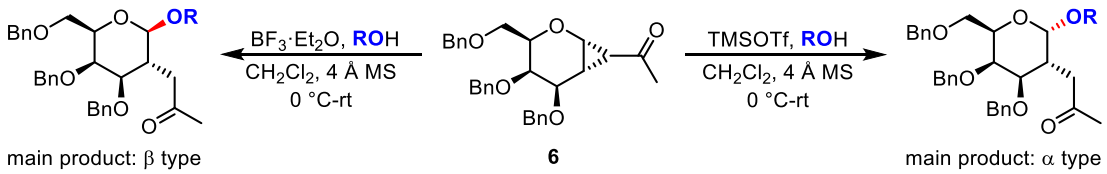

Scheme 6. Catalytic ring opening reaction via donor-acceptor cyclopropanated sugar.[19]

Shao and co-workers first disclosed $BiCl_3$ promoted ring opening of D-A cyclopropanes **7** in the presence of *C*-nucleophilic allylsilanes (Scheme 7).[20] Surprisingly, instead of *C*-glycosylation, the reaction underwent a recyclization addition tandem pathway to create a quaternary carbon center in a stereoselective manner. A range of nucleophilic allylsilanes and silyl enol ethers were investigated and afforded only one diastereomer in high yields. In addition, various carbohydrate substrates **6** and **8**–**10** yielded the desired products **11a**–**11j** in moderate to good yields.

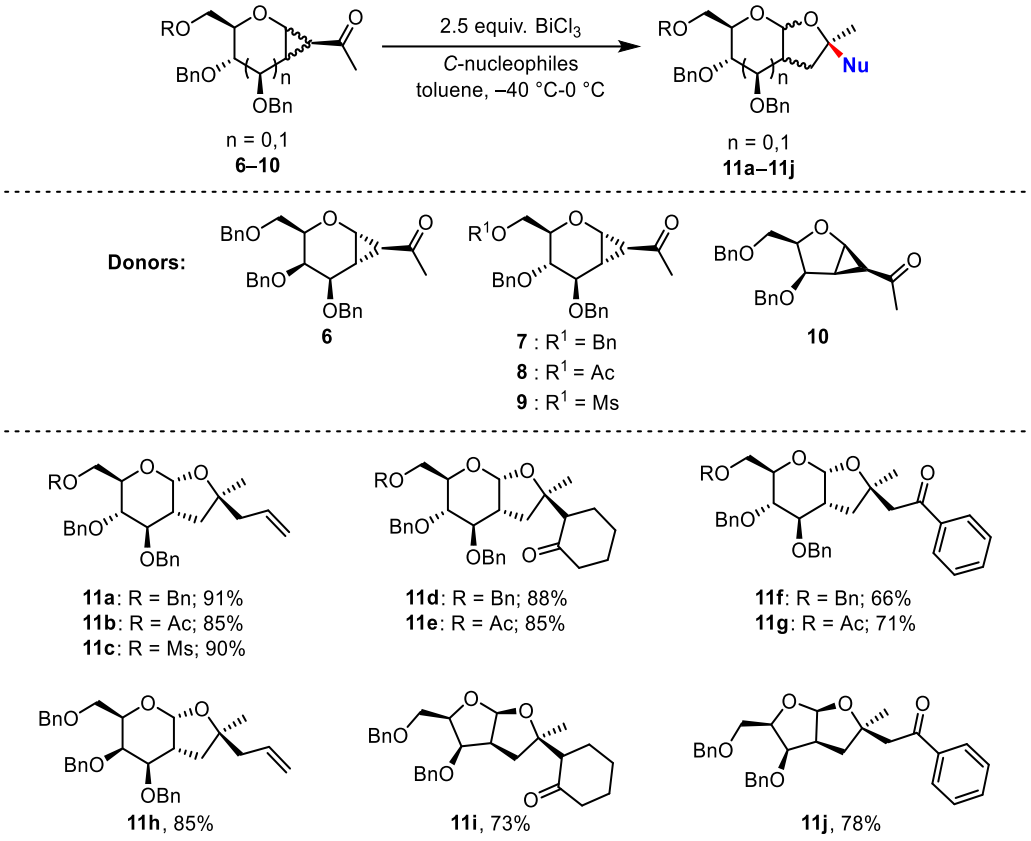

Scheme 7. $BiCl_3$ promoted D-A cyclopropane ring opening.[20]

A plausible mechanism proposed that $BiCl_3$ coordinated to the carbonyl group. This led to the activation of the cyclopropane causing the ring opening (Scheme 8). In pathway one, water attacked the anomeric carbon and generated the hemiacetal intermediate **III** which further formed the bicyclic ring intermediate **VI**. A second possible reaction pathway was due to the neighboring group participation (Scheme 8; path 2). The nucleophilic intramolecular attack via the carbonyl oxygen at the anomeric carbon formed the pseudo bicyclic ring intermediate **VI**. The intermediate was trapped by the nucleophile at the convex face to generate the pyran derivatives as one

diastereomer. The preliminary mechanistic studies revealed that the reaction underwent a stepwise process.[20]

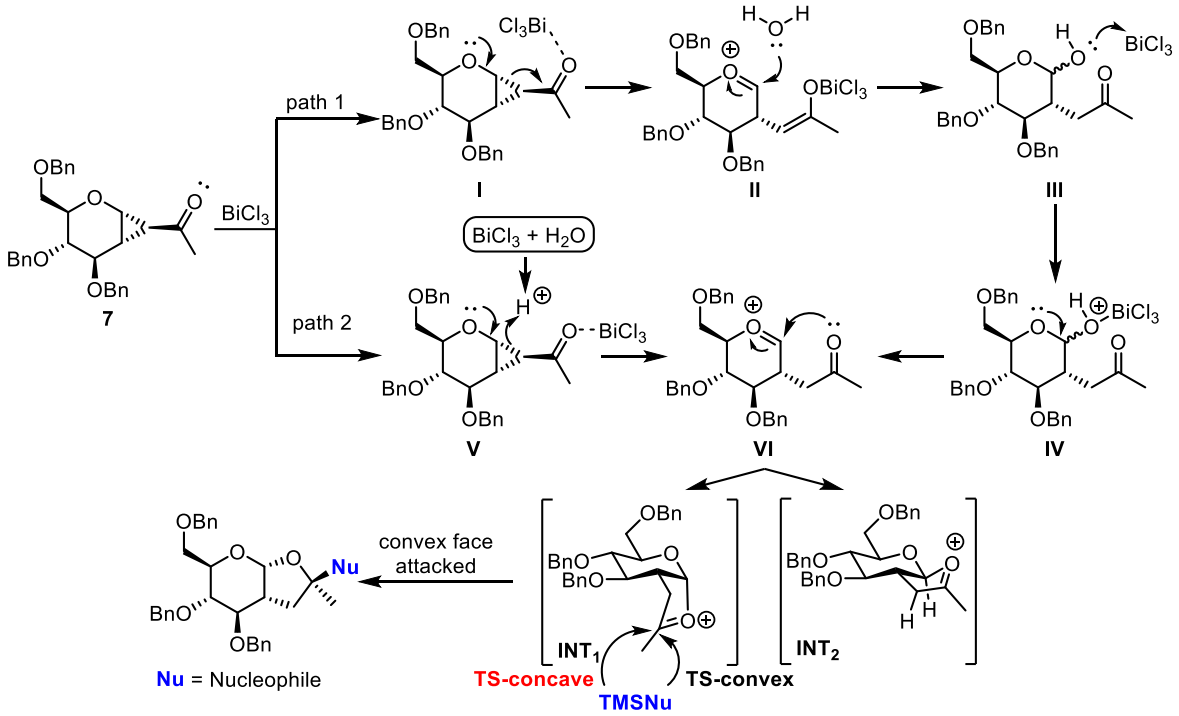

Scheme 8. The proposed mechanism of $BiCl_3$ promoted recyclization addition tandem pathway reaction.[20]

In 2018, our research group developed an ultra-low thiourea catalyzed strain-release glycosylation via non-covalent hydrogen bonding interactions (Scheme 9).[9] The reaction could be performed with as little as 0.2 mol% of the hydrogen bond Kass catalyst **15** to trigger the reaction between D-A cyclopropnated sugars and 1,3,5-trimethoxybenezene **14** to generate the corresponding Friedel-Crafts type *C*-glycosides **16a**–**16c** in moderate yields and good stereoselectivity. However, other less reactive *C*-nucleophiles including mesitylene, 1,3-dimethylbenzene, 3-cyanocoumarin and anthracene were unsuccessful. *In situ* NMR monitoring was performed to reveal the reaction mechanism where the rapid disappearance of donor **10** corresponded to the immediate formation of product **18**. Concomitantly, two non-isolable intermediates, **17a** and **17b** could only be detected by NMR measurements.[9] The disappearance of intermediate **17a** corresponded to the steep increase in the formation of **18** in the initial fast formation phase. Whereas the depletion of intermediate **17b** was consistent with the slow generation of **20** afterwards. Therefore, a plausible mechanism according to these results was proposed. The simultaneous hydrogen bond activation of the oxygen on the alcohol nucleophile

by the thiourea catalyst weakened the O-H bond. This led to the resulting acidic alcohol proton to activate the carbonyl of **10** in the rate limiting step. Owing to the anchimeric assistance by the *C*-2 ketone moiety, the bicyclic intermediates **17a** and **17b** were formed and attacked by nucleophile in a highly stereoselective manner.[9]

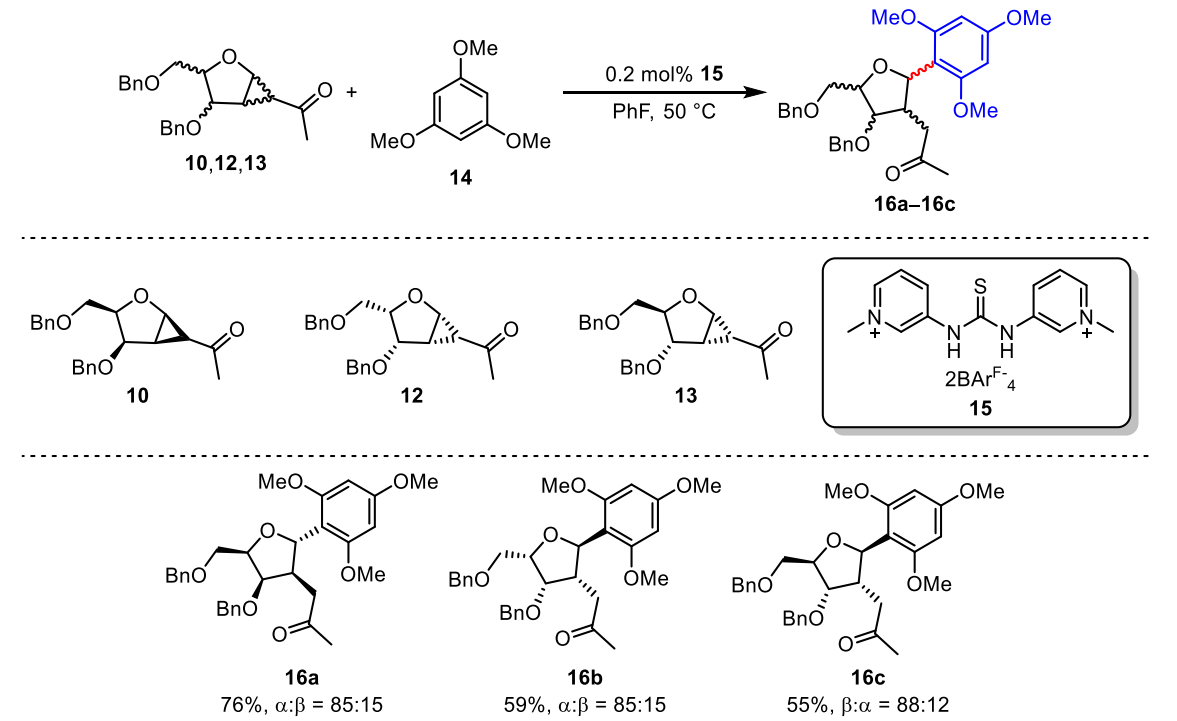

Proposed mechanism

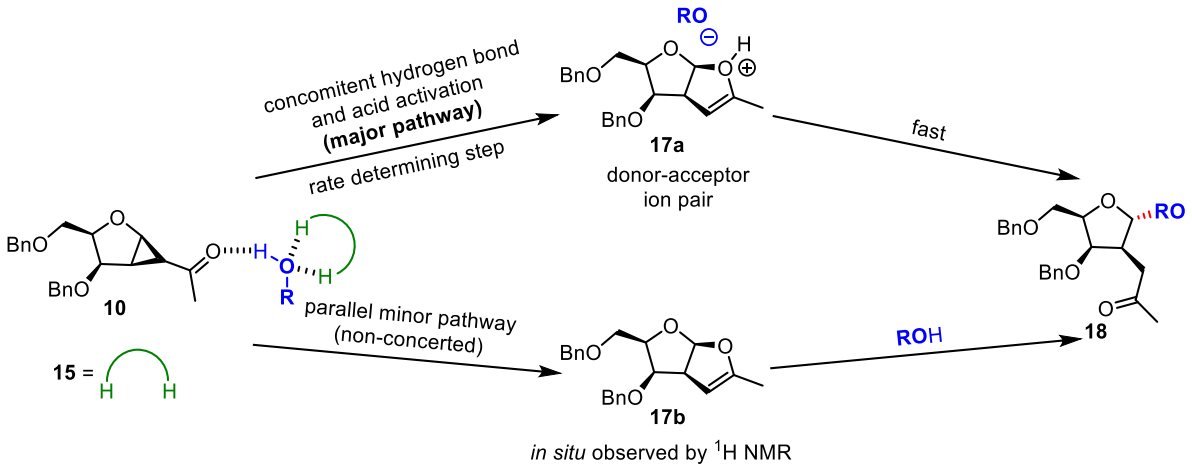

Scheme 9. Ultra-low thiourea catalyzed strain-release glycosylation and the proposed mechanism.[9]

1.1.3 *C*-glycosylation via glycosyl imidates

In 1980, Schmidt introduced the glycosyl trichloroacetimidate strategy which has become one of the most popular glycosyl donors as only catalytic amounts of promoters are needed to trigger the glycosylation.[21] Glycosyl trichloroacetimidates exhibit beneficial donor properties such as generation of high product yields and highly anomeric stereocontrol. The use of sodium hydride or DBU for the formation of glycosyl trichloroacetimidates generates the thermodynamically favored α-anomers, whereas the use of K_2CO_3 generally yields kinetically controlled β-anomers (Scheme 10).[21,22]

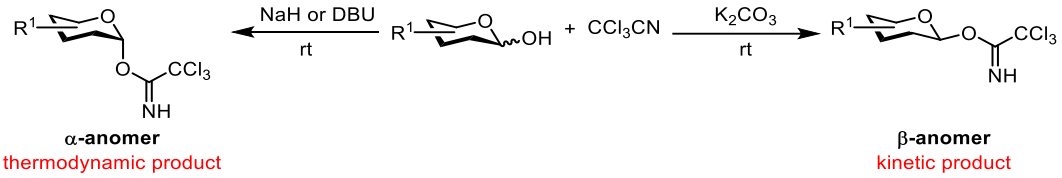

Scheme 10. The formation of glycosyl trichloroacetimidates.[21,22]

Regardless of their broad application for the synthesis of *O*-glycosides, glycosyl trichloroacetimidates are less commonly used for *C*-glycosylation. Schmidt *et al*. reported a Fries-type rearrangement from *O*-aryl glycosides to α-hydroxyaryl *C*-glycosides **20a**–**20g** using the glycosyl trichloroacetimidate **19** and electron rich phenol derivatives mediated by TMSOTf catalysis (Scheme 11).[11] However, the less electron rich phenol derivatives, naphthol and umbelliferone, only afforded the *O*-glycosides.

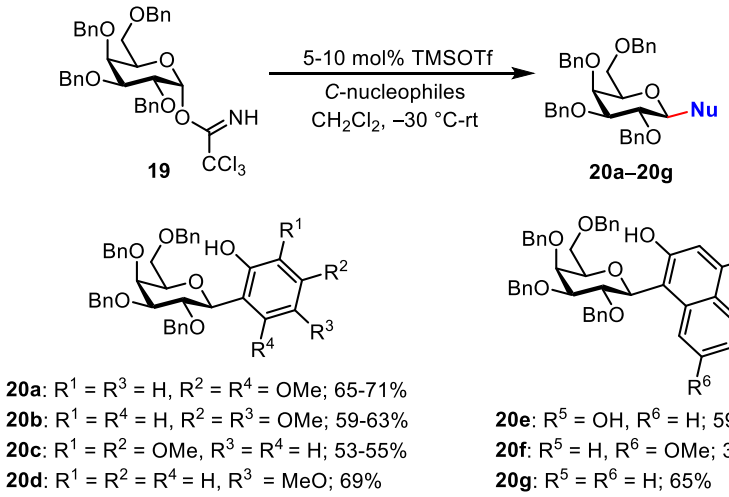

Scheme 11. TMSOTf catalyzed *C*-glycosylation of glycosyl trichloroacetimidate.[11]

C-glycosylation of mannosyl trichloroacetimidate **21** with 2-napththol (**22**) in the presence of stoichiometric amount of TMSOTf afforded the exclusive formation of aryl β-*C*-glycosides **20g**, whereas a preference for the generation of the α-anomer **23** was observed by a $ZnCl_2$ promoted reaction (Scheme 12).[23]

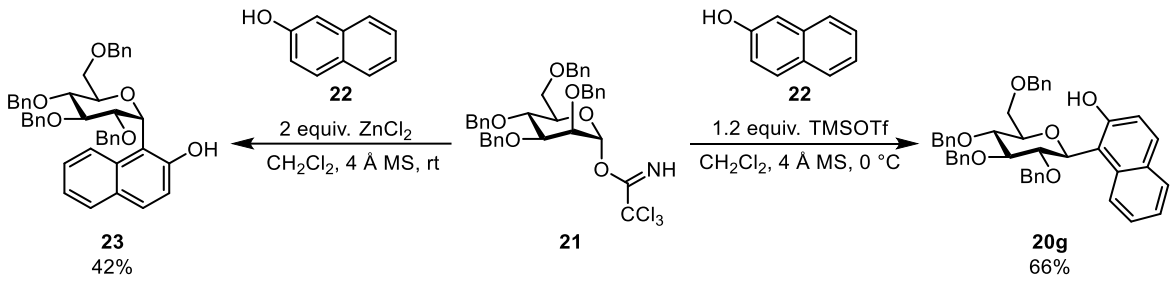

Scheme 12. Formation of aryl *C*-glycosides by different catalysts.[23]

1.2 The concept of vinylogy

Vinylogy is a π-conjugated system which transmits electrons of a functional group to a remote position in the molecule through internal conjugated double bonds. The atom-economic reactions show efficiency in constructing pivotal building blocks and stereocenters at γ- or even more distant positions in complex, bioactive compound.[24] A large amount of biologically active molecules such as polyene macrolide antibiotic **24** contain extended and highly unsaturated conjugated olefins (Figure 3).[25]

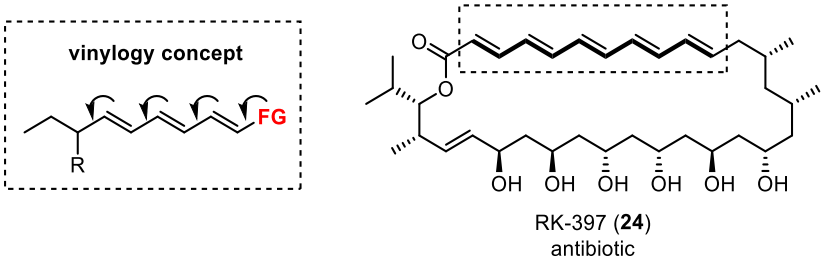

Figure 3. The vinylogy concept and bioactive natural product RK-397 (24).[24]

1.2.1 Vinylogous dioxinone dienolates

The cyclic dienolate **26** derived from dioxinone **25** is particularly useful in generating γ-functionalized product **27** (Scheme 13).[26] Dioxinone **25** is stable at room temperature. However, it rapidly undergoes a retro [4+2] cycloaddition to afford acyl ketene **28** while heating.[24] The

unstable ketene intermediate reacts with nucleophiles such as amines and alcohols to generate the corresponding β-keto-amides and esters **29**.[24,26]

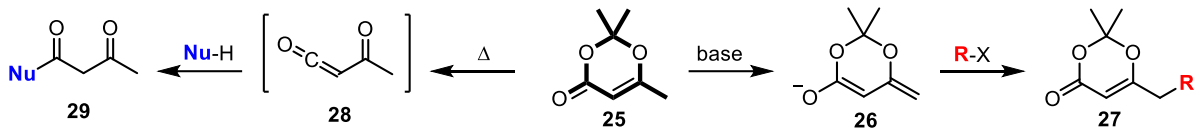

Scheme 13. Transformation of dioxinone 25 to γ-functionalized product and ketenes.[24,26]

The site selectivity of vinylogous dienol ethers is involved in various factors which determine whether the functionalization occurs at the *C*-3 or *C*-5 position (Figure 4).[27] For example, metallodienolates and silyl dienol ethers, highly electron-rich species, possess different electronic properties at the *C*-3 and *C*-5 carbons in the molecule. By calculating the HOMO orbital coefficients (OCs) and electrophilic susceptibilities (ESs), Denmark and co-workers have proved that metalllodienolates are easier to react at the *C*-3 position (higher values of OC and ES at the *C*-3 position, Figure 4; a).[27,28] In contrast, the silyl dienol ethers are prone to undergo the *C*-5 addition (higher values of OC and ES at the *C*-5 position, Figure 4; b). In addition, the reactivity and site selectivity can be modified by the surrounding functional groups and by certain steric environments.

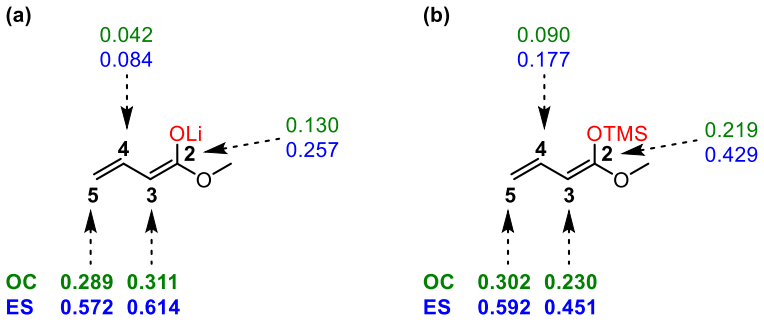

Figure 4. Computationally calculated homo orbital coefficients (OCs, green) and electrophilic susceptibilities (ESs, blue) of a lithium dienolate (a) and a silyl ketene acetal (b).[27,28]

In 2014, Hartwig *et al.* reported an iridium catalyzed, γ-selective asymmetric allylation between a variety of allylic trichloroethyl carbonates **30** and the unstable silyl dioxinone dienolates **31** (Scheme 14).[29] The protocol afforded the desired products in moderate yields and high enantiomeric excess with excellent γ- and branch/linear (b/l) selectivity. Subsequently, the higher γ-selectivity was achieved via methyl substitution at the α-position of dioxinone with γ-selectivity greater than 20:1. However, the formation of the unexpected S_N2 linear side product **34** presumably

originated from the sterical hinderance of the α-methyl substitution leading to lower diastereoselectivity in comparison to the non-substituted dienolate. According to control experiments, the reason of the high regioselectivity and good b/l selectivity of this reaction indicated the importance for the leaving group of the electrophiles together with the addition of chiral phosphoramidite ligand.

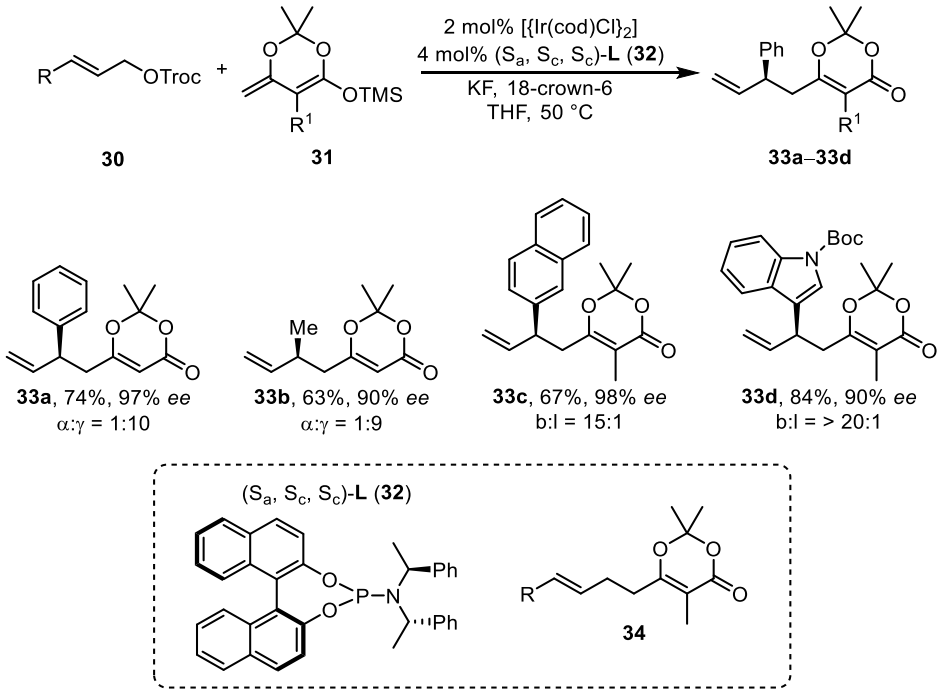

Scheme 14. Iridium catalyzed allylic substitution of dioxinone dienolates.[29]

A further application of vinylogous dienolates is the *C*-glycosylation of glycosyl *ortho*-alkynylbenzoates **35**–**37** with the vinylogous dienolates **38**–**39** catalyzed by PPh_3AuNTf_2 to provide *C*-glycosides **40a**–**40f** (Scheme 15).[30] The *C*-glycosylation of glycosyl *ortho*-alkynylbenzoate with allyltrimethylsilane and simple silyl enol ethers generated α-anomers as the major products, whereas the reaction with dioxinone dienolate **38** and linear dienolate **39** yielded *C*-glycosides **40a**–**40f** in poor stereoselectivity with α/β ratio of almost 1:1. In addition, the reaction of 2-deoxyribofuranosyl *o*-alkynylbenzoates **36** with dioxinone dienolate **38** produced anomers **40b** with higher β-ratio meaning inversed stereoselectivity. The control experiments disclosed the importance of moisture which was sequestered by molecular sieves to regenerate the active catalytic gold (I) species.

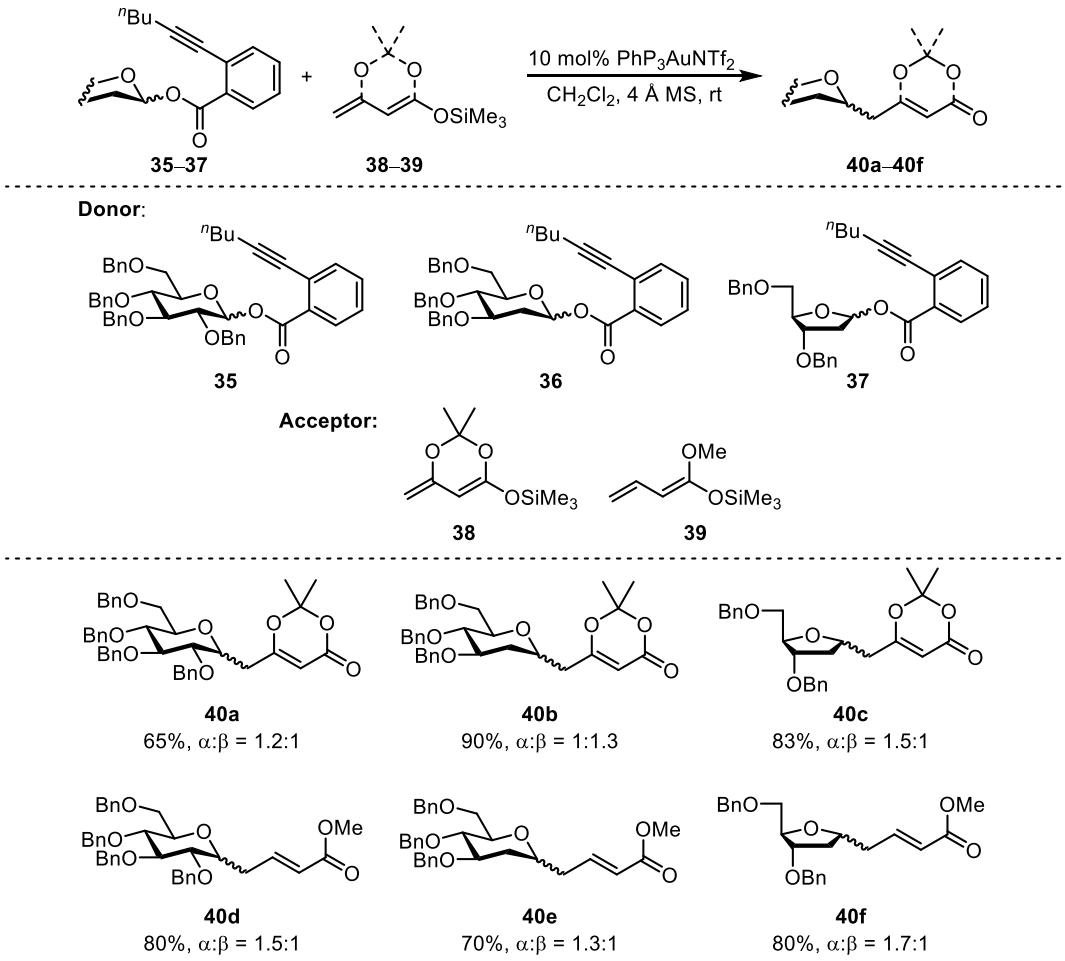

Scheme 15. Gold catalyzed *C*-glycosylation with glycosyl ortho-alkynylbenzoates and dioxinone dienolates.[30]

1.2.2 Vinylogous coumarin dienolates

Additional to dioxinone dienolates, 4-methylcoumarins are another class of inherent vinylogous donors with an exocyclic nucleophilic site. The cyclic units of 4-methylcoumarins play important roles in promoting γ–vinylogous addition reactions. Furthermore, the core is a privileged structure class of heterocycles present in various natural derived and clinically known substances (Figure 5).[31,32]

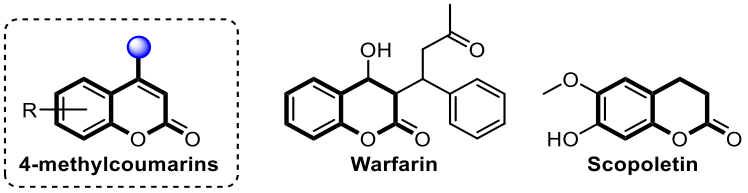

Figure 5. 4-Methylcoumarins and compounds bearing the coumarin scaffold.[31,32]

In 2019, Zhang and co-workers have established a palladium-catalyzed Heck type vinylogous *C*-glycosylation of α,β-unsaturated lactones to attain 2,3-unsaturated *C*-glycosides **46a**–**46d** in moderate to good yields and exclusive β-selectivity (Scheme 16).[33] Diverse *O*-6 substituted D-Galactals including distinct electronic or steric functional groups were evaluated. Interestingly, the reaction between 3,4-*O*-carbonate D-allal **42** and 4-methylcoumarin generated the corresponding *C*-glycoside **46c** with α-stereo preference which is inversed to the other results obtained.

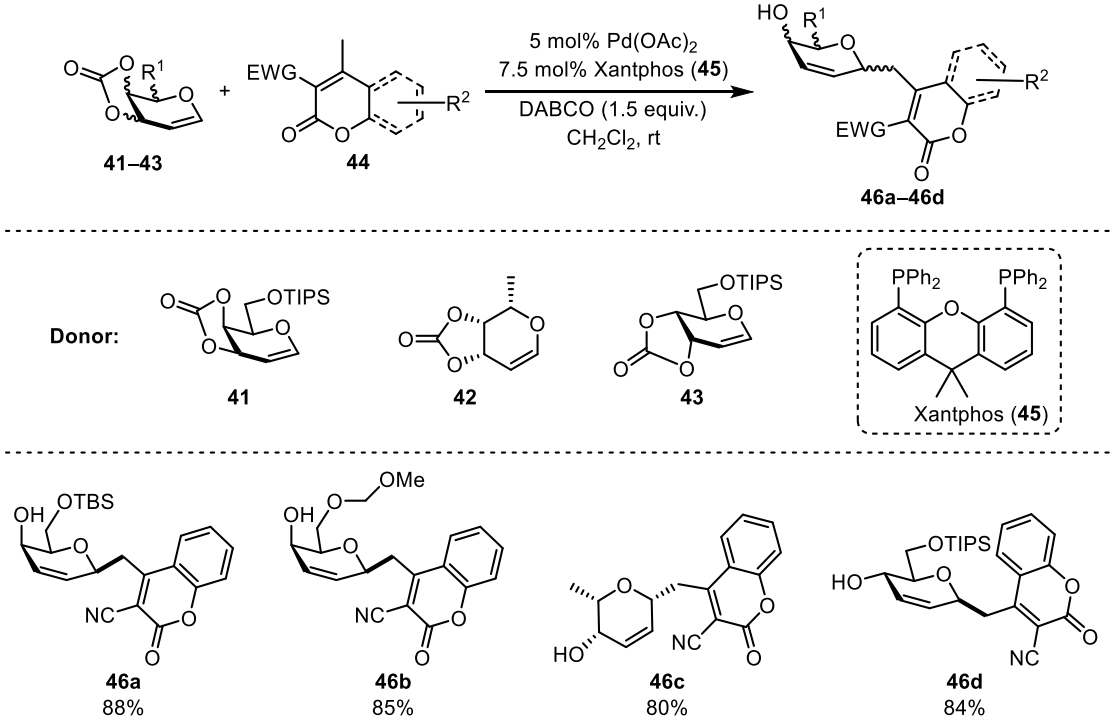

Scheme 16. Palladium-catalyzed Heck type *C*-glycosylation.[33]

1.2.3 Vinylogous oxindole dienolates

The oxindole moiety is a core structure in several natural products and nature-inspired synthetic drugs. A common feature of this complex compound family is the substitution of the *C*-3 position, such as 3,3-spirofused oxindoles in spirotrypostantin B and Gelsemine (Figure 6).[31,32] Similar to coumarins, 3-alkylidene oxindole structures have potential vinylogous nucleophilic character. They possess the dual functional features of a lactam carbonyl moiety fused with a pronucleophilic exocyclic double bond. This enables intermediates to proceed into a useful nitrogen heterocycle of varied complexity.

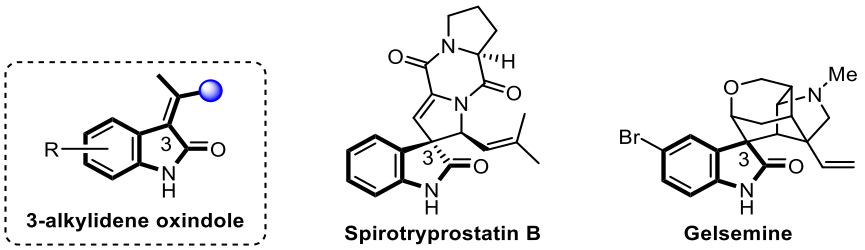

Figure 6. 3-Alkylidene oxindoles and compounds bearing the oxindole scaffold.[31,32]

Li *et al*. demonstrated the bismuth-catalyzed vinylogous nucleophilic 1,6-conjugate addition of 3-alkylidene oxindoles **48** to *para*-quinone methides **47** in complete *Z*-selectivity and excellent diastereoselectivity (Scheme 17).[34] Diverse electronic properties on *para*-quinone methides **47** were employed under the optimized condition. Investigation of different substitution patterns at the C_β-position of 3-alkylidene oxindoles did not affect the *Z*/*E* values on the diastereoselectivity.

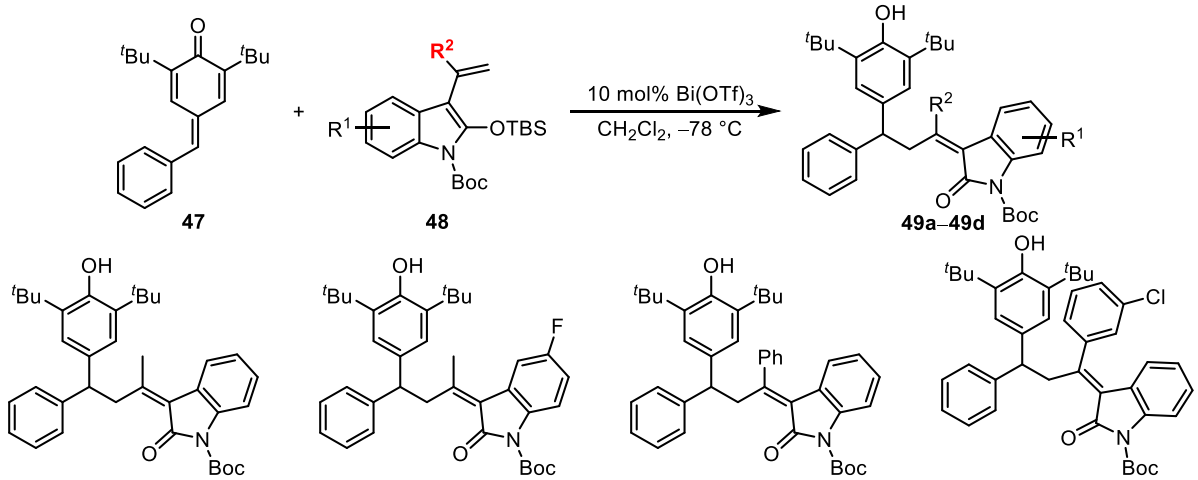

Scheme 17. Bismuth-catalyzed vinylogous nucleophilic 1,6-conjugate addition.[34]

1.3 Calcium-based Lewis acid catalysts and halogen bond catalysts

Transition metal catalysis has attracted tremendous attention. However, there are some inherent disadvantages of transition-metal catalysts such as cost, high toxicity and their availability. Therefore, it is necessary to develop sustainable alternatives which are inexpensive and non-toxic to the environment. Therefore, early main group metals such as calcium and organo-catalysis are acquiring more attention, especially in recent years.[35]

1.3.1 Calcium-based Lewis acid catalysts

Calcium is the fifth most common element in the Earth crust and its common salts are free of toxicity.[35] Therefore, it is logical to create catalysts from calcium compounds both from an economic and ecological point of view. Despite their apparent benefits, the catalytic potential of calcium remains surprisingly undeveloped. In addition, the first calcium-catalyzed transformations were only reported in the last fifteen years.[35]

The low reduction potential ($E° = -2.869$ V) of calcium ions means they are considered as inert towards redox processes under organic reaction conditions. This is an advantage as unwanted side reactions involving redox activity cannot disrupt the desired reaction pathway. The reactivity of calcium (II) compounds can be subdivided into two components (Figure 7).[35] As a result of its low electronegativity, calcium (II) as an alkaline-earth metal ion possesses high ionic character. Therefore, the anionic counterpart has highly nucleophilic character with strong basicity. In addition, the calcium center itself acts as Lewis acid, in a similar fashion to metal centers of conventional group 3 elements.

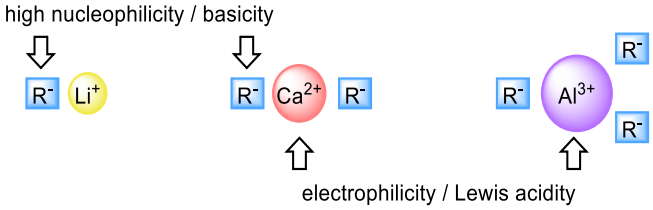

Figure 7. Reactivity of calcium compounds.[35]

When the counterions are adequately chosen, the highly basic character of the calcium ion is vanquished. Therefore, the best results are achieved by pairing Ca^{2+} with weakly coordinating and non-basic anions such as TfO^-, F^-, F_6iPrO^- or a mixture of 1:1 triflimidate (NTf_2^-) and hexafluorophosphate (PF_6^-; Figure 8). Due to the strong coordination to the hydroxyl groups, the

high oxyphilic calcium is generally higher in reactivity towards alcohol compounds. The oxophilic properties can activate the hydroxyl moiety by increasing its leaving group ability as the calcium ion can coordinate to the departing OH^- in its calcium-hydroxide form. In addition, partial or full hydration of the calcium ions result in strong acidification of the coordinated water molecules which can further produce a Lewis acid/Brønsted acid cooperative catalytic system. Also, the presence of water molecules might lead to aggregation of the active catalytic calcium species due to the nature of early main group metals.[35]

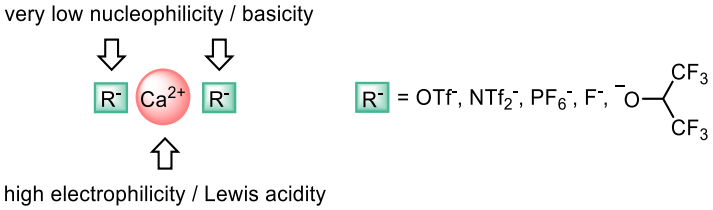

Figure 8. Best coordination system for calcium catalyzed reactions.[35]

Niggemann *et al.* reported a calcium-catalyzed hydroarylation of a series of different styrenes **50a**–**50b** and alkenes **50c**–**50d** with resorcinol dimethyl ether **51** and other electron rich arenes (Scheme 18).[36] The high reactivity of the $Ca(NTf_2)_2/Bu_4NPF_6$ system resulted in the arylation of dienes and even trisubstituted olefins. The reactions proceeded at room temperature with no special precautions for the moisture in the air.[36]

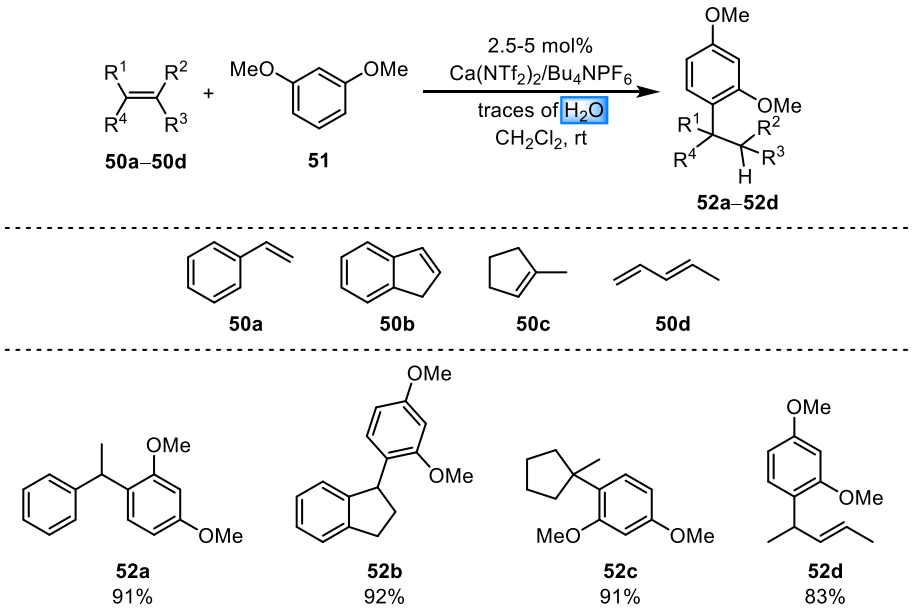

Scheme 18. Calcium triflimide catalyzed hydroarylation.[36]

A further enhancement of the $Ca(NTf_2)_2$ usage was the activation of cyclopropanes to enable Friedel-Crafts alkylation with benzofuran.[37] The addition of dimethyl aryl-, and heteroaryl-cyclopropanes **53** with different electronic properties of benzofuran **54** were achieved with complete regioselectivity to provide the expected products **55d**–**55d** in moderate to good yields.

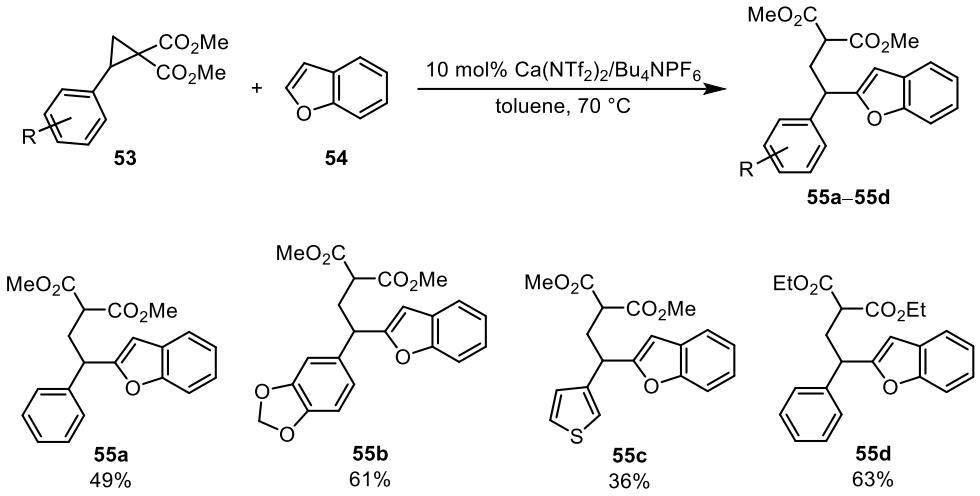

Scheme 19. Calcium triflimide catalyzed Friedel-Crafts alkylation.[37]

The proposed mechanism started with the coordination of the carbonyl group of the cyclopropane **56** leading to the reduction of the C-C cyclopropyl bond (Scheme 20).[37] The benzofuran **54** attacked the newly generated electrophile to form a zwitterionic intermediate **57**. Proton transfer and rearomatization of the intermediate afford the desired product **55a** (Scheme 20; path a), whereas addition of the calcium enolate to the carbocation on the benzofuran generated the unwanted side product **58** (Scheme 20; path b).

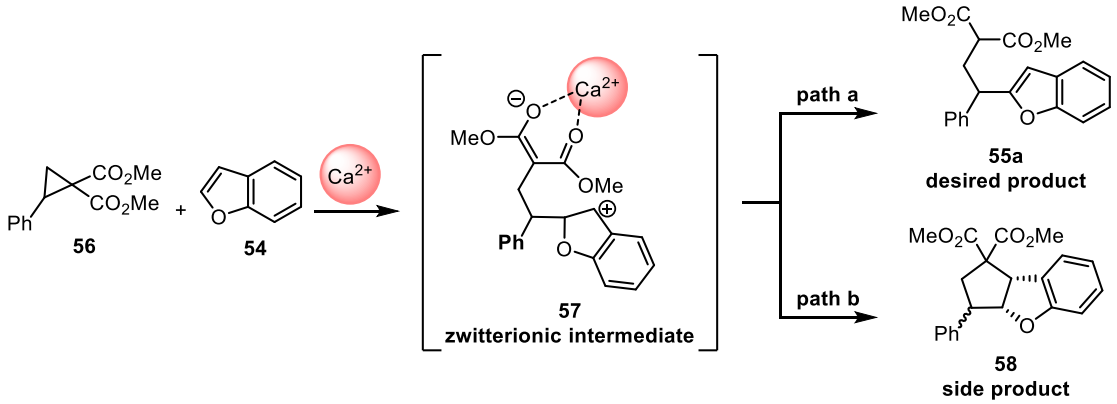

Scheme 20. Proposed mechanism of the Friedel-Crafts alkylation catalyzed by calcium ion.[37]

1.3.2 Halogen bond catalysts

In the last twenty years, the emergence of organocatalysts such as hydrogen bond and halogen bond catalysts had tremendous impact as alternatives to transition metal catalysts. Halogen bonding (XB) is a non-covalent interaction mode. It takes place between an electrophilic halogen atom X and a Lewis base LB (Figure 9; a).[38] The halogen-derived Lewis acid is usually referred to as a XB "donor." The XB interactions are the attractive force from a nonbonding orbital of the Lewis base to the antibonding orbital of the R-X bond by an n→σ* partial electron transfer (Figure 9; b).[39] The interaction angle of such XB adducts is generally close to 180°.[40] The Lewis acidity of XB donors R-X becomes higher in the order X = Cl <Br <I with the more polarizable the halogen atom.[41,42] The more Lewis-acidic XB donors are generated when the electron-withdrawing character of the halogen-bearing group is increasing. In general, the iodine-based halogen-bond donors are predominant since a strong XB is required.

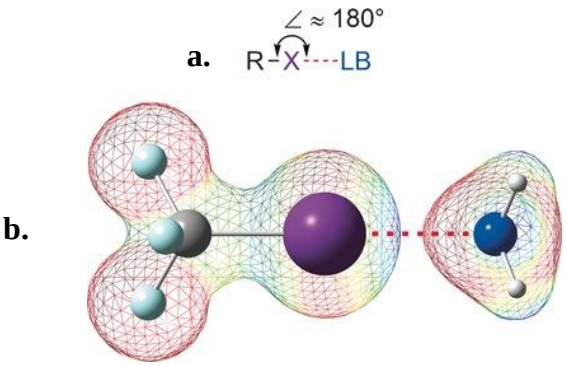

Figure 9. (a.) Depictive model of a halogen bond. (b.) halogen bond between trifluoroiodomethane and ammonia, illustrating the mapped electrostatic potential of the core characteristics of a halogen bond with blue showing low and red showing high electron potential.[42]

The non-covalent interaction of XB is similar to hydrogen bonding (HB) because both of them consist of a pair of electron donors and acceptors (Figure 10). The electron donors in XB and HB are similar since they are both electron-rich but the electron acceptors are different. The electron acceptor in a HB is the electron-deficient hydrogen atom, whereas the electron acceptor in XB is an electron-rich halogen atom which provides an σ-hole to attract electrons.[43]

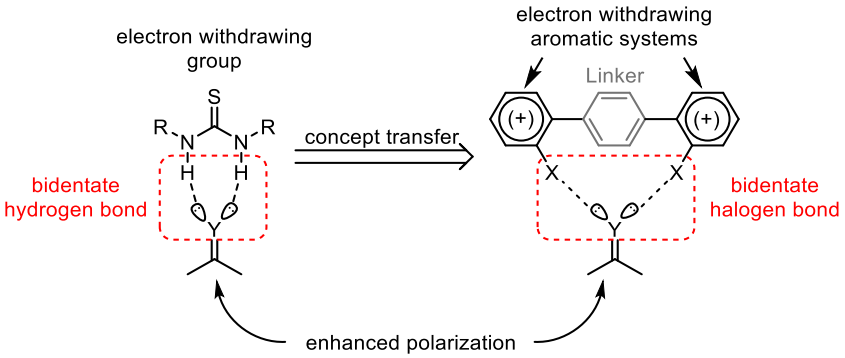

Figure 10. Concept transfer from hydrogen bonding to halogen bonding.[40]

The actual catalytic mode of the XB donor will slightly change according to the nature of the substrates. The coordination of neutral substrates such as carbonyl compounds will lower the LUMO of substrates and stabilize the partial negative charge in the transition state of the reaction (Figure 11; a). Since the coordination is relatively weak, the formation process of product is less inhibitory which is an outstanding advantage of non-covalent catalysts compared to metal catalysts. In the anionic binding mode, the coordination of the anionic leaving group facilitates S_N1 reactions (Figure 11; b). The reaction rate will be accelerated by extraction of the anion from the dissociation equilibrium. However, the stronger affinity of XB donor to the anion might lead to a higher risk of catalyst restriction by anion coordination and therefore a special reaction design is required.

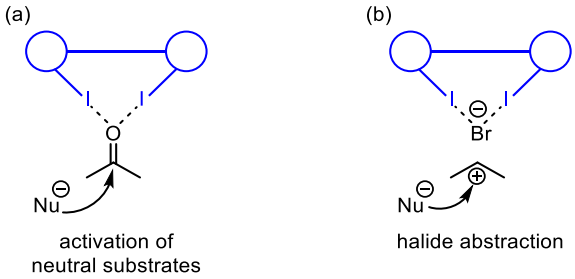

Figure 11. Different mode of activation of halogen bonding catalyzed reactions.[40]

Takemoto *et al.* reported a cooperative catalytic system between Schreiner's thiourea **62** and XB donor **63**.[44] The directly coupled glycosyl trichloroacetimidates **59**, **60** with various amides **61**, including asparagine residues of dipeptides and tripeptides generated hereby unique *N*-acylorthoamides **64a**–**64d** in moderate to good yields (Scheme 21).[44] According to the results, the XB or HB donor on its own was not able to activate the coupling reaction, which revealed the importance of the combination of both, HB catalyst **62** and XB catalyst **63** for the successful

reaction. Additionally, the control experiments indicated that the azolium cation or the triflate anion could not accelerate the reaction by itself. The proposed mechanism showed that the XB donor interacted with the soft sulfur moiety of the thiourea to increase the HB-donating ability of the thiourea resulting in the activation of the trichloroacetimidate leaving group.

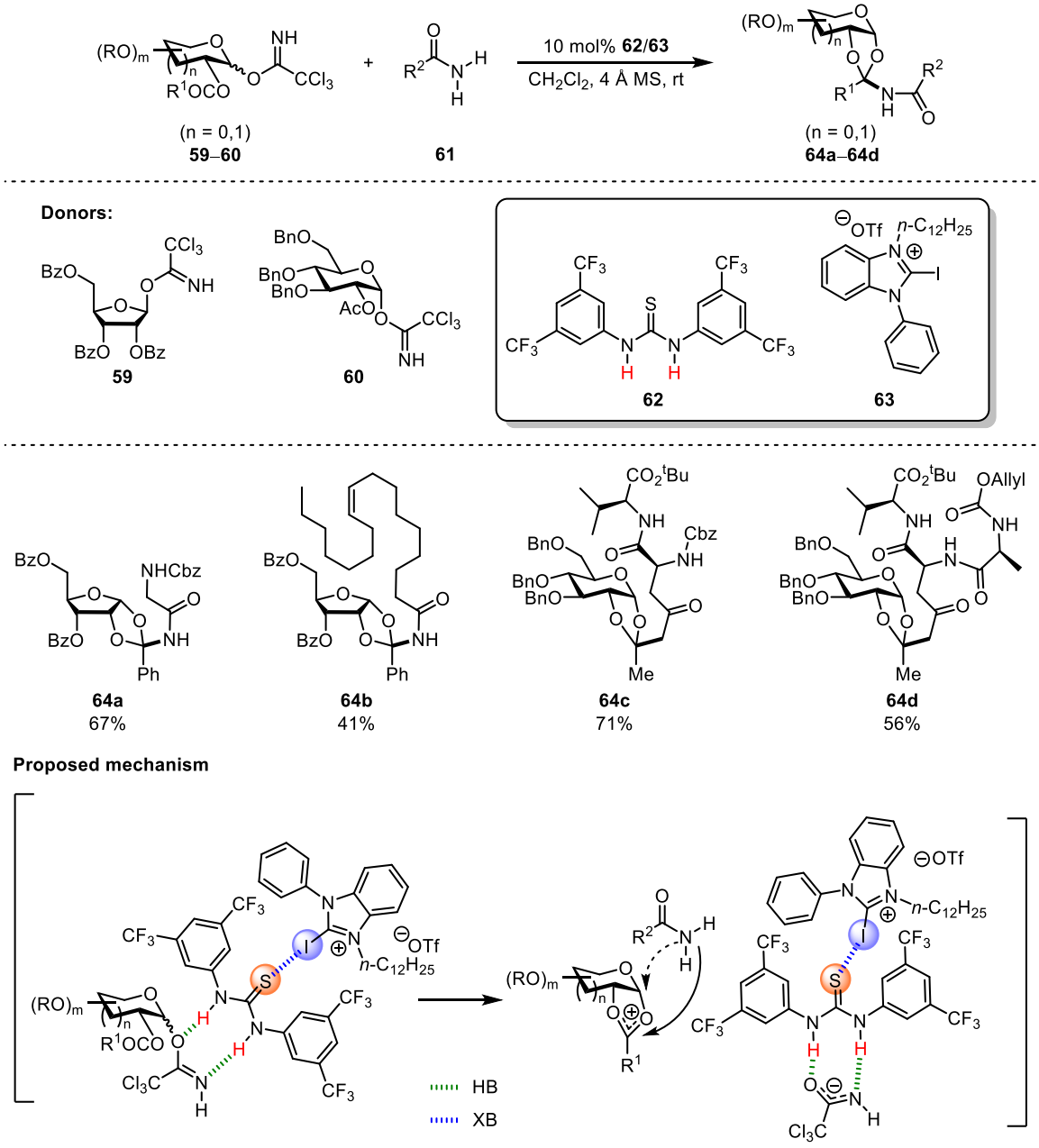

Scheme 21. XB and HB donor cooperative catalyzed *N*-acyl-orthoamidation.[44]

In 2019, our research group developed the first strain-release glycosylation by bidentate benzoimidazolium XB catalysis **65** to generate *O*, *N*-glycosides in excellent anomeric selectivity

(Scheme 22).[45] A wide range of different oxygenated acceptors were tolerated under this condition. Regioisomers **66e** and **66f** were obtained when benzotriazoles are used as *N*-nucleophiles. The steroid derivative **66c** was shown to be a potent inhibitor of the hedgehog signaling pathway via a non-smoothened mode of action. This opened a new opportunity for a potential new mode of action for cancer therapy.

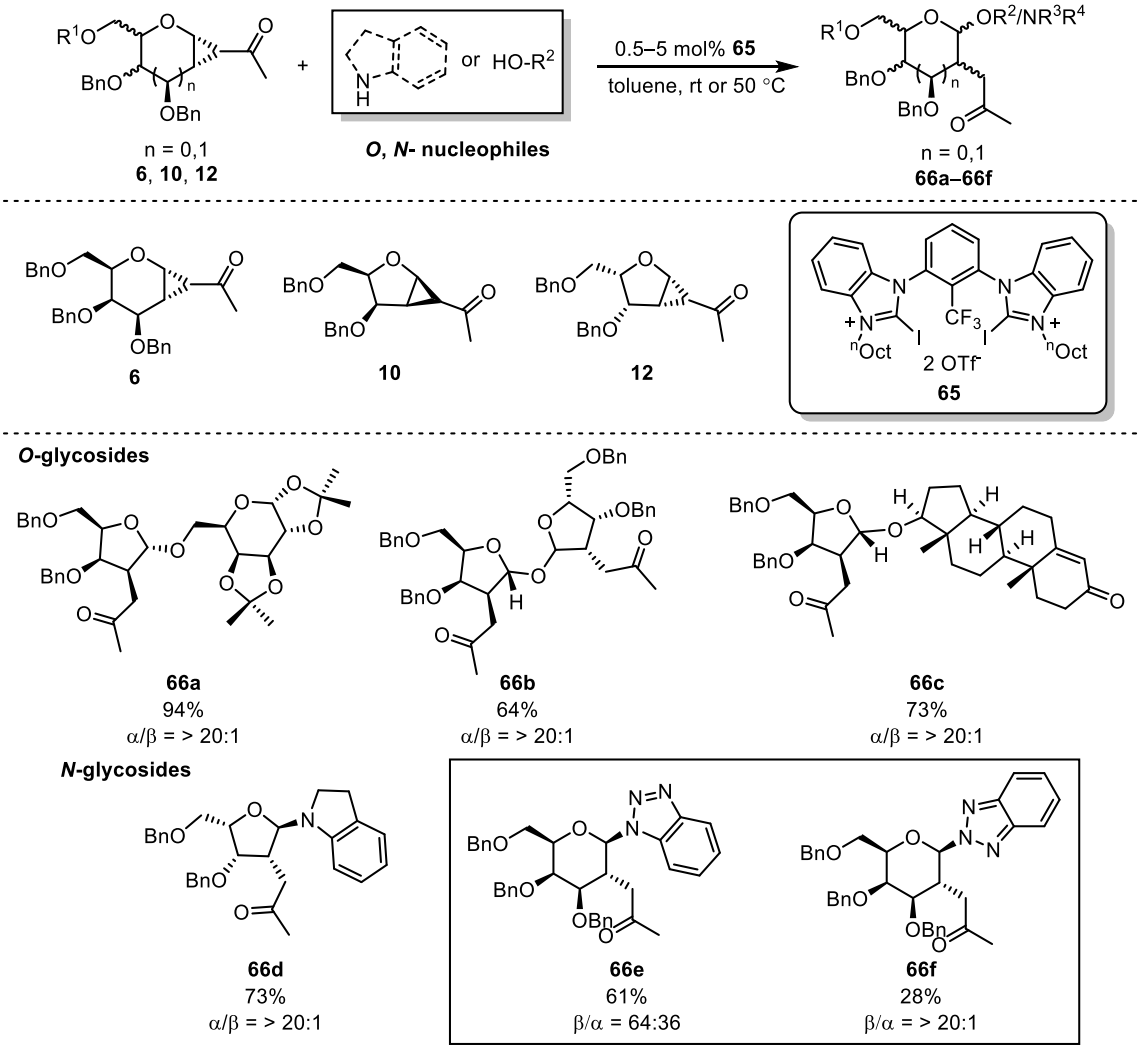

Scheme 22. Solely XB catalyzed strain-release glycosylation.[45]

Similar to HB catalyzed activation mode previous discussed, the XB catalyzed mechanism was involved simultaneous in two different pathways. The attenuation of the O-H bond in the acceptor via XB resulted in an acidic proton attaching to the carbonyl oxygen which activated the ring opening of **10** (Scheme 23; a). The donor-acceptor ion pair **17a** was attacked by the acceptor anion

at the anomeric center to generate **18**. At the same time, the XB catalyst **65** activated the ketone functional group causing the ring opening and forming the intermediate **17b** (Scheme 23; b). Furthermore, the XB catalyst **65** was utilized again in an XB-OH activation mode and facilitated the addition of the acceptor through an alkene transition state **67c** generating the ketal **67d** which underwent rearrangement to provide product **18**.

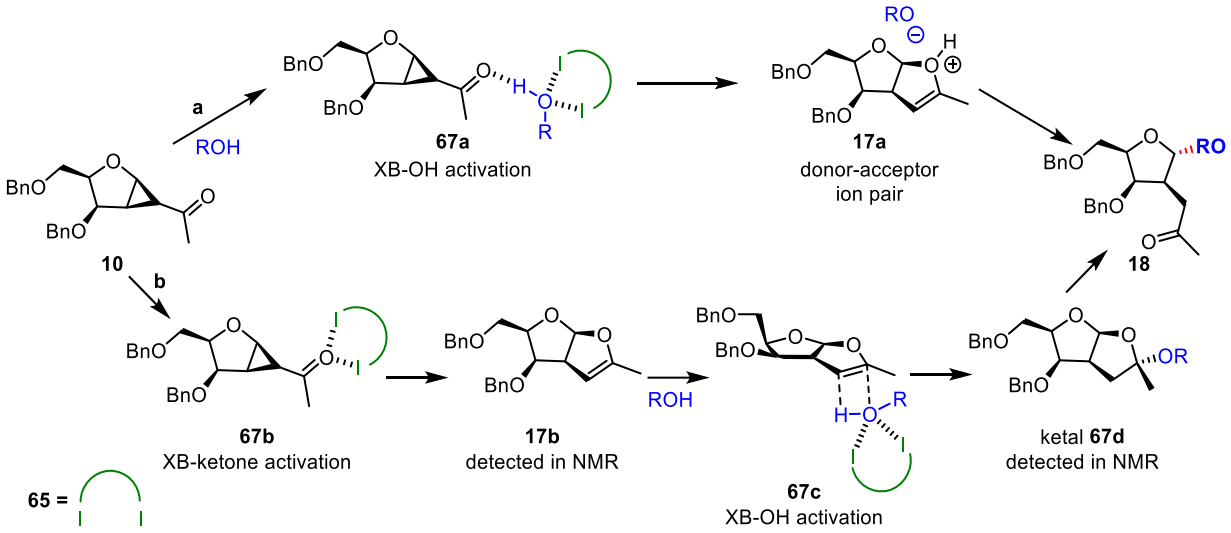

Scheme 23. Proposed mechanism of strain-release furanosylation via halogen bond catalysis (compare with Scheme 9).[45]

2 Design and aim of the project

Over the last twenty years, significant developments in transition metal and organocatalysis have led to milder conditions for C-C, C-O and C-N bond formation. However, utilizing these catalytic methods in carbohydrate chemistry is still a significant challenge. To bridge the gap between these research areas, we aimed to develop novel catalytic *C*-glycosylation methodologies between carbohydrate substrates and commonly found natural product derivatives containing conjugated vinylogous dienolates.

My project aimed to establish convenient ways to generate *C*-glycosides. A key objective of our research was to focus on modern catalytic methods including mild Lewis acid and halogen-bond (XB) catalysis. Distinct carbohydrate precursors could be prepared for feasible C-C bond formation. In addition, various cyclic and acyclic vinylogous dienolates could be synthesized. One approach was used a zinc catalyzed Ferrier rearrangement to give γ-regioselective 2,3-unsaturated glycals. In addition, the development of strain-release donor-acceptor (D-A) cyclopropanes via calcium catalysis was attempted to gain the thermodynamic stable *C*-glycosides. Furthermore, the *C*-glycosylation of glycosyl imidates was tried to establish by halogen-bond (XB) catalysis.

A variety of naturally-occurring carbohydrates such as gluco-, manno- and malto- sugars, could afford diverse mono and disaccharides. This, in turn, could provide an opportunity to generate eventual tool compounds allowing elucidation of various biological pathways. In order to screen for potential bioactivity, our glycosidic analogues could be submitted to Compound Management and Screening Center (COMAS) in Dortmund (Figure 12).

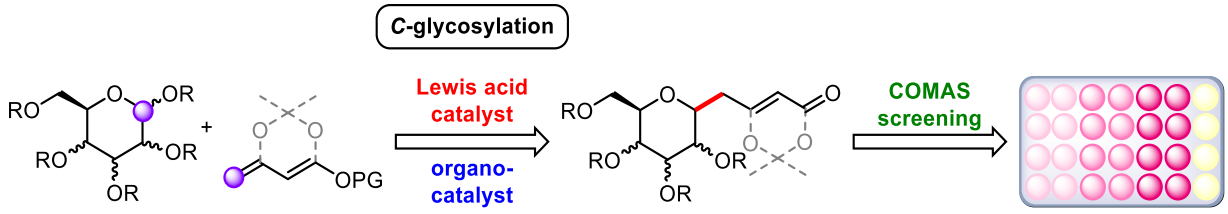

Figure 12. Novel catalytic vinylogous *C*-glycosylation to provide possible bioactive molecules for COMAS biological screening.

3 Results and discussion of $Zn(OTf)_2$ catalyzed Ferrier rearrangement via γ-vinylogous *C*-glycosylation

We were curious to introduce the vinylogous nucleophiles to the Ferreir rearrangement since the *C*-glycosylation of this reaction type was underrepresented. Instead of harsh catalytic condition, mild Lewis acids were decided to be used.

3.1 Synthesis of *O*-acetylated glycals

The unprotected carbohydrate substrates **68** underwent acetylation and subsequent bromination at the anomeric position (Scheme 24). The brominated substrates were reacted according to the Fischer–Zach method by zinc promoted elimination of the glycosyl halides under acidic condition.[46,47,48] Various *O*-acetylated glycals including pyranoses **70**–**72** (D-Xylal, D-Arabinal, L-Arabinal) and disaccharides **73**–**74** (D-Lactal and D-Maltal) were obtained over two steps in moderate to good yields. In addition, the biologically relevant furanose **77** was obtained in moderate yield as well.

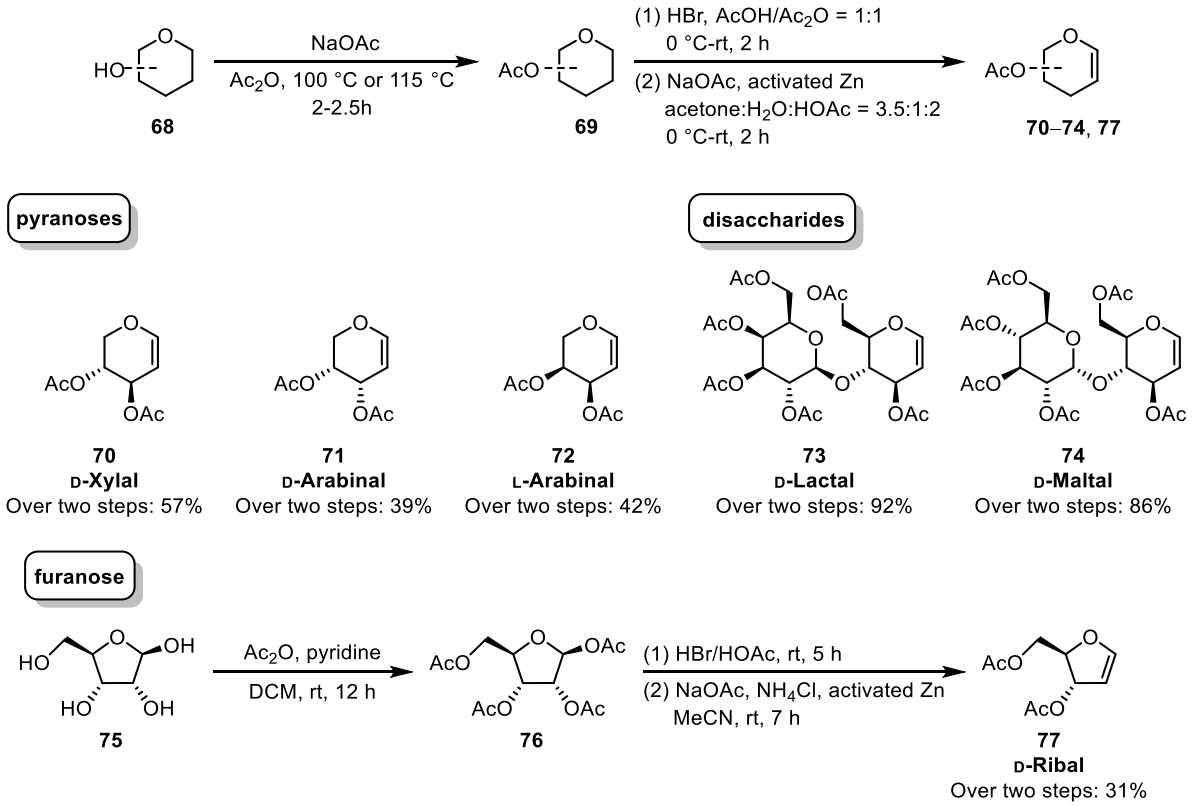

Scheme 24. Synthesis of the *O*-acetylated glycals.

3.2 Reaction scope of the glycals with dioxinone dienolate

The reaction was optimized by my supervisor, Dr. Charles Loh. The γ-vinylogous Ferrier rearrangement *C*-glycosylation took place as 20 mol% of $Zn(OTf)_2$ catalyst. The D-Glucal derivative **79a** was obtained in good yield and excellent regioselectivity in regard to the γ-position (Scheme 25). With the optimized conditions in hand, the substrate scope was expanded to different glycals. The investigation revealed that the *C*-glycosylation proceeded in moderate to good yields and absolute regioselectivity. This protocol tolerated not only pyranosides such as D-Galactal **4** and D-Arabinal **71** but also disaccharides and furanose derivatives. We noticed in our investigation that the anomeric selectivity is highly dependent on the steric properties of carbohydrate substrates. When D-Glucal **1**, D-Galactal **4**, and D-Arabinal **71** were employed, anomeric selectivity was slightly biased towards the disfavored β-anomer. In contrast, when L-Rhamnal, D-Lactal **73**, D-Maltal **74** and D-Ribal **77** were utilized, the major anomers generated were the α-anomers. The anomeric preference was hardly controlled since the *C*-glycosylation is lacking a thermodynamic anomeric effect and the carbohydrate substrates are absent of anchimeric assistance from the functional groups.

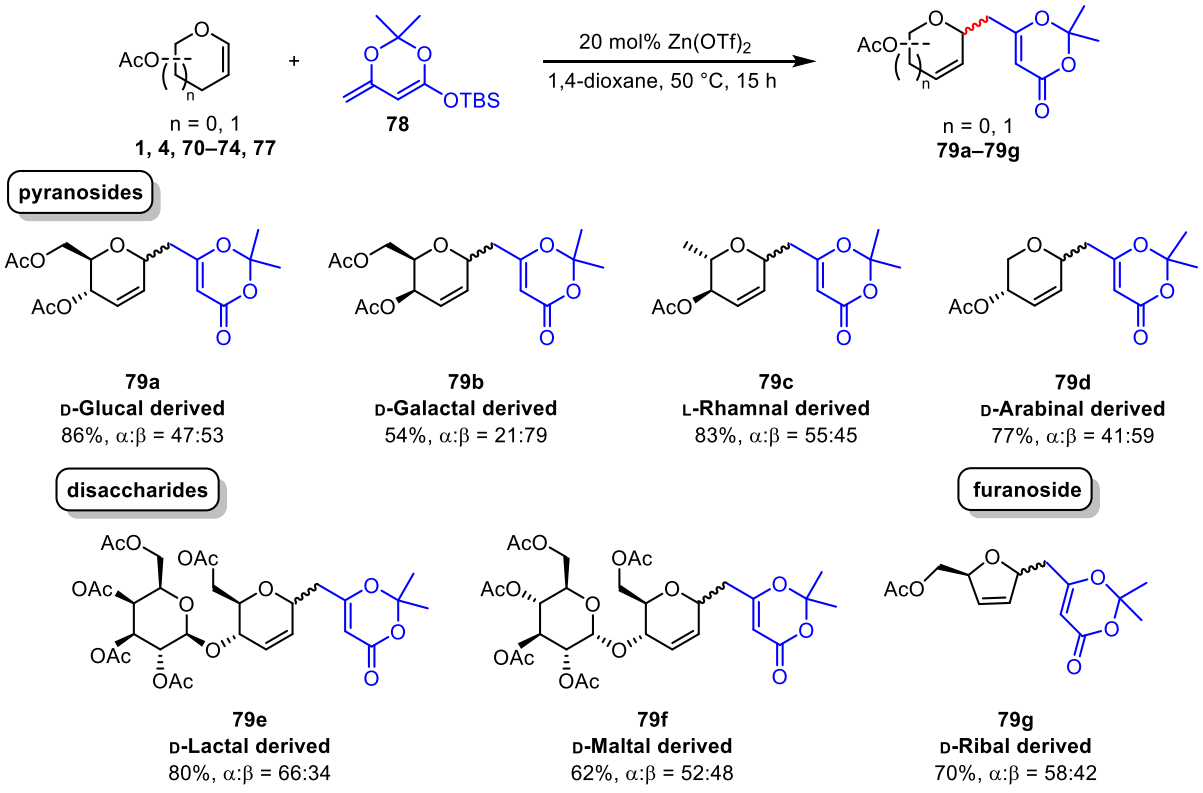

α:β ratio was determined by ^{1}H NMR of the crude reaction mixture; performed by Dr. Charles Loh.

Scheme 25. Reaction scope of glycals with dioxinone dienolate.

3.3 Synthesis of various linear dienolates and their reactivity

In order to further broaden the substrate scope, we synthesized various acyclic dienolates. The simple dienolate **81**, α- and β-methyl substituted dienolates **82** and **83** were obtained by deprotonation with freshly prepared lithium diisopropylamide (LDA) and protection with *tert*-butyldimethylsilyl chloride (Scheme 26).[49] In addition, the rarely found ε reactive trienolate **84** was accessed under the same reported procedure.

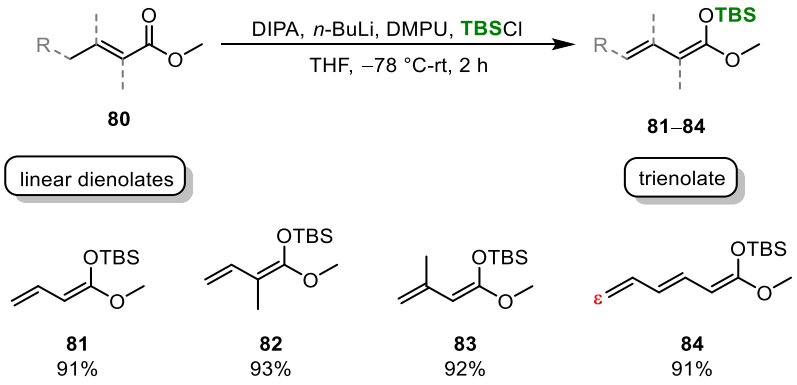

Performed/provided by Dr. Walter Hofer.

Scheme 26. Synthesis of linear dienolates.

We tested our *C*-glycosylation methodology by employing the newly obtained acyclic enolates **81**–**84**. The linear dienolate **81** underwent the reaction but did not display anomeric or regioselectivity (Table 2; entry 1). However, the β-methyl substituted dienolate **83** revealed slightly higher γ'-selectivity with no obvious anomeric selectivity (Table 2; entry 3). Similar to substrate **81**, the trienolate **84** yielded product also without anomeric or regioselectivity (Table 2; entry 4).

Table 2. Reactivity of the linear dienolates.

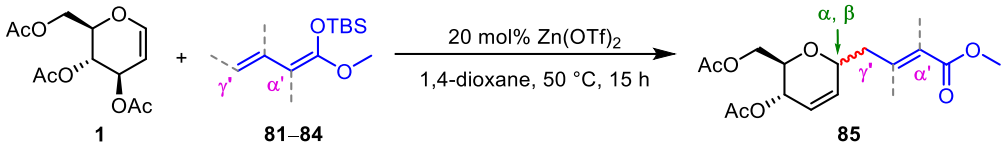

Entry	Linear dienolate	α:β ratio[a]	α':γ':(ε') ratio[a]
1	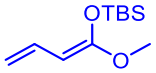 **81**	ca. 1:1	ca. 1:1
2	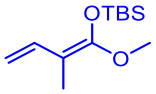 **82**	ca. 1:1	ca. 1:1
3	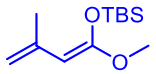 **83**	ca. 1:1	ca. 1:2.2
4	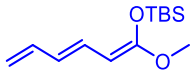 **84**	ca. 1:1	ca. 1:1:1

[a] α:β and α':γ':(ε') ratios were determined by ^{1}H NMR of the crude reaction mixture; in cooperation with Dr. Walter Hofer

3.4 Synthesis of mesityl dienolates and reaction optimization of Ferrier rearrangement with tri-*O*-acetyl Glucal and mesityl dienolate

In order to increase regioselectivity, the α-shielded mesityl dienolates **88** and **89** were synthesized through Friedel–Craft acylation and protection under basic condition (Scheme 27).[50,51]

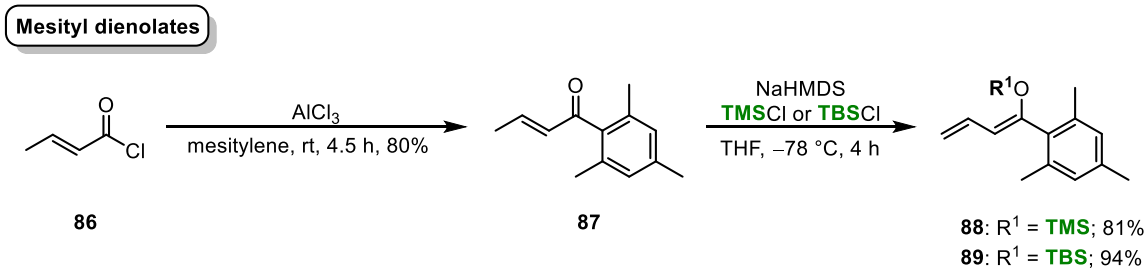

Scheme 27. Synthesis of the mesityl dienolates 88 and 89.

With the newly obtained mesityl dienolates in hand, the optimized protocol was applied. The relatively unstable dienolate **88** only provided trace amount of product (Table 3; entry 1). However, when the TBS protected dienolate **89** was used, the desired product **90a** was formed (Table 3; entry 2). The α-shielding mesityl dienolate **89** effectively prevented the formation of the unwanted α'-regioisomer and therefore generated excellent regioselectivity, analogous to a concept previously published by Schneider group.[50] With this promising result, we further studied the solvent effects. To our delight, with the change of solvent to dichloroethane, the yield increased to 53% (Table 3; entry 3). Optimal conditions were achieved when the reaction concentration was increased from 1 M to 2 M (Table 3; entry 7).

Table 3. **Reaction optimization of mestiyl dienolate with tri-*O*-acetyl Glucal.**

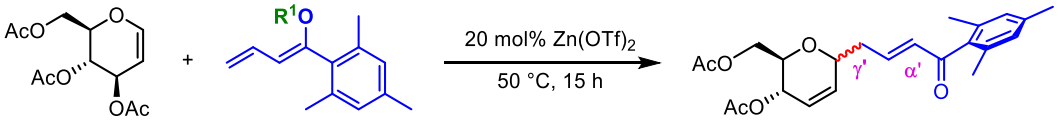

1 **88**: R^1 = TMS; **89**: R^1 = TBS; **90a** γ':α' = > 99:1

Entry	R^1	Solvent	Conc. (M)	Yield[a]
1	TMS	1,4-dioxane	1	trace
2	TBS	1,4-dioxane	1	26%
3	TBS	dichloroethane	1	61% (53%)[b]
4	TBS	chlorobenzene	1	66%
5	TBS	fluorobenzene	1	52%
6	TBS	1,4-dioxane	2	33%
7	**TBS**	**dichloroethane**	**2**	**79% (79%)[b]**
8	TBS	chlorobenzene	2	69%

[a] α':γ' ratio and yields were determined by ^{1}H NMR in the crude reaction mixture; [b] Isolated yield.

3.5 Reaction scope of glycals with mestiyl dieonlate

After optimizing conditions for the mesityl dienolate **89** for γ-vinylogous *C*-glycosylation, a thorough investigation of the substrate scope was carried out (Scheme 28). A wide range of pyranoside donors such as D-Galactal **4**, D-Arabinal **71** and L-Arabinal **72** and furanose **77** were also tolerated in this protocol. Moreover, the disaccharides bearing another sugar at *C*-4 including D-Lactal **73** and D-Maltal **74** were found to be suitable for this methodology. Interestingly, our

investigation revealed a general trend of increased anomeric selectivity than the previously mentioned dioxinone dienolate which gave inferior anomeric selectivity and was also more substrate dependent (Scheme 25 vs Scheme 28). The anomeric preference was thought to originate from the addition of the sterically hindered mesityl group on the less hindered α face of the favored chair transition state (Scheme 2). The anomeric selectivity of the L-Rhanmal derivative **90c** was slightly decreased. We postulated that the *C*-5 methyl substituted group would clash during the addition of the bulky mesityl dienolate from the α face.

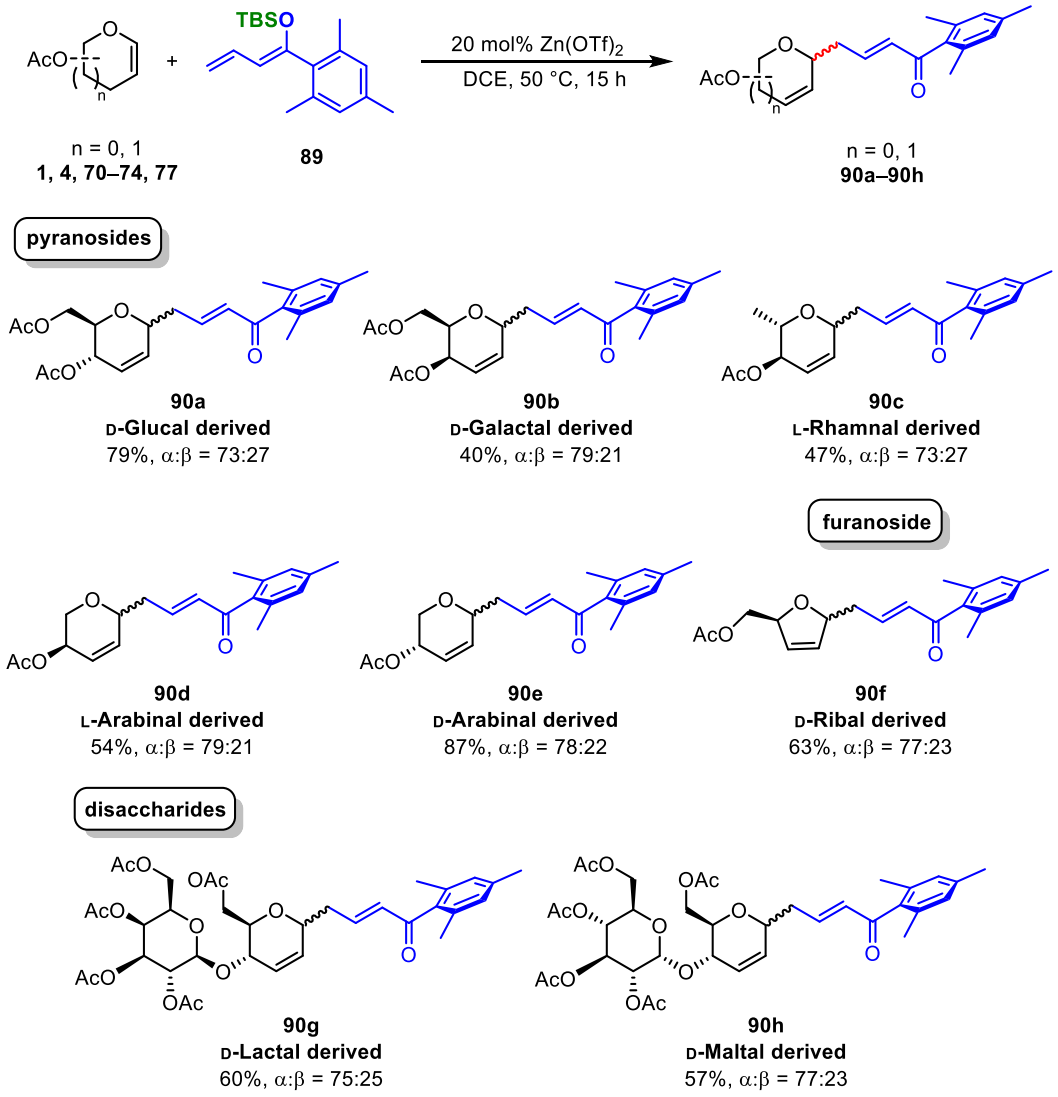

α:β ratio was determined by ^{1}H NMR in the crude reaction mixture.

Scheme 28. Reaction scope of glycals with the mesityl dienolate 89

3.6 Conclusion of $Zn(OTf)_2$ catalyzed Ferrier rearrangement via γ-vinylogous *C*-glycosylation

We showed that an α-anomeric selective and γ-regioselective vinylogous *C*-glycosylation via non-toxic and mild $Zn(OTf)_2$ catalysis was possible with diverse glycal substrates which included monosaccharides and disaccharides (Scheme 29). Additionally, not only the cyclic dioxinone dienolate but also the α-shielded mesityl dienolate generated the corresponding Ferrier type *C*-glycosides.

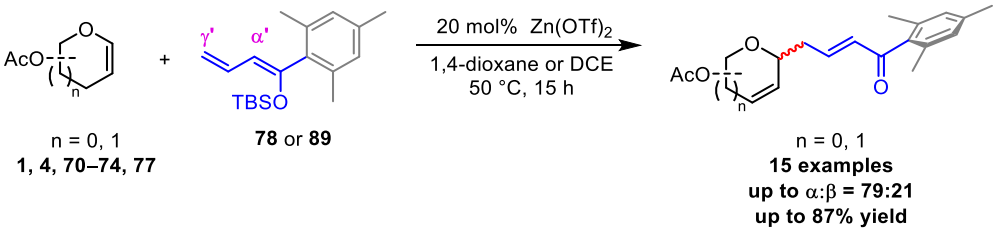

Scheme 29. $Zn(OTf)_2$ catalyzed γ-vinylogous Ferrier rearrangement.

4 Results and discussion of $Ca(NTf_2)_2$ catalyzed strain-release γ-vinylogous *C*-pyranosylation

The strain-release *C*-glycosylation was limited to reactive *C*-nucleophiles. The vinylogous dienolate has never been reported to be used in such sugar substrates. Mild catalysts as well as the counter anions were screened.

4.1 Synthesis of the D-Galactose derived D-A cyclopropanes

The commercially available methyl-α-D-Galactose **91** was used as starting material which underwent benzylation in basic conditions and subsequent allylation of *C*-1 to form the allylic compound **93** (Scheme 30).[52,53] The alcohol **95** was generated in a one-pot reaction. Initially, an iodination constructed the cyclic compound **94** followed by elimination via Zn catalysis. In order to undergo the cyclopropanation in the last step, the hydroxyl group at *C*-2 needed to be in axial orientation. Therefore, the hydroxyl group of **95** was oxidized by 2-iodoxybenzoic acid (IBX) and selectively reduced with L-Selectride to afford the axial alcohol compound **97**. This in turn was activated using 4-toluenesulfonyl chloride affording alkene **98** in a good yield. The alkene was submitted to oxymercuration and oxidation achieved by Jones reagent. In the last step, the α-proton of the resulting ketone was abstracted under basic conditions and underwent a tandem S_N2 elimination to afford the desired cyclopropanated substrate **6** with an overall yield of 27%.[52,53]

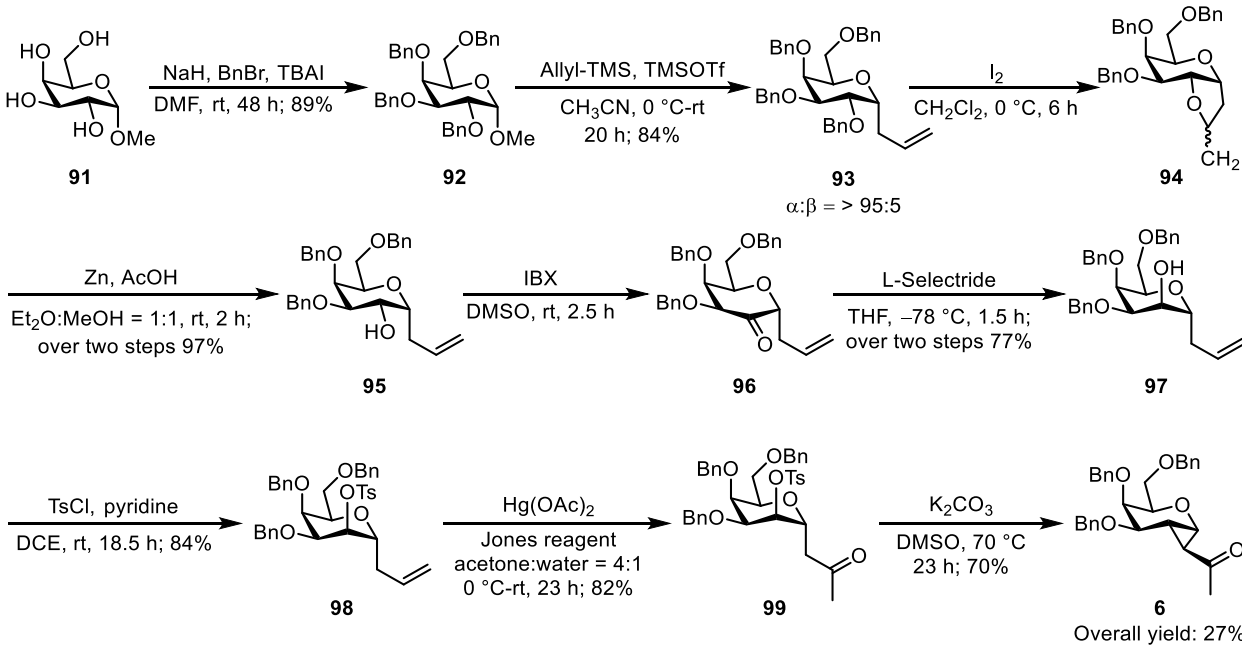

Scheme 30. Synthesis of the D-Galactose derived D-A cyclopropane.[52,53]

As a result of successful generation of **6**, we were curious to investigate the effects of various functional groups at the *O*-6 position of the D-Galactose derived cyclopropane. Therefore, D-A cyclopropanes, equipped with different electronic and steric groups, were prepared (Scheme 31). The acetylated cyclopropane **101** was obtained through a one-pot Zn-activated debenzylation and acetylation of tosyl compound **99** and subsequent cyclopropanation.[19] Furthermore, the acetyl group of compound **100** was removed under mild basic conditions to be further converted into different functional groups to obtain the critical compounds **102**–**107** before undergoing cyclopropanation.[33] The target D-A cyclopropane substrates **108**–**113** were successfully generated under weak basic conditions. To our delight, the natural product and drug derived substrates **112** and **113** could be accessed through the conventional cyclopropanation procedure.

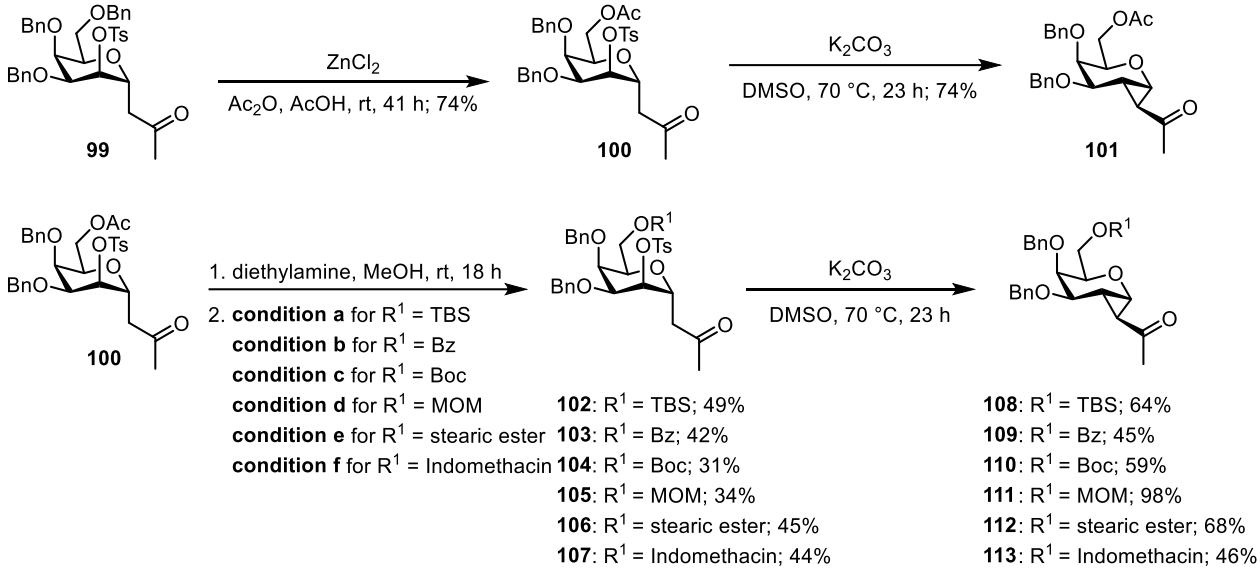

Condition a: TBSCl, triethylamine, CH_2Cl_2, 0 ºC-rt, 64 h; condition b: benzoyl chloride, triethylamine, CH_2Cl_2, 0 ºC-rt, 45 h; condition c: di-*tert*-butyl dicarbonate, DMAP, triethylamine, THF, rt, 17 h; condition d: MOMCl, DIPEA, CH_2Cl_2, rt, 19 h; condition e: stearic acid, EDC, DMAP, DIPEA, CH_2Cl_2, rt, 19 h; condition f: Indomethacin, EDC, DMAP, DIPEA, CH_2Cl_2, rt, 16 h

Scheme 31. Conversion of distinct functional groups at *O*-6 substituted of the D-Galactose derived cyclopropanes.

4.2 Synthesis of various dioxinone dienolates

Different silyl protected dienolates **38**, **116** and diethyl dienolate **117** were synthesized. The sterically strained cyclohexyl dienolate **118** was generated to verify the steric effect at the reaction center of the acceptor on the developed reaction (Scheme 32).[54] In addition, the γ-dimethyl substituted compound **119** was obtained to identify broader application. Diverse α-substituted dienolates **120**–**122** including methyl, benzyl and triisopropylsily (TIPS) were synthesized in order to understand the influence of the α-position for the established reaction.

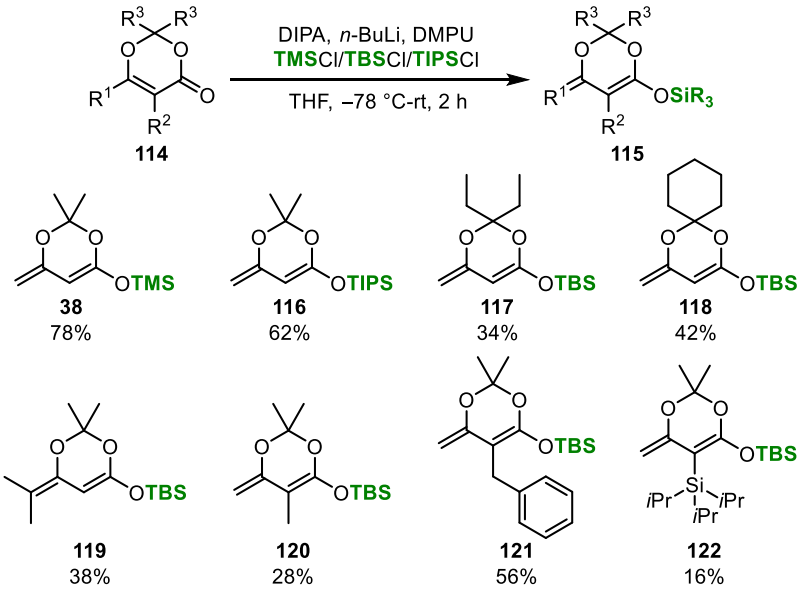

TMS dioxinone dienolate **38** was prepared by Dr. Walter Hofer

Scheme 32. Synthesis of various dioxinone dienolates.

4.3 Reaction optimization of D-A-ring opening reaction with D-Galactose derived cyclopropane and dioxinone dienolate

With all the essential donors and acceptors in hand, we initiated our investigation by utilizing the D-Galactose derived acceptor **6** and the TMS-protected dioxinone **38** as the model pyranosylation reaction. We hypothesized that such cyclopropane fused pyranoside might undergo ring opening through thermodynamic strain release. On the other hand, the ketone may be activated by a catalyst. Initial screening of strong Lewis acids such as $BF_3{\cdot}OEt_2$, TMSOTf and mild Lewis acids including $Yb(OTf)_3$, $Zn(OTf)_2$, and Kass catalyst **15** gave no transformation (Table 4; entry 1–13). Fortunately, the combination of $Ca(NTf_2)_2$ and Bu_4NPF_6 successfully yielded the desired

C-glycoside **123a** with excellent β-stereocontrol and regioselectivity in 62% yield (Table 4; entry 14).

Table 4. Optimization of D-A-ring opening reaction of D-Galactose derived cyclopropane with TMS protected dioxinone dienolate regarding catalysts

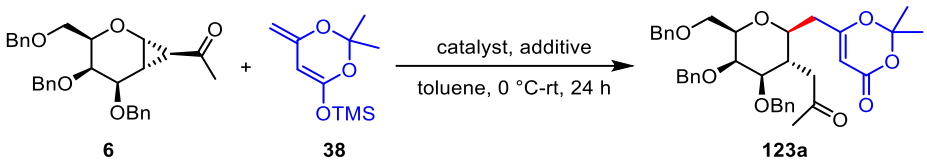

6 **38** **123a**

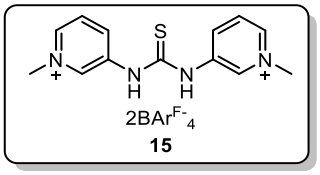

15

Entry	Catalyst[a]	Additive	Yield[c]	β:α[c]
1	$BiBr_3$[b]	–	40% (38%)[d]	79:21
2	$BF_3{\cdot}OEt_2$	–	decomposed	–
3	TMSOTf	–	decomposed	–
4	$Sc(OTf)_3$	–	52%	> 95:5
5	$Mg(OTf)_2$	–	–	–
6	$Ca(OTf)_2$	–	–	–
7	$ZnCl_2$	–	–	–
8	$Ca(OMe)_2$	–	–	–
9	$Bi(OTf)_3$	–	–	–
10	$Yb(OTf)_3$	–	39%	> 95:5
11	$Cu(OTf)_2$	–	–	–
12	$Zn(OTf)_2$	–	–	–
13	**15**	–	–	–
14	**$Ca(NTf_2)_2$**	**Bu_4NPF_6**	**50% (62%)[d]**	**> 95:5**

[a] 20 mol% catalyst; [b] 50 mol% catalyst; [c] α:β ratio and yields were determined by ^{1}H NMR of the crude reaction mixture; [d] isolated yield.

With this promising result in hand, we further probed the counter anion effect. Changing the additive to $NaBF_4$ (Table 5; entry 2) or $Bu_4NB(C_6H_5)_4$ (Table 5; entry 5) stopped the reaction which identified the importance of the counter anion in this catalytic system. In addition, when the

relatively unstable TMS-protected dienolate **38** was replaced by TBS-protected dienolate **78**, the yield was slightly increased (Table 5; entry 7). However, the highly stable TIPS-protected dienolate **116** was not able to generate the desired product under these catalytic conditions even after 24 h (Table 5; entry 8).

Table 5. Optimization of D-A-ring opening reaction of D-Galactose derived cyclopropane with various dioxinone dienolates regarding counter anion

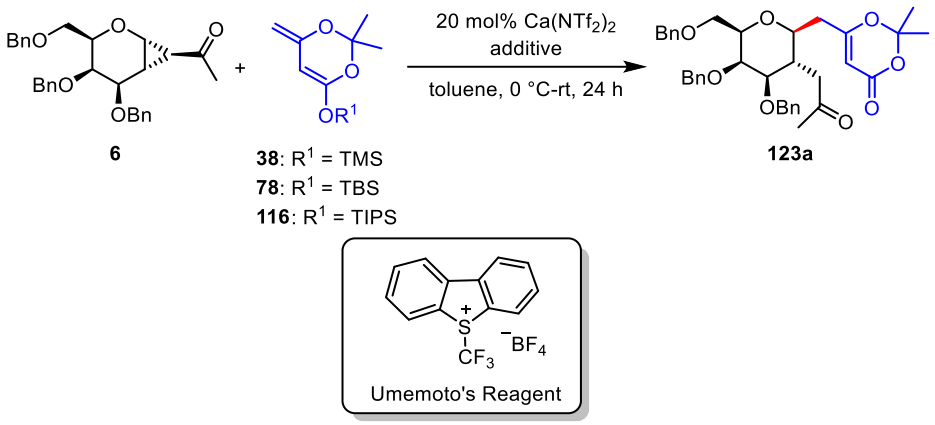

Entry	Additive	R^1	Yield[a]	β:α[a]
1	Bu_4NPF_6	TMS	50% (62%)[b]	> 95:5
2	$NaBF_4$	TMS	–	–
3	Umemoto's reagent	TMS	–	–
4	$NaB(C_6H_5)_4$	TMS	–	–
5	$Bu_4NB(C_6H_5)_4$	TMS	–	–
6	$NH_4B(C_6H_5)_4$	TMS	–	–
7	**Bu_4NPF_6**	**TBS**	**65%**	**> 95:5**
8	Bu_4NPF_6	TIPS	–	–

[a] α:β ratio and yields were determined by ^{1}H NMR of the crude reaction mixture; [b] isolated yield.

Further, the effect of the solvent was investigated (Table 6; entry 1–7). The most suitable solvent found was toluene (Table 6; entry 1). When the temperature was increased to 50 °C, the yield decreased and therefore the optimized temperature was set at room temperature (Table 6; entry 8). Interestingly, when 3 Å molecular sieves were added, the yield was not obviously affected (Table 6; entry 9). However, when excess water was added, a higher yield was observed (Table 6; entry 10–13). To deepen the understanding of the role of water, we tested different equivalent of

water in the reaction. To our delight, 0.5 equivalent of water gave the best yield whilst preserving the α/β ratio (Table 6; entry 12). In addition, when the amount of dienolate **78** or catalyst was lower, the yield decreased (Table 6; entry 14–17).

Table 6. Optimization of D-A-ring opening reaction of D-Galactose derived cyclopropane with dioxinone dienolate regarding solvent effects and additional conditions.

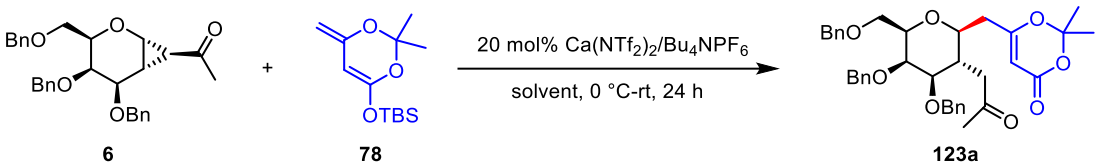

6 **78** **123a**

Entry	Solvent	Temp. (°C)	Extra condition	Yield[a]	β:α[a]
1	toluene	0-rt	–	65%	> 95:5
2	chlorobenzene	0-rt	–	33%	> 95:5
3	fluorobenzene	0-rt	–	54%	> 95:5
4	dichloroethane	0-rt	–	27%	> 95:5
5	chloroform	0-rt	–	42%	> 95:5
6	1,4-dioxane	0-rt	–	–	> 95:5
7	acetonitrile	0-rt	–	–	> 95:5
8	toluene	0-50	–	42%	> 95:5
9	toluene	0-rt	3 Å MS	63%	> 95:5
10	toluene	0-rt	2 equiv. H_2O	76%	> 95:5
11	toluene	0-rt	1 equiv. H_2O	74%	> 95:5
12	**toluene**	**0-rt**	**0.5 equiv. H_2O**	**84% (88%)[b]**	**> 95:5**
13	toluene	0-rt	0.25 equiv. H_2O	74%	> 95:5
14[c]	toluene	0-rt	0.5 equiv. H_2O	52%	> 95:5
15[d]	toluene	0-rt	0.5 equiv. H_2O	54%	> 95:5
16[e]	toluene	0-rt	0.5 equiv. H_2O	63%	> 95:5
17[f]	toluene	0-rt	0.5 equiv. H_2O	60%	> 95:5

[a] α:β ratio and yields were determined by ^1H NMR of the crude reaction mixture; [b] isolated yield; [c] acceptor (3 mmol, 3 equiv.) ; [d] acceptor (2 mmol, 2 equiv.); [e] 10 mol% $Ca(NTf_2)_2$ and Bu_4NPF_6; [f] 5 mol% $Ca(NTf_2)_2$ and Bu_4NPF_6.

4.4 Reaction scope of D-A-ring opening reaction with D-Galactose derived cyclopropanes and dioxinone dienolates

With an optimized pyranosylation protocol, we further expanded the substrate scope of this calcium catalyzed reaction (Scheme 33). Our investigation revealed that the *C*-glycosylation proceeded with good to excellent β-anomeric selectivity. This protocol also tolerated glucosyl donors **7**–**8** and different *O*-6 protected D-Galactose-derivatives **6**, **101** and **108**–**113**. The disarmed donor **101** was much more stable and the product **123b** was generated in good yields. In contrast, the armed donor **108** was relatively reactive leading to side reactions and consequently to a lower yields and anomeric selectivity of *C*-glycoside **123c**. However, the *C*-6 anchimeric assistance of the acetyl group resulted in the formation of the unwanted α-anomer. The β-*C*-glycosides, **123d** and **123e**, derived from Glucose, were obtained in moderate yields and good β-stereocontrol. Product **123f** bearing an acid labile MOM group was generated in moderate yields. Furthermore, the desired *C*-glycosides **123g** and **123h** were obtained when the D-A cyclopropanes were functionalized with different ester groups. However, the sterically hindered Boc group disturbed the addition of dienolate **78** from the β face leading to a lower anomeric selectivity of *C*-glycoside **123g**. To further investigate the versatility of this strain-release vinylogous glycosylation protocol, we applied the optimal conditions to commercially available natural product or drug derived D-A cyclopropanes, **112** and **113** respectively. To our delight, both of the substrates yielded the desired *C*-glycosides **123i** and **123j** in moderate yields and exclusive β-stereoselectivity.

Subsequently, we explored the reaction scope by utilizing various dioxinone dienolates **117**–**122**. The dienolate **117** protected with diethyl groups were compatible with our optimized reaction conditions generating *C*-glyosidic products **123k**–**123n** in moderate yields and good β-stereoselectivity. However, *C*-glycosides **123o**–**123q** were obtained in poor yields and moderate stereoselectivity. The steric hinderance of the cyclohexyl group might have resulted in the impeded nucleophilic addition at the β face. γ-Dimethyl substituted dienolate **119** was not able to generate the corresponding *C*-glycoside **123r** since the γ-position was sterically hindered. When the α-methyl substituted dienolate **120** was employed, the *C*-glycosides **123s**–**123v** were obtained in slightly lower yields and poor anomeric selectivity likely due to the higher steric demand of the dienolate. In addition, the bulky triisopropyl dienolate **122** was unable to generated desired *C*-

glycoside **123x** which further pointed to the importance of the steric influence at α-position of the acceptor.

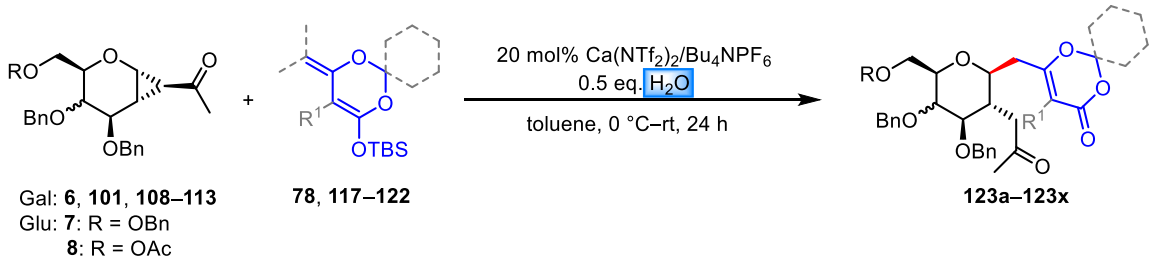

Gal: **6**, **101**, **108–113**
Glu: **7**: R = OBn
8: R = OAc

78, **117–122**

123a–123x

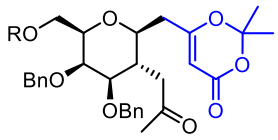

123a: R = OBn; 88%, β:α = > 95:5
123b: R = OAc; 73%, β:α = 93:7
123c: R = OTBS; 39%, β:α = 88:12

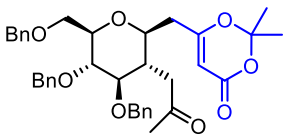

123d: R = OBn; 58%, β:α = 91:9
123e: R = OAc; 48%, β:α = 90:10

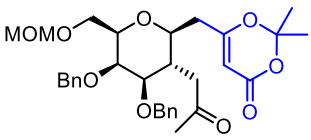

123f: 60%, β:α = > 95:5

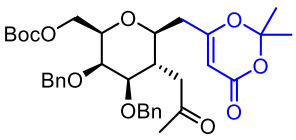

123g: 48%, β:α = 78:22

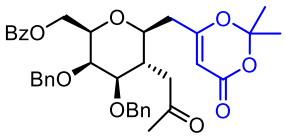

123h: 44%, β:α = > 95:5

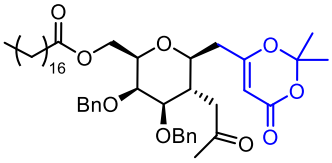

123i: 52%, β:α = > 95:5

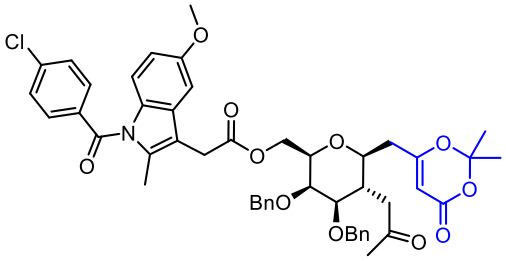

123j: 55%, β:α = > 95:5

different protecting dienolates

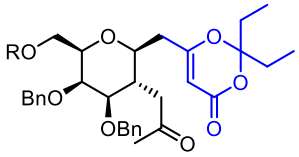

123k: R = OBn; 57%, β:α = > 95:5
123l: R = OTBS; 46%, β:α = > 95:5
123m: R = OAc; 41%, β:α = 93:7

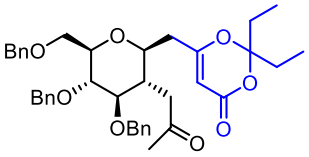

123n: 50%, β:α = 84:16

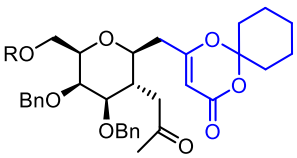

123o: R = OBn; 42%, β:α = > 95:5
123p: R = OTBS; 15%, β:α = 81:19
123q: R = OAc; 30%, β:α = 80:20

γ-substituted dienolate

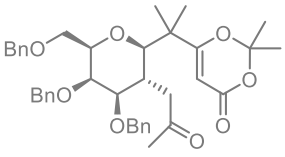

123r: n.d.

α-substituted dienolates

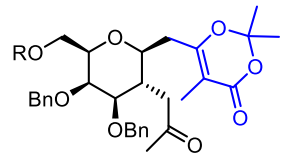

123s: R = OBn; 59%, β:α = > 95:5
123t: R = OTBS; 23%, β:α = 82:18
123u: R = OAc; 35%, β:α = 88:12

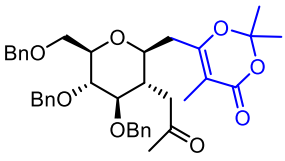

123v: 45%, β:α = 80:20

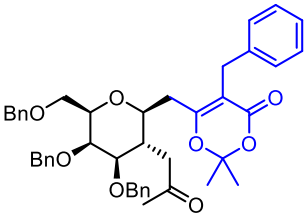

123w: 32%, β:α = 84:16

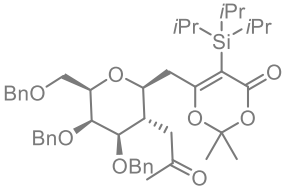

123x: n.d.

α:β ratio was determined by ^{1}H NMR of the crude reaction mixture; n.d. not detected

Scheme 33. Reaction scope of D-A-ring opening reaction with D-Galactose derived cyclopropanes and dioxinone dienolates.

4.5 Mechanistic studies

For further understanding of the mechanistic intricacies of the calcium-catalyzed strain release pyranosylation, an *in situ* NMR monitoring of the reaction was conducted (Figure 13; a). Two distinctive intermediates **124a** and **124b** were detected during room temperature NMR studies with evidence of the strain-release pyranosylation. The proposed structures **124a** and **124b** were based on *in situ* ^{1}H, ^{13}C, COSY and HSQC elucidation from the reaction mixture (Supplementary Figure 1–11) since they were both non-isolable. According to the reaction monitoring profile (Figure 13; b and Supplementary Table 1), donor **6** was not observed in the first 8 minutes which was consistent with the rapid formation of intermediate **124a**. Simultaneously, we observed the depletion of the short life-time intermediate **124a** until ~270 mins, which may correspond with the steep increase of product formation **123a**. Interestingly, we noticed gradual formation of a second intermediate **124b** increasing until the maximum whereby the intermediate **124a** totally disappeared. In addition, there was continuous generation of **123a** and depletion of a second, non-isolable intermediates **124b** with a slightly different rate. This could be attributed to a competitive side reaction. Therefore, the formation of product **123a** (64%) was postulated to be originated from intermediate **124a** and **124b**. Furthermore, unidentifiable intermediates were observed but their structures could not be determined from the crude NMR mixture.

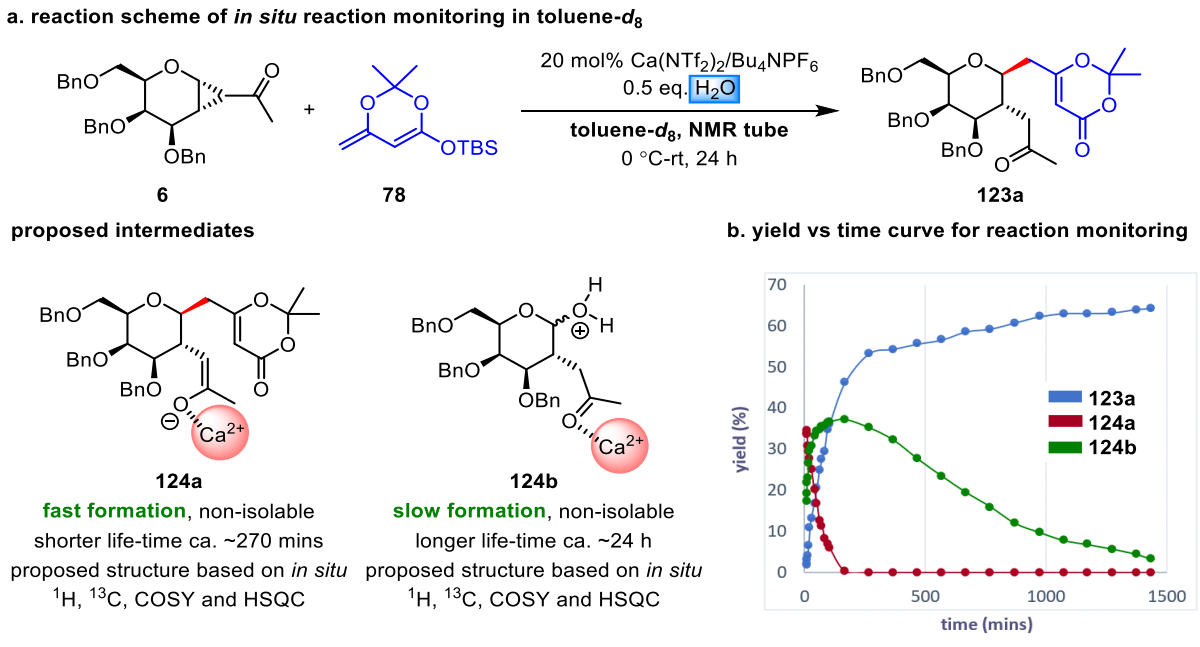

Figure 13. *In situ* reaction monitoring profile in toluene-d_8.

According to these results, we proposed a mechanism involving activation of **6** by calcium catalysis in two different routes (Figure 14) which are deviating from those previously reported in the literature (Scheme 8, Scheme 9 and Scheme 23).[9,33,45] In pathway one (Figure 14), calcium activated the cyclopropane ring which then weakened the C-C bond. The acceptor **78** was also simultaneously activated by water assistance. The activated acceptor attacked at the anomeric center of D-A cyclopropanated sugar **6** to generate the enol intermediate **124a** in a highly stereoselective formation. Keto-enol tautomerism of **124a** further led to the stable product **123a**. Meanwhile, **123a** was also generated through a second route (Figure 14; pathway 2). Water attached to the anomeric position leading to the slow formation of the hydronium intermediate **124b** underlining the important role of water as discovered during the reaction optimization. The activated acceptor **78** replaced the water to afford **123a**. In addition, pathway two could also account for the slow formation of intermediate **124b** over time since water had to attack first to form **124b** and then be substituted by an acceptor. However, the generation of intermediate **124b** might be responsible for the formation of the undesired α-anomer since acceptor **78** could attack from the α face.

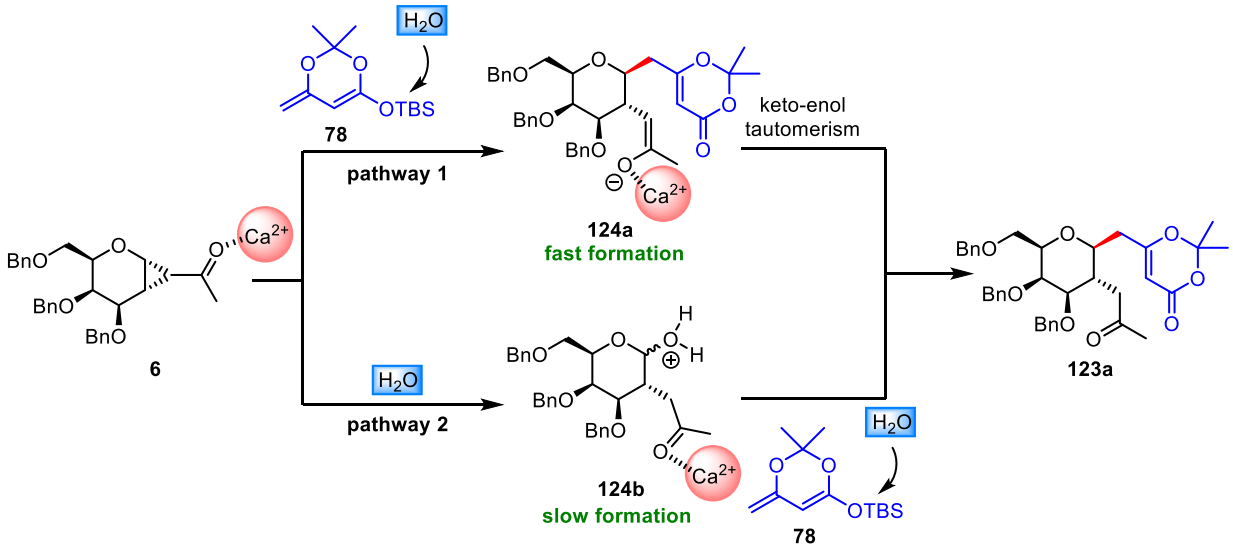

Figure 14. Proposed mechanism for the calcium catalyzed strain-release pyranosylation.

Additionally, a series of control experiments were conducted to gain a thorough understanding of the reaction mechanism (Scheme 34). When the isolated enol side product **125** was treated under the standard reaction conditions without dioxinone dienolate **78**, the expected *C*-glycoside **123a** was not generated (Scheme 34; a). The result suggested that once the TBS group attached to the

molecule, it formed a stable side product. It was assumed that the calcium was chelated with the enol structure **124a** and activated the intermediate. Additionally, the *O*-glyosidic side products **126** and **127** were employed under identical optimized conditions but no product was found (Scheme 34; b and c). Hence, the putative structure **124b** might be the active hydronium intermediate. In order to prove our hypothesis of water as the proton source, we used deuterium oxide under the optimized condition (Scheme 34; d). We couldn't see clearly a splitting of signals by the attachment in the NMR spectrum but could confirm a small fraction of deuterium incorporation by HRMS (Supplementary Figure 12). This outcome could be explained by the not absolute anhydrous reaction conditions.

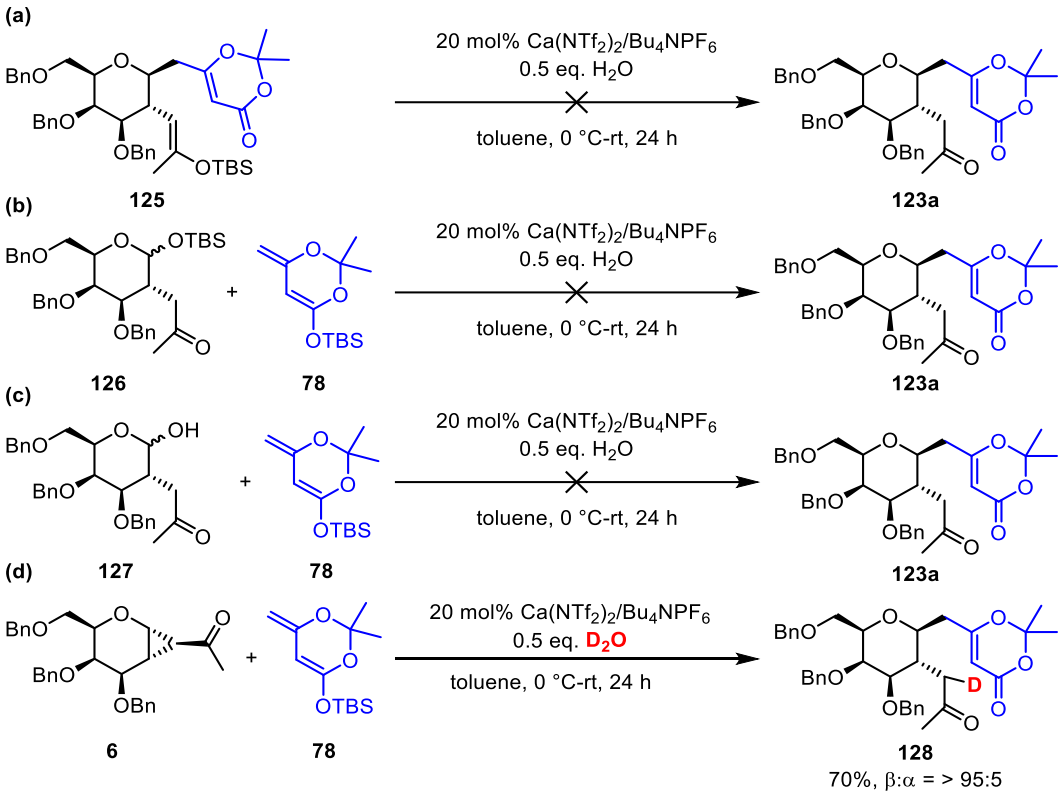

Scheme 34. Control experiments for mechanistic studies.

4.6 Further transformations

To demonstrate the synthetic utility of our methodology, a number of transformations using D-A cyclopropane **123a** were conducted (Scheme 35).[55] The treatment of **123a** with MeOH at 90 °C provided the β-keto ester **129** in 74% yield.[56] Similarly, the treatment of **123a** with *i*PrOH under the same reaction conditions gave the target product **130** in 77% yield. An attempted hydrogenolysis of the benzyl protection groups furnished the hydroxyl product **131** in 86% yield.

Surprisingly, when **123a** was treated with K_2CO_3 at high temperature, the eliminated product **132** was obtained.

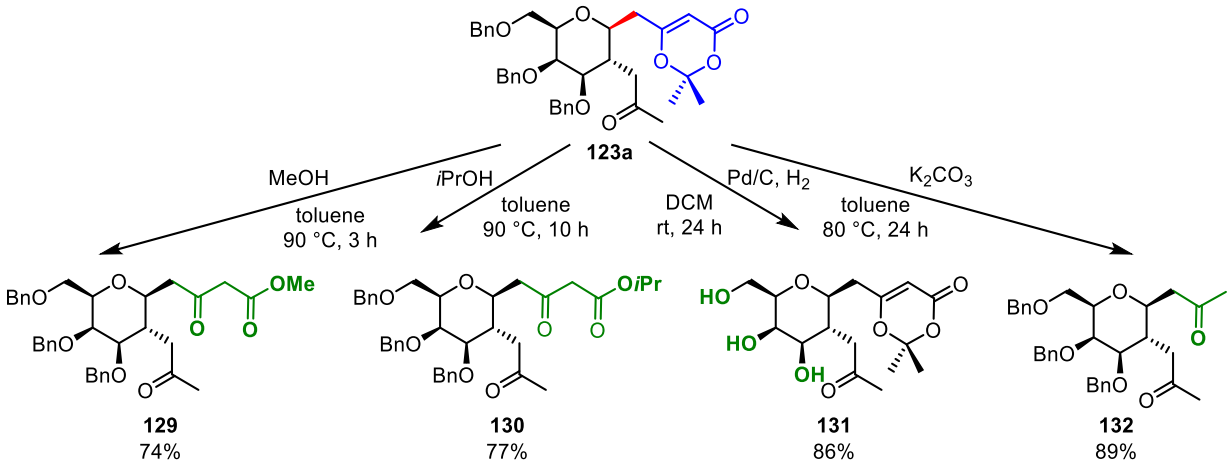

Scheme 35. Further transformation of 123a.

4.7 Dienolate diversification

With this simple and effective pyranosylation protocol in hand, we were curious to extend the scope using a variety of dienolates (Figure 15). The biologically privileged coumarin derivatives and oxindole derivatives are extremely attractive as they possess inherent vinylogous nucleophilicity as well as possible biological activity. In addition, both structures can be substituted by either electron withdrawing or electron donating groups which could allow for a deeper understanding about the character of the cyclopropanted sugar **6** and its ring opening.

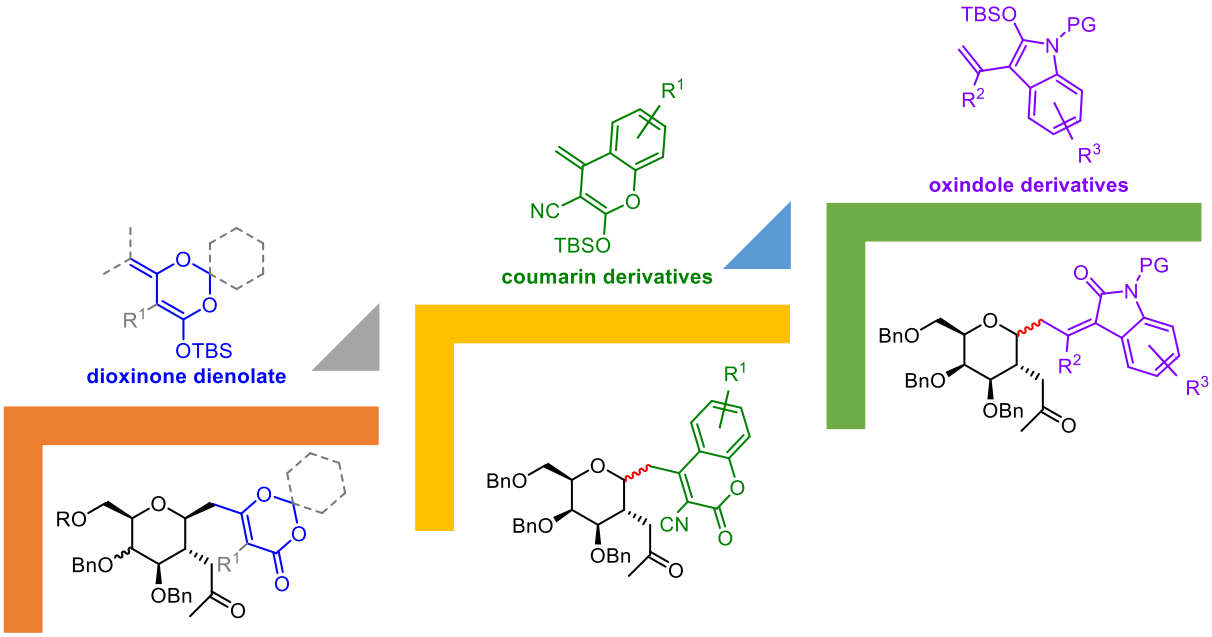

Figure 15. Possible dienolate alternatives based on a biologically privileged scaffold.

4.7.1 Synthesis of coumarin dienolates and reaction optimization of D-A-ring opening reaction with D-Galactose derived cyclopropane and coumarin derivatives

We continued investigating the strain-release pyranosylation with the potential vinylogous coumarin derivative **135** which was obtained through the treatment of *o*-hydroxyacetophenone **133**, ethyl cyanoacetate **134** and ammonium acetate under reflux (Scheme 36).[57]

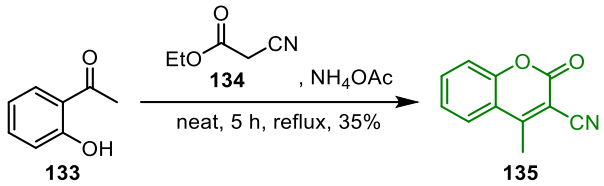

Scheme 36. Synthesis of coumarin derivative 135.

With the coumarin derivative **135** in hand, we further applied the optimized protocol on the cyclopropanated sugar **6** (Table 7). Unexpectedly, instead of the desired product **136**, the hydrolyzed side product **127** was obtained (Table 7; entry 1). Furthermore, when water was excluded in the reaction, no desired product **136** was observed (Table 7; entry 2). Since the base was necessary to trigger the γ-nucleophilicity of the coumarin derivative **135**, triethylamine as external base was used (Table 7; entry 3). However, the cyclopropanated sugar **6** seemed to be sensitive to basic conditions, only decomposition of the **6** was observed.

Table 7. D-A ringopening reaction optimization of D-Galactose derived cyclopropane and coumarin derivative.

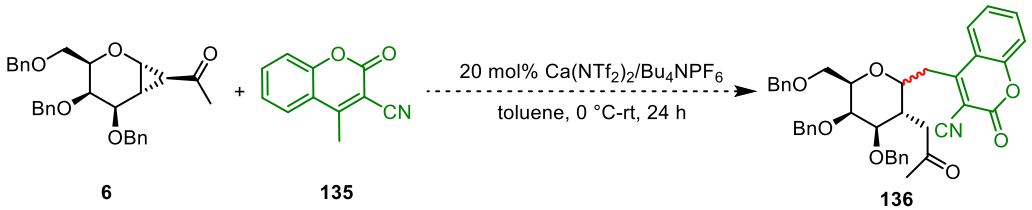

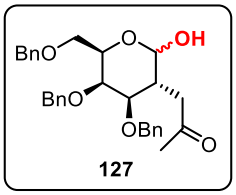

Entry	Extra condition	Results[a]
1	0.5 eq. H_2O	**127**
2	anhydrous	–
3	1.2 eq. Et_3N	decomposed

[a] results was determined by ^{1}H NMR of the crude reaction mixture.

Since the *in situ* generation of the γ-nucleophile was not compatible with the cyclopropanated sugar **6**, we intended to obtain the coumarin dienolate **137** separately (Table 8). The coumarin derivative **135** was retained at 0 °C (Table 8; entry 1). Therefore, we further decreased the temperature to –78 °C, but only starting material **135** was observed (Table 8; entry 2). We concluded that the reaction equilibrium was too rapid at 0 °C leading to the reverse reaction formation of **135**. Hence, the effect of temperature was studied. Reducing the temperature to –20 °C gave total conversion to product **137** (Table 8; entry 4). Unfortunately, conventional isolation in silica, aluminum oxide, extraction and silica-9 gave only back formation of coumarin derivative **135**. Since the conditions of the *in situ* generation of the coumarin dienolate were ineffective and isolation of coumarin **137** was unsuccessful, we decided to postpone the investigation of the coumarin type dienolates.

Table 8. Synthesis of coumarin dienolate.

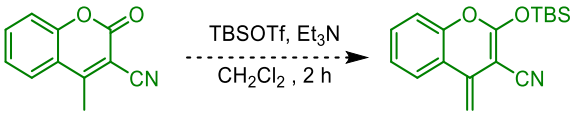

135 **137**

Entry	Temp. (°C)	Result[a]
1	0	s.m.
2	–78	s.m.
3	–40	66% conversion
4	–20	100% converstion

[a] results were checked directly from crude mixture by ^{1}H NMR without further work up; s.m.: starting material.

4.7.2 Synthesis of various oxindole dienolates

In order to expand substrate scope further, we explored the use of vinylogous oxindole dienolates. The investigation was initiated by synthesizing various oxindole dienolates (Scheme 37).[58] The oxindoles substituted with electron withdrawing groups underwent aldol condensation. These were then protected by a Moc or Boc group to afford the vinylogous precursors. Subsequently, the γ-proton was abstracted under basic conditions and replaced by a TBS group to obtain the dienolate **140**, **141 and 143**–**147**. Additionally, the formation of oxindole dienolate **142** was obtained from isatin which underwent benzylation, a Wittig olefination and finally protection with TBS group.

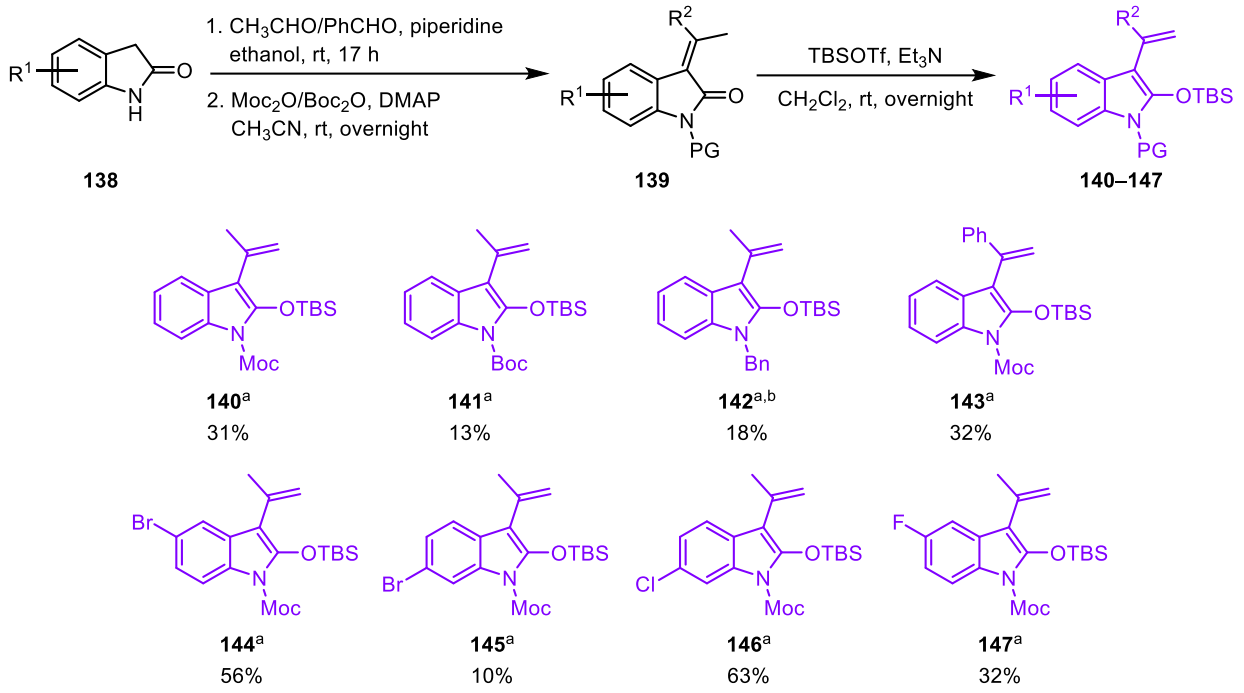

[a] yield over three steps; [b] this reaction was performed by isatin as starting material via benzylation and Wittig olefination; in cooperation with Adrian Weide.

Scheme 37. Synthesis of diverse oxindole dienolates.

4.7.3 Reaction optimization of D-A-ring opening reaction with D-Galactose derived cyclopropane and oxindole dienolate

We employed the optimized conditions without the addition of water to the cyclopropanated sugar **6** with the oxindole dienolates **140**, since it may lead to the hydrolyzed side product **127**. The application of the optimized conditions was incompatible with the oxindole dienolate **140** (Table 9; entry 1). To our surprise when the solvent was changed to CH_2Cl_2, instead of the expected *C*-glycoside **148a**, the rearrangement product **148b** was obtained (Table 9; entry 2). The addition of 0.5 eq. water led to the expected, hydrolyzed side product **127** (Table 9; entry 3). Since the protecting group on the oxindole has a strong influence on the reactivity, the Boc protected oxindole **141** was used but neither *C*-glycoside **148a** nor the rearrangement product **148b** were observed (Table 9; entry 4). We further altered different calcium sources ($CaCl_2$ or $Ca(OTf)_2$; Table 9; entry 5–7). Interestingly, only starting material was observed without Bu_4NPF_6 (Table 9; entry 6) while rearrangement product **148b** was detected in the presence of Bu_4NPF_6 (Table 9; entry 7). This finding highlighted the importance of the PF_6^- anion for the reaction. Different alkali and alkaline triflimides were employed (Table 9; entry 8–11). When $Mg(NTf_2)_2$, which exhibits a

similar character as $Ca(NTf_2)_2$, was utilized, the *C*-glycoside **148b** was generated in 43% yield (Table 9; entry 11). We further studied the solvent effect (Table 9; entry 13–17). The previously used CH_2Cl_2 gave the best results. The reaction temperature was reduced to –20 ºC to lower the possible side reactions but the yield decreased (Table 9; entry 17). Since the preliminary screening was not optimal regarding yield, we decided to hold the promising results for further investigation.

Table 9. Reaction optimization of D-Galactose derived D-A cyclopropane with oxindole dienolates.

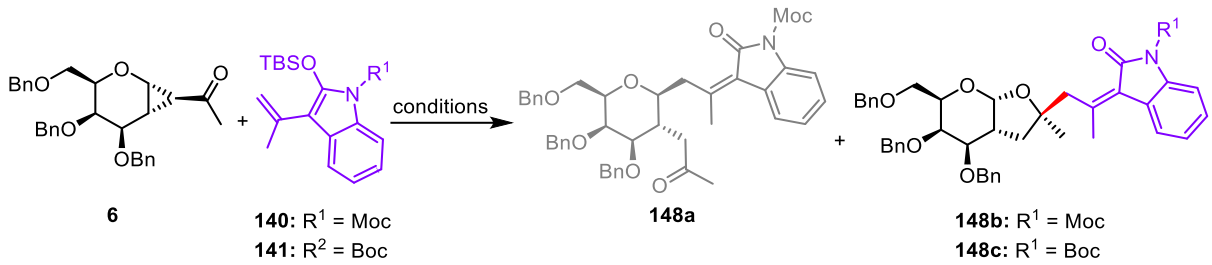

6 | **140:** R^1 = Moc, **141:** R^2 = Boc | **148a** | **148b:** R^1 = Moc, **148c:** R^1 = Boc

Entry	Catalyst	R^1	Solvent	Temp. (ºC)	Time (h)	Results[e]
1[a]	$Ca(NTf_2)_2$	Moc	toluene	0-rt	24	–
2[a]	**$Ca(NTf_2)_2$**	**Moc**	**CH_2Cl_2**	**0-rt**	**3**	**148b: 43% (35%)[f]**
3[a,b]	$Ca(NTf_2)_2$	Moc	CH_2Cl_2	0-rt	2	**127**
4[a]	$Ca(NTf_2)_2$	Boc	CH_2Cl_2	0	3	–
5	$CaCl_2$	Moc	CH_2Cl_2	0-50	17	s.m.
6	$Ca(OTf)_2$	Moc	CH_2Cl_2	0-50	17	s.m.
7[a]	$Ca(OTf)_2$	Moc	CH_2Cl_2	0	2	**148b:** 8%
8[a,c]	$Li(NTf_2)$	Moc	CH_2Cl_2	0	6	–
9[a,c]	$Na(NTf_2)$	Moc	CH_2Cl_2	0-rt	19	–
10[a,c]	$Ba(NTf_2)_2$	Moc	CH_2Cl_2	0	4	**148b:** 26%
11[a,d]	$Mg(NTf_2)_2$	Moc	CH_2Cl_2	0	4	**148b:** 43%
12[d]	$Mg(NTf_2)_2$	Moc	CH_2Cl_2	0	2	–
13[a,d]	$Mg(NTf_2)_2$	Moc	toluene	0	4	–
14[a,d]	$Mg(NTf_2)_2$	Moc	THF	0	4	–
15[a,d]	$Mg(NTf_2)_2$	Moc	dichloroethane	0	4	–
16[a,d]	$Mg(NTf_2)_2$	Moc	dibromomethane	0	4	**148b:** 26%
17[a,d]	$Mg(NTf_2)_2$	Moc	CH_2Cl_2	–20	4	**148b:** 29%

reaction conditions: 20 mol% catalyst; [a] 20 mol% Bu_4NPF_6; [b] 0.5 equiv. H_2O; [c] reaction performed in glove box; [d] $Mg(NTf_2)_2$ was weighed in the glove box but the reaction was performed outside the glove box under argon; [e] yields were determined by ^1H NMR of the crude reaction mixture; [f] isolated yield; s.m.: starting material.

To our surprise, the addition of different dienolates to the cyclopropanated sugar **6** led to distinct product types. As mentioned before, water played a crucial role in the strain-release pyranosylation with dioxinone dienolate **78**. The direct attack of acceptor **78** to sugar **6** in high β-stereoselectivity led to product **123a** (Figure 16). However, water was disadvantageous in the reaction with oxindole dienolate because it caused the formation of the undesired hydrolyzed side product **127**. The generation of the rearrangement product **148b** could be referred to as the plausible bicyclic intermediate **149** which has been reported in numerous literature sources.[9,20,45] We reasoned that oxindole dienolate **140**, which is relatively bulky compared to the dioxinone dienolate **78**, was hindered at the side of the direct addition to the anomeric position. Therefore, the anchimeric assistance from the ketone functional group formed the putative intermediate **149** first and the oxindole dienolate **140** attacked later to generate the rearrangement product **148b**.

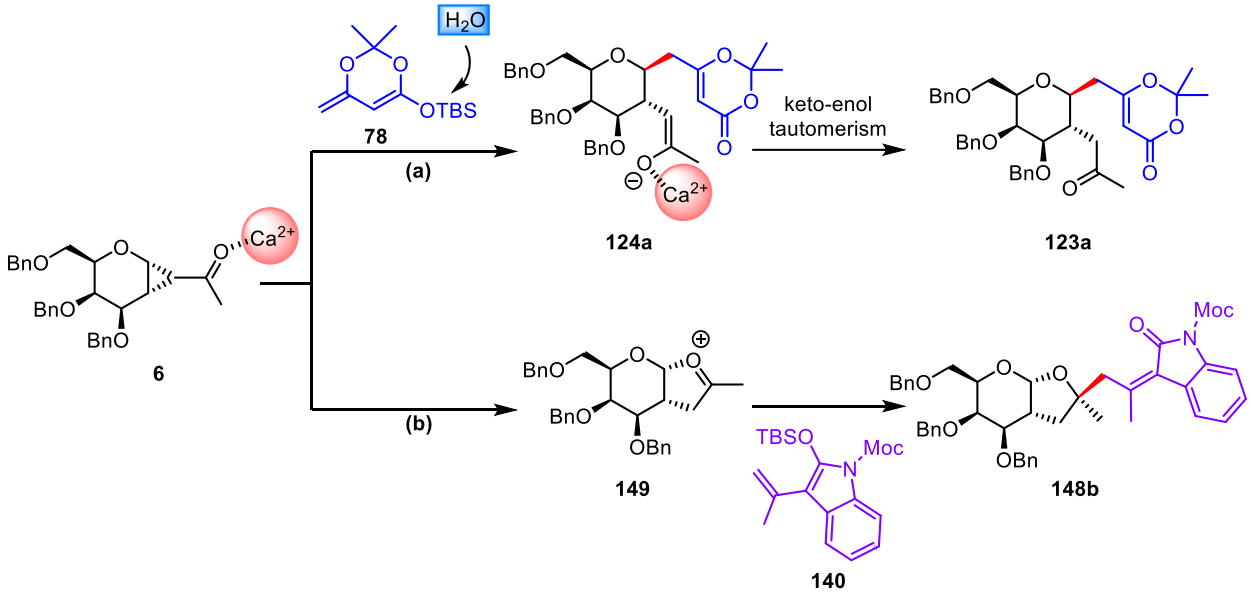

Figure 16. Comparison between the reaction involving the dioxinone dienolate 78 and oxindole dienolate 140 in the calcium catalyzed strain-release pyranosylation.

4.8 Conclusion of $Ca(NTf_2)_2$ catalyzed strain-release γ-vinylogous *C*-pyranosylation

A calcium catalyzed strain-release vinylogous pyranosylation of cyclopropanated sugars with high β-anomeric and γ-regioselectivity was reported in this section (Scheme 38). Moreover, distinct *O*-6 substituted functional groups on the carbohydrates, not only D-Galactose derived but also D-Glucose derived cyclopropanated sugars, were tolerated in our optimized protocol. We further investigated the influence of protecting groups and α-/γ-substituted on dioxinone dienolates in this reaction. We have concluded that the substitution at the γ-position of the dioxinone dienolate was incompatible with our conditions as the nucleophilic γ-position was sterically hindered. In addition, the sterically hindered α-substituted dioxinone dienolate influenced the addition to the cyclopropanated sugar and led to lower stereoselectivity and yields. Furthermore, the *in situ* NMR monitoring and *in situ* characterization of non-isolable intermediates provided a thorough understanding of the mechanism for the calcium catalyzed strain-release *C*-glycosylation and the importance of the addition of water. To demonstrate the value of our protocol, we have successfully performed a number of further transformations such as β-keto ester formation or debenzylation.

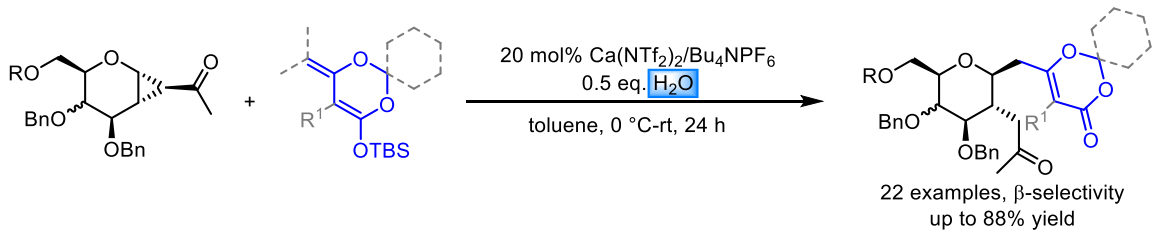

Scheme 38. General scheme for calcium catalyzed γ-vinylogous strain release pyranosylation.

We further attempted to extend our substrate scope to coumarin derivative (Scheme 39). However, the *in situ* generation of γ-vinylogous nucleophilic addition was incompatible with the base sensitive cyclopropanated sugar. In addition, the isolation of the coumarin dienolate was impossible through conventional purification method due to its instability. Therefore, a deeper investigation of such vinylogous coumarins with cyclopropanated sugars have to be performed in the future. However, the preliminary results provided promise in developing *in situ* generation of coumarin dienolate under mild conditions.

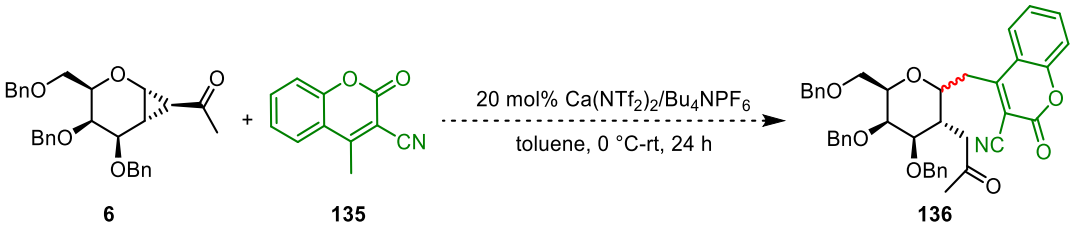

Scheme 39. Attempted calcium catalyzed vinylogous pyranosylation with coumarin dienolate 135.

We were also curious to incorporate the biologically privileged oxindole moiety into our substrate scope (Scheme 40). To our delight, the addition of oxindole dienolate to the cyclopropanated sugar was conducted under slightly modified conditions. However, instead of the expected *C*-glycosides, we obtained a rearrangement product, albeit in poor yield. With the promising results at this stage, we have preliminary understanding in establishing the rearrangement between the cyclopropanated sugars and oxindole dienolates in the future.

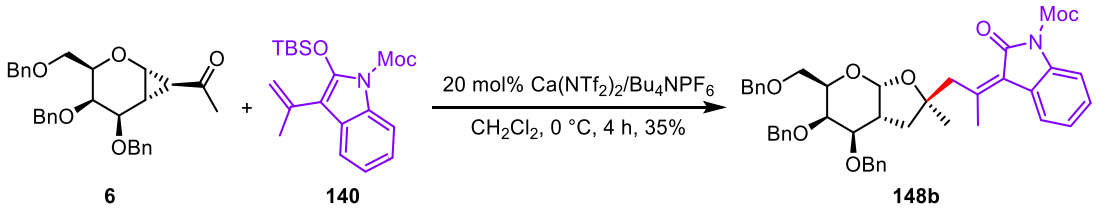

Scheme 40. **General scheme for calcium catalyzed vinylogous pyranosylation with oxindole dienolate.**

5 Results and discussion of halogen bond catalyzed γ-vinylogous *C*-glycosylation with glycosyl imidates

Glycosyl imidates are one of the most frequently used donors in glycoside synthesis. Inspired by Takemoto *et al*., we decided to explore the *C*-vinylogous glycosylation through non-covalent XB catalytic method.[44]

5.1 Synthesis of diverse glycosyl imidates

We initiated our investigation by synthesizing glycosyl imidates (Scheme 41). Conventionally, the use of DBU as base for the reaction of glycosyl hemiacetals **150** and **151** with trichloroacetonitrile (CCl_3CN) generated the thermodynamically favored α-glycosyl trichloroacetimidates (TCAI) **152** and **19**,[59] whereas K_2CO_3 produced the kinetically controlled β-glycosyl TCAIs **153** and **154**.[60] Since the *C*-2 anchimeric assistance of acetyl group are commonly used for the generation of highly stereocontrolled products, the acyl substituted glycosyl TCAIs **60** and 1**57** were synthesized. The treatment of the glycosyl acetals **155** and **156** under acidic condition provided the glycosyl hemiacetal intermediate which further generated the glycosyl TCAIs **60** and **157** by treatment with DBU and trichloroacetonitrile.[61] In addition, the benzoxazolyl (BOX) imidate **158**, which was found to be more reactive than glycosyl TCAIs, was obtained from the glycosyl hemiacetal **150** by treatment with KOH and 2-chlorobenzoxazole.[62]

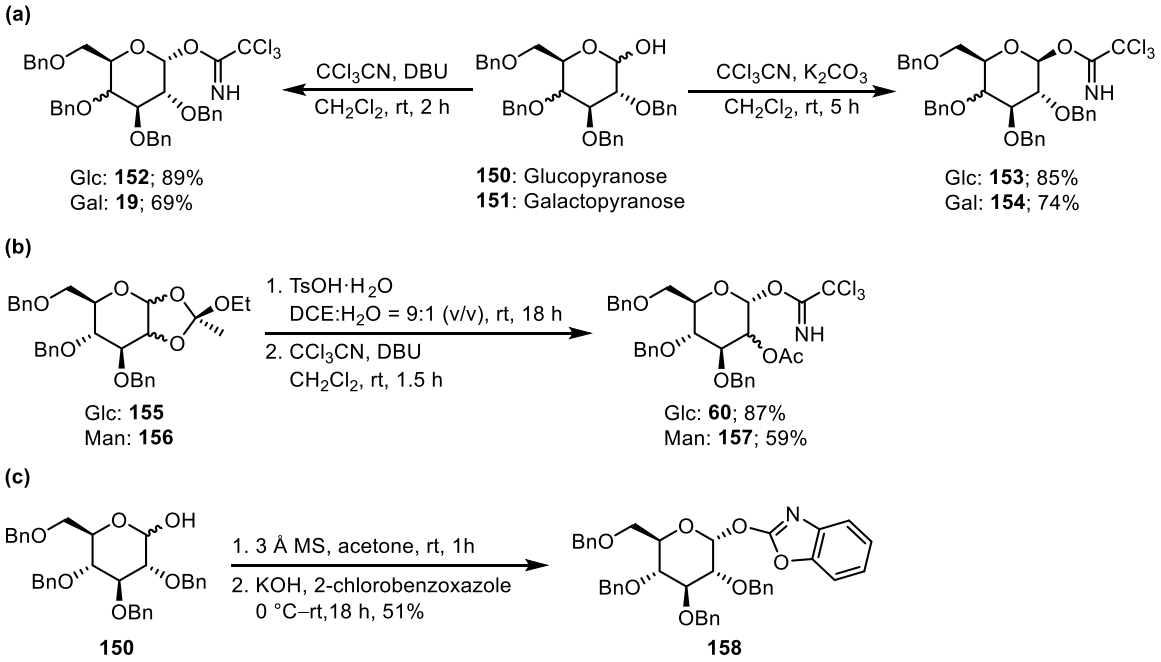

Scheme 41. Synthesis of various glycosyl imidates.

5.2 Synthesis of halogen bond catalysts

We continued our investigation by synthesizing the XB catalysts bearing different electronic properties (Scheme 42). The benzimidazole derivatives **161**–**163** were obtained by copper catalysis under high temperature. To our surprise, the high electron withdrawing *p*-nitro substituted intermediate **162** was generated in high yields because the copper catalyzed coupling reaction is generally assumed to be less efficient. The iodo substituted compounds **164**–**166** were obtained through deprotonation by a strong base and subsequent iodination. The conditions were too harsh for the treatment of the *p*-nitro compound **162** and therefore LiHMDS was used instead. The XB catalysts **167**–**169** were synthesized via S_N2 displacement with octyl triflate.[63]

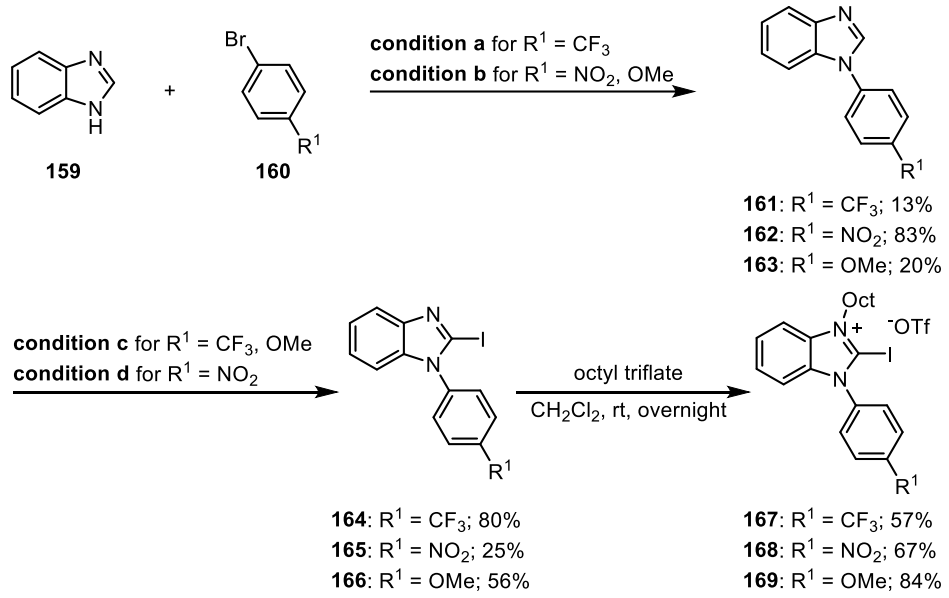

Condition a: CuI, ninhydrin, KOH, DMSO, 110 ºC, overnight; condition b: CuI, Cs_2CO_3, DMSO 120 ºC, overnight; condition c: *n*-BuLi, I_2, THF, –60 ºC-rt, 18.5 h; condition d: LiHMDS, I_2, THF, –78 ºC-rt, 18 h.

Scheme 42. Synthesis of different XB catalysts.

5.3 Optimization of glycosyl imidate with dioxinone dienolate

With all the required donors and catalysts in hands, we started our investigation by utilizing the α-glycosyl TCAIs **152** and relatively stable TBS-protected dioxinone **78** as the model *C*-glycosylation (Table 10). To our delight, the combination of HB catalyst **62** and XB catalyst **167** led to the *C*-glycoside **40a**, albeit with poor yield (Table 10; entry 1). When the HB catalyst **62** was solely used, the target product **40a** was not found indicating an activation of HB catalyst by the XB catalyst (Table 10; entry 2). Furthermore, the XB catalyst **167** was sufficient enough to catalyze the reaction by itself and increased the yield demonstrating the first XB catalyzed glycosyl

imidate substitution (Table 10; entry 3). Surprisingly, inversion of the anomeric selectivity was observed when $Ca(NTf_2)_2$ was used (Table 10; entry 4). The effect of different solvents was also studied (Table 10; entry 5–9). We identified 1,4-dioxane as optimal solvent. We observed that dioxane and ether gave better anomeric selectivity in our study (Table 10; entry 6 and 9) while acetonitrile increased the formation of the β-anomer (Table 10; entry 5). This indicated the participation of acetonitrile from the α face. We further probed the temperature effect. Elevated temperatures led to higher α-selectivity (Table 10; entry 9–12) with the optimum at 80 °C (Table 10; entry 11). With this promising preliminary result, we further studied the donor effects to increase the yields and maintain anomeric selectivity.

Table 10. Reaction optimization of α-glycosyl TCAI 152 with dioxinone dienolate.

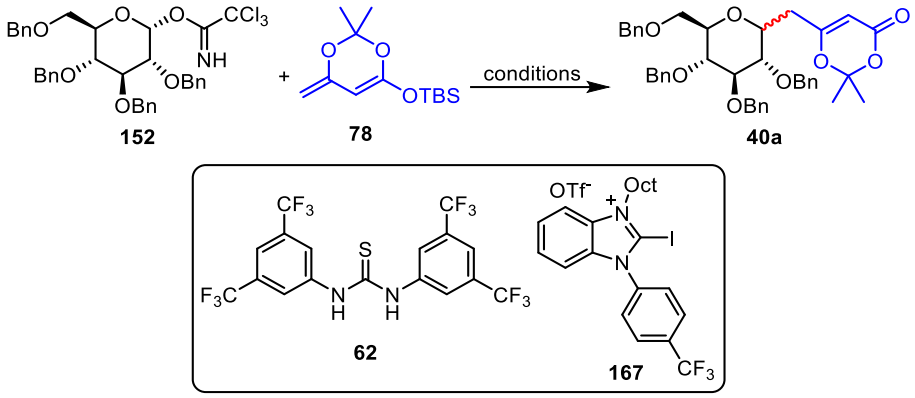

Entry	Catalyst	Solvent	Temp. (°C)	Time (h)	Yield[d]	α:β ratio[d]
1[a]	**62+167**	CH_2Cl_2	rt	2	22%	80:20
2[b]	**62**	CH_2Cl_2	rt	24	s.m.	–
3[a]	**167**	CH_2Cl_2	rt	3	31%	74:26
4[b]	$Ca(NTf_2)_2/Bu_4NPF_6$	CH_2Cl_2	rt	1.5	56% (54%)[e]	37:63
5[c]	**167**	CH_3CN	rt	23	28%	24:76
6[c]	**167**	Et_2O	rt	2	30%	> 95:5
7[c]	**167**	toluene	rt	2	34%	94:6
8[c]	**167**	fluorobenzene	rt	3	39%	87:13
9[c]	**167**	1,4-dioxane	rt	2	40%	94:6
10[c]	**167**	1,4-dioxane	50	2	48%	95:5
11[c]	**167**	**1,4-dioxane**	**80**	**1**	**50%**	**> 95:5**
12[c]	**167**	1,4-dioxane	110	1	21%	> 95:5

[a] 10 mol% catalyst; [b] 20 mol% catalyst; [c] 5 mol% catalyst; [d] α:β ratio and yields were determined by ^{1}H NMR of the crude reaction mixture; [e] isolated yield; s.m.: starting material

Different solvents were used with the glycosyl TCAI **60** to gain *C*-2 anchimeric assistance (Table 11). To our surprise, not only *C*-glycoside **170a** but also the product **170b** was formed, albeit in low yield. However, we were more interested in the development of *C*-glycosylation. Therefore, we decided to postpone further investigation with the acyl glycosyl TCAI **60**.

Table 11. Reaction optimization of acetyl glycosyl TCAI 60 with dioxinone dienolate 78.

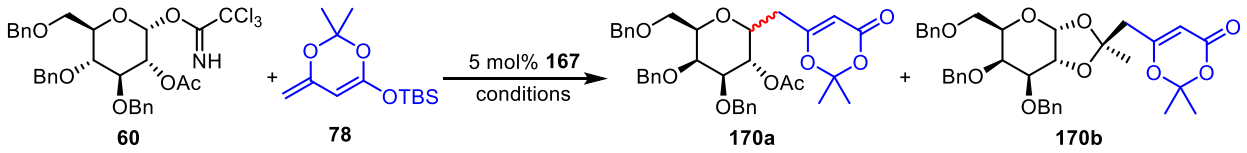

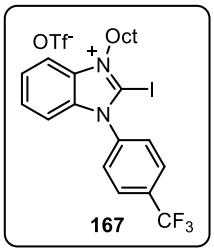

Entry	Solvent	Temp. (°C)	Time (h)	Yield[a]
1	CH_2Cl_2	rt	24	**170a** (10%)[b];**170b** (36%)[b]
2	1,4-dioxane	80	3	**170a** (trace);**170b** (36%)
3	CH_3CN	80	23	**170a** (trace);**170b** (24%)

[a] yields were determined by ^{1}H NMR in the crude reaction mixture; [b] isolated yield.

We further investigated the tetrabenzyl glycosyl imidates including β-gluco-derivative **153** and α-/β-galacto-derivatives **19** and **154** with the dioxinone dienolate **78** (Table 12). The *C*-glycoside **171** was observed in higher yield but the anomeric selectivity decreased significantly (Table 12; entry 2). In addition, the expected higher α-selective attack at β-gluco-derivative **153** gave lower yield but maintained high anomeric selectivity (Table 12; entry 5–7). We observed the generation of an undesired amide side product **172** through back attack of the leaving trichloroacetonitrile up to ~36% in all the reaction examples. Therefore, the BOX imidate **158** with relatively stable leaving group was examined. In this case, the *C*-glycoside **40a** was observed in a slightly lower yield (Table 12; entry 11). As a result, we decided to keep the α-gluco-derivative **152** as the reaction donor for further investigation.

Table 12. Reaction optimization of distinct glycosyl imidates with dioxinone dienolate 78.

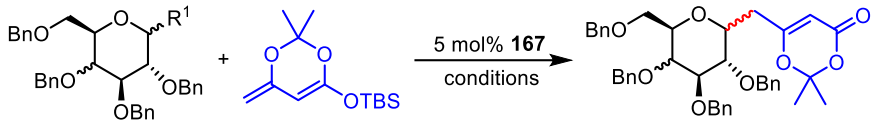

152: R^1 = TCAI, Glc-α
19: R^1 = TCAI, Gal-α
153: R^1 = TCAI, Glc-β
154: R^1 = TCAI, Gal-β
158: R^1 = BOX, Glc-α

78

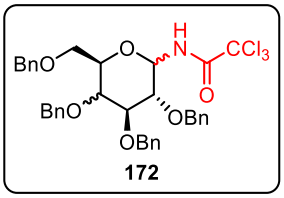

172

Entry	Substrate	Solvent	Temp. (°C)	Time (h)	Yield[a]	α:β-ratio[a]
1	**152**	**1,4-dioxane**	**80**	**1**	**40a: 50%**	**> 95:5**
2	**19**	1,4-dioxane	80	1	**171**: 57% (59%)[b]	62:38
3	**19**	Et_2O	rt	2	**171**: 38%	64:36
4	**19**	CH_3CN	rt	2	**171**: 43%	79:21
5	**153**	1,4-dioxane	80	1	**40a**: 41%	> 95:5
6	**153**	Et_2O	rt	2	**40a**: 31%	> 95:5
7	**153**	CH_3CN	rt	2	**40a**: 28%	27:73
8	**154**	1,4-dioxane	80	1	**171**: 51%	61:39
9	**154**	Et_2O	rt	2	**171**: 40%	70:30
10	**154**	CH_3CN	rt	2	**171**: 42%	79:21
11	**158**	1,4-dioxane	80	1	**40a**: 22% (31%)[b]	> 95:5

[a] α:β ratio and yields were determined by ^{1}H NMR of the crude reaction mixture; [b] isolated yield.

We further investigated the effect of different substituted patterns on the catalysts to the reaction (Table 13; entry 1–5). To our delight, the strongly electron withdrawing nitro group on the XB catalyst **168** increased the formation of *C*-glycoside **40a** (Table 13; entry 2). In contrast, the imidazole XB catalyst **174** was less efficient for catalyzing of the *C*-glycosylation (Table 13; entry 5). Since we observed that ethereal solvents providing increased yields and anomeric selectivity, those solvents were screened but neither of them increased the reaction performance (Table 13; entry 6–8). Since the reaction was relatively active, the protection group of the enolate was changed to the more stable TIPS **116** (Table 13; entry 9). However, the bulky TIPS hindered the addition reaction and resulted in a lower yields and anomeric selectivity. In order to decrease the

competition of side reaction, we added an equivalent of different additive to stabilize the glycosyl oxocarbenium intermediate (Table 13; entry 10–12). Interestingly, when acetonitrile was added, the yields were unaffected but β-anomeric selectivity was increased. The catalyst loading was also varied to 2 mol% or 20 mol% but no significant effect could be identified (Table 13; entry 13–14). When the limiting reagent was changed from imidate **152** to dioxinone dienolate **78**, 74% of *C*-glycoside **40a** was generated (Table 13; entry 15).

Table 13. Reaction optimization toward various XB catalysts.

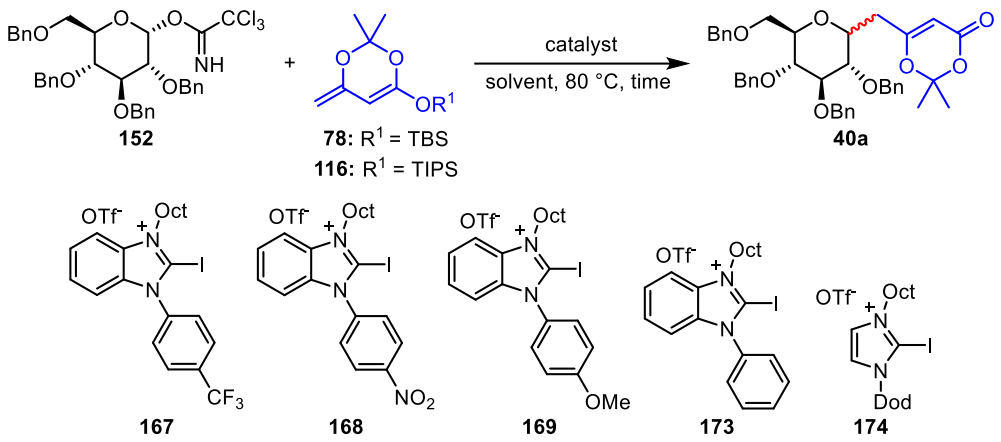

Entry	Cat.	Acceptor	Solvent	Additive	Time (h)	Yield[d]	α:β ratio[d]
1	**167**	**78**	1,4-dioxane	–	1	50%	> 95:5
2	**168**	**78**	1,4-dioxane	–	1	61%	> 95:5
3	**169**	**78**	1,4-dioxane	–	1	48%	> 95:5
4	**173**	**78**	1,4-dioxane	–	1	50%	> 95:5
5	**174**	**78**	1,4-dioxane	–	3	16%	> 95:5
6	**168**	**78**	tetrahydropyrane	–	3	18%	> 95:5
7	**168**	**78**	diethylene glycol diethyl ehter	–	3	46%	82:18
8	**168**	**78**	anisole	–	2	28%	87:13
9	**168**	**116**	1,4-dioxane	–	2	35%	84:16
10	**168**	**78**	1,4-dioxane	H_2O (1 eq.)	1	19%	> 95:5
11	**168**	**78**	1,4-dioxane	CH_3CN (1 eq.)	2	61%	79:21
12	**168**	**78**	1,4-dioxane	DMF(1 eq.)	1	43%	> 95:5
13[a]	**168**	**78**	1,4-dioxane	–	2	52%	> 95:5
14[b]	**168**	**78**	1,4-dioxane	–	2	52%	> 95:5
15[c]	**168**	**78**	**1,4-dioxane**	–	**1**	**74%**	**> 95:5**

General reaction conditions: glycosyl TCAI **152** (0.1 mmol, 1 equiv.), dioxinone dienolate **78** (0.12 mmol, 1.2 equiv.) and 5 mol% catalyst; [a] 2 mol% catalyst; [b] 20 mol% catalyst; [c] glycosyl TCAI **152** (0.2 mmol, 2 equiv.), dioxinone dienolate **78** (0.1 mmol, 1 equiv.); [d] α:β ratio and yields were determined by ^{1}H NMR of the crude reaction mixture.

5.4 Conclusion of halogen bond catalyzed γ-vinylogous *C*-glycosylation with glycosyl imidates

The first halogen bond catalyzed *C*-glycosylation with high α-anomeric and γ-regioselectivity through the vinylogous concept was revealed in this section (Scheme 43). We investigated different XB catalysts bearing distinct electronic properties and observed the nitro substituted XB catalyst as the most potent for this *C*-glyosidic bond formation. We proposed that the highly electron withdrawing nitro group enhanced the electronegativity on the iodo atom and therefore led to a stronger XB interaction.

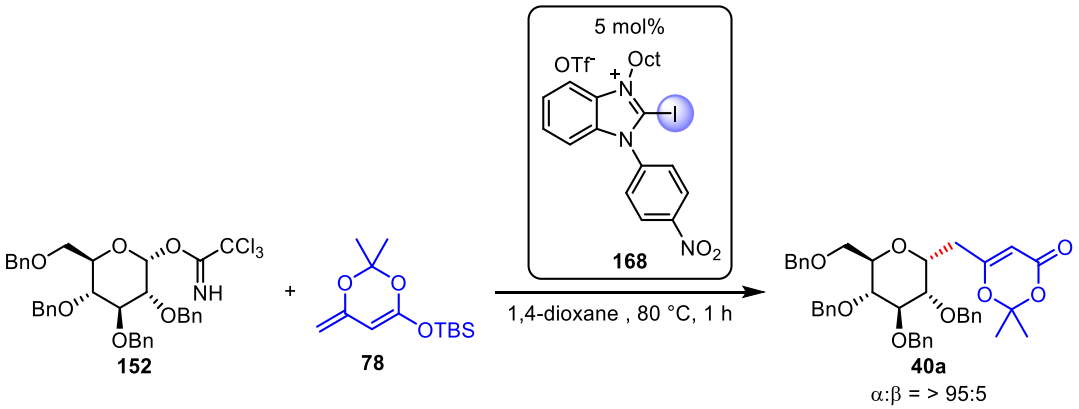

Scheme 43. Halogen bond catalyzed γ- vinylogous *C*-glycosylation with glycosyl imidate.

6 Cell-based screening of the carbohydrate derived compound collection

The carbohydrate derived compound collection was prepared from two distinct *C*-glycosylation projects including the Ferrier rearrangement *C*-glycosides **90a**–**90h** and the strain-release *C*-glycosides **123a**–**123w** and **129**–**132** (Figure 17). In total, 37 compounds were submitted to the COMAS in Dortmund for cell-based screening to assess possible biological activities. The screening revealed that most of the *C*-glycosides showed inhibition of the Hedgehog (Hh) signaling pathway (Table 14). The Hh osteogenesis assay showed compound **90c** from the Ferrier rearrangement cluster as the most potent molecule with a half-maximal inhibitory concentration (IC_{50}) of 1.88 ± 0.41 µM. In addition, compound **123q** from the strain-release project cluster exhibited the highest inhibition with an IC_{50} value of 3.61 ± 0.95 µM for the Hh pathway. We have showed that the developed *C*-glycosylation defines a new class of glycosides that have the potential to be inhibitors in the Hh signaling pathway.

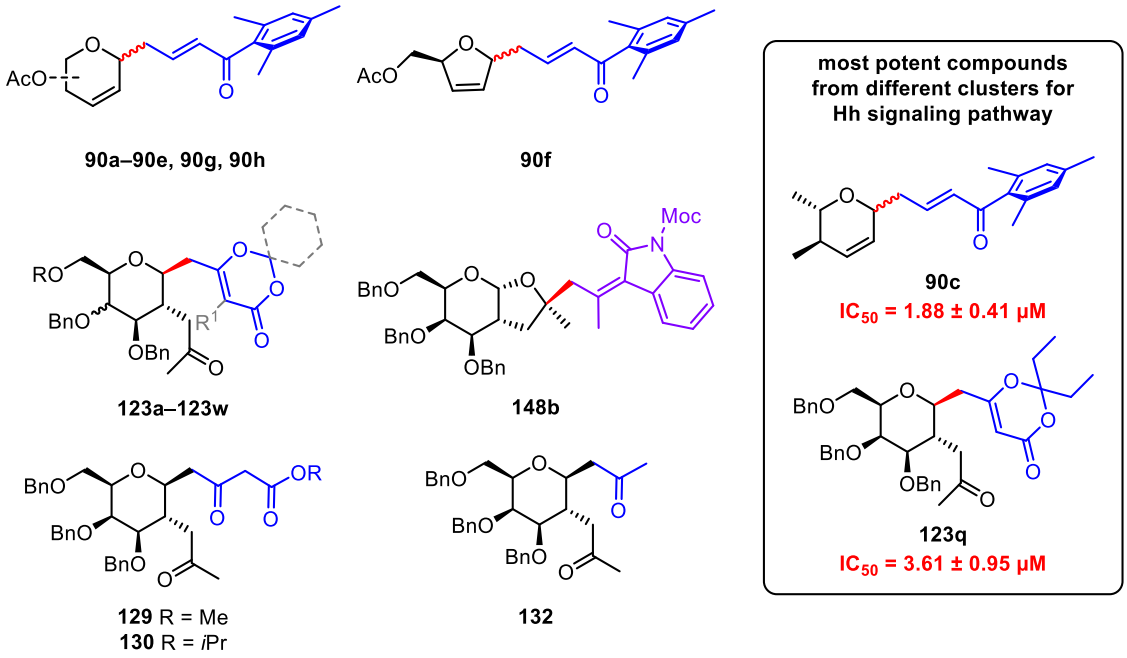

Figure 17. Generated carbohydrate compounds for COMAS biological screening.

Table 14. Biological screening results of generated carbohydrate compounds in Hh signaling pathway.

Compound	IC_{50} [µM]	Compound	IC_{50} [µM]
90a	3.00 ± 0.18	**123h**	9.33 ± 0.42
90b	2.70 ± 1.13	**123i**	–
90c	**1.88 ± 0.41**	**123j**	9.43 ± –
90d-α	2.78 ± 0.33	**123k**	**3.61 ± 0.95**
90d-β	3.42 ± 0.86	**123l**	8.11 ± 1.52
90e-α	3.45 ± 0.56	**123m**	–
90e-β	4.32 ± 0.91	**123n**	4.23 ± 0.37
90f-α	3.26 ±0.12	**123o**	4.95 ± 0.94
90f-β	2.50 ± 0.46	**123p**	5.26 ±0.91
90g	2.91 ± 0.38	**123s**	8.71 ± 1.09
90h	4.21 ± 0.22	**123t**	7.79 ± –
123a	3.86 ± 1.13	**123v**	6.65 ± 2.88
123b	6.24 ± 0.78	**123w**	9.57± –
123c	6.30 ± 0.44	**148b**	4.38±1.29
123d	8.52 ± 0.81	**129**	–
123e	–	**130**	–
123f	8.77 ±1.47	**132**	–
123g	–		

Data are mean values of three independent experiments (n = 3) ± standard deviation

7 Summary

Carbohydrates play important roles in cells and are therefore promising candidates as biological active molecules. *C*-glycosides are more stable than the naturally occurring, more labile *O*-glycosides. Therefore, *C*-glycosylation can provide a potential alternative reaction type for the discovery of distinct biological pathways. The purpose of this thesis was the development of efficient *C*-glycosylation reactions including a challenging vinylogous concept catalyzed by a Lewis acid or halogen bonding effects. Firstly, the α-anomeric and γ-regioselective vinylogous *C*-glycosylation using non-toxic and mild $Zn(OTf)_2$ with diverse glycal substrates was discovered (Scheme 44; a). The protocol was compatible with not only the cyclic dioxinone dienolate but also the α-shielded mesityl dienolate, hence opening up a promising concept for accessing *C*-glycosides.

In the second part of this dissertation, a calcium catalyzed strain-release vinylogous pyranosylation with high β-anomeric and γ-regioselectivity was developed (Scheme 44; b). Moreover, various *O*-6 substituted functional groups on the donor carbohydrates and the influence of the protecting groups as well as α-/γ-substitution of dioxinone dienolates were investigated. Through the use of *in situ* NMR monitoring and *in situ* characterization of non-isolable intermediates, a deeper insight into the mechanism of the calcium catalyzed strain-release *C*-glycosylation was gained. We attempted to extend our substrate scope to coumarin derivates but the developed method was unsuccessful. However, the preliminary results provided promising insights for the future development of *in situ* generated coumarin dienolates under milder conditions. We also sought for the possiblity to incorporate the biologically privileged oxindole moiety into our substrate scope. Surprisingly, instead of the expected *C*-glycosides, we obtained rearrangement bicyclic products. With these early promising results, we have a preliminary idea for establishing a selective rearrangement of the cyclopropanated sugar by oxindole dienolates.

The main focus on the third part of this work was the development of a halogen bond catalyzed *C*-glycosylation with high α-anomeric and γ-regioselectivity by vinylogous substrates (Scheme 44; c). The investigation into distinct XB catalysts bearing different electronic properties revealed a nitro substituted XB catalyst as the most potent for this *C*-glyosidic bond formation. We further demonstrated that the developed *C*-glycosylation gives access to a new class of glycosides that may be potential Hh signaling pathway inhibitors.

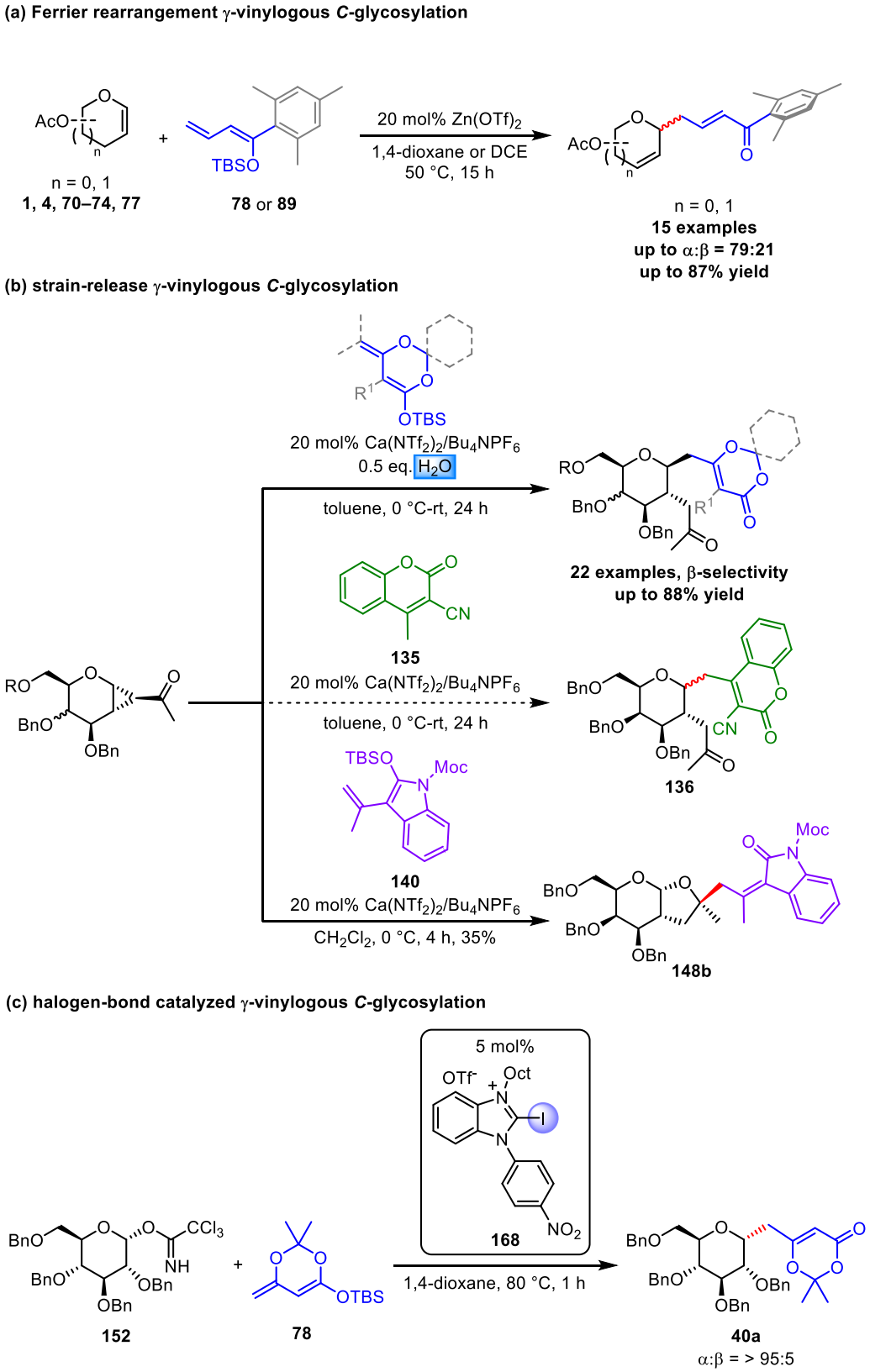

Scheme 44. Summary of *C*-glycosylation with vinylogous concepts in this thesis.

8 Supplementary Information

8.1 *In situ* NMR reaction monitoring at rt for strain-release pyranosylation with D-Galactose derived cyclopropane 6

Supplementary Table 1. Experiment integrations over time.

Time (mins)	Yield (%)			
	6	**124a**	**124b**	**123a**
8	0	34.50904	17.19955	1.95993
9	0	33.86370	19.28854	2.20850
10	0	33.69639	21.71694	2.99247
12	0	30.87601	22.89289	4.03458
17	0	29.24114	26.46857	6.59683
22	0	27.72100	29.58533	10.91344
28	0	25.01535	30.84733	13.24155
40	0	20.04383	33.24704	16.91751
51	0	16.85059	34.26047	20.54576
61	0	12.58655	34.78630	24.76200
72	0	11.46797	35.57983	27.45331
82	0	8.365539	35.83797	29.46582
94	0	6.850181	36.44507	34.88669
103	0	6.037529	36.59326	35.99572
167	0	0.315500	37.18124	46.13475
268	0	0	35.15438	53.20961
368	0	0	32.16669	54.28040
468	0	0	27.60150	55.52328
569	0	0	23.37571	56.53192
669	0	0	19.44151	58.52053
770	0	0	15.93277	59.18977
870	0	0	11.98423	60.66211
971	0	0	9.775730	62.15834
1071	0	0	7.815804	62.92319
1171	0	0	6.792818	62.96144
1272	0	0	5.722029	63.10485
1372	0	0	4.436126	63.93184
1432	0	0	3.274511	64.12305

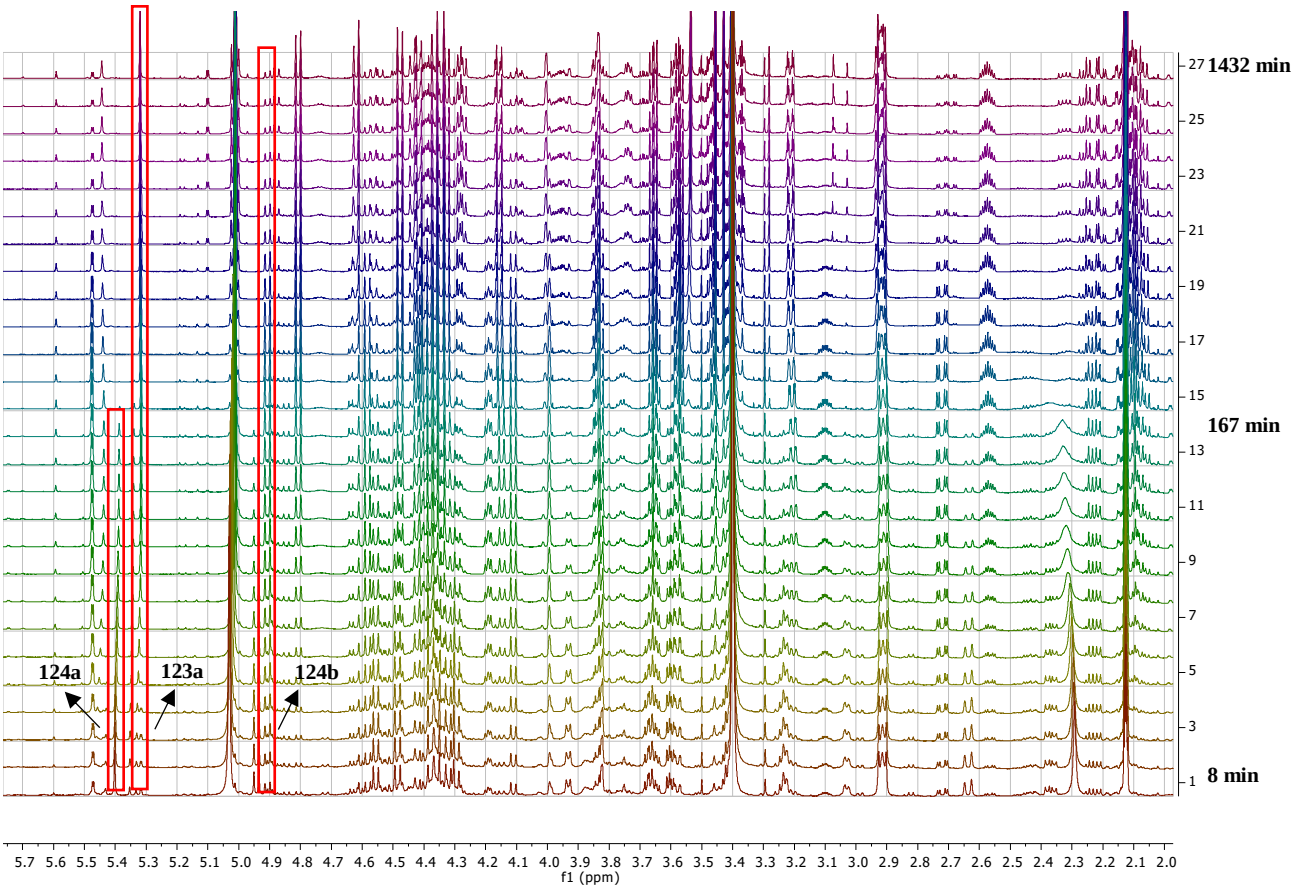

Supplementary Figure 1. Stacked ^{1}H spectra plot for reaction monitoring.

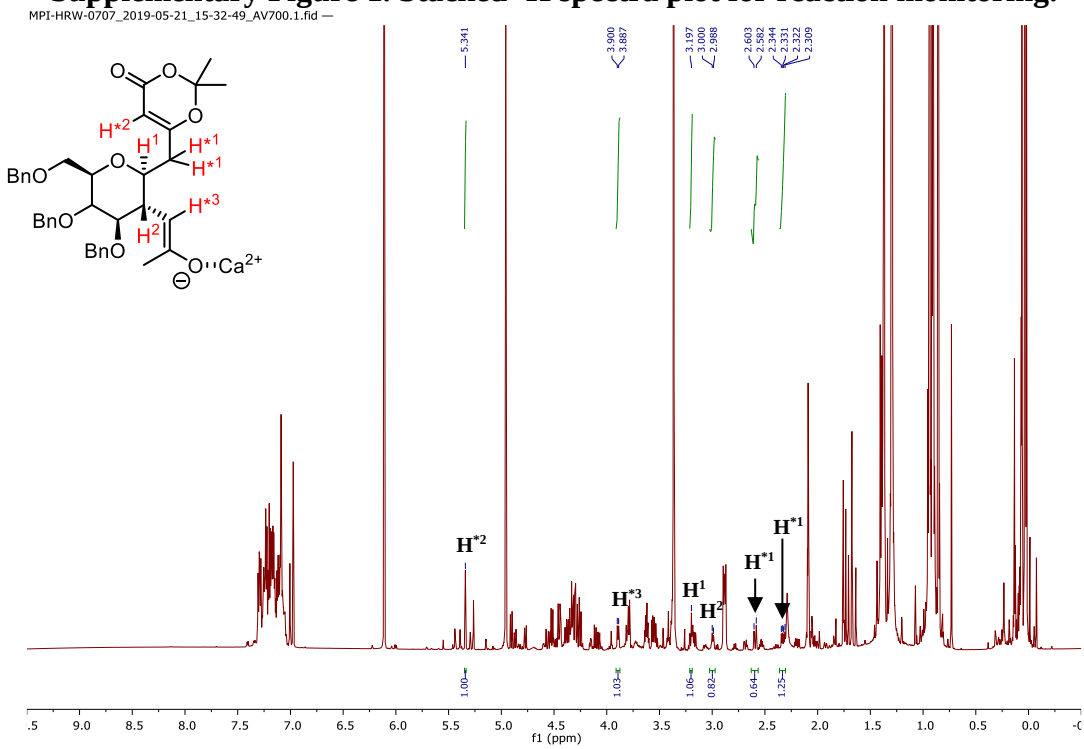

Supplementary Figure 2. *In situ* ^{1}H spectrum of intermediate 124a.

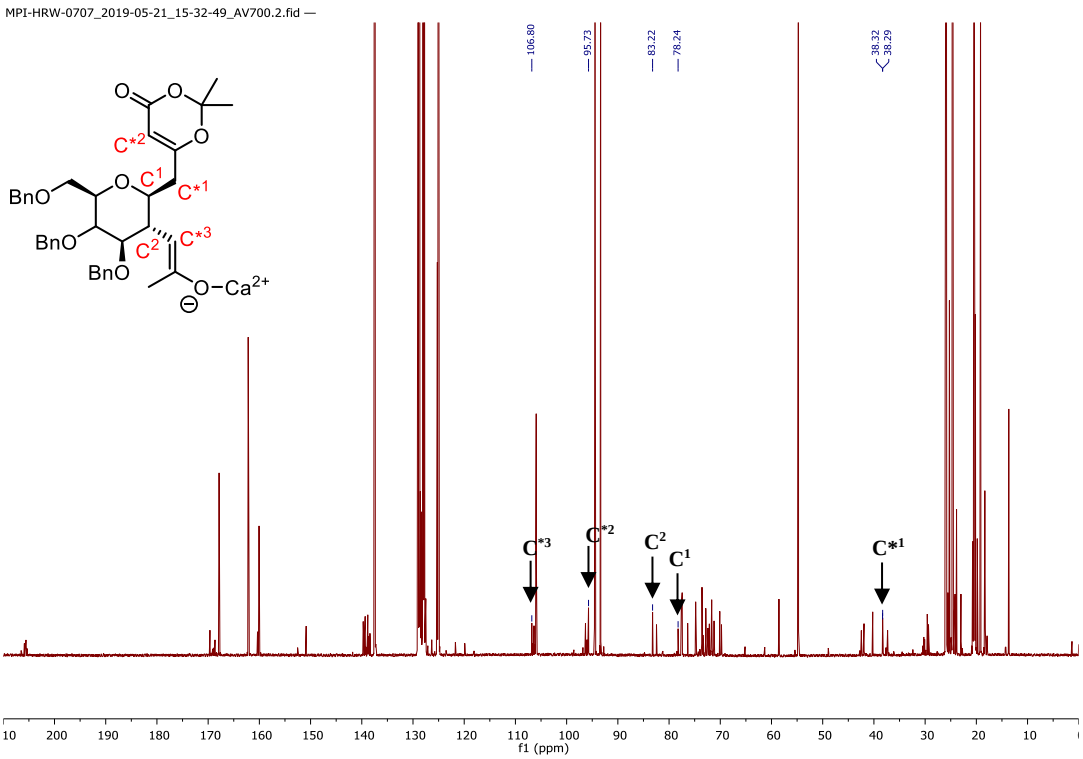

Supplementary Figure 3. ***In situ*** **^{13}C spectrum of intermediate 124a.**

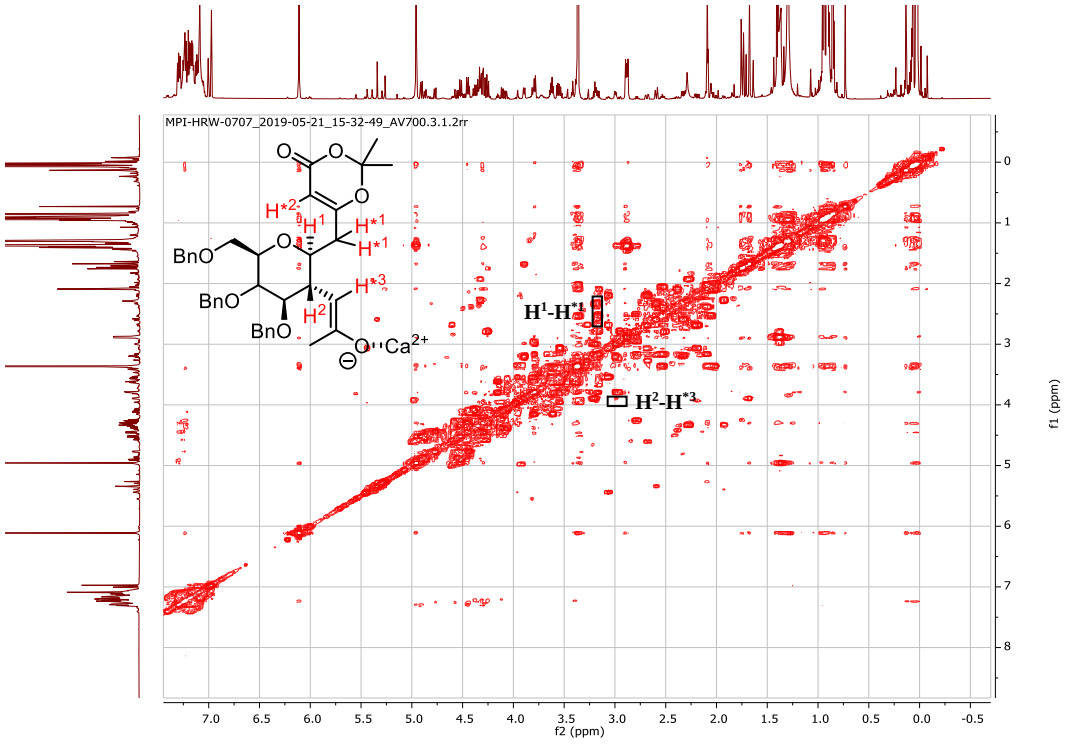

Supplementary Figure 4. ***In situ*** **COSY spectrum of intermediate 124a.**

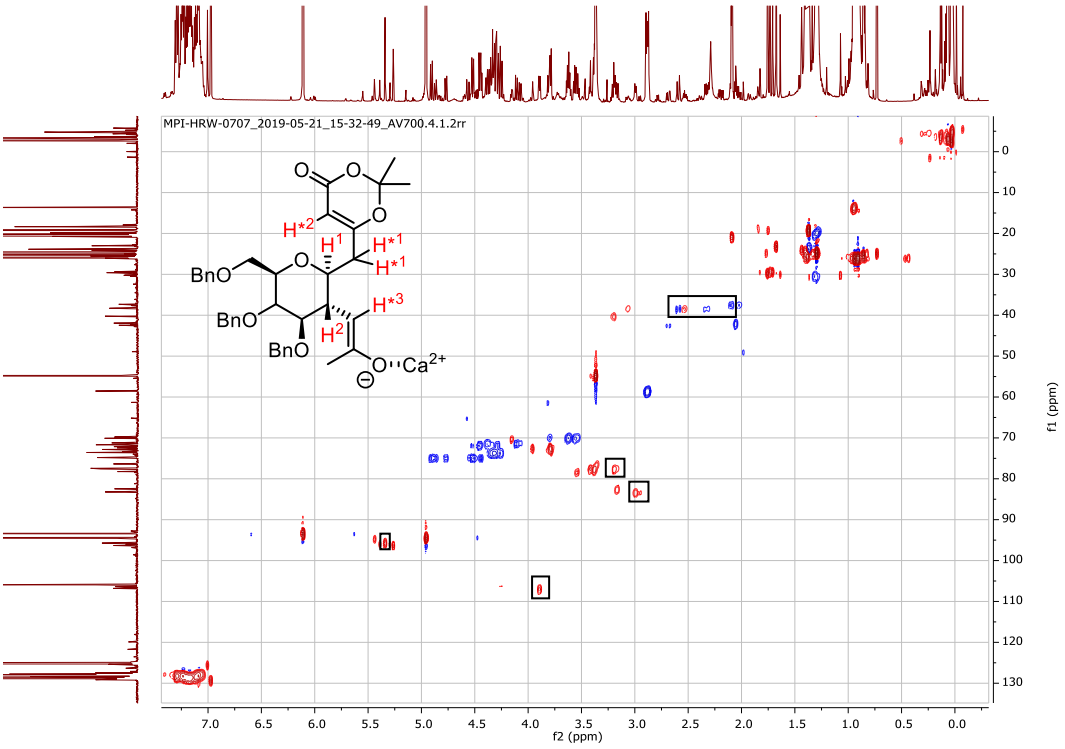

Supplementary Figure 5. ***In situ*** **HSQC spectrum of intermediate 124a.**

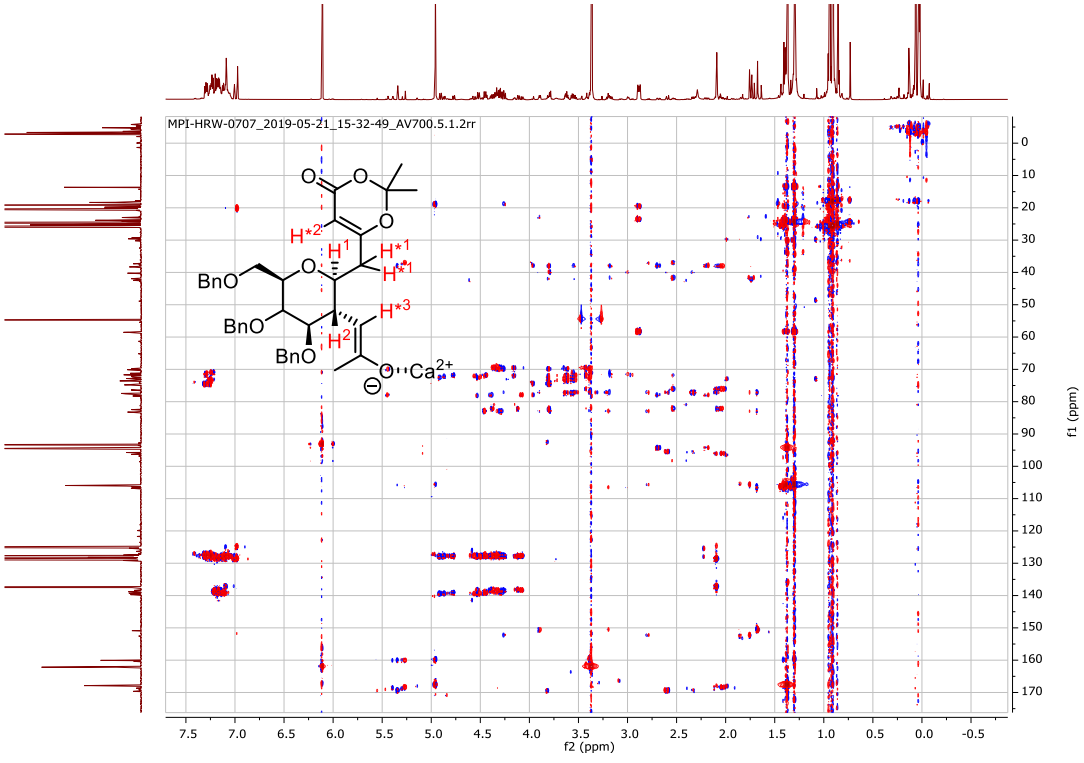

Supplementary Figure 6. ***In situ*** **HMBC spectrum of intermediate 124a.**

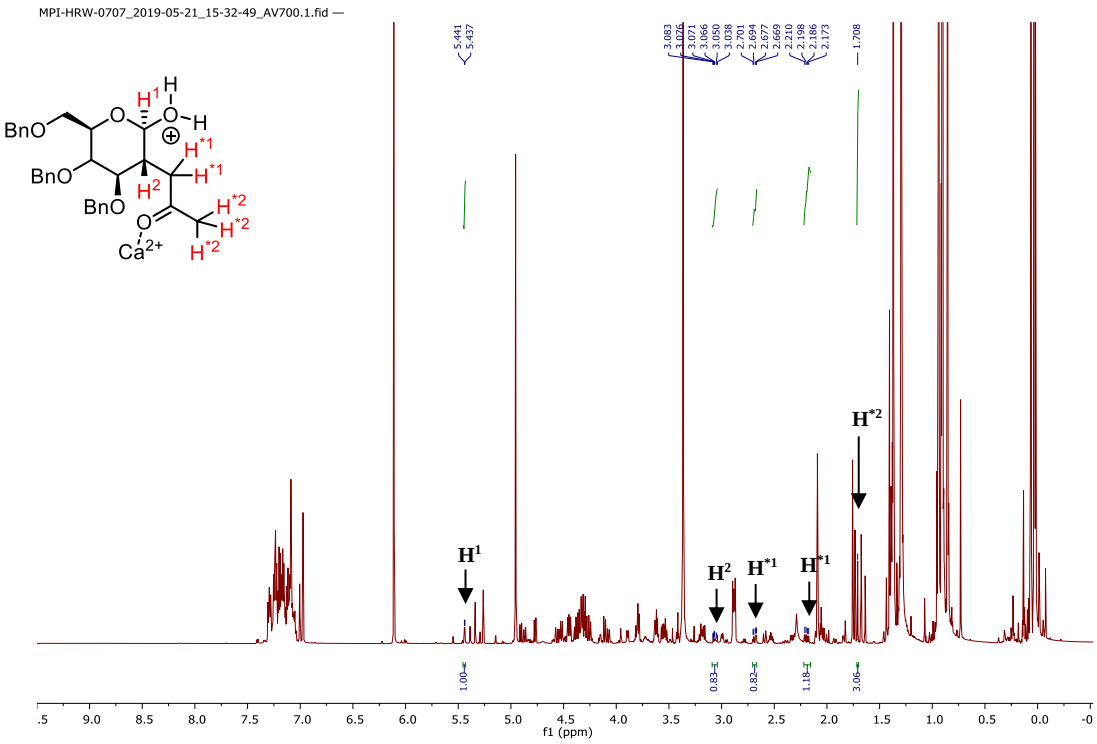

Supplementary Figure 7. ***In situ*** **^{1}H spectrum of intermediate 124b.**

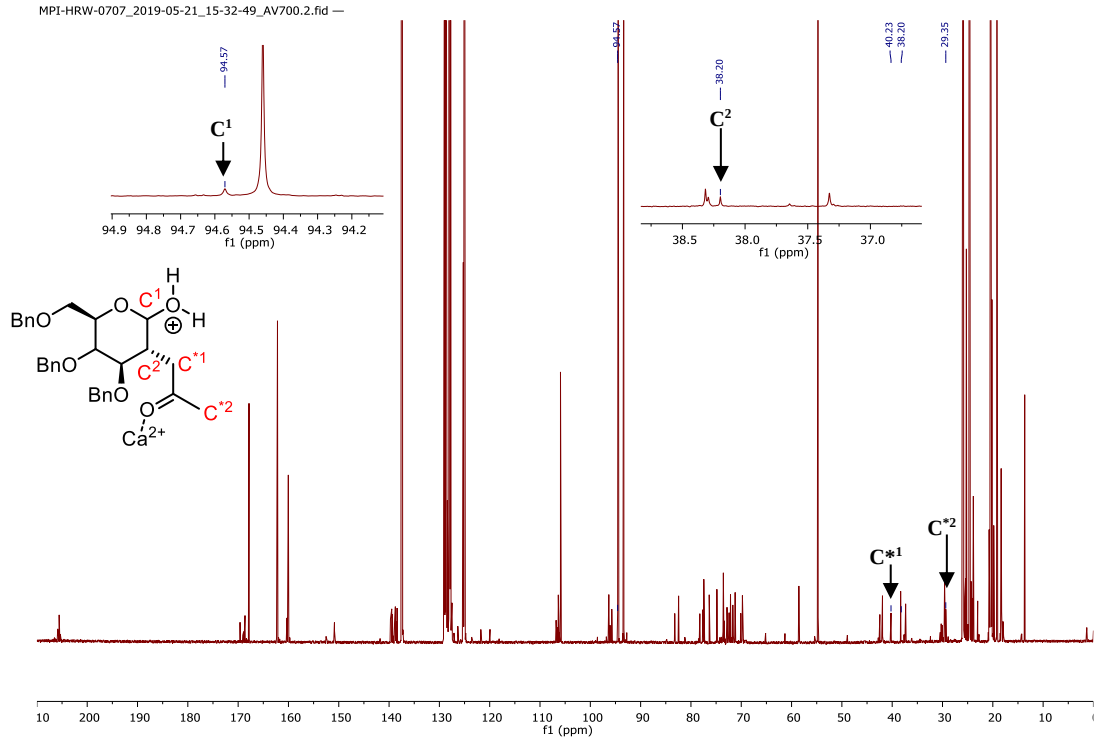

Supplementary Figure 8. ***In situ*** **^{13}C spectrum of intermediate 124b.**

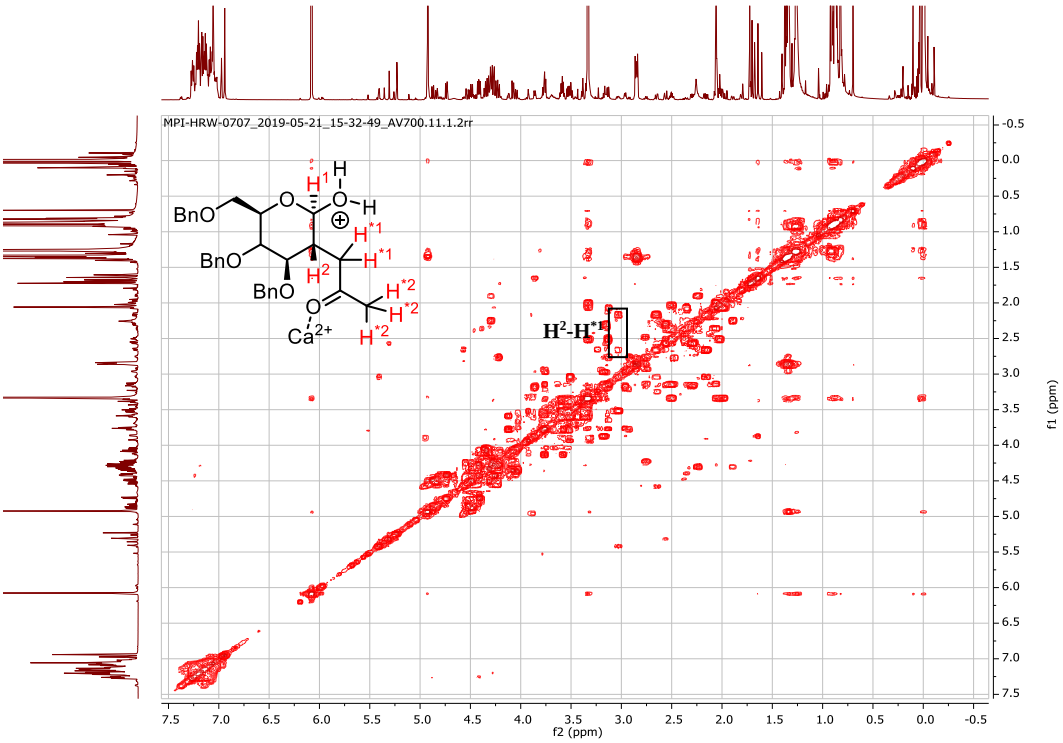

Supplementary Figure 9. ***In situ*** **COSY spectrum of intermediate 124b.**

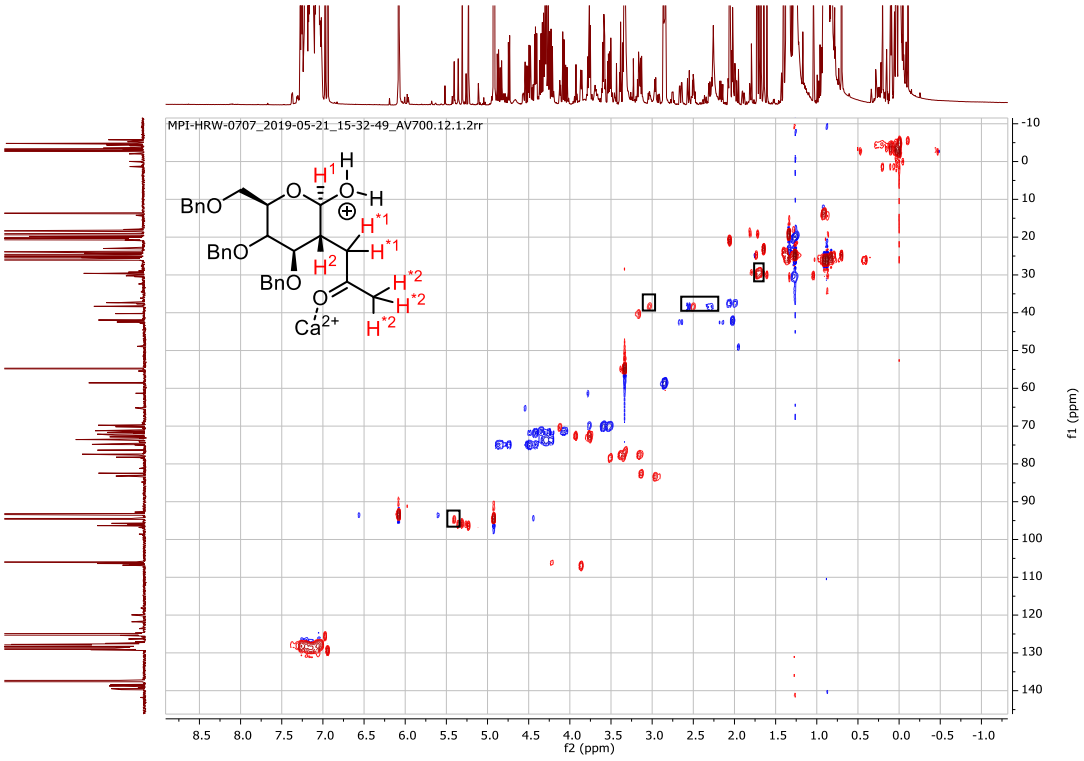

Supplementary Figure 10. ***In situ*** **HSQC spectrum of intermediate 124b.**

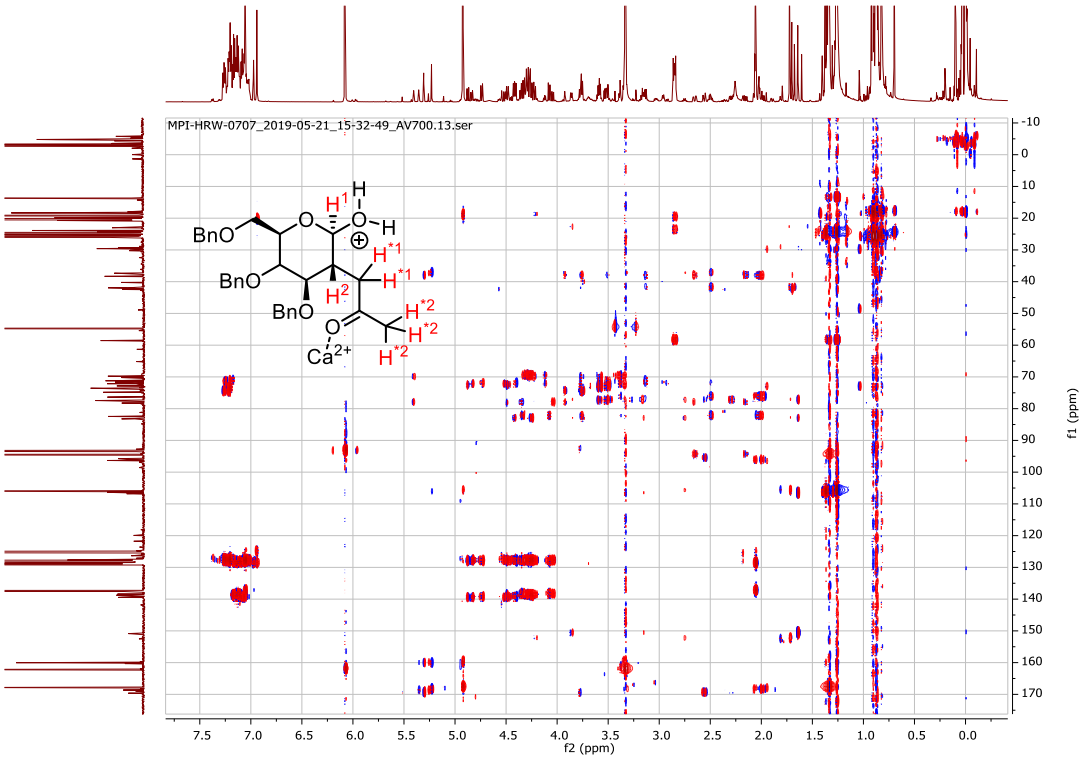

Supplementary Figure 11. *In situ* HBMC spectrum of intermediate 124b.

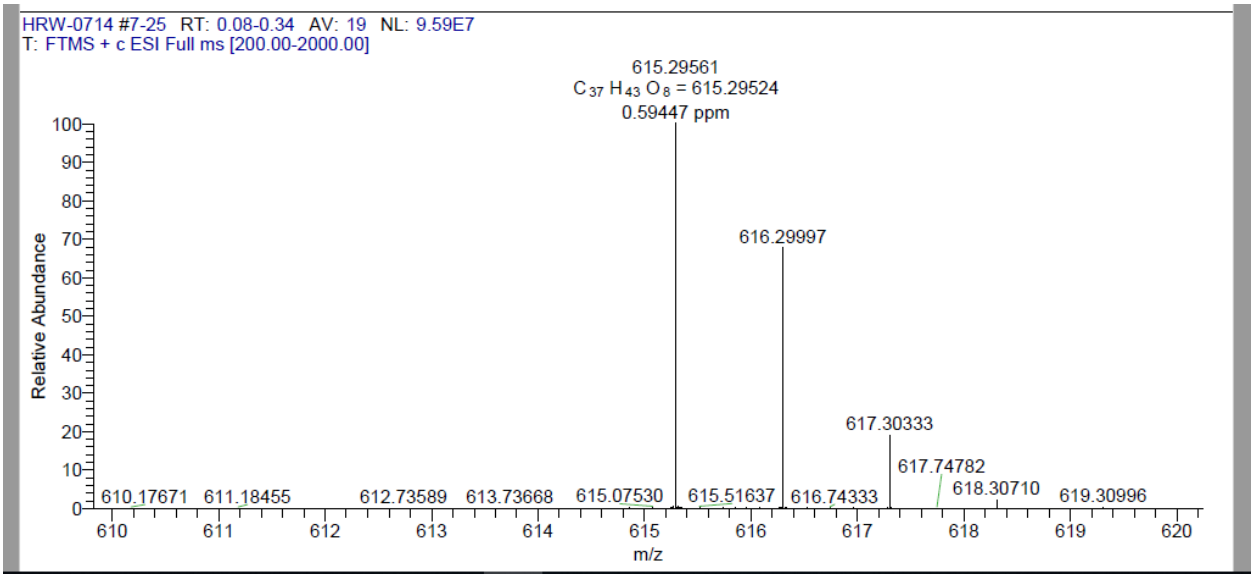

Supplementary Figure 12. HRMS spectrum of deuterium compound 128.

9 Experimental section

9.1 General information

Unless otherwise stated, all reactions were conducted under inert atmosphere (argon) utilizing glassware that were oven dried and cooled under argon purging. Silica gel flash column chromatography was performed on *Silica gel Merck 60* (*particle size 40-63 µm*) [triethylamine (1% v/v) was used as the deactivating reagent]. Starting materials were purchased directly from commercial suppliers (Sigma Aldrich, Acros, Alfa Aesar, VWR, TCI Deutschland GmbH, abcr GmbH, Santa cruz biotechnology) and used without further purifications unless otherwise stated. All solvents were dried according to standard procedures or bought from commercial suppliers. Reactions were monitored using thin-layer chromatography (TLC) on *Merck silica gel aluminum plates with F_{254} indicator*. Visualization of the developed plates was performed under UV light (254 nm) or $KMnO_4$ stain or H_2SO_4-EtOH (10% H_2SO_4 v/v).

NMR characterization data (^{1}H NMR, ^{13}C NMR, ^{19}F NMR and 2D spectra) were collected at 300 K on a *Bruker DRX400* (400 MHz), *Bruker DRX500* (500 MHz), *INOVA500* (500 MHz) and *Bruker RX700* (700 MHz) using toluene-d_8, acetone-d_6, CD_3OD, CD_2Cl_2 or $CDCl_3$ as solvent. Data for ^{1}H NMR were reported as following: chemical shift (δ ppm), multiplicity (s = singlet, d = doublet, t = triplet, q = quartet, pent = pentet, sept = septet, m = multiplet, br = broad), coupling constant (Hz), integration with the solvent resonance as internal standard (acetone-d_6: δ = 2.05 ppm for ^{1}H, δ = 29.92 ppm for ^{13}C; CD_2Cl_2: δ = 5.32 ppm for ^{1}H, δ = 54.00 ppm for ^{13}C; $CDCl_3$: δ = 7.26 ppm for ^{1}H, δ = 77.00 ppm for ^{13}C; CD_3OD: δ = 3.31 ppm for ^{1}H, δ = 49.00 ppm for ^{13}C; toluene-d_8: δ = 2.09 ppm for ^{1}H, δ = 20.40 ppm for ^{13}C). The ratio of anomers was determined by ^{1}H-NMR of the crude reaction mixture via integration of characteristic signals of the anomeric protons in the ^{1}H NMR spectrum. Chemical yields refer to isolated substances after flash column chromatography. Combined yields of both anomers were reported. NMR yields were determined using dibromomethane or 1,3,5-trimethoxybenzene as internal standard.

High resolution mass specta were recorded on a *LTQ Orbitrap* mass spectrometer coupled to an *Accela HPLC-System* (HPLC column: *Hypersyl GOLD*, 50 mm x 1 mm, particle size 1.9 µm, ionization method: electron spray ionization). Optical rotations were measured in a *Schmidt + Haensch Polartronic HH8* polarimeter equipped with a sodium lamp source (589 nm), and were

reported as follows: $[\alpha]_D^{T\,°C}$ (c = g/100 mL, solvent). Kugelrohr distillation was performed on a *GKR-51* under reduced pressure and heating.

9.2 Synthesis of *O*-acetylated glycals

General procedure for synthesis of glycals (procedure A)[64]

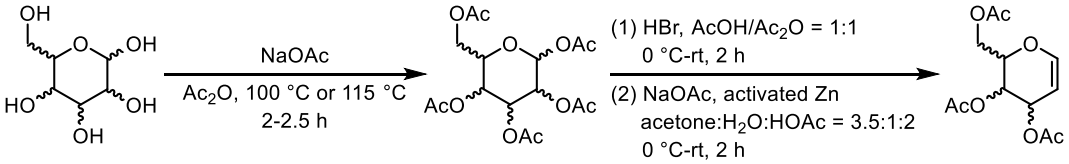

NaOAc (0.53 mol, 1.58 equiv.) was added in acetic anhydride (2.5 mol, 7.6 equiv.) and raised to 115 ºC. Carbohydrate substrate (0.33 mol, 1 equiv.) was added in portions at 115 ºC (the temperature must be kept below 118 ºC) and stirred for 2 h at 115 ºC. After cooling to room temperature, the reaction was poured into 1000 mL ice water and 500 mL CH_2Cl_2 and stirred for another 12 h. The water phase was separated and extracted three times with 250 mL CH_2Cl_2 each time. The combined organic phases were washed with saturated $NaHCO_3$ until neutral, extracted with 1000 mL of water. The organic phase was dried over $MgSO_4$, filtered and the solvent was removed to provide the crude mixture. The crude mixture (0.03 mol) was dissolved in acetic anhydride (2.6 mL) and glacial acetic acid (2.6 mL). After cooling to 0 ºC, a hydrogen bromide solution (33 wt. % in glacial acetic acid, 17.8 mL) was added dropwise and stirred at room temperature for 2 h. The previous mentioned solution was dropwise added through an addition funnel to a solution of sodium acetate (5.1 g), acetone (53.4 mL), distilled water (14.2 mL), acetic acid (14.2 mL) and activated zinc powder (44.64 g) at 0 ºC over 1.5 h (the temperature must not exceed 10 ºC). When the addition was complete, the mixture was stirred at 0 ºC for 1 h and then at rt for a further 18 h. The zinc was filtered off and the filter residue was washed with an acetic acid: H_2O mixture of 1:1. The solution was then extracted once with ice water and three times with cold chloroform and combined organic phases were neutralized using sat. $NaHCO_3$. The solution was dried over $MgSO_4$ and the solvent was removed under reduced pressure. Purification of the product was carried out by silica flash column chromatography.

3,4-Di-*O*-acetyl-D-Xylal (70)

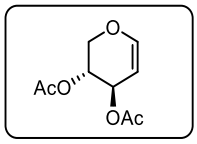

Synthesis according to **procedure A** by using D-Xylose (10.0 g, 31.42 mmol) as starting material to afford **70** (3.61 g, 18.01 mmol, 57%) as a white solid. The analytical data was in accordance to the literature.[65] ^{1}H NMR (700 MHz, $CDCl_3$) δ 6.60 (d, *J* = 6.1 Hz, 1H), 4.99–4.98 (m, 1H), 4.97–4.95 (m, 2H), 4.20 (ddd, *J* = 12.3, 3.2, 1.8 Hz, 1H), 3.98 (dd, *J* = 12.3, 1.6 Hz, 1H), 2.10 (s, 3H), 2.07 (s, 3H); ^{13}C NMR (176 MHz, $CDCl_3$) δ 169.9, 169.8, 148.0, 97.4, 67.2, 63.6, 63.4, 21.1, 20.9; $[\alpha]_D^{20}$ = –283.17 (c = 0.81, CH_2Cl_2).

3,4-Di-*O*-acetyl-D-Arabinal (71)

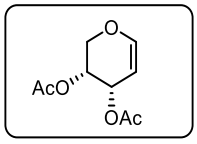

Synthesis according to **procedure A** by using D-Arabinose (5.0 g, 15.71 mmol) as starting material to afford **71** (1.22 g, 6.10 mmol, 39%) as a colorless syrup. The analytical data was in accordance to the literature.[65] ^{1}H NMR (400 MHz, $CDCl_3$) δ 6.50 (dd, *J* = 6.0, 0.8 Hz, 1H), 5.46–5.43 (m, 1H), 5.19 (dt, *J* = 9.2, 4.2 Hz, 1H), 4.85 (dd, *J* = 6.0, 5.0 Hz, 1H), 4.05–3.96 (m, 2H), 2.08 (s, 3H), 2.07 (s, 3H); ^{13}C NMR (176 MHz, $CDCl_3$) δ 170.2, 169.6, 147.6, 97.4, 65.8, 62.7 (2×C), 20.9, 20.6; $[\alpha]_D^{20}$ = +260.73 (c = 2.96, CH_2Cl_2).

3,4-Di-*O*-acetyl-L-Arabinal (72)

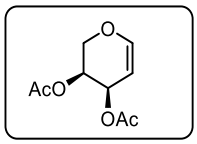

Synthesis according to **procedure A** by using L-Arabinose (10.0 g, 31.42 mmol) as starting material to afford **72** (2.63 g, 13.12 mmol, 42%) as a pale-yellow syrup. The analytical data was in accordance to the literature.[66] ^{1}H NMR (400 MHz, $CDCl_3$) δ 6.50 (d, *J* = 6.0 Hz, 1H), 5.45–5.43 (m, 1H), 5.21–5.17 (m, 1H), 4.85 (dd, *J* = 6.0, 5.1 Hz, 1H), 4.05–3.96 (m, 2H), 2.08 (s, 3H), 2.07 (s, 3H); ^{13}C NMR (176 MHz, $CDCl_3$) δ 170.3, 169.3, 147.7, 97.4, 65.9, 62.8, 62.8, 21.0, 20.7; ESI-

HRMS: *m/z* calcd for $C_9H_{12}O_5Na$ $[M + Na]^+$: 223.05769; found: 223.05690; $[\alpha]_D^{20}$ = –171.72 (c = 1.47, CH_2Cl_2).

Hexa-*O*-acetyl-D-Lactal (73)

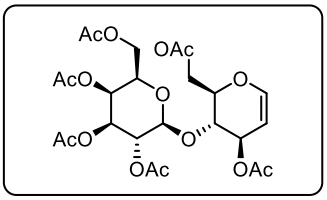

Synthesis according to **procedure A** by using D-Lactose (10.0 g, 14.74 mmol) as starting material to afford **73** (7.57 g, 13.51 mmol, 92%) as a white solid. The analytical data was in accordance to the literature.[65] ^{1}H NMR (400 MHz, $CDCl_3$) δ 6.46 (dt, *J* = 6.3, 1.9 Hz, 2H), 6.57–5.54 (m, 1H), 5.44–5.42 (m, 1H), 5.36–5.33 (m, 1H), 5.22 (dd, *J* = 7.6, 5.7 Hz, 1H), 4.85 (dd, *J* = 6.2, 3.3 Hz, 1H), 4.73 (dddd, *J* = 6.3, 2.7, 1.5, 0.4 Hz, 1H), 4.40 (dd, *J* = 12.0, 5.7 Hz, 1H), 4.34–4.30 (m, 1H), 4.28–4.18 (m, 4H), 2.13 (s, 3H), 2.09 (s, 3H), 2.08 (s, 3H), 2.07 (s, 3H), 2.05 (s, 3H), 2.03 (s, 3H); ^{13}C NMR (176 MHz, $CDCl_3$) δ 170.3, 170.3, 170.1, 170.0, 169.8, 169.2, 145.3, 100.9, 98.9, 74.5, 74.1, 70.71, 70.6, 68.8, 68.7, 66.6, 61.7, 60.9, 21.0, 20.7, 20.5, 20.5 (2×C), 20.4; ESI-HRMS: *m/z* calcd for $C_{24}H_{32}O_{15}Na$ $[M + Na]^+$: 583.16334; found: 583.16318; $[\alpha]_D^{20}$ = –3.77 (c = 0.69, CH_2Cl_2).

Hexa-*O*-acetyl-D-Maltal (74)

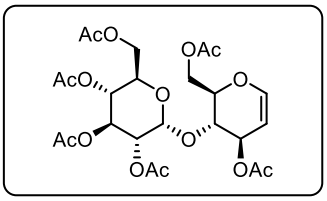

Synthesis according to **procedure A** by using D-Maltose (10.0 g, 14.74 mmol) as starting material to afford **74** (7.14 g, 12.74 mmol, 86%) as a white solid. The analytical data was in accordance to the literature.[65] ^{1}H NMR (400 MHz, $CDCl_3$) δ 6.44 (d, *J* = 6.1 Hz, 1H), 5.50 (d, *J* = 4.0 Hz, 1H), 5.43–5.38 (m, 1H), 5.17 (t, *J* = 4.4 Hz, 1H), 5.05 (t, *J* = 9.9 Hz, 1H), 4.85–4.81 (m, 2H), 4.40–4.35 (m, 2H), 4.32–4.27 (m, 1H), 4.24 (dd, *J* = 12.4, 4.2 Hz, 1H), 4.12–4.08 (m, 1H), 4.05–4.01 (m, 2H), 2.12 (s, 3H), 2.12 (s, 3H), 2.05 (s, 3H), 2.04 (s, 3H), 2.03 (s, 3H), 2.01 (s, 3H); ^{13}C NMR (176 MHz, $CDCl_3$) δ 170.5, 170.4, 170.3 (2×C), 170.0, 169.5, 145.6, 98.6, 95.8, 74.1, 72.5, 70.4, 69.6,

69.5, 68.2, 68.2, 61.8, 61.6, 21.1, 20.8, 20.6, 20.6, 20.6, 20.5; ESI-HRMS: *m/z* calcd for $C_{24}H_{32}O_{15}Na$ $[M + Na]^+$: 583.16334; found: 583.16341; $[\alpha]_D^{20}$ = +63.74 (c = 2.22, CH_2Cl_2).

((2*R*,3*S*)-3-Acetoxy-2,3-dihydrofuran-2-yl)methyl acetate (77)[48]

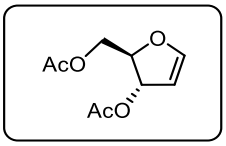

Acetic anhydride (69.3 mL, 0.73 mol, 5.5 equiv.) was added to a solution of D-Ribose (20.0 g, 0.13 mol, 1 equiv.) and pyridine (64.7 mL, 0.80 mol, 6 equiv.) in CH_2Cl_2 (133.3 mL). The resulting solution was stirred for 13.5 hours at rt. The reaction was quenched with water, extracted with CH_2Cl_2, washed with water, dried over with $MgSO_4$, filtered and the solvents were removed under vacuum. The mixture was filtered through a plug of silica, washed with 20% ethyl acetate in hexane and concentrated. The remained pyridine was extracted with $CuSO_{4(aq.)}$ x 2 and concentrated to afford the crude product (41.6 g, 0.13 mol, 98%). The crude product (41.6 g, 0.13 mol, 1 equiv.) was mixed in HBr (33 wt% in acetic acid, 69.1 mL, 3 equiv.), and stirred 5 hours at rt. The reaction was diluted with CH_3CN (133.3 mL), and NaOAc (21.9 g, 0.27 mol, 2 equiv.), NH_4Cl (21.4 g, 0.40 mol, 3 equiv.), and activated Zn dust (17.4 g, 0.27 mol, 2 equiv.) were added sequentially. The reaction was stirred for 2 hours at rt, then quenched with water, extracted with EtOAc, washed with water, dried with $MgSO_4$, filtered and the solvents were removed under vacuum. Purification by silica gel flash column chromatography (EtOAc:*c*-hex = 1:9, R_f = 0.61 (EtOAc:c-hex =1:2)) to afford **77** (8.27 g, 41.33 mmol, 32%) as a pale-yellow syrup. The analytical data was in accordance to the literature.[67] ^{1}H NMR (700 MHz, $CDCl_3$) δ 6.48 (d, *J* = 6.1 Hz, 1H), 5.42 (t, *J* = 4.4 Hz, 1H), 5.17 (dt, *J* = 9.6, 4.0 Hz, 1H), 4.83 (dd, *J* = 6.1, 5.0 Hz, 1H), 4.02–3.95 (m, 2H), 2.06 (s, 3H), 2.05 (s, 3H); ^{13}C NMR (176 MHz, $CDCl_3$) δ 170.4, 169.8, 147.7, 97.4, 65.9, 62.8, 62.8, 21.0, 20.7; $[\alpha]_D^{20}$ = +228.57 (c = 3.16, CH_2Cl_2).

9.3 Synthesis of dioxinone dienolate 78

***Tert*-butyl((2,2-dimethyl-4-methylene-4*H*-1,3-dioxin-6-yl)oxy)dimethylsilane (78)**[68]

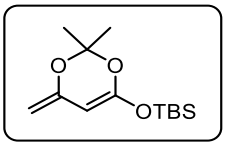

A flame dried flask was charged with anhydrous THF (112.7 mL, 0.5 M regarding the dioxinone) and freshly distilled diisopropylamine (10.85 mL, 77.4 mmol, 1.1 equiv.) at 0 ºC. The solution was cooled in an ice bath followed by slow addition of *n*-butyl lithium (1.6 M in hexane, 48.4 mL, 77.4 mmol, 1.1 equiv.). The reaction was stirred for 30 mins. DMPU (10.2 mL, 84.4 mmol, 1.2 equiv.) was added at –78 ºC and stirred 30 mins upon the mixture turned turbid. Afterwards, the corresponding dioxinone (9.35 mL, 70.4 mmol, 1 equiv.) was added dropwise and the resulting mixture was stirred 30 mins at –78 ºC, where upon the turbidity vanished. The *tert*-butyldimethylsilyl chloride (12.7 g, 84.4 mmol, 1.2 equiv.) dissolved in 8.1 mL THF was added slowly. After complete addition, the cooling was removed and the mixture was stirred for 2 h while reaching room temperature. Afterwards, pentane (200 mL) was added, causing precipitation. The liquid was transferred to a separation funnel and washed quickly five times with 100 mL ice cold water. The organic layer was dried over $MgSO_4$. The solvent was removed to obtain quantitative amounts of crude product. Kugelrohr distillation (0.31 mbar, 80 ºC) was performed to provide **78** (11.17 g, 43.6 mmol, 62%) as colorless oil. The analytical data was in accordance to the literature.[68] ^{1}H NMR (400 MHz, CD_2Cl_2) δ 4.66 (s, 1H), 4.01 (s, 1H), 3.85 (s, 1H), 1.53 (s, 6H), 0.94 (s, 9H), 0.22 (s, 6H); ^{13}C NMR (176 MHz, CD_2Cl_2) δ 154.2, 152.6, 103.1, 85.0, 77.2, 25.8 (3×C), 24.9 (2×C), 18.5, –4.00 (2×C).

9.4 Synthesis of mestiyl dienolates

(*E*)-1-mesitylbut-2-en-1-one (87)[51]

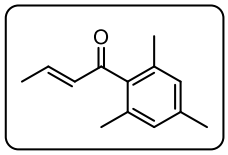

To a stirring mixture of anhydrous aluminum chloride (20.0 g, 0.15 mol, 1.5 equiv.) and mesitylene (250 mL) was added a solution of 2-alkenoyl chloride (10.6 mL, 0.10 mol, 1 equiv.) in the mesitylene (80 mL) dropwise during 3 h at rt. The resulting solution was further stirred for another 1.5 h. It was poured into 1500 mL of 1 mol/L HCl to decompose the $AlCl_3$-complex. After phase separation, the aqueous phase was extracted with EtOAc (×3). Afterwards, the organic phase was dried over $MgSO_4$ and the solvent was evaporated. The residue was purified on silica gel column chromatography (pentane:Et_2O = 79:1; R_f = 0.35 (pentane:Et_2O = 19:1)) as eluent to afford the desired product **87** (15.0 g, 0.08 mol, 80%) as an yellow oil. The analytical data was in accordance to the literature.[51] ^{1}H NMR (700 MHz, $CDCl_3$) δ 6.83 (s, 2H), 6.50 (dq, *J* = 15.8, 6.8 Hz, 1H), 6.32 (dq, *J* = 15.8, 1.6 Hz, 1H), 2.28 (s, 3H), 2.14 (s, 6H), 1.91 (dd, *J* = 6.9, 1.6 Hz, 3H); ^{13}C NMR (176 MHz, $CDCl_3$) δ 201.5, 147.8, 138.1, 137.2, 134.1 (2×C), 133.9, 128.2 (2×C), 21.1, 19.2 (2×C), 18.5; ESI-HRMS: *m/z* calcd for $C_{13}H_{17}O$ $[M + H]^+$: 189.12739; found: 189.12671.

(*Z*)-((1-mesitylbuta-1,3-dien-1-yl)oxy)trimethylsilane (88)[50]

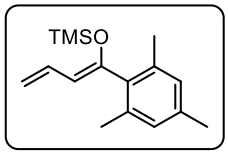

To a solution of **87** (10 g, 53.1 mmol) in THF (200 mL) at –78 ºC, NaHMDS (2 M in THF, 29.2 mL, 58.5 mmol, 1.1 equiv.) was added dropwise under argon for 5 mins and stirred at the same temperature for 2 h. TMSCl (8.3 mL, 63.8 mmol, 1.2 equiv.) was added and stirred for 2 hours more. The reaction mixture was quenched with water and warmed to rt. To the reaction mixture, cold water was added and was extracted with pentane (×3). The combined pentane layers were washed with ice cold water (×5), dried over $MgSO_4$ and concentrated *in vacuo*. Kugelrohr distillation (1.1 mbar, 112.5°C) was performed to provide the pure product **88** (11.2 g, 43.0 mmol, 81%) as pale-yellow oil. The analytical data was in accordance to the literature.[50] ^{1}H NMR (400

MHz, $CDCl_3$) δ 6.88 (s, 2H), 5.83–5.75 (m, 2H), 5.05–4.99 (m, 1H), 4.75–4.70 (m, 1H), 2.30 (s, 3H), 2.25 (s, 6H), 0.20 (s, 9H); ^{13}C NMR (176 MHz, $CDCl_3$) δ 152.6, 137.6, 136.3, 133.7 (2×C), 133.5, 128.0 (2×C), 111.6, 111.6, 21.1, 19.7 (2×C), 0.46 (3×C); ESI-HRMS: *m/z* calcd for $C_{16}H_{25}OSi$ $[M + H]^+$: 261.16692; found: 261.16583.

(*Z*)-*tert*-butyl((1-mesitylbuta-1,3-dien-1-yl)oxy)dimethylsilane (89)[50]

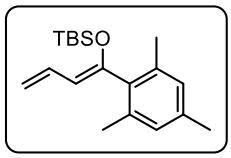

To a solution of **87** (4.91 g, 26.1 mmol) in THF (100 mL) at –78 ºC, NaHMDS (2 M in THF, 14.4 mL, 28.7 mmol, 1.1 equiv.) was added dropwise under argon for 5 mins and stirred at the same temperature for 2 h. TBSCl (4.72 g, 31.3 mmol, 1.2 equiv.) was added and stirred for further 2 hours. The reaction mixture was quenched with water and warmed to rt. To the reaction mixture, cold water was added and extracted with pentane (×3). The combined pentane layers were washed with ice cold water (×5), dried over $MgSO_4$ and concentrated *in vacuo*. Kugelrohr distillation (1.1 mbar, 150 °C) was performed to provide the pure product **89** (7.42 g, 24.5 mmol, 94%) as pale-yellow oil. ^1H NMR (400 MHz, $CDCl_3$) δ 6.85 (s, 2H), 5.82–5.72 (m, 2H), 5.01–4.95 (m, 1H), 4.72–4.67 (m, 1H), 2.28 (s, 3H), 2.22 (s, 6H), 0.90 (s, 9H), 0.09 (s, 6H); ^{13}C NMR (126 MHz, CD_2Cl_2) δ 153.5, 138.2, 136.8, 134.4, 134.3, 128.6 (3×C), 112.4, 112.1, 26.0 (3×C), 21.5, 20.1, 18.7, –4.04 (2×C); ESI-HRMS: *m/z* calcd for $C_{19}H31OSi$ $[M + H]^+$: 303.21387; found: 303.21319.

9.5 Synthesis of *C*-glycosides via Ferrier rearrangement

General procedure for *C*-glycosylation by Ferrier rearrangement (procedure B)

An oven dried tube with a stirring bar was charged with glycal (1 mmol, 1.0 equiv.), mesityl dienolate (2 mmol, 2.0 equiv.) and anhydrous dichloroethane (0.5 mL). Then, $Zn(OTf)_2$ (0.2 mmole, 20 mol%) and dichloroethane (0.5 mL) were added. The tube was purged with argon and sealed with a rubber stopper and parafilm and stirred at 50 ºC for 15 h. Upon completion of the reaction, the reaction mixture was flushed through a short pad of silica gel by EtOAc and subjected to flash column chromatography.

((2*R*,3*S*)-3-acetoxy-6-((*E*)-4-mesityl-4-oxobut-2-en-1-yl)-3,6-dihydro-2*H*-pyran-2-yl)methyl acetate (90a)

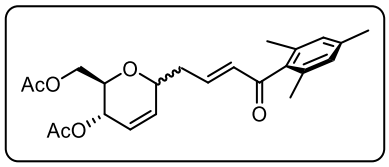

Synthesis according to the **procedure B** by using the corresponding acetylated carbohydrate substrate (272.3 mg, 1.0 mmol) as starting material to afford **90a** (316.4 mg, 0.79 mmol, 79%) as pale-yellow syrup. The α-anomer was assigned based on NOESY spectrum. (data for α-anomer) ^{1}H NMR (700 MHz, $CDCl_3$) δ 6.79 (s, 2H), 6.46–6.40 (m, 2H), 5.82–5.78 (m, 2H), 5.03–5.02 (m, 1H), 4.31–4.28 (m, 1H), 4.18–4.14 (m, 1H), 4.09–4.03 (m, 1H), 3.91–3.88 (m, 1H), 2.59–2.40 (m, 2H), 2.24 (s, 3H), 2.10 (s, 6H), 2.03 (s, 3H), 2.00 (s, 3H); ^{13}C NMR (176 MHz, $CDCl_3$) δ 201.1 170.6, 170.2, 146.9, 138.1, 136.8, 134.7, 133.8, 132.1, 128.1 (2×C), 124.2 (2×C), 70.1, 69.9, 64.4, 62.4, 36.4, 20.9, 20.8, 20.5, 19.1(2×C); ESI-HRMS: *m/z* calcd for $C_{23}H_{28}O_6Na$ $[M + Na]^+$: 423.17781; found: 423.17727.

((2*R*,3*R*)-3-acetoxy-6-((*E*)-4-mesityl-4-oxobut-2-en-1-yl)-3,6-dihydro-2*H*-pyran-2-yl)methyl acetate (90b)

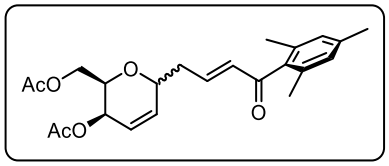

Synthesis according to the **procedure B** by using the corresponding acetylated carbohydrate substrate (272.3 mg, 1.0 mmol) as starting material to afford **90b** (160.2 mg, 0.40 mmol, 40%) as pale-yellow syrup. The α-anomer was assigned based on NOESY spectrum. The integration of ^{1}H NMR spectrum was influenced by the β-anomer since both anomers were inseparable. (data for α-anomer) ^{1}H NMR (700 MHz, $CDCl_3$) δ 6.81 (s, 2H), 6.49–6.31 (m, 2H), 6.01–5.87 (m, 2H), 5.03 (s, 1H), 4.36–4.35 (m, 1H), 4.16–4.13 (m, 1H), 4.12–4.08 (m, 1H), 4.07–4.05 (m, 1H), 2.61–2.49 (m, 1H), 2.40–2.37 (m, 1H), 2.25 (s, 3H), 2.11 (s, 6H), 2.04 (s, 3H), 1.98 (s, 3H); ^{13}C NMR (176 MHz, $CDCl_3$) δ 201.1, 170.7, 170.3, 147.0, 138.2, 136.8, 134.9, 133.8, 133.7, 128.2 (2×C), 122.9 (2×C), 71.3, 68.1, 63.6, 62.7, 35.3, 21.0, 20.8, 20.6, 19.1 (2×C); ESI-HRMS: *m/z* calcd for $C_{23}H_{28}O_6Na$ $[M + Na]^+$: 423.17781; found: 423.17703.

(2*S*,3*R*)-6-((*E*)-4-mesityl-4-oxobut-2-en-1-yl)-2-methyl-3,6-dihydro-2*H*-pyran-3-yl acetate (90c)

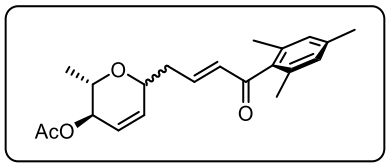

Synthesis according to the **procedure B** by using the corresponding acetylated carbohydrate substrate (214.2 mg, 1.0 mmol) as starting material to afford **90c** (160.9 mg, 0.47 mmol, 47%) as pale-yellow syrup. The α-anomer was assigned based on NOESY spectrum. The integration of ^{1}H NMR spectrum was influenced by the β-anomer since both anomers were inseparable. (data for α-anomer) ^{1}H NMR (700 MHz, $CDCl_3$) δ 6.82 (s, 2H), 6.51–6.47 (m, 1H), 6.36 (d, *J* = 15.9 Hz, 1H), 5.83 (d, *J* = 11.3 Hz, 1H), 5.79 (d, *J* = 11.3 Hz, 1H), 4.84 (s, 1H), 4.25 (t, *J* = 6.1 Hz, 1H), 3.87–3.84 (m, 1H), 2.60–2.56 (m, 1H), 2.50–2.46 (m, 1H), 2.27 (s, 3H), 2.13 (s, 6H), 2.05 (s, 3H), 1.19 (d, *J* = 6.6 Hz, 3H); ^{13}C NMR (176 MHz, $CDCl_3$) δ 201.3, 170.6, 147.5, 138.2, 136.9, 134.6, 133.9, 132.6, 128.2 (2×C), 123.8 (2×C), 69.0, 68.8, 68.7, 37.0, 21.1, 21.0, 19.2 (2×C), 16.7; ESI-HRMS: *m/z* calcd for $C_{21}H_{26}O_4Na$ $[M + Na]^+$: 365.17233; found: 365.17195.

(3*R*)-6-((*E*)-4-mesityl-4-oxobut-2-en-1-yl)-3,6-dihydro-2*H*-pyran-3-yl acetate (90d)

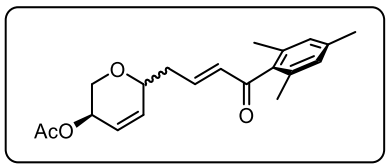

Synthesis according to the **procedure B** by using the corresponding acetylated carbohydrate substrate (200.2 mg, 1.0 mmol) as starting material to afford **90d-α** (135.6 mg, 0.41 mmol, 41%) as pale-yellow syrup and **90d-β** (42.0 mg, 0.13 mmol, 13%) as pale-yellow syrup. The α-anomer was assigned based on NOESY spectrum. (data for α-anomer) ^{1}H NMR (700 MHz, $CDCl_3$) δ 6.82 (s, 2H), 6.46–6.42 (m, 1H), 6.34 (d, *J* = 15.9 Hz, 1H), 5.85–5.79 (m, 2H), 5.16 (s, 1H), 4.23 (s, 1H), 4.04 (dd, *J* = 11.4, 5.0 Hz, 1H), 3.48 (ddd, *J* = 11.4, 6.9, 1.1 Hz, 1H), 2.50–2.43 (m, 2H), 2.27 (s, 3H), 2.12 (s, 6H), 2.05 (s, 3H); ^{13}C NMR (176 MHz, $CDCl_3$) δ 201.1, 170.3, 147.0, 138.1, 136.8, 134.6, 133.7, 132.5, 128.1 (2×C), 125.3 (2×C), 72.0, 64.8, 64.5, 37.0, 20.9, 20.8, 19.1 (2×C); ESI-HRMS: *m/z* calcd for $C_{20}H_{24}O_4Na$ $[M + Na]^+$: 351.15668; found: 351.15627; $[\alpha]_D^{20}$ = –79.08 (c = 0.50, CH_2Cl_2).

The β-anomer was assigned based on NOESY spectrum. (data for β-anomer) ^{1}H NMR (700 MHz, $CDCl_3$) δ 6.82 (s, 2H), 6.50 (dt, *J* = 15.8, 7.0 Hz, 1H), 6.38 (d, *J* = 16.0 Hz, 1H), 5.95–5.93 (m, 1H), 5.90 (d, *J* = 10.3 Hz, 1H), 4.96 (s, 1H), 4.13, (t, *J* = 5.2 Hz, 1H), 3.99 (d, *J* = 13.0 Hz, 1H), 3.71 (dd, *J* = 13.0, 2.7 Hz, 1H), 2.55–2.53 (m, 2H), 2.27 (s, 3H), 2.13 (s, 6H), 2.06 (s, 3H); ^{13}C NMR (176 MHz, $CDCl_3$) δ 201.3, 170.7, 147.0, 138.1, 136.9, 134.8, 134.8, 133.9, 128.2 (2×C), 123.3 (2×C), 72.4, 67.8, 64.2, 37.6, 21.1, 21.0, 19.2 (2×C); ESI-HRMS: *m/z* calcd for $C_{20}H_{24}O_4Na$ $[M + Na]^+$: 351.15668; found: 351.15638; $[\alpha]_D^{20}$ = –51.75 (c = 0.23, CH_2Cl_2).

(3*S*)-6-((*E*)-4-mesityl-4-oxobut-2-en-1-yl)-3,6-dihydro-2*H*-pyran-3-yl acetate (90e)

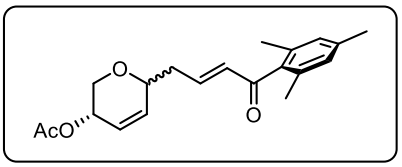

Synthesis according to the **procedure B** by using the corresponding acetylated carbohydrate substrate (200.2 mg, 1.0 mmol) as starting material to afford **90e-α** (223.6 mg, 0.68 mmol, 68%) as pale-yellow syrup and **90e-β** (63.8 mg, 0.19 mmol, 19%) as pale-yellow syrup. The α-anomer was assigned based on NOESY spectrum. (data for α-anomer) ^{1}H NMR (700 MHz, $CDCl_3$) δ 6.76 (s, 2H), 6.40–6.36 (m, 1H), 6.27 (d, *J* = 15.9 Hz, 1H), 5.76 (dd, *J* = 28.4, 10.4 Hz, 2H), 5.10 (s, 1H), 4.18–4.16 (m, 1H), 3.98 (dd, *J* = 11.4, 5.0 Hz, 1H), 3.41 (dd, *J* = 11.4, 6.9 Hz, 1H), 2.44–2.37 (m, 2H), 2.21 (s, 3H), 2.06 (s, 6H), 1.98 (s, 3H); ^{13}C NMR (176 MHz, $CDCl_3$) δ 201.2, 170.4, 147.0, 138.3, 136.8, 134.7, 133.8, 132.5, 128.2 (2×C), 125.4 (2×C), 72.1, 64.9, 64.5, 37.1, 21.0, 20.9, 19.1 (2×C); ESI-HRMS: *m/z* calcd for $C_{20}H_{24}O_4Na$ $[M + Na]^+$: 351.15668; found: 351.15639; $[\alpha]_D^{20}$ = +67.01 (c = 0.78, CH_2Cl_2).

The β-anomer was assigned based on NOESY spectrum. (data for β-anomer) ^{1}H NMR (700 MHz, $CDCl_3$) δ 6.81 (s, 2H), 6.49 (dt, *J* = 15.8, 7.0 Hz, 1H), 6.37 (d, *J* = 16.0 Hz, 1H), 5.94 (dd, *J* = 10.2, 4.9 Hz, 1H), 5.89 (d, *J* = 10.3 Hz, 1H), 4.96 (s, 1H), 4.13 (t, *J* = 5.1 Hz, 1H), 3.99 (d, *J* = 13.0 Hz, 1H), 3.71 (dd, *J* = 13.0, 2.7 Hz, 1H), 2.57–2.50 (m, 2H), 2.27 (s, 3H), 2.12 (s, 6H), 2.05 (s, 3H); ^{13}C NMR (176 MHz, $CDCl_3$) δ 201.3, 170.7, 147.0, 138.1, 136.9, 134.8, 134.8, 133.9, 128.2 (2×C), 123.3 (2×C), 72.4, 67.8, 64.2, 37.6, 21.1, 21.0, 19.2 (2×C); ESI-HRMS: *m/z* calcd for $C_{20}H_{24}O_4Na$ $[M + Na]^+$: 351.15668; found: 351.15634; $[\alpha]_D^{20}$ = +40.36 (c = 0.17, CH_2Cl_2).

((2*S*)-5-((*E*)-4-mesityl-4-oxobut-2-en-1-yl)-2,5-dihydrofuran-2-yl)methyl acetate (90f)

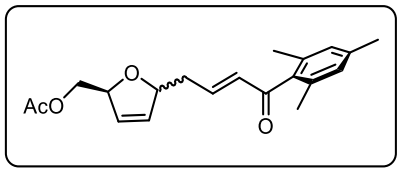

Synthesis according to the **procedure B** by using the corresponding acetylated carbohydrate substrate (200.2 mg, 1.0 mmol) as starting material to afford **90f-α** (158.0 mg, 0.48 mmol, 48%) as pale-yellow syrup and **90f-β** (49.5 mg, 0.15 mmol, 15%) as pale-yellow syrup. The α-anomer was assigned based on NOESY spectrum. (data for α-anomer) ^{1}H NMR (700 MHz, $CDCl_3$) δ 6.82 (s, 2H), 6.46–6,42 (m, 1H), 6.34 (d, *J* = 16.0 Hz, 1H), 5.84 (d, *J* = 10.4 Hz, 1H), 5.80 (d, *J* = 10.4 Hz, 1H), 5.16 (s, 1H), 4.23 (t, *J* = 7.1 Hz, 1H), 4.04 (dd, *J* = 11.4, 5.0 Hz, 1H), 3.48 (dd, *J* = 11.4, 6.9 Hz, 1H), 2.50–2.43 (m, 2H), 2.27 (s, 3H), 2.12 (s, 6H), 2.05 (s, 3H); ^{13}C NMR (176 MHz, $CDCl_3$) δ 201.2, 170.4, 147.0, 138.2, 136.8, 134.7, 133.8, 132.6, 128.2 (2×C), 125.4 (2×C), 72.1, 64.9, 64.5, 37.1, 21.0, 20.9, 19.2 (2×C); ESI-HRMS: *m/z* calcd for $C_{20}H_{25}O_4$ $[M + H]^+$: 329.17474; found: 329.17490; $[\alpha]_D^{20}$ = +54.76 (c = 0.87, CH_2Cl_2).

The β-anomer was assigned based on NOESY spectrum. (data for β-anomer) ^{1}H NMR (700 MHz, $CDCl_3$) δ 6.82 (s, 2H), 6.52–6.48 (m, 1H), 6.38 (d, *J* = 16.0 Hz, 1H), 5.96 –5.93 (m, 1H), 5.90 (d, *J* = 10.3 Hz, 1H), 4.97 (s, 1H), 4.14 (t, *J* = 0.7 Hz, 1H), 4.00 (d, *J* = 13.0 Hz, 1H), 3.71 (dd, *J* = 13.0, 2.8 Hz, 1H), 2.55–2.53 (m, 2H), 2.27 (s, 3H), 2.13 (s, 6H), 2.06 (s, 3H); ^{13}C NMR (176 MHz, $CDCl_3$) δ 201.3, 170.8, 147.0, 138.2, 136.9, 134.8, 134.8, 133.9, 128.3 (2×C), 123.3 (2×C), 72.5, 67.8, 64.3, 37.7, 21.1, 21.1, 19.2 (2×C); ESI-HRMS: *m/z* calcd for $C_{20}H_{24}O_4Na$ $[M + Na]^+$: 351.15668; found: 351.15619; $[\alpha]_D^{20}$ = +33.72 (c = 0.09, CH_2Cl_2).

(2*R*,3*S*,4*S*,5*R*,6*R*)-2-(acetoxymethyl)-6-(((2*R*,3*S*)-2-(acetoxymethyl)-6-((*E*)-4-mesityl-4-oxobut-2-en-1-yl)-3,6-dihydro-2*H*-pyran-3-yl)oxy)tetrahydro-2*H*-pyran-3,4,5-triyl triacetate (90g)

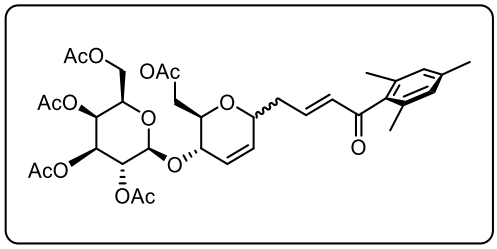

Synthesis according to the **procedure B** by using the corresponding acetylated carbohydrate substrate (560.5 mg, 1.0 mmol) as starting material to afford **90g** (414.6 mg, 0.60 mmol, 60%) as pale-yellow syrup. The α-anomer was assigned based on NOESY spectrum. The integration of ^{1}H NMR spectrum was influenced by the β-anomer since both anomers were inseparable. (data for α-anomer) ^{1}H NMR (700 MHz, $CDCl_3$) δ 6.80 (s, 2H), 6.44–6.39 (m, 1H), 6.33 (d, *J* = 15.9 Hz, 1H), 5.97 (d, *J* = 10.5 Hz, 1H), 5.71 (d, *J* = 10.5 Hz, 1H), 5.35 (s, 1H), 5.19–5.15 (m, 1H), 4.99–4.97 (m, 1H), 4.55–4.53 (m, 1H), 4.25–4.23 (m, 1H), 4.17–4.13 (m, 2H), 4.10–4.03 (m, 2H), 3.96–3.95 (m, 1H), 3.92–3.88 (m, 1H), 3.71 (t, *J* = 7.2 Hz, 1H), 2.61–2.57 (m, 1H), 2.40–2.36 (m, 1H), 2.24 (s, 3H), 2.11 (s, 3H), 2.10 (s, 6H), 2.03 (s, 3H), 2.01 (s, 6H), 1.94 (s, 3H); ^{13}C NMR (176 MHz, $CDCl_3$) δ 201.0, 170.7, 170.2, 170.1, 169.9, 169.3, 147.0, 138.2, 136.8, 134.6, 133.8, 130.3, 128.2, 128.1 (2×C), 127.6 (2×C), 102.2, 72.8, 71.3, 70.7, 70.7, 69.2, 68.7, 66.8, 63.1, 61.2, 35.9, 20.9, 20.6, 20.5 (2×C), 20.5, 20.4, 19.1; ESI-HRMS: *m/z* calcd for $C_{35}H_{44}O_{14}Na$ $[M + Na]^+$: 711.26233; found: 711.26135.

(2*R*,3*R*,4*S*,5*R*,6*S*)-2-(acetoxymethyl)-6-(((2*R*,3*S*)-2-(acetoxymethyl)-6-((*E*)-4-mesityl-4-oxobut-2-en-1-yl)-3,6-dihydro-2*H*-pyran-3-yl)oxy)tetrahydro-2*H*-pyran-3,4,5-triyl triacetate (90h)

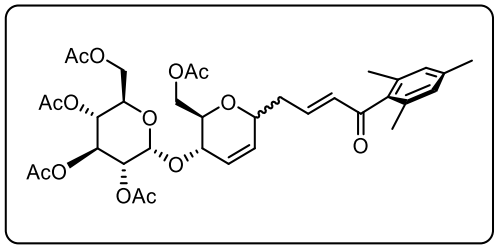

Synthesis according to the **procedure B** by using the corresponding acetylated carbohydrate substrate (560.5 mg, 1.0 mmol) as starting material to afford **90h** (392.6 mg, 0.57 mmol, 57%) as pale-yellow syrup. The α-anomer was assigned based on NOESY spectrum. The integration of ^{1}H NMR spectrum was influenced by the β-anomer since both anomers were inseparable. (data for α-anomer) ^{1}H NMR (700 MHz, $CDCl_3$) δ 6.77 (s, 2H), 6.41–6.37 (m, 1H), 6.33–6.25 (m, 1H), 5.77 (d, *J* = 10.6 Hz, 1H), 5.71 (d, *J* = 10.5 Hz, 1H), 5.38 (t, *J* = 9.8 Hz, 1H), 5.23 (d, *J* = 3.9 Hz, 1H), 5.00–4.97 (m, 1H), 4.76 (dd, *J* = 10.3, 4.2 Hz, 1H), 4.29–4.17 (m, 3H), 4.13 (d, *J* = 5.1 Hz, 1H), 4.04–3.99 (m, 2H), 3.97–3.96 (m, 1H), 3.80 (q, *J* = 5.5 Hz, 1H), 2.56–2.52 (m, 1H), 2.45–2.35 (m, 1H), 2.21 (s, 3H), 2.07 (s, 6H), 2.01 (s, 3H), 1.97–1.96 (m, 9H), 1.94 (s, 3H); ^{13}C NMR (176 MHz, $CDCl_3$) δ 200.9, 170.4, 170.3, 170.0, 169.8, 169.3, 146.9, 138.0, 136.7, 134.5, 133.7, 131.8, 128.1 (2×C), 124.1 (2×C), 94.0, 70.5, 70.4, 70.2, 69.6, 69.4, 68.1, 67.8, 62.9, 61.6, 36.2, 20.8, 20.5, 20.4, 20.4, 20.4, 20.3, 19.0 (2×C); ESI-HRMS: *m/z* calcd for $C_{35}H_{44}O_{14}Na$ $[M + Na]^+$: 711.26233; found: 711.26139.

9.6 Synthesis of donor-acceptor cyclopropanated carbohydrates

Methyl-2,3,4,6-tetra-*O*-benzyl-α-D-galactopyranoside (92)[52]

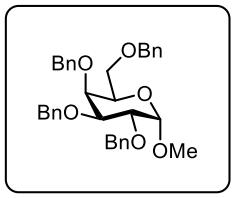

Methyl α-D-galactopyranoside (10 g, 51.5 mmol, 1 equiv.) was dissolved in anhydrous DMF (200 mL). The resulting solution was cooled at 0 ºC and sodium hydride (60% in oil, 16.5 g, 412 mmol, 8 equiv.) was slowly added and stirred for 30 mins. Then, benzyl bromide (49.0 mL, 412.0 mmol,

8 equiv.) and tetrabutylammonium iodide (3.8 g, 10.3 mmol, 0.2 equiv.) were slowly added. The resulting suspension gradually turned yellow. The solution was stirred for 39 h at room temperature under argon and then poured into an Erlenmeyer flask (1 L) containing ice. The water layer was reextracted with further CH_2Cl_2 (2 x 200 mL). The combined organic phases were washed with 2 x 200 mL water and 200 mL brine, dried over $MgSO_4$, filtered and concentrated *in vacuo* to give the crude product which was purified by silica flash column chromatography (EtOAc:*c*-hex = 1:8, R_f = 0.15 (EtOAc:*c*-hex = 1:8)) to afford desired **92** (27.5 g, 46.0 mmol, 89%) as colorless syrup. The analytical data was in accordance to the literature.[52] ^{1}H NMR (700 MHz, $CDCl_3$) δ 7.40–7.24 (m, 20H), 4.95 (d, *J* = 11.5 Hz, 1H), 4.84 (t, *J* = 11.4 Hz, 2H), 4.74 (d, *J* = 11.7 Hz, 1H), 4.70–4.68 (m, 2H), 4.58 (d, *J* = 11.4 Hz, 1H), 4.48 (d, *J* = 11.8 Hz, 1H), 4.40 (d, *J* = 11.8 Hz, 1H), 4.05–4.03 (m, 1H), 3.95–3.93 (m, 2H), 3.90 (t, *J* = 6.4 Hz, 1H), 3.53 (d, *J* = 6.5 Hz, 2H), 3.37 (s, 3H); ^{13}C NMR (176 MHz, $CDCl_3$) δ 138.8, 138.7, 138.5, 138.0, 128.4 (2×C), 128.4 (2×C), 128.3 (2×C), 128.2 (2×C), 128.2 (2×C), 128.1 (2×C), 127.7 (2×C), 127.7, 127.7, 127.6, 127.5 (3×C), 98.8, 79.1, 76.5, 75.2, 74.7, 73.6, 73.5, 73.3, 69.2, 69.1, 55.3; ESI-HRMS: *m/z* calcd for $C_{35}H_{38}O_6Na$ $[M + Na]^+$: 577.25606; found: 577.25546; $[\alpha]_D^{20}$ = +42.82 (c = 0.34, CH_2Cl_2).

3-*C*-(2′,3′,4′,6′-Tetra-*O*-benzyl-α-D-galactopyranosyl)-propene (93)[53]

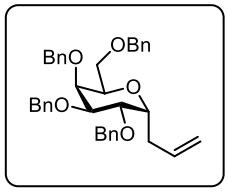

To a stirring solution of methyl 2,3,4,6-tetra-*O*-benzyl-α-D-galactopyranoside **92** (31.1g, 56.0 mmol, 1 equiv.) in anhydrous CH_3CN (115 mL) at 0 ºC under argon was added allyltrimethylsilane (18.4 mL, 112.0 mmol, 2 equiv.). Then trimethylsilyl triflate (5.12 mL, 28.0 mmol, 0.5 equiv.) was added dropwise. The reaction mixture was allowed to stir at 0 ºC for 16 h then for 5.5 h at rt. The yellow mixture was diluted with CH_2Cl_2 (400 mL), and neutralized with saturated $NaHCO_3$ solution (2 x 150 mL). The water layer was reextracted with further CH_2Cl_2 (2 x 80 mL). The combined organic phases were dried over anhydrous $MgSO_4$ and concentrated to give an orange syrup. The crude material was purified by silica gel flash column chromatography (pentane:Et_2O = 9:1 to 4:1; R_f = 0.2 (pentane:Et_2O = 4:1)) to yield **93** (26.7 g, 47.3 mmol, 84%) as pale-yellow syrup. The analytical data was in accordance to the literature.[53] ^{1}H NMR (700 MHz, $CDCl_3$) δ

7.31–7.23 (m, 20H), 5.80–5.71 (m, 1H), 5.08 (dq, *J* = 17.1, 1.6 Hz, 1H), 5.04–5.02 (m, 1H), 4.70–4.67 (m, 2H), 4.60–4.55 (m, 3H), 4.51–4.47 (m, 3H), 4.07 (br, 1H), 4.03–4.00 (m, 2H), 3.86 (br, 1H), 3.76 (br, 1H), 3.72 (dd, *J* = 6.8, 2.8 Hz, 1H), 3.69 (dd, *J* =10.6, 4.7 Hz, 1H), 2.46–2.42 (m, 1H), 2.37–2.33 (m, 1H); ^{13}C NMR (176 MHz, $CDCl_3$) δ 138.6, 138.5, 138.4, 138.2, 135.1, 128.3 (2×C), 128.3 (2×C), 128.3 (2×C), 128.2 (2×C), 127.9 (2×C), 127.8 (2×C), 127.7 (2×C), 127.7, 127.7, 127.5, 127.5 (2×C), 127.4 (2×C), 116.7, 76.4, 74.2, 73.1, 73.0 (2×C), 73.0, 72.5, 70.8, 67.2, 32.2; ESI-HRMS: m/z calcd for $C_{37}H_{41}O_5$ $[M + H]^+$: 565.29485; found: 565.29463; $[\alpha]_D^{20}$ = +45.83 (c = 0.68, CH_2Cl_2).

3-*C*-(3′,4′,6′-Tri-*O*-benzyl-α-D-galactopyranosyl)-propene (95)[53]

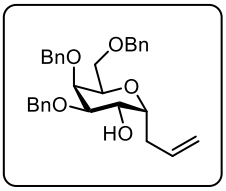

Under argon atmosphere, I_2 (32.0 g, 126.1 mmol, 2 equiv.) was added to a solution of **93** (35.6 g, 63.0 mmol, 1 equiv.) in anhydrous CH_2Cl_2 (105.8 mL) at 0 ºC. After 6 h, the reaction was complete; aqueous $Na_2S_2O_3$ was added and the mixture stirred until the organic phase became colorless. The organic layer was washed with water, then dried over $MgSO_4$, filtered and concentrated to dryness. The crude cyclic iodoether (yellowish oil) was dissolved in a 1:1 mixture of Et_2O:MeOH (220 mL), and activated Zn (41.2 g, 630.7 mmol, 10 equiv.) and glacial AcOH (8.1 mL) were added. After 18 h the reaction mixture was filtered over a celite pad and the solvent was evaporated. The residue was dissolved in CH_2Cl_2, and the organic phase was washed sequentially with 5% HCl and water. The crude material was purified by silica flash column chromatography (MeOH:CH_2Cl_2 = 1:99; R_f = 0.1 (MeOH:CH_2Cl_2 = 1:99)) to afford **95** (28.9 g, 60.9 mmol, 97%) as colorless syrup. The analytical data was in accordance to the literature.[53] ^{1}H NMR (700 MHz, $CDCl_3$) δ 7.44–7.31 (m, 15H), 5.90 (ddt, *J* = 17.1, 10.2, 6.9 Hz, 1H), 5.21 (dq, *J* = 17.1, 1.7 Hz, 1H), 5.15–5.14 (m, 1H), 4.80–4.77 (m, 2H), 4.64 (d, *J* = 11.7 Hz, 1H), 4.62–4.57 (m, 3H), 4.16–4.08 (m, 4H), 3.93 (br, 1H), 3.79 (dd, *J* = 10.4, 5.2 Hz, 1H), 3.76–3.75 (m, 1H), 2.48–2.41 (m, 3H); ^{13}C NMR (176 MHz, $CDCl_3$) δ 138.2, 138.1, 138.0, 134.7, 128.3 (2×C), 128.2 (2×C), 128.2 (2×C), 127.7 (2×C), 127.6, 127.6 (2×C), 127.5, 127.5, 127.4 (2×C), 116.8, 78.2, 73.2 (2×C), 73.1, 73.0, 72.3, 68.5, 67.1, 31.4;

ESI-HRMS: m/z calcd for $C_{30}H_{35}O_5$ $[M + H]^+$: 475.24790; found: 475.24720; $[\alpha]_D^{20}$ = +52.96 (c = 0.30, CH_2Cl_2).

3-*C*-(3′,4′,6′-Tri-*O*-benzyl-α-D-talopyranosyl)-propene (97)[53]

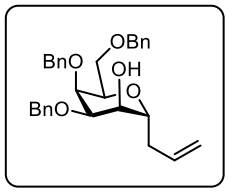

To a stirring solution of **95** (29.5 g, 62.3 mmol, 1 equiv.) in DMSO (76.6 mL) was added IBX (34.9 g, 124.5 mmol, 2 equiv.). The reaction mixture was allowed to stir at rt for 2.5 h. The mixture was diluted with CH_2Cl_2, and extracted with water. The organic layer was collected, and the aqueous layer was reextracted with further CH_2Cl_2. The combined organic phases were dried over anhydrous $MgSO_4$ and concentrated to give a colorless syrup ketone intermediate. To a solution of the ketone intermediate was added anhydrous THF (163.7 mL) at –78 ºC and L-selectride (1 mol/L in THF, 74.7 mL, 74.7 mmol, 1.2 equiv.) in anhydrous THF (224 mL) and stirred for 3 h at –78 ºC. To the mixture, water (613 mL), 2 M NaOH (11.8 mL) and 30% H_2O_2 (11.8 mL) were added and extracted three times with CH_2Cl_2. The organic phases were concentrated *in vacuo* and after silica flash column chromatography (EtOAc:*c*-hex = 9:1; R_f = 0.34 (EtOAc:*c*-hex = 1:4)) afforded **97** (22.8 g, 47.9 mmol, 77%) as a pale-yellow syrup. The analytical data was in accordance to the literature.[53] ^{1}H NMR (700 MHz, $CDCl_3$) δ 7.42–7.32 (m, 15H), 5.91–5.85 (m, 1H), 5.13–5.11 (m, 2H), 4.89 (d, *J* = 11.4 Hz, 1H), 4.79 (d, *J* = 11.9 Hz, 1H), 4.74 (d, *J* = 11.7 Hz, 1H), 4.66 (d, *J* = 11.3 Hz, 1H), 4.60 (d, *J* = 12.0 Hz, 1H), 4.53 (d, *J* = 11.9 Hz, 1H), 4.04 (br, 1H), 3.97 (br, 1H), 3.92 (s, 1H), 3.84 (br, 1H), 3.80 (br, 1H), 3.78–3.76 (m, 1H), 3.72 (br, 1H), 2.35 (t, *J* = 7.1 Hz, 2H); ^{13}C NMR (176 MHz, $CDCl_3$) δ 138.1, 137.8, 137.7, 134.2, 128.4 (2×C), 128.3 (2×C), 128.2 (2×C), 127.8 (2×C), 127.7, 127.7, 127.7 (2×C), 127.7 (2×C), 127.5, 117.1, 76.3, 74.6, 74.0, 73.2 (2×C), 71.9, 71.3, 69.0, 67.6, 26.8; ESI-HRMS: m/z calcd for $C_{30}H_{35}O_5$ $[M + H]^+$: 475.24790; found: 475.24718; $[\alpha]_D^{20}$ = +11.52 (c = 0.78, CH_2Cl_2).

3-*C*-(3′,4′,6′-Tri-*O*-benzyl-2′-*O*-tosyl-α-D-talopyranosyl)-propene (98)[53]

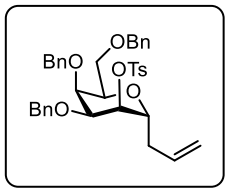

To a solution of **97** (17.3 g, 36.5 mmol, 1 equiv.) in 1,2-dichloroethane (103.8 mL) cooled to 0 ºC, pyridine (29.5 mL, 364.5 mmol, 10 equiv.) and TsCl (34.7 g, 182.3 mmol, 5 equiv.) were sequentially added. After 10 mins at 0 ºC, the reaction mixture was allowed to stir at 70 ºC for 18.5 h. The mixture was diluted by CH_2Cl_2 and washed with 10 % HCl, water, and brine, then dried over $MgSO_4$. The organic phase was concentrated *in vacuo* and after silica flash column chromatography (EtOAc:*c*-hex = 1:19 to 1:9; R_f = 0.47 (EtOAc:*c*-hex = 1:4)) afforded **98** (19.3 g, 30.8 mmol, 84%) as a colorless syrup. The analytical data was in accordance to the literature.[53] ^{1}H NMR (700 MHz, $CDCl_3$) δ 7.79 (d, *J* = 8.3 Hz, 2H), 7.37–7.25 (m, 17H), 5.76 (ddt, *J* = 17.1, 10.3, 6.8 Hz, 1H), 5.05–5.00 (m, 2H), 4.72 (d, *J* = 11.3 Hz, 1H), 4.58–4.50 (m, 5H), 4.30–4.26 (m, 2H), 4.24–4.23 (m, 1H), 4.05 (dd, *J* = 12.0, 8.7 Hz, 1H), 3.92 (td, *J* = 8.5, 3.4 Hz, 1H), 3.77 (dd, *J* = 12.0, 2.3 Hz, 1H), 3.68 (dd, *J* = 6.2, 2.5 Hz, 1H), 2.45 (s, 3H), 2.30–2.26 (m, 1H), 1.99–1.95 (m, 1H); ^{13}C NMR (176 MHz, $CDCl_3$) δ 145.0, 138.4, 138.3, 137.6, 133.6, 133.4, 129.8 (2×C), 128.4 (2×C), 128.2 (2×C), 128.1 (2×C), 127.8 (2×C), 127.8, 127.7 (2×C), 127.5 (2×C), 127.4, 127.4, 127.4 (2×C), 117.5, 78.1, 75.8, 75.7, 74.8, 74.6, 73.0, 71.4, 66.3, 66.0, 34.9, 21.6; ESI-HRMS: m/z calcd for $C_{37}H_{41}O_7S$ $[M + H]^+$: 629.25675; found: 629.25596; $[\alpha]_D^{20}$ = +34.45 (c = 0.98, CH_2Cl_2).

1-*C*-(3′,4′,6′-Tri-*O*-benzyl-2′-*O*-tosyl-α-D-talopyranosyl)-acetone (99)[53]

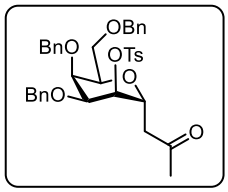

To a solution of **98** (19.3 g, 30.8 mmol, 1 equiv.) and $Hg(OAc)_2$ (2.45 g, 7.69 mmol, 0.25 equiv.) in acetone/water (4:1, 181.7 mL) was added dropwise a solution of Jones reagent (2 M, 34.8 mL) at 0 ºC. The dark greenish-brown mixture was stirred for 23 h at room temperature and then poured into water (500 mL). The aqueous mixture was extracted with CH_2Cl_2 (5 x 100 mL). The organic

layers were successively washed with water (2 x 120 mL), brine (2 x 120 mL), dried over anhydrous $MgSO_4$. The filtrate was concentrated *in vacuo* and the residue was purified by silica gel flash column chromatography (EtOAc:*c*-hex = 1:4; R_f = 0.28 (EtOAc:*c*-hex = 1:2)) to afford **99** (16.3 g, 25.4 mmol, 82%) as a colorless syrup. The analytical data was in accordance to the literature.[53] ^{1}H NMR (600 MHz, $CDCl_3$) δ 7.83 (d, *J* = 8.3 Hz, 2H), 7.40–7.29 (m, 17H), 4.78 (d, *J* = 11.4 Hz, 1H), 4.66 (d, *J* = 11.4 Hz, 1H), 4.61 (d, *J* = 12.0 Hz, 1H), 4.56–4.54 (m, 3H), 4.48 (td, *J* = 9.4, 3.0 Hz, 1H), 4.39 (dd, *J* = 9.6, 2.8 Hz, 1H), 4.34–4.32 (m, 1H), 4.26 (t, *J* = 2.7 Hz, 1H), 4.21 (dd, *J* = 12.0, 8.8 Hz, 1H), 3.87 (dd, *J* = 12.0, 2.0 Hz, 1H), 3.73 (dd, *J* = 6.4, 2.5 Hz, 1H), 2.59 (dd, *J* = 16.0, 3.0 Hz, 1H), 2.45 (s, 3H), 2.38 (dd, *J* = 16.0, 9.2 Hz, 1H), 2.13 (s, 3H); ^{13}C NMR (151 MHz, $CDCl_3$) δ 205.2, 145.1, 138.1, 137.9, 137.3, 133.0, 129.7 (2×C), 128.1 (2×C), 128.0 (2×C), 127.9 (2×C), 127.6 (2×C), 127.5, 127.5 (2×C), 127.3 (2×C), 127.2, 127.2, 127.1, 77.8, 75.4, 74.7, 74.6, 72.9 (2×C), 71.1, 65.5, 63.1, 44.7, 29.9, 26.6, 21.3; $[\alpha]_D^{20}$ = +30.18 (c = 1.68, CH_2Cl_2).

General procedure for the synthesis of cyclopropanated sugar (procedure C)[53]

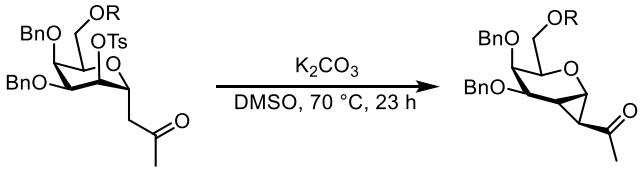

To a solution of tosyl precursor (1 mmol, 1 equiv.) in anhydrous DMSO (10 mL) was added flame dried K_2CO_3 (5 mmol, 5 equiv.) and stirred at 70 ºC for 23 h. The mixture was cooled to room temperature, diluted with EtOAc, washed with water, brine, and dried over $MgSO_4$. The filtrate was concentrated *in vacuo*, and purified by silica gel flash column chromatography (triethylamine (1% v/v) was used as the deactivating reagent) to afford the desired cyclopropanated sugar.

1-*C*-Acetyl-3,4,6-tri-*O*-benzyl-1,2-cyclopropane-1,2-deoxy-α-D-galctopyranose (6)[53]

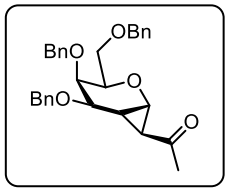

Synthesis according to the **procedure C** by using the corresponding tosyl precursor **99** (16.3 g, 25.35 mmol) as starting material to afford **6** (8.40 g, 17.8 mmol, 70%) as a pale-yellow solid. The

analytical data was in accordance to the literature.[53] ^{1}H NMR (700 MHz, toluene-d_8) δ 7.27–7.09 (m, 15H), 4.79 (d, *J* = 11.7 Hz, 1H), 4.49–4.46 (m, 2H), 4.34–4.31 (m, 2H), 4.26 (d, *J* = 11.9 Hz, 1H), 3.97 (dd, *J* = 7.5, 2.1 Hz, 1H), 3.76 (dd, *J* = 9.8, 6.0 Hz, 1H), 3.69–3.67 (m, 1H), 3.63–3.61 (m, 1H), 3.60–3.59 (m, 1H), 3.36 (t, *J* = 2.8 Hz, 1H), 2.19 (ddd, *J* = 7.5, 5.8, 2.8 Hz, 1H), 1.79 (s, 3H), 1.58 (dd, *J* = 5.8, 2.0 Hz, 1H); ^{13}C NMR (176 MHz, toluene-d_8) δ 202.5, 139.3, 139.0, 138.6, 129.2, 129.1, 128.6 (2×C), 128.5 (3×C), 128.2, 128.2, 128.0 (2×C), 127.9 (2×C), 127.7, 127.7, 76.3, 75.0, 73.8, 73.5, 72.7, 71.3, 69.5, 60.9, 34.4, 30.1, 26.2; ESI-HRMS: m/z calcd for $C_{30}H_{32}O_5Na$ $[M + Na]^+$: 495.21420; found: 495.21230; $[\alpha]_D^{20}$ = +28.57 (c = 0.55, CH_2Cl_2).

1-*C*-(3′,4′-Di-*O*-benzyl-6′-*O*-acetyl -2′-*O*-tosyl-α-D-talopyranosyl)-acetone (100)[19]

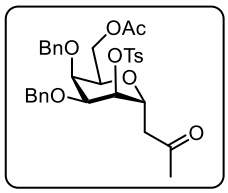

To the solution of **99** (3.00 g, 4.65 mmol, 1 equiv.) in Ac_2O (10.6 mL) and AcOH (21.1 mL), powdered anhydrous $ZnCl_2$ (4.12 g, 30.2 mmol, 6.5 equiv.) was added under argon atmosphere at 0 ºC. After stirring at room temperature for 41 h, the mixture was extracted with CH_2Cl_2 and water, then the organic layer was successively washed with water (2 × 100 mL), saturated aqueous $NaHCO_3$ (3 × 100 mL), brine (2 × 100 mL) and dried over anhydrous $MgSO_4$. The filtrate was concentrated *in vacuo*. The residue was purified by silica gel flash column chromatography (EtOAc:*c*-hex = 1:3, R_f = 0.18 (EtOAc:*c*-hex = 1:3)) to afford the **100** (2.05 g, 3.44 mmol, 74%) as colorless syrup. ^{1}H NMR (500 MHz, $CDCl_3$) δ 7.75 (d, *J* = 8.1 Hz, 2H), 7.37–7.27 (m, 12H), 4.80 (dd, *J* = 13.2, 10.0 Hz, 1H), 4.76 (d, *J* = 11.5 Hz, 1H), 4.62 (d, *J* = 11.5 Hz, 1H), 4.56–4.50 (m, 2H), 4.44–4.41 (m, 1H), 4.38 (dd, *J* = 9.3, 2.9 Hz, 1H), 4.29 (dd, *J* = 9.7, 2.7 Hz, 1H), 4.23–4.22 (m, 1H), 4.20–4.16 (m, 1H), 3.65 (dd, *J* = 6.5, 2.4 Hz, 1H), 2.53 (dd, *J* = 15.9, 2.9 Hz, 1H), 2.46 (s, 3H), 2.24 (dd, *J* = 15.9, 9.1 Hz, 1H), 2.08 (s, 3H), 2.03 (s, 3H); ^{13}C NMR (126 MHz, $CDCl_3$) δ 205.4, 171.0, 145.4, 138.0, 137.3, 133.2, 130.0 (2×C), 128.5 (2×C), 128.2 (2×C), 128.0, 127.8 (2×C), 127.8 (2×C), 127.6, 127.5 (2×C), 77.8, 75.5, 75.4, 75.2, 73.4, 71.3, 63.1, 60.3, 45.0, 29.9, 21.7, 21.0; ESI-HRMS: m/z calcd for $C_{32}H_{37}O_9S$ $[M + H]^+$: 597.21528; found: 597.21439; $[\alpha]_D^{20}$ = +32.85 (c = 0.41, CH_2Cl_2).

1-*C*-Acetyl-6-*O*-acetyl-3,4-di-*O*-benzyl-1,2-cyclopropane-1,2-deoxy-α-D-galctopyranose (101)[19]

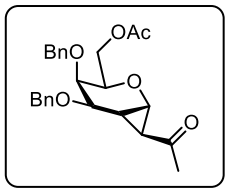

Synthesis according to the **procedure C** by using the corresponding tosyl precursor **100** (77.7 mg, 0.13 mmol) as starting material to afford **101** (41.0 mg, 0.10 mmol, 74%) as a pale-yellow solid. ^{1}H NMR (500 MHz, acetone-d_6) δ 7.44–7.27 (m, 10H), 4.86–4.81 (m, 2H), 4.74 (d, *J* = 12.0 Hz, 1H), 4.67 (d, *J* = 11.6 Hz, 1H), 4.46 (dd, *J* = 11.9, 7.9 Hz, 1H), 4.15–4.12 (m, 1H), 4.04 (t, *J* = 2.8 Hz, 1H), 3.85–3.82 (m, 2H), 3.70 (dd, *J* = 7.3, 2.0 Hz, 1H), 2.22 (dd, *J* = 5.9, 2.0 Hz, 1H), 2.20 (s, 3H), 2.04–2.02 (m, 1H), 1.98 (s, 3H); ^{13}C NMR (126 MHz, acetone-d_6) δ 204.5, 170.9, 139.7, 139.6, 129.1 (2×C), 129.1 (2×C), 128.6 (2×C), 128.4 (2×C), 128.4, 128.3, 74.9, 73.9 (2×C), 73.5, 72.4, 63.8, 59.0, 34.5, 30.7, 27.7, 20.8; ESI-HRMS: m/z calcd for $C_{25}H_{28}O_6Na$ $[M + Na]^+$: 447.17781; found: 447.17663; $[\alpha]_D^{20}$ = +10.9 (c = 0.19, CH_2Cl_2); m.p. = 85.0 ºC.

1-*C*-(3′,4′-Di-*O*-benzyl-6′-*O*- benzoyl -2′-*O*-tosyl-α-D-talopyranosyl)-acetone (103)[33]

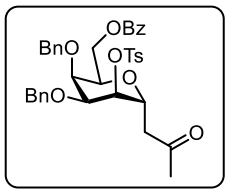

To a solution of **100** (1.30 g, 2.18 mmol, 1 equiv.) in anhydrous MeOH (50 mL), diethylamine (3.9 mL) was added. The mixture was stirred at room temperature for 18 h. After the reaction was complete, the mixture was concentrated and purified by flash column chromatography on silica gel (EtOAc:*c*-hex = 1:2, R_f = 0.3 (EtOAc:*c*-hex = 1:1)) to afford the hydroxyl substrate. The hydroxyl substrate (150.0 mg, 0.27 mmol, 1 equiv.) was dissolved in anhydrous CH_2Cl_2 (6 mL) and cooled to 0 ºC. Triethylamine (0.085 mL, 0.61 mmol, 2.25 equiv.) was added to that mixture, followed by the dropwise addition of benzoyl chloride (0.075 mL, 0.65 mmol, 2.4 equiv.). It was stirred at 0 ºC for another 1 h and raised to rt for 44 h. After adding H_2O (10 mL), the mixture was diluted with CH_2Cl_2 (20 mL) and washed with brine (20 mL). The mixture was evaporated under reduced pressure, and the residue was purified by silica flash column chromatography on silica gel

(EtOAc:*c*-hex = 1:4, R_f = 0.67 (EtOAc:*c*-hex = 1:1)) to afford **103** (156.2 mg, 0.24 mmol, 88%) as a pale-yellow syrup. ^{1}H NMR (700 MHz, $CDCl_3$) δ 8.00 (d, *J* = 7.2 Hz, 2H), 7.76 (d, *J* = 8.3 Hz, 2H), 7.53 (t, *J* = 7.4 Hz, 1H), 7.41 (t, *J* = 7.8 Hz, 2H), 7.37–7.27 (m, 12H), 4.99 (dd, *J* = 13.1, 10.0 Hz, 1H), 4.80 (d, *J* = 11.4 Hz, 1H), 4.74 (dd, *J* = 13.2, 2.1 Hz, 1H), 4.66 (d, *J* = 11.4 Hz, 1H), 4.62 (d, *J* = 11.8 Hz, 1H), 4.57 (d, *J* = 11.9 Hz, 1H), 4.49 (td, *J* = 9.5, 3.1 Hz, 1H), 4.35–4.32 (m, 2H), 4.27 (t, *J* = 2.6 Hz, 1H), 3.71 (dd, *J* = 6.5, 2.5 Hz, 1H), 2.53 (dd, *J* = 15.6, 3.0 Hz, 1H), 2.46 (s, 3H), 2.26 (dd, *J* = 15.6, 9.3 Hz, 1H), 2.06 (s, 3H); ^{13}C NMR (176 MHz, $CDCl_3$) δ 205.5, 166.5, 145.4, 138.0, 137.4, 133.3, 132.9, 130.2, 130.0 (2×C), 129.6 (2×C), 128.5 (2×C), 128.3 (3×C), 128.0, 127.9 (2×C), 127.8 (2×C), 127.7, 127.6 (2×C), 77.9, 75.7, 75.5, 75.3, 73.5, 71.4, 63.4, 60.8, 45.1, 30.0, 21.7; ESI-HRMS: m/z calcd for $C_{37}H_{39}O_9S$ $[M + H]^+$: 659.23093; found: 659.23010; $[\alpha]_D^{20}$ = +36.0 (c = 0.24, CH_2Cl_2).

1-*C*-(3′,4′-Di-*O*-benzyl-6′-*O*-tert-butoxycarbonyl-2′-*O*-tosyl-α-D-talopyranosyl)-acetone (104)[33]

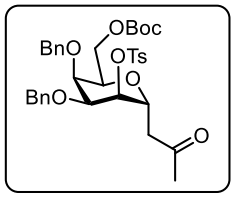

To a solution of **100** (1.30 g, 2.18 mmol, 1 equiv.) in anhydrous MeOH (50 mL), diethylamine (3.9 mL) was added. The mixture was stirred at room temperature for 18 h. After the reaction was complete, the mixture was concentrated and purified by flash column chromatography on silica gel (EtOAc:*c*-hex = 1:2, R_f = 0.3 (EtOAc:*c*-hex = 1:1)) to afford the hydroxyl substrate. A solution of hydroxyl substrate (300 mg, 0.54 mmol, 1 equiv.) in THF (12 mL) was treated with triethylamine (0.17 mL, 1.22 mmol, 2.25 equiv.), DMAP (99.1 mg, 0.81 mmol, 1.5 equiv.) and di-*tert*-butyl dicarbonate (354.1 mg, 1.62 mmol, 3 equiv.) After stirring for 17 h, the mixture was diluted with ethyl acetate (20 mL) and washed with brine (20 mL). The residue was purified by flash column chromatography on silica gel (EtOAc:*c*-hex = 1:4, R_f = 0.72 (EtOAc:*c*-hex = 1:1)) to afford **104** (230.6 mg, 0.35 mmol, 65%) as a pale-yellow syrup. ^{1}H NMR (700 MHz, $CDCl_3$) δ 7.74 (d, *J* = 8.3 Hz, 2H), 7.36–7.26 (m, 12H), 4.84 (dd, *J* = 13.1, 9.7 Hz, 1H), 4.75 (d, *J* = 11.6 Hz, 1H), 4.65 (d, *J* = 11.6 Hz, 1H), 4.53–4.49 (m, 2H), 4.39 (td, *J* = 9.1, 3.4 Hz, 1H), 4.36–4.31 (m, 2H), 4.24–4.21 (m, 2H), 3.64 (dd, *J* = 6.6, 2.5 Hz, 1H), 2.51 (dd, *J* = 15.8, 3.3 Hz, 1H), 2.45 (s,

3H), 2.23 (dd, *J* = 15.8, 8.5 Hz, 1H), 2.07 (s, 3H), 1.46 (s, 9H); ^{13}C NMR (176 MHz, $CDCl_3$) δ 205.5, 153.5, 145.4, 138.1, 137.3, 133.2, 130.0 (2×C), 128.5 (2×C), 128.3 (2×C), 128.0, 127.9 (2×C), 127.9 (2×C), 127.6, 127.5 (2×C), 82.0, 77.9, 75.5, 75.3, 75.1, 73.5, 71.3, 63.3, 62.8, 45.0, 30.0, 27.8 (3×C), 21.7; ESI-HRMS: m/z calcd for $C_{35}H_{42}O_{10}NaS$ $[M + Na]^+$: 677.23909; found: 677.23807; $[\alpha]_D^{20}$ = +32.3 (c = 0.31, CH_2Cl_2).

((2*R*,3*S*,4*S*,5*S*,6*S*)-3,4-bis(benzyloxy)-6-(2-oxopropyl)-5-(tosyloxy)tetrahydro-2*H*-pyran-2-yl)methyl stearate (106)[33]

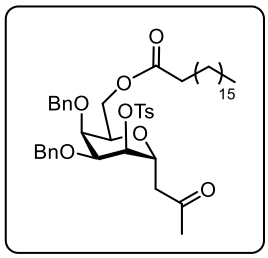

To a solution of **100** (1.30 g, 2.18 mmol, 1 equiv.) in anhydrous MeOH (50 mL), diethylamine (3.9 mL) was added. The mixture was stirred at room temperature for 18 h. After the reaction was complete, the mixture was concentrated and purified by flash column chromatography on silica gel (EtOAc:*c*-hex = 1:2, R_f = 0.3 (EtOAc:*c*-Hex = 1:1)) to afford the hydroxyl substrate. In an oven dried 25 mL round-bottom flask, hydroxyl substrate (100 mg, 0.18 mmol, 1 equiv.) and the stearic acid (115.4 mg, 0.41 mmol, 2.25 equiv.) were dissolved in 5 mL anhydrous CH_2Cl_2. To this, EDC (86.9 mg, 0.45 mmol, 2.5 equiv.), DMAP (6.61 mg, 0.05 mmol, 0.3 equiv.) and DIPEA (0.10 mL, 0.59 mmol, 3.3 equiv.) were added. The resulting solution was stirred at 25 ºC for 19 h. After adding H_2O (10 mL), the mixture was diluted with CH_2Cl_2 (20 mL) and washed with brine (20 mL). After removal of the solvents *in vacuo*, the residue was purified by flash column chromatography on silica gel (pentane:Et_2O = 2:1, R_f = 0.39 (EtOAc:*c*-hex = 1:9)) to afford **106** (138.6 mg, 0.175 mmol, 89%) as a colorless syrup. ^{1}H NMR (500 MHz, $CDCl_3$) δ 7.75 (d, *J* = 8.3 Hz, 2H), 7.36–7.27 (m, 12H), 4.80–4.74 (m, 2H), 4.62 (d, *J* = 11.5 Hz, 1H), 4.53 (q, *J* = 11.9 Hz, 2H), 4.44 (dd, *J* = 13.3, 2.1 Hz, 1H), 4.39 (td, *J* = 9.4, 3.1 Hz, 1H), 4.29 (dd, *J* = 9.7, 2.7 Hz, 1H), 4.22 (t, *J* = 2.6 Hz, 1H), 4.18 (ddd, *J* = 10.0, 6.4, 2.1 Hz, 1H), 3.64 (dd, *J* = 6.5, 2.5 Hz, 1H), 2.52 (dd, *J* = 15.7, 3.0 Hz, 1H), 2.46 (s, 3H), 2.28–2.20 (m, 3H), 2.08 (s, 3H), 1.56–1.54 (m, 2H), 1.31–1.24 (m, 28H), 0.88 (t, *J* = 6.9 Hz, 3H); ^{13}C NMR (126 MHz, $CDCl_3$) δ 205.4, 173.8, 145.4, 138.0, 137.3, 133.2, 130.0 (2×C), 128.5 (2×C), 128.3 (2×C), 127.9, 127.8 (2×C), 127.8 (2×C), 127.6,

127.5 (2×C), 77.8, 75.5, 75.4, 75.2, 73.4, 71.3, 63.1, 60.1, 45.1, 34.2, 31.9, 29.9, 29.7 (3×C), 29.7 (2×C), 29.6 (2×C), 29.6, 29.5, 29.4, 29.3, 29.1, 24.9, 22.7, 21.7, 14.1; ESI-HRMS: m/z calcd for $C_{48}H_{69}O_9S$ $[M + H]^+$: 821.46568; found: 821.46622; $[\alpha]_D^{20}$ = +29.0 (c = 0.82, CH_2Cl_2).

((2*R*,3*S*,4*S*,5*R*,6*R*)-3,4-bis(benzyloxy)-6-(2-oxopropyl)-5-(tosyloxy)tetrahydro-2*H*-pyran-2-yl)methyl 2-(1-(4-chlorobenzoyl)-5-methoxy-2-methyl-1*H*-indol-3-yl)acetate (107)[33]

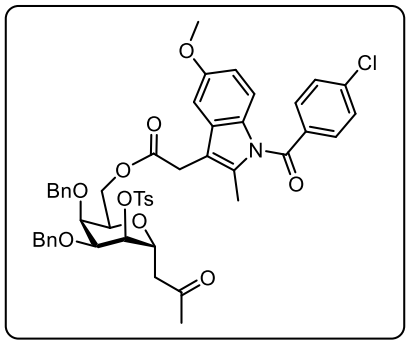

To a solution of **100** (1.30 g, 2.18 mmol, 1 equiv.) in anhydrous MeOH (50 mL), diethylamine (3.9 mL) was added. The mixture was stirred at room temperature for 18 h. After the reaction was complete, the mixture was concentrated and purified by flash column chromatography on silica gel (EtOAc:*c*-hex = 1:2, R_f = 0.3 (EtOAc:*c*-hex = 1:1)) to afford the hydroxyl substrate. In an oven dried 25 mL round-bottom flask, hydroxyl substrate (150 mg, 0.27 mmol, 1 equiv.) and Indomethacin (217.7 mg, 0.61 mmol, 2.25 equiv.) were dissolved in 5 mL anhydrous CH_2Cl_2. To this, EDC (130.3 mg, 0.68 mmole, 2.5 equiv.), DMAP (9.9mg, 0.08 mmol, 0.3 equiv.) and DIPEA (0.16 mL, 0.89 mmol, 3.3 equiv.) were added. The resulting solution was stirred at 25 ºC for 17 h. After adding H_2O (10 mL), the mixture was diluted with CH_2Cl_2 (20 mL) and washed with brine (20 mL). The solvents were concentrated *in vacuo*, the residue was purified by silica gel flash column chromatography (pentane:Et_2O = 1:1, R_f = 0.32 (EtOAc:*c*-hex = 1:2)) to afford the desired product **107** (220.0 mg, 0.25 mmol, 91%) as yellow solid. ^{1}H NMR (500 MHz, $CDCl_3$) δ 7.72 (d, *J* = 8.3 Hz, 2H), 7.63 (d, *J* = 8.5 Hz, 2H), 7.43 (d, *J* = 8.5 Hz, 2H), 7.32–7.22 (m, 12H), 6.93 (d, *J* = 2.5 Hz, 1H), 6.85 (d, *J* = 9.0 Hz, 1H), 6.63 (dd, *J* = 9.0, 2.5 Hz, 1H), 4.87 (dd, *J* = 13.1, 10.0 Hz, 1H), 4.71 (d, *J* = 11.5 Hz, 1H), 4.59 (d, *J* = 11.5 Hz, 1H), 4.48 (s, 2H), 4.39 (dd, *J* = 13.2, 2.1 Hz, 1H), 4.35 (dd, *J* = 8.9, 3.0 Hz, 1H), 4.30 (dd, *J* = 9.8, 2.6 Hz, 1H), 4.19 (t, *J* = 2.6 Hz, 1H), 4.14 (ddd, *J* = 10.2, 6.5, 2.1 Hz, 1H), 3.78 (s, 3H), 3.64–3.60 (m, 3H), 2.48–2.42 (m, 1H), 2.43 (s, 3H), 2.31 (s, 3H), 2.21 (dd, *J* = 16.1, 8.7 Hz, 1H), 1.97 (s, 3H); ^{13}C NMR (126 MHz, $CDCl_3$) δ 205.1, 170.8, 168.3, 156.0, 145.4, 139.1, 138.0, 137.2, 135.9, 133.9, 133.2, 131.2 (2×C), 130.7, 130.7,

130.0 (2×C), 129.1 (2×C), 128.5 (2×C), 128.3 (2×C), 128.0, 127.8 (2×C), 127.8 (3×C), 127.6, 127.4 (2×C), 114.9, 112.6, 111.6, 101.2, 75.5, 75.4, 75.2, 73.3, 71.3, 63.0, 60.8, 55.7, 44.7, 30.1, 30.0, 21.7, 13.4; ESI-HRMS: m/z calcd for $C_{49}H_{49}O_{11}NClS$ $[M + H]^+$: 894.27094; found: 894.27034; $[\alpha]_D^{20}$ = +28.9 (c = 0.53, CH_2Cl_2); m.p. = 69.2 ºC.

1-*C*-Acetyl-3,4-di-*O*-benzyl-6-*O*-tert-butyldimethylsilyl-1,2-cyclopropane-1,2-deoxy-α-D-galctopyranose (108)[20]

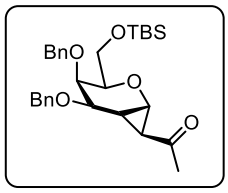

To a solution of **100** (4.00 g, 6.70 mmol, 1 equiv.) in anhydrous MeOH (200 mL) diethylamine (3.9 mL) was added. The mixture was stirred at room temperature for overnight. After the reaction was complete, the mixture was concentrated. The crude oil was dissolved in anhydrous CH_2Cl_2 (44 mL) and cooled to 0 ºC. TBSCl (3.03 g, 20.1 mmol, 3 equiv.) and triethylamine (1.87 mL, 13.4 mmol, 2 equiv.) were added and the solution was warmed to room temperature slowly. The reaction was stirred at this temperature for 64 h. Then H_2O (200 mL) was added and extracted with CH_2Cl_2 (3 x 100 mL), the organic phases were washed with brine (2 x 100 mL), dried over $MgSO_4$, and evaporated under reduced pressure. The residue was purified by flash column chromatography on silica gel (pentane:Et_2O = 2:1, R_f = 0.33 (pentane:Et_2O = 2:1)) to afford tosyl substrate **102** (2.20 g, 3.29 mmol, 49%) as a colorless syrup. The tosyl substrate **102** (1.0 g, 1.49 mmol, 1 equiv.) then underwent **procedure C** to afford **108** (477.8 mg, 0.96 mmol, 64%) as colorless syrup. ^{1}H NMR (500 MHz, CD_2Cl_2) δ 7.39–7.26 (m, 10H), 4.89 (d, *J* = 11.3 Hz, 1H), 4.77 (d, *J* = 11.8 Hz, 1H), 4.63 (d, *J* = 11.8 Hz, 1H), 4.60 (d, *J* = 11.3 Hz, 1H), 3.81 (dd, *J* = 6.9, 2.9 Hz, 1H), 3.77 (t, *J* = 2.6 Hz, 1H), 3.73 (dd, *J* = 6.4, 1.8 Hz, 2H), 3.69 (t, *J* = 2.6 Hz, 1H), 3.47 (td, *J* = 6.4, 2.3 Hz, 1H), 2.22 (s, 3H), 2.03–1.99 (m, 2H), 0.89 (s, 9H), 0.054 (s, 3H), 0.050 (s, 3H); ^{13}C NMR (126 MHz, CD_2Cl_2) δ 205.2, 139.4, 138.8, 128.9 (2×C), 128.8 (2×C), 128.4 (2×C), 128.1, 128.1, 128.0 (2×C), 76.7, 74.4, 72.4, 71.7, 62.4, 61.6, 34.5, 31.2, 26.5, 26.2 (3×C), 18.7, –5.10, –5.15; ESI-HRMS: m/z calcd for $C_{29}H_{40}O_5NaSi$ $[M + Na]^+$: 519.25372; found: 519.25247; $[\alpha]_D^{20}$ = +32.6 (c = 0.93, CH_2Cl_2).

1-*C*-Acetyl-3,4-di-*O*-benzyl-6-*O*-benzoyl-1,2-cyclopropane-1,2-deoxy-α-D-galctopyranose (109)

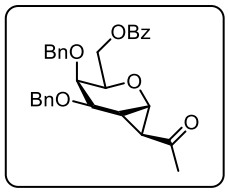

Synthesis according to the **procedure C** by using the corresponding tosyl precursor **103** (146.0 mg, 0.22 mmol) as starting material to afford **109** (48.3 mg, 0.10 mmol, 45%) as a pale-yellow solid. ^{1}H NMR (700 MHz, CD_2Cl_2) δ 8.00 (d, *J* = 7.3 Hz, 2H), 7.58 (t, *J* = 7.4 Hz, 1H), 7.45 (t, *J* = 7.8 Hz, 2H), 7.41–7.27 (m, 10H), 4.82 (t, *J* = 11.8 Hz, 2H), 4.70–4.65 (m, 3H), 4.41 (dd, *J* = 11.9, 4.2 Hz, 1H), 3.93 (dt, *J* = 7.8, 3.8 Hz, 1H), 3.89 (t, *J* = 2.8 Hz, 1H), 3.85 (dd, *J* = 7.2, 2.0 Hz, 1H), 3.75 (t, *J* = 3.2 Hz, 1H), 2.23 (s, 3H), 2.16–2.14 (m, 1H), 2.00 (dd, *J* = 5.9, 2.0 Hz, 1H); ^{13}C NMR (176 MHz, CD_2Cl_2) δ 204.9, 166.7, 138.8, 138.8, 133.5, 130.8, 130.1 (2×C), 128.9 (2×C), 128.9 (2×C), 128.9 (2×C), 128.5 (2×C), 128.3, 128.2, 128.2 (2×C), 74.8, 73.9, 73.6, 73.5, 72.4, 64.2, 60.3, 34.9, 31.2, 27.5; ESI-HRMS: m/z calcd for $C_{30}H_{31}O_6$ $[M + H]^+$: 487.21152; found: 487.21154; $[\alpha]_D^{20}$ = +31.5 (c = 0.74, CH_2Cl_2); m.p. = 82.6 ºC.

1-*C*-Acetyl-3,4-di-*O*-benzyl-6-*O*-tert-butoxycarbonyl-1,2-cyclopropane-1,2-deoxy-α-D-galctopyranose (110)

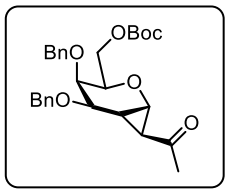

Synthesis according to the **procedure C** by using the corresponding tosyl precursor **104** (63.0 mg, 0.10 mmol) as starting material to afford **110** (27.6 mg, 0.06 mmol, 59%) as a colorless syrup. ^{1}H NMR (700 MHz, CD_2Cl_2) δ 7.39–7.29 (m, 10H), 4.78 (dd, *J* = 11.7, 4.1 Hz, 2H), 4.67 (d, *J* = 11.9 Hz, 1H), 4.60 (d, *J* = 11.5 Hz, 1H), 4.40 (dd, *J* = 11.9, 8.5 Hz, 1H), 4.15 (dd, *J* = 12.0, 3.5 Hz, 1H), 3.87 (t, *J* = 2.8 Hz, 1H), 3.80–3.78 (m, 2H), 3.65 (t, *J* = 3.3 Hz, 1H), 2.23 (s, 3H), 2.12–2.11 (m, 1H), 1.98 (dd, *J* = 6.0, 2.0 Hz, 1H), 1.46 (s, 9H); ^{13}C NMR (176 MHz, CD_2Cl_2) δ 204.8, 153.9, 138.8, 138.8, 128.9 (2×C), 128.9 (2×C), 128.4 (2×C), 128.3, 128.2, 128.1 (2×C), 82.5, 74.2, 73.7,

73.6, 73.4, 72.4, 66.2, 60.1, 34.8, 31.3, 28.0 (3×C), 27.6; ESI-HRMS: m/z calcd for $C_{28}H_{34}O_7Na$ $[M + Na]^+$: 505.21967; found: 505.21773; $[\alpha]_D^{20}$ = +26.2 (c = 0.24, CH_2Cl_2).

1-*C*-Acetyl-3,4-di-*O*-benzyl-6-*O*-methoxymethyl-1,2-cyclopropane-1,2-deoxy-α-D-galctopyranose (111)

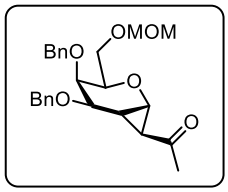

To a solution of **100** (1.30 g, 2.18 mmol, 1 equiv.) in anhydrous MeOH (50 mL), diethylamine (3.9 mL) was added. The mixture was stirred at room temperature for 18 h. After the reaction was complete, the mixture was concentrated and purified by flash column chromatography on silica gel (EtOAc:*c*-hex = 1:2, R_f = 0.3 (EtOAc:*c*-hex = 1:1)) to afford the hydroxyl substrate. To a solution of hydroxyl substrate (150 mg, 0.27 mmol, 1 equiv.) in anhydrous CH_2Cl_2 (6 mL) was added DIPEA (0.28 mL, 1.62 mmol, 6 equiv.), followed by the addition of MOMCl (0.041 mL, 0.54 mmol, 2 equiv.). After stirring for 19 h at 25 ºC, the solvents were evaporated under reduced pressure. The residue was purified by silica gel column chromatography (pentane: Et_2O = 1:1, R_f = 0.69 (EtOAc:*c*-hex = 1:1)) to afford the tosyl substrate **105** (114.5 mg, 0.19 mmol, 71%) as colorless syrup. The tosyl substrate **105** (114.5 mg, 0.19 mmol, 1 equiv.) then underwent **procedure C** to afford **111** (80.3 mg, 0.19 mmol, 98%) as a colorless syrup. ^{1}H NMR (700 MHz, CD_2Cl_2) δ 7.39–7.29 (m, 10H), 4.86 (d, *J* = 11.4 Hz, 1H), 4.78 (d, *J* = 12.0 Hz, 1H), 4.65 (d, *J* = 11.9 Hz, 1H), 4.60 (d, *J* = 11.5 Hz, 1H), 4.59–4.55 (m, 2H), 3.82 (dd, *J* = 7.4, 2.1 Hz, 1H), 3.77 (t, *J* = 2.8 Hz, 1H), 3.76–3.74 (m, 1H), 3.70 (t, *J* = 2.9 Hz, 1H), 3.67–3.65 (m, 1H), 3.64–3.62 (m, 1H), 3.32 (s, 3H), 2.23 (s, 3H), 2.06 (ddd, *J* = 7.7, 5.8, 2.5 Hz, 1H), 2.00 (dd, *J* = 5.8, 2.1 Hz, 1H); ^{13}C NMR (176 MHz, CD_2Cl_2) δ 205.1, 139.1, 138.8, 128.9 (2×C), 128.9 (2×C), 128.4 (2×C), 128.2 (2×C), 128.1 (2×C), 97.3, 75.8, 74.9, 74.0, 73.1, 71.9, 67.4, 61.1, 55.6, 34.6, 31.2, 26.9; ESI-HRMS: m/z calcd for $C_{25}H_{31}O_6$ $[M + H]^+$: 427.21152; found: 427.21019; $[\alpha]_D^{20}$ = +31.2 (c = 1.61, CH_2Cl_2).

((3*R*,4*R*,5*R*)-7-acetyl-4,5-bis(benzyloxy)-2-oxabicyclo[4.1.0]heptan-3-yl)methyl stearate (112)

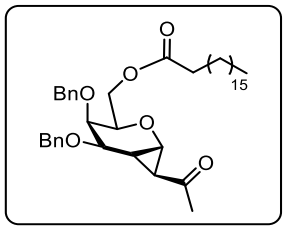

Synthesis according to the **procedure C** by using the corresponding tosyl precursor **106** (211.6 mg, 0.26 mmol) as starting material to afford **112** (113.4 mg, 0.17 mmol, 68%) as a pale-yellow syrup. ^{1}H NMR (700 MHz, CD_2Cl_2) δ 7.38–7.28 (m, 10H), 4.78 (dt, *J* = 12.1, 5.9 Hz, 2H), 4.80–4.77 (m, 1H), 4.61– 4.57 (m, 2H), 4.39 (dd, *J* = 12.0, 8.2 Hz, 1H), 4.16 (dd, *J* = 12.0, 4.0 Hz, 1H), 3.83 (t, *J* = 2.8 Hz, 1H), 3.77–3.73 (m, 2H), 3.66–3.62 (m, 2H), 2.22 (s, 3H), 2.10 (ddd, *J* = 7.5, 5.9, 2.5 Hz, 1H), 2.27 (td, *J* = 7.4, 1.1 Hz, 2H), 1.97 (dd, *J* = 5.9, 2.0 Hz, 1H), 1.58 (t, *J* = 7.4 Hz, 2H), 1.31–1.26 (m, 26H), 0.88 (t, *J* = 7.0 Hz, 3H); ^{13}C NMR (176 MHz, CD_2Cl_2) δ 204.9, 174.0, 138.9, 138.8, 128.9 (2×C), 128.9, 128.4, 128.4 (2×C), 128.3, 128.2, 128.2, 128.1, 97.3, 74.9, 73.9, 73.6, 73.5, 72.3, 63.5, 60.3, 55.6, 34.9, 34.7, 32.5, 31.2, 30.3 (2×C), 30.2, 30.2, 30.2, 30.1, 29.9, 29.9, 29.7, 27.5, 25.5, 23.3, 14.5; ESI-HRMS: m/z calcd for $C_{41}H_{61}O_6$ $[M + H]^+$: 649.44627; found: 649.44466; $[\alpha]_D^{20}$ = +24.3 (c = 0.52, CH_2Cl_2).

((1*S*,3*R*,4*R*,5*R*,6*S*,7*S*)-7-(1-(l1-oxidaneyl)vinyl)-4,5-bis(benzyloxy)-2-oxabicyclo[4.1.0]heptan-3-yl)methyl 2-(1-(4-chlorobenzoyl)-5-methoxy-2-methyl-1*H*-indol-3-yl)acetate (113)

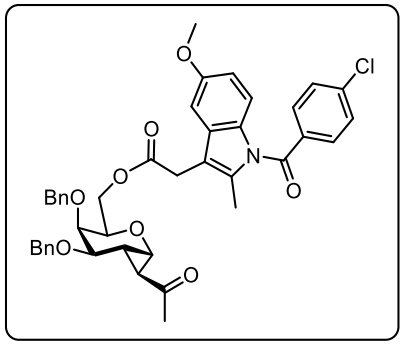

Synthesis according to the **procedure C** by using the corresponding tosyl precursor **107** (396.0 mg, 0.44 mmol) as starting material with stirring time reduced to 3 h to afford **113** (147.0 mg, 0.20 mmol, 46%) as a yellow solid. ^{1}H NMR (700 MHz, CD_2Cl_2) δ 7.61 (d, *J* = 8.5 Hz, 2H), 7.46 (d, *J* = 8.5 Hz, 2H), 7.37–7.27 (m, 10H), 6.97 (d, *J* = 2.6 Hz, 1H), 6.93 (d, *J* = 9.0 Hz, 1H), 6.66 (dd, *J*

= 9.0, 2.6 Hz, 1H), 4.75 (d, *J* = 11.8 Hz, 1H), 4.70 (d, *J* = 11.5 Hz, 1H), 4.63 (d, *J* = 11.9 Hz, 1H), 4.50 (dd, *J* = 12.0, 8.3 Hz, 1H), 4.46 (d, *J* = 11.4 Hz, 1H), 4.20 (dd, *J* = 12.0, 4.1 Hz, 1H), 3.82 (t, *J* = 2.8 Hz, 1H), 3.80 (s, 3H), 3.78–3.76 (m, 2H), 3.68 (s, 2H), 3.58 (t, *J* = 3.3 Hz, 1H), 2.32 (s, 3H), 2.22 (s, 3H), 2.09 (ddd, *J* = 7.3, 5.9, 2.5 Hz, 1H), 1.95 (dd, *J* = 5.9, 2.0 Hz, 1H); ^{13}C NMR (176 MHz, CD_2Cl_2) δ 204.8, 171.1, 168.8, 156.6, 139.6, 138.8, 138.8, 136.5, 134.6, 131.7 (2×C), 131.4, 131.2, 129.6 (2×C), 128.9 (2×C), 128.9 (2×C), 128.3 (2×C), 128.3, 128.2, 128.1 (2×C), 115.5, 113.2, 112.0, 101.9, 74.4, 73.7, 73.6, 73.5, 72.3, 64.1, 60.0, 56.2, 34.9, 31.2, 30.7, 27.6, 13.8; $[\alpha]_D^{20}$ = +22.1 (c = 0.36, CH_2Cl_2); ESI-HRMS: m/z calcd for $C_{42}H_{41}O_8N^{37}Cl$ $[M + H]^+$: 724.24857; found: 724.24825; m.p. = 63.4 ºC.

9.7 Synthesis of dioxinone dienoaltes

General procedure for synthesis of the dioxinone dienolates (procedure D)[68]

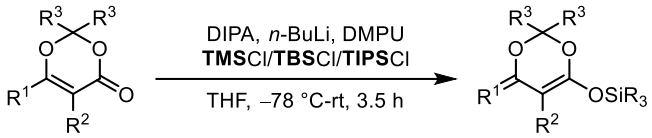

A flame dried flask was charged with anhydrous THF (35 mL, 0.5 M regarding the dioxinone) and freshly distilled diisopropylamine (0.02 mmol, 1.1 equiv.) at 0 ºC. The solution was cooled in an ice bath followed by slow addition of *n*-butyl lithium (2.5 M in hexane, 20.70 mmol, 1.1 equiv.). The reaction was stirred for 30 mins. DMPU (22.6 mmol, 1.2 equiv.) was added at –78 ºC. The mixture was stirred 30 min where upon it turned turbid. Afterwards, the corresponding dioxinone (18.8 mmol) was added dropwise and the resulting mixture was stirred 30 mins at –78 ºC. The turbidity vanished. The silane chloride (22.6 mmol, 1.2 equiv.) was dissolved in 2.5 mL THF and added slowly. After complete addition, the cooling was removed and the mixture was stirred 2 h while reaching room temperature. Following, pentane (200 mL) was added, causing precipitation. The liquid was transferred to a separation funnel and washed quickly five times with 100 mL ice cold water. The organic layer was dried over $MgSO_4$. Removal of the solvent yielded in quantitative amounts of the crude product. The mixture was purified by Kugelrohr distillation.

((2,2-Dimethyl-4-methylene-4*H*-1,3-dioxin-6-yl)oxy)triisopropylsilane (116)

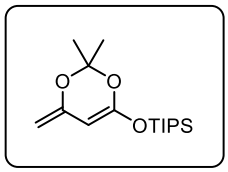

Synthesis according to **procedure D** by using the 2,2,6-trimethyl-4*H*-1,3-dioxin-4-one (2.5 mL, 18.82 mmol, 1 equiv.) as starting material to afford **116** (3.48 g, 11.67 mmol, 62%) as a pale-yellow oil. ^{1}H NMR (400 MHz, $CDCl_3$) δ 4.69 (s, 1H), 4.05 (s, 1H), 3.86 (s, 1H), 1.54 (s, 6H), 1.22–1.17 (m, 3H), 1.09–1.05 (m, 18H); ^{13}C NMR (176 MHz, CD_2Cl_2) δ 154.1, 152.8, 103.1, 84.8, 76.5, 24.9 (2×C), 18.1 (6×C), 13.1 (3×C); ESI-HRMS: m/z calcd for $C_{16}H_{31}O_3Si$ $[M + H]^+$: 299.20370; found: 299.20318; b.p. = 113–117 ºC (1.1 mbar).

Synthesis of 4-methyl-1,5-dioxaspiro[5.5]undec-3-en-2-one (s2)[69]

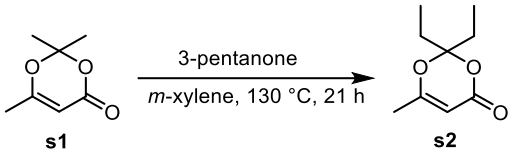

A solution of 2,2,6-trimethyl-4*H*-1,3-dioxin-4-one (10 mL, 75.3 mmol, 1 mmol) and 3-pentanone (17.5 mL, 165.6 mmol, 2.2 equiv.) in 7.5 mL of *m*-xylene was heated at 130 ºC for 21 h and the volatile parts were allowed to distill out by putting a needle in the septum. The crude mixture was evaporated and purified by silica gel column chromatography (pentane:Et_2O = 4:1, (R_f = 0.47 (pentane:Et_2O = 2:1)) to afford **s2** (6.52 g, 38.3 mmol, 51 %). ^{1}H NMR (700 MHz, $CDCl_3$) δ 5.16 (q, *J* = 0.9 Hz, 1H), 1.98–1.89 (m, 4H), 0.95 (t, *J* = 7.5 Hz, 1H); ^{13}C NMR (176 MHz, $CDCl_3$) δ 168.6, 161.3, 110.5, 93.6, 28.1 (2×C), 19.9 (2×C), 7.43; ESI-HRMS: m/z calcd for $C_9H_{14}O_3Na$ $[M + Na]^+$: 193.08352; found: 193.08276.

***Tert*-butyl((2,2-diethyl-4-methylene-4*H*-1,3-dioxin-6-yl)oxy)dimethylsilane (117)**

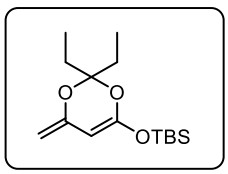

Synthesis according to **procedure D** by using the dioxinone precursor **s2** (1.0 g, 5.88 mmol, 1 equiv.) as starting material to afford **117** (575.7 mg, 2.02 mmol, 34%) as a pale-yellow oil. ^{1}H

NMR (500 MHz, $CDCl_3$) δ 4.63 (s, 3H), 4.04 (d, *J* = 0.9 Hz, 1H), 3.85 (d, *J* = 0.9 Hz, 1H), 1.94–1.75 (m, 4H), 0.97–0.93 (m, 15H), 0.20 (s, 6H); ^{13}C NMR (126 MHz, $CDCl_3$) δ 153.5, 151.9, 106.5, 84.5, 76.4, 27.2 (2×C), 25.5 (3×C), 18.0, 7.36 (2×C), –4.27 (2×C); ESI-HRMS: m/z calcd for $C_{15}H_{29}O_3Si$ $[M + H]^+$: 285.18805; found: 285.18741; b.p. = 103–107 ºC (0.54 mbar).

Synthesis of 4-methyl-1,5-dioxaspiro[5.5]undec-3-en-2-one (s3)[69]

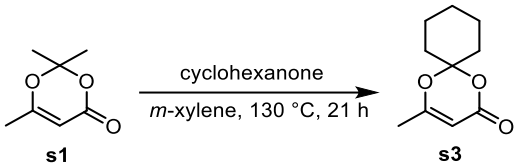

s1 **s3**

A solution of 2,2,6-trimethyl-4*H*-1,3-dioxin-4-one (10 mL, 75.3 mmol, 1 equiv.) and cyclohexanone (7.8 mL, 75.3 mmol, 1 equiv.) in 7.5 mL of *m*-xylene was heated at 130 ºC for 21 h and the volatile parts were allowed to distill out by putting a needle in the septum. The crude mixture was evaporated and purification by silica gel column chromatography (pentane:Et_2O = 4:1, (R_f = 0.43 (pentane:Et_2O = 2:1)) to afford **s3** (5.90 g, 32.4 mmol, 43 %). The analytical data was in accordance to the literature.[69] ^{1}H NMR (400 MHz, $CDCl_3$) δ 5.20 (s, 1H), 2.01–1.93 (m, 6H), 1.73–1.67 (m, 2H), 1.63–1.56 (m, 3H), 1.49–1.44 (m, 2H); ^{13}C NMR (126 MHz, CD_2Cl_2) δ 169.0, 161.2, 107.3, 94.5, 34.2 (2×C), 25.2, 22.8 (2×C), 20.3; ESI-HRMS: m/z calcd for $C_{10}H_{14}O_3Na$ $[M + Na]^+$: 205.08352; found: 205.08271.

***Tert*-butyldimethyl((4-methylene-1,5-dioxaspiro[5.5]undec-2-en-2-yl)oxy)silane (118)**

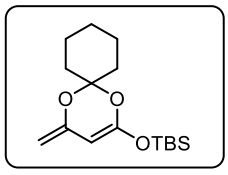

Synthesis according to **procedure D** by using the dioxinone precursor **s3** (1.0 g, 5.49 mmol, 1 equiv.) as starting material to afford **118** (686.7 mg, 2.32 mmol, 42%) as a pale-yellow oil. ^{1}H NMR (500 MHz, CD_2Cl_2) δ 4.62 (s, 1H), 4.02 (d, *J* = 0.7 Hz, 1H), 3.85 (d, *J* = 0.7 Hz, 1H), 1.89–1.85 (m, 2H), 1.78–1.73 (m, 2H), 1.63–1.57 (m, 4H), 1.51–1.46 (m, 1H), 1.45–1.39 (m, 1H), 0.94 (s, 9H), 0.22 (s, 6H); ^{13}C NMR (176 MHz, CD_2Cl_2) δ 154.0, 152.2, 103.7, 85.0, 77.1, 33.8 (2×C), 25.8 (3×C), 25.7, 22.9 (2×C), 18.4, –4.02 (2×C); ESI-HRMS: m/z calcd for $C_{16}H_{29}O_3Si$ $[M + H]^+$: 297.18805; found: 297.18830; b.p. 135–139 ºC (0.47 mbar).

Synthesis of 6-isopropyl-2,2-dimethyl-4*H*-1,3-dioxin-4-one (s6)[70]

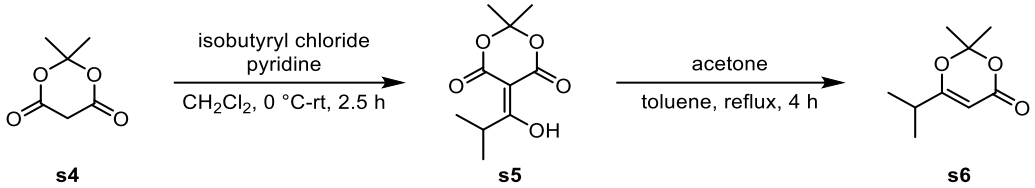

s4 **s5** **s6**

To a stirred solution of Meldrum's acid (10.0 g, 69.4 mmol, 1 equiv.) in CH_2Cl_2 (50 mL) at 0 ºC was added pyridine (11.2 mL, 0.14 mol, 2 equiv.) and stirred for 10 mins followed by dropwise addition of isobutyryl chloride (8.72 mL, 83.3 mmol, 1.2 equiv.) over 30 mins. The resulting mixture was stirred for 1 h at 0 ºC and warmed to rt for 1 h. The reaction mixture was poured into an ice cold solution of 2 M aqueous hydrochloric acid (50 mL), diluted with CH_2Cl_2 (80 mL) and the phases were separated. The organic layers were washed with 2 M aqueous hydrochloric acid (50 mL), water (50 mL x 2), brine (50 mL) and dried over $MgSO_4$. After filtering and evaporation of the solvent under reduced pressure, purification by silica gel column chromatography (pentane: Et_2O = 1:1 (R_f = 0.12 (pentane:Et_2O = 1:1)) to afford desired product **s5** (7.63 g, 35.6 mmol, 51%) as colorless oil. The analytical data was in accordance to the literature.[70] ^{1}H NMR (500 MHz, $CDCl_3$) δ 15.50 (s, 1H), 4.04 (hept, *J* = 6.8 Hz, 1H), 1.69 (s, 6H), 1.20 (s, 3H), 1.18 (s, 3H); ^{13}C NMR (126 MHz, $CDCl_3$) δ 202.3, 170.8, 159.9, 104.6, 90.0, 32.9, 26.6 (2×C), 18.9 (2×C).

To a stirring solution of **s5** (6.53 g, 30.5 mmol, 1 equiv.) in toluene (10 mL), anhydrous acetone (1.12 mL, 15.3 mmol, 0.5 equiv.) was added. The resulting mixture was heated at reflux for 4 h before being allowed to cool to rt and concentrated *in vacuo*. Silica gel chromatographic purification (EtOAc:*c*-hex = 1:9, R_f = 0.14 (pentane:Et_2O = 9:1)) was performed to provide **s6** (2.02 g, 11.9 mmol, 39%) as a colorless oil. The analytical data was in accordance to the literature.[70] ^{1}H NMR (400 MHz, $CDCl_3$) δ 5.23 (s, 1H), 2.43 (sept, *J* = 7 Hz, 1H), 1.68 (s, 6H), 1.14 (s, 3H), 1.13 (s, 3H); ^{13}C NMR (126 MHz, CD_2Cl_2) δ 176.9, 162.0, 106.6, 91.6, 33.0, 25.2 (2×C), 19.3 (2×C).

***Tert*-butyl((2,2-dimethyl-4-(propan-2-ylidene)-4*H*-1,3-dioxin-6-yl)oxy)dimethylsilane (119)**

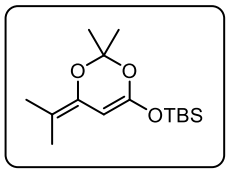

Synthesis according to **procedure D** by using the dioxinone precursor **s6** (1.0 g, 5.88 mmol, 1 equiv.) as starting material to afford **119** (636.1 mg, 2.24 mmol, 38%) as a pale-yellow oil. ^{1}H NMR (500 MHz, $CDCl_3$) δ 4.77 (s, 1H), 1.64 (s, 3H), 1.59 (s, 3H), 1.48 (s, 6H), 0.93 (s, 9H), 0.20 (s, 6H); ^{13}C NMR (126 MHz, $CDCl_3$) δ 152.4, 139.0, 104.3, 102.3, 74.0, 25.8 (3×C), 24.9, 19.3, 18.4, 17.6, 16.7 , –4.09 (2×C); ESI-HRMS: m/z calcd for $C_{15}H_{29}O_3Si$ $[M + H]^+$: 285.18805; found: 285.18806; b.p. = 123–127 ºC (0.47mbar).

Synthesis of 2,2,5,6-tetramethyl-4*H*-1,3-dioxin-4-one (s9)[49]

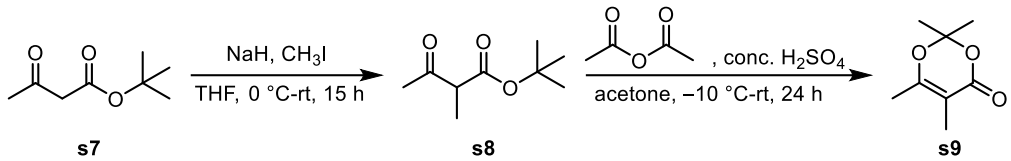

To a stirred solution of NaH (60% in oil, 2.65 g, 66.3 mmol, 1.1 equiv.) in 250 mL anhydrous THF at 0 ºC, *tert*-butyl-acetoacetate **s7** (10.0 mL, 60.31 mmol, 1 equiv.) was added and the mixture was stirred for 1 h. MeI (7.51 mL, 120.6 mmol, 2 equiv.) was added slowly and the solution was stirred at rt for another 14 h. The reaction was quenched with sat. NH_4Cl (250 mL) and extracted three times with Et_2O (250 mL). The organic layers were dried over $MgSO_4$ and the solvent was evaporated. Purification by silica gel column chromatography (pentane:Et_2O = 15:1 to 9:1 (R_f = 0.39 (pentane:Et_2O = 9:1)) was perform to afford the product **s8** (8.84 g, 51.3 mmol, 85%) as a colorless liquid. The analytical data was in accordance to the literature.[49] ^{1}H NMR (400 MHz, $CDCl_3$) δ 3.40 (q, *J* = 7.1 Hz, 1H), 2.23 (s, 3H), 1.46 (s, 9H), 1.29 (d, *J* = 7.1 Hz, 3H); ^{13}C NMR (126 MHz, CD_2Cl_2) δ 204.4, 170.2, 82.0, 55.1, 28.8, 28.2 (3×C), 13.0.

To a stirred solution of **s8** (5.0 g, 29.0 mmol, 1 equiv.) in 17 mL anhydrous acetone at –10 ºC, acetic anhydride (11.0 mL, 116.1 mmol, 4 equiv.) and catalytic amount of 0.5 mL conc. H_2SO_4 was added. The mixture was allowed to warm to rt for 24 h. Ice water (32 mL) was added to the

resulting mixture and stirred for 1 h. The aqueous layer was extracted five times with 20 mL CH_2Cl_2. The combined organic layers were washed with brine and dried over $MgSO_4$ and the solvent was evaporated. Purification by silica gel column chromatography (pentane:Et_2O = 4:1, R_f = 0.34 (pentane:Et_2O = 2:1)) afforded product **s9** (3.36 g, 21.5 mmol, 74%) as colorless oil. The analytical data was in accordance to the literature.[49] ^{1}H NMR (700 MHz, $CDCl_3$) δ 1.97 (s, 3H), 1.82 (s, 3H), 1.64 (s, 6H); ^{13}C NMR (126 MHz, CD_2Cl_2) δ 163.3, 162.8, 105.1, 100.9, 25.4 (2×C), 17.8, 10.6.

***Tert*-butyldimethyl((2,2,5-trimethyl-4-methylene-4*H*-1,3-dioxin-6-yl)oxy)silane (120)**

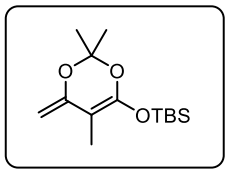

Synthesis according to **procedure D** by using the dioxinone precursor **s9** (3.0 g, 19.21 mmol, 1 equiv.) as starting material to afford **120** (2.55 g, 9.44 mmol, 28%) as a pale-yellow oil. ^{1}H NMR (400 MHz, $CDCl_3$) δ 4.05 (d, *J* = 1.0 Hz, 1H), 3.90 (d, *J* = 1.0 Hz, 1H), 1.66 (s, 3H), 1.49 (s, 6H), 0.96 (s, 9H), 0.20 (s, 6H); ^{13}C NMR (176 MHz, CD_2Cl_2) δ 154.9, 150.2, 102.0, 84.1, 82.2, 25.9 (3×C), 25.0 (2×C), 18.5, 9.67, –3.70 (2×C); ESI-HRMS: m/z calcd for $C_{14}H_{27}O_3Si$ $[M + H]^+$: 271.17240; found: 271.17255; b.p. 85–89 ºC (0.73 mbar).

Synthesis of 5-benzyl-2,2,6-trimethyl-4*H*-1,3-dioxin-4-one (s11)[71]

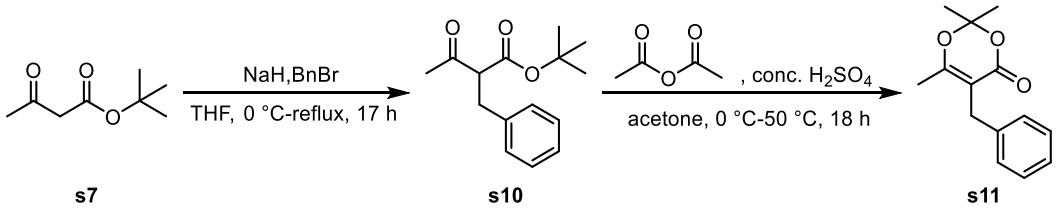

To *tert*-butylacetoacetate **s7** (10.0 g, 63.2 mmol, 1 equiv.), 208 mL anhydrous THF was added under an argon atmosphere in a 500 mL round bottom flask equipped with a stirring bar. The solution was cooled to 0 °C and NaH (60% in oil, 3.29 g, 82.2 mmol, 1.3 equiv.) was added slowly. Upon complete addition of the NaH, the slurry was warmed to room temperature and stirred until the solution was clear. The mixture was cooled back to 0 °C and BnBr (8.27 mL, 69.5 mmol, 1.1 equiv.) was added dropwise. The flask was subsequently equipped with a condenser and refluxed for 17 h. After completion of the reaction, the reaction mixture was quenched with sat. NH_4Cl

(100 mL) and H_2O (10 mL). The product was extracted with CH_2Cl_2 (3 × 150 mL) and dried with $MgSO_4$. The volatile parts were evaporated and the residue was purified by silica gel column chromatography (EtOAc:*c*-hex = 1:19, R_f = 0.30 (EtOAc:*c*-hex = 1:9)) to give product **s10** (7.64 g, 30.8 mmol, 49%) as clear colorless oil. The analytical data was in accordance to the literature.[71] ^{1}H NMR (500 MHz, $CDCl_3$) δ 7.34–7.24 (m, 5H), 3.76 (t, *J* = 7.75 Hz, 1H), 3.22–3.15 (m, 2H), 2.26 (s, 3H), 1.46 (s, 9H); ^{13}C NMR (126 MHz, $CDCl_3$) δ 202.8, 168.3, 138.3, 128.8 (2×C), 128.4 (2×C), 126.5, 82.0, 62.3, 33.8, 29.4, 27.8 (3×C).

Tert-butyl 2-benzyl-3-oxobutanoate **s10** (2.00 g, 8.05 mmol, 1 equiv.), acetic anhydride (5.92 mL, 80.5 mmol, 10.0 equiv.) and acetone (1.90 mL, 20.1 mmol, 2.5 equiv.) were added to a 25 mL round bottom flask equipped with a stirring bar. The solution was cooled to 0 °C, 20 drops of concentrated H_2SO_4 was added and the solution was allowed to warm to room temperature over 15 hours. The light red solution was subsequently heated at 50 °C for 3 hours, wherein a dark red colour persisted. The reaction was poured into 100 mL sat. $NaHCO_3$ and extracted with Et_2O (3 × 30 mL). The organic layers were combined, washed with 50 mL brine, dried over $MgSO_4$, concentrated and purified by silica gel flash column chromatography (EtOAc:*c*-hex = 1:19, R_f = 0.15 (EtOAc:*c*-hex = 1:9)) to afford **s11** (1.31 g, 5.64 mmol, 70%) as a clear oil. The analytical data was in accordance to the literature.[71] ^{1}H NMR (500 MHz, $CDCl_3$) δ 7.29–7.17 (m, 5H), 3.64 (s, 2H), 2.01 (s, 3H), 1.65 (s, 6H); ^{13}C NMR (126 MHz, $CDCl_3$) δ 164.5, 162.3, 139.8, 128.5 (2×C), 128.0 (2×C), 126.2, 105.0, 104.8, 30.7, 25.2 (2×C), 17.8.

((5-Benzyl-2,2-dimethyl-4-methylene-4*H*-1,3-dioxin-6-yl)oxy)(tert-butyl)dimethylsilane (121)

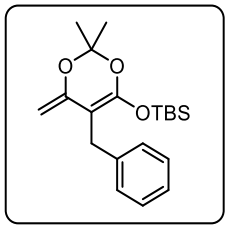

Synthesis according to **procedure D** by using the dioxinone precursor **s11** (1.0 g, 4.31 mmol, 1 equiv.) as starting material to afford **121** (836.0 mg, 2.41 mmol, 56%) as a pale-yellow oil. ^{1}H NMR (500 MHz, $CDCl_3$) δ 7.25–7.13 (m, 5H), 4.09 (d, *J* = 1.3 Hz, 1H), 3.92 (d, *J* = 1.3 Hz, 1H), 3.51 (s, 2H), 1.54 (s, 6H), 0.90 (s, 9H), 0.20 (s, 6H); ^{13}C NMR (126 MHz, $CDCl_3$) δ 153.0, 151.0, 141.3, 128.1 (2×C), 127.9 (2×C), 125.6, 101.7, 85.3, 85.1, 30.2, 25.5 (3×C), 24.7 (2×C), 17.9, –

3.93 (2×C); ESI-HRMS: m/z calcd for $C_{20}H_{31}O_3Si$ $[M + H]^+$: 347.20370; found: 347.20386; b.p. 153–157 ºC (0.54 mbar).

Synthesis of 2,2,6-trimethyl-5-(triisopropylsilyl)-4*H*-1,3-dioxin-4-one (s13)[26,72]

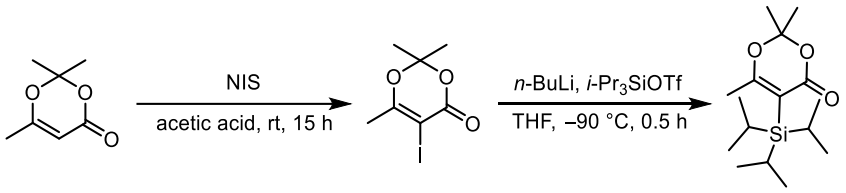

s1 **s12** **s13**

A solution of 2,2,6-trimethyl-4*H*-1,3-dioxin-4-one **s1** (10 g, 70.4 mmol, 1 equiv.) and *N*-iodosuccinimide (23.7 g, 105.5 mmol, 1.5 equiv.) in acetic acid (60 mL) was stirred for 15 h at room temperature in the dark. The reaction mixture was diluted with water and extracted with CH_2Cl_2. The organic layer was washed with water and dried over $MgSO_4$. The residue obtained after evaporation of the solvent was purified by chromatography on silica gel (EtOAc:*c*-hex = 1:9, R_f = 0.45 (EtOAc:*c*-hex = 1:4)) to give compound **s12** (12.8 g, 62.6 mmol, 89%) as pale-yellow prisms. The analytical data was in accordance to the literature.[72] ^{1}H NMR (400 MHz, $CDCl_3$) δ 2.30 (s, 3H), 1.69 (s, 6H); ^{13}C NMR (176 MHz, $CDCl_3$) δ 169.5, 158.1, 106.6, 62.4, 25.0 (2×C), 24.1.

To a solution of **s12** (3.0 g, 11.2 mmol, 1 equiv.) and *i*-Pr_3SiOTf (3.61 mL, 13.4 mmol, 1.2 equiv.) in anhydrous THF (111.6 mL), *n*-BuLi (1.6 M in THF, 3.61 mL, 12.9 mmol, 1.15 equiv.) was added at –90 ºC. After stirring for 0.5 h, the reaction mixture was poured into sat. $NaHCO_3$. The crude products were extracted with EtOAc (x 3), and the combined organic phases were washed with brine, dried by $MgSO_4$ and concentrated *in vacuo*. The residue was recrystallized in *c*-hexane to afford product **s13** (2.00 g, 6.72 mmol, 60%) as colorless prisms. The analytical data was in accordance to the literature.[26] ^{1}H NMR (500 MHz, $CDCl_3$) δ 2.07 (s, 3H), 1.66 (s, 6H), 1.50 (q, *J* = 7.5 Hz, 3H), 1.10 (s, 9H), 1.08 (s, 9H); ^{13}C NMR (126 MHz, $CDCl_3$) 172.9, 163.8, 103.9, 98.2, 24.8 (3×C), 21.8, 19.0 (6×C), 12.3 (2×C).

***Tert*-butyl((2,2-dimethyl-4-methylene-5-(triisopropylsilyl)-4*H*-1,3-dioxin-6-yl)oxy)dimethylsilane (122)**

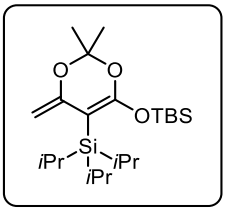

Synthesis according to **procedure D** by using the dioxinone precursor **s13** (1.2 g, 4.02 mmol, 1 equiv.) as starting material to afford **122** (270.5 mg, 0.6 mmol, 16%) as a pale-yellow oil. ^{1}H NMR (700 MHz, CD_2Cl_2) δ 4.76 (s, 2H), 1.32 (sept, J = 7.4 Hz, 3H), 1.09 (s, 3H), 1.08 (s, 9H), 1.07 (s, 9H), 0.94 (s, 9H), 0.93 (s, 3H), 0.25 (s, 6H); ^{13}C NMR (176 MHz, CD_2Cl_2) δ 220.0, 168.4, 101.9, 92.4, 71.7, 25.9 (2×C), 18.9 (6×C), 18.4, 18.2 (3×C), 12.1 (3×C), –4.54 (2×C).

9.8 Synthesis of *C*-glycosides via strain-release pyranosylation

General procedure for *C*-glycosylation via strain-release pyranosylation (procedure E)

An oven dried tube with a stirring bar was charged with D-A cyclopropanated carbohydrate (47.3 mg, 0.1 mmol, 1.0 equiv.), vinylogous enolate (0.4 mmol, 4.0 equiv.) and anhydrous toluene (0.5 mL). Then, the tube was purged with argon and sealed with a rubber stopper. After stirring for 10 mins at 0 °C, calcium (II) bis(trifluoromethanesulfonimide) (0.02 mmol, 20 mol%) and tetrabutylammonium hexafluorophosphate (0.02 mmol, 20 mol%), distillated water (0.05 mmol, 0.5 equiv.) and anhydrous toluene (0.5 mL) were added. The tube was sealed with parafilm and stirred at room temperature for 24 h. Upon completion of the reaction, the reaction mixture was flushed through a short pad of silica gel by EtOAc, the solvent evaporated and subjected to silica flash column chromatography.

6-(((2*S*,3*S*,4*R*,5*R*,6*R*)-4,5-bis(benzyloxy)-6-((benzyloxy)methyl)-3-(2-oxopropyl)tetrahydro-2*H*-pyran-2-yl)methyl)-2,2-dimethyl-4*H*-1,3-dioxin-4-one (123a)

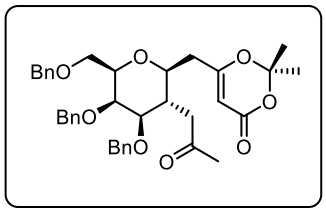

Synthesis according to the **procedure E** by using D-A cyclopropanated carbohydrate **6** (47.3 mg, 0.1 mmol) to afford **123a** (54.1 mg, 0.09 mmol, 88%) as a pale-yellow syrup. The β-anomer was assigned based on NOESY spectrum. (data for β-anomer) ^{1}H NMR (700 MHz, $CDCl_3$) δ 7.36–7.25 (m, 15H), 5.31 (s, 1H), 4.83 (d, *J* = 11.4 Hz, 1H), 4.68 (*d*, *J* = 11.5 Hz, 1H), 4.55 (*d*, *J* = 11.5 Hz, 1H), 4.46–4.42 (m, 2H), 4.35 (d, *J* = 11.5 Hz, 1H), 3.96 (d, *J* = 2.5 Hz, 1H), 3.57–3.54 (m, 2H), 3.53–3.49 (m, 2H), 3.43 (dd, *J* = 10.9, 2.5 Hz, 1H), 2.56 (sept, *J* = 4.9 Hz, 1H), 2.44–2.43 (m, 2H), 2.39–2.38 (m, 2H), 2.05 (s, 3H), 1.60 (s, 3H), 1.55 (s, 3H); ^{13}C NMR (176 MHz, $CDCl_3$) δ 207.0, 168.6, 161.1, 138.5, 137.7, 137.5, 128.5 (2×C), 128.4 (2×C), 128.2 (2×C), 128.1 (2×C), 127.9 (3×C), 127.9 (2×C), 127.8, 127.6, 106.5, 95.7, 81.7, 77.2, 76.2, 74.4, 73.5, 71.1, 71.0, 69.1, 41.8, 37.9, 37.2, 30.0, 25.6, 24.1; ESI-HRMS: m/z calcd for $C_{37}H_{43}O_8$ $[M + H]^+$: 615.29524; found: 615.29447; $[\alpha]_D^{20}$ = +1.38 (c = 0.29, CH_2Cl_2).

((2*R*,3*R*,4*R*,5*S*,6*S*)-3,4-bis(benzyloxy)-6-((2,2-dimethyl-4-oxo-4*H*-1,3-dioxin-6-yl)methyl)-5-(2-oxopropyl)tetrahydro-2*H*-pyran-2-yl)methyl acetate (123b)

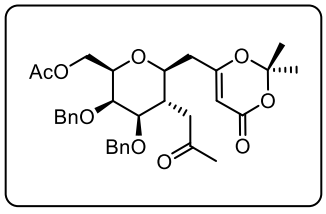

Synthesis according to the **procedure E** by using D-A cyclopropanated carbohydrate **101** (42.4 mg, 0.1 mmol) to afford **123b** (41.5 mg, 0.07 mmol, 73%) as a pale-yellow syrup. The β-anomer was assigned based on NOESY spectrum. (data for β-anomer) ^{1}H NMR (700 MHz, $CDCl_3$) δ 7.38–7.28 (m, 10H), 5.34 (s, 1H), 4.88 (d, *J* = 11.5 Hz, 1H), 4.73 (d, *J* = 11.5 Hz, 1H), 4.58 (d, *J* = 11.5 Hz, 1H), 4.40 (d, *J* = 11.5 Hz, 1H), 4.13 (dd, *J* = 11.4, 7.1 Hz, 1H), 4.06 (dd, *J* = 11.4, 5.1 Hz, 1H), 3.85 (d, *J* = 1.4 Hz, 1H), 3.59 (td, *J* = 9.6, 3.1 Hz, 1H), 3.57–3.51 (m, 1H), 3.48 (dd, *J* = 10.9, 2.5 Hz, 1H), 2.56 (sept, *J* = 5.3 Hz, 1H), 2.46 (d, *J* = 5.2 Hz, 2H), 2.41 (dd, *J* = 15.4, 9.1Hz, 1H), 2.37

(dd, *J* = 15.4, 2.8 Hz, 1H), 2.06 (s, 3H), 1.98 (s, 3H), 1.63 (*d*, *J* = 3.6 Hz, 6H); ^{13}C NMR (176 MHz, $CDCl_3$) δ 206.9, 170.7, 168.4, 161.1, 138.0, 137.3, 128.6 (2×C), 128.4 (2×C), 128.3 (2×C), 128.0, 127.9 (2×C), 127.9, 106.5, 95.6, 81.6, 76.1, 76.1, 74.2, 71.5, 70.7, 64.1, 41.4, 37.8, 37.2, 30.1, 25.6, 24.3, 20.8; ESI-HRMS: m/z calcd for $C_{32}H_{39}O_9$ $[M + H]^+$: 567.25886; found: 567.25847; $[\alpha]_D^{20}$ = +10.94 (c = 0.19, CH_2Cl_2).

6-(((2*S*,3*S*,4*R*,5*R*,6*R*)-4,5-bis(benzyloxy)-6-(((tert-butyldimethylsilyl)oxy)methyl)-3-(2-oxopropyl)tetrahydro-2*H*-pyran-2-yl)methyl)-2,2-dimethyl-4*H*-1,3-dioxin-4-one (123c)

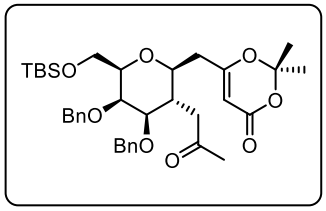

Synthesis according to the **procedure E** by using D-A cyclopropanated carbohydrate **108** (49.7 mg, 0.1 mmol) to afford **123c** (25.0 mg, 0.04 mmol, 39%) as a pale-yellow syrup. The β-anomer was assigned based on NOESY spectrum. (data for β-anomer) ^{1}H NMR (500 MHz, $CDCl_3$) δ 7.36–7.24 (m, 10H), 5.31 (s, 1H), 4.83 (d, *J* = 11.4 Hz, 1H), 4.64 (d, *J* = 11.5 Hz, 1H), 4.61 (d, *J* = 11.3 Hz, 1H), 4.38 (s, 1H), 3.95 (s, 1H), 3.66 (dd, *J* = 9.9, 7.8 Hz, 1H), 3.60 (dd, *J* = 9.9, 5.6 Hz, 1H), 3.58–3.53 (m, 1H) 3.43 (dd, *J* = 10.9, 2.5 Hz, 1H), 3.35 (t, *J* = 6.8 Hz, 1H), 2.55 (sept, *J* = 5.5 Hz, 1H), 2.44 (d, *J* = 5.4 Hz, 2H), 2.39– 2.37 (m, 2H), 2.06 (s, 3H), 1.62 (s, 3H), 1.61 (s, 3H), 0.89 (s, 9H), 0.04 (s, 3H), 0.03 (s, 3H); ^{13}C NMR (126 MHz, $CDCl_3$) δ 207.2, 168.6, 161.2, 138.7, 137.6, 128.5 (2×C), 128.2 (2×C), 128.0 (2×C), 128.0 (2×C), 127.9, 127.6, 106.5, 95.7, 81.7, 78.9, 76.0, 74.5, 71.2, 70.8, 61.7, 41.9, 38.0, 37.2, 30.0, 25.9 (3×C), 25.6, 24.3, 18.2 (2×C); ESI-HRMS: m/z calcd for $C_{36}H_{51}O_8Si$ $[M + H]^+$: 639.33477; found: 639.33417; $[\alpha]_D^{20}$ = +2.82 (c = 0.14, CH_2Cl_2).

6-(((2*S*,3*S*,4*R*,5*S*,6*R*)-4,5-bis(benzyloxy)-6-((benzyloxy)methyl)-3-(2-oxopropyl)tetrahydro-2*H*-pyran-2-yl)methyl)-2,2-dimethyl-4*H*-1,3-dioxin-4-one (123d)

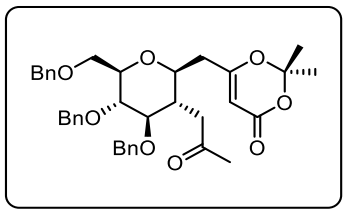

Synthesis according to the **procedure E** by using D-A cyclopropanated carbohydrate **7** (47.3 mg, 0.1 mmol) to afford **123d** (35.7 mg, 0.06 mmol, 58%) as a pale-yellow syrup. The β-anomer was assigned based on NOESY spectrum. (data for β-anomer) ^{1}H NMR (700 MHz, $CDCl_3$) δ 7.35–7.27 (m, 13H), 7.20–7.19 (m, 2H), 5.35 (s, 1H), 4.93 (d, *J* = 11.5 Hz, 1H), 4.78 (d, *J* = 10.9 Hz, 1H), 4.62 (d, *J* = 10.9 Hz, 1H), 4.58–4.53 (m, 3H), 3.68 (dd, *J* = 10.8, 4.1 Hz, 1H), 3.65 (t, *J* = 9.2 Hz, 1H), 3.61 (dd, *J* = 10.8, 2.0 Hz, 1H), 3.54 (td, *J* = 9.8, 3.2 Hz, 1H), 3.47 (dd, *J* = 10.7, 8.8 Hz, 1H), 3.37 (ddd, *J* = 9.7, 4.1, 1.9 Hz, 1H), 2.44 (dd, *J* = 17.6, 4.6 Hz, 1H), 2.37–2.34 (m, 2H), 2.32–2.27 (m, 1H), 2.13 (sept, *J* = 5.6 Hz, 1H), 2.00 (s, 3H), 1.65 (s, 3H), 1.57 (s, 3H); ^{13}C NMR (176 MHz, $CDCl_3$) δ 206.4, 168.5, 161.1, 138.3, 138.0, 137.9, 128.5 (2×C), 128.4 (2×C), 128.4 (2×C), 127.8 (2×C), 127.8, 127.8 (2×C), 127.7, 127.7 (2×C), 127.7, 106.6, 95.6, 83.3, 79.8, 79.2, 75.8, 74.6, 74.6, 73.4, 68.6, 42.6, 41.8, 37.6, 29.9, 26.0, 23.9; ESI-HRMS: m/z calcd for $C_{37}H_{43}O_8$ $[M + H]^+$: 615.29524; found: 615.29412; $[\alpha]_D^{20}$ = +1.59 (c = 0.63, CH_2Cl_2).

((2*R*,3*S*,4*R*,5*S*,6*S*)-3,4-bis(benzyloxy)-6-((2,2-dimethyl-4-oxo-4*H*-1,3-dioxin-6-yl)methyl)-5-(2-oxopropyl)tetrahydro-2*H*-pyran-2-yl)methyl acetate (123e)

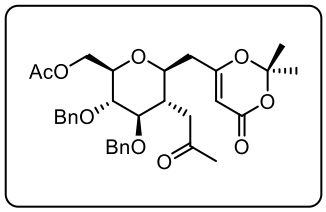

Synthesis according to the **procedure E** by using D-A cyclopropanated carbohydrate **8** (42.4 mg, 0.1 mmol) to afford **123e** (27.2 mg, 0.05 mmol, 48%) as a pale-yellow syrup. The β-anomer was assigned based on NOESY spectrum. (data for β-anomer) ^{1}H NMR (700 MHz, $CDCl_3$) δ 7.35–7.27 (m, 10H), 5.32 (s, 1H), 4.94 (d, *J* = 11.6 Hz, 1H), 4.82 (d, *J* = 10.8 Hz, 1H), 4.59 (d, *J* = 3.5 Hz, 1H), 4.57 (d, *J* = 4.3 Hz, 1H), 4.31 (dd, *J* = 11.8, 1.8 Hz, 1H), 4.14 (dd, *J* = 11.8, 5.5 Hz, 1H), 3.56 (td, *J* = 9.4, 3.7 Hz, 1H), 3.52–3.50 (m, 1H), 3.48–3.44 (m, 2H), 2.45 (dd, *J* = 17.9, 4.4 Hz, 1H), 2.37 (dd, *J* = 17.9, 5.4 Hz, 1H), 2.32–2.26 (m, 2H), 2.11 (sept, *J* = 4.9 Hz, 1H), 2.04 (s, 3H), 2.00 (s, 3H), 1.68 (s, 3H), 1.66 (s, 3H); ^{13}C NMR (176 MHz, $CDCl_3$) δ 206.3, 170.7, 168.1, 161.0, 138.0, 137.5, 128.6 (2×C), 128.6 (2×C), 128.1, 127.9 (3×C), 127.8 (2×C), 106.5, 95.6, 83.2, 80.1, 77.0, 75.6, 74.9, 74.8, 63.5, 42.4, 41.3, 37.4, 30.0, 25.8, 24.1, 20.8; ESI-HRMS: m/z calcd for $C_{32}H_{39}O_9$ $[M + H]^+$: 567.25886; found: 567.25764; $[\alpha]_D^{20}$ = +7.22 (c = 0.18, CH_2Cl_2).

6-(((2*S*,3*S*,4*R*,5*R*,6*R*)-4,5-bis(benzyloxy)-6-((methoxymethoxy)methyl)-3-(2-oxopropyl)tetrahydro-2*H*-pyran-2-yl)methyl)-2,2-dimethyl-4*H*-1,3-dioxin-4-one (123f)

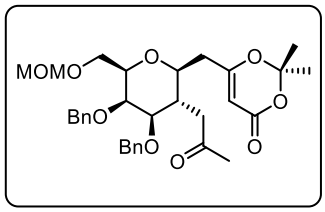

Synthesis according to the **procedure E** by using D-A cyclopropanated carbohydrate **111** (42.7 mg, 0.1 mmol) to afford **123f** (34.1 mg, 0.06 mmol, 60%) as a pale-yellow syrup. The β-anomer was assigned based on NOESY spectrum. (data for β-anomer) ^{1}H NMR (700 MHz, $CDCl_3$) δ 7.37–7.27 (m, 10H), 5.32 (s, 1H), 4.87 (d, *J* = 11.4 Hz, 1H), 4.70 (d, *J* = 11.4 Hz, 1H), 4.60 (d, *J* = 11.4 Hz, 1H), 4.54 (d, *J* = 6.4 Hz, 1H), 4.51 (d, *J* = 6.4 Hz, 1H), 4.37 (d, *J* = 11.4 Hz, 1H), 3.93 (s, 1H), 3.63 (dd, *J* = 9.8, 6.1 Hz, 1H), 3.60–3.57 (m, 1H), 3.55–3.53 (m, 1H), 3.51–3.49 (m, 1H), 3.46 (dd, *J* = 10.9, 2.5 Hz, 1H), 3.32 (s, 3H), 2.58 (sept, *J* = 5.3 Hz, 1H), 2.45 (d, *J* = 5.3 Hz, 2H), 2.41–2.39 (m, 2H), 2.05 (s, 3H), 1.62 (s, 3H), 1.61 (s, 3H); ^{13}C NMR (176 MHz, $CDCl_3$) δ 207.0, 168.6, 161.1, 138.4, 137.4, 128.5 (2×C), 128.3 (2×C), 128.1 (2×C), 128.0, 127.9 (2×C), 127.7, 106.6, 96.8, 95.6, 81.8, 77.4, 76.1, 74.4, 71.2, 71.1, 67.1, 55.4, 41.7, 37.9, 37.2, 30.1, 25.5, 24.3; ESI-HRMS: m/z calcd for $C_{32}H_{41}O_9$ $[M + H]^+$: 569.27451; found: 569.27623; $[\alpha]_D^{20}$ = +20.92 (c = 0.35, CH_2Cl_2).

((2*R*,3*R*,4*R*,5*S*,6*S*)-3,4-bis(benzyloxy)-6-((2,2-dimethyl-4-oxo-4*H*-1,3-dioxin-6-yl)methyl)-5-(2-oxopropyl)tetrahydro-2*H*-pyran-2-yl)methyl tert-butyl carbonate (123g)

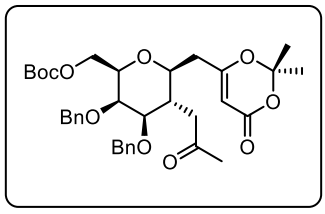

Synthesis according to the **procedure E** by using D-A cyclopropanated carbohydrate **110** (48.3 mg, 0.1 mmol) to afford **123g** (30.1 mg, 0.05 mmol, 48%) as a pale-yellow syrup. The β-anomer was assigned based on NOESY spectrum. (data for β-anomer) ^{1}H NMR (700 MHz, $CDCl_3$) δ 7.37–7.27 (m, 10H), 5,30 (s, 1H), 4.87 (d, *J* = 11.3 Hz, 1H), 4.71 (d, *J* = 11.4 Hz, 1H), 4.58 (d, *J* = 11.3 Hz, 1H), 4.37 (d, *J* = 11.5 Hz, 1H), 4.15 (dd, *J* = 11.1, 6.8 Hz, 1H), 4.08 (dd, *J* = 11.1, 5.4 Hz, 1H), 3.90 (s, 1H), 3.60 (dt, *J* = 10.1, 6.1 Hz, 1H), 3.56 (t, *J* = 6.0 Hz, 1H), 3.47 (dd, *J* = 10.9, 2.5 Hz,

1H), 2.56 (sept, *J* = 5.3 Hz, 1H), 2.49–2.45 (m, 2H), 2.40 (d, *J* = 6.1 Hz, 2H), 2.05 (s, 3H), 1.63 (s, 6H), 1.47 (s, 9H); ^{13}C NMR (176 MHz, $CDCl_3$) δ 206.9, 168.3, 161.1, 153.2, 138.1, 137.3, 128.6 (2×C), 128.4 (2×C), 128.2 (2×C), 128.0, 127.9 (2×C), 127.8, 106.7, 95.8, 82.4, 81.7, 76.1, 76.1, 74.4, 71.3, 71.0, 66.2, 41.5, 37.8, 37.3, 30.1, 27.7 (3×C), 25.8, 24.1; ESI-HRMS: m/z calcd for $C_{35}H_{45}O_{10}$ $[M + H]^+$: 625.30072; found: 625.30190; $[\alpha]_D^{20}$ = +6.25 (c = 0.14, CH_2Cl_2).

((2*R*,3*R*,4*R*,5*S*,6*S*)-3,4-bis(benzyloxy)-6-((2,2-dimethyl-4-oxo-4*H*-1,3-dioxin-6-yl)methyl)-5-(2-oxopropyl)tetrahydro-2*H*-pyran-2-yl)methyl benzoate (123h)

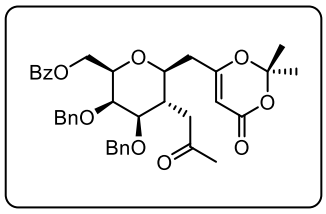

Synthesis according to the **procedure E** by using D-A cyclopropanated carbohydrate **109** (48.6 mg, 0.1 mmol) to afford **123h** (27.6 mg, 0.04 mmol, 44%) as a pale-yellow syrup. The β-anomer was assigned based on NOESY spectrum. (data for β-anomer) ^{1}H NMR (700 MHz, $CDCl_3$) δ 7.93 (d, *J* = 7.5 Hz, 2H), 7.57 (t, *J* = 7.4 Hz, 1H), 7.44 (t, *J* = 7.7 Hz, 2H), 7.37–7.24 (m, 10H), 5.36 (s, 1H), 4.92 (d, *J* = 11.5 Hz, 1H), 4.73 (d, *J* = 11.5 Hz, 1H), 4.62 (d, *J* = 11.5 Hz, 1H), 4.42 (d, *J* = 11.4 Hz, 1H), 4.37 (qd, *J* = 11.3, 6.0 Hz, 2H), 3.92 (s, 1H), 3.69 (t, *J* = 6.2 Hz, 1H), 3.61 (td, *J* = 9.7, 2.9 Hz, 1H), 3.51 (dd, *J* = 10.9, 2.5 Hz, 1H), 2.60 (sept, *J* = 4.9 Hz, 1H), 2.47 (d, *J* = 4.9 Hz, 2H), 2.45–2.42 (m, 1H), 2.39–2.36 (m, 1H), 2.07 (s, 3H), 1.58 (s, 3H), 1.49 (s, 3H); ^{13}C NMR (176 MHz, $CDCl_3$) δ 206.9, 168.4, 166.3, 161.0, 138.1, 137.3, 133.2, 129.7, 129.6 (2×C), 128.6 (2×C), 128.5 (2×C), 128.4 (2×C), 128.3 (2×C), 128.0, 128.0, 127.9 (2×C), 106.5, 95.6, 81.8, 76.1, 76.1, 74.4, 71.6, 70.9, 64.3, 41.5, 37.8, 37.3, 30.1, 25.6, 24.1; ESI-HRMS: m/z calcd for $C_{37}H_{41}O_9$ $[M + H]^+$: 629.27451; found: 629.27604; $[\alpha]_D^{20}$ = +3.45 (c = 0.20, CH_2Cl_2).

((2*R*,3*R*,4*R*,5*S*,6*S*)-3,4-bis(benzyloxy)-6-((2,2-dimethyl-4-oxo-4*H*-1,3-dioxin-6-yl)methyl)-5-(2-oxopropyl)tetrahydro-2*H*-pyran-2-yl)methyl stearate (123i)

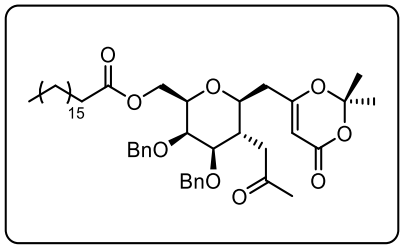

Synthesis according to the **procedure E** by using D-A cyclopropanated carbohydrate **112** (64.9 mg, 0.1 mmol) to afford **123i** (41.3 mg, 0.05 mmol, 52%) as a pale-yellow syrup. The β-anomer was assigned based on NOESY spectrum. (data for β-anomer) ^{1}H NMR (700 MHz, $CDCl_3$) δ 7.38–7.27 (m, 10H), 5.33 (s, 1H), 4.88 (d, *J* = 11.4 Hz, 1H), 4.72 (d, *J* = 11.4 Hz, 1H), 4.58 (d, *J* = 11.4 Hz, 1H), 4.39 (d, *J* = 11.4 Hz, 1H), 4.14 (dd, *J* = 11.3, 6.8 Hz, 1H), 4.09 (dd, *J* = 11.3, 5.5 Hz, 1H), 3.85 (s, 1H), 3.59 (td, *J* = 9.3, 3.4 Hz, 1H), 3.53 (t, *J* = 6.2 Hz, 1H), 3.48 (dd, *J* = 10.9, 2.4 Hz, 1H), 2.56 (sept, *J* = 5.3 Hz, 1H), 2.48–2.45 (m, 2H), 2.43–2.36 (m, 2H), 2.25–2.19 (m, 2H), 2.06 (s, 3H), 1.66 (s, 3H), 1.65 (s, 3H), 1.33–1.25 (m, 30H), 0.88 (t, *J* = 7.1 Hz, 3H); ^{13}C NMR (176 MHz, $CDCl_3$) δ 207.0, 173.65, 168.4, 161.1, 138.1, 137.3, 128.6 (2×C), 128.4 (2×C), 128.2 (2×C), 128.1, 127.9 (2×C), 127.9, 106.5, 95.7, 81.7, 76.1, 76.1, 74.4, 71.4, 70.9, 63.7, 41.5, 37.9, 37.2, 34.0, 31.9, 30.1, 29.7 (5×C), 29.7, 29.7, 29.6, 29.5, 29.4, 29.3, 29.2, 25.7, 24.9, 24.3, 22.7, 14.1; ESI-HRMS: m/z calcd for $C_{48}H_{71}O_9$ $[M + H]^+$: 791.50926; found: 791.50734; $[\alpha]_D^{20}$ = +10.86 (c = 0.35, CH_2Cl_2).

((2*R*,3*R*,4*R*,5*S*,6*S*)-3,4-bis(benzyloxy)-6-((2,2-dimethyl-4-oxo-4*H*-1,3-dioxin-6-yl)methyl)-5-(2-oxopropyl)tetrahydro-2*H*-pyran-2-yl)methyl 2-(1-(4-chlorobenzoyl)-5-methoxy-2-methyl-1*H*-indol-3-yl)acetate (123j)

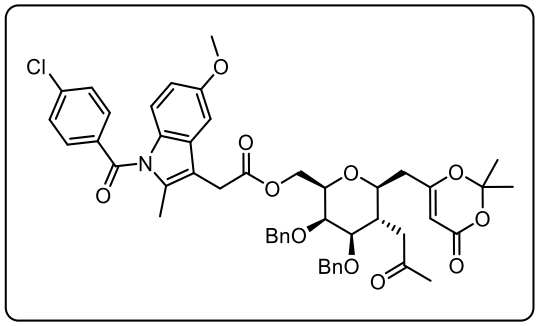

Synthesis according to the **procedure E** by using D-A cyclopropanated carbohydrate **113** (72.2 mg, 0.1 mmol) to afford **123j** (47.9 mg, 0.06 mmol, 55%) as a yellow solid. The β-anomer was assigned based on NOESY spectrum. (data for β-anomer) ^{1}H NMR (700 MHz, $CDCl_3$) δ 7.52 (d, *J* = 8.0 Hz, 2H), 7.39–7.23 (m, 10H), 7.19–7.18 (m, 2H), 6.98 (d, *J* = 2.5 Hz, 1H), 6.81 (d, *J* = 9.0 Hz, 1H), 6.63 (dd, *J* = 9.0, 2.5 Hz, 1H), 5.31 (s, 1H), 4.63 (d, *J* = 11.1 Hz, 1H), 4.51 (d, *J* = 11.3 Hz, 1H), 4.23–4.20 (m, 2H), 4.18 (d, *J* = 11.1, 1Hz), 4.14–4.10 (m, 1H), 3.78 (s, 3H), 3.66 (s, 2H), 3.63 (s, 1H), 3.61–3.58 (m, 1H), 3.56 (t, *J* = 6.7 Hz, 1H), 3.38 (dd, *J* = 10.8, 2.5 Hz, 1H), 2.51–2.47 (m, 1H), 2.43 (dd, *J* = 15.3, 5.1 Hz, 2H), 2.38 (s, 3H), 2.36–2.33 (m, 2H), 2.02 (s, 3H), 1.62 (s, 3H), 1.61 (s, 3H); ^{13}C NMR (176 MHz, $CDCl_3$) δ 207.0, 170.3, 168.4, 168.2, 161.1, 156.0, 139.3, 138.2, 137.3, 136.1, 133.7, 131.0 (2×C), 130.8, 130.6, 129.1 (2×C), 128.5 (2×C), 128.3 (2×C), 128.0, 128.0 (2×C), 127.9 (2×C), 127.8, 115.0, 112.3, 111.3, 106.5, 101.7, 95.6, 81.4, 76.0, 75.4, 74.4, 71.0, 70.8, 63.4, 55.7, 55.7, 41.4, 37.7, 37.0, 30.1, 25.3, 24.5, 13.3; ESI-HRMS: m/z calcd for $C_{49}H_{51}O_{11}NCl$ $[M + H]^+$: 864.31452; found: 864.31223; $[\alpha]_D^{20}$ = +1.50 (c = 0.13, CH_2Cl_2); b.p. = 78–81 ºC.

6-(((2*S*,3*S*,4*R*,5*R*,6*R*)-4,5-bis(benzyloxy)-6-((benzyloxy)methyl)-3-(2-oxopropyl)tetrahydro-2*H*-pyran-2-yl)methyl)-2,2-diethyl-4*H*-1,3-dioxin-4-one (123k)

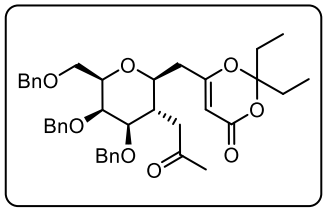

Synthesis according to the **procedure E** by using D-A cyclopropanated carbohydrate **6** (47.3 mg, 0.1 mmol) to afford **123k** (42.7 mg, 0.07 mmol, 57%) as a pale-yellow syrup. The β-anomer was assigned based on NOESY spectrum. (data for β-anomer) ^{1}H NMR (500 MHz, $CDCl_3$) δ 7.37–7.27 (m, 15H), 5.26 (s, 1H), 4.84 (d, *J* = 11.6 Hz, 1H), 4.67 (d, *J* = 11.5 Hz, 1H), 4.57 (d, *J* = 11.5 Hz, 1H), 4.44 (s, 2H), 4.34 (d, *J* = 11.5 Hz, 1H), 3.97 (d, *J* = 2.5 Hz, 1H), 3.58–3.53 (m, 2H), 3.52–3.46 (m, 2H), 3.42 (dd, *J* = 10.9, 2.5 Hz, 1H), 2.55 (sept, *J* = 5.3 Hz, 1H), 2.48–2.42 (m, 2H), 2.40–2.38 (m, 2H), 2.05 (s, 3H), 1.93–1.84 (m, 4H), 0.92 (t, *J* = 7.4 Hz, 3H), 0.84 (t, *J* = 7.5 Hz, 3H); ^{13}C NMR (126 MHz, $CDCl_3$) δ 207.1, 168.6, 161.2, 138.5, 137.7, 137.5, 128.5 (2×C), 128.4 (2×C), 128.2 (2×C), 128.1 (2×C), 127.9 (3×C), 127.9 (2×C), 127.8, 127.6, 110.6, 95.1, 81.6, 77.1, 76.2, 74.4, 73.5, 71.1, 70.9, 68.8, 41.8, 38.0, 37.5, 30.1, 28.4, 27.3, 7.56, 7.19; ESI-HRMS: m/z calcd for $C_{39}H_{47}O_8$ = $[M + H]^+$: 643.32654; found: 643.32806; $[\alpha]_D^{20}$ = +8.82 (c = 0.10, CH_2Cl_2).

6-(((2*S*,3*S*,4*R*,5*R*,6*R*)-4,5-bis(benzyloxy)-6-(((tert-butyldimethylsilyl)oxy)methyl)-3-(2-oxopropyl)tetrahydro-2*H*-pyran-2-yl)methyl)-2,2-diethyl-4*H*-1,3-dioxin-4-one (123l)

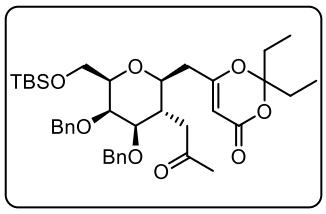

Synthesis according to the **procedure E** by using D-A cyclopropanated carbohydrate **108** (49.7 mg, 0.1 mmol) to afford **123l** (30.7 mg, 0.05 mmol, 46%) as a pale-yellow syrup. The β-anomer was assigned based on NOESY spectrum. (data for β-anomer) ^{1}H NMR (500 MHz, $CDCl_3$) δ 7.36–7.24 (m, 10H), 5.24 (s, 1H), 4.83 (d, *J* = 11.4 Hz, 1H), 4.64 (d, *J* = 8.0 Hz, 1H), 4.62 (d, *J* = 7.8 Hz, 1H), 4.36 (d, *J* = 11.5 Hz, 1H), 3.97 (d, *J* = 1.7 Hz, 1H), 3.69 (dd, *J* = 9.8, 8.2 Hz, 1H), 3.61–3.54 (m, 2H), 3.43 (dd, *J* = 10.8, 2.6 Hz, 1H), 3.35 (dd, *J* = 8.0, 6.2 Hz, 1H), 2.54 (sept, *J* = 5.3 Hz, 1H), 2.45–2.44 (m, 2H), 2.38 (d, *J* = 6.2 Hz, 2H), 2.06 (s, 3H), 1.98–1.87 (m, 4H), 0.93 (td, *J*

= 7.5, 5.5 Hz, 6H), 0.91–0.89 (m, 9H), 0.05 (d, *J* = 4.3 Hz, 6H); ^{13}C NMR (126 MHz, $CDCl_3$) δ 207.2, 168.6, 161.2, 138.8, 137.5, 128.5 (2×C), 128.2 (2×C), 128.0 (2×C), 127.9 (2×C), 128.0, 127.5, 110.5, 95.1, 81.6, 78.7, 76.1, 74.6, 71.1, 70.8, 61.5, 41.9, 38.2, 37.5, 30.1, 28.4, 27.4, 25.9 (3×C), 18.2, 7.59, 7.23, –5.43 (2×C); ESI-HRMS: m/z calcd for $C_{38}H_{55}O_8Si$ = $[M + H]^+$: 667.36607; found: 667.36853; $[\alpha]_D^{20}$ = +8.05 (c = 0.20, CH_2Cl_2).

((2*R*,3*R*,4*R*,5*S*,6*S*)-3,4-bis(benzyloxy)-6-((2,2-diethyl-4-oxo-4*H*-1,3-dioxin-6-yl)methyl)-5-(2-oxopropyl)tetrahydro-2*H*-pyran-2-yl)methyl acetate (123m)

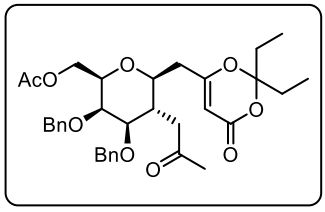

Synthesis according to the **procedure E** by using D-A cyclopropanated carbohydrate **101** (42.4 mg, 0.1 mmol) to afford **123m** (24.1mg, 0.04 mmol, 41%) as a pale-yellow syrup. The β-anomer was assigned based on NOESY spectrum. (data for β-anomer) ^{1}H NMR (700 MHz, $CDCl_3$) δ 7.38–7.28 (m, 10H), 5.29 (s, 1H), 4.88 (d, *J* = 11.6 Hz, 1H), 4.73 (d, *J* = 11.5 Hz, 1H), 4.58 (d, *J* = 11.6 Hz, 1H), 4.40 (d, *J* = 11.4 Hz, 1H), 4.15 (dd, *J* = 11.3, 7.0 Hz, 1H), 4.05 (dd, *J* = 11.4, 5.3 Hz, 1H), 3.85 (s, 1H), 3.59 (td, *J* = 9.8, 3.1 Hz, 1H), 3.52 (t, *J* = 6.3 Hz, 1H), 3.48 (dd, *J* = 10.9, 2.4 Hz, 1H), 2.55 (sept, *J* = 5.3 Hz, 1H), 2.47 (d, *J* = 4.9 Hz, 2H), 2.73–2.34 (m, 2H), 2.06 (s, 3H), 1.99 (s, 3H), 1.98–1.90 (m, 4H), 0.94 (q, *J* = 7.3 Hz, 6H); ^{13}C NMR (176 MHz, $CDCl_3$) δ 206.9, 170.7, 168.4, 161.1, 138.1, 137.3, 128.6 (2×C), 128.4 (2×C), 128.3 (2×C), 128.1, 127.9 (2×C), 127.9, 110.6, 95.0, 81.7, 76.2, 76.0, 74.3, 71.5, 70.7, 63.9, 41.5, 38.0, 37.4, 30.1, 28.3, 27.5, 20.8, 7.6, 7.3; ESI-HRMS: m/z calcd for $C_{34}H_{43}O_9$ = $[M + H]^+$: 595.29016; found: 595.29144; $[\alpha]_D^{20}$ = +6.44 (c = 0.20, CH_2Cl_2).

6-(((2*S*,3*S*,4*R*,5*S*,6*R*)-4,5-bis(benzyloxy)-6-((benzyloxy)methyl)-3-(2-oxopropyl)tetrahydro-2*H*-pyran-2-yl)methyl)-2,2-diethyl-4*H*-1,3-dioxin-4-one (123n)

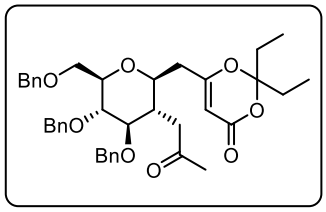

Synthesis according to the **procedure E** by using D-A cyclopropanated carbohydrate **7** (47.3 mg, 0.1 mmol) to afford **123n** (32.0 mg, 0.05 mmol, 50%) as a pale-yellow syrup. The β-anomer was assigned based on NOESY spectrum. (data for β-anomer) ^{1}H NMR (700 MHz, $CDCl_3$) δ 7.35–7.19 (m, 15H), 5.29 (s, 1H), 4.93 (d, *J* = 11.6 Hz, 1H), 4.78 (d, *J* = 10.9 Hz, 1H), 4.62 (d, *J* = 10.8 Hz, 1H), 4.59–4.54 (m, 3H), 3.70–3.66 (m, 2H), 3.61 (dd, *J* = 10.8, 2.0 Hz, 1H), 3.54 (td, *J* = 9.7, 3.5 Hz, 1H), 3.47 (dd, *J* = 10.7, 8.8 Hz, 1H), 3.36 (ddd, *J* = 9.7, 4.0, 2.0 Hz, 1H), 2.45 (dd, *J* = 17.6, 4.6 Hz, 1H), 2.37– 2.30 (m, 3H), 2.12 (sept, *J* = 4.9 Hz, 1H), 2.00 (s, 3H), 1.94–1.88 (m, 4H), 0.96 (t, *J* = 7.4 Hz, 3H), 0.84 (t, *J* = 7.5 Hz, 3H); ^{13}C NMR (176 MHz, $CDCl_3$) δ 206.4, 168.4, 161.1, 138.3, 138.0, 137.9, 128.5 (2×C), 128.5 (2×C), 128.4 (2×C), 127.8 (4×C), 127.8, 127.8, 127.7 (2×C), 127.7, 110.7, 95.1, 83.3, 79.8, 79.2, 75.9, 74.7, 74.6, 73.4, 68.5, 42.7, 41.7, 37.8, 29.9, 28.6, 27.2, 7.67, 7.17; ESI-HRMS: m/z calcd for $C_{39}H_{47}O_8$ = $[M + H]^+$: 643.32654; found: 643.32825; $[\alpha]_D^{20}$ = +0.59 (c = 0.34, CH_2Cl_2).

4-(((2*S*,3*S*,4*R*,5*R*,6*R*)-4,5-bis(benzyloxy)-6-((benzyloxy)methyl)-3-(2-oxopropyl)tetrahydro-2*H*-pyran-2-yl)methyl)-1,5-dioxaspiro[5.5]undec-3-en-2-one (123o)

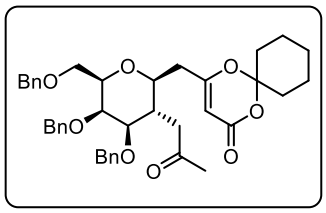

Synthesis according to the **procedure E** by using D-A cyclopropanated carbohydrate **6** (47.3 mg, 0.1 mmol) to afford **123o** (27.7 mg, 0.04 mmol, 42%) as a pale-yellow syrup. The β-anomer was assigned based on NOESY spectrum. (data for β-anomer) ^{1}H NMR (500 MHz, $CDCl_3$) δ 7.37–7.27 (m, 15H), 5.28 (s, 1H), 4.84 (d, *J* = 11.6 Hz, 1H), 4.67 (d, *J* = 11.5 Hz, 1H), 4.57 (d, *J* = 11.6 Hz, 1H), 4.43 (s, 2H), 4.35 (d, *J* = 11.4 Hz, 1H), 3.97 (d, *J* = 2.1 Hz, 1H), 3.61–3.54 (m, 2H), 3.52–3.49 (m, 1H), 3.48–3.43 (m, 2H), 2.58–2.50 (m, 1H), 2.45 (dd, *J* = 5.2, 2.1 Hz, 2H), 2.39 (d, *J* =

6.2 Hz, 2H), 2.05 (s, 3H), 1.92–1.86 (m, 3H), 1.71–1.65 (m, 1H), 1.58–1.52 (m, 3H), 1.43–1.39 (m, 3H); ^{13}C NMR (126 MHz, $CDCl_3$) δ 207.1, 168.3, 161.2, 138.5, 137.7, 137.5, 128.5 (2×C), 128.4 (2×C), 128.2 (2×C), 128.1 (2×C), 127.9 (2×C), 127.9 (3×C), 127.8, 127.6, 107.1, 95.7, 81.6, 77.1, 76.2, 74.4, 73.5, 71.1, 70.9, 68.9, 41.8, 38.1, 37.5, 34.7, 32.6, 30.1, 24.6, 22.3, 22.1; ESI-HRMS: m/z calcd for $C_{40}H_{46}O_8Na$ $[M + Na]^+$: 677.30849; found: 677.30844; $[\alpha]_D^{20}$ = +0.64 (c = 0.16, CH_2Cl_2).

4-(((2*S*,3*S*,4*R*,5*R*,6*R*)-4,5-bis(benzyloxy)-6-(((tert-butyldimethylsilyl)oxy)methyl)-3-(2-oxopropyl)tetrahydro-2*H*-pyran-2-yl)methyl)-1,5-dioxaspiro[5.5]undec-3-en-2-one (123p)

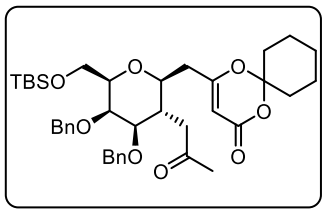

Synthesis according to the **procedure E** by using D-A cyclopropanated carbohydrate **108** (49.7 mg, 0.1 mmol) to afford **123p** (10.1 mg. 0.01 mmol, 15%) as a pale-yellow syrup. The β-anomer was assigned based on NOESY spectrum. (data for β-anomer) ^{1}H NMR (400 MHz, $CDCl_3$) δ 7.37–7.27 (m, 10H), 5.27 (s, 1H), 4.83 (d, *J* = 11.4 Hz, 1H), 4.64 (d, *J* = 8.1 Hz, 1H), 4.61 (d, *J* = 8.1 Hz, 1H), 4.37 (d, *J* = 11.5 Hz, 1H), 3.97 (d, *J* = 2.3 Hz, 1H), 3.69 (dd, *J* = 9.7, 8.2 Hz, 1H), 3.62–3.56 (m, 2H), 3.45 (dd, *J* = 10.8, 2.5 Hz, 1H), 3.37–3.33 (m, 1H), 2.53 (sept, *J* = 5.2 Hz, 1H), 2.46 (d, *J* = 5.3 Hz, 2H), 2.40–2.38 (m, 2H), 2.06 (s, 3H), 1.97–1.91 (m, 4H), 1.70–1.62 (m, 3H), 1.45–1.40 (m, 3H), 0.89 (s, 9H), 0.07–0.04 (m, 6H); ^{13}C NMR (126 MHz, $CDCl_3$) δ 207.2, 168.4, 161.2, 138.8, 137.6, 128.5 (2×C), 128.3 (2×C), 128.0 (2×C), 128.0 (2×C), 127.9, 127.6, 107.1, 95.8, 81.7, 78.7, 76.1, 74.6, 71.2, 70.9, 61.5, 41.9, 38.3, 37.6, 34.7, 32.8, 30.1, 26.0 (3×C), 24.7, 22.4, 22.2, 18.3, –5.37 (2×C); ESI-HRMS: m/z calcd for $C_{39}H_{55}O_8Si$ = $[M + H]^+$: 679.36607; found: 679.36524; $[\alpha]_D^{20}$ = +5.14 (c = 0.21, CH_2Cl_2).

6-(((2*S*,3*S*,4*R*,5*R*,6*R*)-4,5-bis(benzyloxy)-6-((benzyloxy)methyl)-3-(2-oxopropyl)tetrahydro-2*H*-pyran-2-yl)methyl)-2,2,5-trimethyl-4*H*-1,3-dioxin-4-one (123s)

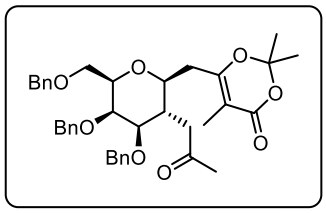

Synthesis according to the **procedure E** by using D-A cyclopropanated carbohydrate **6** (94.5 mg, 0.2 mmol) to afford **123s** (74.2 mg, 0.12 mmol, 59%) as a pale-yellow syrup. The β-anomer was assigned based on NOESY spectrum. (data for β-anomer) ^{1}H NMR (700 MHz, $CDCl_3$) δ 7.36–7.24 (m, 15H), 4.83 (d, *J* = 11.5 Hz, 1H), 4.68 (d, *J* = 11.4 Hz, 1H), 4.54 (d, *J* = 11.5 Hz, 1H), 4.43 (d, *J* = 5.8 Hz, 2H), 4.36 (d, *J* = 11.4 Hz, 1H), 3.94 (s, 1H), 3.58–3.54 (m, 2H), 3.51–3.47 (m, 2H), 3.42 (dd, *J* = 10.9, 2.6 Hz, 1H), 2.61–2.55 (m, 2H), 2.45 (d, *J* = 5.4 Hz, 2H), 2.33 (dd, *J* = 14.5, 3.1 Hz, 1H), 2.06 (s, 3H), 1.81 (s, 3H), 1.58 (s, 3H), 1.53 (s, 3H); ^{13}C NMR (176 MHz, $CDCl_3$) δ 207.1, 162.8, 162.6, 138.7, 137.8, 137.5, 128.5 (2×C), 128.4 (2×C), 128.2 (2×C), 127.9 (2×C), 127.9 (2×C), 127.9, 127.8 (2×C), 127.8, 127.7, 127.5, 104.9, 102.9, 81.9, 77.1, 74.4, 73.5, 71.3, 71.1, 69.3, 41.9, 38.1, 34.6, 30.0, 25.8, 24.0, 10.4; ESI-HRMS: m/z calcd for $C_{38}H_{45}O_8$ $[M + H]^+$: 629.31089; found: 629.31015; $[\alpha]_D^{20}$ = +11.92 (c = 0.41, CH_2Cl_2)

6-(((2*S*,3*S*,4*R*,5*R*,6*R*)-4,5-bis(benzyloxy)-6-(((tert-butyldimethylsilyl)oxy)methyl)-3-(2-oxopropyl)tetrahydro-2*H*-pyran-2-yl)methyl)-2,2,5-trimethyl-4*H*-1,3-dioxin-4-one (123t)

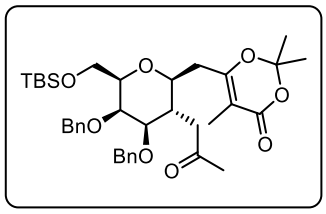

Synthesis according to the **procedure E** by using D-A cyclopropanated carbohydrate **108** (49.7 mg, 0.1 mmol) to afford **123t** (15.0 mg, 0.02 mmol, 23%) as a pale-yellow syrup. The β-anomer was assigned based on NOESY spectrum. (data for β-anomer) ^{1}H NMR (600 MHz, $CDCl_3$) δ 7.36–7.28 (m, 10H), 4.82 (d, *J* = 11.4 Hz, 1H), 4.64 (d, *J* = 11.5 Hz, 1H), 4.60 (d, *J* = 11.4 Hz, 1H), 4.37 (d, *J* = 11.5 Hz, 1H), 3.39 (s, 1H), 3.65 (dd, *J* = 9.8, 7.8 Hz, 1H), 3.57–3.55 (m, 2H), 3.42 (dd, *J* = 10.9, 2.5 Hz, 1H), 3.32 (t, *J* = 6.6 Hz, 1H), 2.60–2.54 (m, 2H), 2.45 (t, *J* = 4.9 Hz, 2H), 2.31 (dd, *J* = 14.5, 3.1 Hz, 1H), 2.07 (s, 3H), 1.80 (s, 3H), 1.58 (s, 3H), 1.58 (s, 3H), 0.88 (s, 9H), 0.03 (s,

3H), 0.02 (s, 3H); ^{13}C NMR (151 MHz, $CDCl_3$) δ 207.2, 162.8, 162.6, 138.9, 137.6, 128.5 (2×C), 128.2 (2×C), 128.0 (2×C), 127.9, 127.9 (2×C), 127.5, 104.9, 102.9, 81.9, 78.8, 74.5, 71.2, 71.0, 61.8, 42.0, 38.3, 34.6, 30.1, 29.7, 25.9 (3×C), 25.9, 24.1, 18.2, 10.4, –5.4 (2×C); ESI-HRMS: m/z calcd for $C_{37}H_{53}O_8Si$ $[M + H]^+$: 653.35042; found: 653.34964; $[\alpha]_D^{20}$ = +2.34 (c = 0.13, CH_2Cl_2).

((2*R*,3*R*,4*R*,5*S*,6*S*)-3,4-bis(benzyloxy)-5-(2-oxopropyl)-6-((2,2,5-trimethyl-4-oxo-4*H*-1,3-dioxin-6-yl)methyl)tetrahydro-2*H*-pyran-2-yl)methyl acetate (123u)

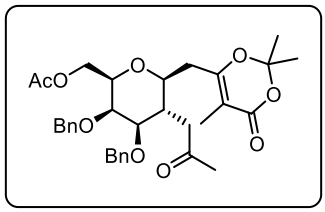

Synthesis according to the **procedure E** by using D-A cyclopropanated carbohydrate **101** (42.4 mg, 0.1 mmol) to afford **123u** (20.1 mg, 0.03 mmol, 35%) as a pale-yellow syrup. The β-anomer was assigned based on NOESY spectrum. (data for β-anomer) ^{1}H NMR (400 MHz, $CDCl_3$) δ 7.39–7.27 (m, 10H), 4.87 (d, *J* = 11.5 Hz, 1H), 4.72 (d, *J* = 11.4 Hz, 1H), 4.56 (d, *J* = 11.4 Hz, 1H), 4.40 (d, *J* = 11.5 Hz, 1H), 4.09 (qd, *J* = 11.3, 6.1 Hz, 2H), 3.83 (s, 1H), 3.58 (td, *J* = 9.9, 3.0 Hz, 1H), 3.52–3.46 (m, 2H), 2.67–2.55 (m, 2H), 2.48–2.46 (m, 2H), 2.30 (dd, *J* = 14.3, 2.7 Hz, 1H), 2.06 (s, 3H), 1.96 (s, 3H), 1.81 (s, 3H), 1.60 (s, 6H); ^{13}C NMR (126 MHz, $CDCl_3$) δ 207.0, 170.7, 162.8, 162.3, 138.2, 137.3, 128.6 (2×C), 128.4 (2×C), 128.1 (2×C), 128.0, 128.0 (2×C), 127.8, 104.9, 103.1, 81.8, 76.9, 75.9, 74.3, 71.4, 70.9, 64.2, 41.6, 38.0, 34.6, 30.1, 26.0, 23.9, 20.8, 10.3; ESI-HRMS: m/z calcd for $C_{33}H_{41}O_9$ $[M + H]^+$: 581.27451; found: 581.27357; $[\alpha]_D^{20}$ = +44.06 (c = 0.14, CH_2Cl_2).

6-(((2*S*,3*S*,4*R*,5*S*,6*R*)-4,5-bis(benzyloxy)-6-((benzyloxy)methyl)-3-(2-oxopropyl)tetrahydro-2*H*-pyran-2-yl)methyl)-2,2,5-trimethyl-4*H*-1,3-dioxin-4-one (123v)

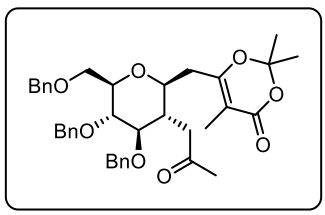

Synthesis according to the **procedure E** by using D-A cyclopropanated carbohydrate **7** (47.3 mg, 0.1 mmol) to afford **123v** (28.2 mg. 0.04 mmol, 45%) as a pale-yellow syrup. The β-anomer was

assigned based on NOESY spectrum. (data for β-anomer) ^{1}H NMR (700 MHz, $CDCl_3$) δ 7.35–7.20 (m, 15H), 4.93 (d, *J* = 11.5 Hz, 1H), 4.78 (d, *J* = 11.0 Hz, 1H), 4.63 (d, *J* = 11.0 Hz, 1H), 4.57–4.54 (m, 2H), 4.50 (d, *J* = 12.0 Hz, 1H), 3.68–3.64 (m, 2H), 3.59 (dd, *J* = 10.8, 1.7 Hz, 1H), 3.51 (td, *J* = 9.9, 2.8 Hz, 1H), 3.46 (dd, *J* = 10.5, 8.9 Hz, 1H), 3.34 (ddd, *J* = 9.8, 4.1, 1.8 Hz, 1H), 2.57 (dd, *J* = 14.2, 9.8 Hz, 1H), 2.45 (dd, *J* = 17.6, 4.7 Hz, 1H), 2.36 (dd, *J* = 17.6, 5.4 Hz, 1H), 2.19–2.14 (m, 2H), 2.00 (s, 3H), 1.85 (s, 3H), 1.61 (s, 3H), 1.53 (s, 3H); ^{13}C NMR (176 MHz, $CDCl_3$) δ 206.5, 162.7, 162.5, 138.3, 138.0, 138.0, 128.5 (2×C), 128.4 (2×C), 128.4 (2×C), 127.8 (5×C), 127.7, 127.7, 127.6 (2×C), 105.0, 102.9, 83.4, 79.9, 79.2, 76.6, 74.7, 74.5, 73.5, 69.0, 42.8, 41.8, 34.9, 30.0, 26.4, 23.6, 10.4; ESI-HRMS: m/z calcd for $C_{38}H_{45}O_8$ $[M + H]^+$: 629.31089; found: 629.31252; $[\alpha]_D^{20}$ = +13.08 (c = 0.26, CH_2Cl_2).

5-Benzyl-6-(((2*S*,3*S*,4*R*,5*R*,6*R*)-4,5-bis(benzyloxy)-6-((benzyloxy)methyl)-3-(2-oxopropyl)tetrahydro-2*H*-pyran-2-yl)methyl)-2,2-dimethyl-4*H*-1,3-dioxin-4-one (123w)

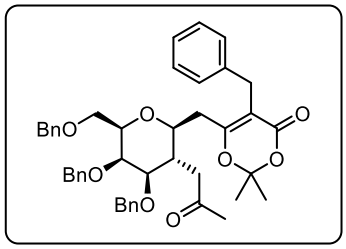

Synthesis according to the **procedure E** by using D-A cyclopropanated carbohydrate **6** (47.3 mg, 0.1 mmol) to afford **123w** (26.5 mg, 0.04 mmol, 32%) as a pale-yellow syrup. The β-anomer was assigned based on NOESY spectrum. (data for β-anomer) ^{1}H NMR (700 MHz, $CDCl_3$) δ 7.36–7.24 (m, 17H), 7.19–7.17 (m, 2H), 7.14–7.12 (m, 1H), 4.85 (d, *J* = 11.4 Hz, 1H), 4.68 (d, *J* = 11.4 Hz, 1H), 4.54 (d, *J* = 11.4 Hz, 1H), 4.41 (q, *J* = 11.7 Hz, 2H), 4.35 (d, *J* = 11.4 Hz, 1H), 3.96 (s, 1H), 3.63 (s, 2H), 3.60 (ddd, *J* = 10.2, 8.7, 3.3 Hz, 1H), 3.57–3.54 (m, 1H), 3.50–3.48 (m, 1H), 3.43–3.40 (m, 2H), 2.64 (dd, *J* = 14.6, 8.7 Hz, 1H), 2.59 (sept, *J* = 5.3 Hz, 1H), 2.45–2.42 (m, 1H), 2.41–2.37 (m, 2H), 2.02 (s, 3H), 1.59 (s, 3H), 1.52 (s, 3H); ^{13}C NMR (176 MHz, $CDCl_3$) δ 207.1, 164.1, 162.3, 139.8, 138.8, 137.8, 137.6, 128.5 (2×C), 128.5 (2×C), 128.4 (2×C), 128.2 (3×C), 128.2 (3×C), 127.9 (3×C), 127.9, 127.9, 127.8 (2×C), 127.6, 126.0, 107.0, 105.2, 81.9, 77.1, 76.8, 74.4, 73.5, 71.4, 71.2, 69.2, 42.0, 38.3, 34.7, 30.5, 30.1, 26.0, 24.3; ESI-HRMS: m/z calcd for $C_{44}H_{49}O_8$ $[M + H]^+$: 705.34219; found: 705.34432; $[\alpha]_D^{20}$ = +5.88 (c = 0.15, CH_2Cl_2).

6-(((2*S*,3*S*,4*R*,5*R*,6*R*)-4,5-bis(benzyloxy)-6-((benzyloxy)methyl)-3-((*E*)-2-((tert-butyldimethylsilyl)oxy)prop-1-en-1-yl)tetrahydro-2*H*-pyran-2-yl)methyl)-2,2-dimethyl-4*H*-1,3-dioxin-4-one (125)

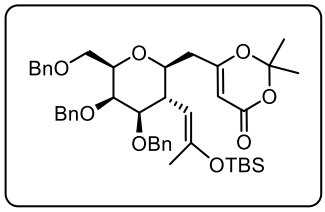

Synthesis according to the **procedure E** to afford **125** as a pale-yellow syrup. (data for β-anomer) ^{1}H NMR (700 MHz, $CDCl_3$) δ 7.35–7.25 (m, 15H), 5.32 (s, 1H), 4.88 (d, *J* = 11.7 Hz, 1H), 4.66 (d, *J* = 12.0 Hz, 1H), 4.61 (d, *J* = 11.7 Hz, 1H), 4.50 (d, *J* = 12.0 Hz, 1H), 4.44–4.38 (m, 2H), 4.00 (d, *J* = 9.8 Hz, 1H), 3.89–3.87 (m, 1H), 3.58–3.55 (m, 1H), 3.53–3.50 (m, 1H), 3.44–3.42 (m, 1H), 3.27–3.24 (m, 1H), 3.21–3.18 (m, 1H), 3.14–3.10 (m, 1H), 2.61–2.59 (m, 1H), 2.35 (dd, *J* = 15.5, 9.9 Hz, 1H), 1.82 (s, 3H), 1.63 (s, 3H), 1.56 (s, 3H), 0.93 (s, 9H), 0.18 (s, 3H), 0.15 (s, 3H); ^{13}C NMR (176 MHz, $CDCl_3$) δ 170.2, 161.4, 150.9, 138.8, 138.7, 137.9, 128.4 (2×C), 128.3 (2×C), 128.1 (2×C), 128.1 (2×C), 127.9 (2×C), 127.7, 127.6 (2×C), 127.4, 127.4, 106.3, 94.9, 82.9, 77.4, 77.4, 74.2, 73.5 (2×C), 71.6, 71.5 (2×C), 69.5, 39.9, 37.8, 25.6 (3×C), 24.0, 23.1, 18.1, –3.58, –3.59; ESI-HRMS: m/z calcd for $C_{43}H_{57}O_8Si$ $[M + H]^+$: 729.38172; found: 729.38437; $[\alpha]_D^{20}$ = +7.75 (c = 0.13, CH_2Cl_2).

1-((3*R*,4*R*,5*R*,6*R*)-4,5-bis(benzyloxy)-6-((benzyloxy)methyl)-2-((tert-butyldimethylsilyl)oxy)tetrahydro-2*H*-pyran-3-yl)propan-2-one (126)

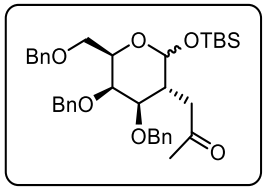

Synthesis according to the **procedure E** to afford **126**. ^{1}H NMR (500 MHz, toluene-d_8) δ 7.35–6.99 (m, 15H), 5.50 (d, *J* = 2.9 Hz, 1H), 4.91 (d, *J* = 11.4 Hz, 1H), 4.58 (d, *J* = 11.6 Hz, 1H), 4.38–4.30 (m, 3H), 4.22–4.19 (m, 1H), 4.05 (d, *J* = 11.6 Hz, 1H), 3.98 (s, 1H), 3.84 (t, *J* = 8.4 Hz, 1H), 3.65 (dd, *J* = 9.1, 5.6 Hz, 1H), 3.57 (dd, *J* = 11.3, 2.3 Hz, 1H), 3.17–3.12 (m, 1H), 2.71 (dd, *J* = 17.1, 5.2 Hz, 1H), 2.19 (dd, *J* = 17.2, 8.9 Hz, 1H), 1.72 (s, 3H), 0.95 (s, 9H), 0.16 (s, 3H), 0.05 (s, 3H); ^{13}C NMR (126 MHz, toluene-d_8) δ 205.5, 139.7, 138.9, 138.6, 137.2, 129.3, 129.2 (2×C),

128.5, 128.5, 128.4 (2×C), 128.4, 128.2 (2×C), 128.1, 128.0, 127.8, 127.4, 125.4, 94.6, 78.3, 74.7, 73.6, 72.3, 71.1, 70.2, 69.8, 42.5, 38.2, 29.3, 26.1, 25.9, 18.3, –4.36, –5.80; ESI-HRMS: m/z calcd for $C_{36}H_{48}O_6NaSi$ $[M + Na]^+$: 627.31124; found: 627.31008; $[\alpha]_D^{20}$ = +39.23 (c = 0.36, CH_2Cl_2).

1-((3*R*,4*R*,5*R*,6*R*)-4,5-bis(benzyloxy)-6-((benzyloxy)methyl)-2-hydroxytetrahydro-2*H*-pyran-3-yl)propan-2-one (127)

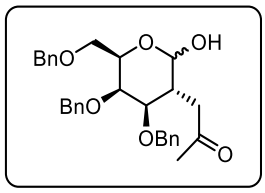

Synthesis according to the **procedure E** to afford **127**. ^{1}H NMR (700 MHz, toluene-d_8) δ 7.30–7.02 (m, 15H), 5.34 (s, 1H), 4.86 (d, *J* = 11.5 Hz, 1H), 4.50 (d, *J* = 11.4 Hz, 1H), 4.41–4.30 (m, 3H), 4.26–4.24 (m, 1H), 4.08 (d, *J* = 11.5 Hz, 1H), 3.86 (s, 1H), 3.78–3.74 (m, 1H), 3.71–3.66 (m, 1H), 3.60 (dd, *J* = 11.5, 2.4 Hz, 1H), 3.34 (s, 1H), 3.10–3.06 (m, 1H), 2.63 (dd, *J* = 16.9, 5.2 Hz, 1H), 2.32 (dd, *J* = 16.9, 8.5 Hz, 1H), 1.70 (s, 3H); ^{13}C NMR (176 MHz, toluene-d_8) δ 206.7, 139.7, 138.9, 138.8, 128.6, 128.6, 128.6 (2×C), 128.5 (2×C), 128.4, 128.4 (2×C), 128.2 (2×C), 128.0 (2×C), 127.8, 127.5, 94.0, 78.5, 74.7, 73.6, 72.8, 71.3, 70.2, 69.9, 42.0, 37.3, 29.6; ESI-HRMS: m/z calcd for $C_{30}H_{34}O_6Na$ $[M + Na]^+$: 513.22476; found: 513.22335; $[\alpha]_D^{20}$ = +60.47 (c = 0.13, CH_2Cl_2).

6-(((2*S*,3*S*,4*R*,5*R*,6*R*)-4,5-bis(benzyloxy)-6-((benzyloxy)methyl)-3-((*R*)-2-oxopropyl-1-d)tetrahydro-2*H*-pyran-2-yl)methyl)-2,2-dimethyl-4*H*-1,3-dioxin-4-one (128)

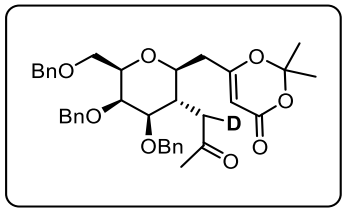

Synthesis according to **procedure E** by using D-A cyclopropanated carbohydrate **6** (47.3 mg, 0.1 mmol) but D_2O (0.9 μL, 0.05 mmol, 0.5 equiv.) was added instead of H_2O to afford **128** (43.1mg, 70.1 μmol, 70%) as a pale-yellow syrup. The β-anomer was assigned based on NOESY spectrum. ^{1}H NMR (700 MHz, $CDCl_3$) δ 7.34–7.23 (m, 15H), 5.29 (s, 1H), 4.81 (d, *J* = 11.5 Hz, 1H), 4.66

(d, *J* = 11.4 Hz, 1H), 4.53 (d, *J* = 11.5 Hz, 1H), 4.42 (q, *J* = 11.7 Hz, 2H), 4.33 (d, *J* = 11.4 Hz, 1H), 3.94 (d, *J* = 1.4 Hz, 1H), 3.56–3.52 (m, 2H), 3.51–3.47 (m, 2H), 3.41 (dd, *J* = 10.9, 2.0 Hz, 1H), 2.54 (sept, *J* = 5.3 Hz, 1H), 2.45–2.41 (m, 2H), 2.39–2.34 (m, 2H), 2.03 (s, 3H), 1.58 (s, 3H), 1.53 (s, 3H); ^{13}C NMR (176 MHz, $CDCl_3$) δ 207.0, 168.6, 161.2, 138.5, 137.8, 137.5, 128.5 (2×C), 128.4 (2×C), 128.2 (2×C), 128.1 (2×C), 127.9 (2×C), 127.9 (3×C), 127.8, 127.6, 106.6, 95.7, 81.7, 77.2, 76.2, 74.4, 73.5, 71.2, 71.0, 69.1, 41.8, 37.9, 37.3, 30.0, 25.6, 24.2; ESI-HRMS: m/z calcd for $C_{37}H_{42}O_8{}^2D$ $[M + H]^+$: 616.30152; found: 616.29997; $[\alpha]_D^{20}$ = –3.11 (c = 0.32, CH_2Cl_2).

Methyl 4-((2*S*,3*S*,4*R*,5*R*,6*R*)-4,5-bis(benzyloxy)-6-((benzyloxy)methyl)-3-(2-oxopropyl)tetrahydro-2*H*-pyran-2-yl)-3-oxobutanoate (129)[55]

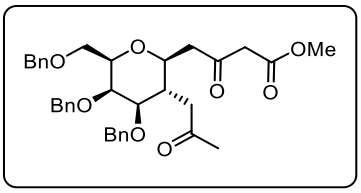

A round bottom flask was charged with a stirring bar, **123a** (50.0 mg, 81.3 μmol, 1 equiv.), anhydrous MeOH (0.033 mL, 0.81 mmol, 10 equiv.) and anhydrous toluene (1 mL) were added. The resulting mixture was heated to 90 °C in an oil bath and stirred for 3 hours. The reaction mixture was cooled to room temperature and directly put onto silica gel and purified by silica flash column chromatography (pentane: Et_2O = 2:1, R_f = 0.42 (EtOAc:*c*-hex = 1:1)) to afford **129** (35.2 mg, 59.8 μmol, 74%) as pale-yellow syrup. ^{1}H NMR (700 MHz, $CDCl_3$) δ 7.33–7.21 (m, 15H), 4.82 (d, *J* = 11.6 Hz, 1H), 4.65 (d, *J* = 11.5 Hz, 1H), 4.53 (d, *J* = 11.6 Hz, 1H), 4.45–4.40 (m, 2H), 4.33 (d, *J* = 11.5 Hz, 1H), 3.93 (d, *J* = 2.1 Hz, 1H), 3.73 (ddd, *J* = 10.4, 8.0, 3.7 Hz, 1H), 3.65 (s, 3H), 3.55–3.48 (m, 3H), 3.47 (s, 2H), 3.37 (dd, *J* = 10.9, 2.4 Hz, 1H), 2.76 (dd, *J* = 15.7, 8.0 Hz, 1H), 2.62 (dd, *J* = 15.7, 3.7 Hz, 1H), 2.53 (sept, *J* = 5.3 Hz, 1H), 2.44 (dd, *J* = 17.1, 5.3 Hz, 1H), 2.32 (dd, *J* = 17.1, 5.5 Hz, 1H), 2.00 (s, 3H); ^{13}C NMR (176 MHz, $CDCl_3$) δ 207.3, 201.6, 167.6, 138.7, 137.9, 137.5, 128.5 (2×C), 128.4 (2×C), 128.2 (2×C), 128.0 (2×C), 127.9 (2×C), 127.8, 127.8 (2×C), 127.8, 127.5, 81.8, 77.1, 76.3, 74.3, 73.5, 71.2, 71.0, 69.0, 52.2, 49.9, 46.9, 41.9, 37.9, 29.9; ESI-HRMS: m/z calcd for $C_{35}H_{41}O_8$ $[M + H]^+$: 589.27959; found: 589.28211; $[\alpha]_D^{20}$ = +20.18 (c = 0.11, CH_2Cl_2).

Isopropyl 4-((2*S*,3*S*,4*R*,5*R*,6*R*)-4,5-bis(benzyloxy)-6-((benzyloxy)methyl)-3-(2-oxopropyl) tetrahydro-2*H*-pyran-2-yl)-3-oxobutanoate (130)[55]

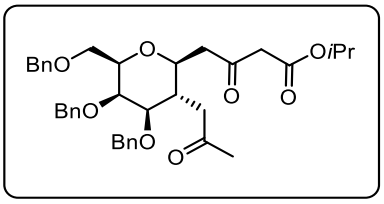

A round bottom flask was charged with a stirring bar, **123a** (20.0 mg, 32.5 μmol, 1 equiv.), isopropanol (0.025 mL, 0.33 mmol, 10 equiv.) and anhydrous toluene (1 mL) were added. The resulting mixture was heated to 90 °C in an oil bath, and stirred for 10 h. The reaction mixture was cooled to room temperature and directly put onto silica gel and purified by silica flash column chromatography (pentane:Et_2O = 1:1, R_f = 0.67 (EtOAc:*c*-hex = 1:1)) to afford **130** (15.5 mg, 25.1 μmol, 77%) as pale-yellow syrup. ^{1}H NMR (700 MHz, $CDCl_3$) δ 7.32–7.21 (m, 15H), 4.98 (pent, *J* = 6.3 Hz, 1H), 4.81 (d, *J* = 11.6 Hz, 1H), 4.64 (d, *J* = 11.5 Hz, 1H), 4.53 (d, *J* = 11.6 Hz, 1H), 4.42 (q, *J* = 11.8 Hz, 2H), 4.32 (d, *J* = 11.5 Hz, 1H), 3.93 (d, *J* = 2.1 Hz, 1H), 3.72 (ddd, *J* = 10.5, 8.1, 3.7 Hz, 1H), 3.55–3.47 (m, 3H), 3.40 (s, 2H), 3.36 (dd, *J* = 10.9, 2.4 Hz, 1H), 2.76 (dd, *J* = 15.9, 8.0 Hz, 1H), 2.61 (dd, *J* = 15.9, 3.7 Hz, 1H), 2,53 (sept, *J* = 5.3 Hz, 1H), 2.43 (dd, *J* = 17.1, 5.4 Hz, 1H), 2.31 (dd, *J* = 17.0, 5.5 Hz, 1H), 2.00 (s, 3H), 1.19 (t, *J* = 5.6 Hz, 6H); ^{13}C NMR (176 MHz, $CDCl_3$) δ 207.3, 201.8, 166.7, 138.7, 137.9, 137.6, 128.5 (2×C), 128.4 (2×C), 128.2 (2×C), 128.0 (2×C), 127.9 (2×C), 127.8 (3×C), 127.8, 127.5, 81.9, 77.1, 76.3, 74.3, 73.5, 71.2, 71,0, 68.9, 68.8, 50.4, 46.9, 41.9, 37.9, 29.9, 21.7, 21.7; ESI-HRMS: m/z calcd for $C_{37}H_{45}O_8$ $[M + H]^+$: 617.31089; found: 617.31398; $[\alpha]_D^{20}$ = +13.21 (c = 0.11, CH_2Cl_2).

6-(((2*S*,3*R*,4*R*,5*R*,6*R*)-4,5-dihydroxy-6-(hydroxymethyl)-3-(2-oxopropyl)tetrahydro-2*H*-pyran-2-yl)methyl)-2,2-dimethyl-4*H*-1,3-dioxin-4-one (131)[55]

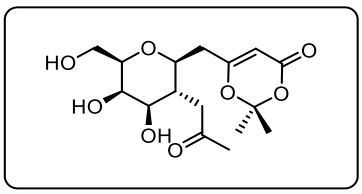

To a solution of **123a** (60.0 mg, 97.6 μmol, 1 equiv.) in CH_2Cl_2 (2.5 mL) was added 10 wt% Pd/C (31 mg, 30 mol%), and the resulting mixture was stirred 24 h at room temperature under hydrogen balloon. The mixture was filtered through a pad of celite, and the resulting filtrate was concentrated

under reduced pressure. The crude product was purified by silica gel column chromatography (MeOH:CH_2Cl_2 = 1:15, R_f = 0.36 (MeOH:CH_2Cl_2 = 1:9)) to afford the title compound **131** (28.9 mg, 83.9 μmol, 86%) as a colorless syrup. ^{1}H NMR (400 MHz, CD_3OD) δ 5.42 (s, 1H), 3.86–3.81 (m, 1H), 3.75–3.66 (m, 3H), 3.62–3.55 (m, 1H), 3.50–3.44 (m, 2H), 3.37–3.36 (m, 1H), 2.93–2.81 (m, 1H), 2.76 (dd, *J* = 17.5, 4.8 Hz, 1H), 2.59–2.52 (m, 2H), 2.46–2.39 (m, 1H), 2.36–2.28 (m, 1H), 2.23 (s, 3H), 1.74 (s, 3H), 1.73 (s, 3H); compound decomposed during ^{13}C NMR measurement, HRMS measurement and optical rotation measurement.

1,1'-((2*S*,3*S*,4*R*,5*R*,6*R*)-4,5-bis(benzyloxy)-6-((benzyloxy)methyl)tetrahydro-2*H*-pyran-2,3-diyl)bis(propan-2-one) (132)

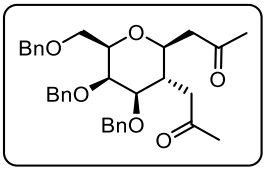

A round bottom flask was charged with a stirring bar, **123a** (20.0 mg, 32.5 μmol), K_2CO_3 (18.0 mg, 0.13 mmol, 4 equiv.) and anhydrous dichloroethane (1 mL) were added. The resulting mixture was heated to 80 °C in an oil bath, and stirred for 24 hours. The reaction mixture was cooled to room temperature, and directly put onto silica gel, and purified by column chromatography (pentane: Et_2O = 2:1, R_f = 0.33 (EtOAc:*c*-hex = 1:1)) to afford **132** (15.3 mg, 28.8 μmol, 89%) as colorless syrup. ^{1}H NMR (700 MHz, $CDCl_3$) δ 7.35–7.23 (m, 15H), 4.84 (d, *J* = 11.6 Hz, 1H), 4.67 (d, *J* = 11.5 Hz, 1H), 4.57 (d, *J* = 11.6 Hz, 1H), 4.44 (q, *J* = 11.8 Hz, 2H), 4.35 (d, *J* = 11.5 Hz, 1H), 3.95 (d, *J* = 2.1 Hz, 1H), 3.73 (ddd, *J* = 10.4, 8.1, 3.7 Hz, 1H), 3.58–3.51 (m, 3H), 3.37 (dd, *J* = 10.9, 2.4 Hz, 1H), 2.72 (dd, *J* = 15.9, 8.0 Hz, 1H), 2.56 (sept, *J* = 5.6 Hz, 1H), 2.51–2.45 (m, 2H), 2.31 (dd, *J* = 17.0, 5.6 Hz, 1H), 2.13 (s, 3H), 2.03 (s, 3H); ^{13}C NMR (176 MHz, $CDCl_3$) δ 207.5 (2×C), 138.7, 138.0, 137.6, 128.5 (2×C), 128.4 (2×C), 128.2 (2×C), 128.1 (2×C), 127.9 (2×C), 127.8 (3×C), 127.8, 127.5, 82.1, 77.1, 76.5, 74.3, 73.5, 71.2, 70.9, 69.1, 47.5, 42.1, 38.0, 31.1, 29.9; ESI-HRMS: m/z calcd for $C_{33}H_{39}O_6$ $[M + H]^+$: 531.27412; found: 531.27557; $[\alpha]_D^{20}$ = +13.25 (c = 0.08, CH_2Cl_2).

9.9 Synthesis of coumarin derivative 135

4-Methyl-2-oxo-2*H*-chromene-3-carbonitrile (135)[57]

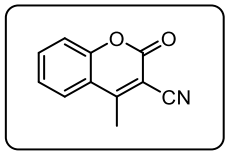

Hydroxyacetophenone (17.7 mL, 146.9 mmol, 1 equiv.), ethyl cyanoacetate (23.4 mL, 220.4 mmol, 1.5 equiv.) and ammonium acetate (28.3 g, 0.37 mol, 2.5 equiv.) were added sequentially into a 250 mL round bottom flask under air, fitted with a reflux condenser and heated to 150–170 ºC for 5 h. The mixture was then cooled to rt, 95% EtOH (100 mL) was added and the mixture was stirred overnight. The precipitated solid was filtered and recrystallized in an acetone/H_2O mixture, filtered, washed with *c*-hexane and dried under a high vacuum to yield coumarin **135** (9.48 g, 51.2 mmol, 35%) as white prism. The analytical data was in accordance to the literature.[57] ^{1}H NMR (500 MHz, $CDCl_3$) δ 7.76–7.69 (m, 2H), 7.44–7.40 (m, 2H), 2.79 (s, 3H); ^{13}C NMR (126 MHz, $CDCl_3$) δ 162.3, 156.7, 153.3, 135.2, 126.0, 125.4, 118.2, 117.7, 113.4, 102.5, 18.3; ESI-HRMS: m/z calcd for $C_{11}H_8O_2N$ $[M + H]^+$: 186.05496; found: 186.05423.

9.10 Synthesis of oxindole dienolates

Synthesis of oxindole derivative precursors s16 and s17[58]

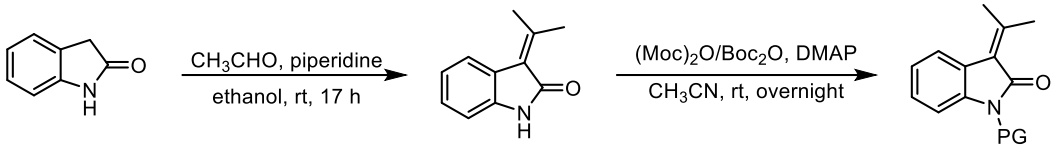

s14 **s15** **s16** PG = Moc **s17** PG = Boc

To a suspension of oxindole **s14** (20.0 g, 0.15 mol), 333 mL 1:1 mixture of acetone/ethanol was added together with piperidine (59.4 mL, 0.60 mmol, 4 equiv.) and stirred for 17 h at room temperature. The mixture was filtered and washed with pentane and vacuum dried to afford **s15** (21.2 g, 0.12 mmol, 81%) as a yellow solid. The analytical data was in accordance to the literature.[58] ^{1}H NMR (400 MHz, $CDCl_3$) δ 8.28 (br, 1H), 7.52 (d, *J* = 7.7 Hz, 1H), 7.19 (t, *J* = 7.7 Hz, 1H), 7.01 (td, *J* = 7.7, 1.2 Hz, 1H), 6.87 (d, *J* = 7.7 Hz, 1H), 2.62 (s, 3H), 2.39 (s, 3H); ^{13}C

NMR (101 MHz, $CDCl_3$) δ 169.6, 155.6, 139.3, 127.5, 124.4, 123.7, 123.0, 121.6, 109.3, 25.3, 23.1; ESI-HRMS: m/z calcd for $C_{11}H_{12}ON$ $[M + H]^+$: 174.09134; found: 174.09054.

To a suspension of **s15** (5.0 g, 28.9 mmol, 1 equiv.) and DMAP (705 mg, 5.77 mmol, 0.2 equiv.) in 60 mL anhydrous acetonitrile, dimethyl decarbonate (6.19 mL, 57.7 mmol, 2 equiv.) was added dropwise. The mixture was stirred for 14 h and the volatile parts were evaporated under vacuum. Purification by silica gel column chromatography by EtOAc:*c*-hex = 1:9 (R_f = 0.32 (EtOAc:*c*-hex = 1:4)) provided **s16** (4.24 g, 18.35 mmol, 64%) as white solid. The analytical data was in accordance to the literature.[58] ^{1}H NMR (400 MHz, $CDCl_3$) δ 8.00 (d, *J* = 8.2 Hz, 1H), 7.59 (d, *J* = 7.8 Hz, 1H), 7.30 (t, *J* = 7.8 Hz, 1H), 7.18 (t, *J* = 7.7 Hz, 1H), 4.03 (s, 3H), 2.61 (s, 3H), 2.42 (s, 3H); ^{13}C NMR (126 MHz, $CDCl_3$) δ 165.5, 157.8, 151.9, 137.4, 127.9, 124.2, 124.0, 123.1, 121.4, 114.7, 53.7, 26.1, 24.2.

To a suspension of oxindole **s15** (500.0 mg, 2.89 mmol, 1 equiv.) in 6 mL anhydrous acetonitrile, DMAP (70.5 mg, 0.58 mmol, 0.2 equiv.) and then di-*tert*-butyl decarbonate (1.26 g, 5.77 mmol, 2 equiv.) solution in 3.1 mL anhydrous acetonitrile were added dropwise at –20 ºC. The mixture was stirred for 3 h at –20 ºC and the volatile parts were evaporated. Precipitation by pentane provided **s17** (549 mg, 2.01 mmol, 70%) as white solid. The analytical data was in accordance to the literature.[58] ^{1}H NMR (400 MHz, $CDCl_3$) δ 7.89 (d, *J* = 8.2 Hz, 1H), 7.58 (d, *J* = 8.1 Hz, 3H), 7.30–7.25 (m, 1H), 7.15 (td, *J* = 7.7, 1.1 Hz, 3H), 2.62 (s, 3H), 2.41 (s, 3H), 1.66 (s, 9H); ^{13}C NMR (126 MHz, CD_2Cl_2) δ 165.9, 157.3, 150.1, 138.5, 128.1, 124.6, 124.0, 123.8, 122.1, 114.8, 84.1, 28.4 (3×C), 26.3, 24.3.

Methyl 2-((tert-butyldimethylsilyl)oxy)-3-(prop-1-en-2-yl)-1*H*-indole-1-carboxylate (140)[58]

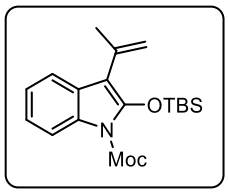

To an ice bath cooled solution of **s16** (3.00 g, 13.0 mmol, 1 equiv.) in freshly distilled CH_2Cl_2 (52 mL), triethylamine (5.43 mL, 38.9 mmol, 3 equiv.) and TBSOTf (3.87 mL, 16.9 mmol, 1.3 equiv.) were sequentially added. After 45 h, the mixture was flushed through a short pad of silica and

precipitation with pentane to afford **140** (4.00 g, 11.6 mmol, 89%) as white solid. The analytical data was in accordance to the literature.[58] ^{1}H NMR (400 MHz, $CDCl_3$) δ 8.05–8.01 (m, 1H), 7.54–7.50 (m, 1H), 7.23–7.18 (m, 2H), 5.30 (s, 1H), 5.22 (s, 1H), 3.99 (s, 3H), 2.13 (s, 3H), 1.04 (s, 9H), 0.16 (s, 6H); ^{13}C NMR (126 MHz, CD_2Cl_2) δ 152.2, 143.6, 137.1, 131.9, 128.4, 123.5, 123.0, 119.1, 116.9, 115.0, 105.7, 53.8, 26.0 (3×C), 23.2, 18.5, –4.11 (2×C).

***Tert*-butyl 2-((tert-butyldimethylsilyl)oxy)-3-(prop-1-en-2-yl)-1*H*-indole-1-carboxylate (141)**[58]

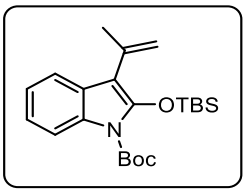

To an ice bath cooled solution of **s17** in freshly distilled CH_2Cl_2 (27 mL), triethylamine (1.07 mL, 7.68 mmol, 1.4 equiv.) and TBSOTf (1.39 mL, 6.04 mmol, 1.1 equiv.) were sequentially added After 7 h, the volatile parts were evaporated, directly filtered through a 5 cm silica column, concentrate solution and recrystallized with pentane to afford **141** (1.37 g, 3.53 mmol, 64%) as white solid. The analytical data was in accordance to the literature.[58] ^{1}H NMR (400 MHz, $CDCl_3$) δ 7.81–7.79 (m, 1H), 7.53–7.51 (m, 1H), 7.20–7.13 (m, 2H), 5.28 (s, 1H), 5.21 (s, 1H), 2.13 (s, 3H), 1.68 (s, 9H), 1.03 (s, 9H), 0.17 (s, 6H); ^{13}C NMR (126 MHz, CD_2Cl_2) δ 149.6, 144.6, 137.2, 131.2, 128.1, 122.9, 122.5, 119.0, 116.5, 114.8, 105.5, 84.2, 28.5 (3×C), 26.1 (3×C), 23.3, 18.6, –4.08 (2×C).

9.11 Synthesis of rearrangement compound via strain-release pyranosylation

Methyl (*Z*)-3-(1-((2*R*,3a*R*,4*R*,5*R*,6*R*,7a*R*)-4,5-bis(benzyloxy)-6-((benzyloxy)methyl)-2-methylhexahydro-4*H*-furo[2,3-b]pyran-2-yl)propan-2-ylidene)-2-oxoindoline-1-carboxylate (148b)

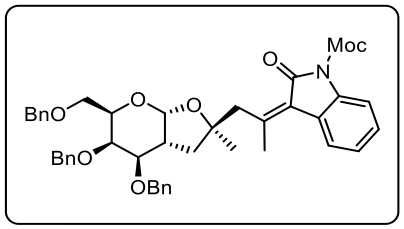

An oven dried tube with a stirring bar was charged with D-A cyclopropanated carbohydrate **6** (47.3 mg, 0.1 mmol, 1.0 equiv.), vinylogous enolate **140** (0.4 mmol, 4.0 equiv.) and anhydrous CH_2Cl_2 (1 mL). The tube was purged with argon and sealed with a rubber stopper. After stirred 10 mins at 0 °C, calcium (II) bis(trifluoromethanesulfonimide) (0.02 mmol, 20 mol%), and tetrabutylammonium hexafluorophosphate (0.02 mmol, 20 mol%) were added. The tube was sealed with parafilm and stirred at room temperature for 24 h. Upon completion of the reaction, the reaction mixture was flushed through a short pad of silica gel with EtOAc and subjected to silica flash column chromatography (pentane:Et_2O = 2:1 to 1:1 to 1:2 (R_f = 0.3 (pentane:Et_2O = 1:1)) to provide **148b** (24.3 mg, 34.5 μmol, 35%) as a pale-yellow syrup. ^{1}H NMR (700 MHz, $CDCl_3$) δ 7.99 (d, *J* = 8.1 Hz, 1H), 7.60 (d, *J* = 7.8 Hz, 1H), 7.36–7.27 (m, 16H), 7.19 (t, *J* = 7.4 Hz, 1H), 5.43 (d, *J* = 4.4 Hz, 1H), 4.87 (d, *J* = 11.6 Hz, 1H), 4.65 (dd, *J* = 17.4, 11.8 Hz, 2H), 4.49 (q, *J* = 11.8 Hz, 2H), 4.39 (d, *J* = 11.9 Hz, 1H), 4.03 (s, 3H), 4.01–3.99 (m, 2H), 3.76 (d, *J* = 12.3 Hz, 1H), 3.68 (t, *J* = 8.5 Hz, 1H), 3.62 (dd, *J* = 9.0, 5.4 Hz, 1H), 3.46 (dd, *J* = 9.8, 1.9 Hz, 1H), 2.94 (d, *J* = 12.3 Hz, 1H), 2.50–2.47 (m, 1H), 2.46 (s, 3H), 2.11 (dd, *J* = 13.6, 8.1 Hz, 1H), 1.89 (dd, *J* = 13.6, 2.6 Hz, 1H), 1.12 (s, 3H); ^{13}C NMR (176 MHz, $CDCl_3$) δ 165.4, 158.9, 151.8, 138.6, 138.0, 137.6, 137.5, 128.6 (2×C), 128.4 (2×C), 128.3 (2×C), 128.3 (2×C), 128.2, 128.1 (2×C), 128.0, 128.0 (2×C), 127.8, 127.6, 124.2, 124.2, 124.0, 123.6, 114.6, 100.8, 81.7, 78.7, 74.0, 73.5, 72.0, 70.7, 70.1, 68.4, 53.8, 46.9, 40.1, 39.6, 27.8, 26.1; ESI-HRMS: m/z calcd for $C_{43}H_{45}O_8NNa$ $[M + H]^+$: 726.30374; found: 726.30340; $[\alpha]_D^{20}$ = +7.78 (c = 0.17, CH_2Cl_2).

9.12 Synthesis of glycosyl imidates

Synthesis of pyranosides 150 and 151

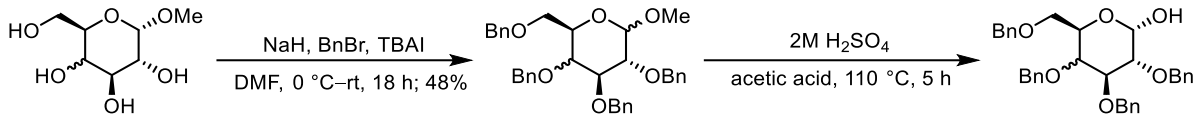

Glc: **s18**
Gal: **s19**

Glc: **s20**
Gal: **92**

Glc: **150**
Gal: **151**

Methyl 2,3,4,6-tetra-*O*-Benzyl-D-glucopyranose (s20)[63]

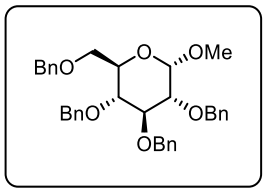

α-D-Methylglucoside (10.8 g, 55.51 mmol) was dissolved in anhydrous DMF (215 mL). The resulting solution was cooled at 0 °C and sodium hydride (60% in oil, 17.8 g, 0.44 mol, 8 equiv.) was added slowly and stirred for 30 mins. Then, benzyl bromide (52.8 mL, 0.44 mmol, 8 equiv.) and tetrabutylammonium iodide (4.1 g, 11.1 mmol, 0.2 equiv.) were added slowly. The solution was stirred for 18 h at room temperature under argon atmosphere. After completion of the reaction, the mixture was cooled in a water bath and quenched with MeOH. The organic layer was extracted four times with CH_2Cl_2 and the combined extracts were washed with brine (3 × 500 mL), water (3 × 500 mL), dried over $MgSO_4$ and concentrated under vacuum. The product was purified by silica flash column chromatography (pentane:Et_2O = 4:1, R_f = 0.18 (pentane:Et_2O = 4:1)) to give product **s20** (14.8 g, 26.68 mmol, 48%) as a pale-yellow syrup. The analytical data was in accordance to the literature.[63] (data for α-anomer) ^{1}H NMR (500 MHz, DMSO–d_6) δ 7.36–7.25 (m, 18 H), 7.19–7.17 (m, 2H), 4.85–4.83 (m, 2H), 4.73 (d, J = 8.0 Hz, 1H), 4.71 (d, J = 8.2 Hz, 1H), 4.68–4.62 (m, 2 H), 4.53–4.45 (m, 3H), 3.76 (t, J = 9.2 Hz, 1H), 3.62–3.60 (m, 3H), 3.49–3.44 (m, 2H), 3.35 (s, 3H); ^{13}C NMR (126 MHz, DMSO–d_6) δ 138.8, 138.5, 138.3, 138.3, 128.3, 128.3, 128.2, 128.2, 127.7, 127.6, 127.5, 127.5, 127.4, 96.8, 81.2, 79.6, 77.5, 74.5, 74.1, 72.3, 71.4, 69.7, 68.7, 54.5; $[\alpha]_D^{20}$ = +46.60 (c = 1.03, CH_2Cl_2).

2,3,4,6-Tetra-*O*-benzyl-D-glucopyranose (150)[59]

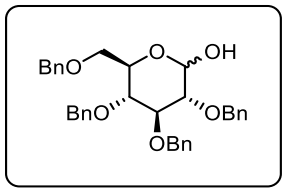

Methyl 2,3,4,6-tetra-*O*-benzyl-α-D-glucopyranoside **s20** (24.3 g, 43.7 mmol, 1 equiv.) was dissolved in a mixture of glacial acetic acid (500 mL) and aqueous H_2SO_4 (2 M, 250 mL). The mixture was refluxed for 5 h at 110 °C and cooled down to room temperature. The reaction mixture was poured into 1.2 L of ice water after the reaction completed. The resulting mixture was extracted with 300 mL dichloromethane for three times. The combined extracts were washed successively with sat. $NaHCO_3$ and brine, dried over $MgSO_4$ and evaporated on a rotary evaporator to afford an oily residue, which was purified by silica flash column chromatography (EtOAc:*c*-hex = 1:4, R_f = 0.42 (EtOAc:*c*-hex = 1:2)) to yield the pure 2,3,4,6-tetra-*O*-benzyl-D-glycopyranoses **150** (anomeric mixtures, 11.9 g, 22.0 mmol, 50%) as white solid. The analytical data was in accordance to the literature.[59] (data for α-anomer) ^{1}H NMR (500 MHz, CD_3OD) δ 7.32–7.12 (m, 20H), 6.58 (d, *J* = 4.4 Hz, 1H), 5.18–5.17 (m, 1H), 4.86–4.82 (m, 1H), 4.80–4.75 (m, 1H), 4.70–4.67 (m, 1H), 4.67–4.65 (m, 1H), 4.63–4.61 (m, 1H), 4.50–4.39 (m, 2H), 3.83–3.77 (m, 2H), 3.62–3.52 (m, 2H), 3.40–3.34 (m, 2H); ^{13}C NMR (126 MHz, CD_3OD) δ 148.3, 148.2, 147.8, 147.7, 137.8 (2×C), 137.7 (2×C), 137.7 (2×C), 137.6 (2×C), 137.2 (2×C), 137.2 (2×C), 137.2 (2×C), 137.1 (2×C), 137.1 (2×C), 137.1 (2×C), 106.2, 93.4, 92.6, 87.4, 84.0, 83.4, 83.0, 81.8, 81.8, 80.7; ESI-HRMS: *m/z* calcd for $C_{34}H_{36}O_6Na$ $[M + Na]^+$: 563.24041; found: 563.23921; $[\alpha]_D^{20}$ = +29.14 (c = 0.53, CH_2Cl_2).

2,3,4,6-Tetra-*O*-benzyl-D-galactopyranose (**151**)[59]

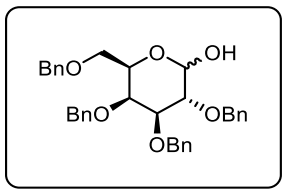

Methyl 2,3,4,6-tetra-*O*-benzyl-α-D-galactopyranoside **92** (20.0 g, 36.1 mmol, 1 equiv.) was dissolved in a mixture of glacial acetic acid (201.6 mL) and aqueous H_2SO_4 (3 M, 31 mL). The solution was refluxed for 7 h at 110 °C and cooled down to room temperature. The mixture was diluted with cold water (240 mL) and ethyl acetate (240 mL). The two layers were separated and

the organic layer was first washed with water to remove excess of AcOH, followed by aqueous sat. $NaHCO_3$, dried over anhydrous $MgSO_4$. The solution was concentrated to get a syrup. The crude syrup was purified by silica gel column chromatography (pentane:Et_2O = 2:1, R_f = 0.52 (EtOAc:*c*-hex = 1:2)) to get 2,3,4,6-tetra-*O*-benzylgalactopyranose **151** (anomeric mixtures, 12.0 g, 22.3 mmol, 62%) as a white solid. The analytical data was in accordance to the literature.[59] (data for α-anomer) ^{1}H NMR (600 MHz, $CDCl_3$) δ 7.37–7.22 (m, 20H), 5.26 (s, 1H), 4.93–4.89 (m, 1H), 4.81–4.76 (m, 2H), 4.76–4.68 (m, 2H), 4.59–4.55 (m, 1H), 4.47–4.44 (m, 1H), 4.39–4.36 (m, 1H), 4.14 (t, *J* = 6.4 Hz, 1H), 4.01 (dd, *J* = 9.8, 3.6 Hz, 1H), 3.93 (m, 2H), 3.59–3.44 (2H); ^{13}C NMR (151 MHz, $CDCl_3$) δ 138.6, 138.5, 138.2, 137.8, 128.4 (2×C), 128.4 (3×C), 128.2 (2×C), 128.2 (2×C), 128.1, 128.0 (2×C), 127.9 (2×C), 127.7, 127.7, 128.6 (2×C), 127.5 (2×C), 91.8, 78.7, 76.5, 74.7, 74.6, 73.5, 73.4, 72.9, 69.4, 69.0; ESI-HRMS: *m/z* calcd for $C_{34}H_{36}O_6Na$ $[M + Na]^+$: 563.24041; found: 563.23952; $[\alpha]_D^{20}$ = +35.04 (c = 1.01, CH_2Cl_2).

2,3,4,6-Tetra-*O*-benzyl-α-D-glucopyranosyl trichloroacetimidate (152)[59]

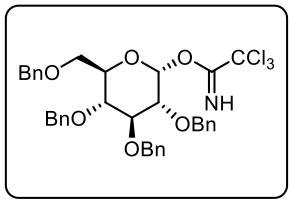

A mixture of 2,3,4,6-tetra-*O*-benzoyl-D-gluctopyranose **150** (1.0 g, 1.85 mmol, 1 equiv.), trichloroacetonitrile (1.8 mL, 18.5 mmol, 10 equiv.), and 1,8-diazabicyclo[5.4.0]undec-7-ene (0.055 mL, 0.37 mmol, 0.2 equiv.) in anhydrous dichloromethane (10 mL) was stirred for 1 h at room temperature and then concentrated. The residue was eluted from a silica gel column chromatography (containing 1% trimethylamine in the eluent, EtOAc:*c*-hex = 1:19, R_f = 0.47 (EtOAc:*c*-hex= 1:2)) to get compound **152** (1.13 g, 1.65 mmol, 89%) as a white solid. The analytical data was in accordance to the literature.[59] ^{1}H NMR (400 MHz, CD_2Cl_2) δ 8.55 (s, 1H), 7.24–7.11 (m, 20H), 6.41 (d, *J* = 3.4 Hz, 1H), 4.85 (d, *J* = 11.0 Hz, 1H), 4.78–4.72 (m, 2H), 4.66 (d, *J* = 11.6 Hz, 1H), 4.59 (d, *J* = 11.6 Hz, 1H), 4.50–4.37 (m, 3H), 3.93 (t, *J* = 9.3 Hz, 1H), 3.88 (ddd, *J* = 10.1, 3.6, 2.0 Hz, 1H), 3.69–3.64 (m, 3H), 3.57 (dd, *J* = 11.0, 2.0 Hz, 1H); ^{13}C NMR (101 MHz, CD_2Cl_2) δ 161.8, 139.5, 139.0, 138.8, 138.8, 129.0 (2×C), 128.9 (2×C), 128.9 (2×C), 128.9 (2×C), 128.6 (2×C), 128.6 (2×C), 128.5 (2×C), 128.3 (4×C), 128.3, 128.1, 92.0, 94.9, 81.9,

80.1, 77.6, 76.2, 75.7, 73.9, 73.9, 73.5, 69.0; ESI-HRMS: *m/z* calcd for $C_{36}H_{36}O_6NCl_2{}^{37}ClNa$ [M + Na]$^+$: 708.14709; found: 708.14671; $[\alpha]_D^{20}$ = +58.33 (c = 0.34, CH_2Cl_2).

2,3,4,6-Tetra-*O*-benzyl-α-D-galactopyranosyl trichloroacetimidate (19)

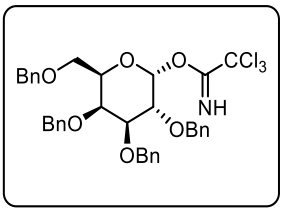

A mixture of 2,3,4,6-tetra-*O*-benzoyl-D-galactopyranose **151** (3.0 g, 5.55 mmol, 1 equiv.), trichloroacetonitrile (5.5 mL, 55.5 mmol, 10 equiv.), and 1,8-diazabicyclo[5.4.0]undec-7-ene (0.17 ml, 1.11 mmol, 0.2 equiv.) in anhydrous dichloromethane 60 mL was stirred for 2 h at room temperature and then concentrated. The residue was eluted from a silica gel column chromatography (containing 1% trimethylamine in the eluent, pentane:Et_2O = 9:1, R_f = 0.17 (pentane:Et_2O = 4:1)) to get compound **19** (2.62 g, 3.83 mmol, 69%) as a white solid. The analytical data was in accordance to the literature.[59] ^{1}H NMR (600 MHz, CD_2Cl_2) δ 8.61 (s, 1H), 7.40–7.28 (m, 20H), 6.52 (d, *J* = 3.5 Hz, 1H), 4.97 (d, *J* = 10.9 Hz, 1H), 4.81 (q, *J* = 11.8 Hz, 2H), 4.76 (s, 2H), 4.57 (d, *J* = 10.9 Hz, 1H), 4.51–4.44 (m, 2H), 4.23–4.18 (m, 2H), 4.10–4.09 (m, 1H), 4.05 (dd, *J* = 10.1, 2.8 Hz, 1H), 3.63 (dd, *J* = 9.4, 7.3 Hz, 1H), 3.57 (dd, *J* = 9.4, 5.8 Hz, 1H); ^{13}C NMR (151 MHz, CD_2Cl_2) δ 161.8, 139.3, 139.2, 139.2, 138.7, 128.9 (2×C), 128.8 (2×C), 128.8 (2×C), 128.8 (2×C), 128.7 (2×C), 128.4 (2×C), 128.2, 128.2, 128.2 (2×C), 128.0 (2×C), 128.0, 128.0, 95.7, 92.0, 78.7, 76.5, 75.6, 75.5, 73.9, 73.5, 73.4, 72.7, 69.0; ESI-HRMS: *m/z* calcd for $C_{36}H_{36}O_6NCl_2{}^{37}ClNa$ [M + Na]$^+$: 708.14709; found: 708.14673; $[\alpha]_D^{20}$ = +58.60 (c = 2.82, CH_2Cl_2).

2,3,4,6-Tetra-*O*-benzyl-β-D-glucopyranosyl trichloroacetimidate (153)[73]

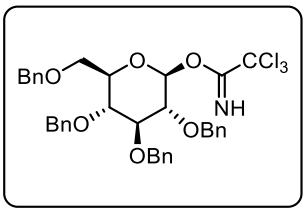

To glucose precursor **150** (3.0 g, 5.55 mmol, 1 equiv.) in 30 mL anhydrous dichloromethane, potassium carbonate (3.07 g, 22.2 mmol, 4 equiv.) and trichloroacetonitrile. (2.78 mL, 27.74 mmol, 5 equiv.) were added. The suspension was strongly stirred for 4 h at room temperature under a

argon atmosphere. The mixture was filtered over celite, washed with dichloromethane (10 mL), the filtrate concentrated under reduced pressure and the oily residue recrystallized from Et_2O:pentane = 1:1 (30 mL) to give compound **153** (3.23 g, 4.72 mmol, 85%) as white solid. The analytical data was in accordance to the literature.[73] ^{1}H NMR (500 MHz, CD_2Cl_2) δ 8.79 (s, 1H), 7.34–7.19 (m, 20H), 5.83 (d, *J* = 7.5 Hz, 1H), 4.94 (d, *J* = 10.9 Hz, 1H), 4.91 (d, *J* = 11.0 Hz, 1H), 4.83 (d, *J* = 10.0 Hz, 2H), 4.77 (d, *J* = 10.9 Hz, 1H), 4.58 (d, *J* = 11.4 Hz, 2H), 4.52 (d, *J* = 11.9 Hz, 1H), 3.77–3.68 (m, 5H), 6.35–3.62 (m, 1H); ^{13}C NMR (126 MHz, CD_2Cl_2) δ 161.6, 139.2, 138.8, 138.7 (2×C), 128.9 (2×C), 128.8 (2×C), 128.8 (4×C), 128.5 (4×C), 128.4 (2×C), 128.3 (2×C), 128.2, 128.2, 128.2, 128.1, 98.8, 91.4, 85.0, 81.4, 77.8, 76.3, 76.0, 75.4, 75.3, 73.8, 68.9; $[\alpha]_D^{20}$ = +22.86 (c = 0.54, CH_2Cl_2).

2,3,4,6-Tetra-*O*-benzyl-β-D-galactopyranosyl trichloroacetimidate (154)[53]

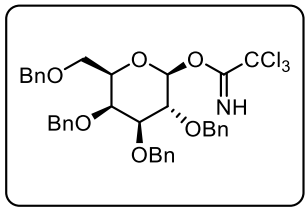

To galactose precursor **151** (3.0 g, 5.55 mmol, 1 equiv.) in 30 mL anhydrous dichloromethane, potassium carbonate (3.07 g, 22.2 mmol, 4 equiv.) and trichloroacetonitrile. (2.78 mL, 27.74 mmol, 5 equiv.) were added. The suspension was strongly stirred for 4 h at room temperature under a nitrogen atmosphere. The mixture was filtered over celite, washed with dichloromethane (10 mL), the filtrate concentrated under reduced pressure, and the oily residue recrystallized from Et_2O:pentane = 1:1 (30 mL) to give compound **154** (2.82 g, 4.12 mmol, 74%) as white solid. The analytical data was in accordance to the literature.[74] ^{1}H NMR (600 MHz, CD_2Cl_2) δ 8.73 (s, 1H), 7.39–7.27 (m, 20H), 5.79 (d, *J* = 8.0 Hz, 1H), 4.95 (d, *J* = 10.9 Hz, 1H), 4.89 (d, *J* = 10.8 Hz, 1H), 4.82 (d, *J* = 10.8 Hz, 1H), 4.79–4.75 (m, 2H), 4.60 (d, *J* = 11.0 Hz, 1H), 4.52 (d, *J* = 11.7 Hz, 1H), 4.47 (d, *J* = 11.8 Hz, 1H), 4.03–4.00 (m, 2H), 3.77 (t, *J* = 6.3 Hz, 1H), 3.69 (dd, *J* = 9.7, 2.9 Hz, 1H), 3.66–3.60 (m, 2H); ^{13}C NMR (151 MHz, CD_2Cl_2) δ 161.8, 139.1, 139.1, 138.9, 138.7, 128.9 (4×C), 128.9 (2×C), 128.9 (2×C), 128.7 (2×C), 128.5 (2×C), 128.5 (2×C), 128.3, 128.3, 128.2 (2×C), 128.2, 128.1, 99.1, 91.5, 82.7, 78.7, 75.7, 75.6, 74.9, 74.3, 73.9, 73.5, 68.9; ESI-HRMS: *m/z* calcd for $C_{36}H_{36}O_6NCl^{37}Cl_2Na$ $[M + Na]^+$: 710.14414; found: 710.14490; $[\alpha]_D^{20}$ = +22.04 (c = 1.18, CH_2Cl_2).

Synthesis of (3a*R*,5*R*,6*R*,7*S*,7a*R*)-6,7-bis(benzyloxy)-5-((benzyloxy)methyl)-2-ethoxy-2-methyltetrahydro-5*H*-[1,3]dioxolo[4,5-b]pyran (155)[61]

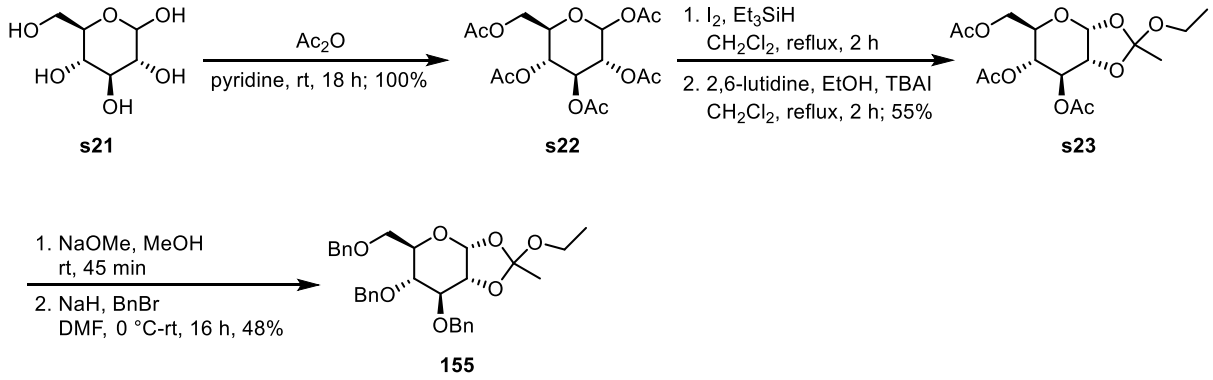

s21 **s22** **s23** **155**

D-Glucose penta acetate (s22)[61]

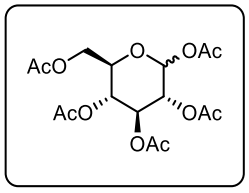

D-Glucose **s21** (10.0 g, 55.5 mmol, 1 equiv.) was dissolved in 215 mL of a 3:2 mixture of pyridine and Ac_2O and stirred at room temperature for 18 h. All volatile parts were removed by repeated use of toluene as an azeotropic entraining agent. The remainder was dissolved in EtOAc and washed with sat. $CuSO_4$, brine, sat. $NaHCO_3$ and again brine. The organic layer was dried over $MgSO_4$ and concentrated. The crude product was used without further purification to yield the mixture of isomers **s22** (21.7 g, 55.5 mmol, 100%) as a white solid. The analytical data was in accordance to the literature.[61] (data for α-anomer) ^{1}H NMR (500 MHz, $CDCl_3$) δ 6.32 (d, *J* = 3.7 Hz, 1H), 5.48–5.44 (m, 1H), 5.15–5.11 (m, 1H), 5.09 (dd, *J* = 10.3, 3.7 Hz, 1H), 4.28–4.24 (m, 1H), 4.12–4.07 (m, 2H), 2.17 (s, 3H), 2.08 (s, 3H), 2.03 (s, 3H), 2.02 (s, 3H), 2.00 (s, 3H); ^{13}C NMR (151 MHz, $CDCl_3$) δ 170.6, 170.2, 169.6, 169.4, 168.7, 89.0, 69.8, 69.1, 67.8, 61.4, 20.9, 20.7, 20.6, 20.5, 20.4.

3,4,6-Tri-*O*-acetyl-α-D-glucopyranose 1,2-(ethyl orthoacetate) (s23)[61]

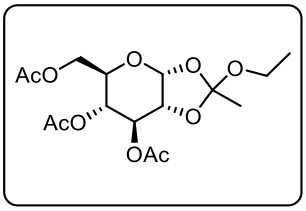

A solution of **s22** (21.7 g, 55.51 mmol, 1 equiv.) in CH_2Cl_2 (256 mL) was treated with I_2 (19.7 g, 77.7 mmol, 1.4 equiv.) and Et_3SiH (12.4 mL, 77.7 mmol, 1.4 equiv.). The mixture was heated at reflux for 2 h, cooled to rt and treated with 2,6-lutidine (25.9 mL, 0.2 mol, 4 equiv.), EtOH (19.4 mL, 0.3 mol, 6 equiv.) and TBAI (5.13 g, 13.9 mmol, 0.25 equiv.). The solution was heated at reflux for 2 h, the volatile parts were removed under reduced pressure and the residue was purified by silica flash chromatography (EtOAc:*c*-hex = 1: 4, R_f = 0.36 (EtOAc:*c*-hex = 1: 2)) to give product **s23** (11.5 g, 30.6 mmol, 55%) as transparent hygroscopic crystals. The analytical data was in accordance to the literature.[61] ^{1}H NMR (400 MHz, $CDCl_3$) δ 5.71 (d, *J* = 5.2 Hz, 1H), 5.19 (t, *J* = 2.9 Hz, 1H), 4.90 (ddd, *J* = 9.6, 2.7, 1.0 Hz, 1H), 4.32 (ddd, *J* = 5.2, 3.0, 1.0 Hz, 1H), 4.20–4.19 (m, 2H), 3.95 (dddd, *J* = 9.6, 4.9, 3.3, 0.7 Hz, 1H), 3.54 (qd, *J* = 7.0, 1.0 Hz, 2H), 2.11 (s, 3H), 2.09 (s, 3H), 2.09 (s, 3H), 1.72 (s, 3H), 1.18 (t, *J* = 7.1 Hz, 3H); ^{13}C NMR (101 MHz, CD_2Cl_2) δ 170.7, 169.6, 169.2, 121.2, 96.9, 73.0, 70.1, 68.2, 66.9, 63.0, 59.1, 20.8 (2×C), 20.7, 20.7, 15.2; ESI-HRMS: *m/z* calcd for $C_{16}H_{24}O_{10}Na$ $[M + Na]^+$: 399.12617; found: 399.12561; $[\alpha]_D^{20}$ = +37.64 (c = 0.83, CH_2Cl_2).

3,4,6-Tri-*O*-benzyl-α-D-glucopyranose 1,2-(ethyl orthoacetate) (155)[61]

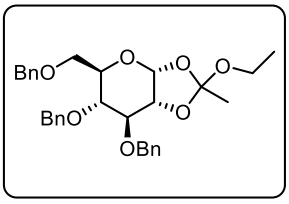

A solution of **s23** (10.0 g, 26.6 mmol, 1 equiv.) in MeOH (105 mL) was treated with NaOMe (287 mg, 5.31 mmol, 0.2 equiv.) in one portion and the resulting mixture was stirred at rt until consumption of the starting material (ca. 45 min). The volatile parts were removed under reduced pressure and the residue was dissolved in anhydrous DMF (105 mL). The mixture was cooled to 0 °C and NaH (60% in mineral oil, 4.25 g, 0.11 mol, 4 equiv.) was added in one portion. BnBr (14.2 mL, 0.12 mol, 4.5 equiv.) was added via syringe and the resulting mixture was stirred for 16

h at rt. The reaction was quenched with 250 g of ice and extracted twice with EtOAc. The combined organic phases were washed with brine, dried, concentrated and the residue was purified by silica flash column chromatography (EtOAc:*c*-hex = 1: 19, R_f = 0.31 (EtOAc:*c*-hex = 1: 4)) to afford **155** (6.63 g, 12.7 mmol, 48%) as a clear oil. The analytical data was in accordance to the literature.[61] ^{1}H NMR (400 MHz, $CDCl_3$) δ 7.30–7.12 (m, 15H), 5.72 (d, *J* = 5.2 Hz, 1H), 4.66 (d, *J* = 11.9 Hz, 1H), 4.56–4.52 (m, 3H), 4.45 (d, *J* = 12.1 Hz, 1H), 4.38–4.32 (m, 2H), 3.84–3.82 (m, 1H), 3.76–3.72 (m, 1H), 3.66 (dd, *J* = 9.8, 4.6 Hz, 1H), 3.61–3.60 (m, 2H) 3.53–3.46 (m, 2H), 1.61 (s, 3H), 1.14 (t, *J* = 7.0 Hz, 3H); ^{13}C NMR (101 MHz, $CDCl_3$) δ 138.1, 137.9, 137.7, 128.4 (2×C), 128.3 (2×C), 128.3 (2×C), 128.0 (2×C), 128.0 (2×C), 127.9, 127.8 (2×C), 127.8, 127.6, 120.9, 97.8, 78.8, 75.4, 74.9, 73.4, 72.9, 71.9, 70.4, 69.1, 58.7, 21.8, 15.3; ESI-HRMS: *m/z* calcd for $C_{31}H_{36}O_7Na$ $[M + Na]^+$: 543.23532; found: 543.23424; $[\alpha]_D^{20}$ = +22.37 (c = 0.78, CH_2Cl_2).

2-*O*-Acetyl-3,4,6-tri-*O*-benzyl-α-D-glucopyranosyl trichloroacetimidate (60)[61]

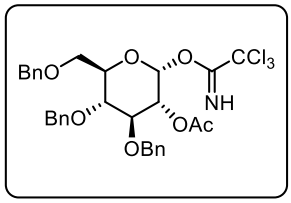

A solution of **155** (6.62 g, 12.7 mmol, 1 equiv.) in 150 mL of a mixture of 10% H_2O in DME was treated with *p*-toluenesulfonic acid monohydrate (1.21 g, 6.36 mmol, 0.5 equiv.) and stirred for 1.5 h. The reaction was quenched with sat. $NaHCO_3$, extracted three times with EtOAc. The combined organic layers were washed with H_2O and brine, dried over $MgSO_4$ and concentrated. The crude product was dissolved in anhydrous CH_2Cl_2 (261.8 mL), treated with CCl_3CN (12.8 mL, 0.12 mol, 10 equiv.) and DBU (0.48 mL, 3.18 mmol, 0.25 equiv.) and stirred at rt for 1.5 h. The solvent was removed and the brownish remainder was purified by silica flash column chromatography (eluent containing 1% triethylamine, EtOAc:*c*-hex = 1:9, R_f = 0.34 (EtOAc:*c*-hex = 1:4)) to remove the 1-*O*-acetyl-2-trichloroimidate by-product and to leave **60** (7.03 g, 11.0 mmol, 87%) as a colourless oil. The analytical data was in accordance to the literature.[61] ^{1}H NMR (400 MHz, $CDCl_3$) δ 8.58 (s, 1H), 7.35–7.18 (m, 15H), 6.54 (d, *J* = 3.5 Hz, 1H), 5.09 (dd, *J* = 10.0, 3.6 Hz, 1H), 4.89–4.84 (m, 2H), 4.78 (d, *J* = 11.5 Hz, 1H), 4.66–4.58 (m, 2H), 4.52 (d, *J* = 12.0 Hz, 1H), 4.14–4.09 (m, 1H), 4.03 (dt, *J* = 10.1, 2.5 Hz, 1H), 3.91 (d, *J* = 9.3 Hz, 1H), 3.87–3.81 (m, 1H), 3.71 (dd, *J* = 11.1, 1.9 Hz, 1H), 1.94 (s, 3H); ^{13}C NMR (101 MHz, $CDCl_3$) δ 170.0, 161.0,

138.2, 137.8, 137.8, 128.4 (2×C), 128.4 (2×C), 128.4 (2×C), 128.1 (2×C), 127.9, 127.9 (2×C), 127.8 (2×C), 127.7 (2×C), 94.0, 91.0, 79.5, 75.4, 75.4, 73.5, 73.4, 72.4, 67.9, 26.9, 20.6; ESI-HRMS: *m/z* calcd for $C_{31}H_{32}O_7NCl_3Na$ $[M + Na]^+$: 658.11366; found: 658.11349; $[\alpha]_D^{20}$ = +61.34 (c = 2.24, CH_2Cl_2).

2-*O*-Acetyl-3,4,6-tri-*O*-benzyl-α-D-mannopyranosyl trichloroacetimidate (157)[61]

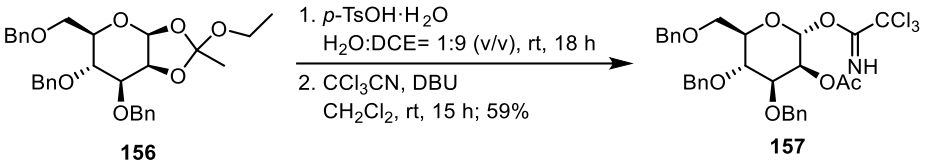

A solution of **156** (500 mg, 0.99 mmol, 1 equiv.) in 11.3 mL of a mixture of 10% H_2O in DCE was treated with *p*-toluenesulfonic acid monohydrate (91.0 mg, 0.49 mmol, 0.5 equiv.) and stirred for 18 h. The reaction was quenched with sat. $NaHCO_3$, extracted three times with CH_2Cl_2, and the combined organic layers were washed with H_2O and brine, dried over $MgSO_4$ and concentrated. The crude product was dissolved in anhydrous CH_2Cl_2 (19.7 mL), treated with CCl_3CN (0.96 mL, 9.87 mmol, 10 equiv.) and DBU (0.036 mL, 0.25 mmol, 0.25 equiv.) and stirred at rt for 1.5 h. The solvent was removed and the brownish remainder was purified by silica gel column chromatography (EtOAc:*c*-hex = 1:9, R_f = 0.46 (EtOAc:*c*-hex = 1: 2)) to remove the 1-*O*-acetyl-2-trichloroimidate by-product and to leave **157** (373 mg, 0.59 mmol, 59%) as a yellow oil. The analytical data was in accordance to the literature.[74] ^{1}H NMR (500 MHz, $CDCl_3$) δ 8.68 (s, 1H), 7.36–7.26 (m, 13H), 7.19–7.17 (m, 2H), 6.31 (d, *J* = 2.0 Hz, 1H), 5.50 (t, *J* = 2.3 Hz, 1H), 4.87 (d, *J* = 10.5 Hz, 1H), 4.74 (d, *J* = 11.2 Hz, 1H), 4.69 (d, *J* = 12.0 Hz, 1H), 4.59 (d, *J* = 11.2 Hz, 1H), 4.52 (t, *J* = 10.8 Hz, 2H), 4.05–4.02 (m, 2H), 4.00–3.98 (m, 1H), 3.85 (dd, *J* = 11.1, 3.7 Hz, 1H), 3.72 (dd, *J* = 11.2, 1.8 Hz, 1H), 2.20 (s, 3H); ^{13}C NMR (126 MHz, $CDCl_3$) δ 170.1, 160.0, 138.1, 138.0, 137.5, 128.5, 128.4, 128.3, 128.3, 128.1, 127.9, 127.8, 127.6, 95.3, 90.8, 77.3, 75.5, 74.3, 73.6, 73.4, 72.1, 68.3, 67.3, 21.0; ESI-HRMS: *m/z* calcd for $C_{31}H_{32}O_7NCl_3Na$ $[M + Na]^+$: 658.11366; found: 658.11352; $[\alpha]_D^{20}$ = +28.25 (c = 0.62, CH_2Cl_2).

2-(((2*R*,3*R*,4*S*,5*R*,6*R*)-3,4,5-Tris(benzyloxy)-6-((benzyloxy)methyl)tetrahydro-2*H*-pyran-2-yl)oxy)benzo[*d*]oxazole (158)[62]

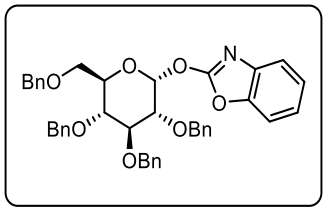

To 2,3,4,6-tetra-*O*-benzyl-D-glucopyranose **150** (500 mg, 0.92 mmol, 1 equiv.) in anhydrous acetone (10 mL), freshly activated 3 Å MS (1.5 g) were added and stirred under argon for 1 h at rt. 2-chlorobenzoxazole (0.53 mL, 4.62 mmol, 5 equiv.) and KOH (51.9 mg, 0.92 mmol, 1 equiv.) were added to the stirring solution at 0 ºC and the resulting reaction was raised to rt and stirred for 18 h. After that, the solid was filtered off and washed successively with CH_2Cl_2. The combined filtrate was washed with water (3 × 75 mL). The organic phase was separated, dried with $MgSO_4$, and concentrated *in vacuo*. The residue was purified by silica gel column chromatography (Et_2O:pentane = 1:4, R_f = 0.20 (Et_2O:pentane = 1:4)) to obtain the title compound **158** (α:β = 1:1) as a colourless syrup. The analytical data was in accordance to the literature.[62] (data for α-anomer) ^{1}H NMR (500 MHz, CD_2Cl_2) δ 7.51–7.20 (m, 24H), 6.48 (d, *J* = 3.5 Hz, 1H), 4.98 (d, *J* = 11.0 Hz, 1H), 4.93–4.80 (m, 3H), 4.75 (s, 1H), 4.59 (d, *J* = 10.9 Hz, 2H), 4.54–4.44 (m, 2H), 4.09 (t, *J* = 9.4 Hz, 1H), 3.99 (ddd, *J* = 10.2, 3.6, 1.9 Hz, 1H), 3.82–3.74 (m, 2H), 3.66–3.62 (m, 1H); ^{13}C NMR (126 MHz, CD_2Cl_2) δ 162.9, 149.0, 141.5, 139.3, 138.9, 138.6, 138.2, 128.9 (2×C), 128.8 (2×C), 128.5 (2×C), 128.5 (2×C), 128.4 (2×C), 128.4 (2×C), 128.4 (2×C), 128.4 (2×C), 128.2, 128.2, 128.2, 128.1, 124.9, 123.6, 118.7, 110.3, 99.1, 81.8, 79.6, 77.3, 76.1, 75.6, 74.0, 74.0, 73.8, 68.7; ESI-HRMS: *m/z* calcd for $C_{41}H_{39}O_7NNa$ $[M + Na]^+$: 680.26187; found: 680.26190; $[\alpha]_D^{20}$ = +28.65 (c = 0.75, CH_2Cl_2).

9.13 Synthesis of halogen bond catalysts

1-(4-(Trifluoromethyl)phenyl)-1*H*-benzo[*d*]imidazole (161)[75]

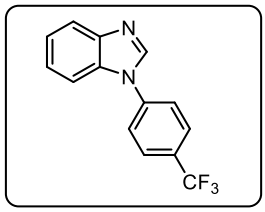

To a three-necked flask (250 mL), benzimidazole (7.88 g, 66.66 mmol, 1.5 equiv.), CuI (1.693 g, 8.89 mmol, 0.2 equiv.), ninhydrin (1.58 g, 8.89 mmol, 0.2 equiv.) and KOH (4.99 g, 88.89 mmol, 2 equiv.) were added under a nitrogen atmosphere. From another flask, 4-bromobenztrifluoride (10.0 g, 44.44 mmol, 1 equiv.) in degassed DMSO (100 mL) was injected, and the resulting mixture was heated to 110 °C and stirred for 23 h. The mixture was allowed to cool to room temperature, extracted with EtOAc, and washed with water twice. The organic layers were dried over $MgSO_4$ and concentrated by vacuum to give a crude product, which was purified by silica flash column chromatography (EtOAc:*c*-Hex = 1:1, R_f = 0.45 (EtOAc:*c*-Hex = 2:1)) to afford pure product **161** (1.52 g, 5.78 mmol, 13%) as pale-yellow solid. The analytical data was in accordance to the literature.[75] ^{1}H NMR (700 MHz, $CDCl_3$) δ 8.24 (s, 1H), 7.92–7.91 (m, 1H), 7.87 (d, *J* = 8.2 Hz, 1H), 7.69 (d, *J* = 8.2 Hz, 1H), 7.58–7.57 (m, 1H), 7.41–7.38 (m, 2H); ^{13}C NMR (176 MHz, $CDCl_3$) δ 143.7, 141.7, 139.3, 133.1, 130.2 (q, *J* = 33.2 Hz), 127.4 (q, *J* = 3.7 Hz), 125.9, 124.4, 124.0, 123.5, 122.8, 121.3, 120.8, 110.3; ESI-HRMS: *m/z* calcd for $C_{14}H_{10}N_2F_3$ $[M + Na]^+$: 263.07906; found: 263.07803.

1-(4-Nitrophenyl)-1*H*-benzo[*d*]imidazole (162)[76]

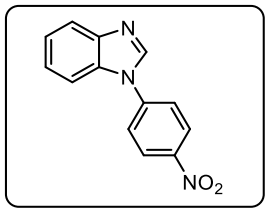

Degassed DMSO (50 mL) was added to a mixture of benzoimidazole (5.91 g, 50.0 mmol, 1.5 equiv.), Cs_2CO_3 (21.72 g, 66.66 mmol, 2 equiv.), CuI (1.27 g, 6.67 mmol, 0.2 equiv.), and 1-bromo-4-nitrobenzene (6.73 g, 33.33 mmol, 1equiv.). The solution was heated at 120 °C for 48 h. After cooling, the solvent was removed completely under vacuum. The residual was washed with

water and extracted with CH_2Cl_2 twice. The extract was washed with water and dried over anhydrous $MgSO_4$. The solvent was removed under vacuum. The solid was washed thoroughly with ether and dried under vacuum. The filtrate was purified by silica flash column chromatography (EtOAc:*c*-Hex = 2:1, R_f = 0.30 (EtOAc:*c*-Hex = 2:1)) to afford pure product **162** (6.59 g, 27.54 mmol, 83%) as pale-yellow solid. ^{1}H NMR (500 MHz, CD_2Cl_2) δ 8.44 (d, *J* = 9.0 Hz, 2H), 8.20 (s, 1H), 7.85 (dd, *J* = 6.9, 1.7 Hz, 1H), 7.77–7.74 (m, 2H), 7.65 (dd, *J* = 7.0, 1.7 Hz, 1H), 7.39 (pd, *J* = 7.2, 1.5 Hz, 2H); ^{13}C NMR (126 MHz, CD_2Cl_2) δ 146.9, 145.1, 142.4, 142.3, 133.4, 126.2 (2×C), 124.8, 124.1 (2×C), 123.9, 121.3, 110.9; ESI-HRMS: *m/z* calcd for $C_{13}H_{10}O_2N_3$ $[M + Na]^+$: 240.07675; found: 240.07590.

1-(4-Methoxyphenyl)-1*H*-benzo[*d*]imidazole (163)[76]

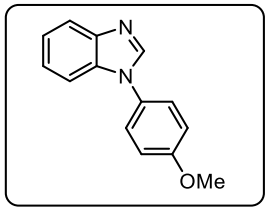

Degassed DMF (50 mL) was added to a mixture of benzoimidazole (5.91 g, 50.0 mmol, 1.5 equiv.), Cs_2CO_3 (21.7 g, 66.66 mmol, 2 equiv.), CuI (1.27 g, 6.67 mmol, 0.2 equiv.) and 4-bromoanisole (4.17 mL, 33.33 mmol, 1 equiv.). The solution was heated at 120 °C for 48 h. After cooling, the solvent was removed completely under vacuum. The residual was washed with water and extracted twice with CH_2Cl_2. The extract was washed with water and dried over anhydrous $MgSO_4$. The solvent was then removed under vacuum. The solid was then washed thoroughly with ether and dried under vacuum. The filtrate was purified by silica flash column chromatography (EtOAc:*c*-hex = 1:1, R_f = 0.53 (EtOAc:*c*-hex = 2:1)) to afford pure product **163** (1.50 g, 6.67 mmol, 20%) as white solid. The analytical data was in accordance to the literature.[76] ^{1}H NMR (500 MHz, CD_2Cl_2) δ 8.05 (s, 1H), 7.82–7.80 (m, 1H), 7.50–7.46 (m, 1H), 7.45–7.42 (m, 2H), 7.33–7.29 (m, 2H), 7.10–7.07 (m, 2H), 3.88 (s, 3H); ^{13}C NMR (126 MHz, CD_2Cl_2) δ 159.8, 144.1, 143.2, 134.8, 129.1, 126.4 (2×C), 123.8, 122.8, 120.7, 115.5 (2×C), 110.9, 56.1; ESI-HRMS: *m/z* calcd for $C_{14}H_{13}ON_2$ $[M + Na]^+$: 225.10224; found: 225.10146.

2-Iodo-1-(4-(trifluoromethyl)phenyl)-1*H*-benzo[*d*]imidazole (164)[75]

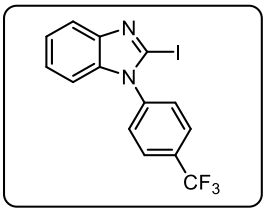

To a three-necked round-bottom flask, **161** (934 mg, 3.56 mmol, 1 equiv.) was added. To the flask, THF (21.5 mL) was injected and the resulting solution was cooled to –60 °C. A hexane solution of *n*-BuLi (1.6 M, 2.89 mL, 4.63 mmol, 1.3 equiv.) was added dropwise to the cooled mixture over 1.5 h. A THF solution (8.4 mL) of iodine (1.18 g, 4.63 mmol, 1.3 equiv.) was added to the mixture at –60 °C, and the resulting mixture was slowly allowed to warm up to room temperature and stirred for 17 h. Volatile components were evaporated under reduced pressure, and the resulting residue was dissolved in CH_2Cl_2 (200 mL), washed with water (100 mL × 2), $Na_2S_2O_3$ (100 mL × 2) and brine (100 mL × 2). The combined organic layer was dried over $MgSO_4$ and solvent was removed under reduced pressure to give a crude solid which was purified by silica flash column chromatography (EtOAc:*c*-hex = 1:9, R_f = 0.59 (EtOAc:*c*-hex = 1:1)) to afford pure product **164** (1.11 g, 2.85 mmol, 80%) as white solid. The analytical data was in accordance to the literature.[75] ^{1}H NMR (500 MHz, $CDCl_3$) δ 7.88 (d, *J* = 8.2 Hz, 2H), 7.79 (d, *J* = 8.0 Hz, 1H), 7.57 (d, *J* = 8.2 Hz, 2H), 7.28 (t, *J* = 7.5 Hz, 1H), 7.22 (t, *J* = 7.5 Hz, 1H), 7.14 (d, *J* = 8.1 Hz, 1H); ^{13}C NMR (126 MHz, $CDCl_3$) δ 145.4, 139.6, 137.1, 131.6 (q, *J* = 33.1 Hz),128.6, 127.0 (q, *J* = 3.7 Hz), 124.0, 124.0 123.1, 122.4, 119.4, 109.9, 102.4, 26.8; ESI-HRMS: *m/z* calcd for $C_{14}H_9N_2F_3I$ $[M + Na]^+$: 388.97570; found: 388.97518.

2-Iodo-1-(4-nitrophenyl)-1*H*-benzo[*d*]imidazole (165)

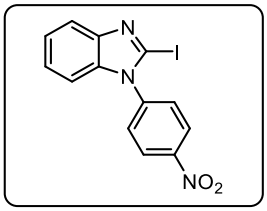

To a three-necked round-bottom flask, (100 mL), **162** (1.00 g, 4.18 mmol, 1 equiv.) was added. To the flask, THF (22 mL) was injected and the resulting solution was cooled to –78 °C. A hexane solution of LiHMDS (1 M, 5.43 mL, 5.43 mmol, 1.3 equiv.) was added dropwise to the cooled mixture over 1 h. A THF solution (10.5 mL) of iodine (1.38 g, 5.43 mmol, 1.3 equiv.) was added

to the mixture at –78 °C, and the resulting mixture was slowly allowed to warm up to room temperature and stirred for 17 h. Volatile components were evaporated under reduced pressure and the resulting residue was dissolved in CH_2Cl_2 (200 mL), washed with water (100 mL × 2), $Na_2S_2O_3$ (100 mL × 2) and brine (100 mL × 2). The combined organic layers were dried over $MgSO_4$ and the solvent was removed under reduced pressure to give a crude solid which was purified by silica flash column chromatography (pentane:Et_2O = 4:1, R_f = 0.56 (EtOAc:*c*-hex = 1:1)) to afford pure product **165** (385 mg, 1.06 mmol, 25%) as white solid. ^{1}H NMR (400 MHz, $CDCl_3$) δ 7.93–7.90 (m, 2H), 7.81–7.79 (m, 1H), 7.61–7.58 (m, 2H), 7.32–7.28 (m, 1H), 7.26–7.22 (m, 1H), 7.15–7.13 (m, 1H); compound decomposed during ^{13}C NMR measurement; ESI-HRMS: *m/z* calcd for $C_{14}H_9N_2F_3I$ $[M + Na]^+$: 388.97570; found: 388.97518.

2-Iodo-1-(4-methoxyphenyl)-1*H*-benzo[*d*]imidazole (166)[75]

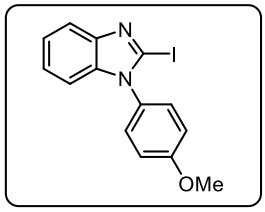

To a three-necked round-bottom flask, **163** (1.00 g, 4.46 mmol, 1 equiv.) was added. To the flask, THF (22 mL) was injected and the resulting solution was cooled to –78 °C. A hexane solution of *n*-BuLi (1.6 M, 3.62 mL, 5.8 mmol, 1.3 equiv.) was added dropwise to the cooled mixture over 1 h. A THF solution (10.5 mL) of iodine (1.47 g, 5.8 mmol, 1.3 equiv.) was added to the mixture at –78 °C, and the resulting mixture was slowly allowed to warm up to room temperature and stirred for 21 h. Volatile components were evaporated under reduced pressure and the resulting residue was dissolved in CH_2Cl_2 (200 mL), washed with water (100 mL × 2), $Na_2S_2O_3$ (100 mL × 2) and brine (100 mL × 2). The combined organic layers were dried over $MgSO_4$ and the solvent was removed under reduced pressure to give a crude solid which was purified by silica flash column chromatography (pentane:Et_2O = 4:1, R_f = 0.62 (EtOAc:*c*-hex = 1:1)) to afford pure product **166** (876 mg, 2.50 mmol, 56%) as yellow solid. ^{1}H NMR (500 MHz, CD_2Cl_2) δ 7.71 (d, *J* = 7.6 Hz, 1H), 7.32–7.29 (m, 2H), 7.25–7.18 (m, 2H), 7.13–7.08 (m, 3H), 3.90 (s, 3H); ^{13}C NMR (126 MHz, CD_2Cl_2) δ 160.9, 146.0, 138.4, 130.0 (2×C), 129.8, 123.9, 122.9, 119.4, 115.3 (2×C), 110.9, 105.3, 56.2; ESI-HRMS: *m/z* calcd for $C_{14}H_{12}ON_2I$ $[M + H]^+$: 350.99888; found: 350.99886.

Octyl trifluoromethanesulfonate (s25)[63]

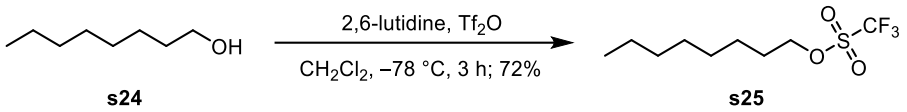

s24 **s25**

According to a literature procedure, a flame-dried round bottom flask was charged with the corresponding octan-1-ol **s24** (6.2 mL, 38.39 mmol, 1 equiv.) in anhydrous CH_2Cl_2 (0.2 M, 191 mL). At –78 °C, 2,6-lutidine (7.2 mL, 61.43 mmol, 1.6 equiv.) was added followed by the slow addition of Tf_2O (7.8 mL, 46.07 mmol, 1.2 equiv.). After 3 hours, the reaction mixture was quenched with 1 M HCl, washed with brine and the aqueous phase was extracted with CH_2Cl_2. The combined organic layers were dried over $MgSO_4$. Evaporation of the solvents at room temperature (due to decomposition of the triflates at higher temperatures) afforded the crude title compound. Purification by silica chromatography with pentane (R_f = 0.26 (pentane)) as eluent afforded pure alkyltriflates **s25** (7.28 g, 27.76 mmol, 72%) as purple oil The analytical data was in accordance to the literature.[63] ^{1}H NMR (500 MHz, $CDCl_3$) δ 4.54 (t, *J* = 6.5 Hz, 2H), 1.82 (dt, *J* = 14.8, 6.7 Hz, 2H), 1.45–1.39 (m, 2H), 1.24–1.24 (m, 8H), 0.88 (t, *J* = 6.9 Hz, 3H); ^{13}C NMR (126 MHz, $CDCl_3$) δ 118.6 (q, ^1J = 319 Hz), 77.8, 31.6, 29.2, 29.0, 28.8, 25.0, 22.6, 14.0; ^{19}F NMR (470 MHz, $CDCl_3$) δ = –75.0.

2-Iodo-3-octanoyl-1-(4-(trifluoromethyl)phenyl)-1*H*-benzo[*d*]imidazol-3-ium trifluoromethanesulfonate (167)[75]

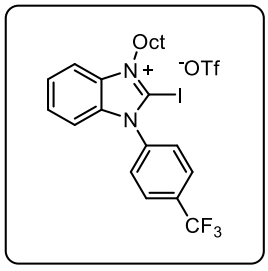

To a flame-dried two-necked flask, **164** (1.10 g, 2.83 mmol, 1 equiv.) and CH_2Cl_2 (100 mL) were added. Octyl triflate **s25** (1.73 mL, 7.93 mmol, 2.8 equiv.) was added to the solution, and the resulting mixture was stirred at room temperature for 15 h. The solvent was removed under reduced pressure and the residue was rinsed with *c*-hexane (10 mL) for five times to remove excessive octyl triflate. The mixture was recrystallized in a 1:10 of CH_3CN-Et_2O system to give **167** (1.05 g, 1.61 mmol, 57%) as a white solid. The analytical data was in accordance to the literature.[75] ^{1}H

NMR (500 MHz, CD_2Cl_2) δ 8.03 (d, *J* = 8.4 Hz, 2H), 7.84 (d, *J* = 8.4 Hz, 1H), 7.76 (d, *J* = 8.3 Hz, 2H), 7.69 (t, *J* = 7.4 Hz, 1H), 7.60 (t, *J* = 7.4 Hz, 1H), 7.36 (d, *J* = 8.4 Hz, 1H), 4.61 (t, *J* = 7.8 Hz, 2H), 2.02 (p, *J* = 7.8 Hz, 2H), 1.53 (p, *J* = 7.2 Hz, 2H), 1.45–1.39 (m, 2H), 1.37–1.28 (m, 6H), 0.89 (t, *J* = 6.8 Hz, 3H); ^{13}C NMR (126 MHz, CD_2Cl_2) δ 137.7, 135.4, 134.3 (q, *J* = 33.4 Hz), 133.7, 129.2, 128.7 (q, *J* = 3.6 Hz), 128.6, 128.3, 124.9, 122.8, 122.3, 120.0, 113.7, 113.6, 112.7, 51.8, 32.2, 29.6, 29.0, 29.6, 27.3, 23.1, 14.4; ESI-HRMS: *m/z* calcd for $C_{22}H_{25}N_2F_3I$ $[M]^+$: 501.10090; found: 501.09975.

2-Iodo-1-(4-nitrophenyl)-3-octanoyl-1*H*-benzo[*d*]imidazol-3-ium trifluoromethanesulfonate (168)[75]

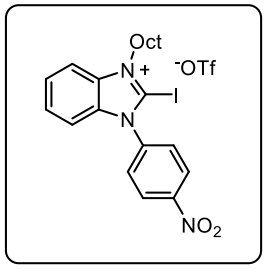

To a flame-dried two-necked flask, **165** (300 mg, 0.82 mmol, 1 equiv.) and CH_2Cl_2 (30 mL) were added. Octyl triflate **s25** (0.50 mL, 2.30 mmol, 2.8 equiv.) was added to the solution and the resulting mixture was stirred at room temperature for 16 h. The solvent was removed under reduced pressure and the residue was rinsed with *c*-hexane (5 mL) for five times to remove excessive octyl triflate. The mixture was recrystallized in a 1:10 of CH_3CN-Et_2O system to give **168** (1.05 g, 1.61 mmol, 57%) as a white solid. ^{1}H NMR (500 MHz, CD_2Cl_2) δ 8.60–8.56 (m, 2H), 7.37–7.83 (m, 3H), 7.71 (t, *J* = 7.8 Hz, 1H), 7.62 (t, *J* = 7.9 Hz, 1H), 7.36 (d, *J* = 8.3 Hz, 1H), 4.63–4.60 (m, 2H), 2.07–1.98 (m, 2H), 1.56–1.50 (m, 2H), 1.45–1.39 (m, 2H), 1.37–1.28 (m, 6H), 0.88 (d, *J* = 7.0 Hz, 3H); ^{13}C NMR (126 MHz, CD_2Cl_2) δ 150.2, 139.5, 135.3, 133.8, 130.1 (2×C), 128.7 (2×C), 128.4, 126.7 (2×C), 113.7, 113.6, 112.6, 51.9, 32.2, 29.6 (2×C), 29.6, 27.3, 23.1, 14.4; ESI-HRMS: *m/z* calcd for $C_{21}H_2O_2N_3I$ $[M + H]^+$: 478.09860; found: 478.09728.

2-Iodo-1-(4-nitrophenyl)-3-octanoyl-1*H*-benzo[*d*]imidazol-3-ium trifluoromethanesulfonate (169)[75]

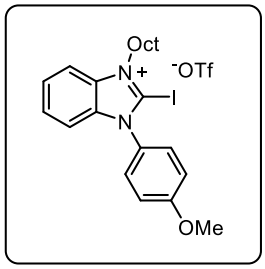

To a flame-dried two-necked flask, **166** (500 mg, 1.43 mmol, 1 equiv.) and CH_2Cl_2 (50 mL) were added. Octyl triflate **s25** (0.87 mL, 4.00 mmol, 2.8 equiv.) was added to the solution and the resulting mixture was stirred at room temperature for 16 h. The solvent was removed under reduced pressure and the residue was rinsed with *c*-hexane (5 mL) for five times to remove excessive octyl triflate. The mixture was recrystallized in a 1:10 of CH_3CN-Et_2O system to give **169** (732 mg, 1.20 mmol, 84%) as a white solid. ^{1}H NMR (500 MHz, CD_2Cl_2) δ 7.81 (d, *J* = 8.4 Hz, 1H), 7.66 (t, *J* = 8.3 Hz, 1H), 7.58 (t, *J* = 7.5 Hz, 1H), 7.44–7.41 (m, 2H), 7.38 (d, *J* = 8.3 Hz, 1H), 7.22–7.19 (m, 2H), 4.59 (t, *J* = 7.8 Hz, 2H), 3.95 (s, 3H), 2.01 (p, *J* = 7.7 Hz, 2H), 1.51 (p, *J* = 7.2 Hz, 2H), 1.44–1.38 (m, 2H), 1.36–1.27 (m, 6H), 0.89 (t, *J* = 6.9 Hz, 3H); ^{13}C NMR (126 MHz, CD_2Cl_2) δ 162.6, 135.8, 133.6, 129.3 (2×C), 128.3 (2×C), 128.0, 126.9, 116.4 (2×C), 114.2, 113.6, 113.3, 56.5, 51.6, 32.2, 29.7, 29.6, 29.6, 27.3, 23.1, 14.4; ESI-HRMS: *m/z* calcd for $C_{22}H_{28}ON_2I$ $[M]^+$: 463.12408; found: 463.12275.

9.14 Synthesis of *C*-glycosides by halogen bond catalyzed

2,2-Dimethyl-6-(((3*S*,4*R*,5*R*,6*R*)-3,4,5-tris(benzyloxy)-6-((benzyloxy)methyl)tetrahydro-2*H*-pyran-2-yl)methyl)-4*H*-1,3-dioxin-4-one (40a)

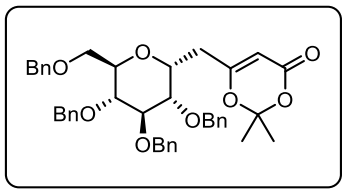

An oven dried tube with a stirring bar was charged with glycosyl imidate (137.0 mg, 0.2 mmol, 2 equiv.), vinylogous enolate (0.1 mmol, 1 equiv.) and anhydrous 1,4-dioxane (1 mL). Then, the tube was purged with argon and sealed with a rubber stopper. After stirring for 10 mins at rt,

halogen-bond catalyst **168** (5 μmol, 5 mol) was added. The tube was further sealed with parafilm and raised to 80 ºC for 1 h. Upon completion of the reaction, the reaction mixture was cooled down to rt and flushed through a short pad of silica gel by EtOAc. The solvent was evaporated and the crude mixture was subjected to flash column chromatography to afford **40a** as a pale-yellow syrup. The analytical data was in accordance to the literature.[30] (data for α-anomer) ^{1}H NMR (700 MHz, $CDCl_3$) δ 7.33–7.13 (m, 20H), 5.26 (s, 1H), 4.94–4.89 (m, 1H), 4.83–4.74 (m, 3H), 4.63–4.56 (m, 2H), 4.51–4.43 (m, 2H), 4.32–4.29 (m, 1H), 3.77–3.61 (m, 4H), 3.58–3.55 (m, 2H), 2.63–2.62 (m, 2H), 1.66 (s, 3H), 1.62 (s, 3H); ^{13}C NMR (176 MHz, $CDCl_3$) δ 168.9, 161.0, 138.4, 137.9, 137.8, 137.7, 128.5 (2×C), 128.4 (4×C), 128.4 (2×C), 128.1, 128.0, 128.0 (2×C), 128.0 (2×C), 127.9 (2×C), 127.9 (2×C), 127.8 (2×C), 106.7, 95.3, 82.1, 79.3, 77.6, 75.5, 75.2, 73.6, 73.5, 71.8, 71.6, 68.5, 30.1, 25.8, 24.2; ESI-HRMS: *m/z* calcd for $C_{41}H_{45}O_8$ $[M + H]^+$: 665.31089; found: 665.31008; $[\alpha]_D^{20}$ = +14.0 (c = 0.28, CH_2Cl_2).

10 References

1. Dwek, R. A. Glycobiology: Toward understanding the function of sugars. *Chem. Rev.* **96**, 683–720 (1996).
2. Lindhorst T. K. *Essentials of carbohydrate chemistry and biochemistry* (Wiley-VCH, Germany, 2007)
3. Wells, L., Whelan, S. A., Hart, G. W. O-GlcNAc: a regulatory post-translational modification. *Biochem. Biophys. Res. Commun.* **302**, 435–441 (2003).
4. Yang, Y., Yu, B. Recent advances in the chemical synthesis of *C*-glycosides. *Chem. Rev.* **117**, 12281–12356 (2017).
5. Chao, E. C., Henry, R. R. SGLT2 inhibition – a novel strategy for diabetes treatment. *Nat. Rev. Drug Discov.* **9**, 551–559 (2010).
6. Ehrenkranz, J. R. L., Lewis, N. G., Ronald Kahn, C., Roth, J. Phlorizin: a review. *Diabetes. Metab. Res. Rev.* **21**, 31–38 (2005).
7. Takhi, M., Abdel Rahman, A. A.-H., Schmidt, R. R. $Yb(OTf)_3$-catalyzed *C*-glycosylation: highly stereoselective synthesis of *C*-pseudoglycals. *Tetrahedron Lett.* **42**, 4053–4056 (2001).
8. Katajisto, J., Lönnberg, H. Solid-phase synthesis of cyclic *C*-glycoside/amino acid hybrids by carbamate coupling chemistry and on-support cyclization. *European J. Org. Chem.* **2005**, 3518–3525 (2005).
9. Xu, C., Loh, C. C. J. An ultra-low thiourea catalyzed strain-release glycosylation and a multicatalytic diversification strategy. *Nat. Commun.* **9**, 4057 (2018).
10. Crich, D., Sharma, I. Is donor–acceptor hydrogen bonding eecessary for 4,6-*O*-benzylidene-directed β-mannopyranosylation? Stereoselective synthesis of β-*C*-mannopyranosides and α-*C*-glucopyranosides. *Org. Lett.* **10**, 4731–4734 (2008).
11. Mahling, J-A., Schmidt, R. R. Aryl *C*-glycosides from *O*- glycosyltrichloroacetimidates and phenol derivatives with trimethylsilyl trifluoromethanesulfonate as the catalyst. *Synthesis.* **3**, 325– 328 (1993).
12. Benett, C. S. *Selective glycosylations: synthetic methods and catalysts* (WileyVCH, Germany, 2017).
13. Gómez, A. M., Lobo, F., Uriel, C., López, J. C. Recent developments in the Ferrier rearrangement. *European J. Org. Chem.* **2013**, 7221–7262 (2013).

14. Anjaiah, S., Chandrasekhar, S., Grée, R., Carbon-Ferrier rearrangements in ionic liquids using $Yb(OTf)_3$ as catalyst. *J. Mol. Catal. A Chem.* **214**, 133–136 (2004).
15. Reddy, T. R., Rao, D. S., Kashyap, S. A mild and efficient Zn-catalyzed *C*-glycosylation: synthesis of C(2)–C(3) unsaturated *C*-linked glycopyranosides. *RSC Adv.* **5**, 28338–28343 (2015).
16. Harvey, J. E., Hewitt, R. J., Moore, P. W., Somarathne, K. K. Reactions of 1,2-cyclopropyl carbohydrates. *Pure Appl. Chem.* **86**, 1377–1399 (2014).
17. Mąkosza, M., Wawrzyniewicz, M. Reactions of organic anions. XXIV. Catalytic method for preparation of dichlorocyclopropane derivatives in aqueous medium. *Tetrahedron Lett.* **10**, 4659–4662 (1969).
18. Doyle, M. P. Catalytic methods for metal carbene transformations. *Chem. Rev.* **86**, 919–939 (1986).
19. Tian, Q., Dong, L., Ma. X., Hu, C., Zou, W., Shao, H. Stereoselective synthesis of 2-*C*-branched (acetylmethyl) oligosaccharides and glycoconjugates: Lewis acid-catalyzed glycosylation from 1,2-cyclopropaneacetylated sugars. *J. Org. Chem.* **76**, 1045–1053 (2011).
20. Ma, X., Tang, Q., Ke, J., Zhang, J., Wang, C., Wang, H., Li, Y., Shao, H., Straightforward and highly diastereoselective synthesis of 2,2-di-substituted perhydrofuro[2,3-b]pyran (and furan) derivatives promoted by $BiCl_3$. *Chem. Commun.* **49**, 7085–7087 (2013).
21. Demchenko, A. V. *Handbook of chemical glycosylation : advances in stereoselectivity and therapeutic relevance*. (Wiley-VCH, 2008).
22. Schmidt, R. R., Kinzy, W. Anomeric-oxygen activation for glycoside synthesis: the trichloroacetimidate method. *Adv. Carbohydr. Chem. Biochem.* **50**, 21–123 (1994).
23. Weck, E. P., Opatz, T. β-Selective *C*-mannosylation of electron-rich phenols. *Synthesis*. **14**, 2393–2398 (2010)
24. Casiraghi, G., Zanardi, F., Appendino, G., Rassu, G. Vinylogous aldol reaction: a valuable, yet understated carbon-carbon bond-forming maneuver. *Chem. Rev.* **100**, 1929–1972 (2000).
25. Curti, C., Sartori, A., Battistini, L., Brindani, N., Rassu, G., Pelosi, G., Lodola, A., Mor, M., Casiraghi, G., Zanardi, F. Pushing the boundaries of vinylogous reactivity: catalytic enantioselective mukaiyama aldol reactions of highly unsaturated 2-silyloxyindoles. *Chem. Eur. J.* **21**, 6433–6442 (2015).

26. Yoshinari, T., Ohmori, K., Suzuki, K. anti-Selective vinylogous aldol reaction by silylated alkyldioxinone dienolate. *Chem. Lett.* **39**, 1042–1044 (2010).
27. Frías, M., Cieślik, W., Fraile, A., Rosado-Abón, A., Garrido-Castro, A. F., Yuste, F., Alemán, José. Development and application of asymmetric organocatalytic mukaiyama and vinylogous mukaiyama-type reactions. *Chem. Eur. J.* **24**, 10906–10933 (2018).
28. Fukui, K., Yonezawa, T., Nagata, C., Shingu, H. Molecular orbital theory of orientation in aromatic, heteroaromatic, and other conjugated molecules. *J. Chem. Phys.* **22**, 1433–1442 (1954).
29. Chen, M., Hartwig, J. F. Iridium-catalyzed regio- and enantioselective allylic substitution of silyl dienolates derived from dioxinones. *Angew. Chem. Int. Ed.* **53**, 12172–12176 (2014).
30. Chen, X., Wang, Q., Yu, B. Gold(i)-catalyzed *C*-glycosylation of glycosyl *ortho*-alkynylbenzoates: the role of the moisture sequestered by molecular sieves. *Chem. Commun.* **52**, 12183–12186 (2016).
31. Li, H., Yin, L. Recent progress on direct catalytic asymmetric vinylogous reactions. *Tetrahedron Lett.* **59**, 4121–4135 (2018).
32. Emami, S., Dadashpour, S. Current developments of coumarin-based anti-cancer agents in medicinal chemistry. *Eur. J. Med. Chem.* **102**, 611–630 (2015).
33. Dai, Y., Tian, B., Chen, H., Zhang, Q. Palladium-catalyzed stereospecific *C*-glycosylation of glycals with vinylogous acceptors. *ACS Catal.* **9**, 2909–2915 (2019).
34. Xie, K.-X., Zhang, Z.-P., Li, X. Bismuth triflate-catalyzed vinylogous nucleophilic 1,6-conjugate addition of *para* -quinone methides with 3-propenyl-2-silyloxyindoles. *Org. Lett.* **19**, 6708–6711 (2017).
35. Begouin, J.-M., Niggemann, M. Calcium-based lewis acid catalysts. *Chem. Eur. J.* **19**, 8030–8041 (2013).
36. Niggemann, M., Bisek, N. Calcium-catalyzed hydroarylation of alkenes at room temperature. *Chem. Eur. J.* **16**, 11246–11249 (2010).
37. Maloney, T. P., Murphy, K. L., Mainsah, T. L., Nolin, K. A. Friedel-Crafts alkylation of benzo[b]furan with activated cyclopropanes catalyzed by a calcium(II) complex. *Tetrahedron Lett.* **59**, 18–21 (2018).
38. Desiraju, G. R., .Ho, P. S., Kloo, L., Legon, A. C., Marquardt, R., Metrangolo, P., Politzer, P., Resnati, G., Rissanen, K. Definition of the halogen bond (IUPAC Recommendations

2013). *Pure Appl. Chem.* **85**, 1711–1713 (2013).

39. Parrish, R. M., Parker, T. M., Sherrill, C. D. Chemical assignment of symmetry-adapted perturbation theory interaction energy components: the functional-group SAPT partition. *J. Chem. Theory Comput.* **10**, 4417–4431 (2014).
40. Bulfield, D., Huber, S. M. Halogen bonding in organic synthesis and organocatalysis. *Chem. Eur. J.* **22**, 14434–14450 (2016).
41. Cavallo, G. Metrangolo, P., Milani, R., Pilati, T., Priimagi, A., Resnati, G., Terraneo, G., The halogen bond. *Chem. Rev.* **116**, 2478–2601 (2016).
42. Metrangolo, P., Meyer, F., Pilati, T., Resnati, G., Terraneo, G. Halogen bonding in supramolecular chemistry. *Chem. Rev.* **115**, 7118–7195 (2015).
43. Zhou, P.-P., Qiu, W.-Y., Liu, S., Jin, N.-Z. Halogen as halogen-bonding donor and hydrogen-bonding acceptor simultaneously in ring-shaped H3N·X(Y)·HF (X = Cl, Br and Y = F, Cl, Br) Complexes. *Phys. Chem. Chem. Phys.* **13**, 7408–7418 (2011).
44. Kobayashi, Y., Nakatsuji, Y., Li, S., Tsuzuki, S., Takemoto, Y. Direct *N*-glycofunctionalization of amides with glycosyl trichloroacetimidate by thiourea/halogen bond donor co-catalysis. *Angew. Chem. Int. Ed.* **57**, 3646–3650 (2018).
45. Xu, C., Loh, C. C. J. A Multistage halogen bond catalyzed strain-release glycosylation unravels new hedgehog signaling inhibitors. *J. Am. Chem. Soc.* **141**, 5381–5391 (2019).
46. Wang, B., Xiong, D.-C., Ye, X.-S. Direct C–H trifluoromethylation of glycals by photoredox catalysis. *Org. Lett.* **17**, 5698–5701 (2015).
47. Salicylic acid glucosides methyl compound, and synthesis method and purposes thereof. China Patent No. CN101863934A (2009).
48. Brawn, R. A., Panek, J. S. Stereoselective *C*-glycosidations with achiral and enantioenriched allenylsilanes. *Org. Lett.* **12**, 4624–4627 (2010).
49. Prantz, K., Mulzer, J. Synthesis of (*Z*)-trisubstituted olefins by decarboxylative grob-type rragmentations: Epothilone D, Discodermolide, and Peloruside. A. *Chem. Eur. J.* **16**, 485–506 (2010).
50. Gupta, V., Sudhir, S., Mandal, T., Schneider, C. Organocatalytic, highly enantioselective vinylogous mukaiyama-michael reaction of acyclic dienol silyl ethers. *Angew. Chem. Int. Ed.* **51**, 12609–12612 (2012).
51. Zhou, Y., Li, X., Hou, S., Xu, J. Facile synthesis of dihydrochalcones via the $AlCl_3$-

promoted tandem Friedel–Crafts acylation and alkylation of arenes with 2-alkenoyl chlorides. *J. Mol. Catal. A Chem.* **365**, 203–211 (2012).

52. Beaton, S. A., Huestis, M. P., Sadeghi-Khomami, A., Thomas, N. R., Jakeman, D. L. Enzyme-catalyzed synthesis of isosteric phosphono-analogues of sugar nucleotides. *Chem. Commun.* **2**, 238–240 (2009)
53. Tian, Q., Xu, L., Ma, X., Zou, W., Shao, H. Stereoselective synthesis of 2-*C*-acetonyl-2-deoxy-D-galactosides using 1,2-cyclopropaneacetylated sugar as novel glycosyl donor. *Org. Lett.* **12**, 540–543 (2010).
54. Evans, D. A., Gauchet-Prunet, J. A. Diastereoselective synthesis of protected syn 1,3-diols by base-catalyzed intramolecular conjugate addition of hemiacetal-derived alkoxide nucleophiles. *J. Org. Chem.* **58**, 2446–2453 (1993).
55. Glukhov, E., Stark, M., Burrows, L. L., Deber, C. M. Basis for selectivity of cationic antimicrobial peptides for bacterial versus mammalian membranes. *J. Biol. Chem.* **280**, 33960–33967 (2005).
56. Wang, Q., van Gemmeren, M., List, B. Asymmetric disulfonimide-catalyzed synthesis of δ-Amino-β-Ketoester derivatives by vinylogous mukaiyama-mannich reactions. *Angew. Chem. Int. Ed.* **53**, 13592–13595 (2014).
57. Loh, C. C. J., Schmid, M., Peters, B., Fang, X., Lautens, M. Exploiting distal reactivity of coumarins: a rhodium-catalyzed vinylogous asymmetric ring-opening reaction. *Angew. Chem. Int. Ed.* **55**, 4600–4604 (2016).
58. Ranieri, B. Sartori, A., Curti, C., Battistini, L., Rassu, G., Pelosi, G., Casiraghi, G., Zanardi, F. 3-Alkenyl-2-silyloxyindoles in vinylogous mannich reactions: Synthesis of aminated indole-based scaffolds and products. *Org. Lett.* **16**, 932–935 (2014).
59. Fernández-Herrera, M. A., Mohan, S., López-Muñoz, H., Hernández-Vázquez, J. M.V., Pérez-Cervantes, E., Escobar-Sánchez, M. L., Sánchez-Sánchez, L., Regla, I., Pinto, B. M., Sandoval-Ramírez, J. Synthesis of the steroidal glycoside (25R)-3β,16β-diacetoxy-12,22-dioxo-5α-cholestan-26-yl β-D-glucopyranoside and its anti-cancer properties on cervicouterine HeLa, CaSki, and ViBo cells. *Eur. J. Med. Chem.* **45**, 4827–4837 (2010).
60. Rathore, H., Hashimoto, T., Igarashi, K., Nukaya, H., Fullerton, D. S. Cardiac glycosides: 5. Stereoselective syntheses of digitoxigenin α-D, β-D, α-L, and β-L-glucosides. *Tetrahedron* **41**, 5427–5438 (1985).

61. Loscher, S., Schobert, R. Total synthesis and absolute configuration of Epicoccamide D, a naturally occurring mannosylated 3-acyltetramic acid. *Chem. Eur. J.* **19**, 10619–10624 (2013).

62. Nigudkar, S. S., Parameswar, A. R., Pornsuriyasak, P., Stine, K. J., Demchenko, A. V. *O*-Benzoxazolyl imidates as versatile glycosyl donors for chemical glycosylation. *Org. Biomol. Chem.* **11**, 4068 (2013).

63. Scharfbier, J., Oestreich, M. Copper-catalyzed Si–B bond activation in the nucleophilic substitution of primary aliphatic triflates. *Synlett.* **27**, 1274–1276 (2016).

64. Nkosana, N. K., Czyzyk, D. J., Siegel, Z. S., Cote, J. M., Taylor, E. A. Synthesis, kinetics and inhibition of *Escherichia coli* Heptosyltransferase I by monosaccharide analogues of Lipid A. *Bioorganic Med. Chem. Lett.* **28**, 594–600 (2018).

65. Chen, H. Xian, T., Zhang. W., Si, W., Luo, X., Zhang, B., Zhang, M., Wang, Z., Zhang, J. An efficient method for the synthesis of pyranoid glycals. *Carbohydr. Res.* **431**, 42–46 (2016).

66. Brimacombe, J. S., Foster, A. B., Stacey, M., Whiffen, D. H. Aspects of stereochemistry–I : Properties and reactions of some diols. *Tetrahedron* **4**, 351–360 (1958).

67. Singh, A. K., Kandasamy, J. Palladium catalyzed stereocontrolled synthesis of *C*-aryl glycosides using glycals and arenediazonium salts at room temperature. *Org. Biomol. Chem.* **16**, 5107–5112 (2018).

68. Fettes, A., Carreira, E. M. Leucascandrolide A: Synthesis and related studies. *J. Org. Chem.* **68**, 9274–9283 (2003).

69. Iwaoka, T., Murohashi, T., Katagiri, N., Sato, M., Kaneko, C. Use of 1,3-dioxin-4-ones and related compounds in synthesis. Part 37. 5-Trifluoromethyl-1,3-dioxin-4-ones as versatile building blocks for trifluoromethylated aliphatic compounds. *J. Chem. Soc. Perkin Trans. 1*. **11**, 1393–1397 (1992).

70. Dieckmann, M. Kretschmer, M., Li, P., Rudolph, S., Herkommer, D., Menche, D. Total Synthesis of Rhizopodin. *Angew. Chem. Int. Ed.* **51**, 5667–5670 (2012).

71. Sato, M., Ogasawara, H., Oi, K., Kato, T. Synthesis of 1,3-dioxin-4-one derivatives. *Chem. Pharm. Bull. (Tokyo).* **31**, 1896–1901 (1983).

72. Sato, M., Sunami, S., Sugita, Y., Kaneko, C. Use of 1,3-dioxin-4-ones and related compounds in synthesis. XLIV. Asymmetric aldol reaction of 4-trimethylsiloxy-6-

methylene-1,3-dioxines: Use of tartaric acid-derived (acyloxy)borane complex as the catalyst. *Chem. Pharm. Bull. (Tokyo).* **42**, 839–845 (1994).

73. Cardona, F., Parmeggiani, C., Faggi, E., Bonaccini, C., Gratteri, P., Sim, L., Gloster, T. M. Roberts, S., Davies, G. J., Rose, D. R., Goti, A. Total syntheses of casuarine and its 6-*O*-α-glucoside: complementary inhibition towards glycoside hydrolases of the GH31 and GH37 families. *Chem. Eur. J.* **15**, 1627–1636 (2009).
74. Gannedi, V., Ali, A., Singh, P. P., Vishwakarma, R. A. Intramolecular aglycon delivery for (1 → 2)–β-mannosylation: towards the synthesis of phospholipomannan of Candida albicans. *Tetrahedron Lett.* **55**, 2945–2947 (2014).
75. Takeda, Y., Hisakuni, D., Lin, C.-H., Minakata, S. 2- Halogenoimidazolium salt catalyzed aza-diels–alder reaction through halogen-bond formation. *Org. Lett.* **17**, 318–321 (2015).
76. Ke, C.-H., Kuo, B.-C., Nandi, D., Lee, H. M. Monodentate palladium complexes bearing abnormal and normal carbene ligands with a formally identical steric environment. *Organometallics* **32**, 4775–4784 (2013).

11 Appendix

11.1 List of abbreviations

Ac	acetyl
ACN	acetonitrile
aq.	aqueous
BOX	benzoxazolyl
Bz	benzoyl
Bn	benzyl
b/l	branch/linear
calcd	calculated
cat.	catalyst
CCl_3CN	trichloroacetonitrile
cod	1,5-cyclooctadiene
COMAS	Compound Management and Screening Center
Conc.	concentration
DBU	1,8-Diazabicyclo(5.4.0)undec-7-ene
DCE	1,2-dichloroethane
DCM	dichloromethane
DMSO	dimethylsulfoxide
DMF	dimethylformamide
D-A	donor-acceptor
eq./equiv.	equivalent
Ess	electrophilic susceptibilities
ESI	electrospray ionization
Et	ethyl
FR	Ferrier rearrangement
Gal	galactose
Glc	glucose
Hh	hedgehog

HPLC	high-performance liquid chromatography
HRMS	high resolution mass spectrometry
Hz	Hertz
HB	hydrogen bonding
IBX	2-iodoxybenzoic acid
IC_{50}	half-maximal inhibitory concentration
*i*Pr	iso-propyl
J	coupling constants
LDA	lithium diisopropylamide
m	meta
Moc	dimethyl dicarbonate
Me	methyl
MOM	methoxymethyl
m.p.	melting point
MS	molecular sieves
NIS	*N*-iodosuccinimide
NMR	nuclear magnetic resonance
Nu	nucleophile
o	ortho
OCs	orbital coefficients
P	para
ppm, δ	parts per million
R_f	retention factor
Rt	room temperature
sat.	saturated
s.d.	standard deviation
SGLTs	sodium glucose co-transporters
TBAI	tetra-n-butylammonium iodide
TBS	*tert*-butyl dimethylsilyl
TCAI	trichloroacetimidate

*t*Bu	*tert*-butyl
TEA	trimethylamine
Temp.	temperature
Tf	trifluoromethanesulfonyl
TIPS	triisopropylsilyl
THF	tetrahydrofuran
TLC	thin-layer chromatography
TMS	trimethylsilyl
Ts	para-tosyl
XB	halogen bonding

11.2 NMR spectra

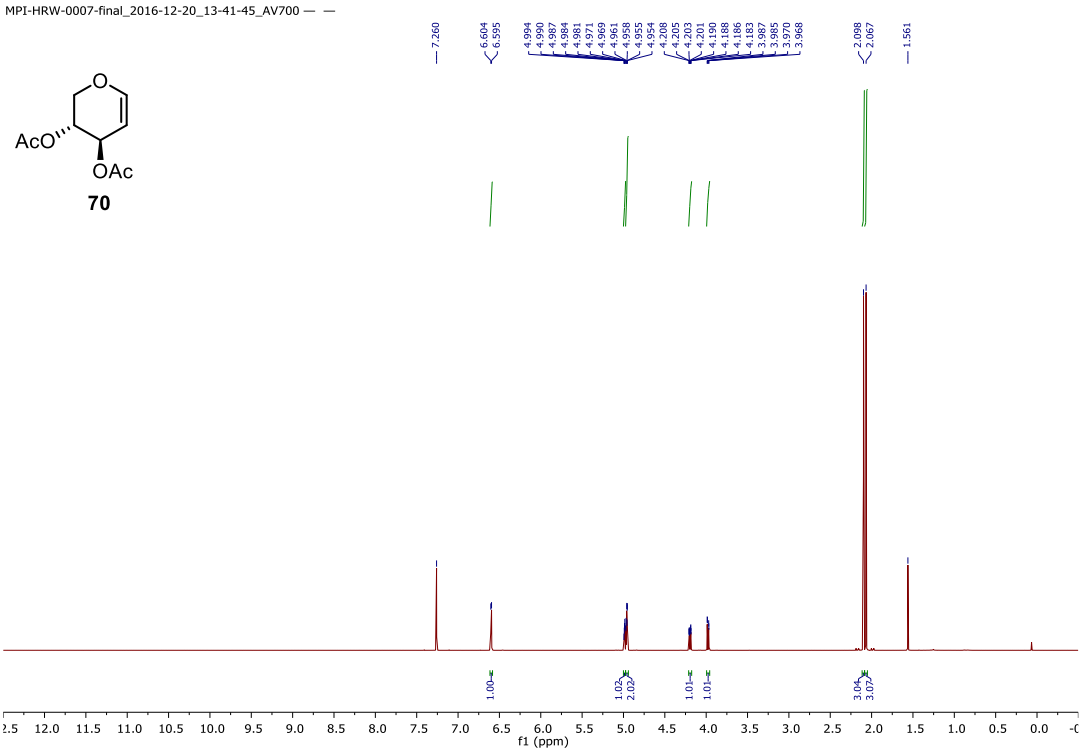

^{1}H NMR spectrum of compound **70** (700 MHz, in $CDCl_3$)

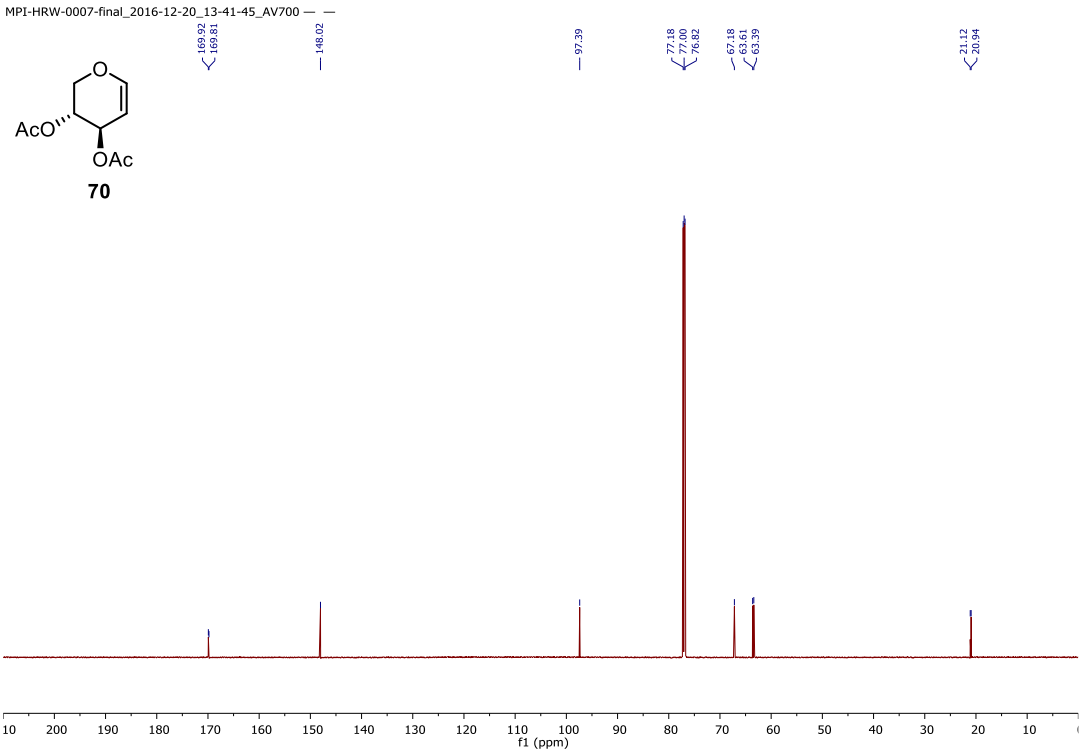

^{13}C NMR spectrum of compound **70** (176 MHz, in $CDCl_3$)

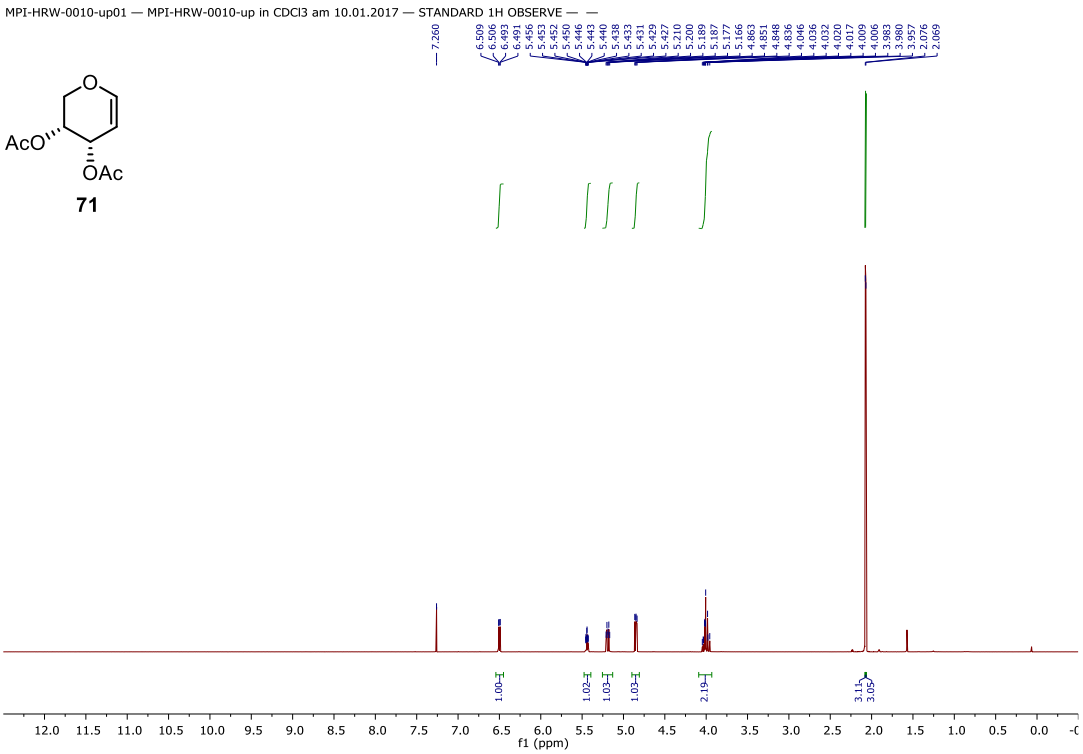

^{1}H NMR spectrum of compound **71** (400 MHz, in $CDCl_3$)

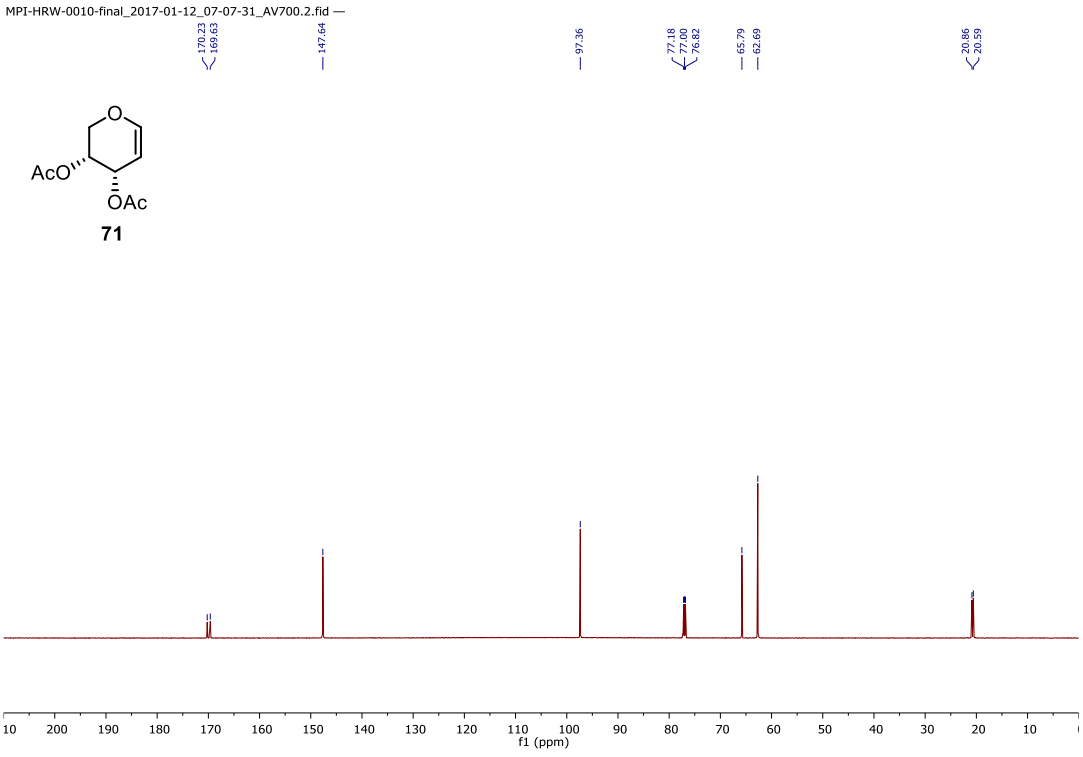

^{13}C NMR spectrum of compound **71** (176 MHz, in $CDCl_3$)

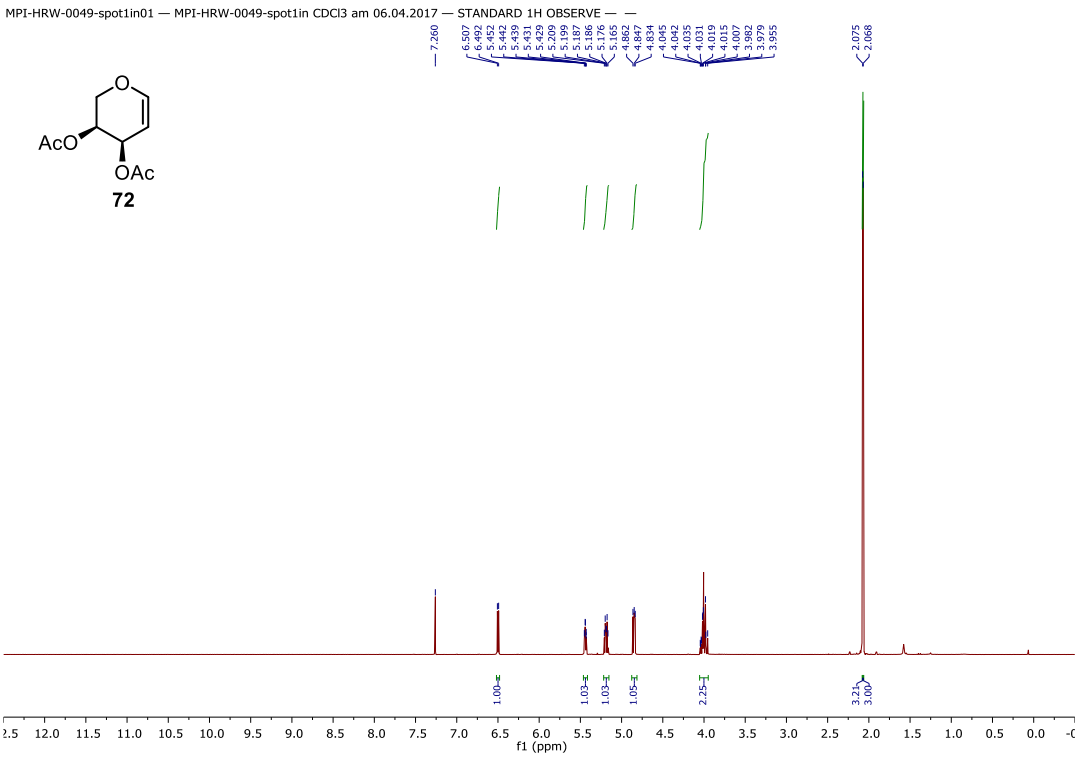

^{1}H NMR spectrum of compound **72** (400 MHz, in $CDCl_3$)

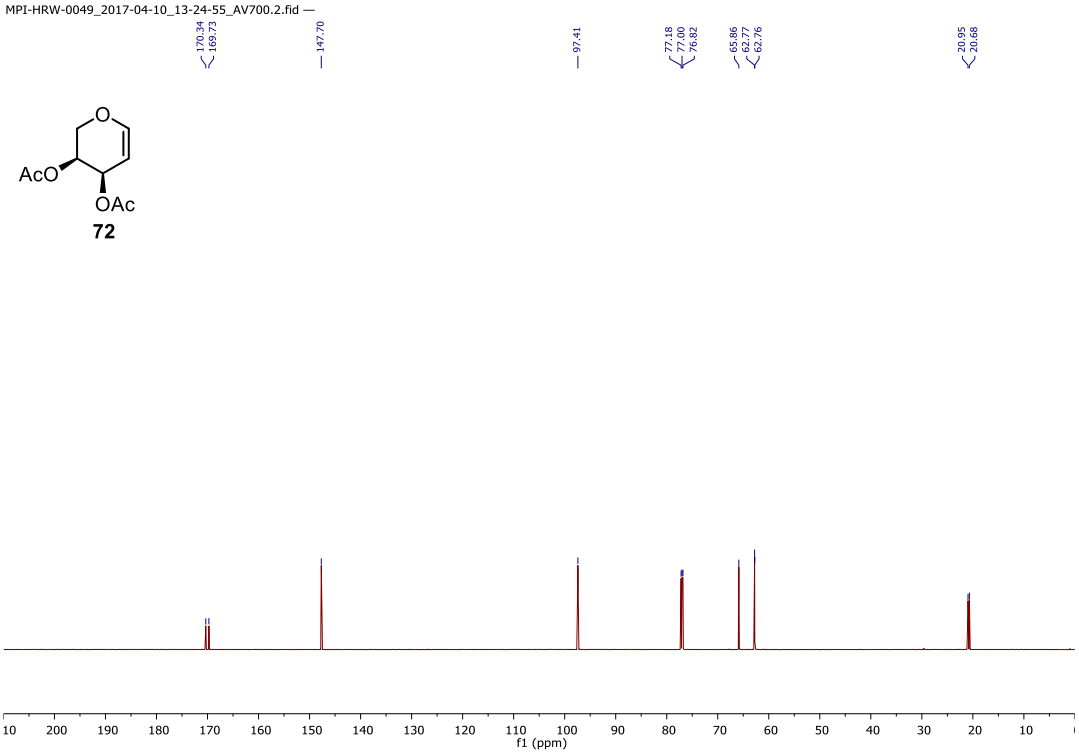

^{13}C NMR spectrum of compound **72** (176 MHz, in $CDCl_3$)

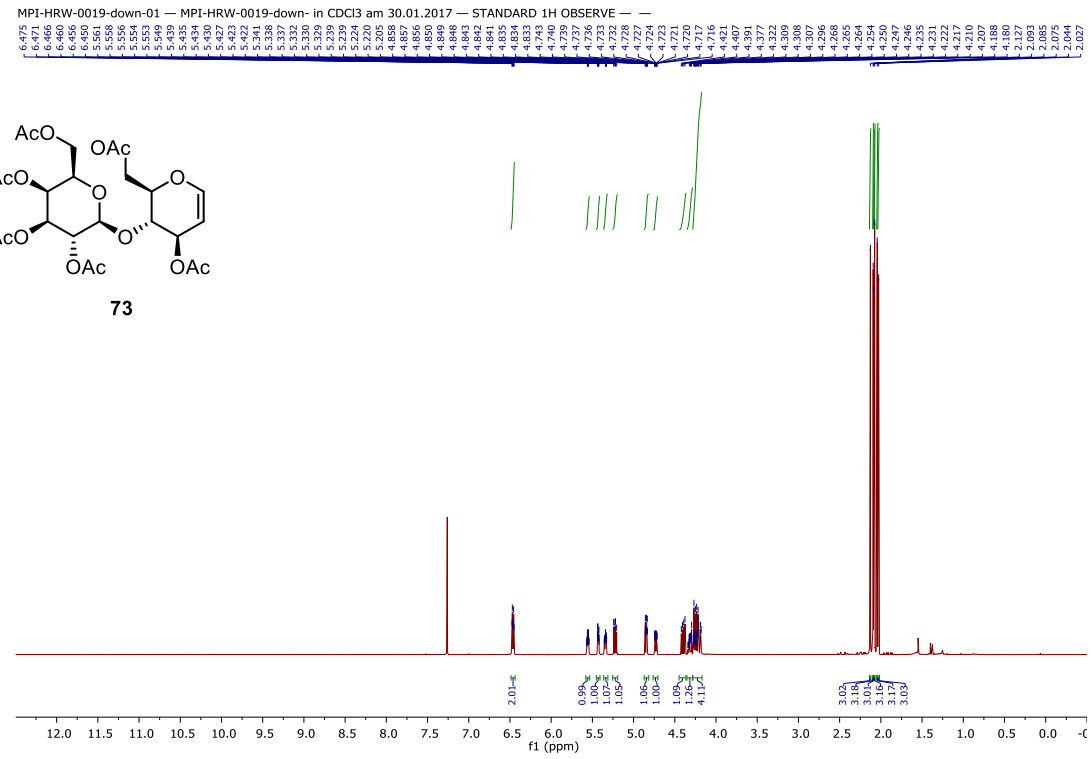

^{1}H NMR spectrum of compound **73** (400 MHz, in $CDCl_3$)

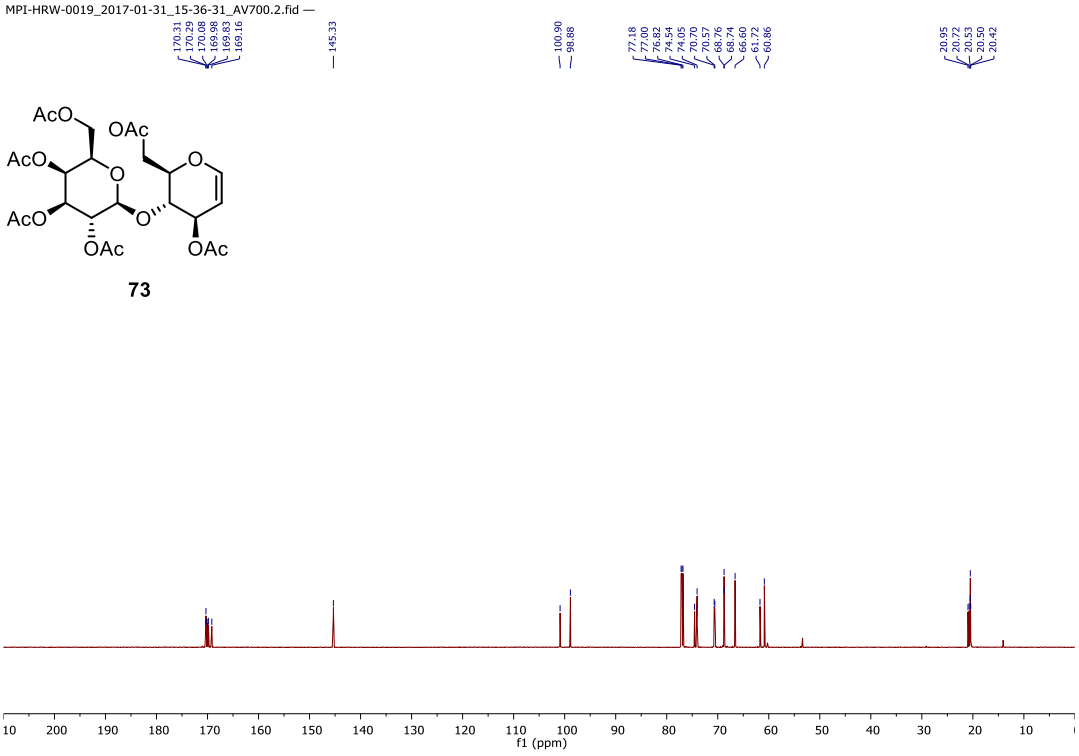

^{13}C NMR spectrum of compound **73** (176 MHz, in $CDCl_3$)

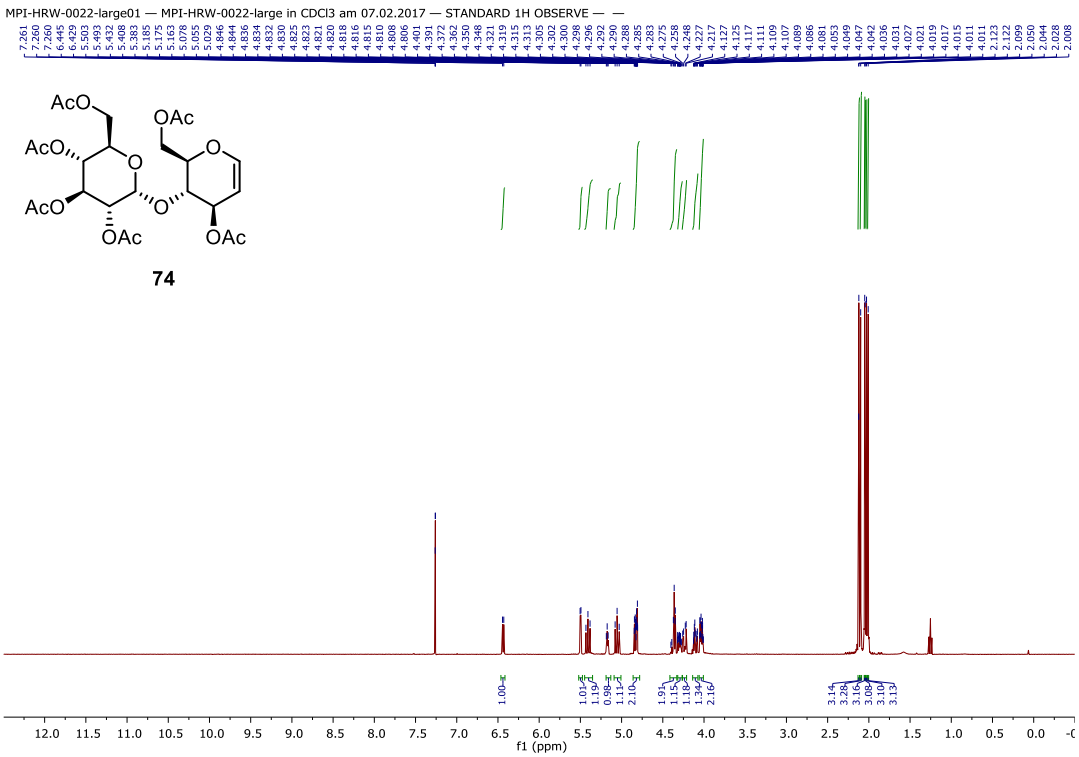

^{1}H NMR spectrum of compound **74** (400 MHz, in $CDCl_3$)

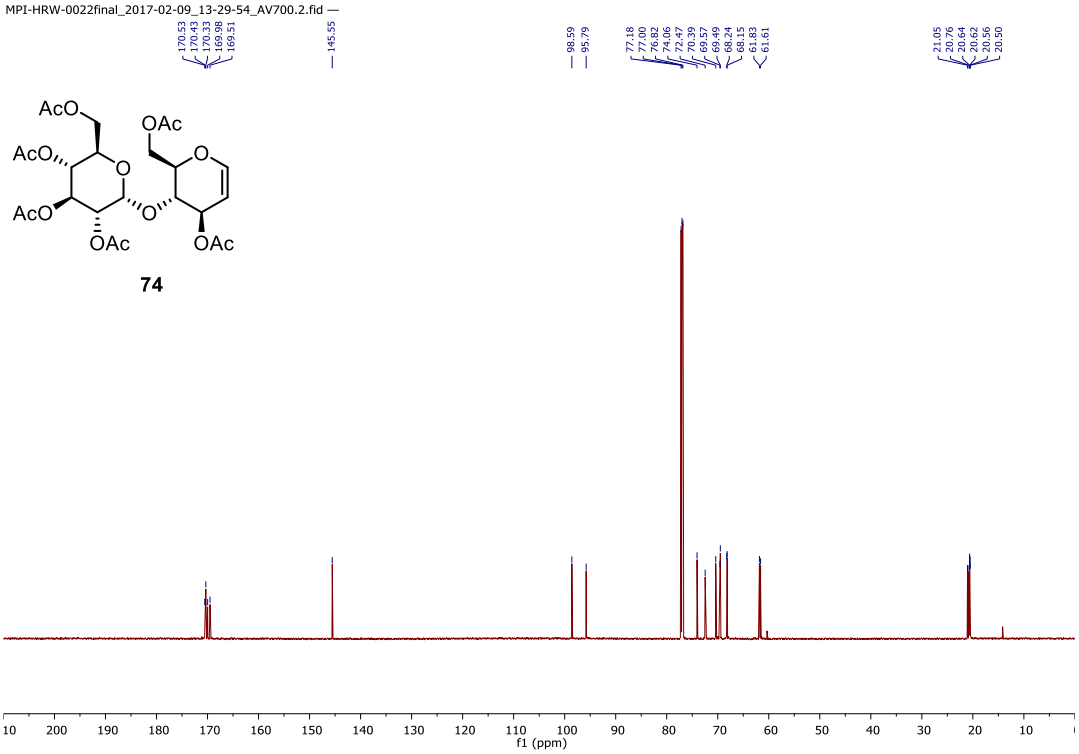

^{13}C NMR spectrum of compound **74** (176 MHz, in $CDCl_3$)

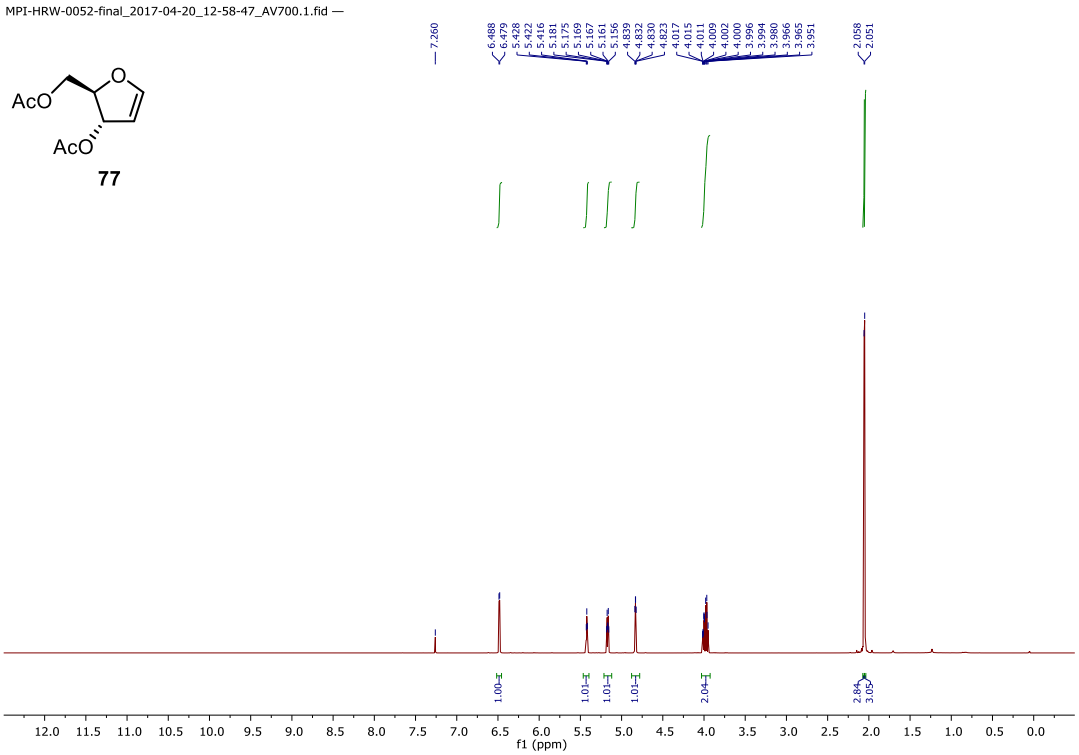

^{1}H NMR spectrum of compound **77** (400 MHz, in $CDCl_3$)

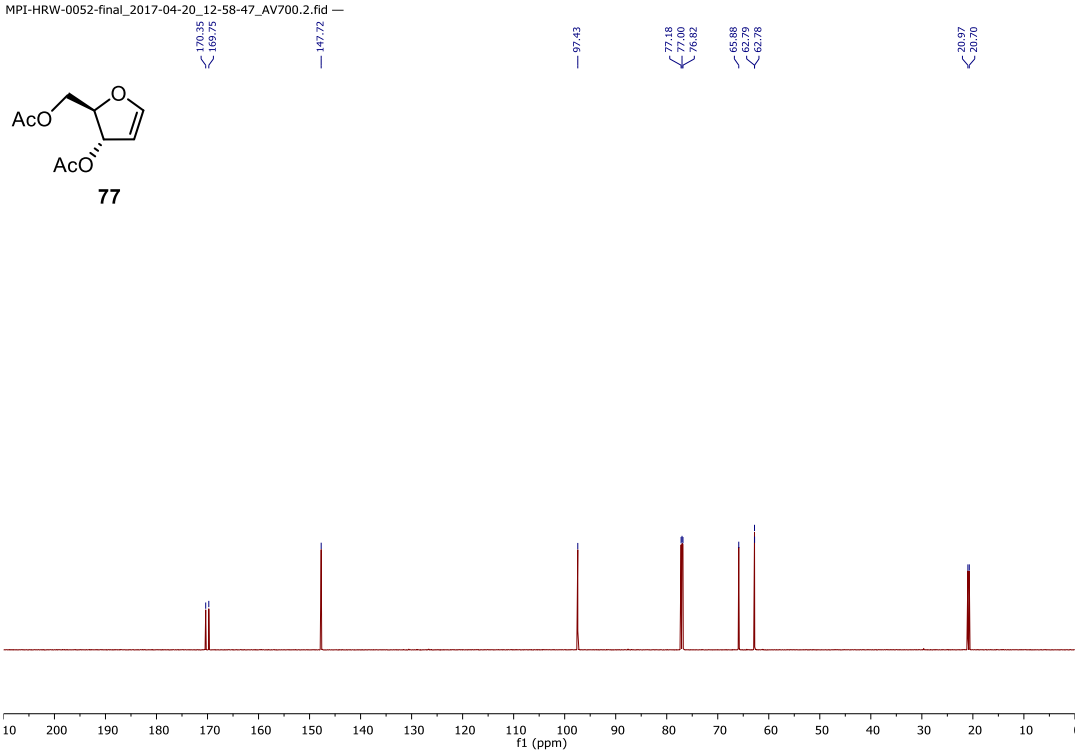

^{13}C NMR spectrum of compound **77** (176 MHz, in $CDCl_3$)

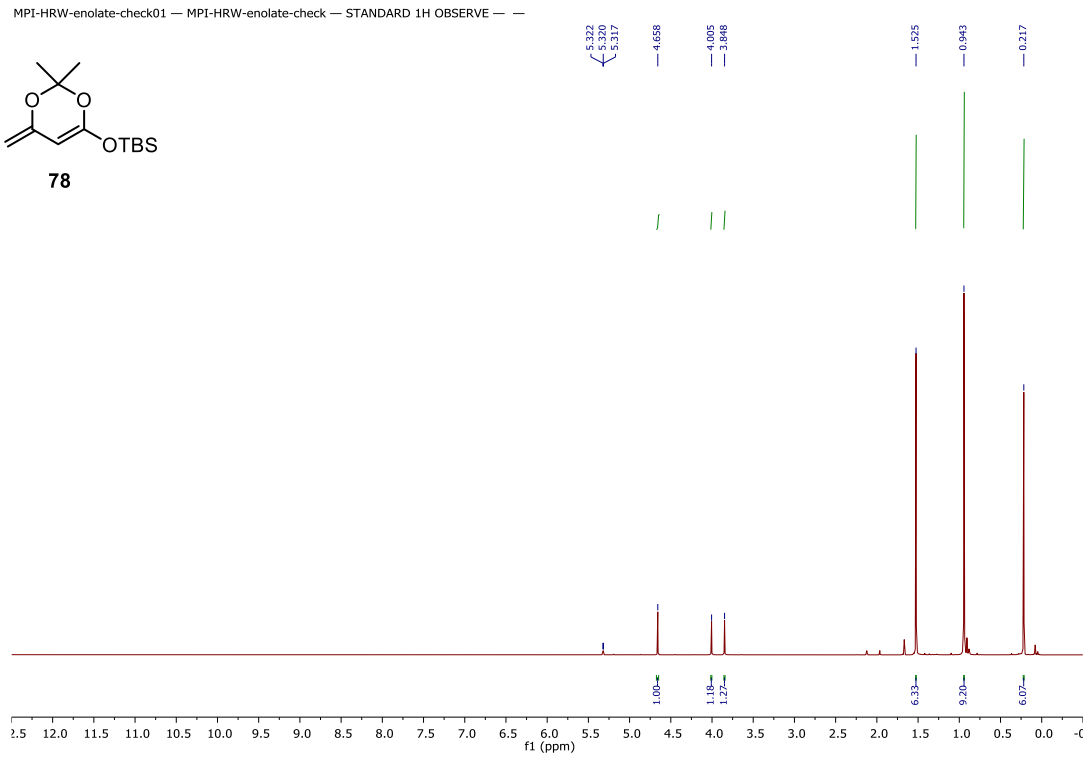

^{1}H NMR spectrum of compound **78** (400 MHz, in CD_2Cl_2)

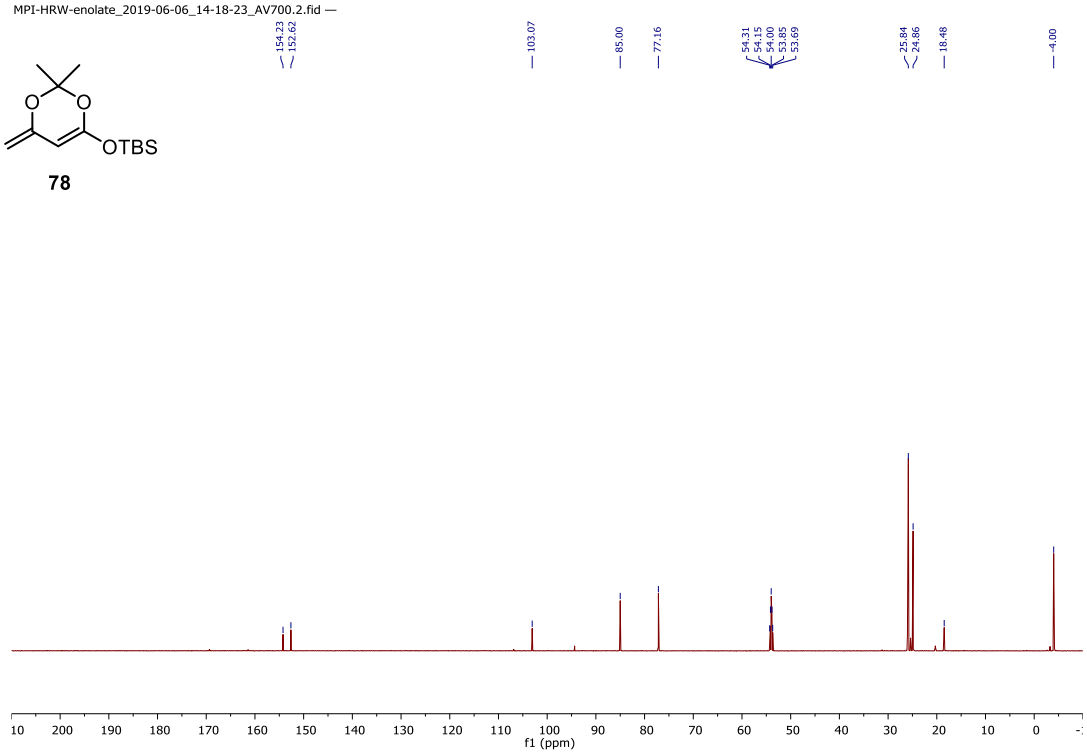

^{13}C NMR spectrum of compound **78** (176 MHz, in CD_2Cl_2)

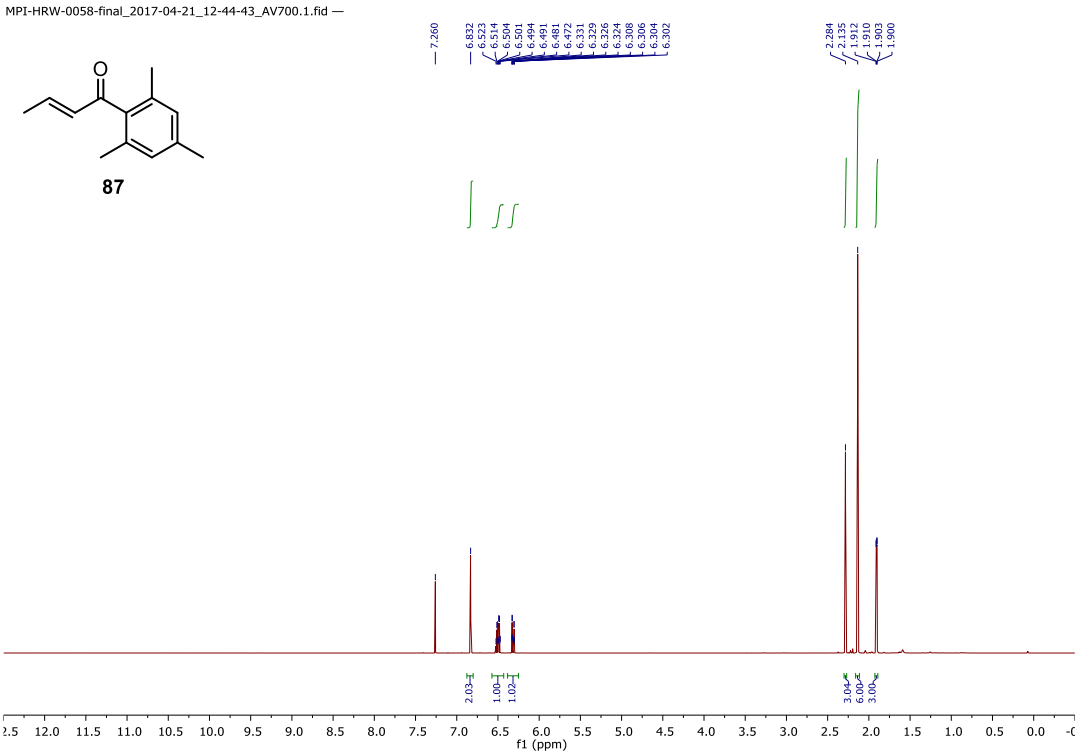

^{1}H NMR spectrum of compound **87** (700 MHz, in $CDCl_3$)

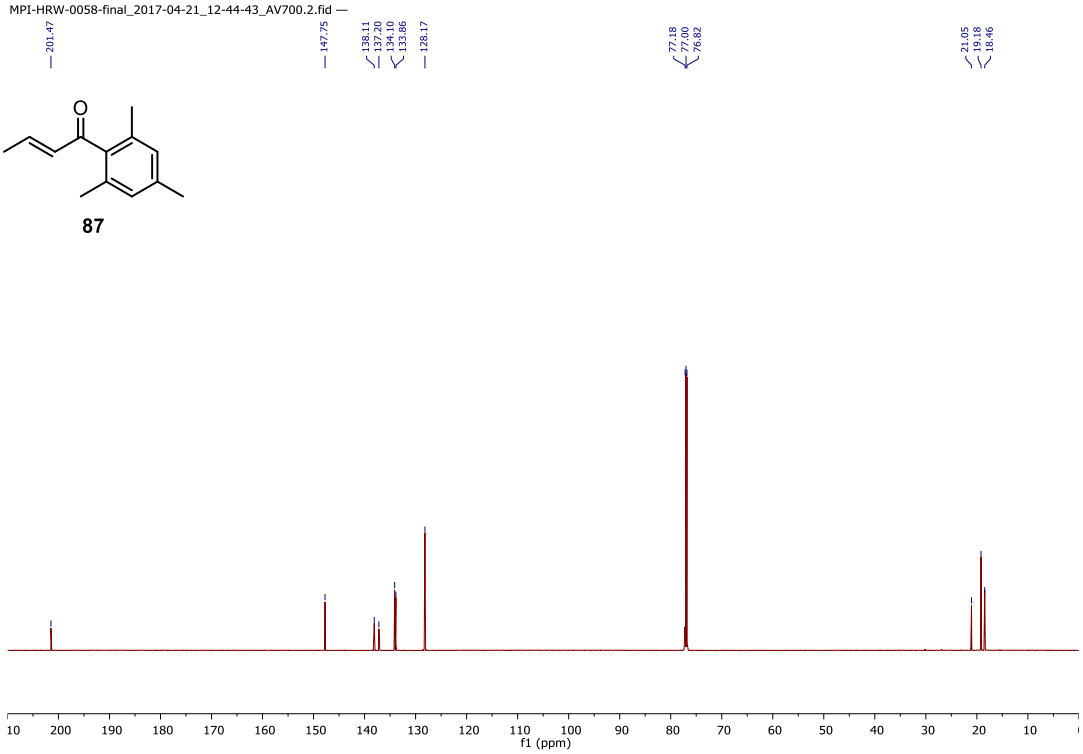

^{13}C NMR spectrum of compound **87** (176 MHz, in $CDCl_3$)

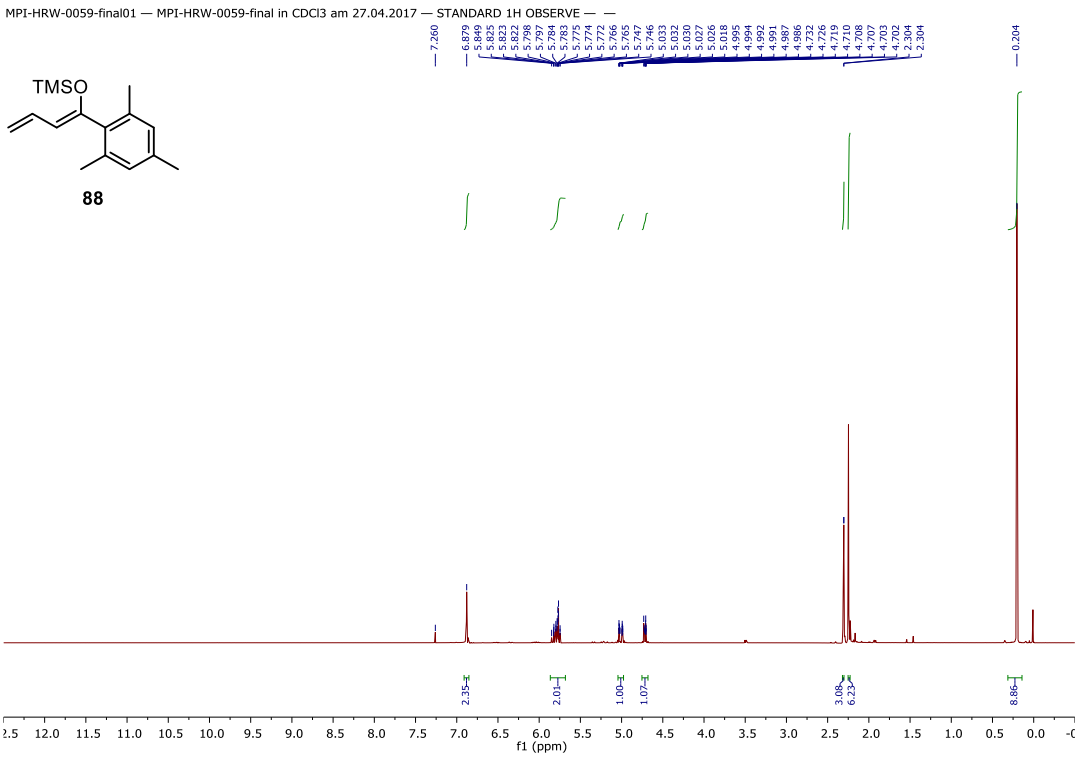

^{1}H NMR spectrum of compound **88** (400 MHz, in $CDCl_3$)

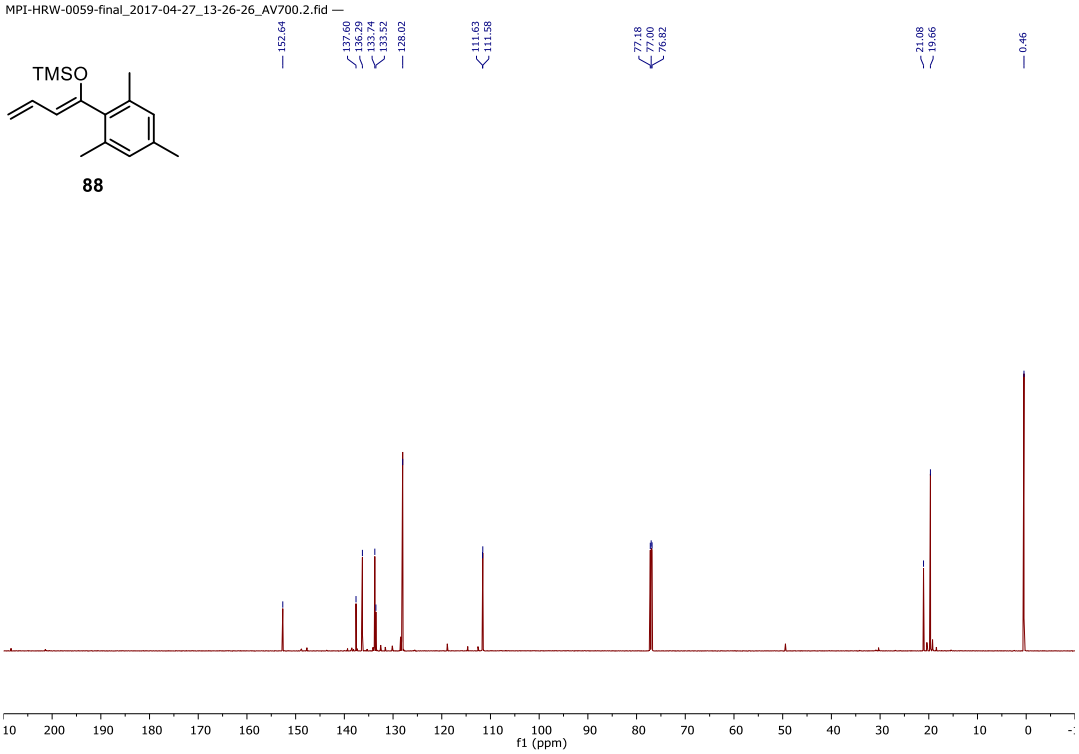

^{13}C NMR spectrum of compound **88** (176 MHz, in $CDCl_3$)

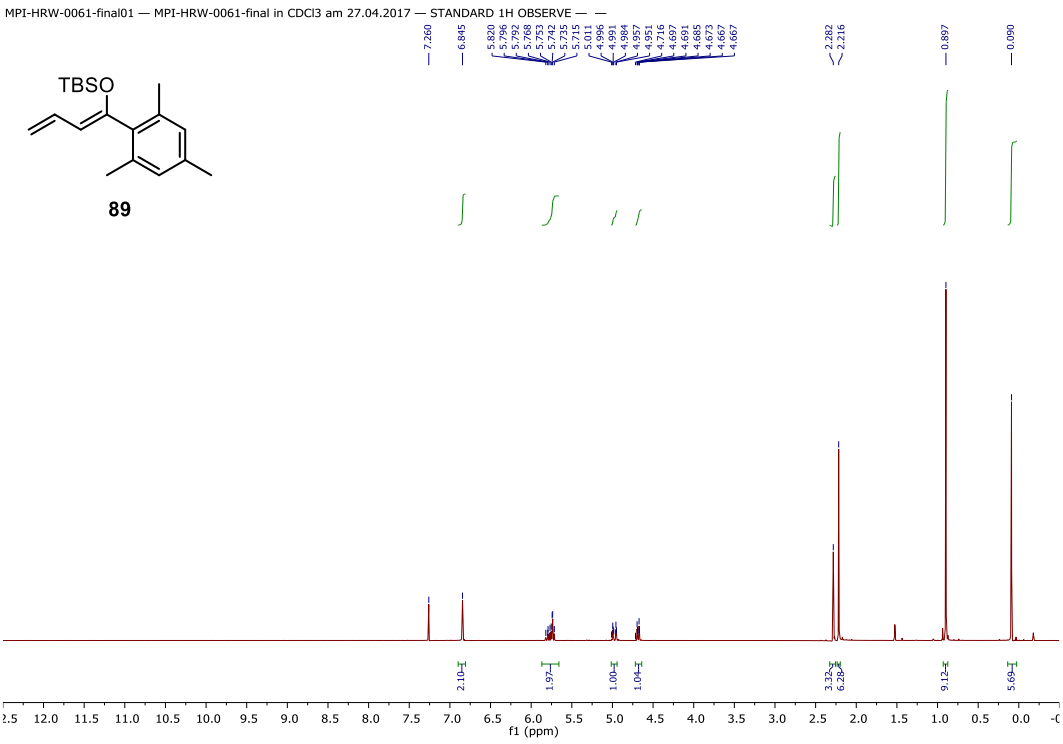

^{1}H NMR spectrum of compound **89** (400 MHz, in $CDCl_3$)

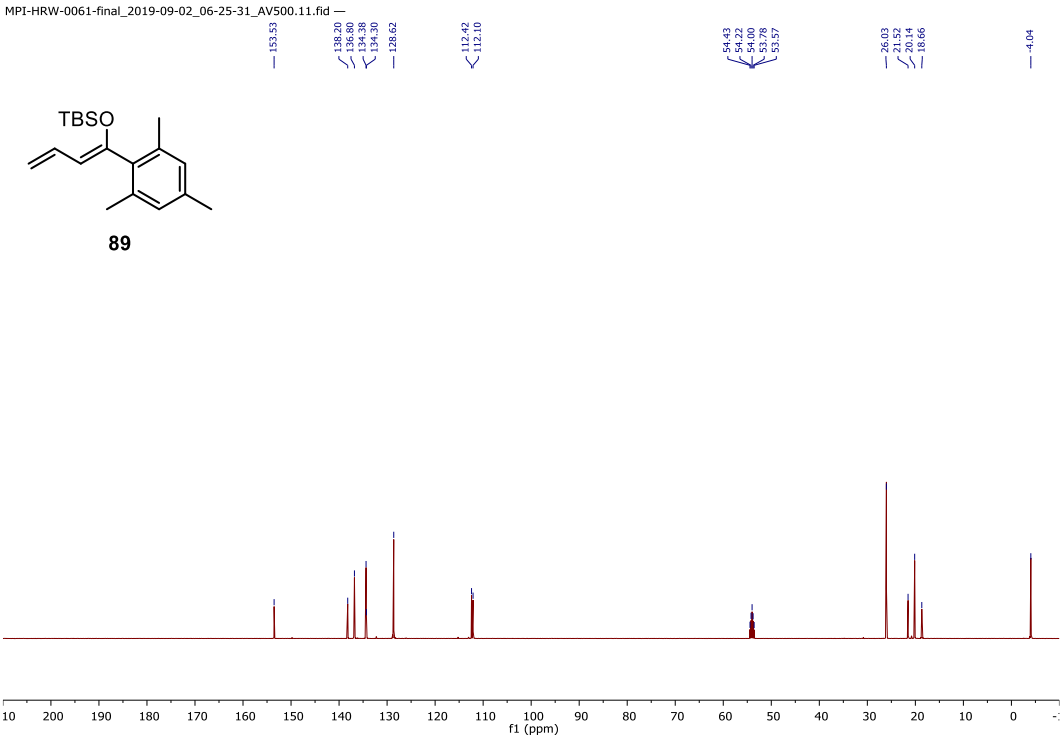

^{13}C NMR spectrum of compound **89** (126 MHz, in CD_2Cl_2)

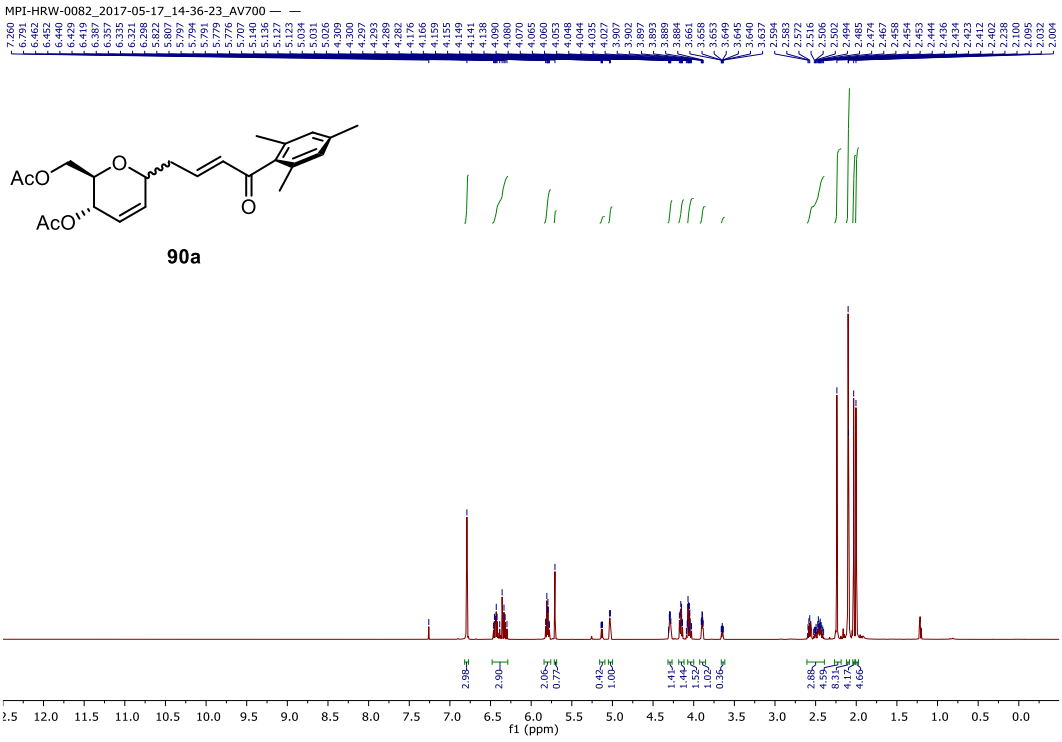

^{1}H NMR spectrum of compound **90a** (700 MHz, in $CDCl_3$)

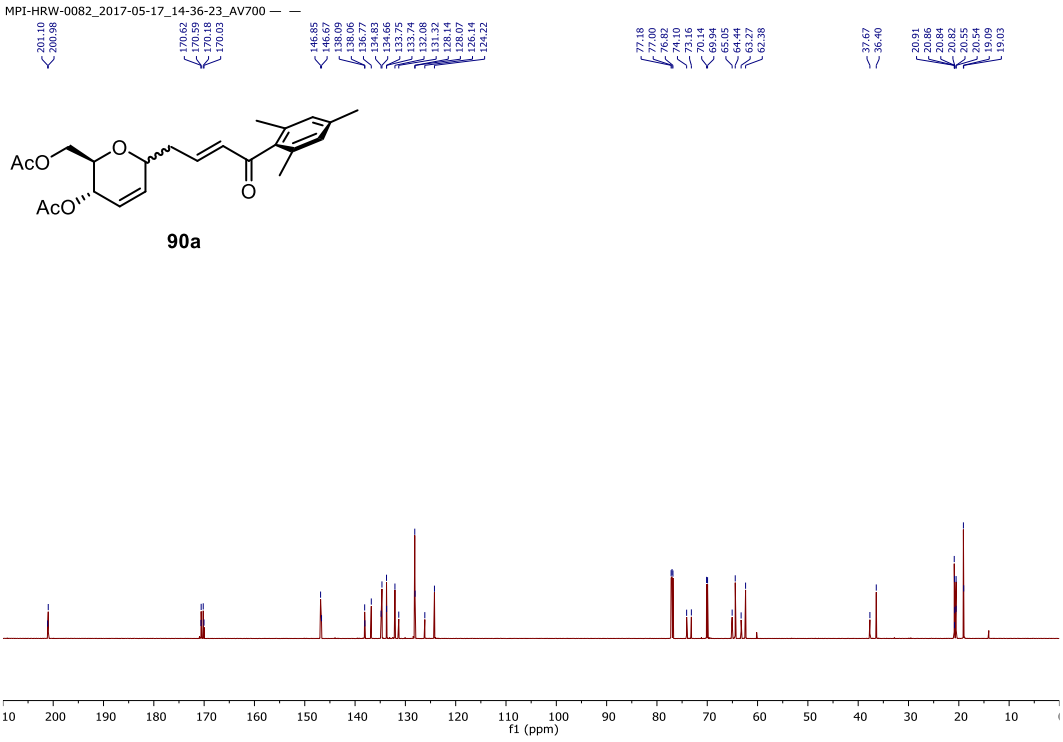

^{13}C NMR spectrum of compound **90a** (176 MHz, in $CDCl_3$)

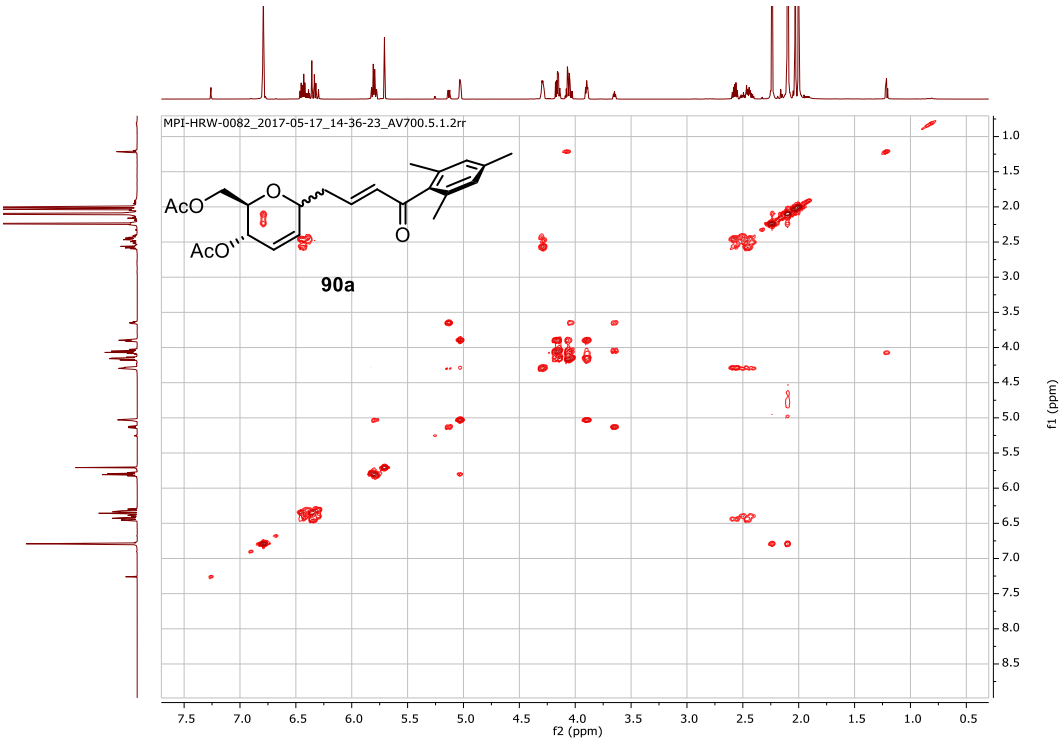

COSY spectrum of compound **90a**

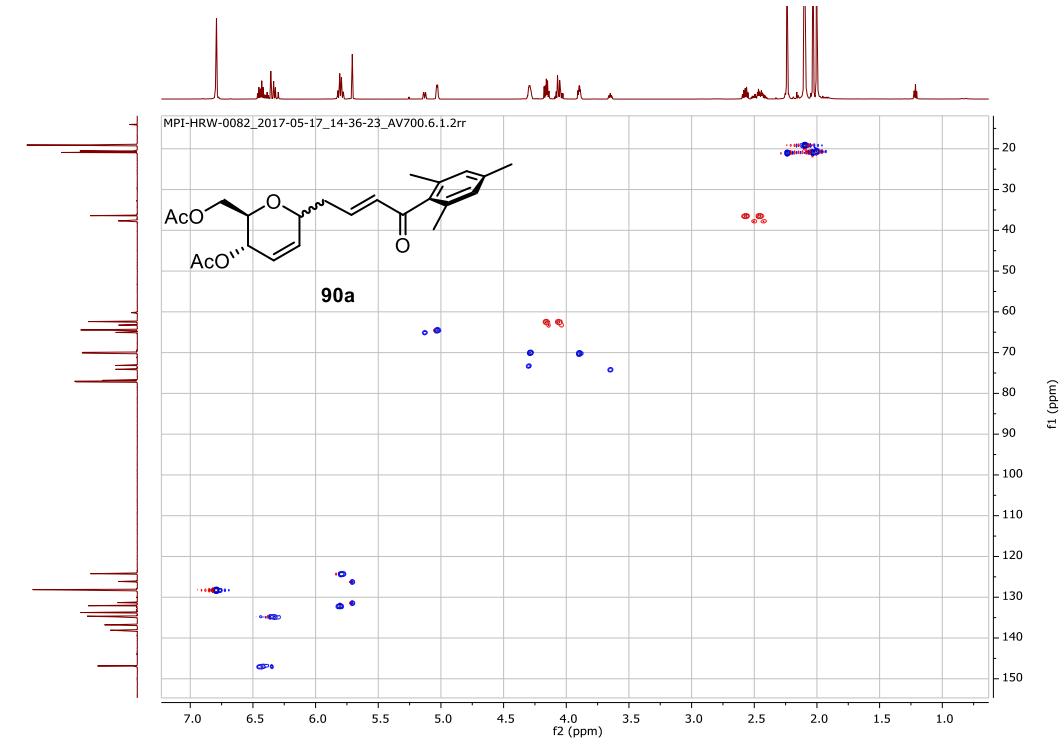

HSQC spectrum of compound **90a**

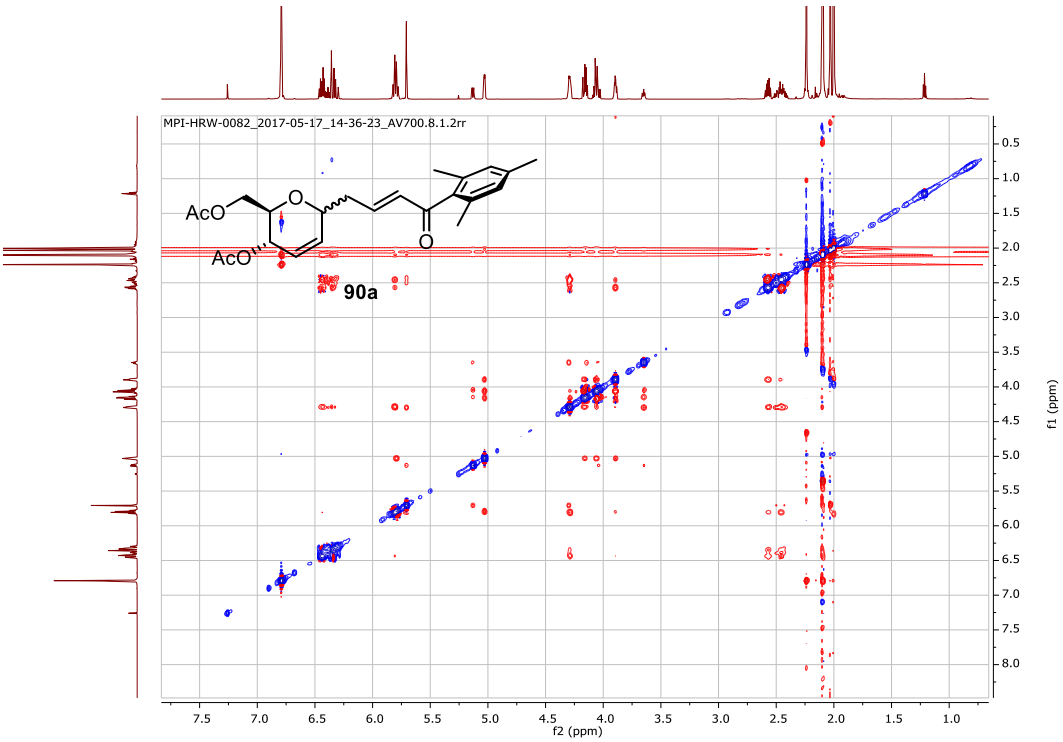

NOESY spectrum of compound **90a**

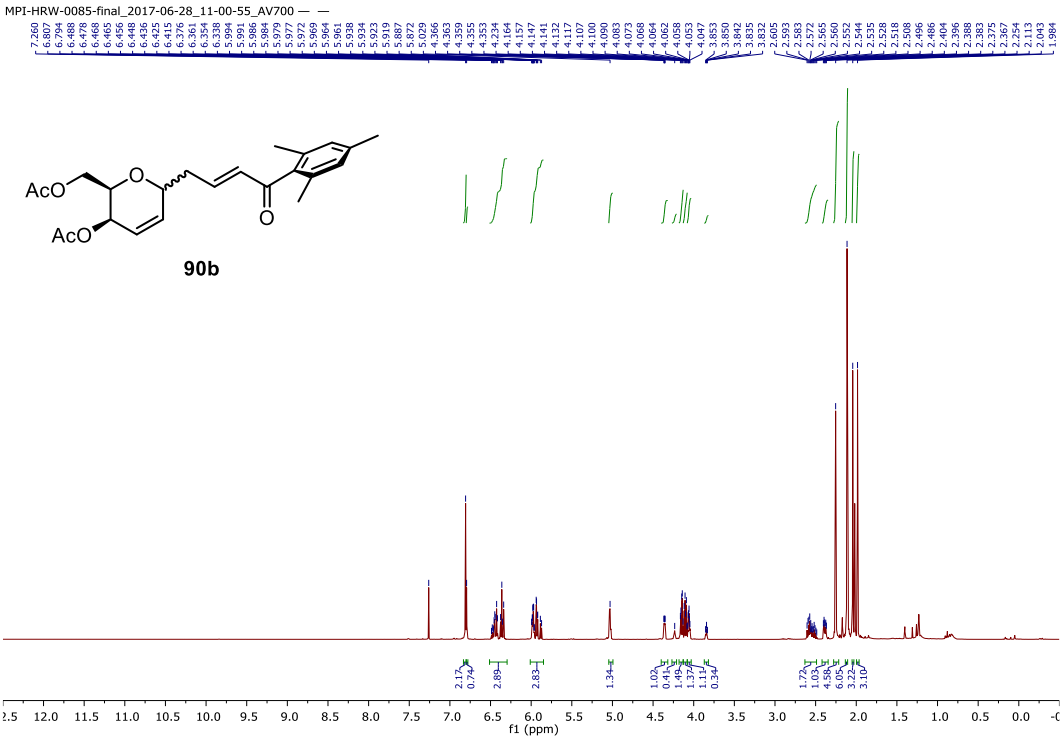

^{1}H NMR spectrum of compound **90b** (700 MHz, in $CDCl_3$)

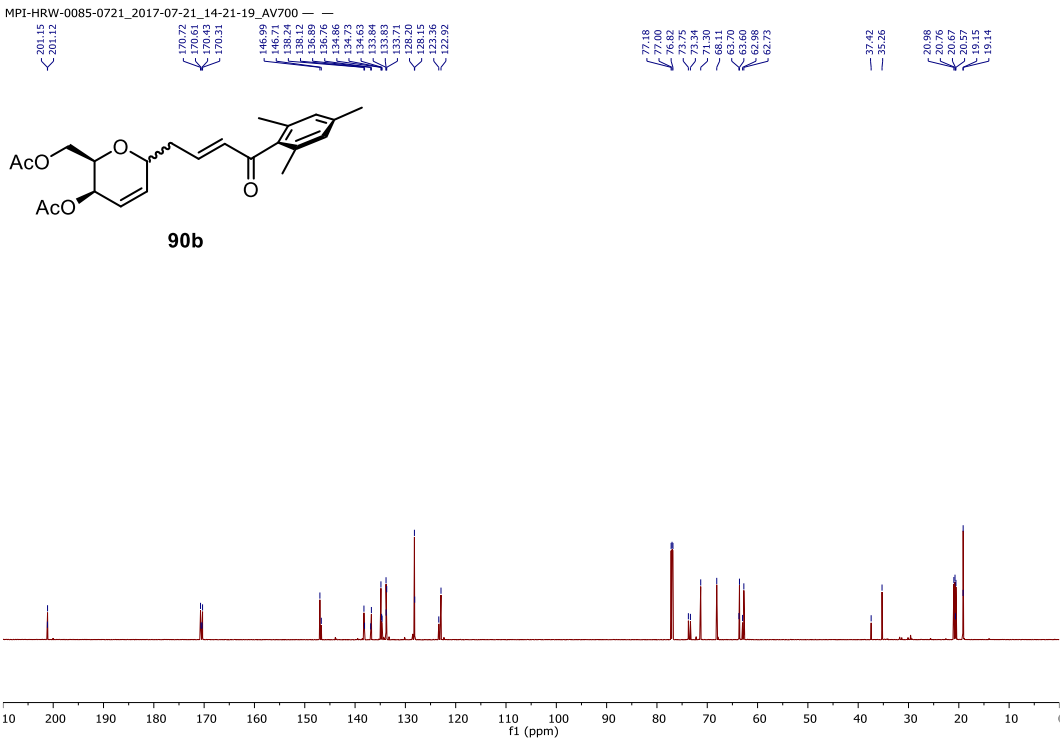

^{13}C NMR spectrum of compound **90b** (176 MHz, in $CDCl_3$)

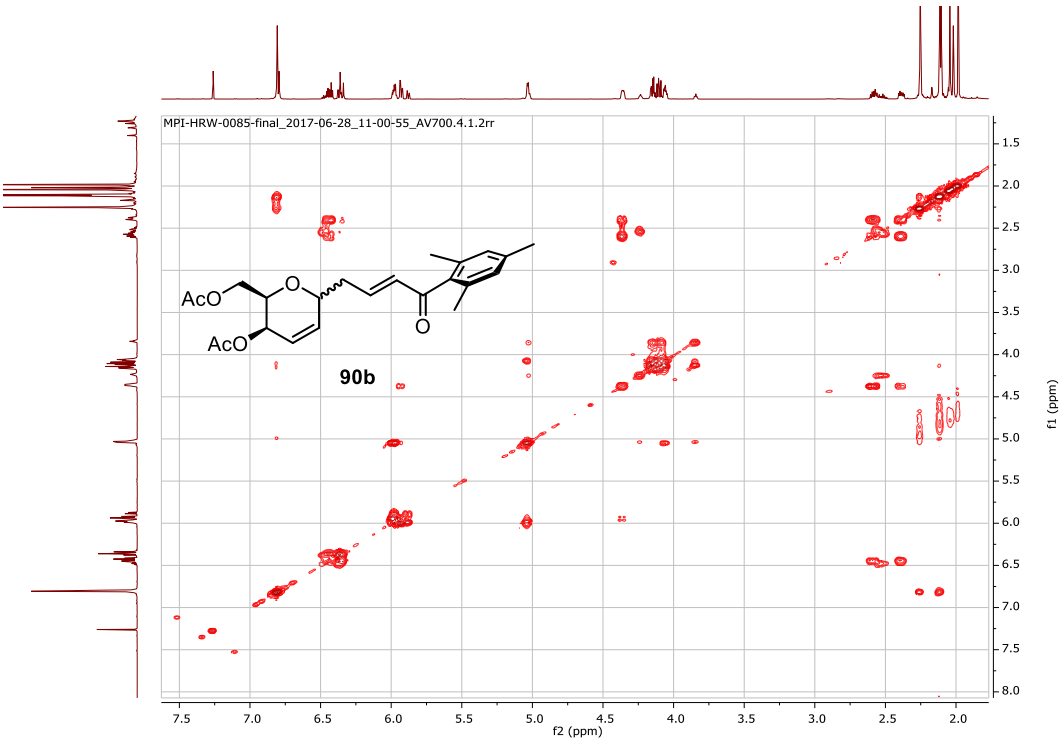

COSY spectrum of compound **90b**

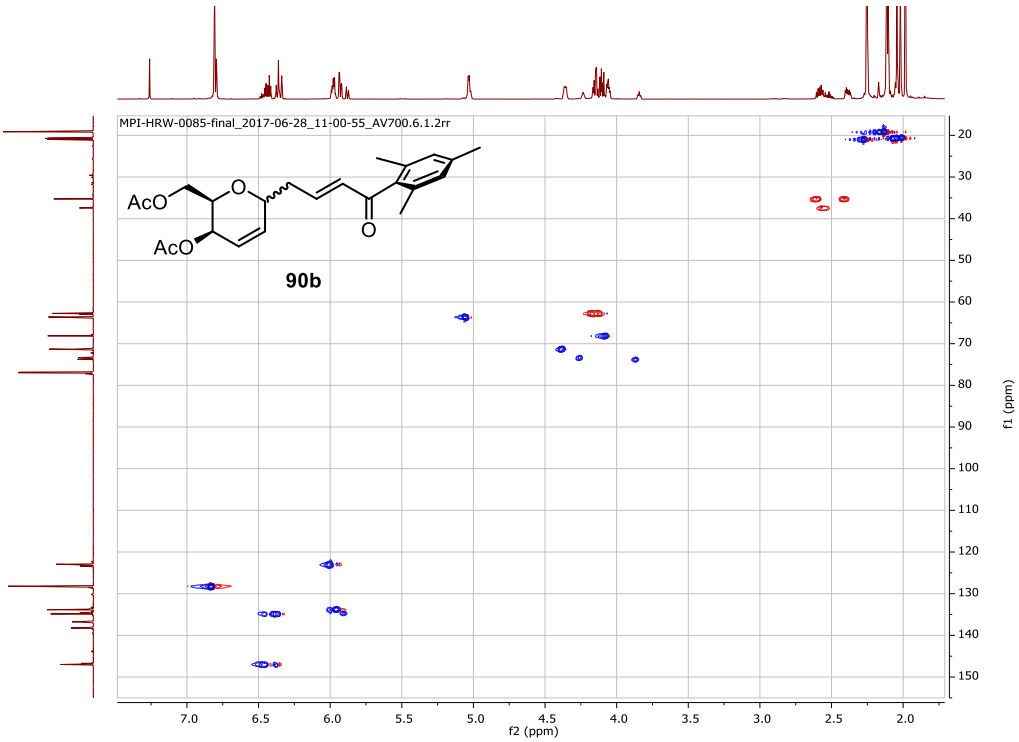

HSQC spectrum of compound **90b**

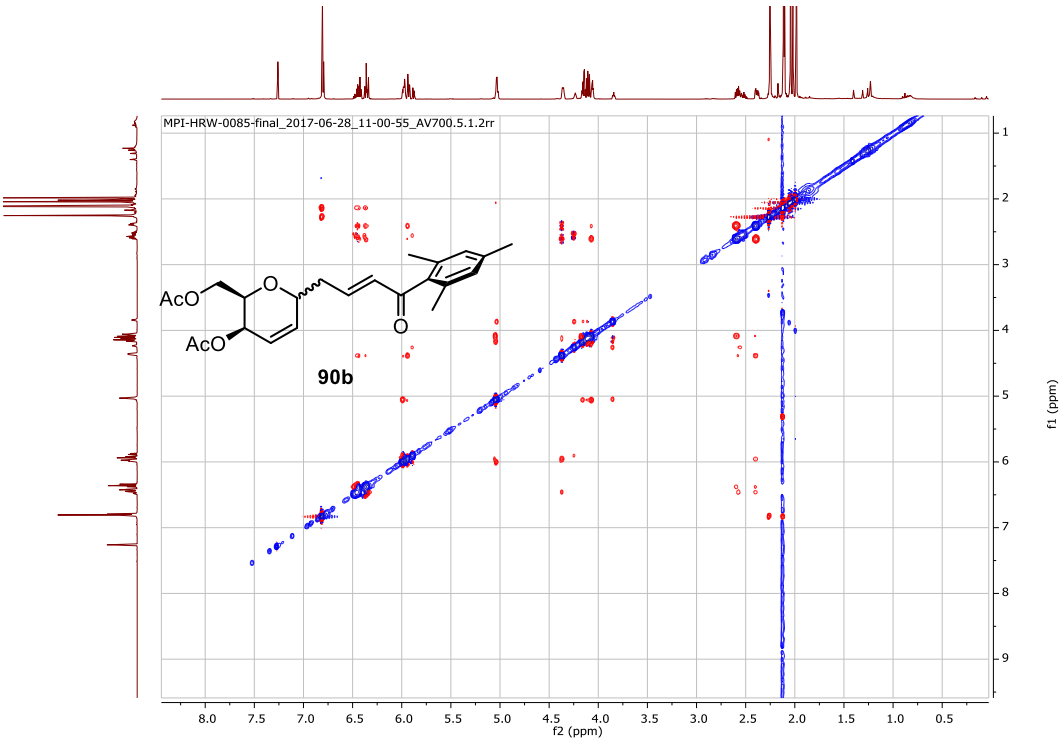

NOESY spectrum of compound **90b**

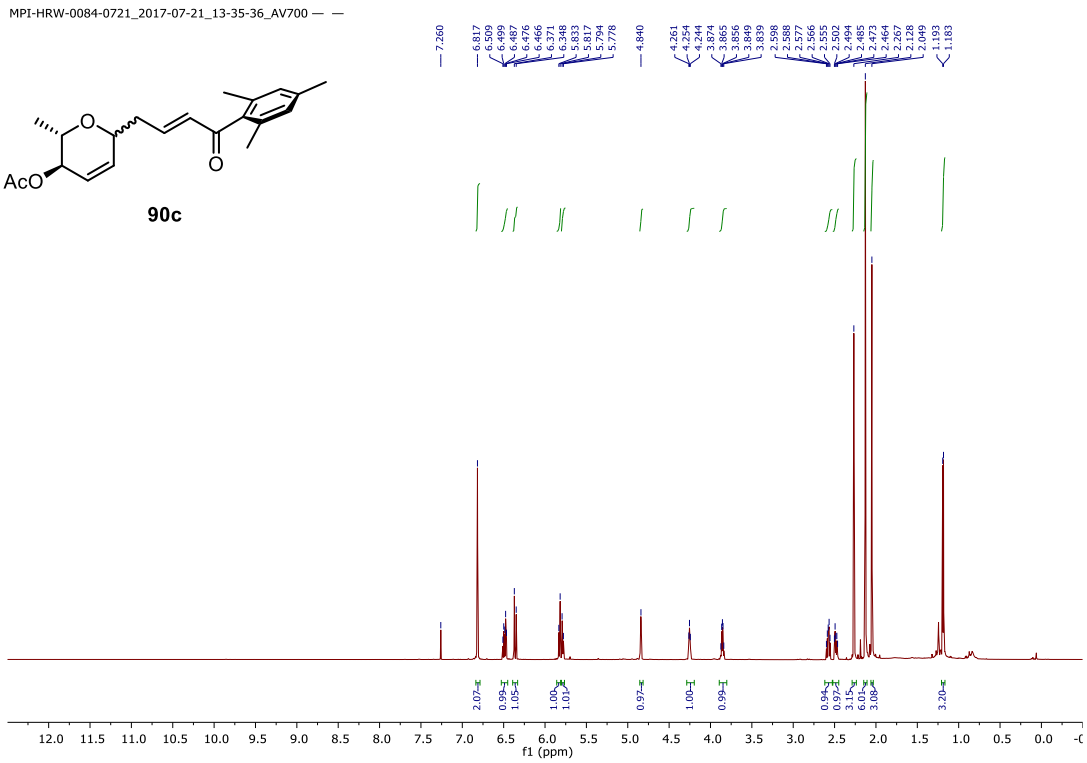

^{1}H NMR spectrum of compound **90c** (700 MHz, in $CDCl_3$)

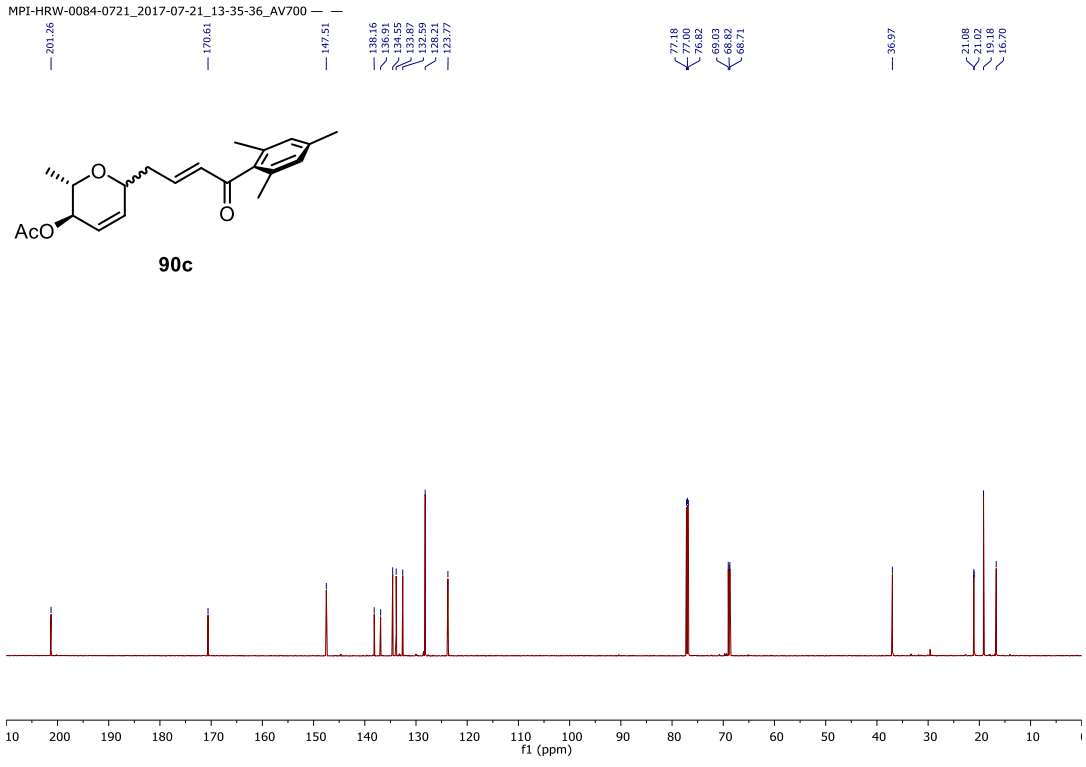

^{13}C NMR spectrum of compound **90c** (176 MHz, in $CDCl_3$)

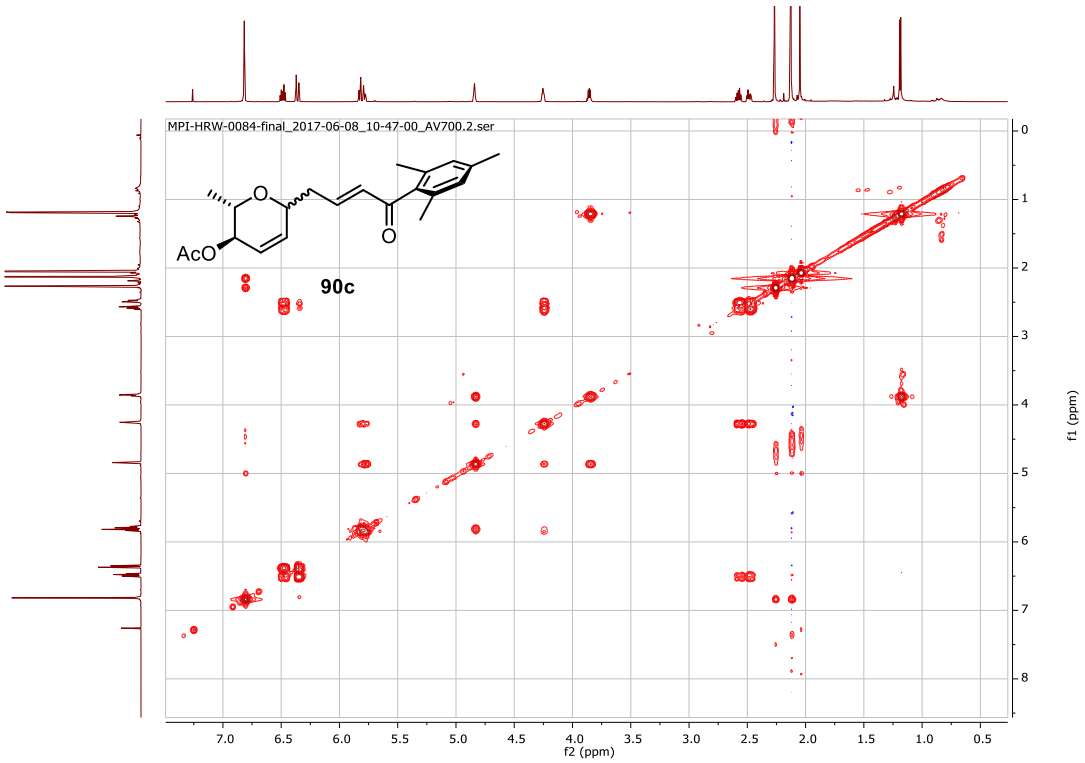

COSY spectrum of compound **90c**

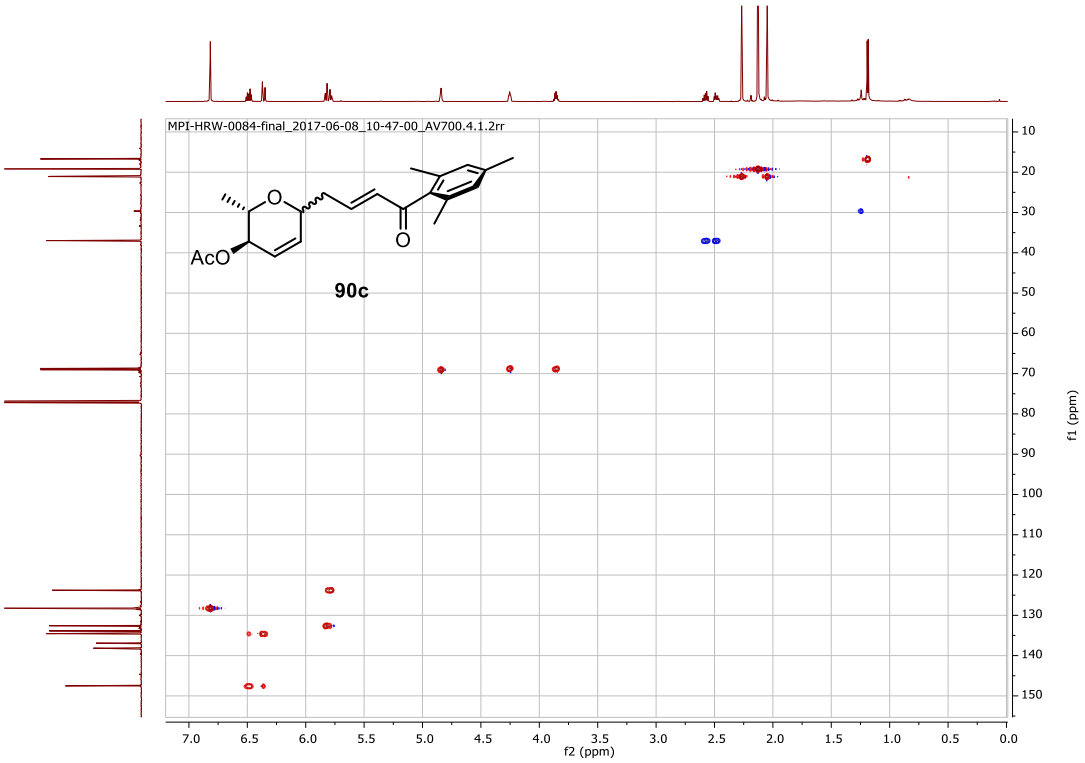

HSQC spectrum of compound **90c**

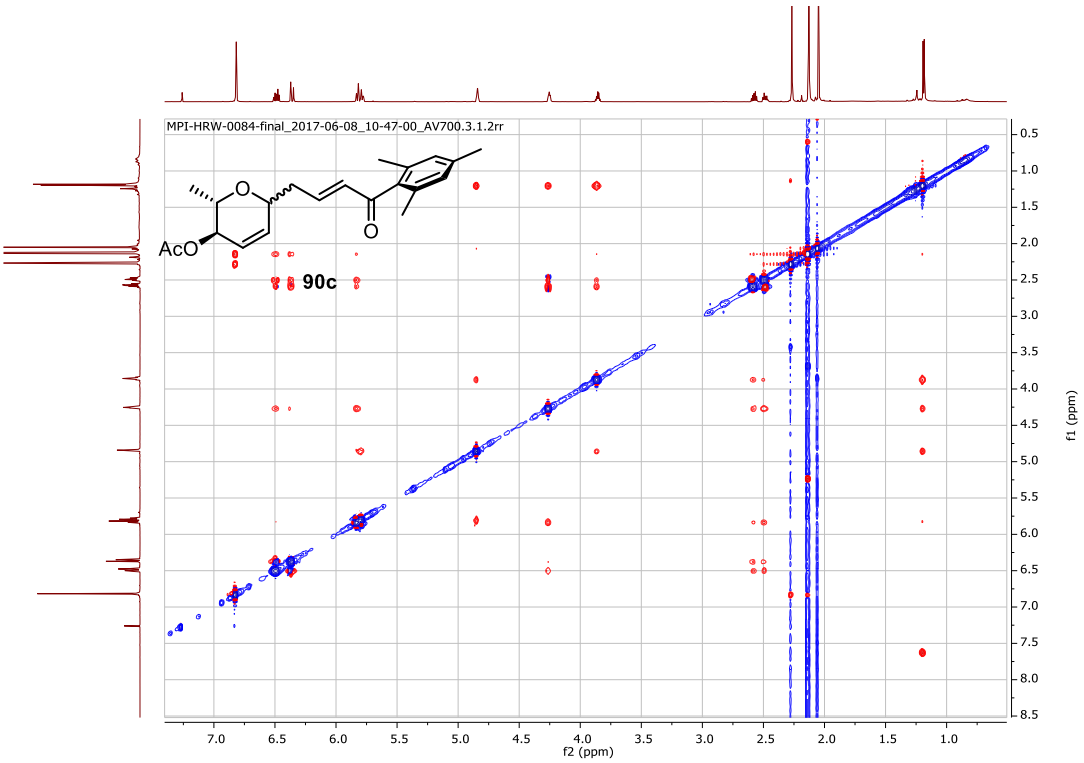

NOESY spectrum of compound **90c**

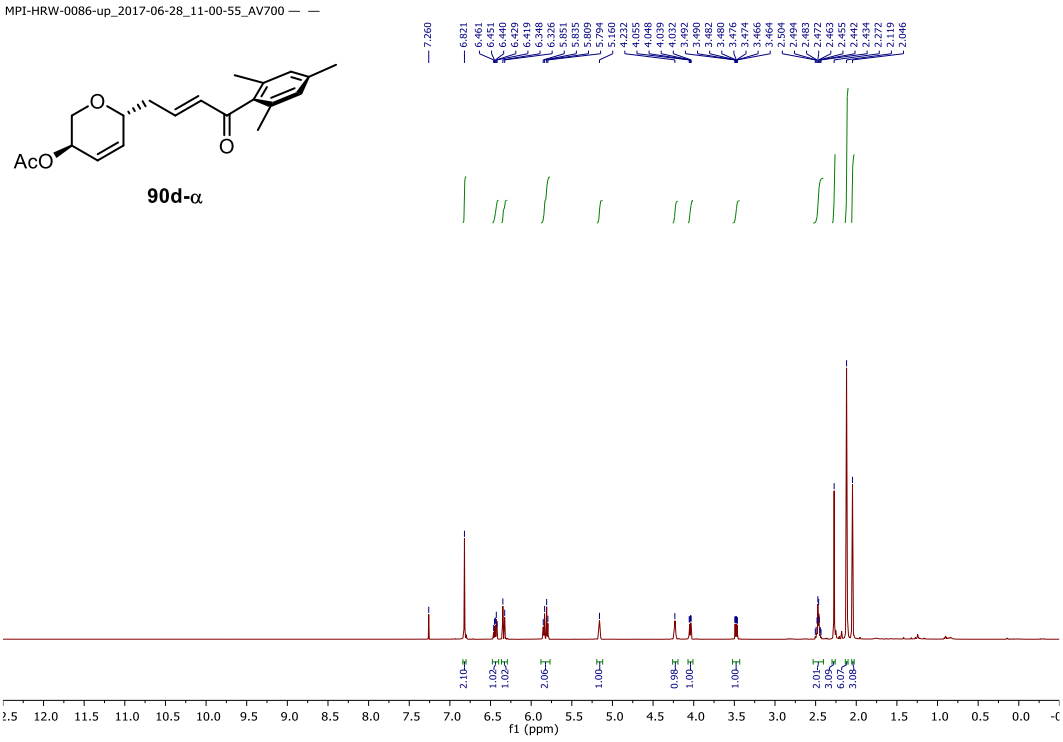

^{1}H NMR spectrum of compound **90d-α** (700 MHz, in $CDCl_3$)

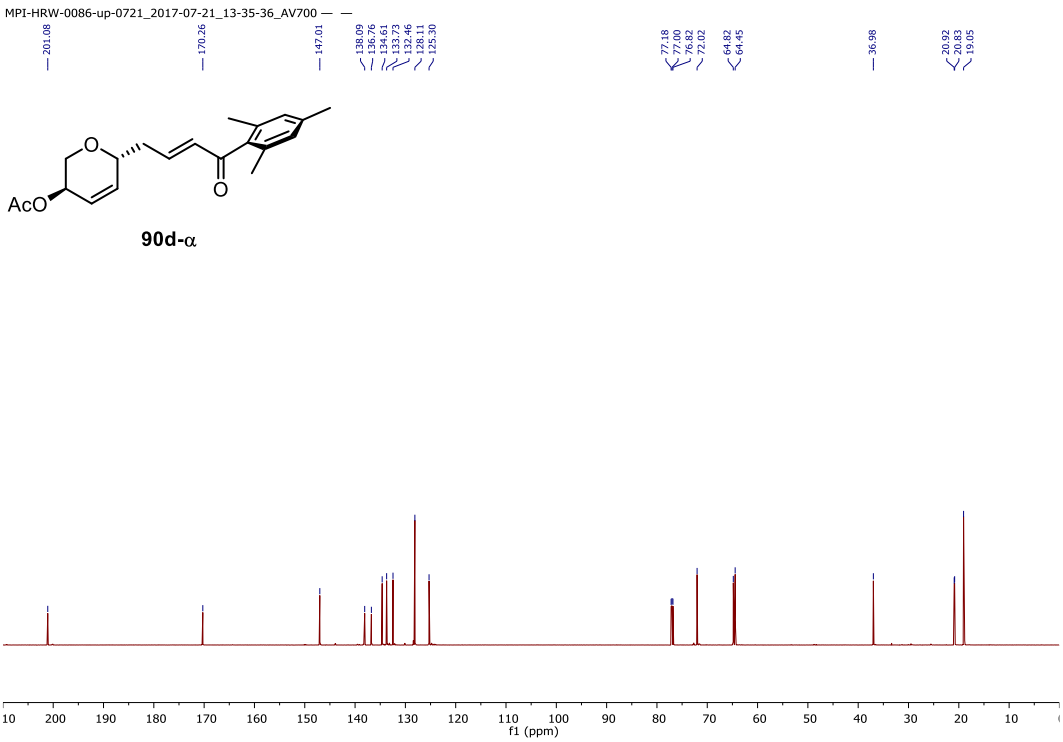

^{13}C NMR spectrum of compound **90d-α** (176 MHz, in $CDCl_3$)

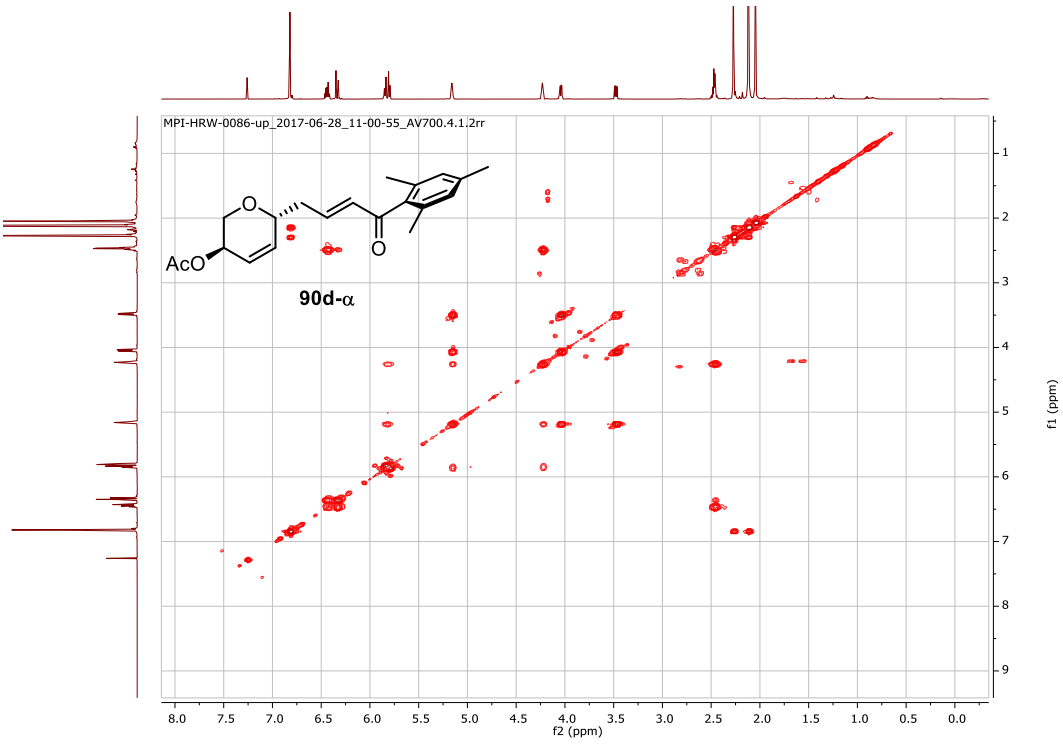

COSY spectrum of compound **90d-α**

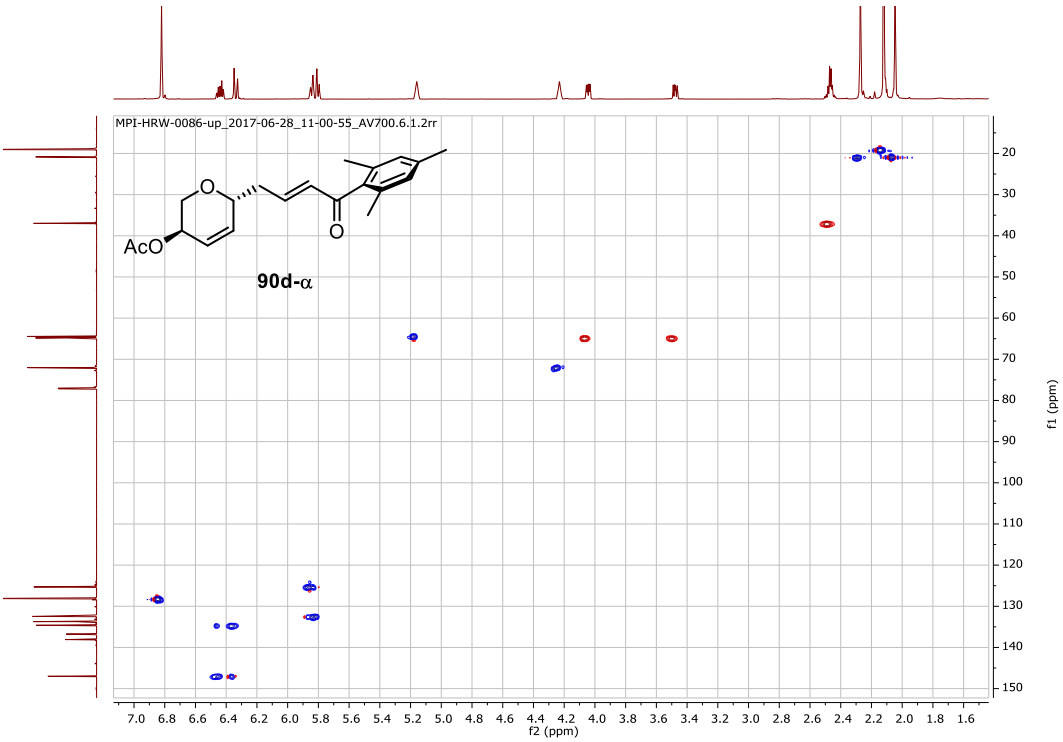

HSQC spectrum of compound **90d-α**

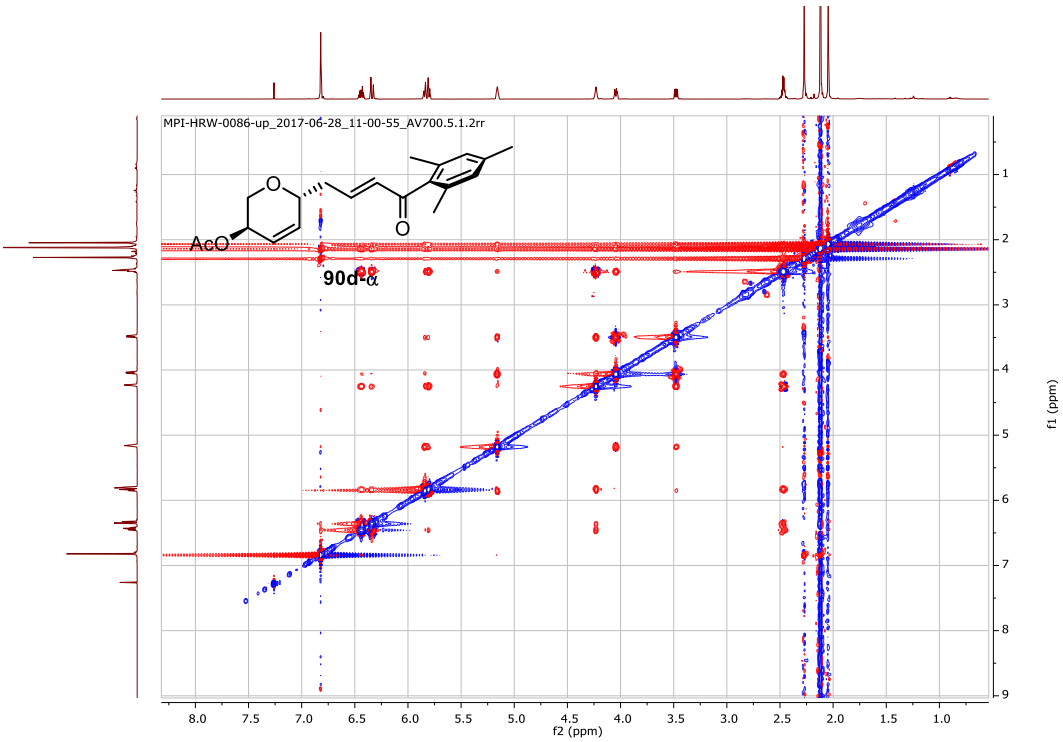

NOESY spectrum of compound **90d-α**

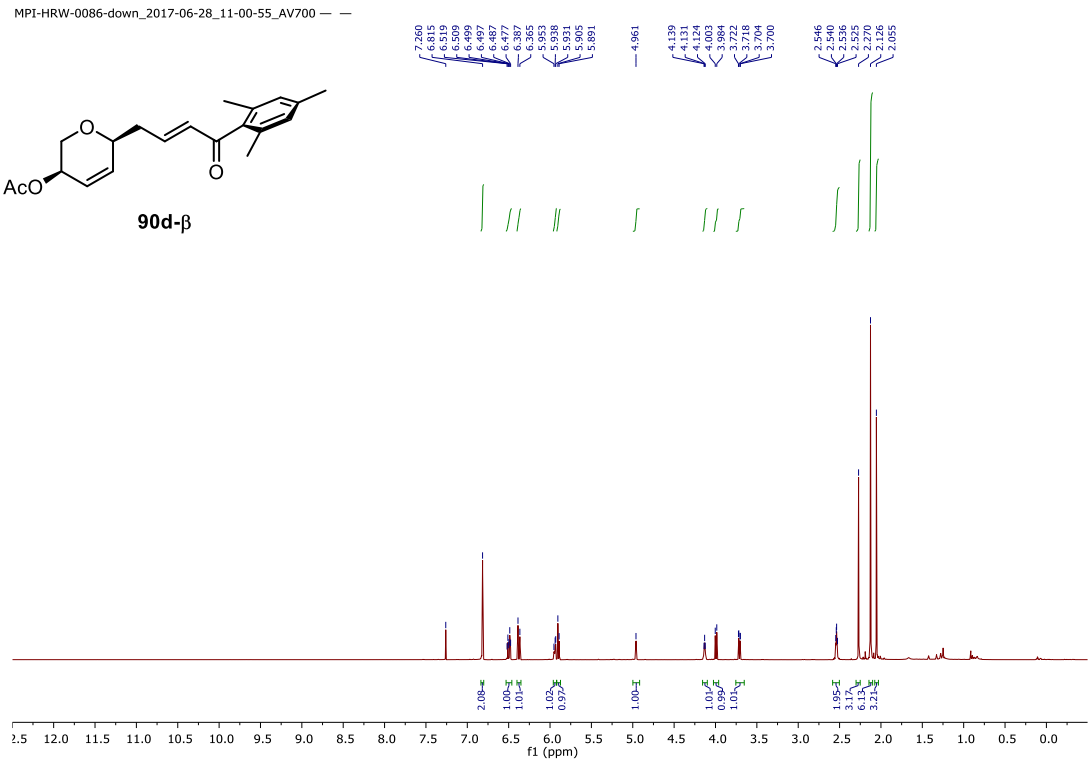

^{1}H NMR spectrum of compound **90d-β** (700 MHz, in $CDCl_3$)

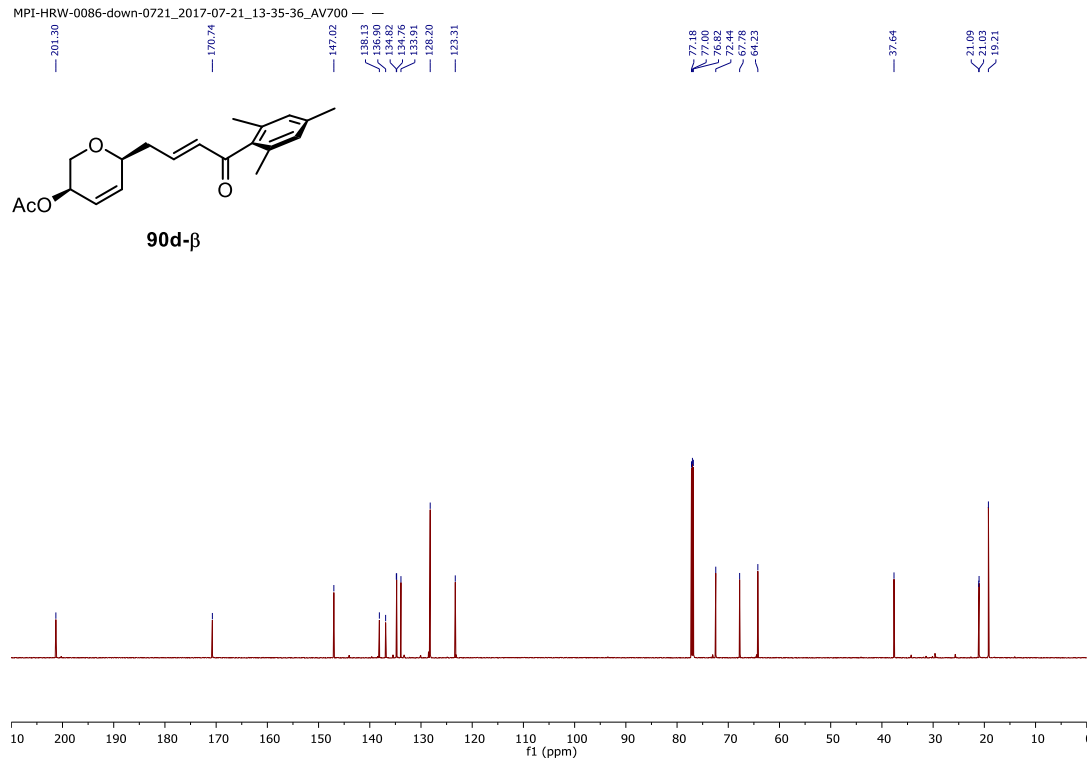

^{13}C NMR spectrum of compound **90d-β** (176 MHz, in $CDCl_3$)

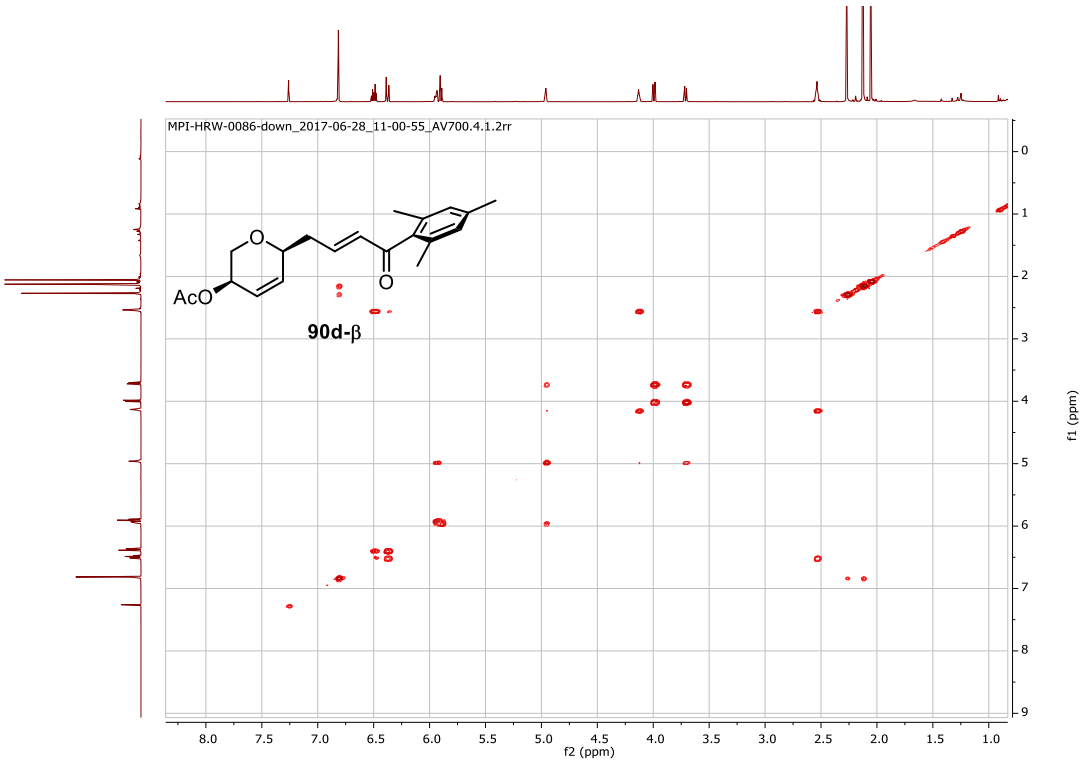

COSY spectrum of compound **90d-β**

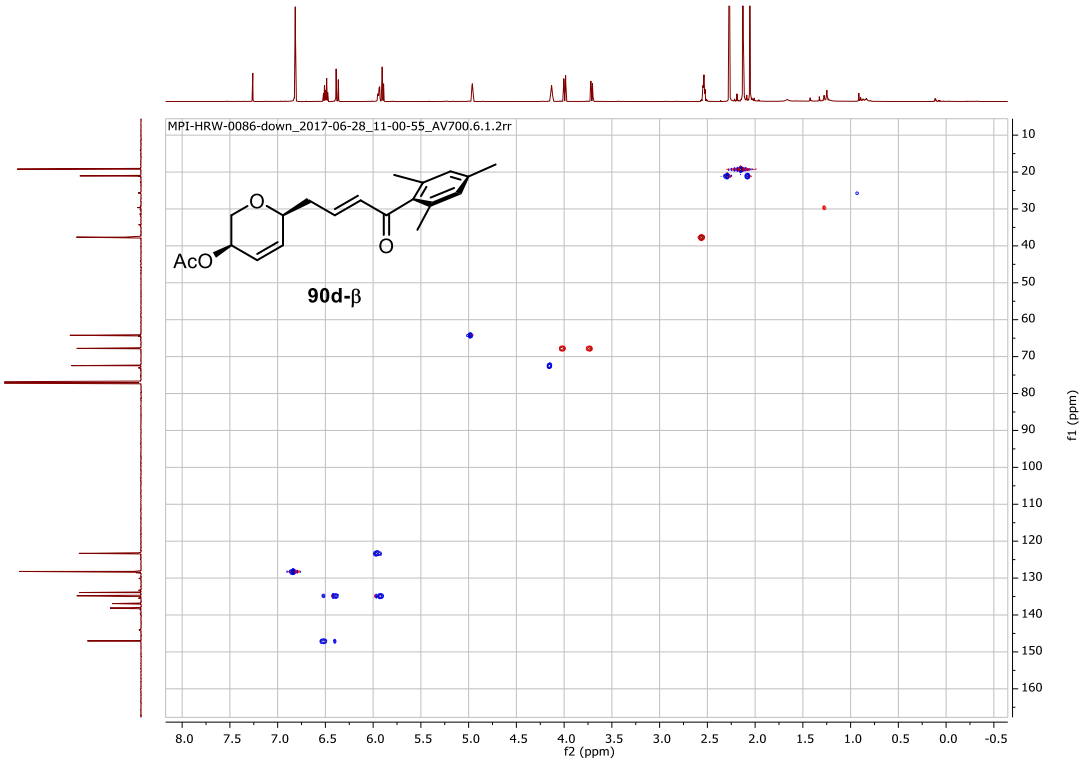

HSQC spectrum of compound **90d-β**

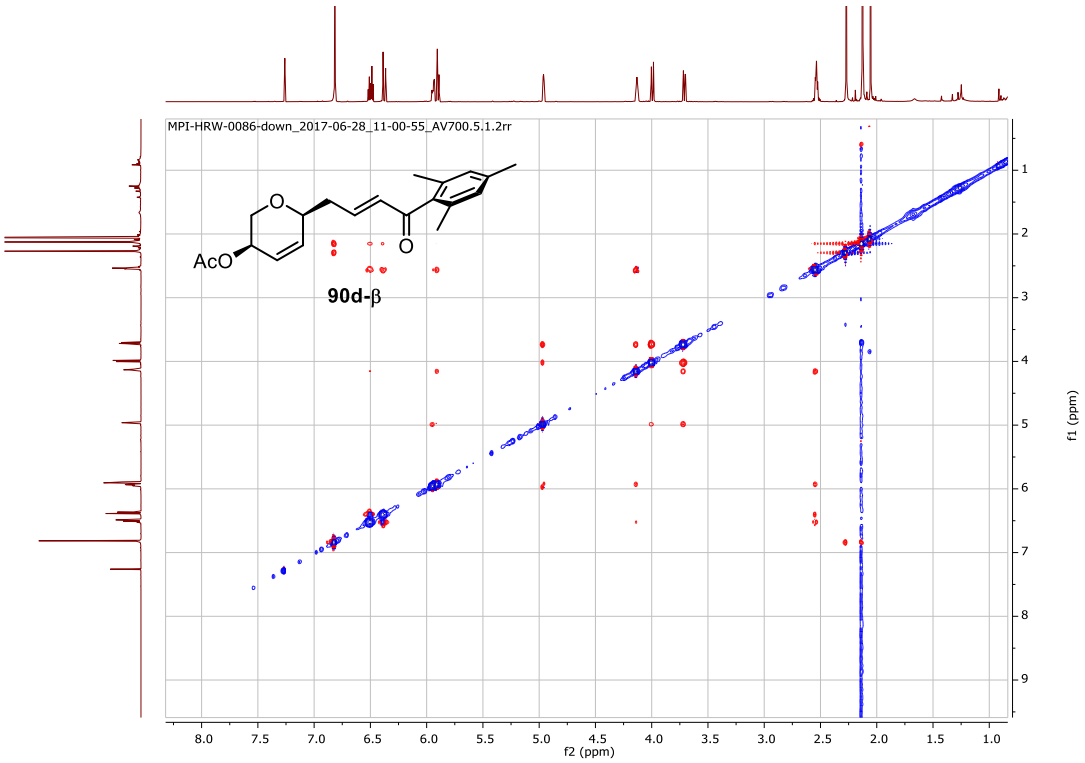

NOESY spectrum of compound **90d-β**

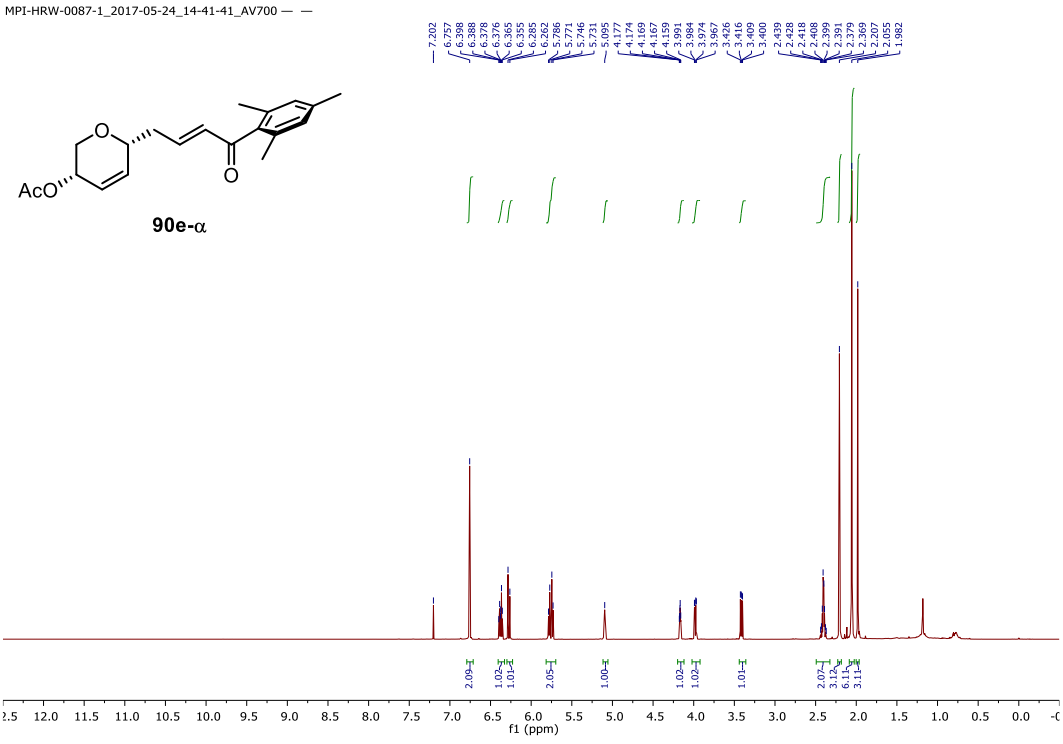

^{1}H NMR spectrum of compound **90e-α** (700 MHz, in $CDCl_3$)

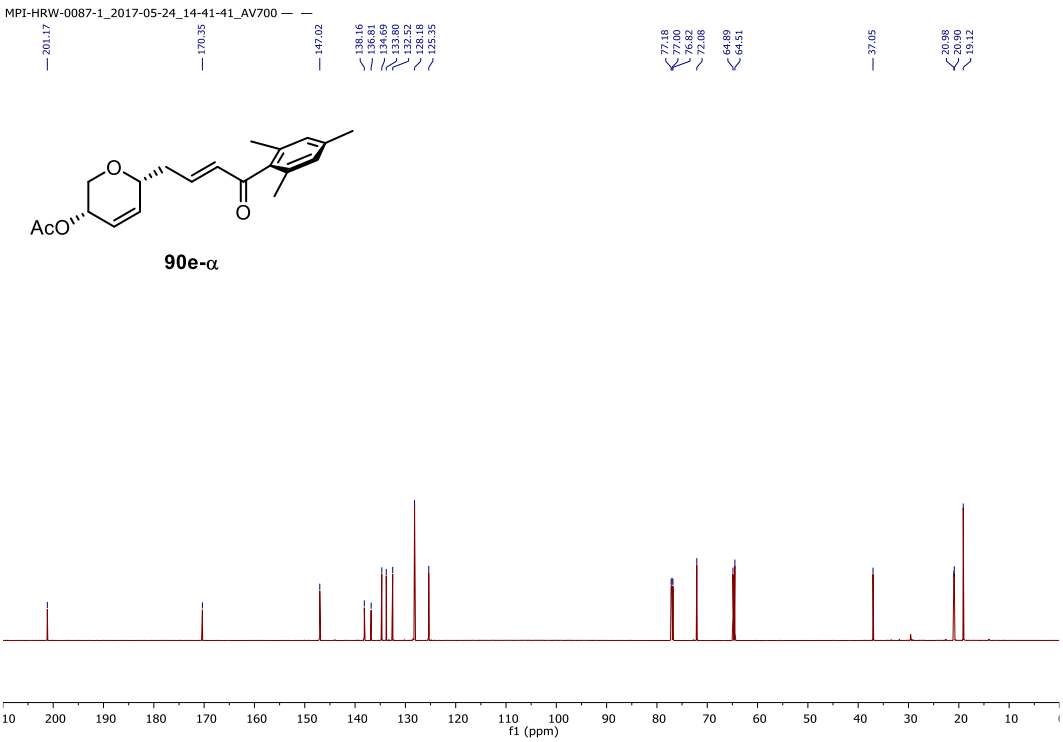

^{13}C NMR spectrum of compound **90e-α** (176 MHz, in $CDCl_3$)

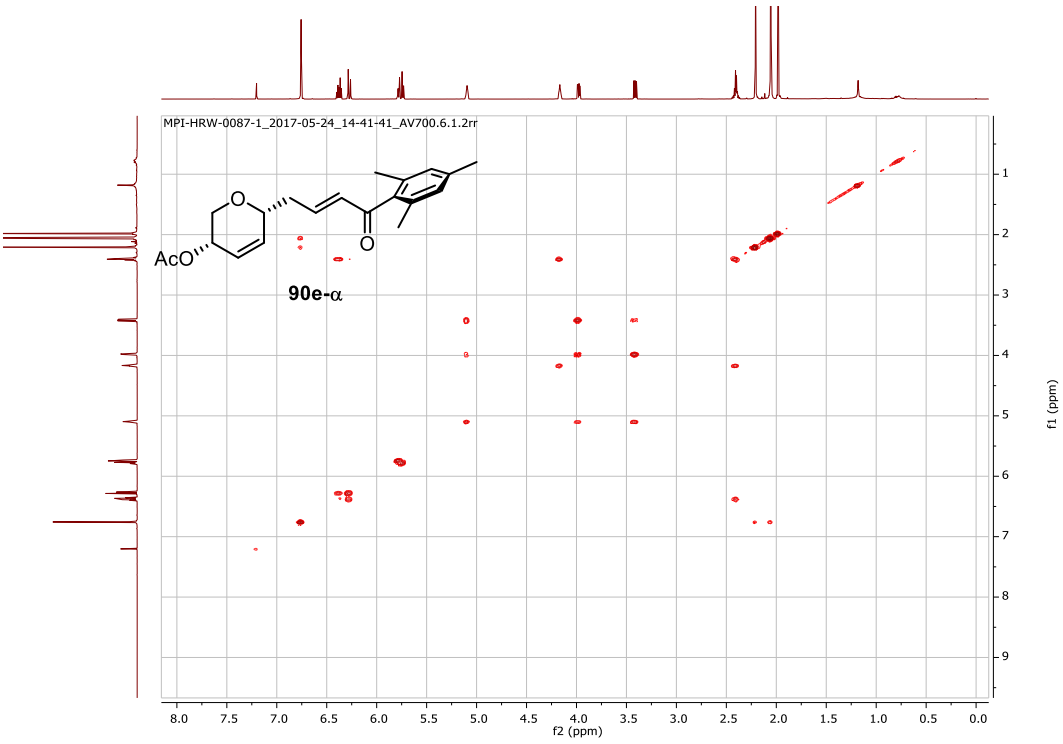

COSY spectrum of compound **90e-α**

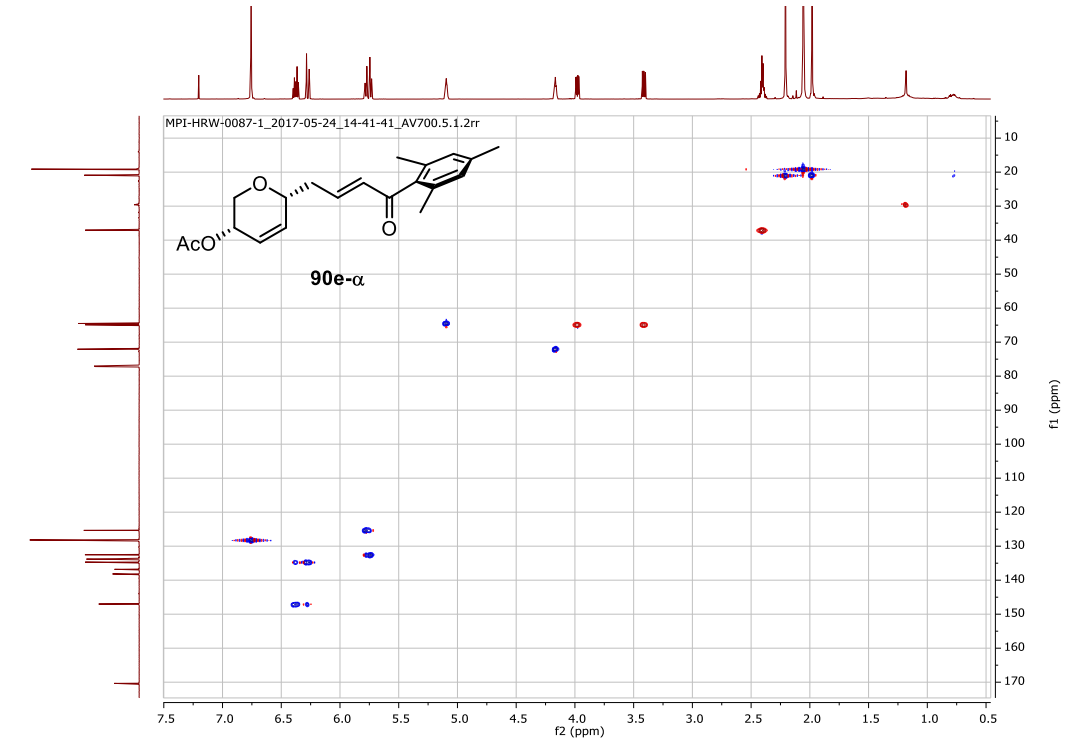

HSQC spectrum of compound **90e-α**

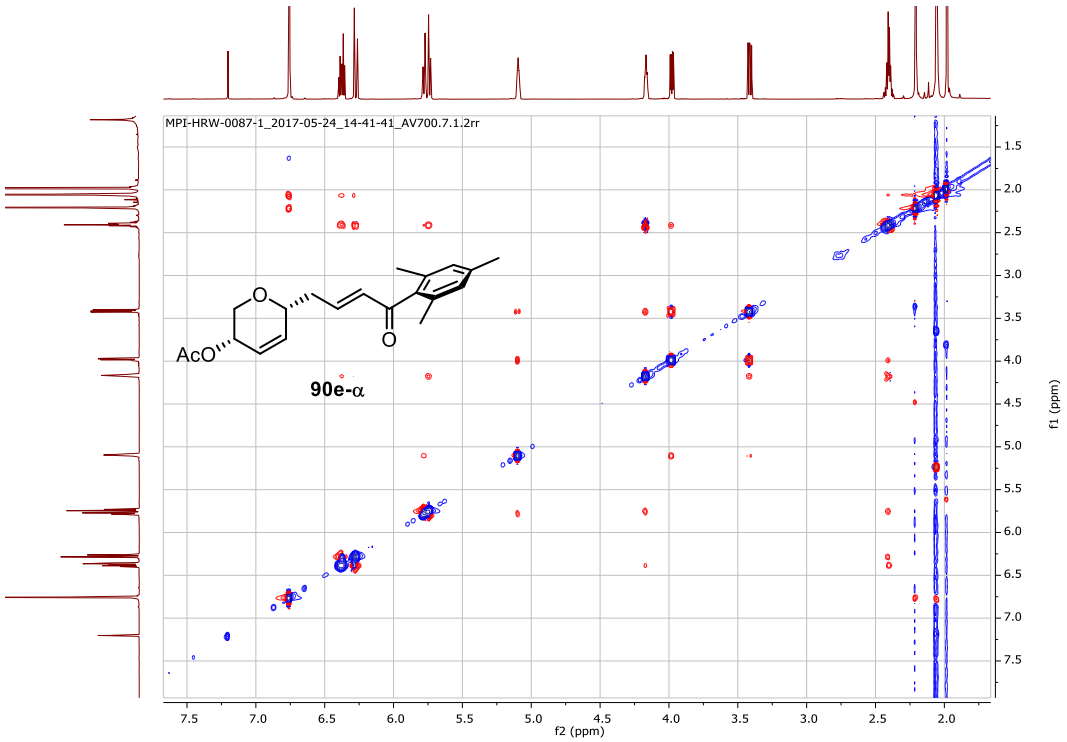

NOESY spectrum of compound **90e-α**

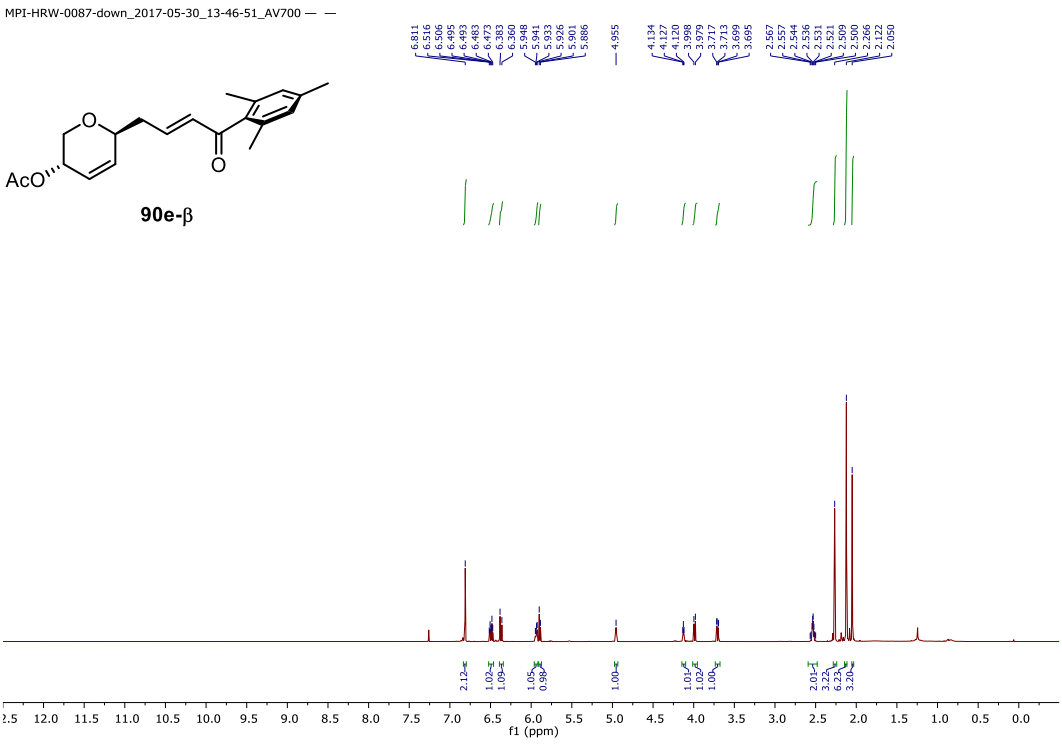

^{1}H NMR spectrum of compound **90e-β** (700 MHz, in $CDCl_3$)

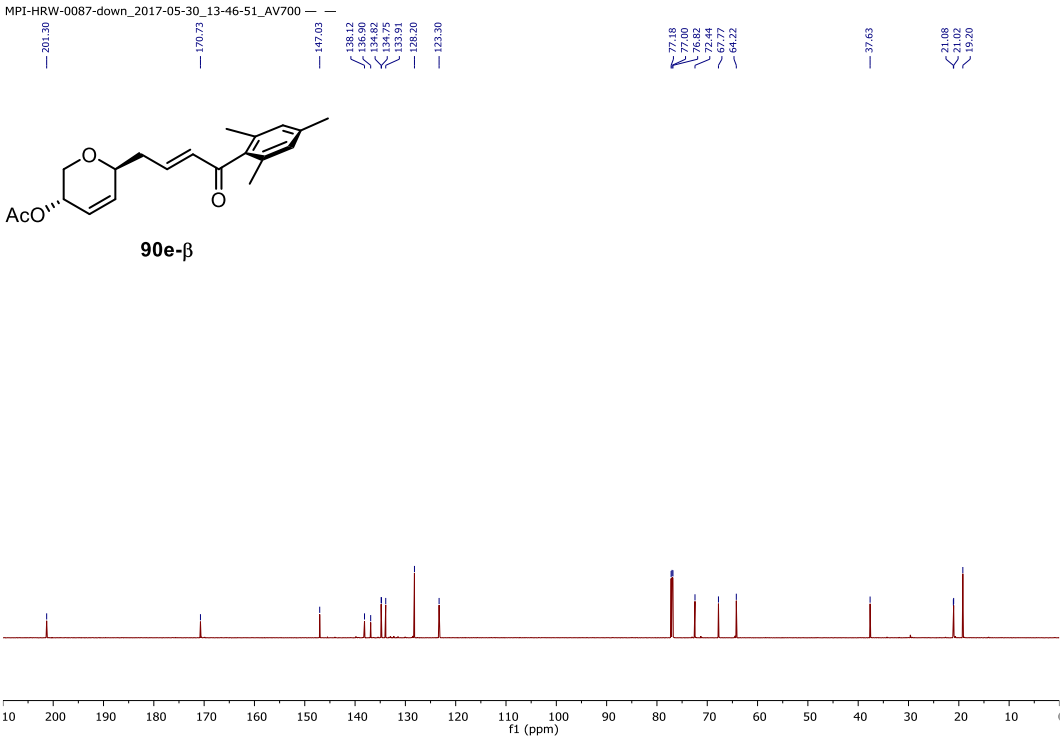

^{13}C NMR spectrum of compound **90e-β** (176 MHz, in $CDCl_3$)

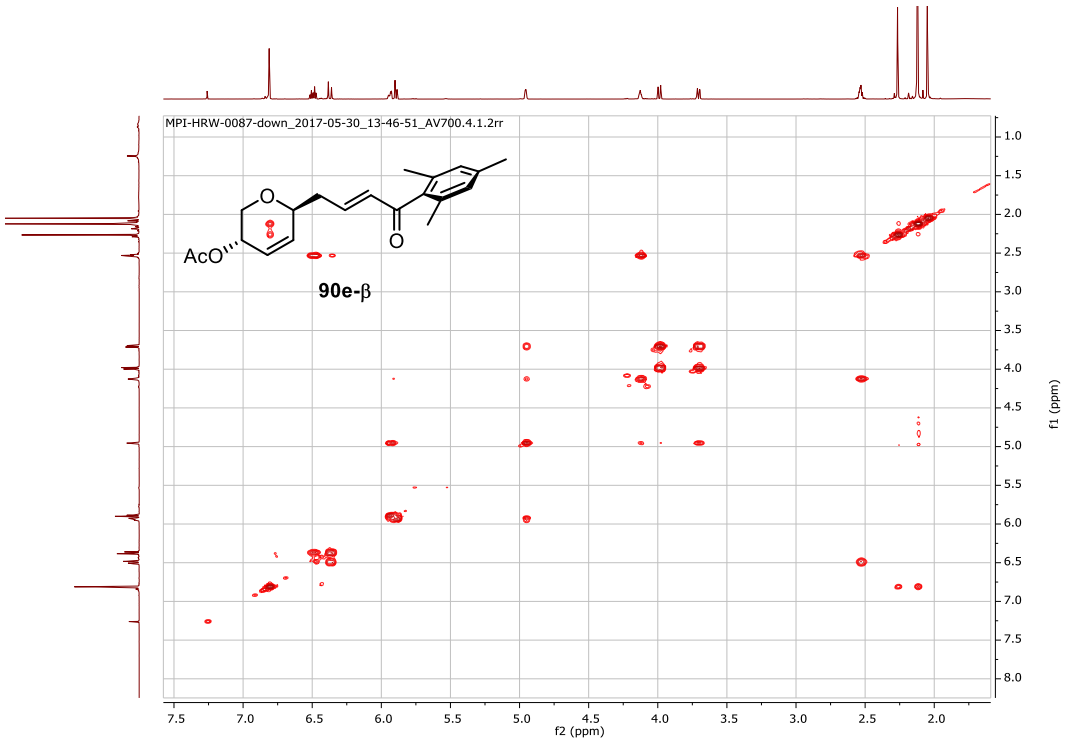

COSY spectrum of compound **90e-β**

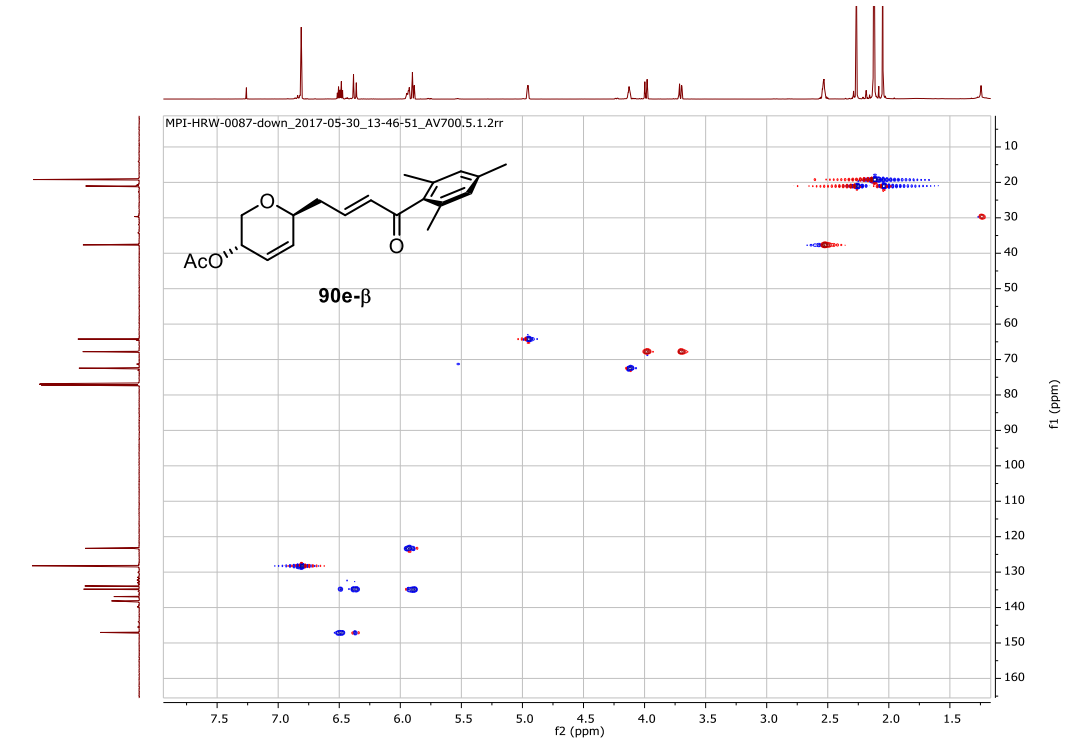

HSQC spectrum of compound **90e-β**

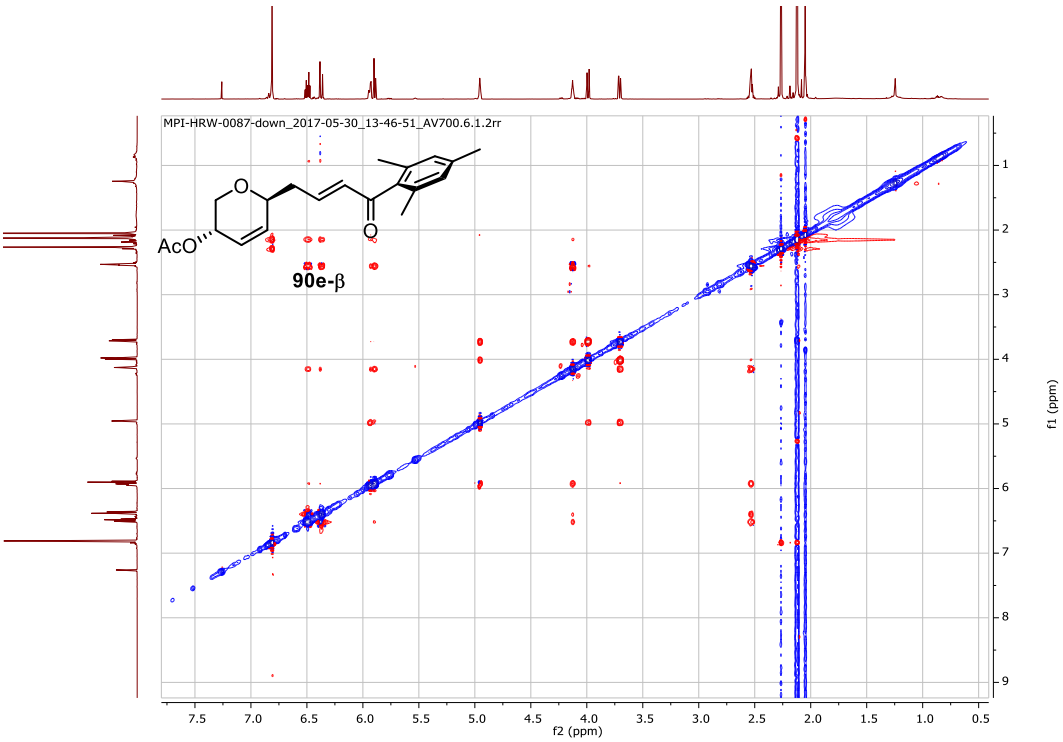

NOESY spectrum of compound **90e-β**

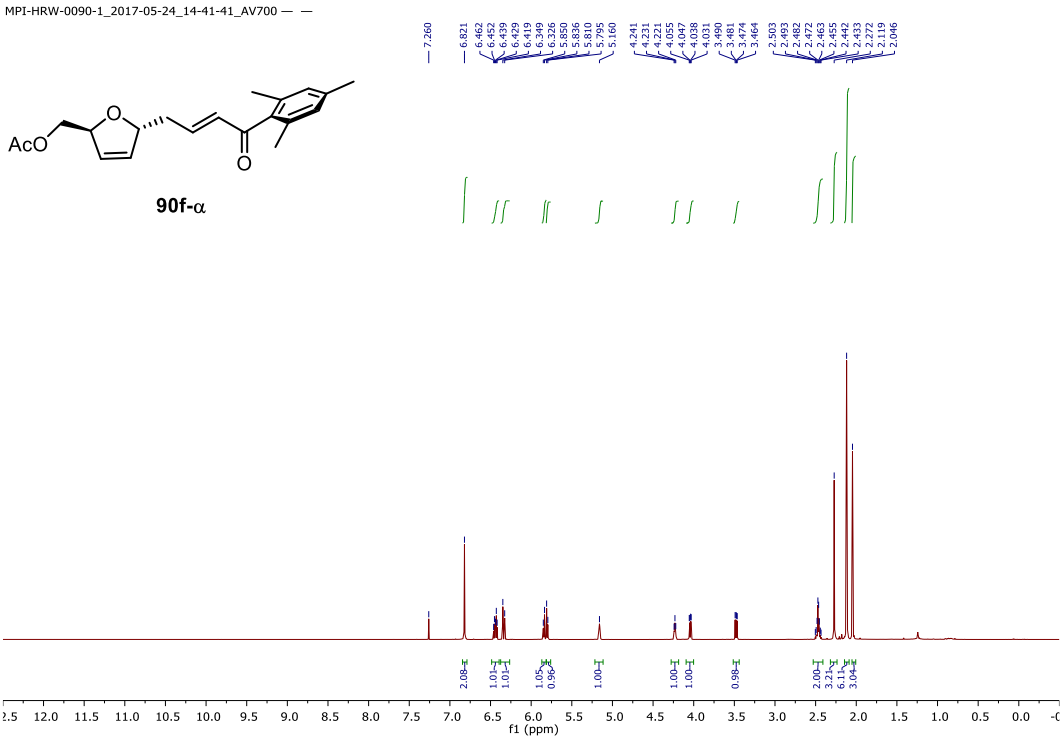

^{1}H NMR spectrum of compound **90f-α** (700 MHz, in $CDCl_3$)

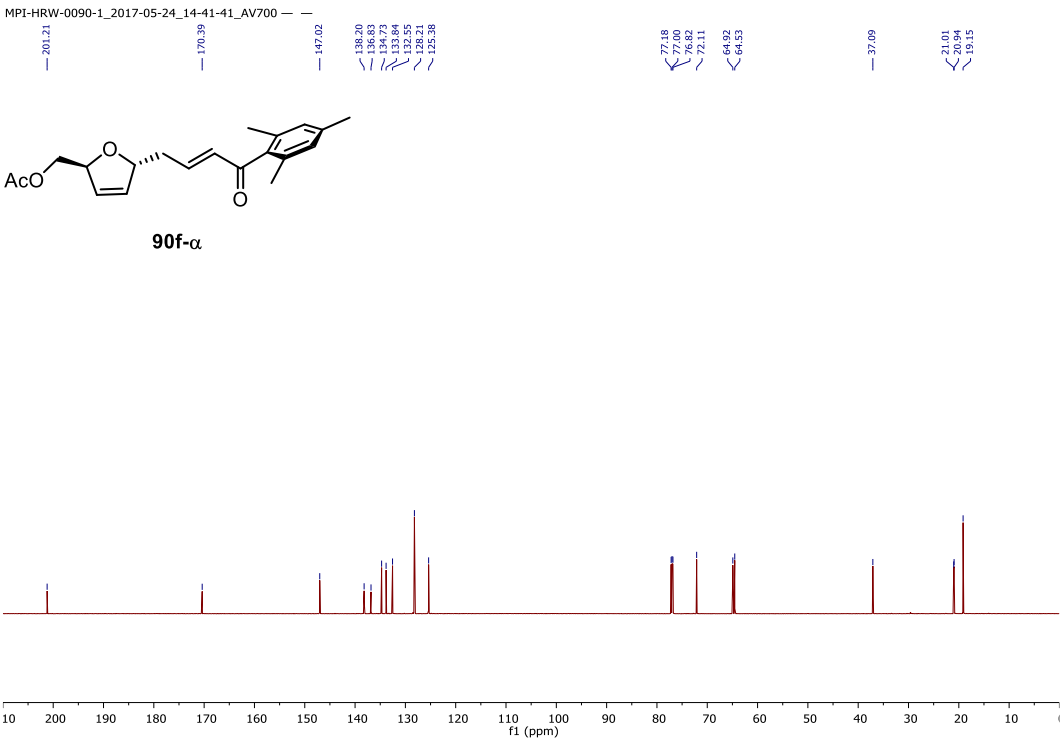

^{13}C NMR spectrum of compound **90f-α** (176 MHz, in $CDCl_3$)

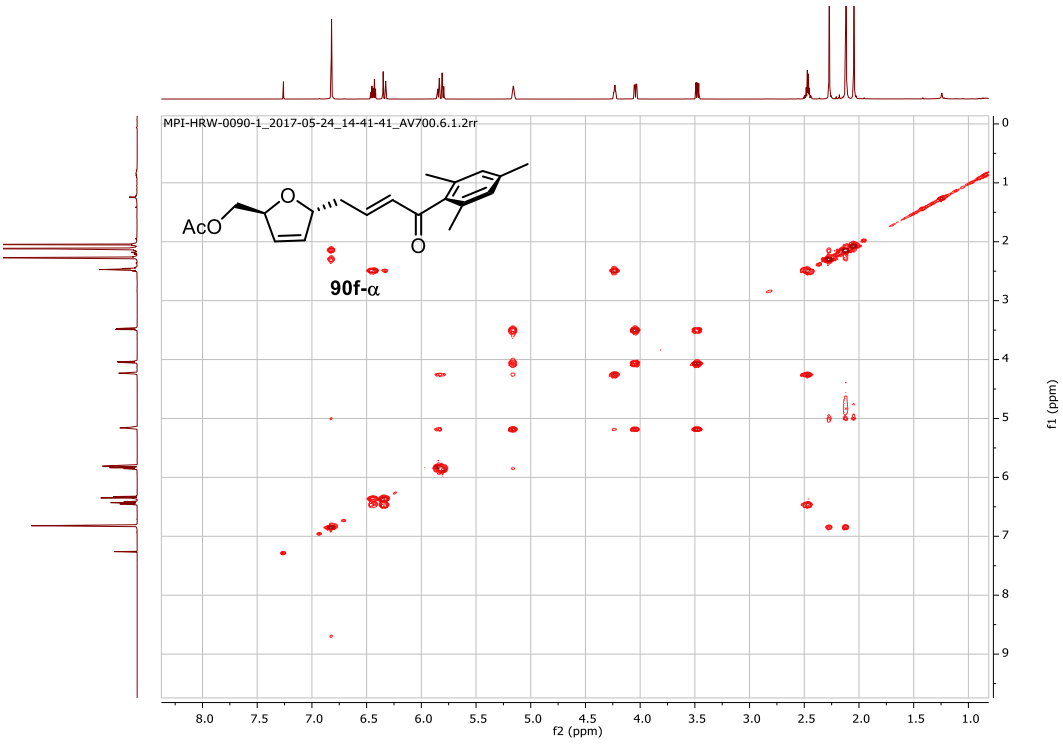

COSY spectrum of compound **90f-α**

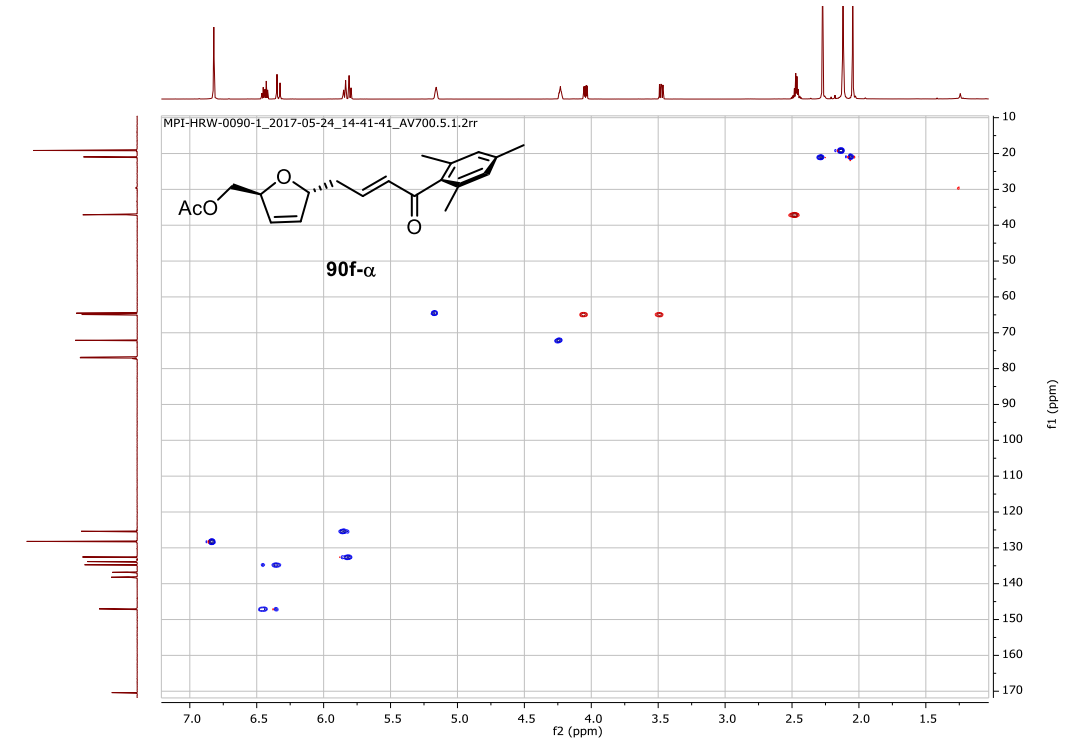

HSQC spectrum of compound **90f-α**

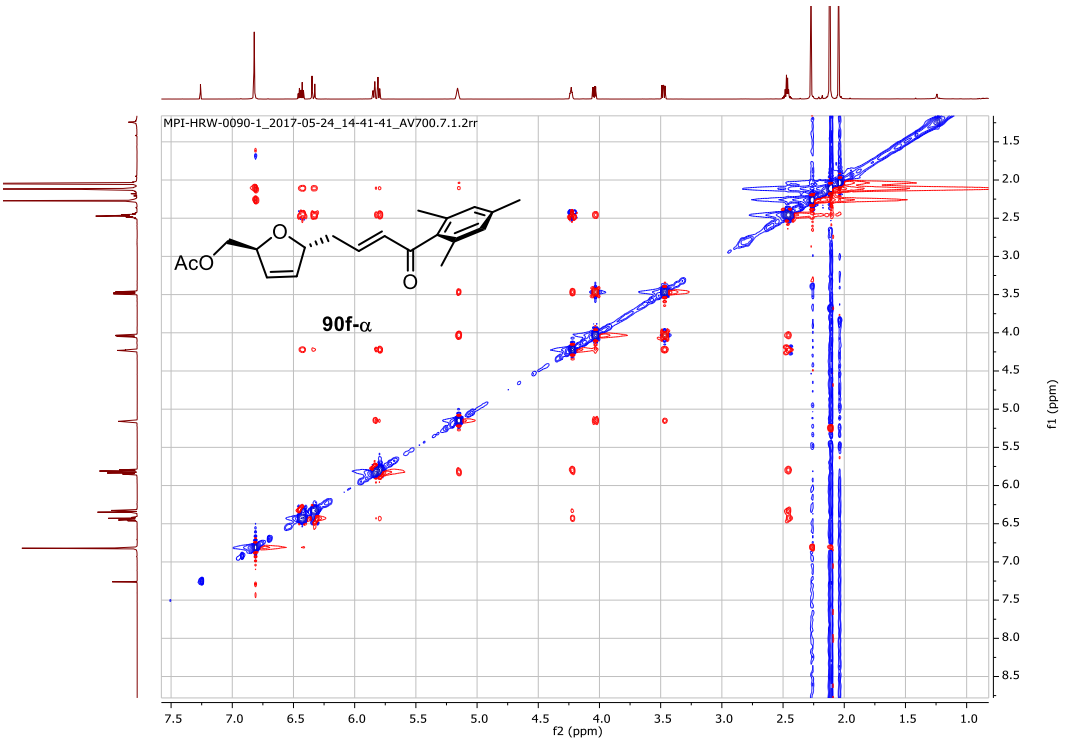

NOESY spectrum of compound **90f-α**

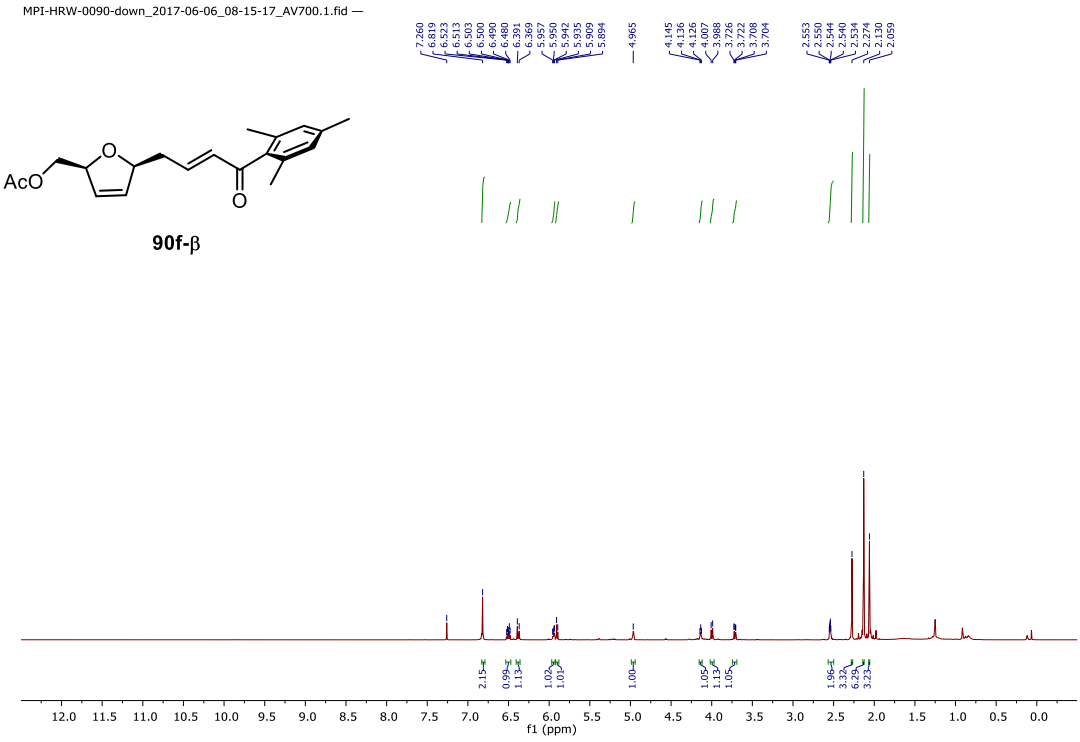

^{1}H NMR spectrum of compound **90f-β** (700 MHz, in $CDCl_3$)

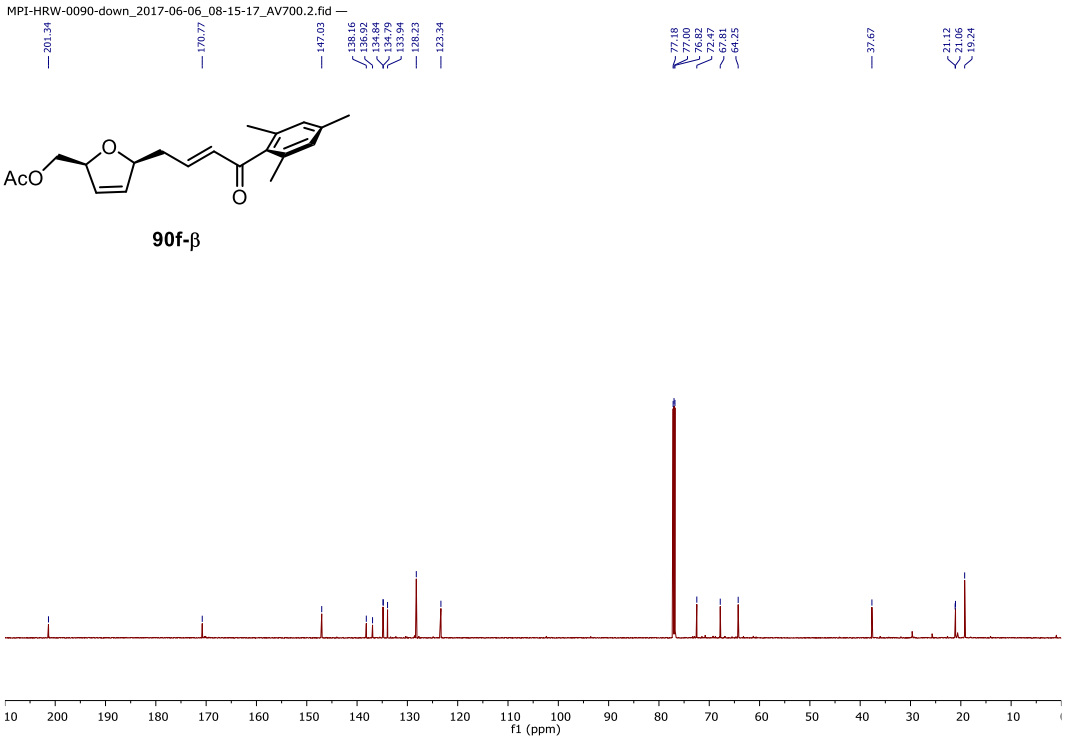

^{13}C NMR spectrum of compound **90f-β** (176 MHz, in $CDCl_3$)

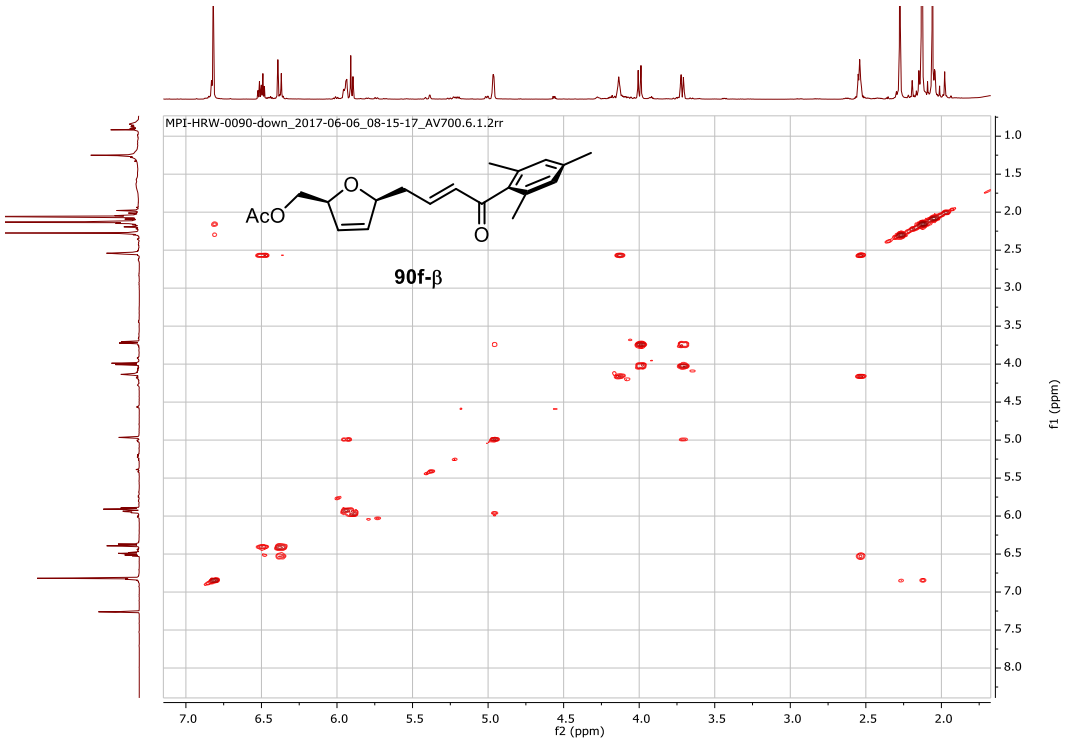

COSY spectrum of compound **90f-β**

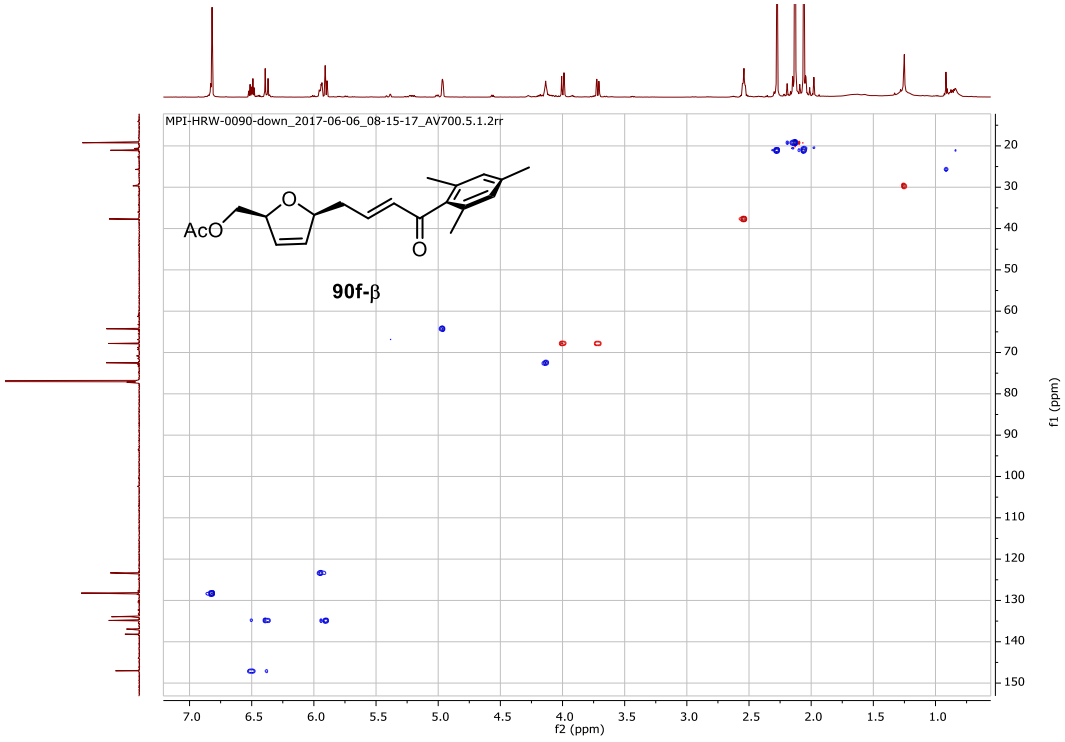

HSQC spectrum of compound **90f-β**

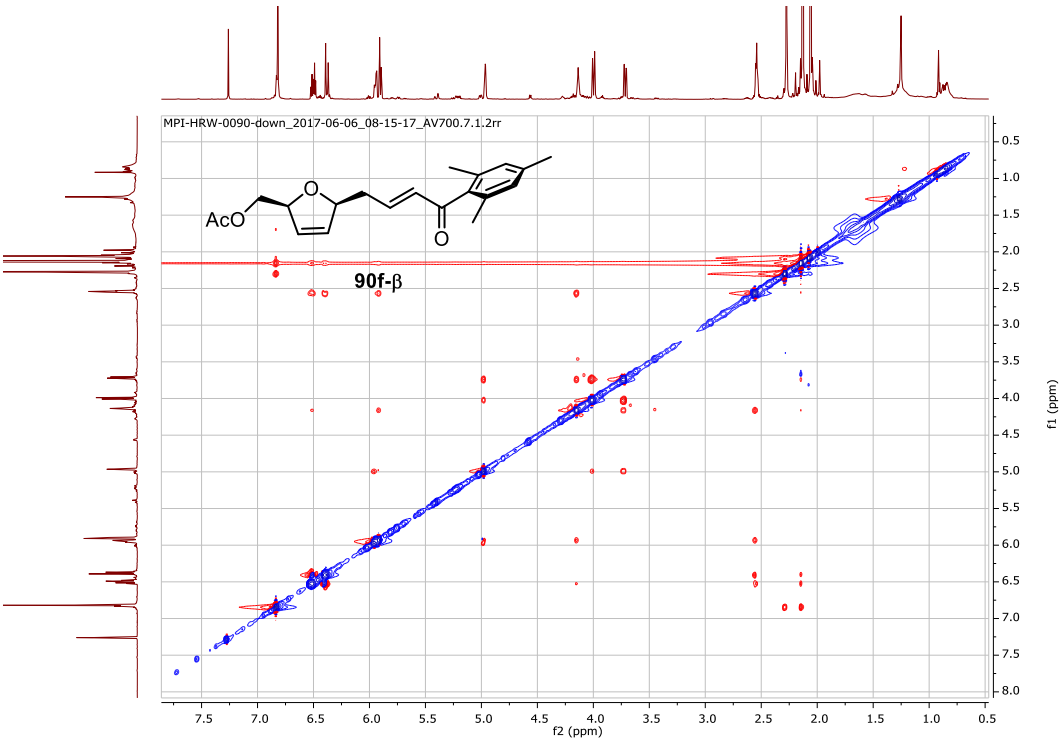

NOESY spectrum of compound **90f-β**

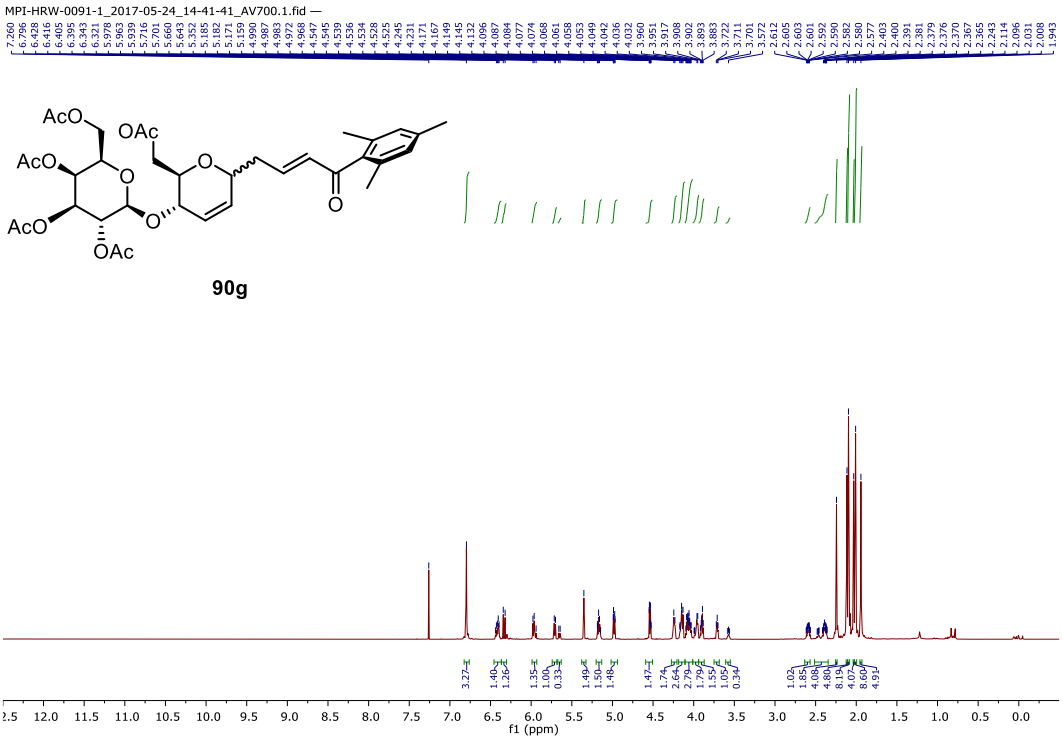

^{1}H NMR spectrum of compound **90g** (700 MHz, in $CDCl_3$)

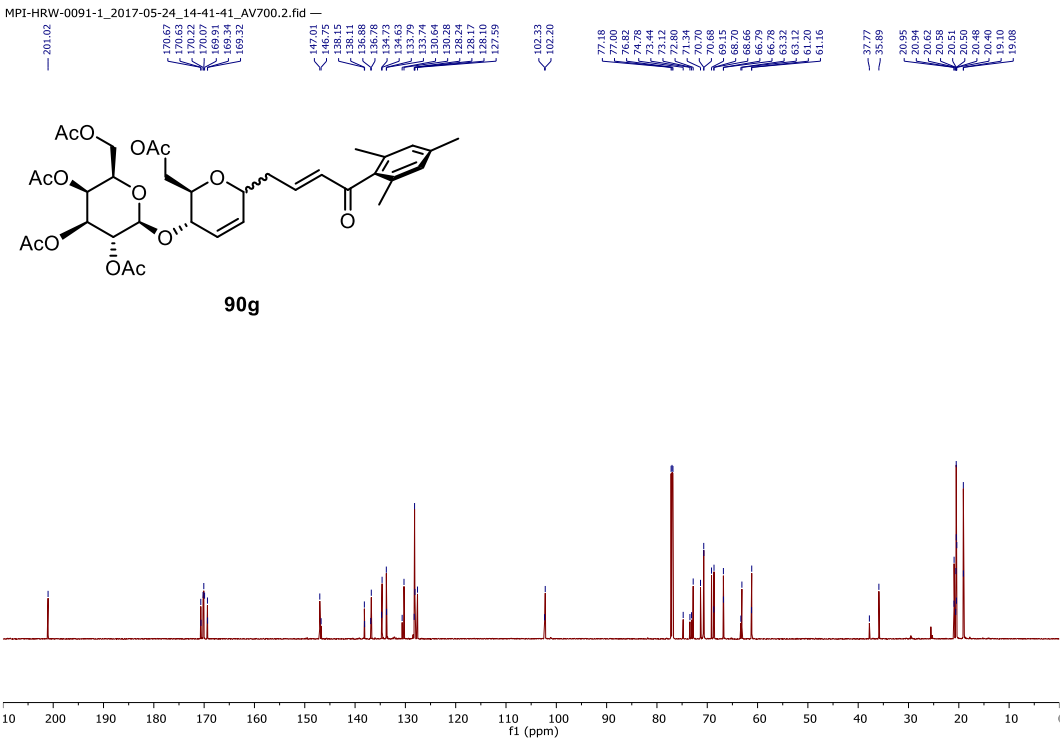

^{13}C NMR spectrum of compound **90g** (176 MHz, in $CDCl_3$)

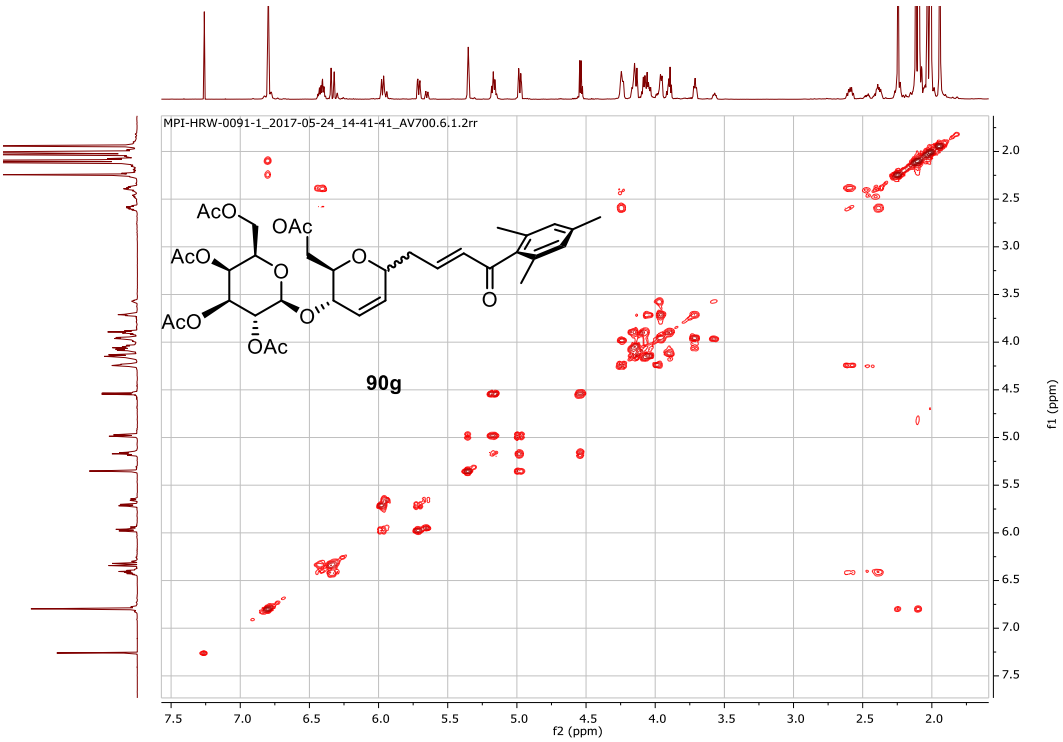

COSY spectrum of compound **90g**

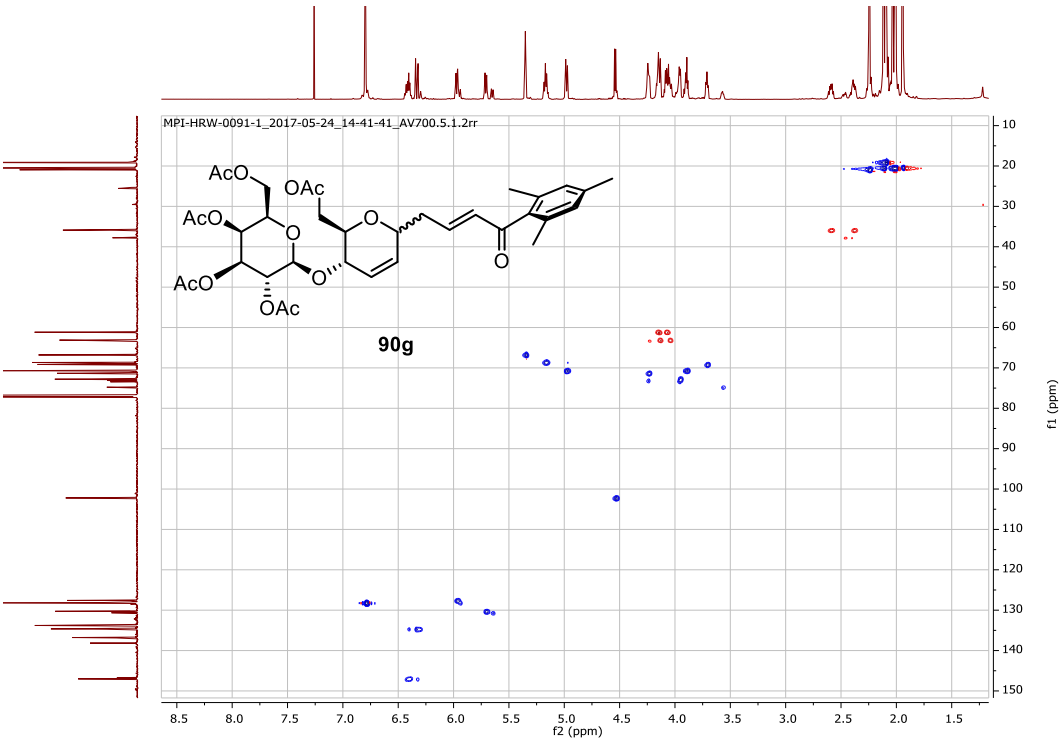

HSQC spectrum of compound **90g**

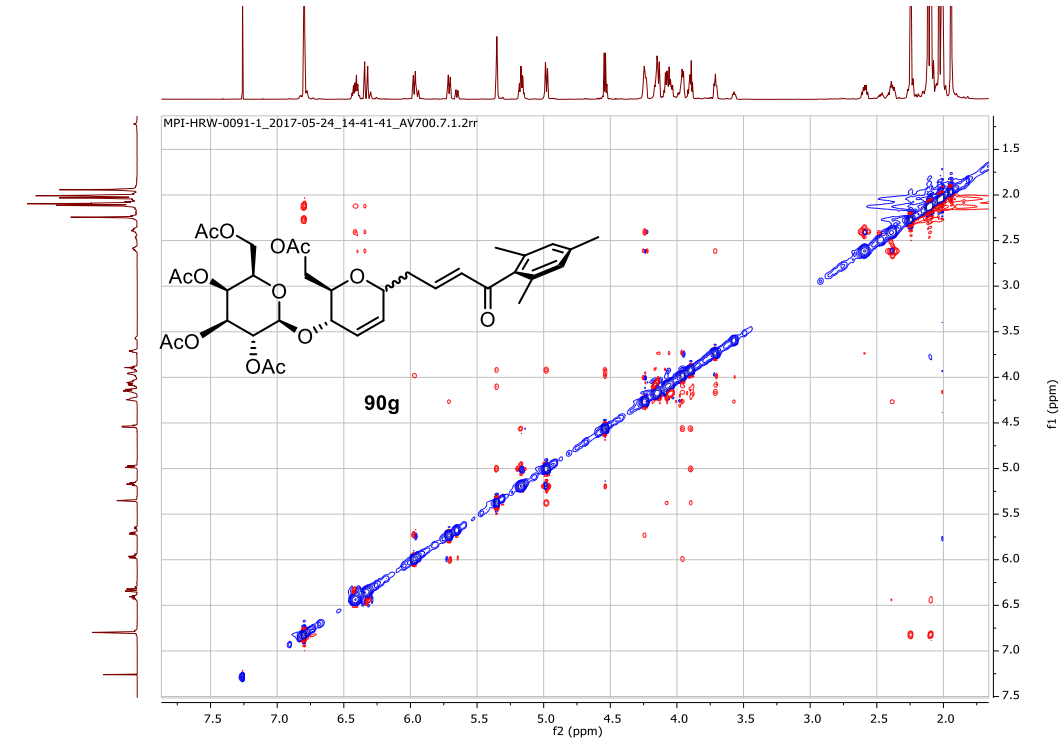

NOESY spectrum of compound **90g**

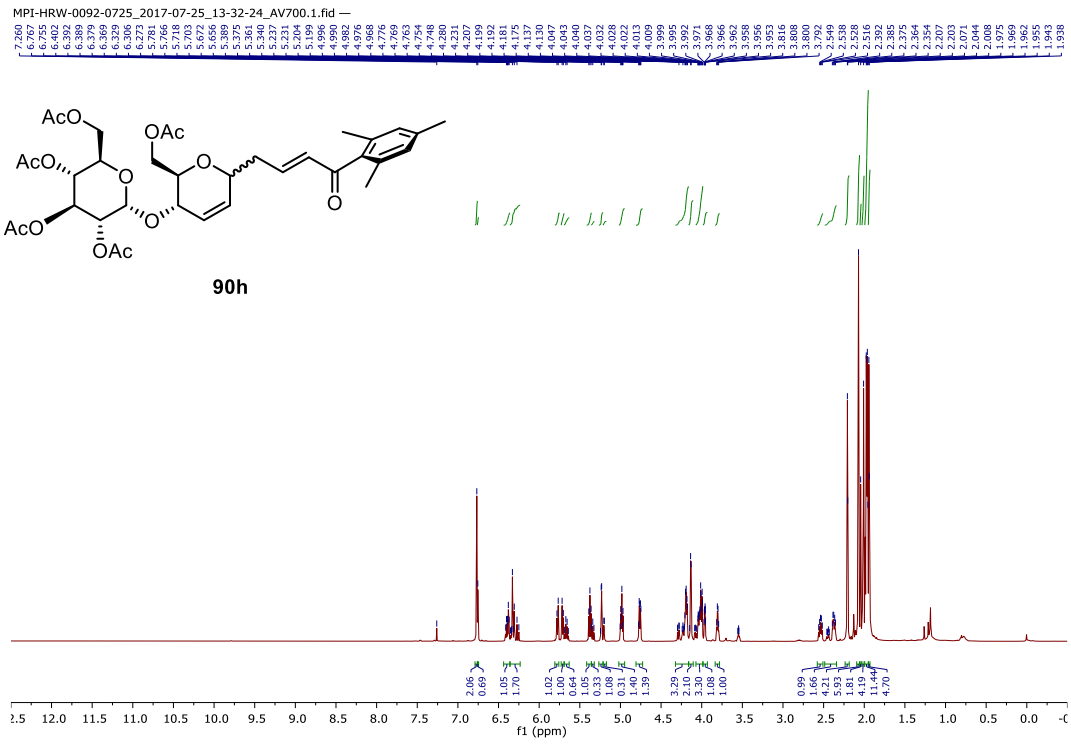

^{1}H NMR spectrum of compound **90h** (700 MHz, in $CDCl_3$)

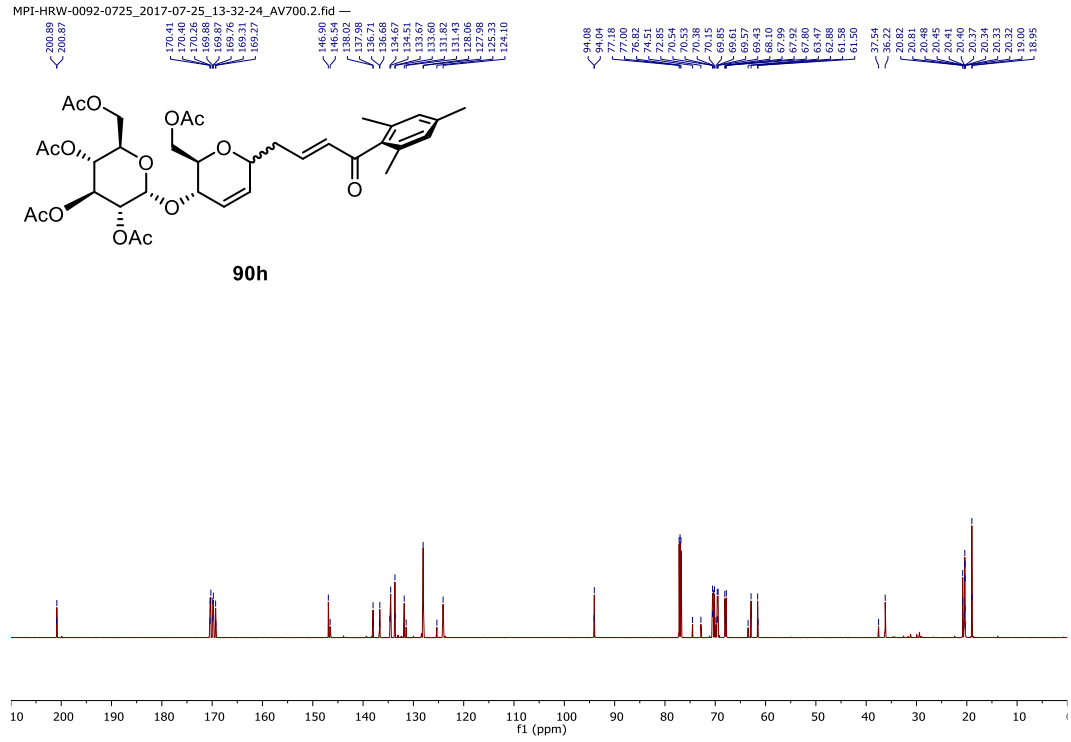

^{13}C NMR spectrum of compound **90h** (176 MHz, in $CDCl_3$)

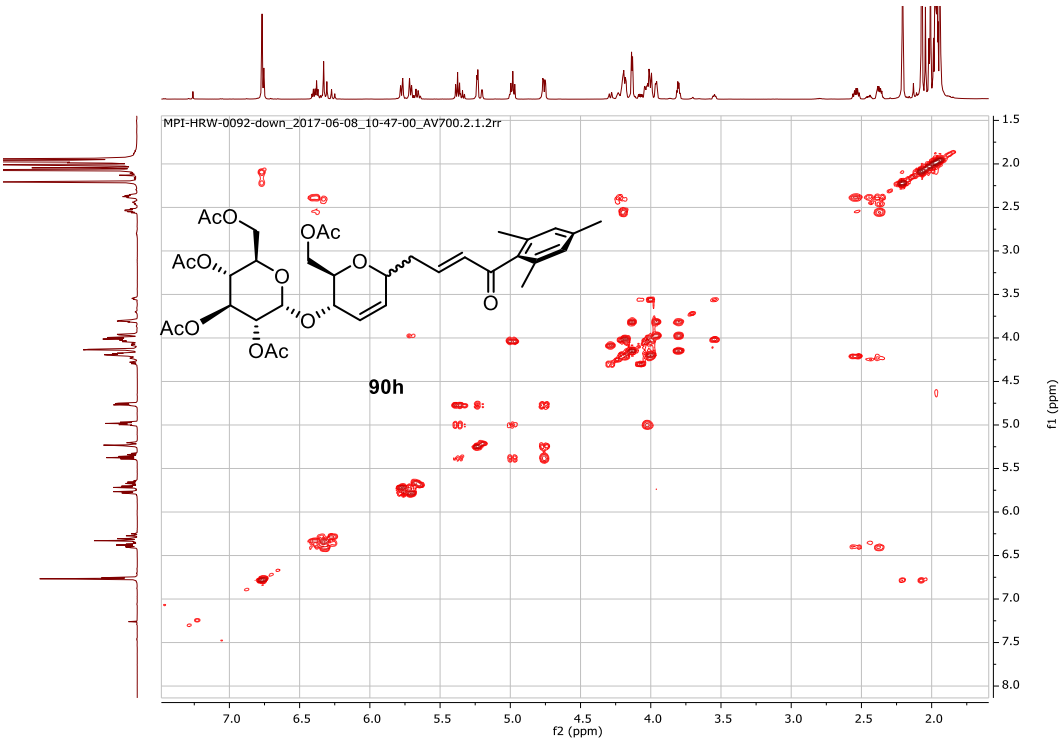

COSY spectrum of compound **90h**

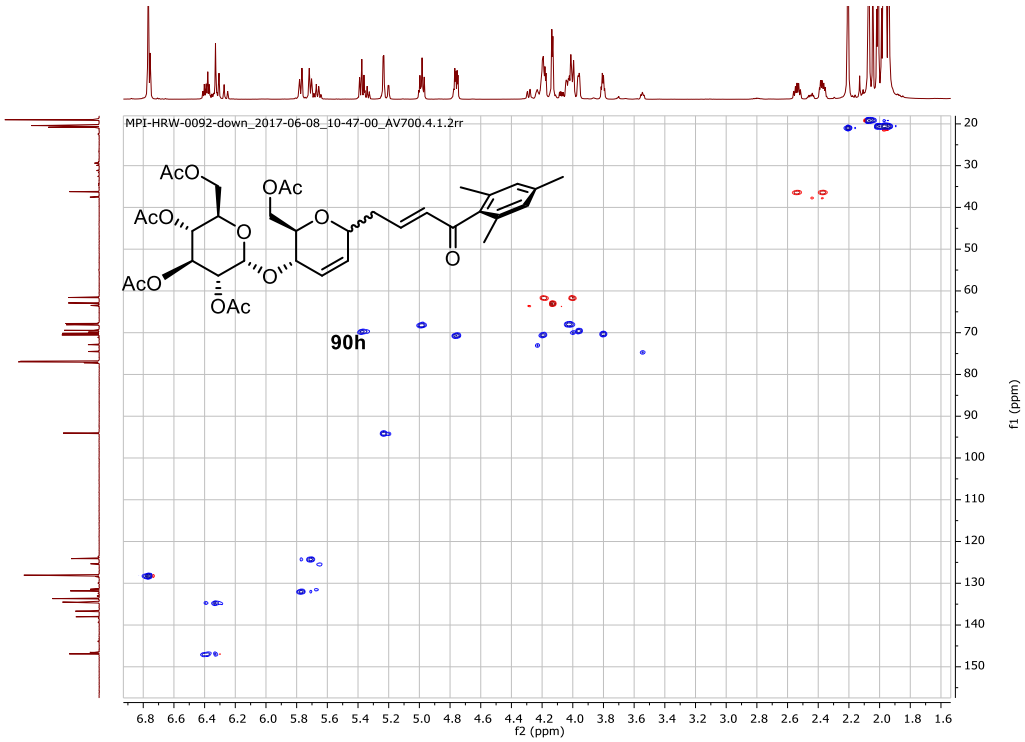

HSQC spectrum of compound **90h**

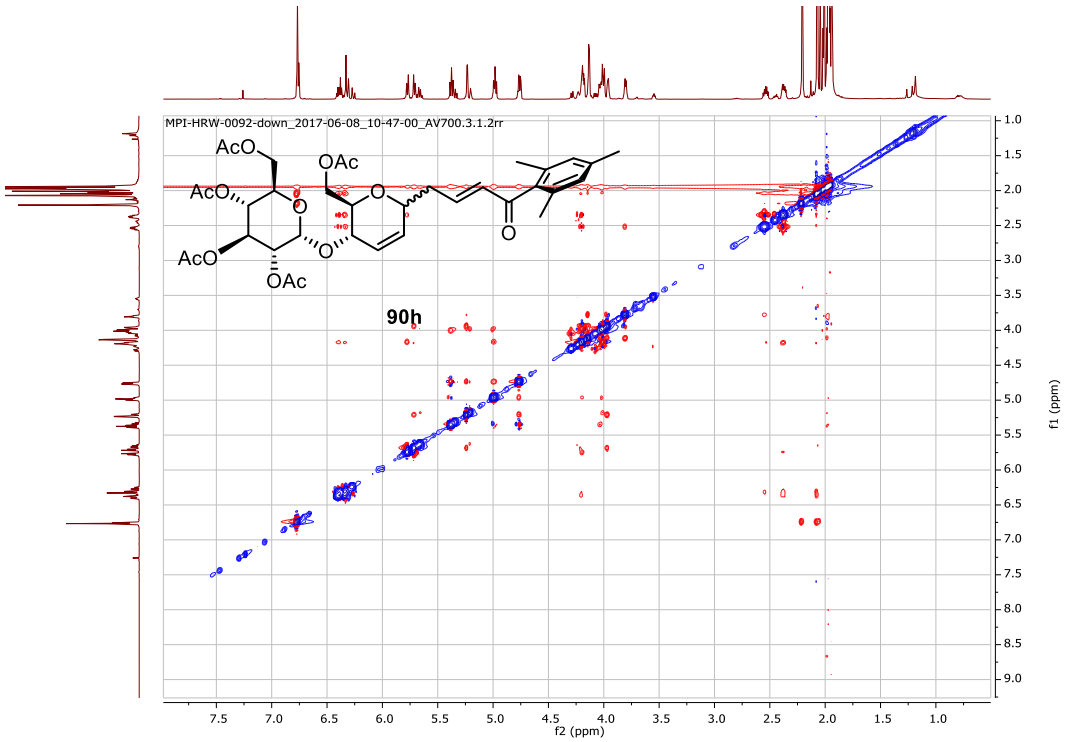

NOESY spectrum of compound **90h**

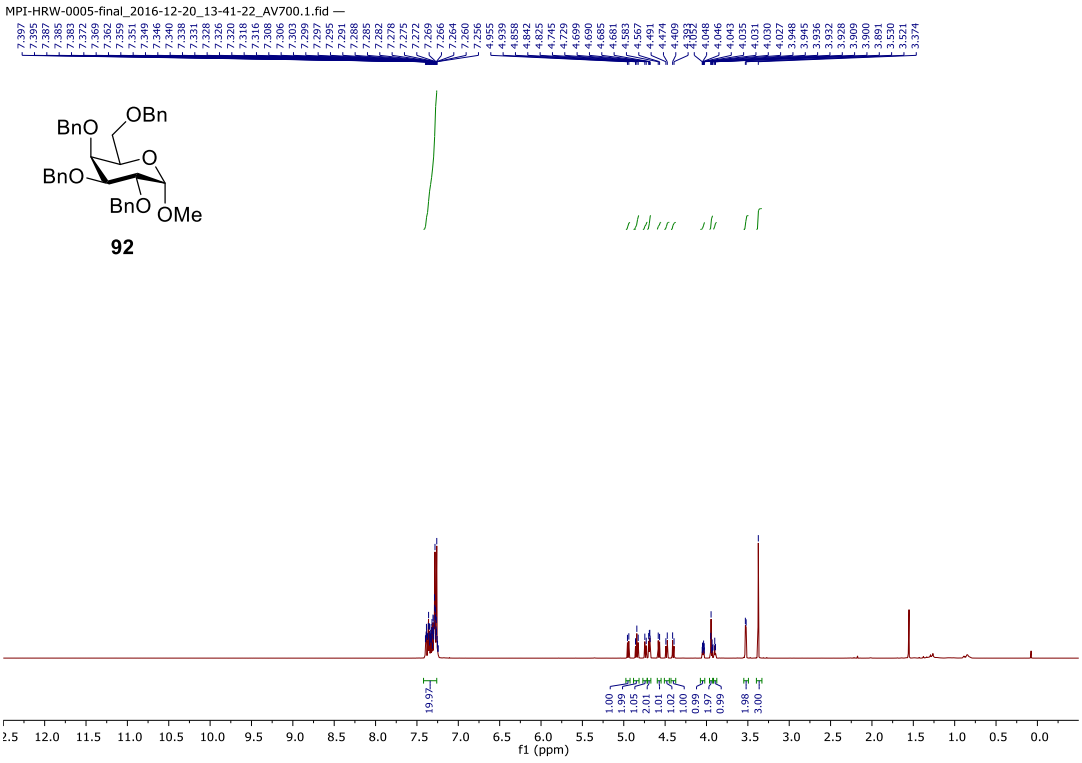

^{1}H NMR spectrum of compound **92** (700 MHz, in $CDCl_3$)

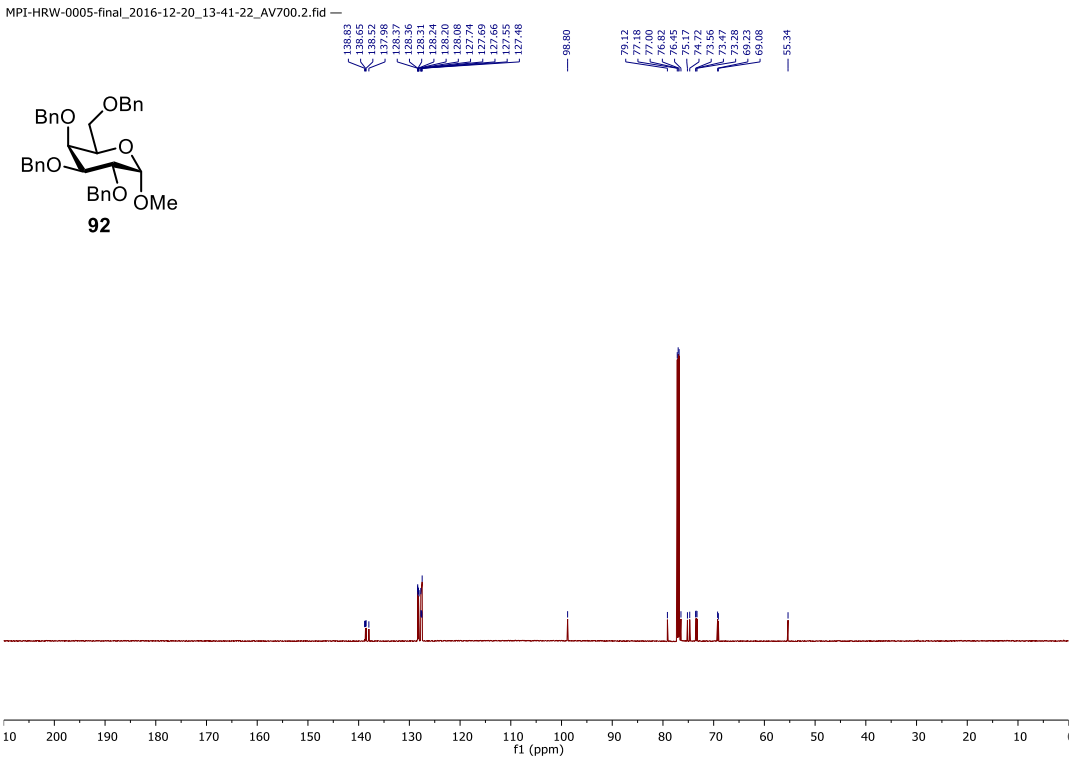

^{13}C NMR spectrum of compound **92** (176 MHz, in $CDCl_3$)

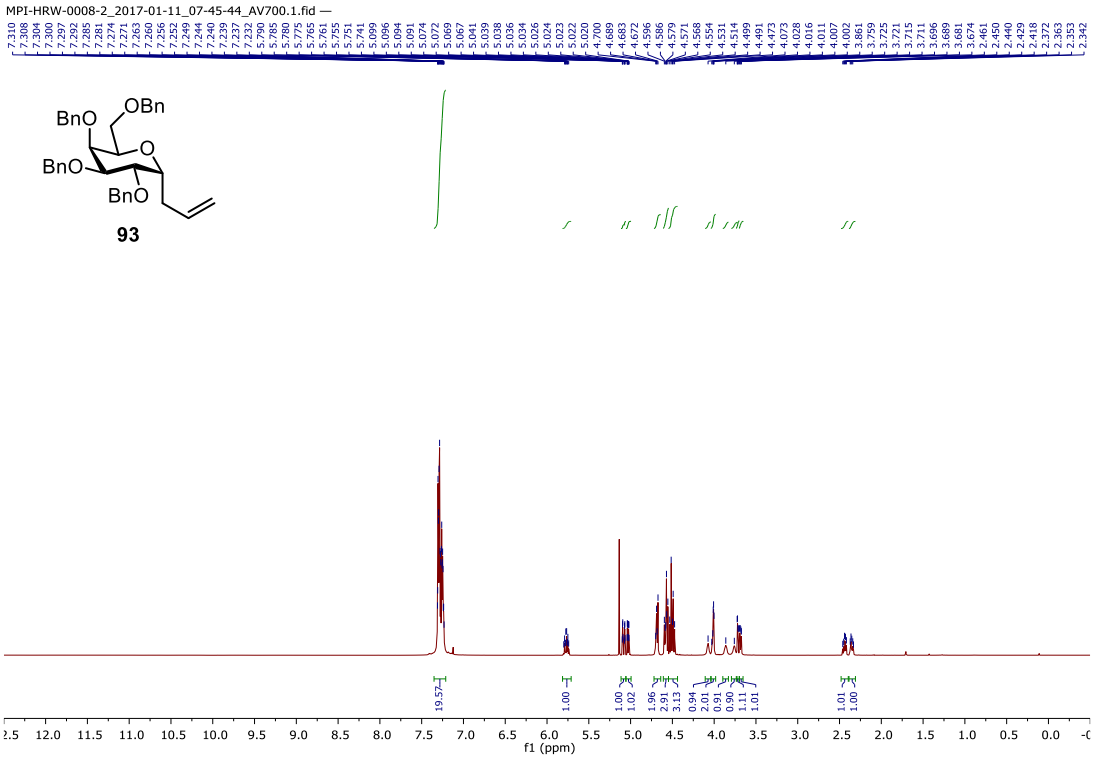

^{1}H NMR spectrum of compound **93** (700 MHz, in $CDCl_3$)

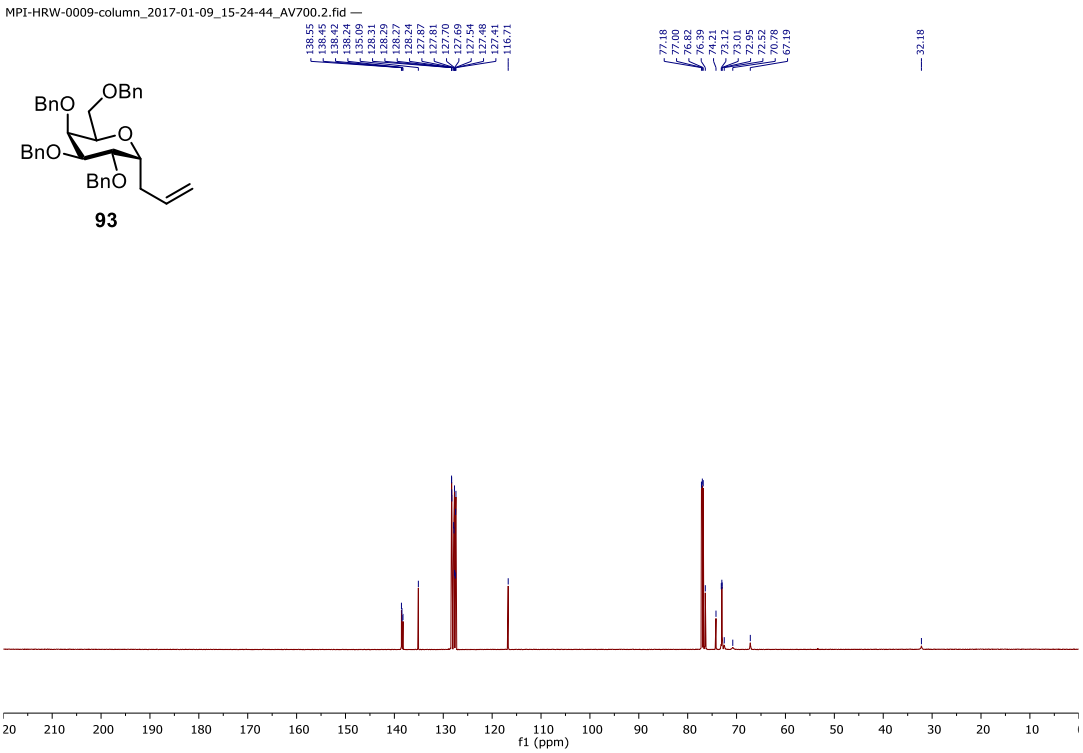

^{13}C NMR spectrum of compound **93** (176 MHz, in $CDCl_3$)

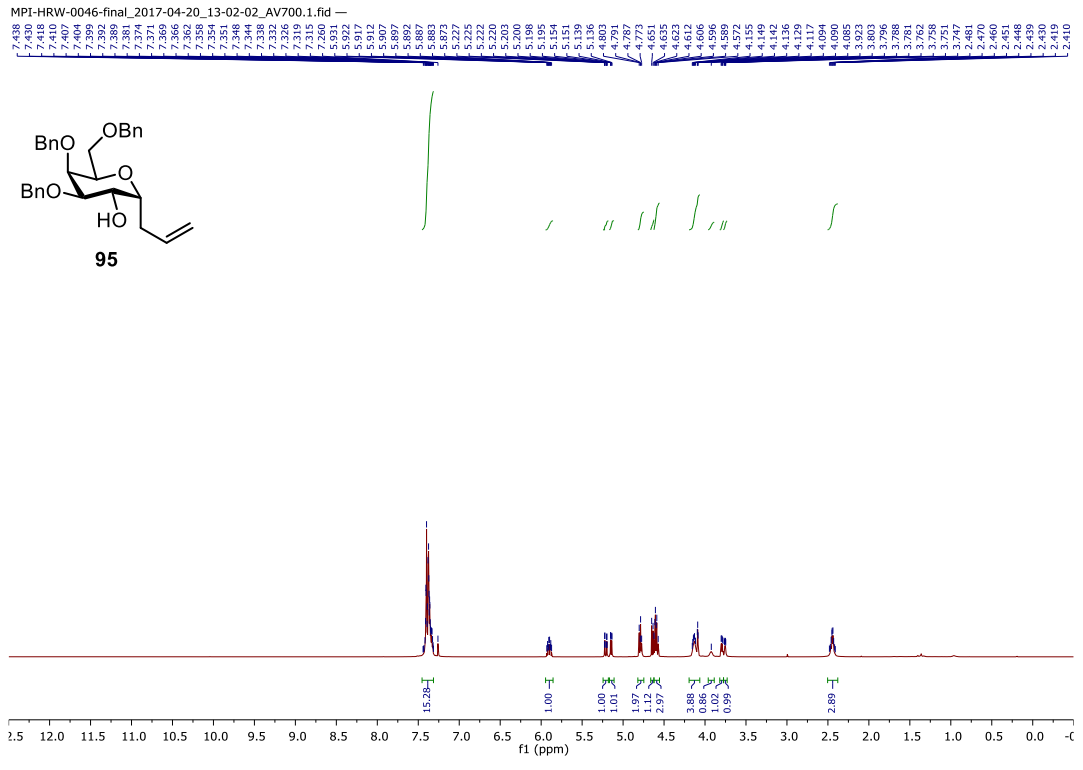

^{1}H NMR spectrum of compound **95** (700 MHz, in $CDCl_3$)

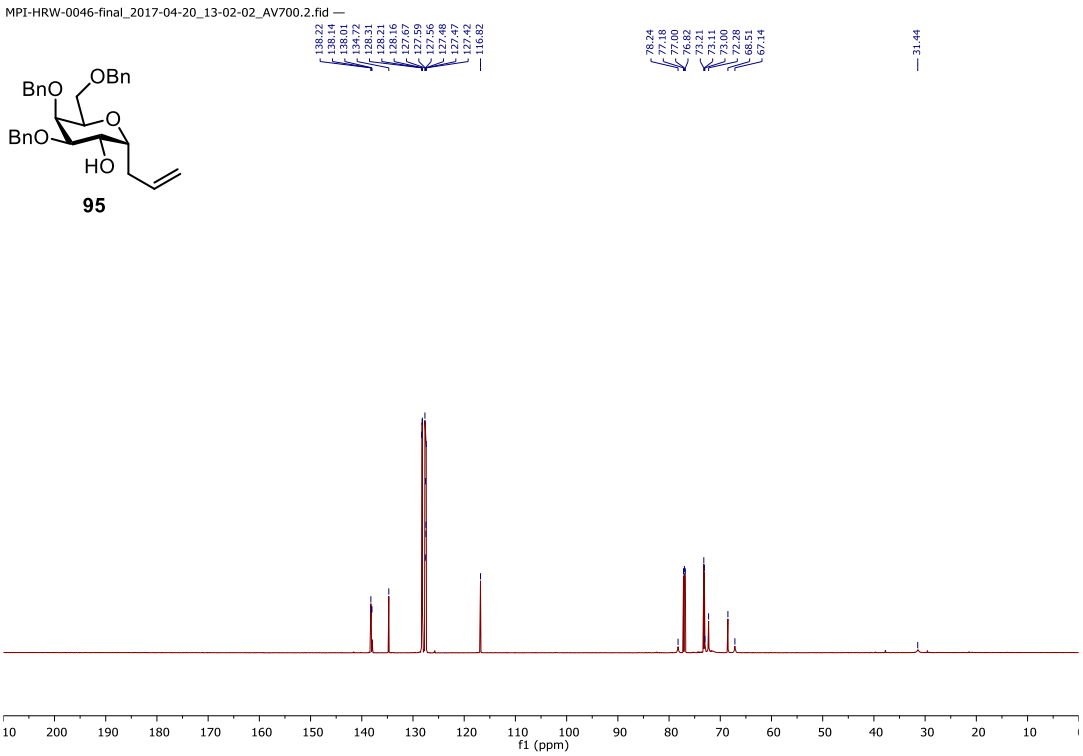

^{13}C NMR spectrum of compound **95** (176 MHz, in $CDCl_3$)

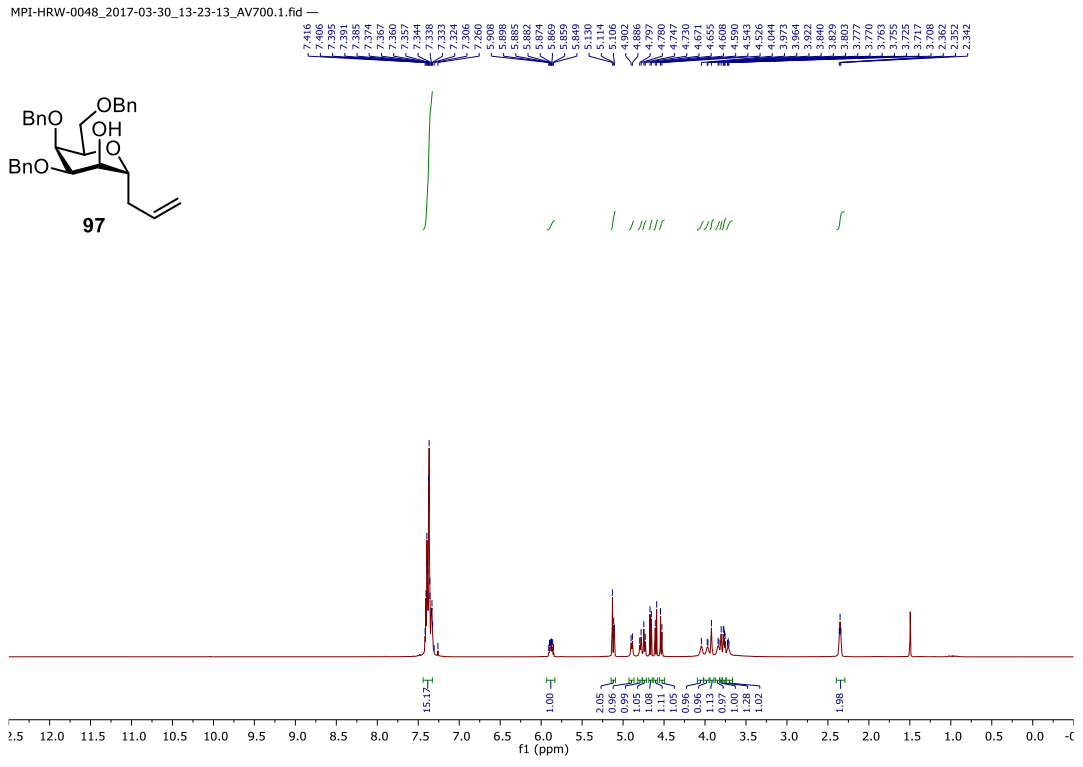

^{1}H NMR spectrum of compound **97** (700 MHz, in $CDCl_3$)

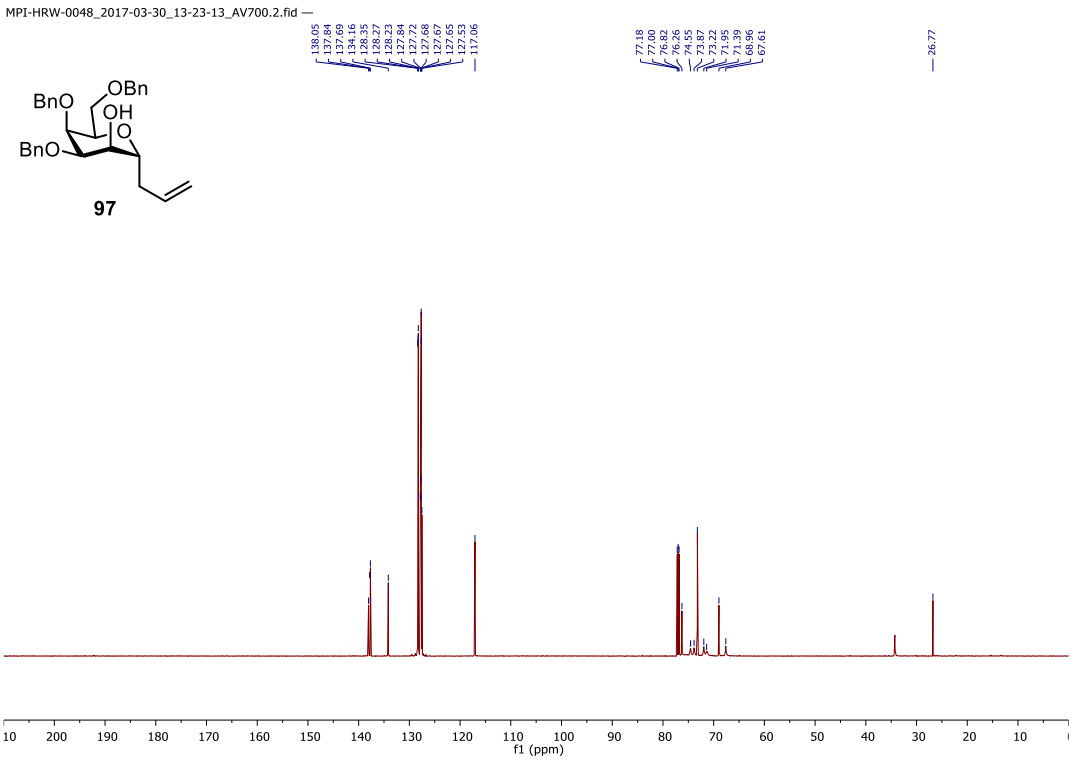

^{13}C NMR spectrum of compound **97** (176 MHz, in $CDCl_3$)

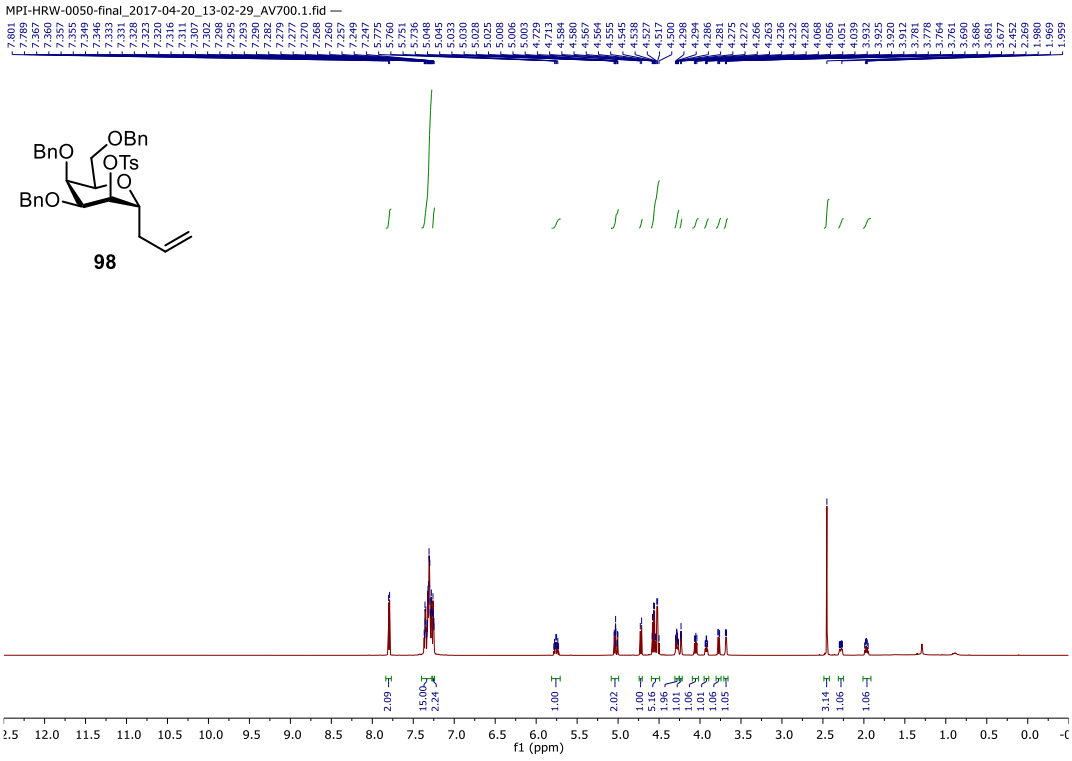

^{1}H NMR spectrum of compound **98** (700 MHz, in $CDCl_3$)

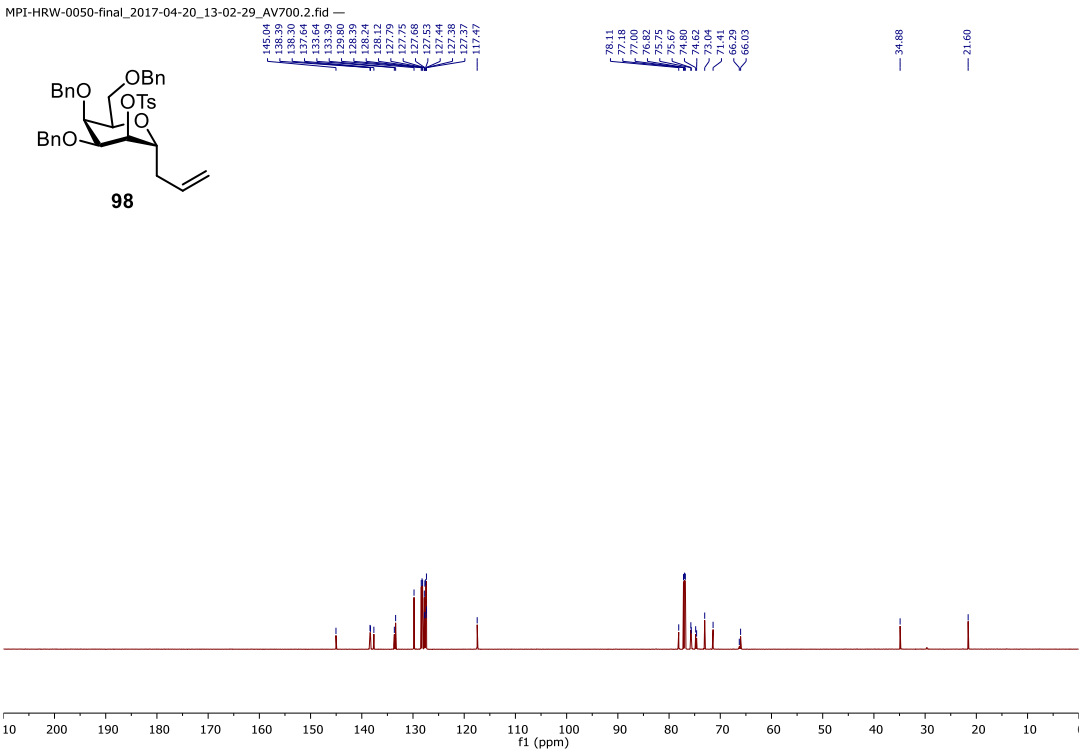

^{13}C NMR spectrum of compound **98** (176 MHz, in $CDCl_3$)

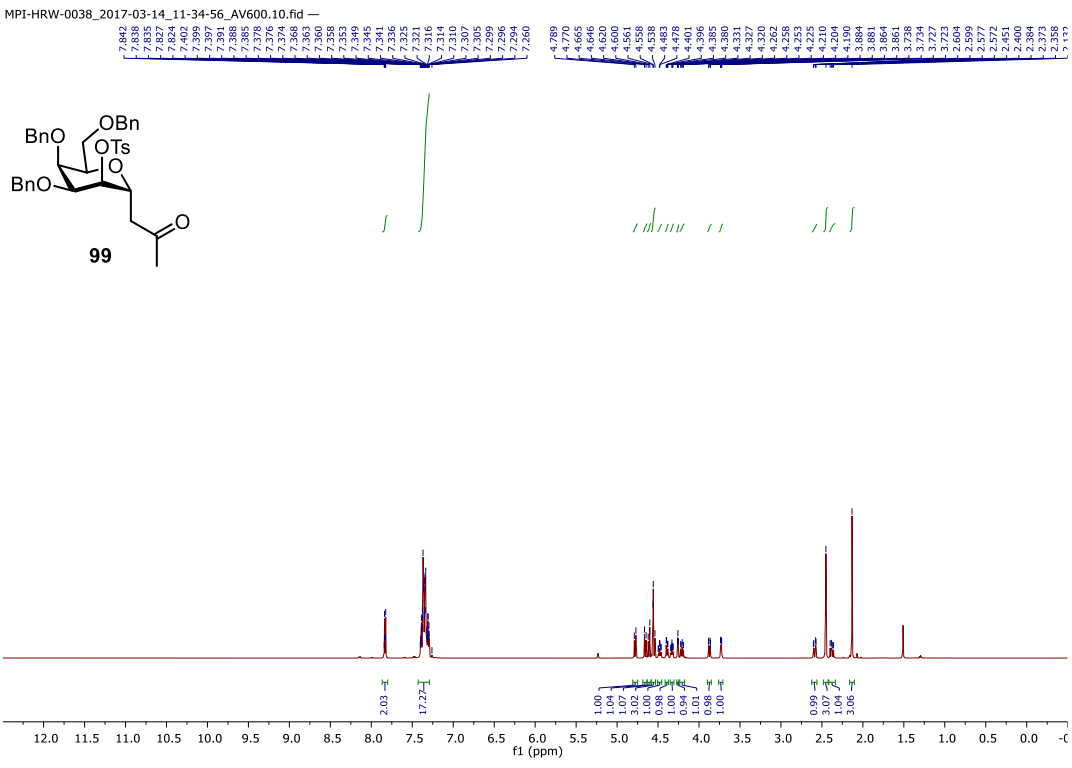

^{1}H NMR spectrum of compound **99** (600 MHz, in $CDCl_3$)

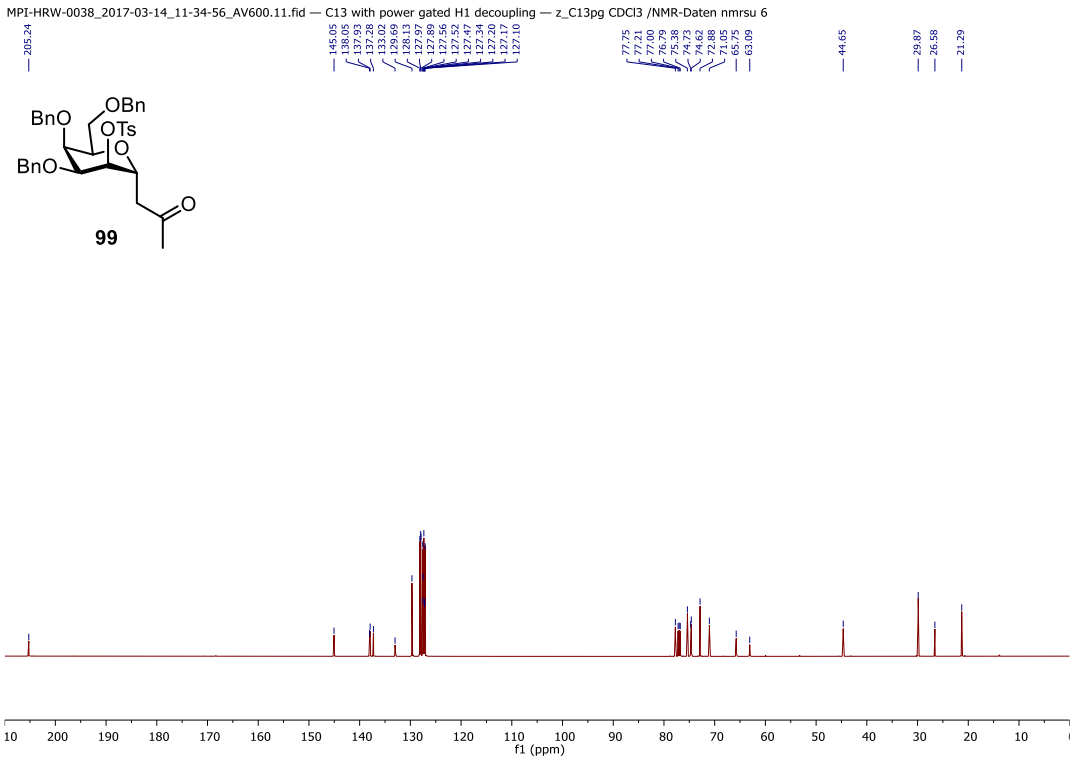

^{13}C NMR spectrum of compound **99** (151 MHz, in $CDCl_3$)

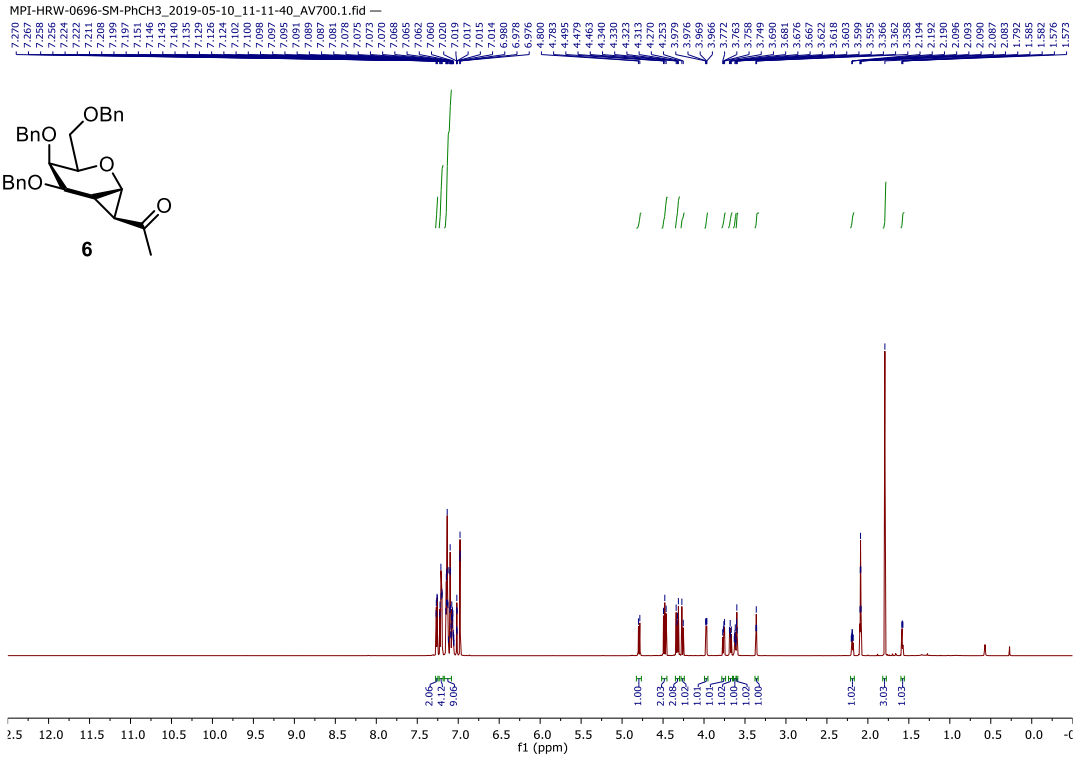

^{1}H NMR spectrum of compound **6** (700 MHz, in toluene-d_8)

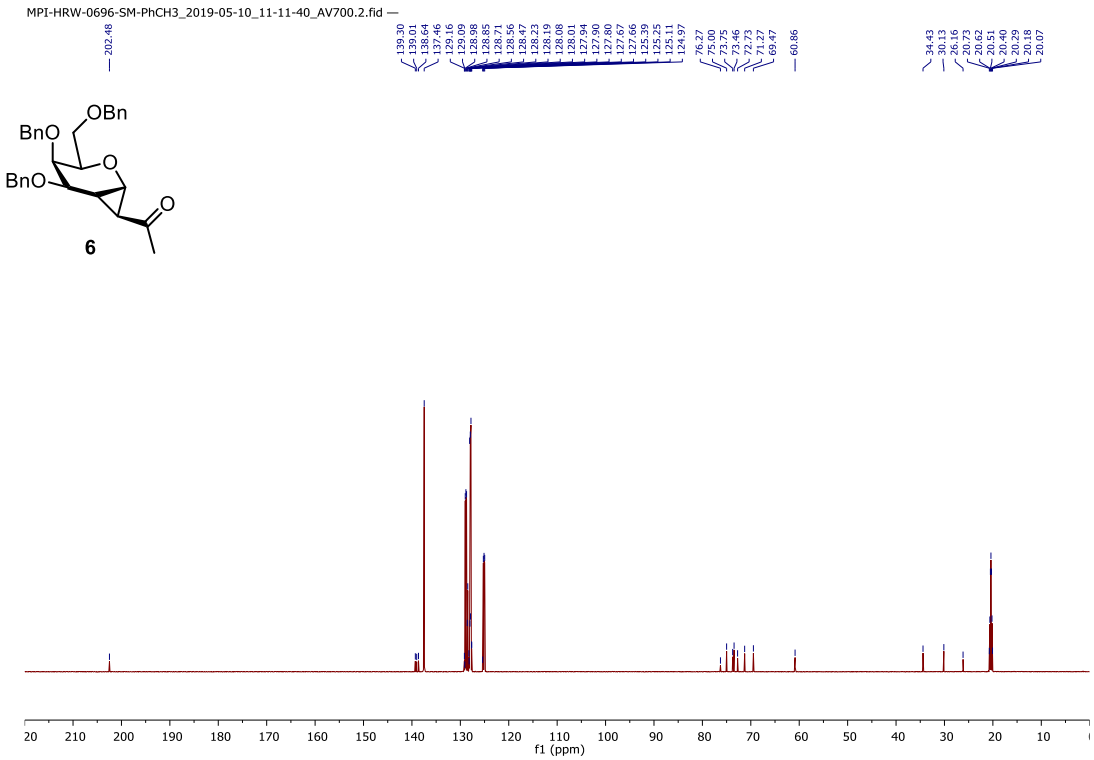

^{13}C NMR spectrum of compound **6** (176 MHz, in toluene-d_8)

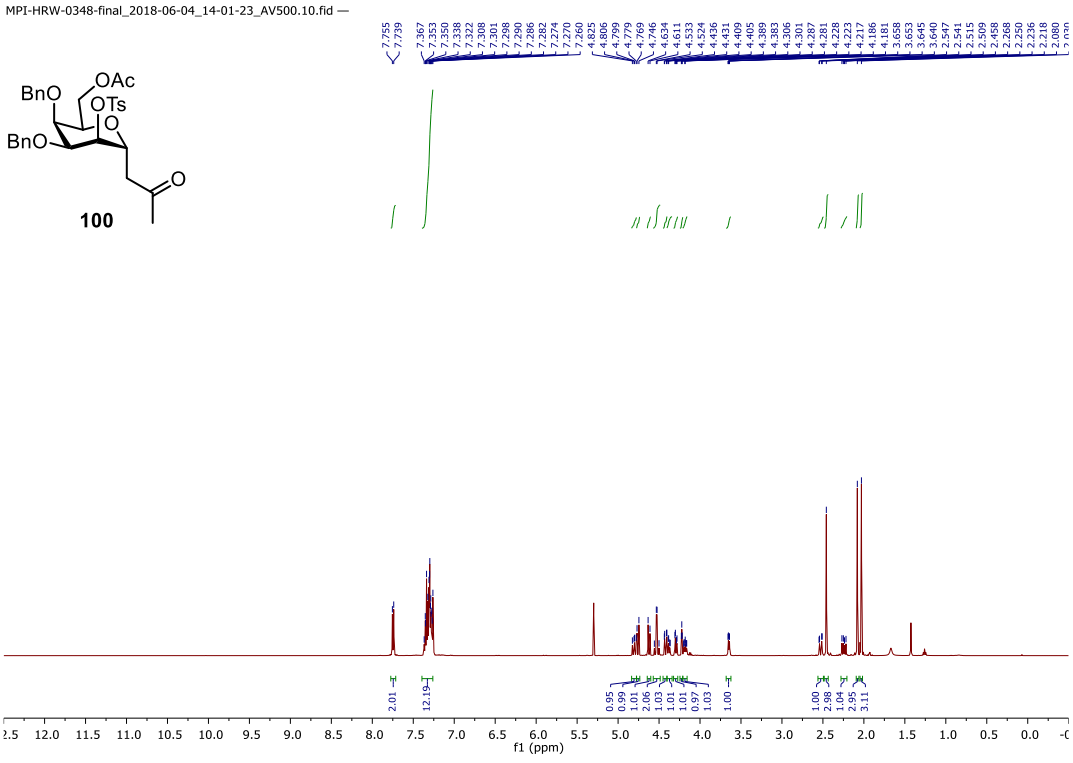

^{1}H NMR spectrum of compound **100** (500 MHz, in $CDCl_3$)

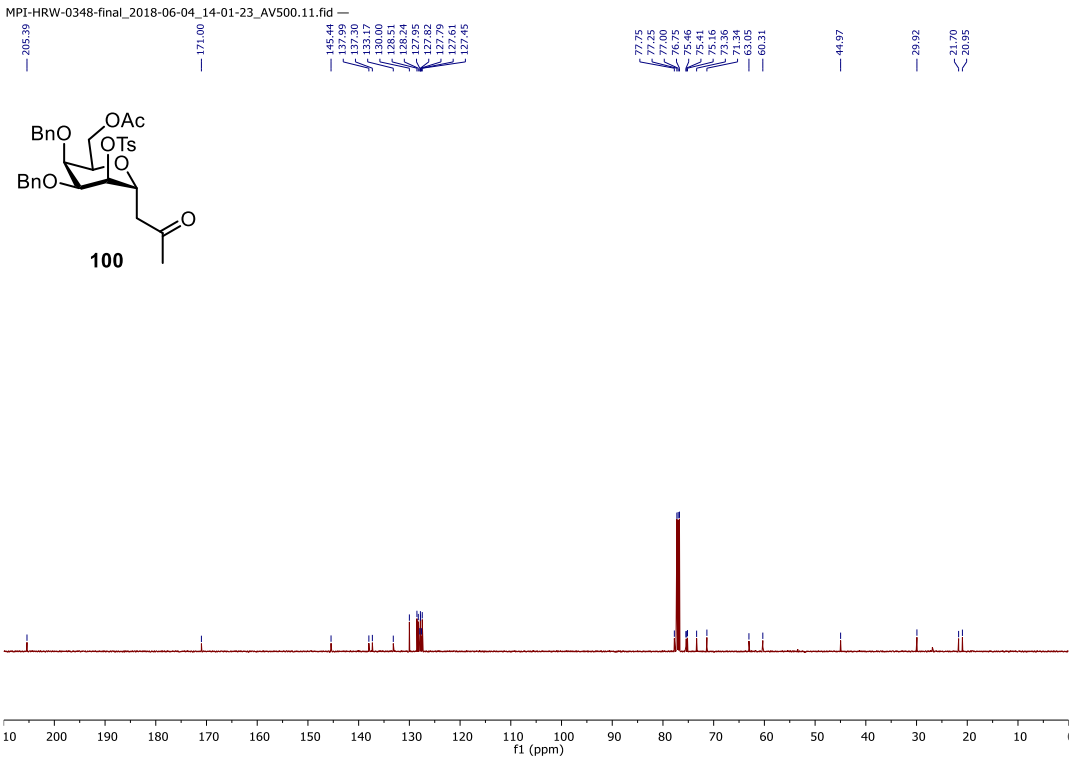

^{13}C NMR spectrum of compound **100** (126 MHz, in $CDCl_3$)

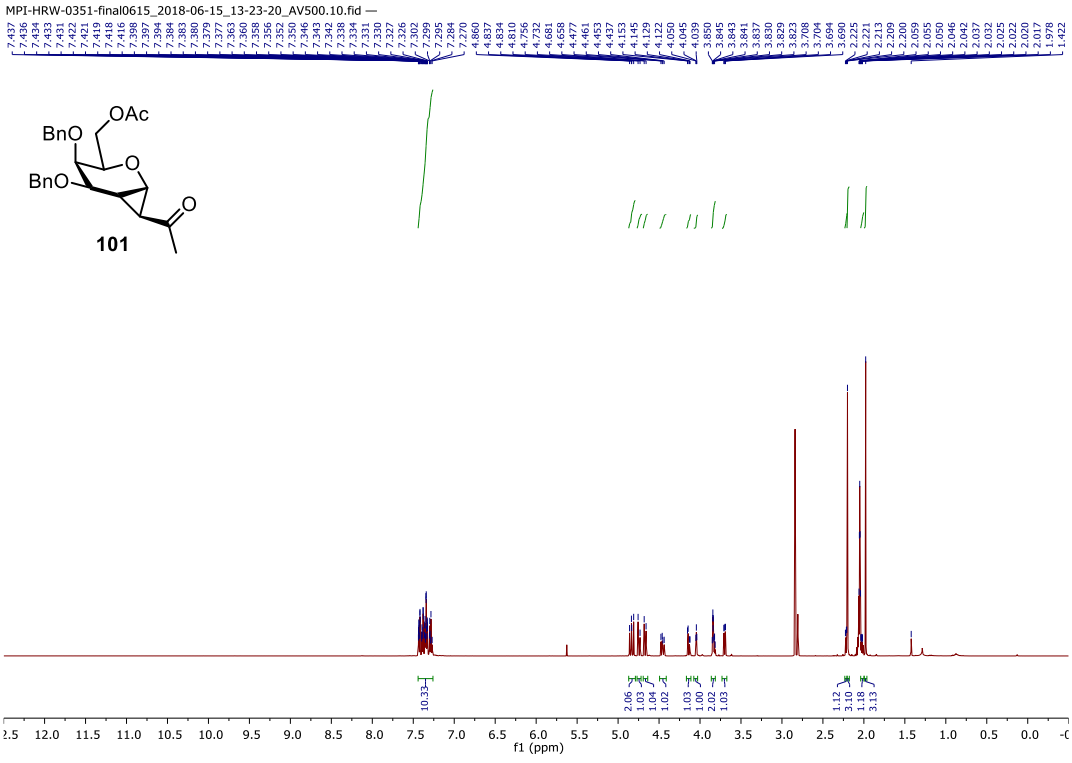

^{1}H NMR spectrum of compound **101** (500 MHz, in acetone-d_6)

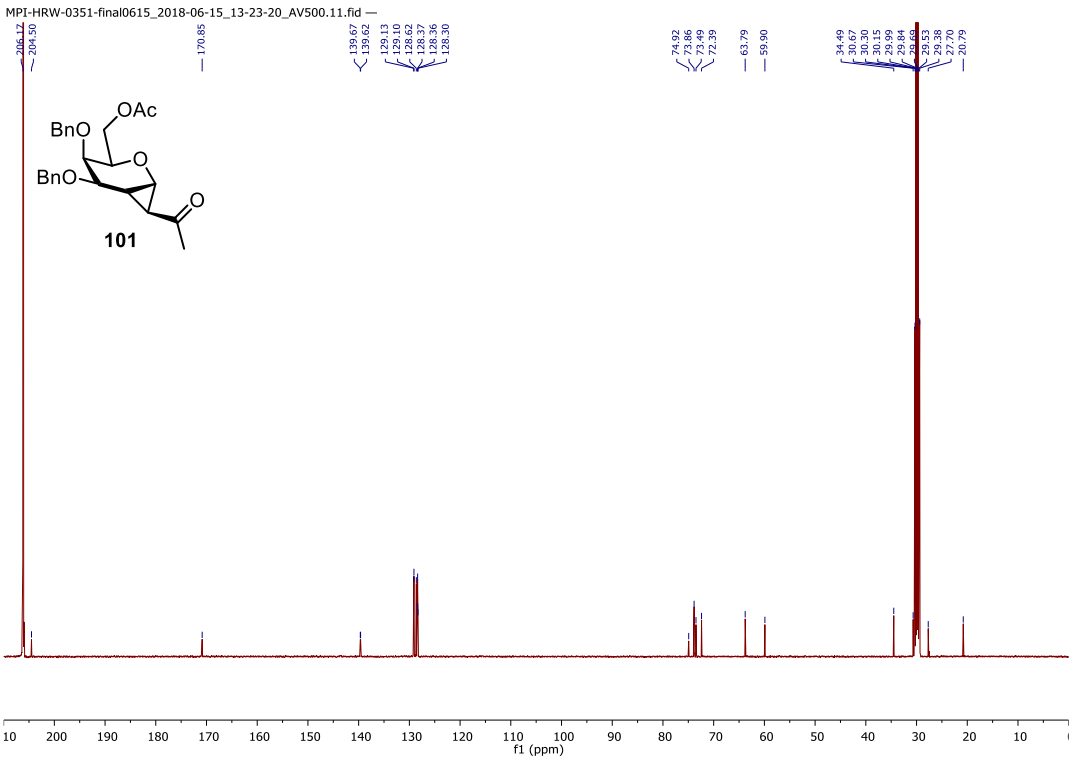

^{13}C NMR spectrum of compound **101** (126 MHz, in in acetone-d_6)

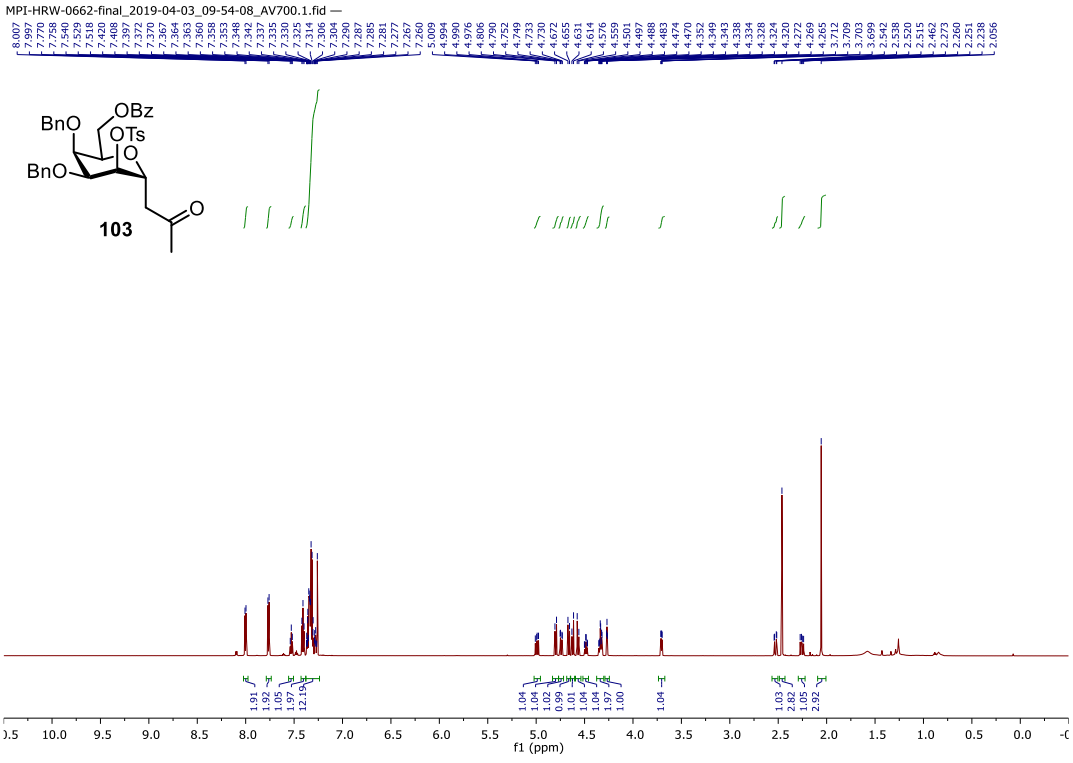

^{1}H NMR spectrum of compound **103** (700 MHz, in $CDCl_3$)

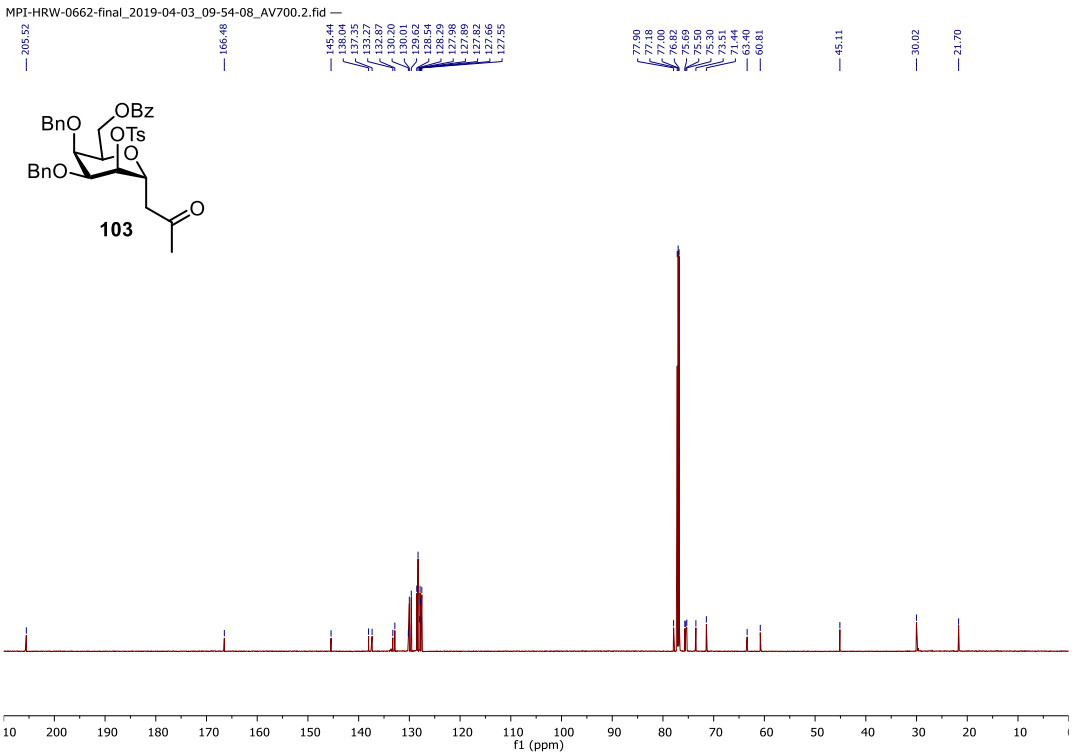

^{13}C NMR spectrum of compound **103** (176 MHz, in $CDCl_3$)

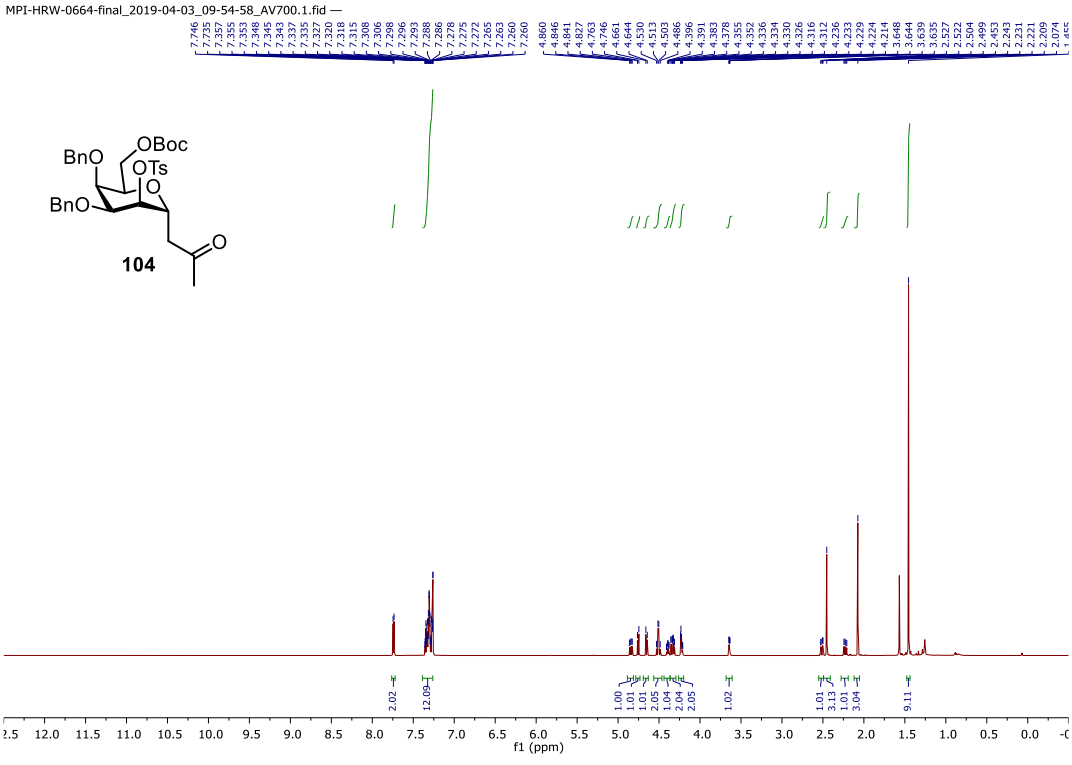

^{1}H NMR spectrum of compound **104** (700 MHz, in $CDCl_3$)

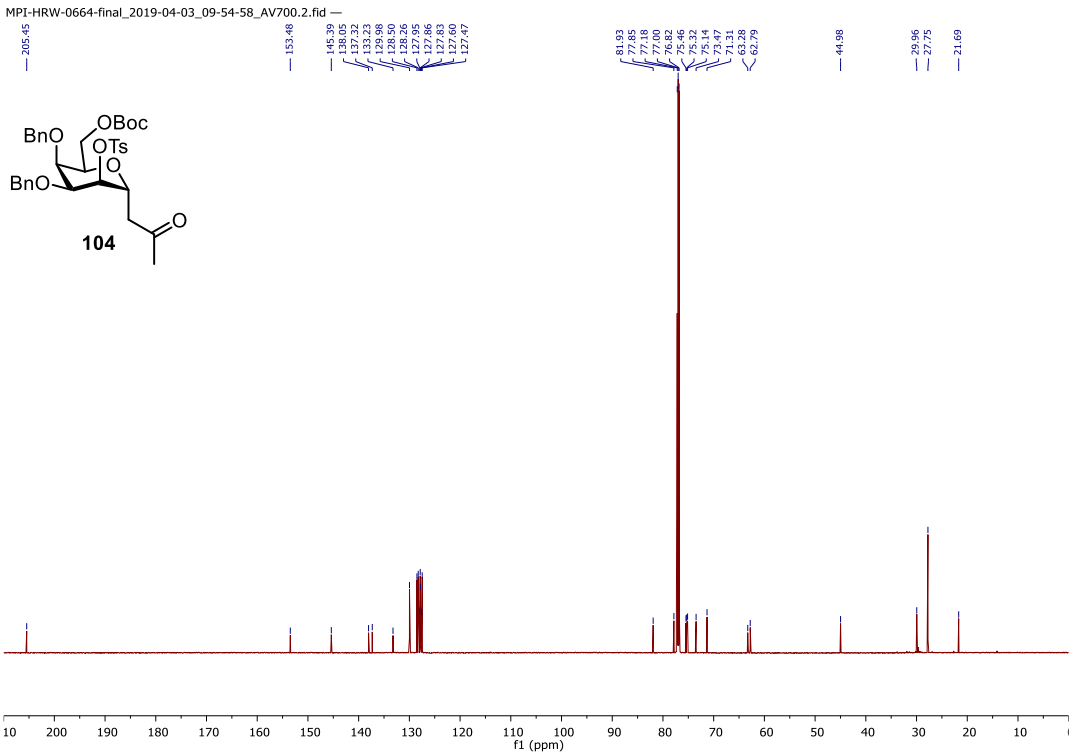

^{13}C NMR spectrum of compound **104** (176 MHz, in $CDCl_3$)

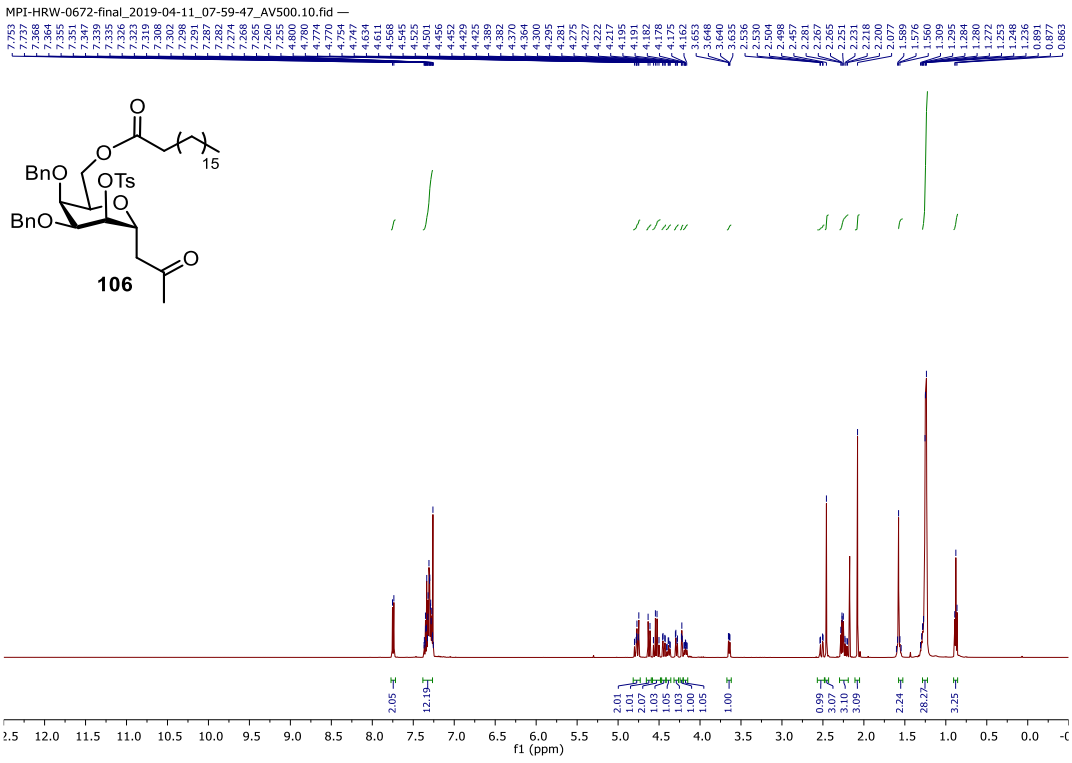

^{1}H NMR spectrum of compound **106** (500 MHz, in $CDCl_3$)

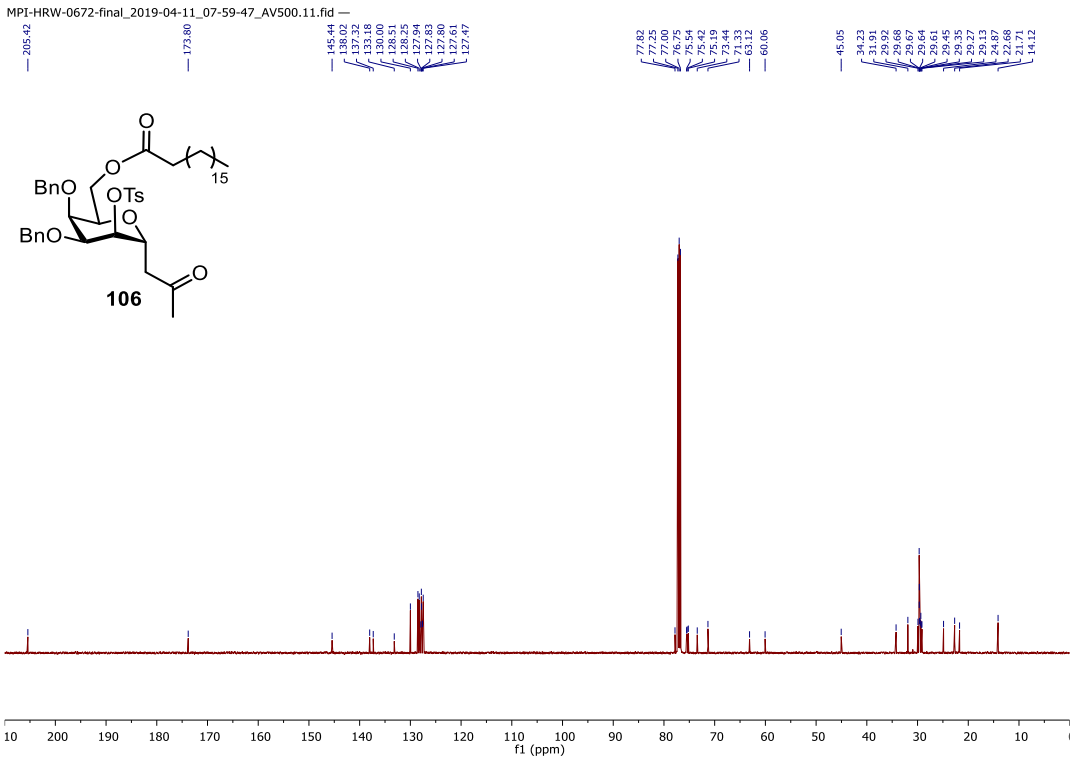

^{13}C NMR spectrum of compound **106** (176 MHz, in $CDCl_3$)

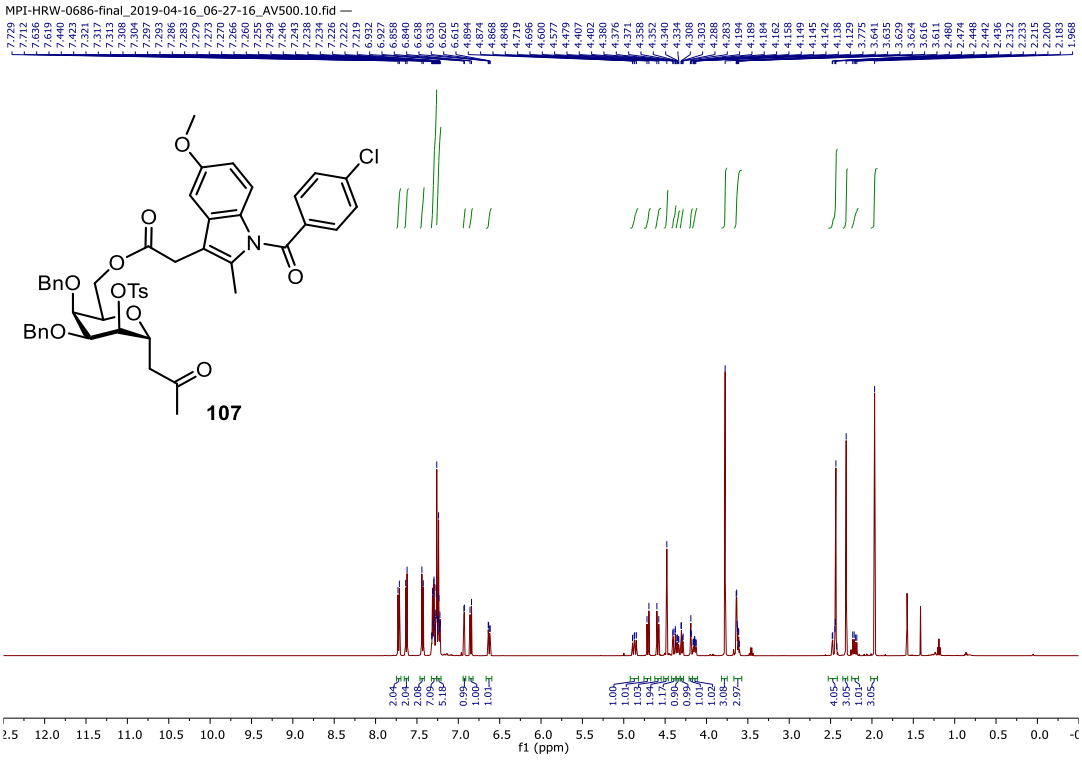

^{1}H NMR spectrum of compound **107** (500 MHz, in $CDCl_3$)

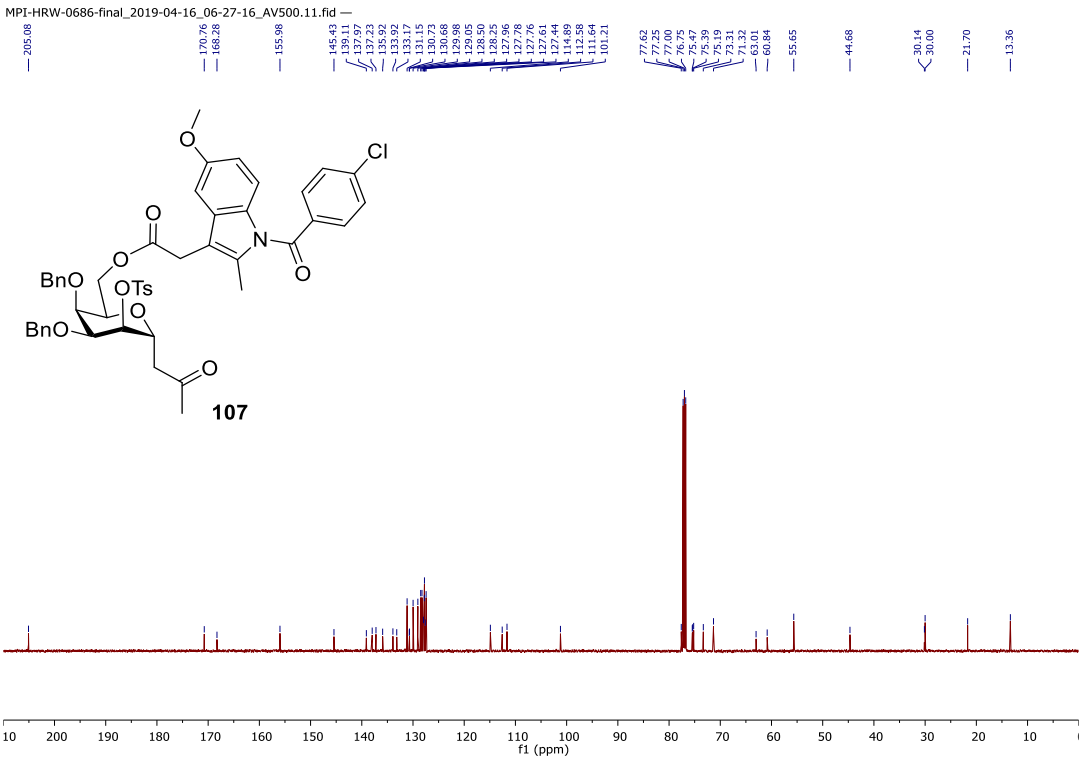

^{13}C NMR spectrum of compound **107** (126 MHz, in $CDCl_3$)

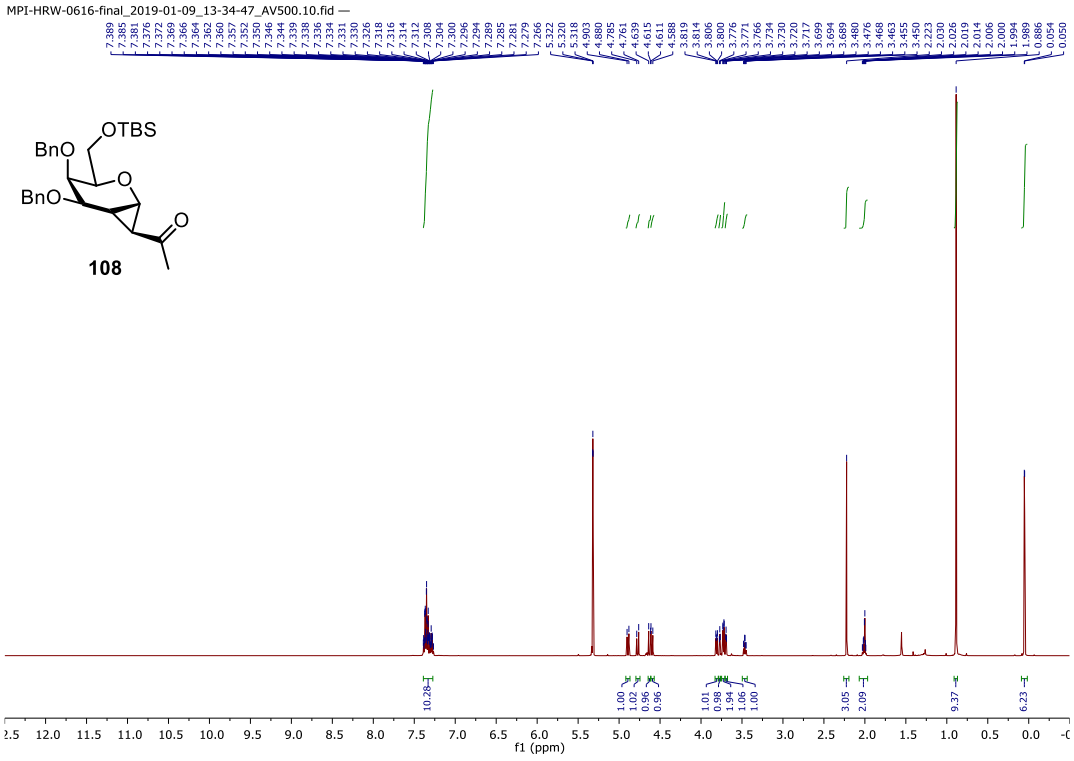

^{1}H NMR spectrum of compound **108** (500 MHz, in CD_2Cl_2)

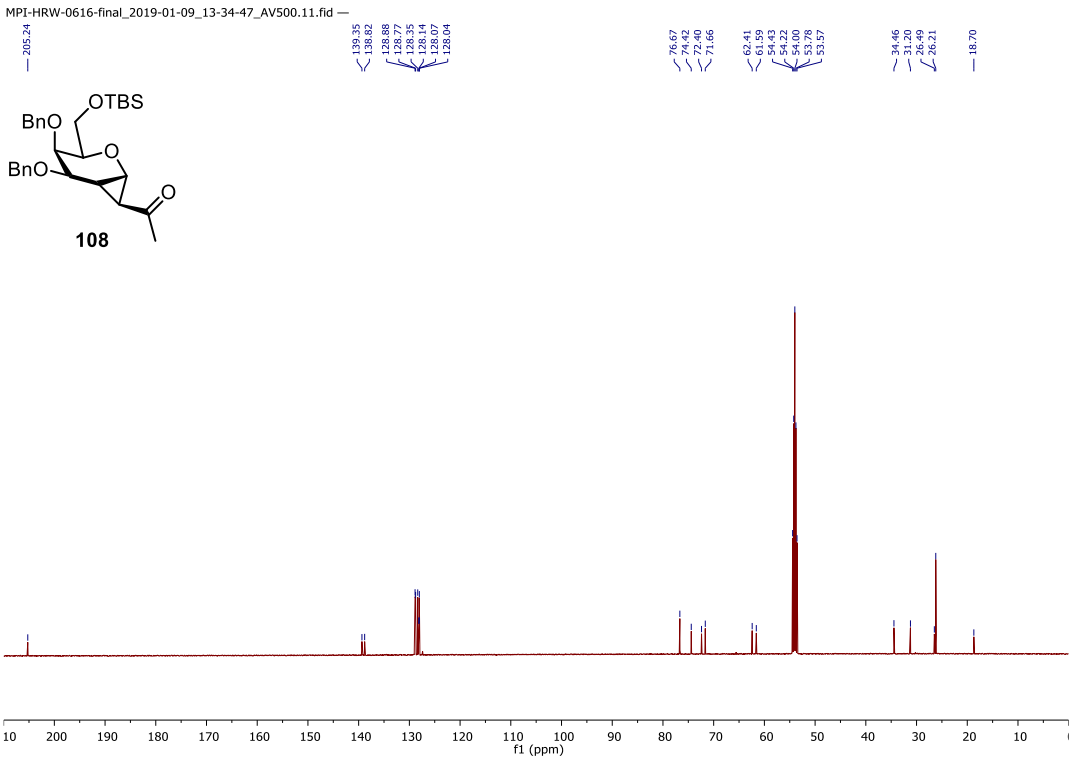

^{13}C NMR spectrum of compound **108** (126 MHz, in CD_2Cl_2)

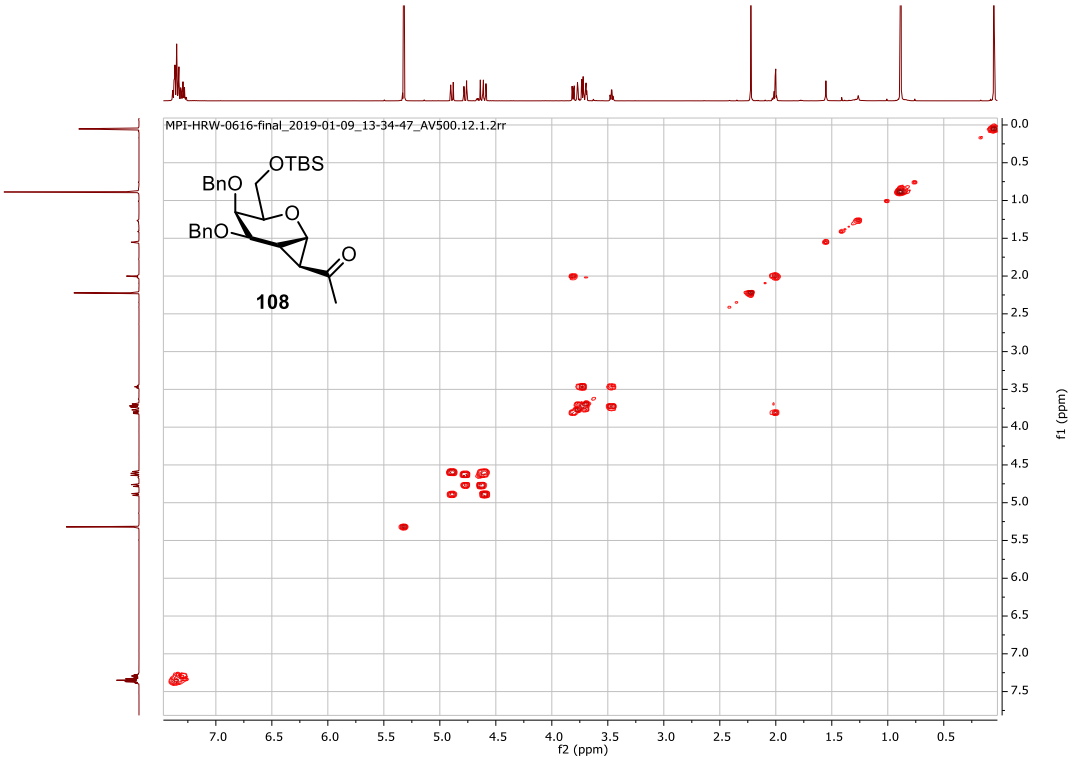

COSY spectrum of compound **108**

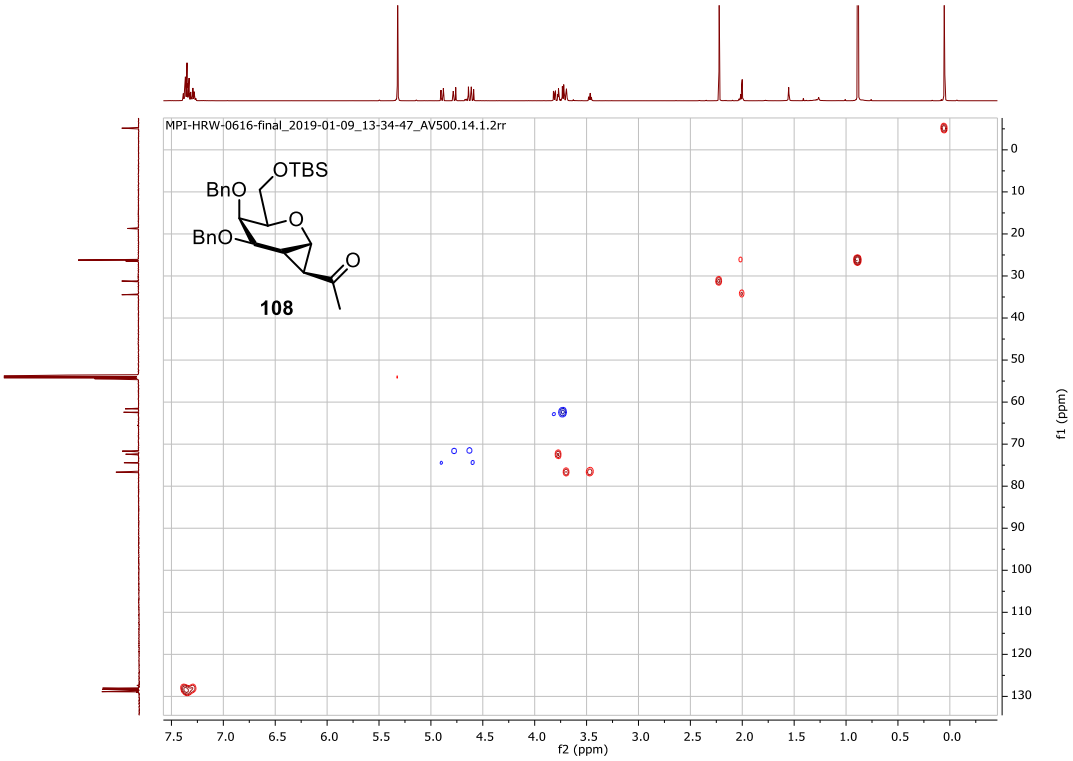

HSQC spectrum of compound **108**

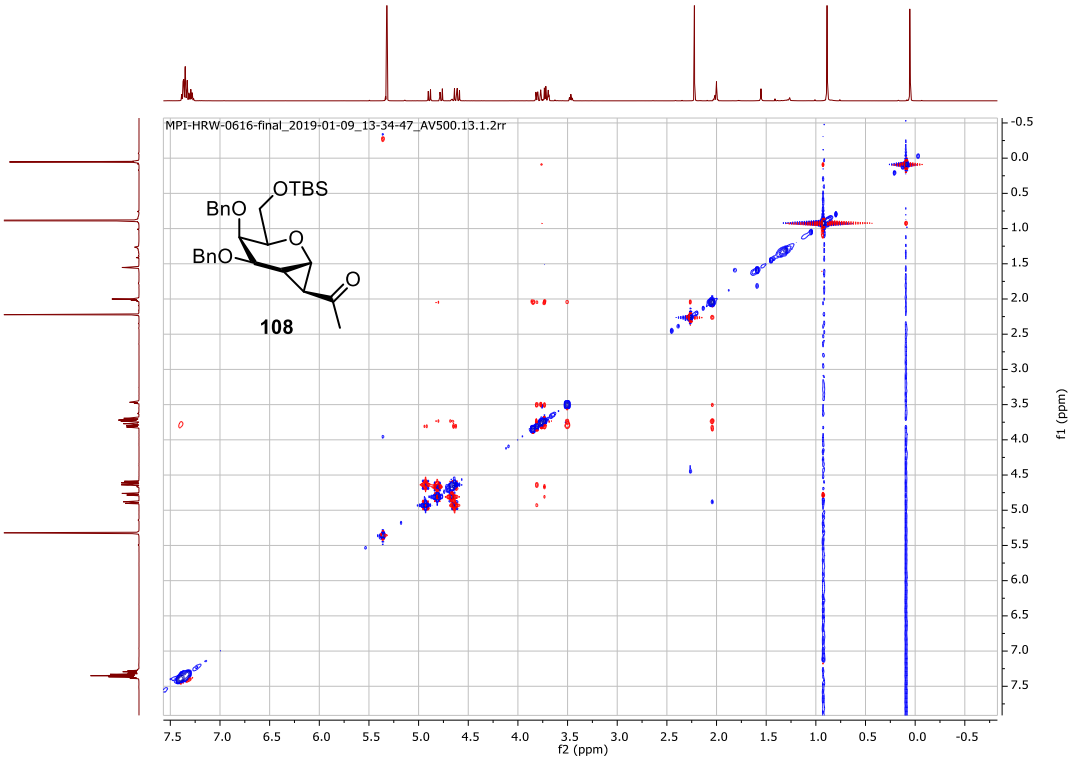

NOESY spectrum of compound **108**

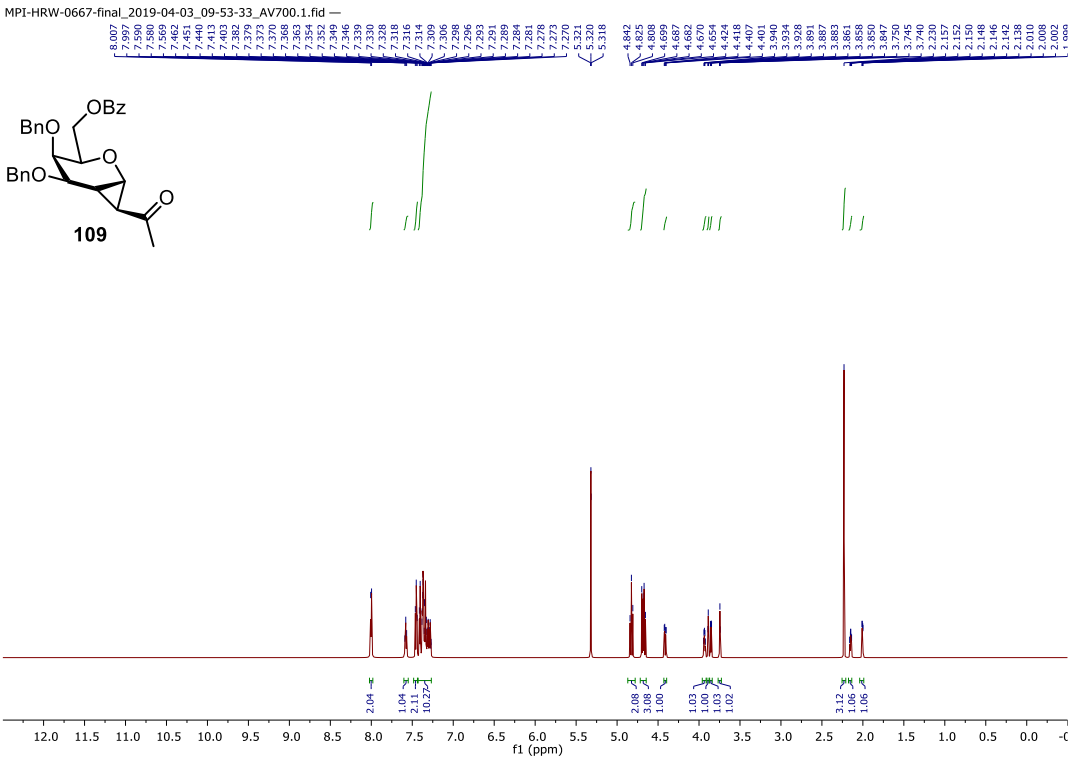

^{1}H NMR spectrum of compound **109** (700 MHz, in CD_2Cl_2)

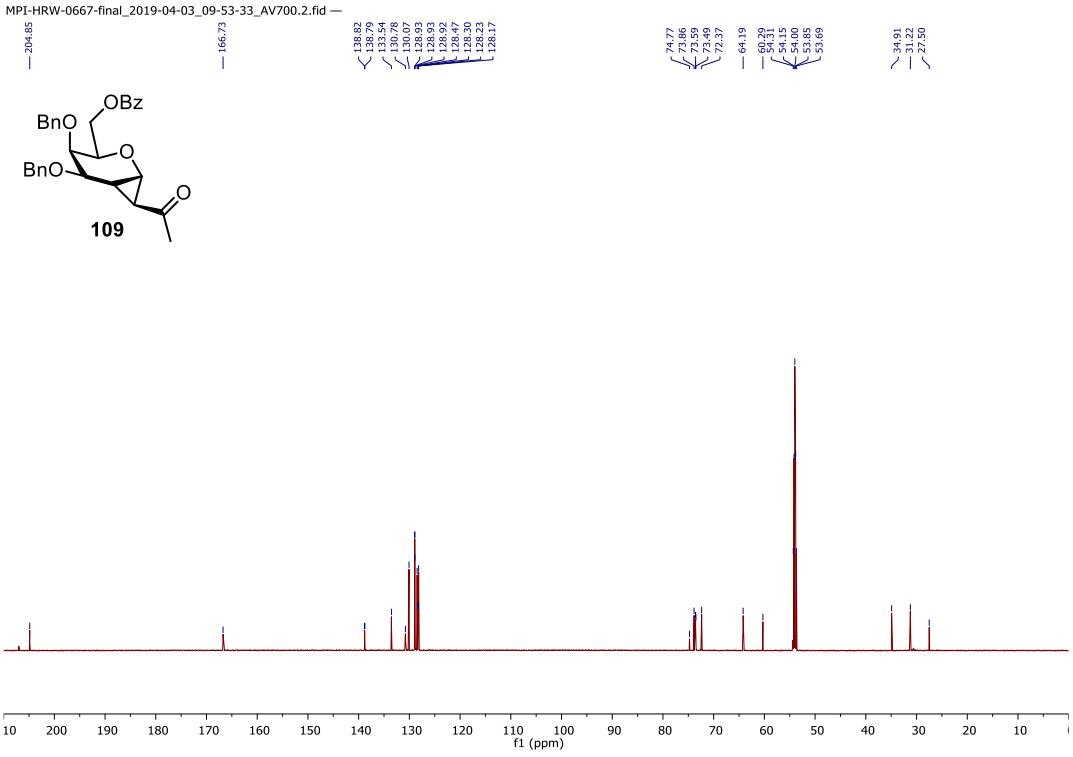

^{13}C NMR spectrum of compound **109** (176 MHz, in CD_2Cl_2)

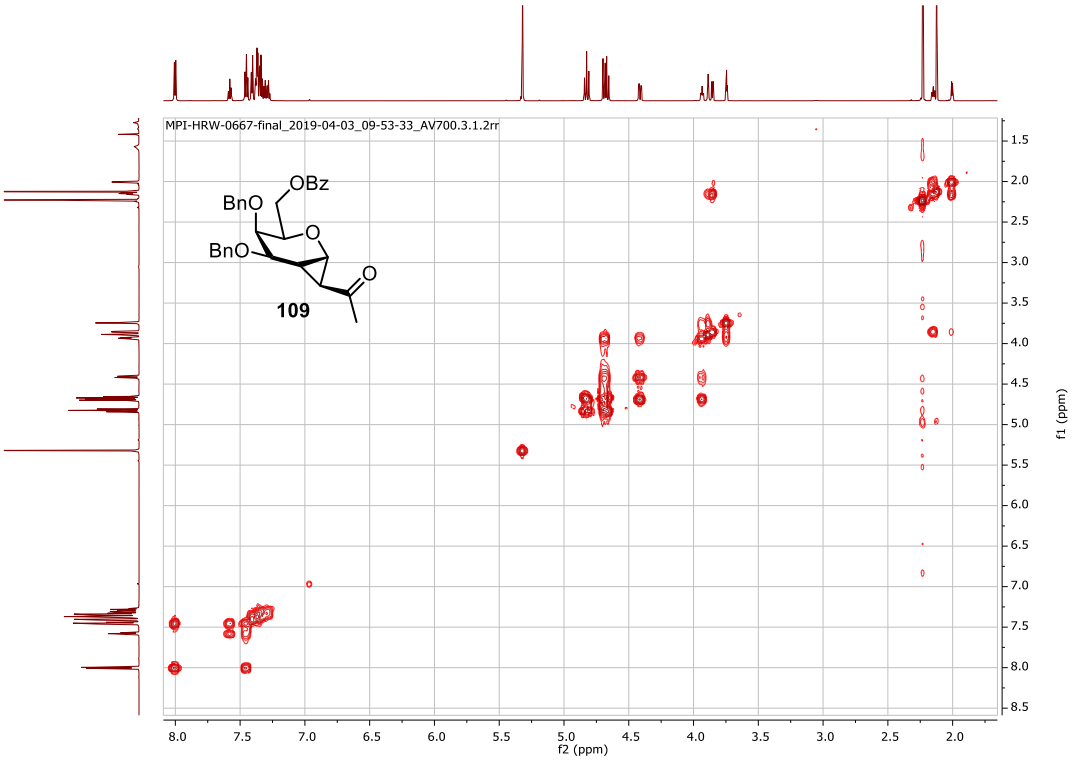

COSY spectrum of compound **109**

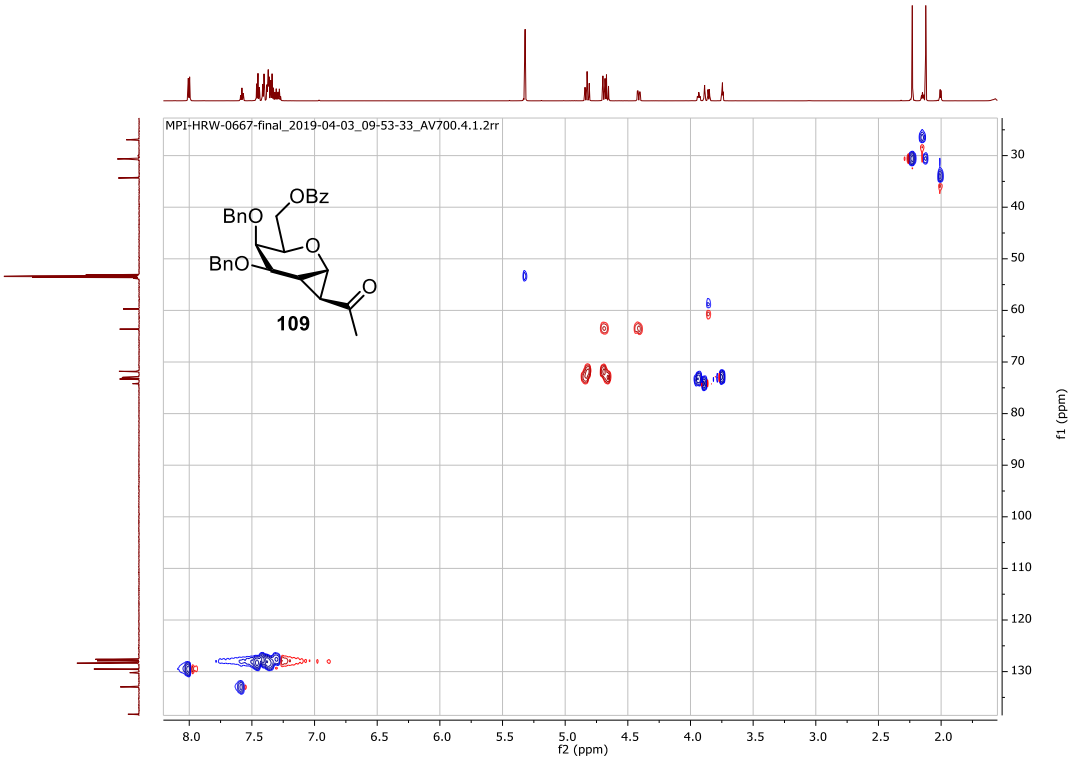

HSQC spectrum of compound **109**

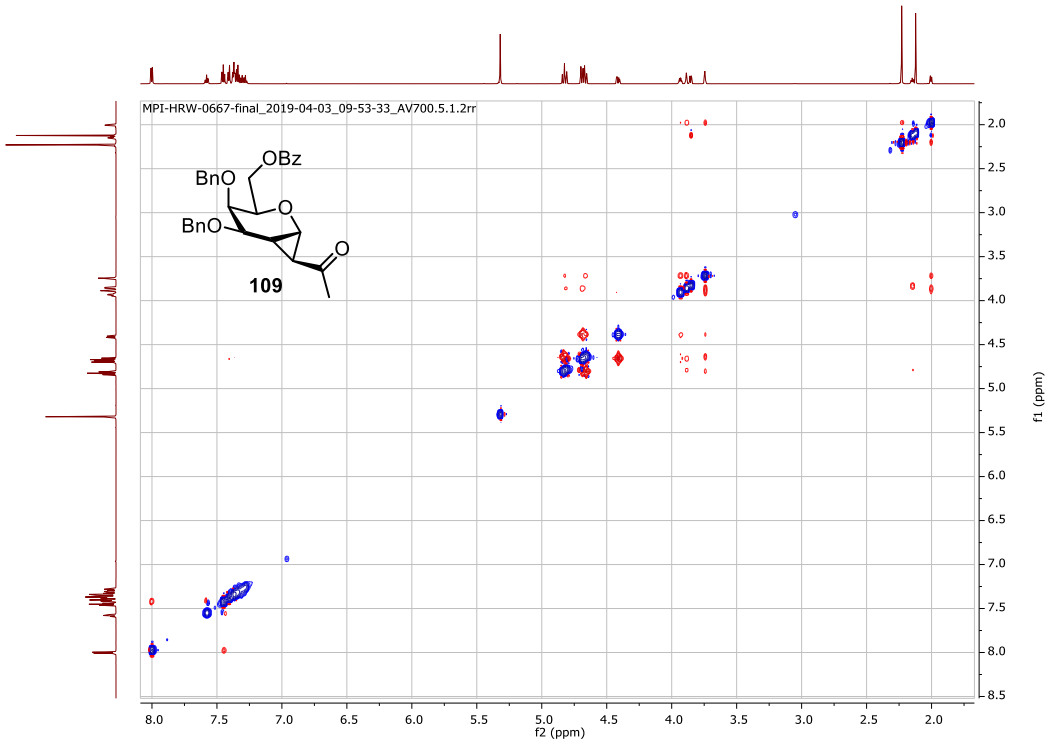

NOESY spectrum of compound **109**

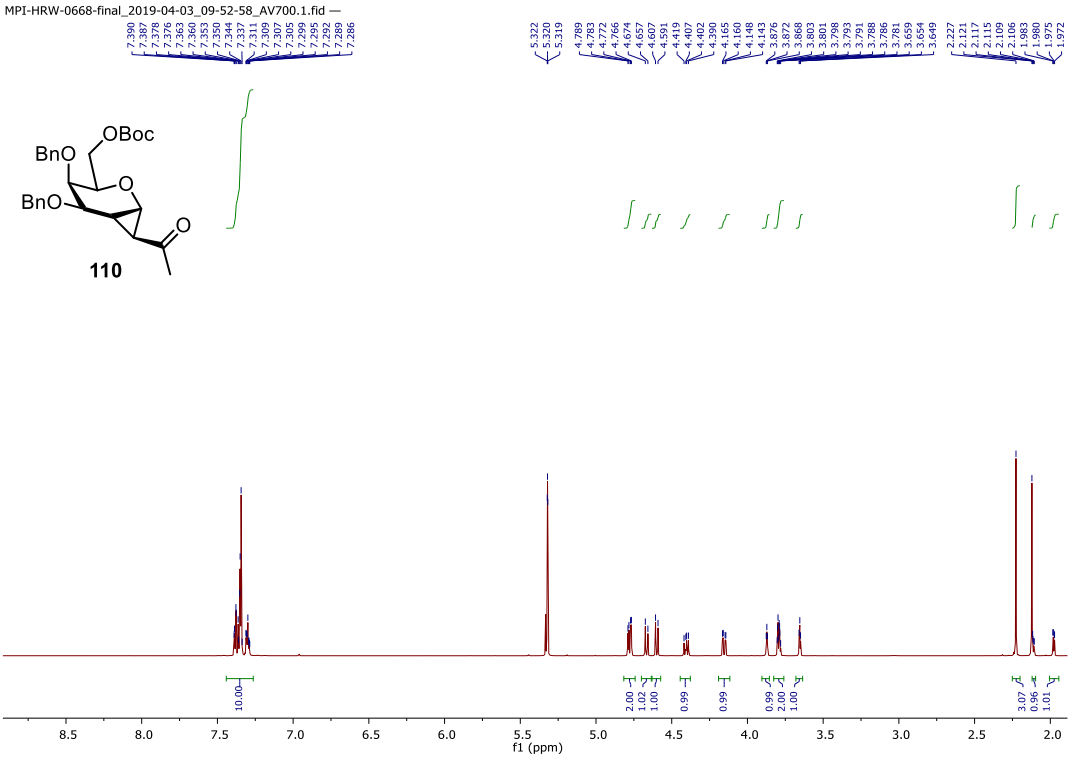

^{1}H NMR spectrum of compound **110** (700 MHz, in CD_2Cl_2)

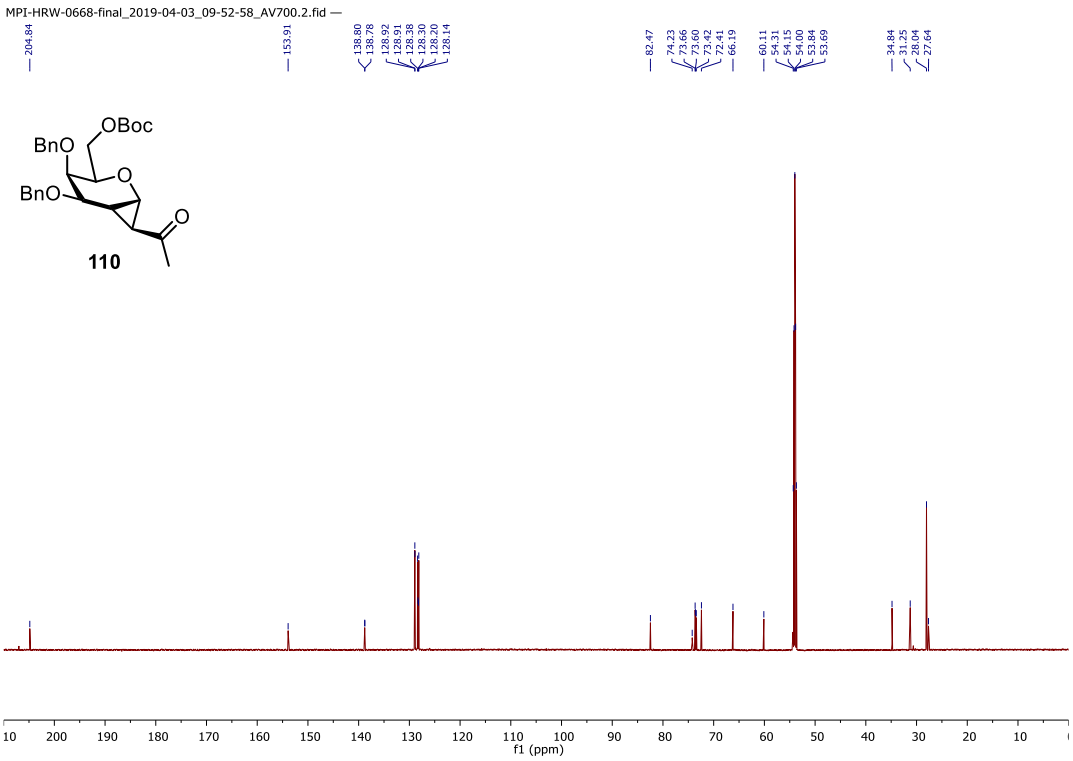

^{13}C NMR spectrum of compound **110** (176 MHz, in CD_2Cl_2)

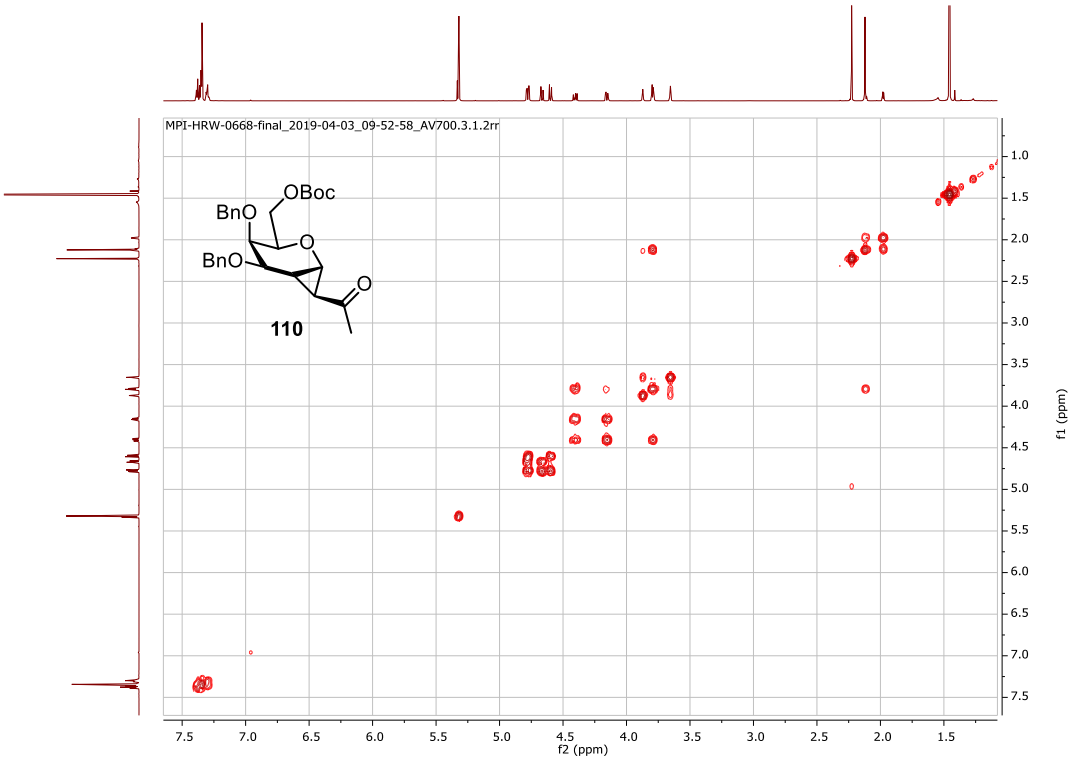

COSY spectrum of compound **110**

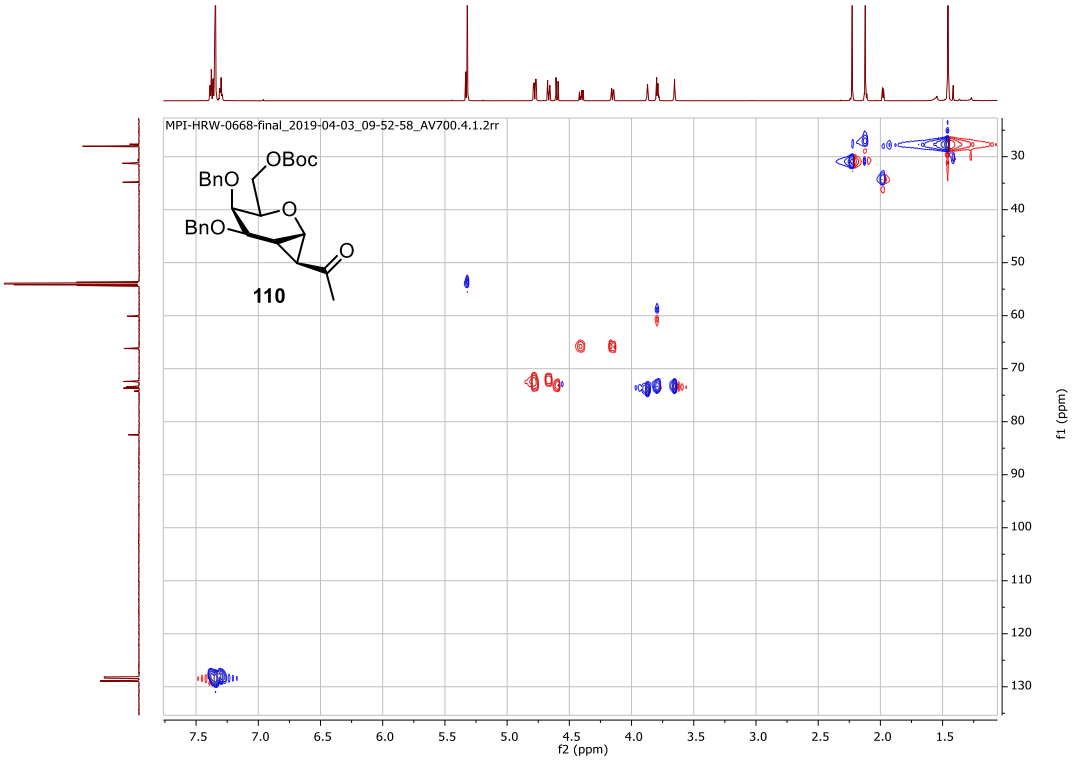

HSQC spectrum of compound **110**

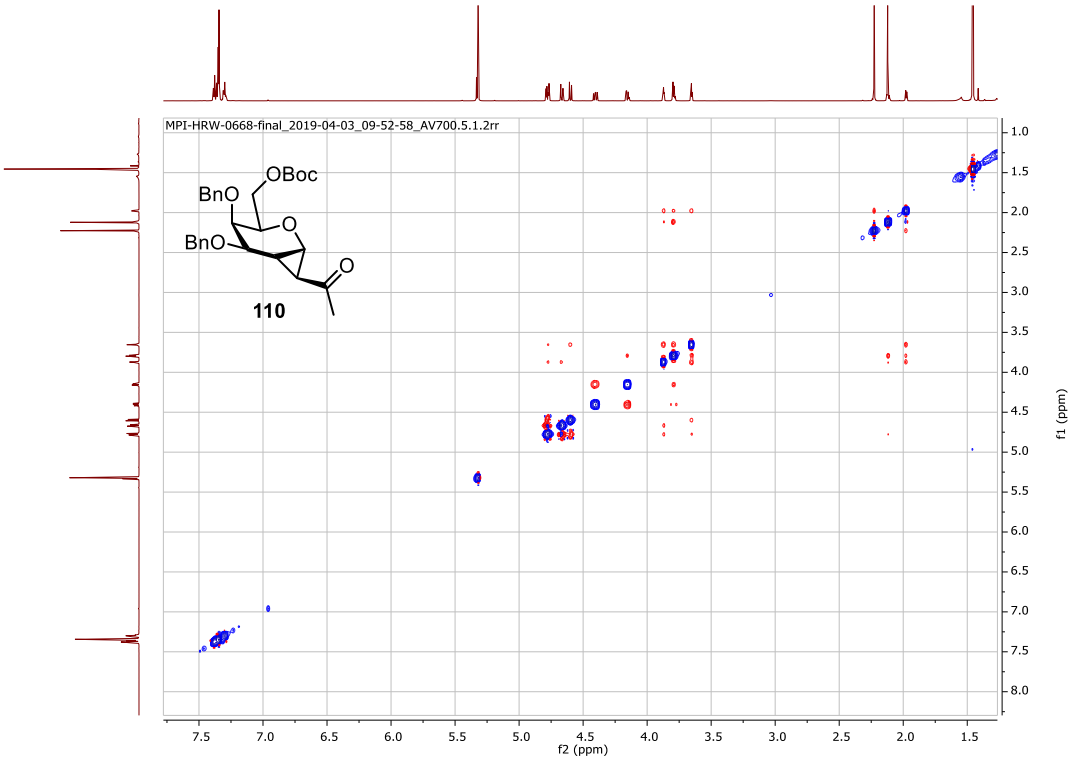

NOESY spectrum of compound **110**

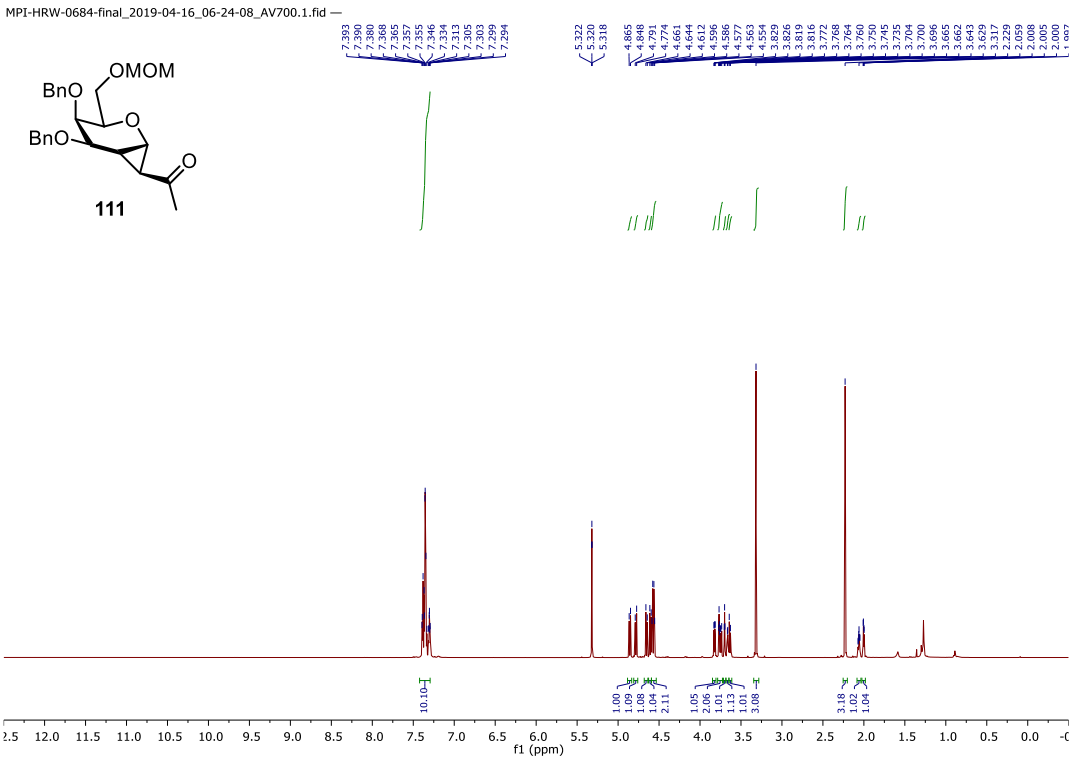

^{1}H NMR spectrum of compound **111** (700 MHz, in CD_2Cl_2)

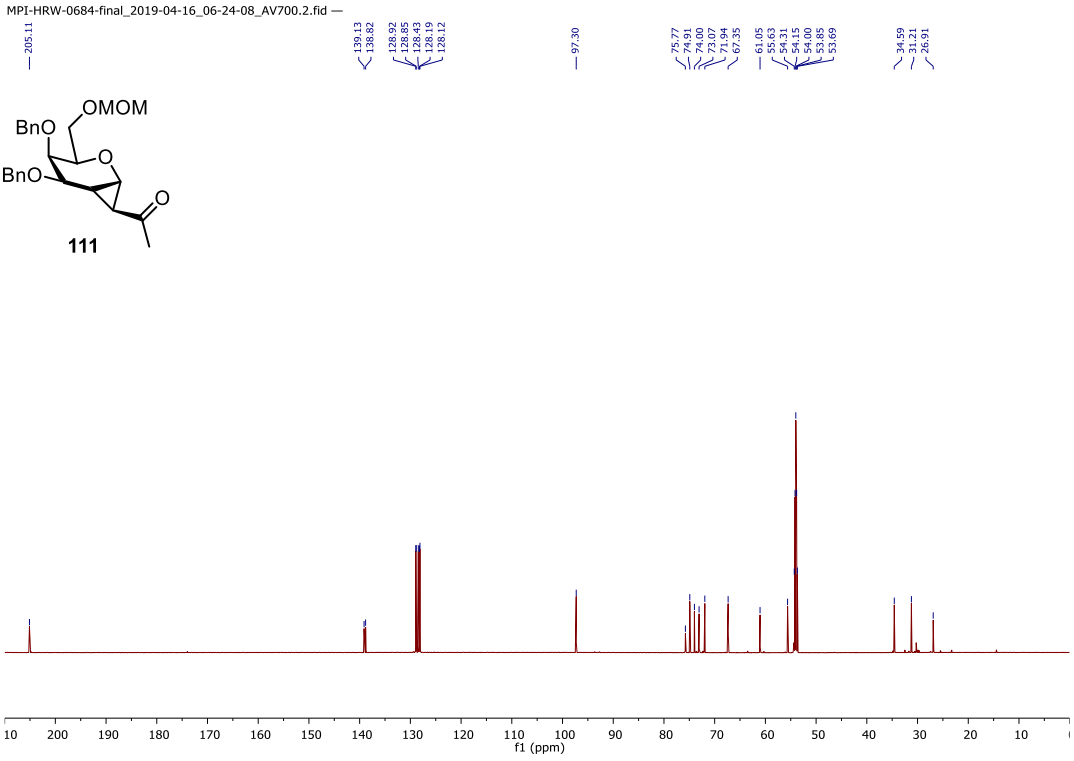

^{13}C NMR spectrum of compound **111** (176 MHz, in CD_2Cl_2)

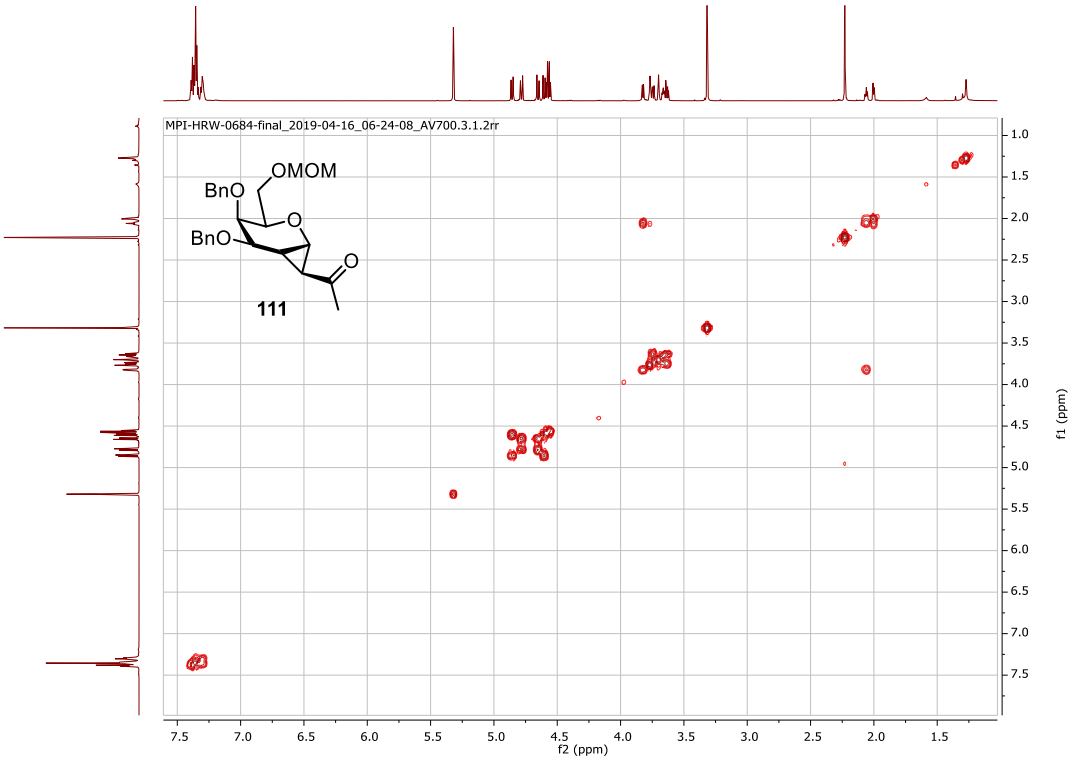

COSY spectrum of compound **111**

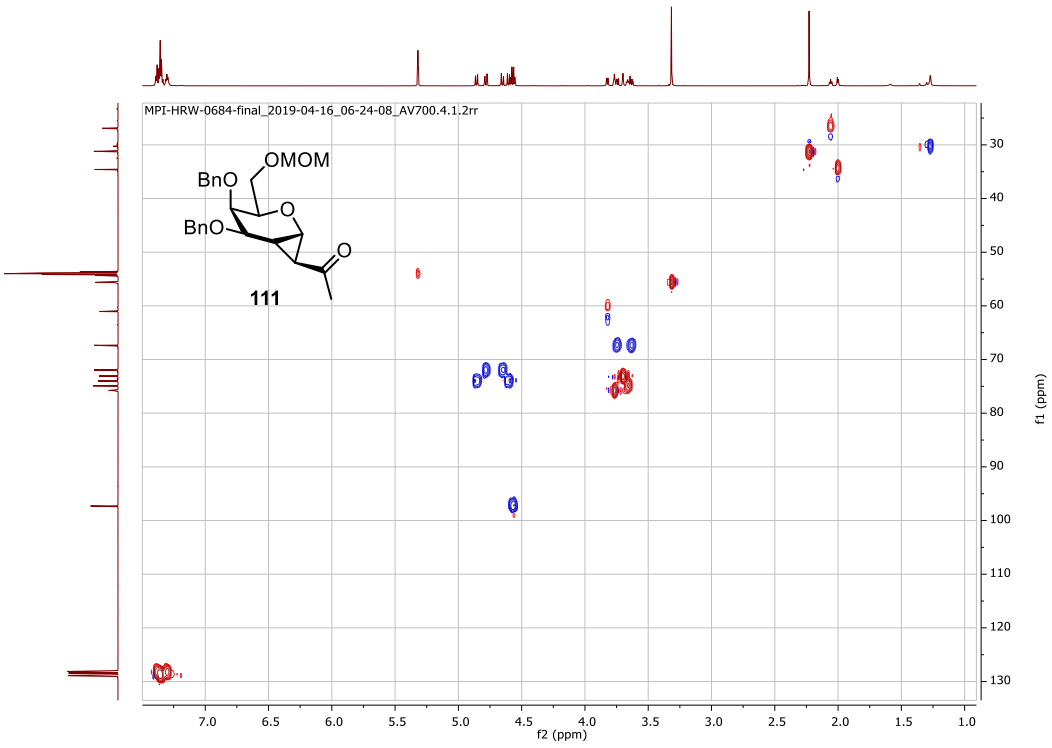

HSQC spectrum of compound **111**

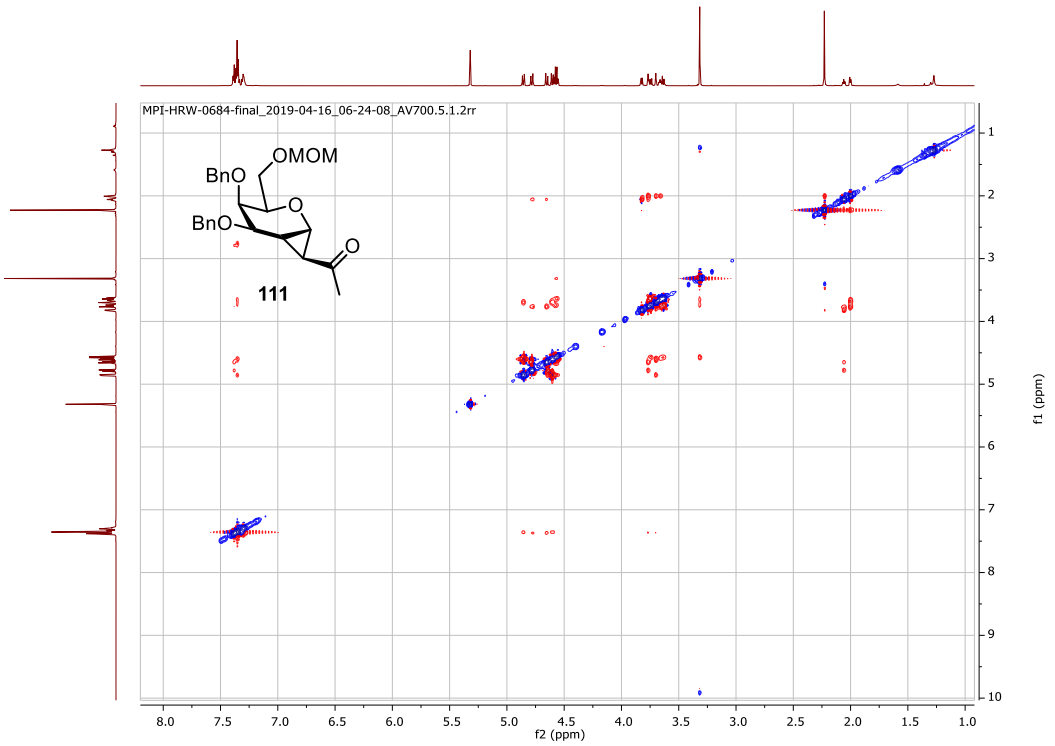

NOESY spectrum of compound **111**

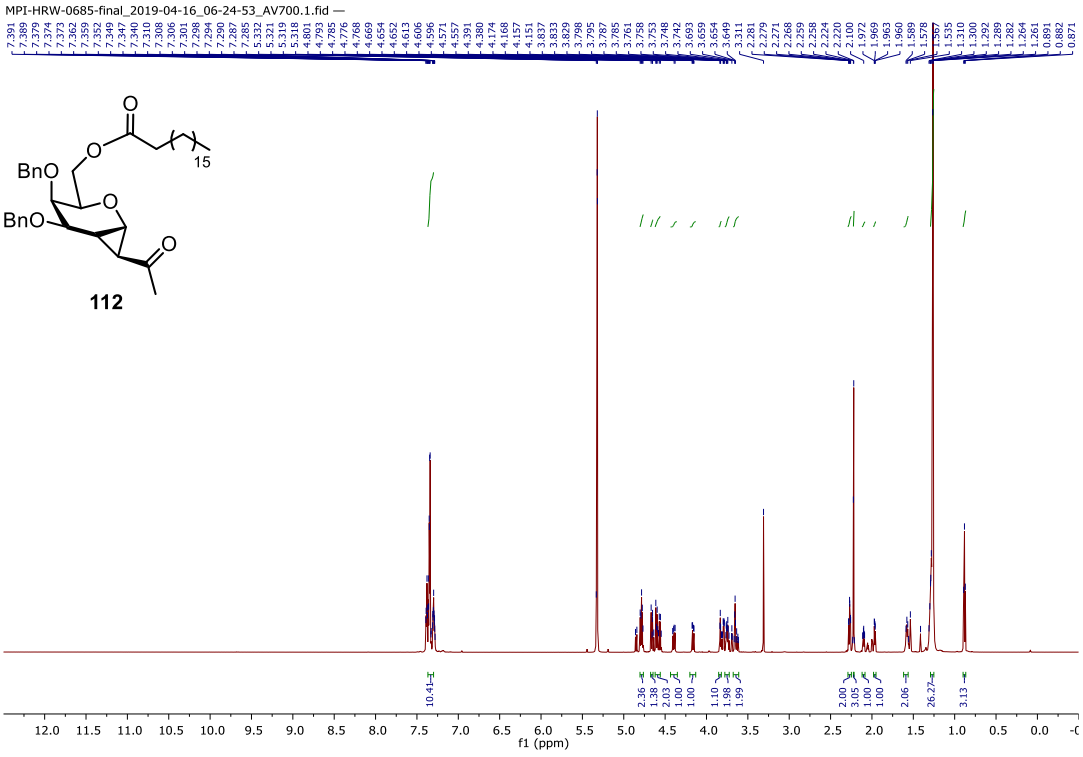

^{1}H NMR spectrum of compound **112** (700 MHz, in CD_2Cl_2)

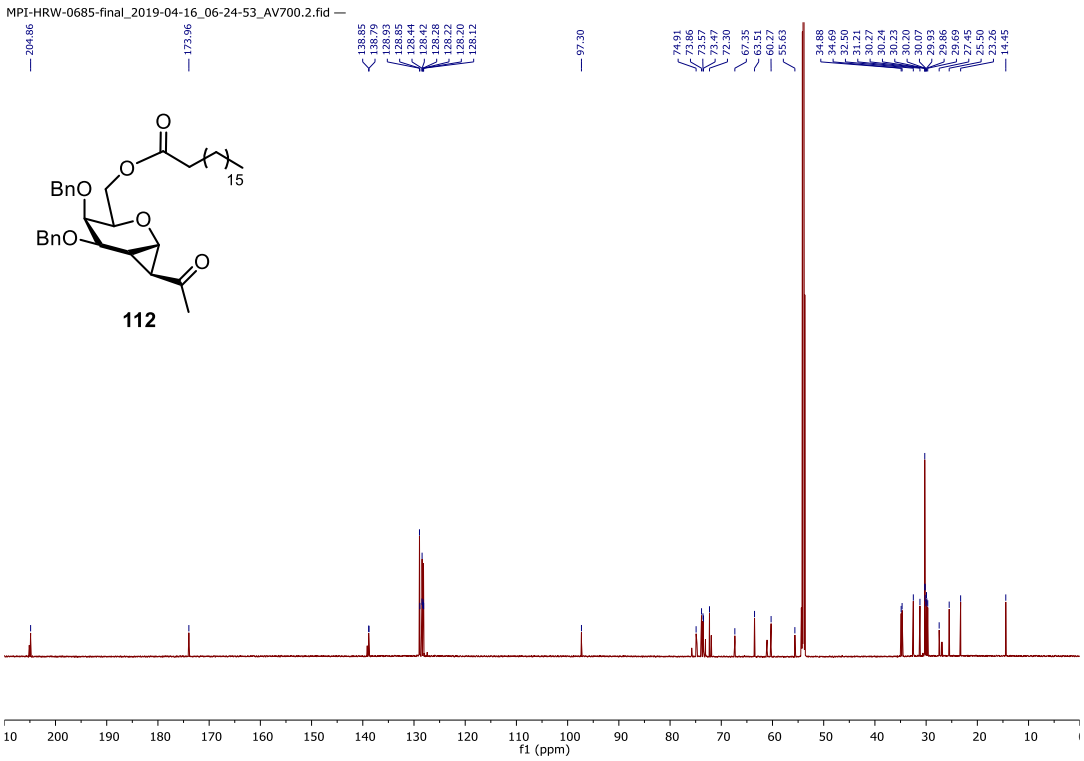

^{13}C NMR spectrum of compound **112** (176 MHz, in CD_2Cl_2)

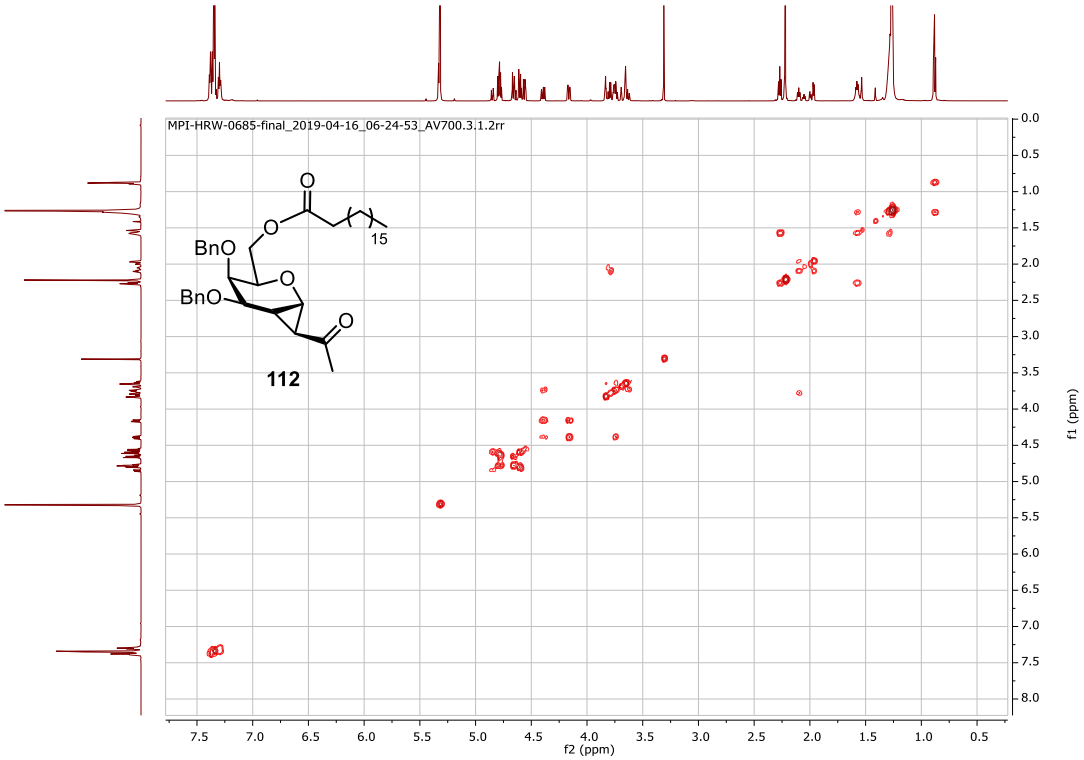

COSY spectrum of compound **112**

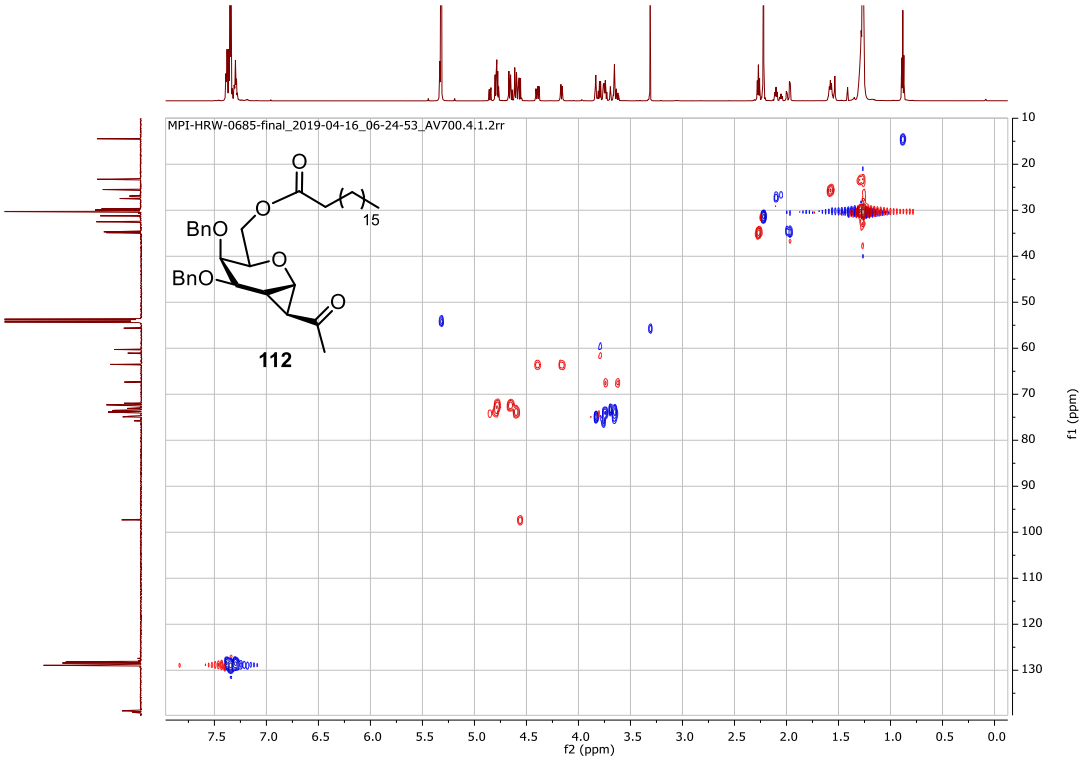

HSQC spectrum of compound **112**

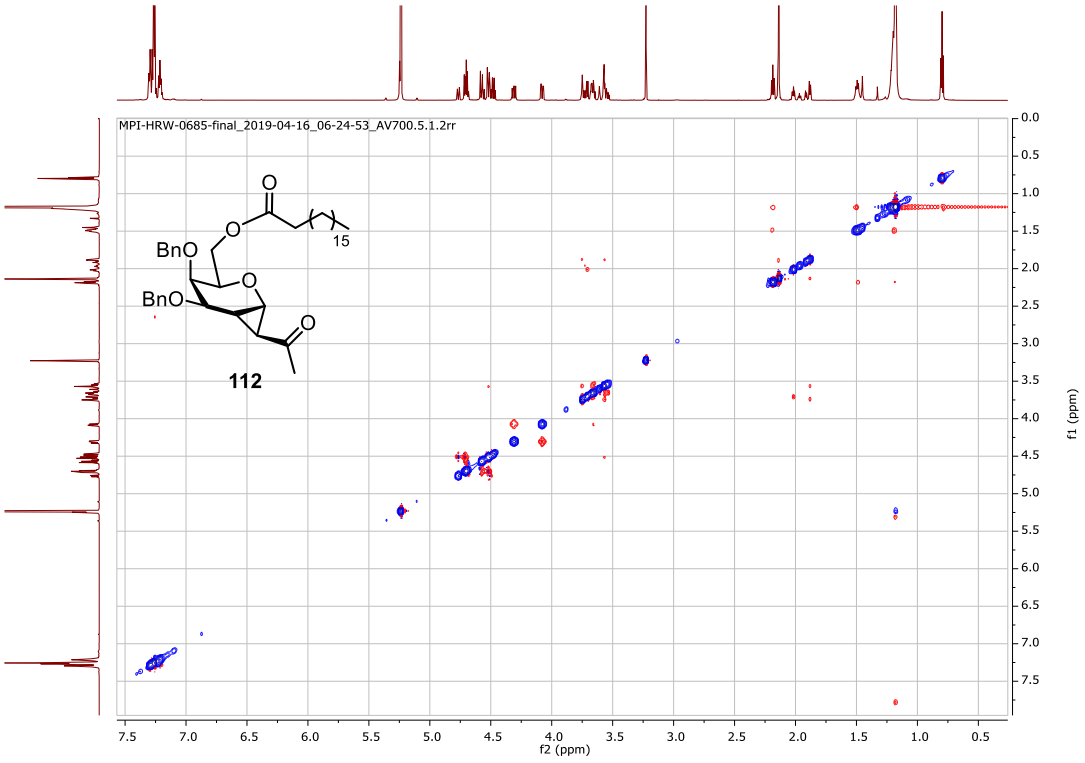

NOESY spectrum of compound **112**

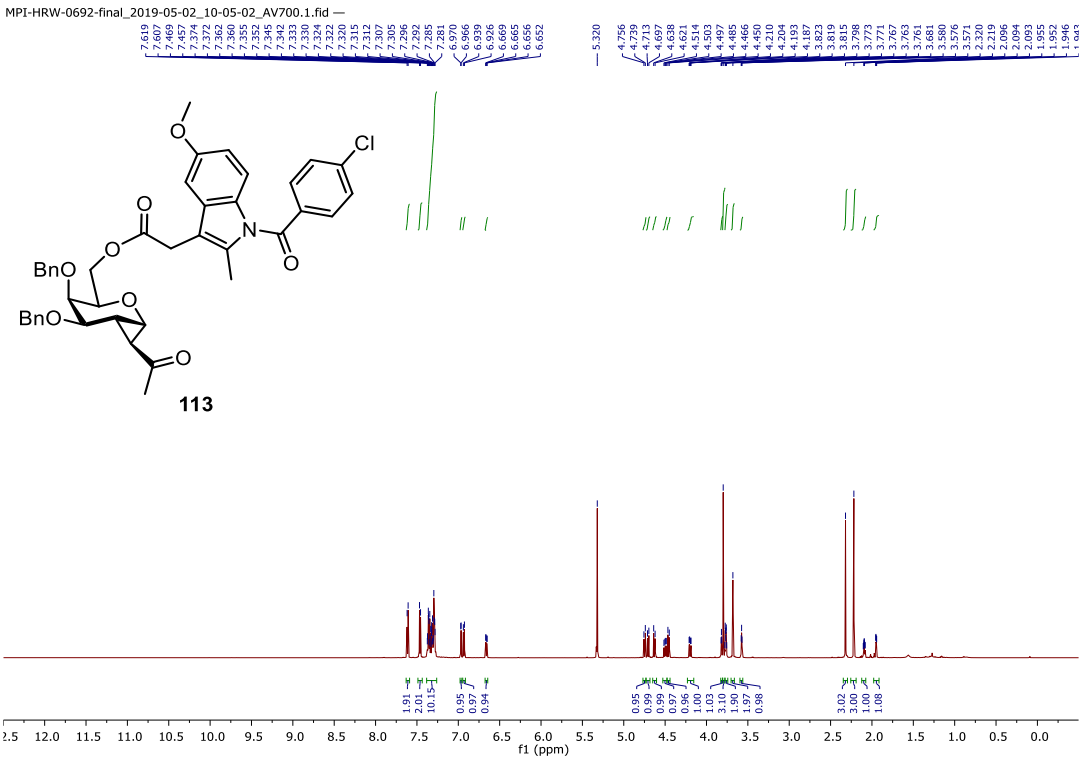

^{1}H NMR spectrum of compound **113** (700 MHz, in CD_2Cl_2)

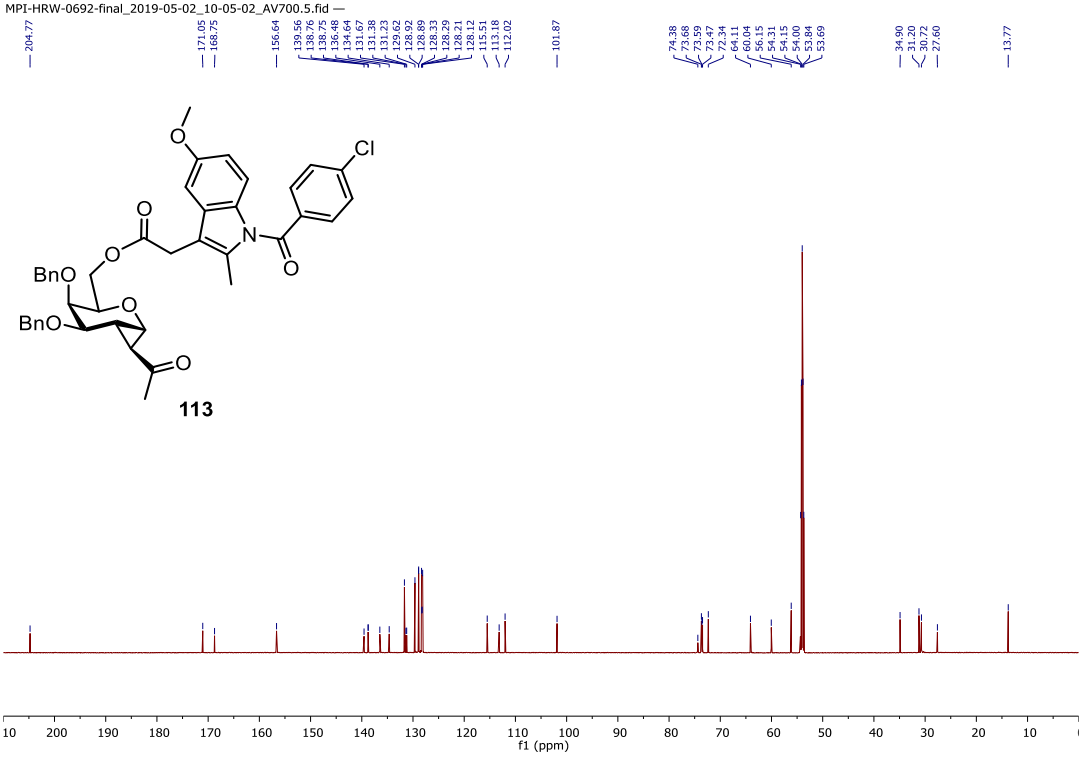

^{13}C NMR spectrum of compound **113** (176 MHz, in CD_2Cl_2)

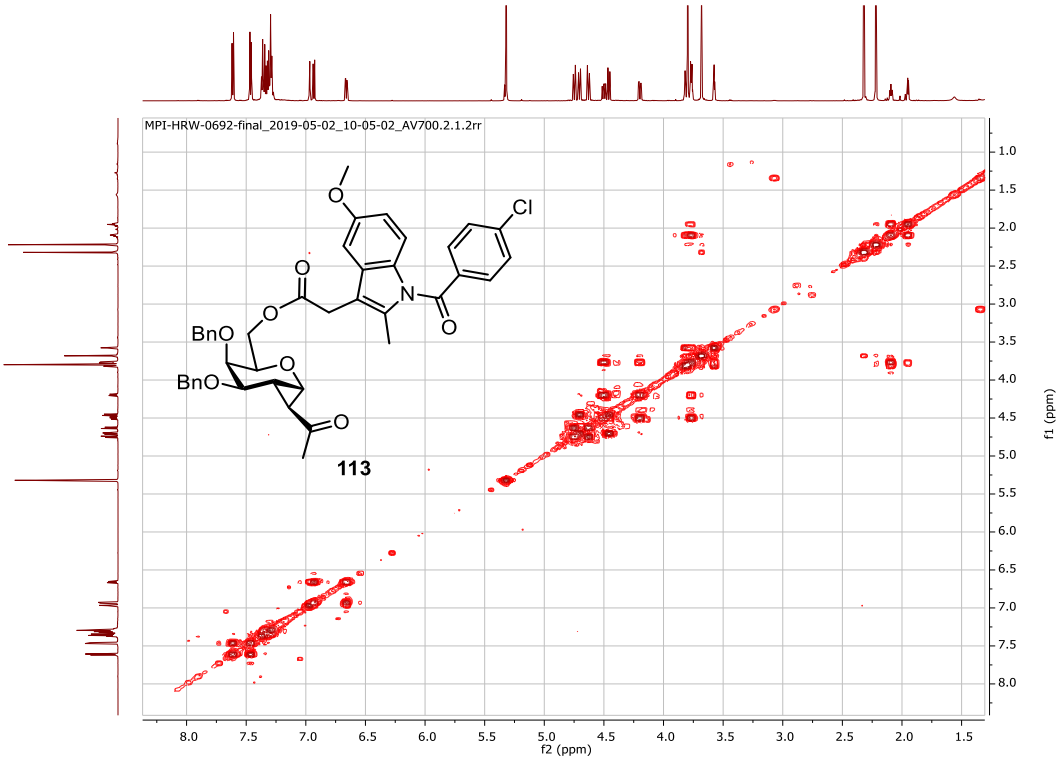

COSY spectrum of compound **113**

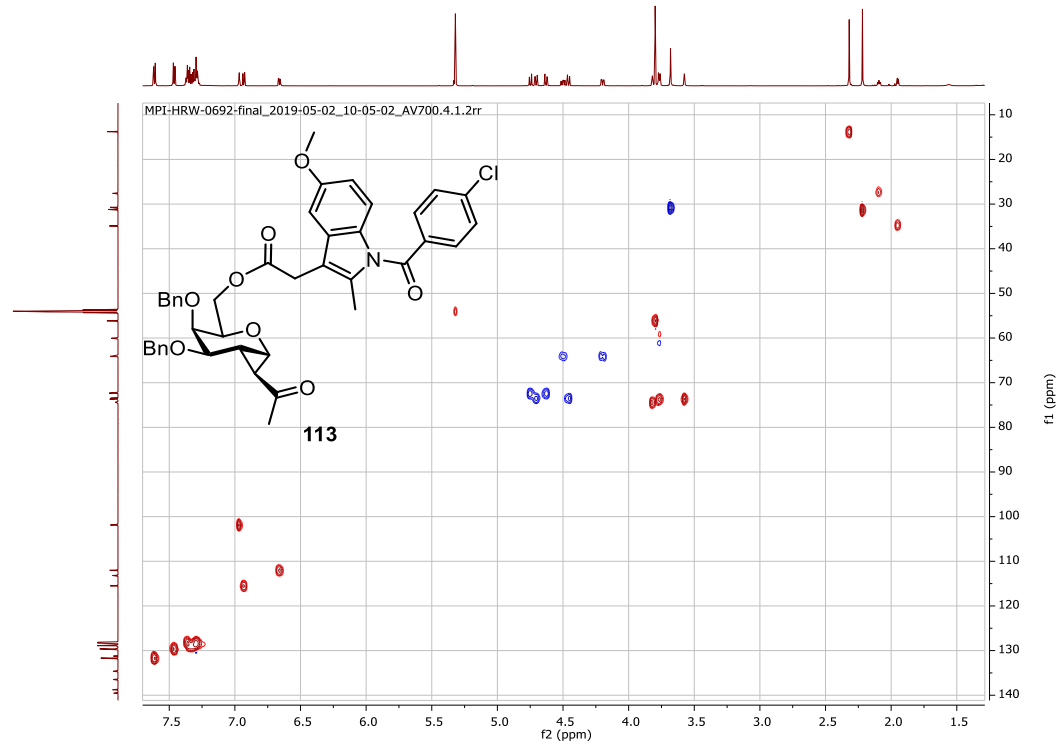

HSQC spectrum of compound **113**

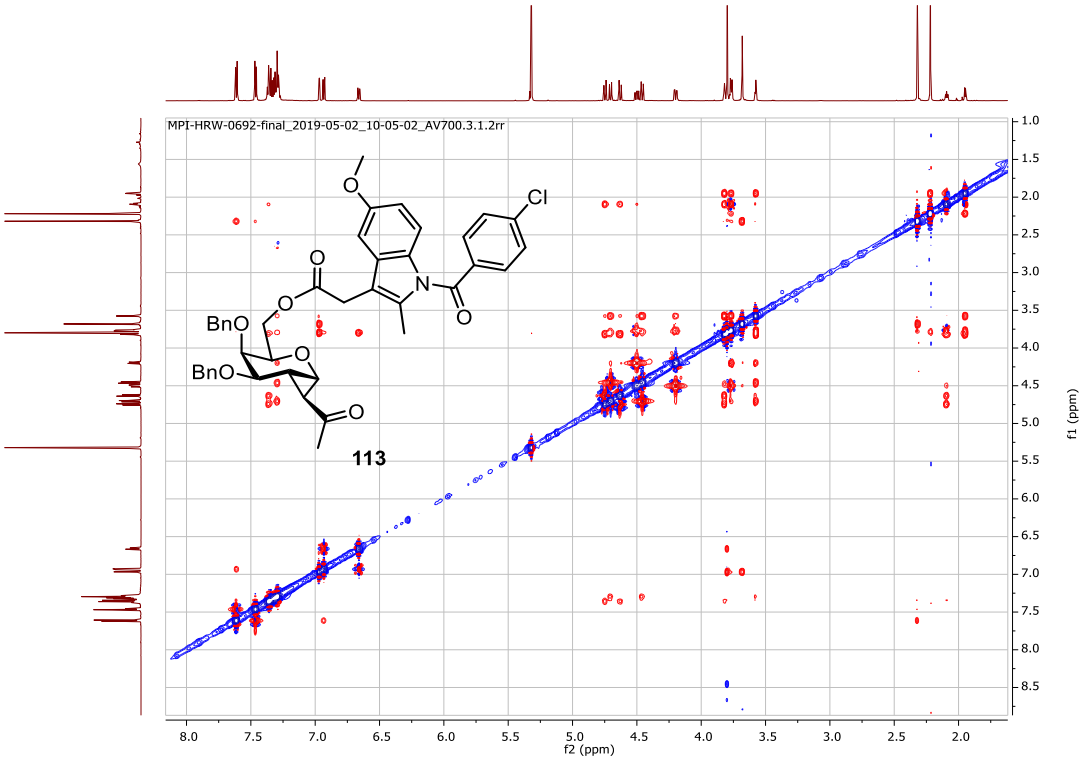

NOESY spectrum of compound **113**

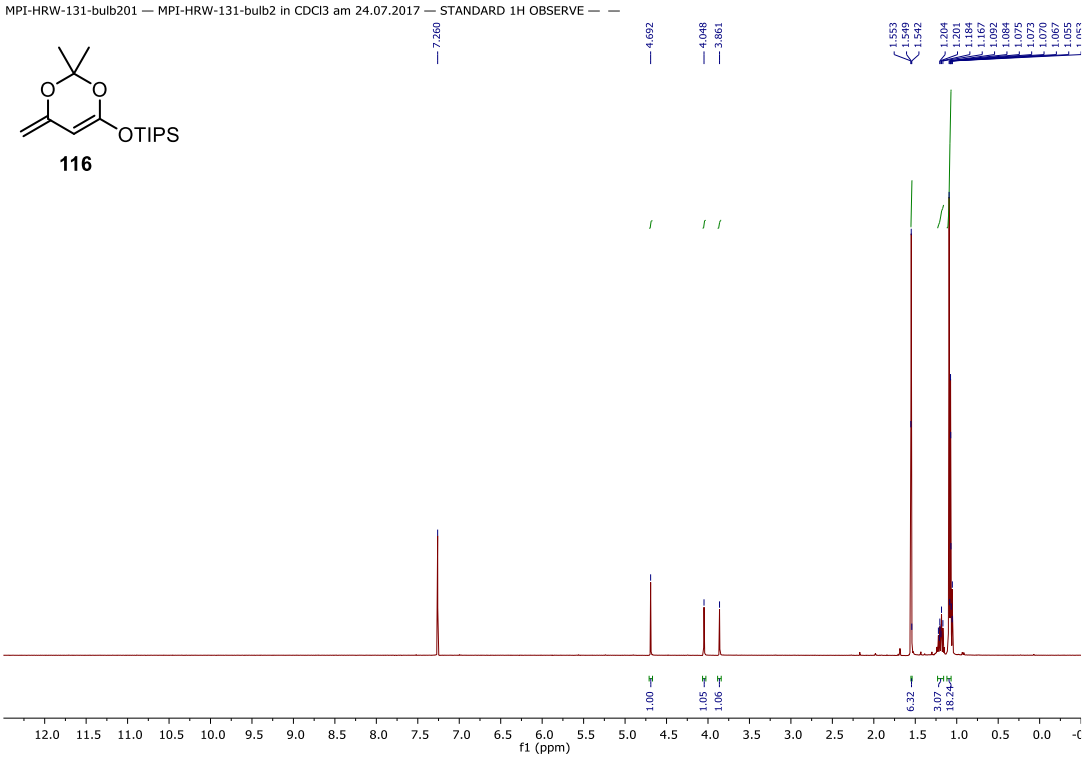

^{1}H NMR spectrum of compound **116** (400 MHz, in $CDCl_3$)

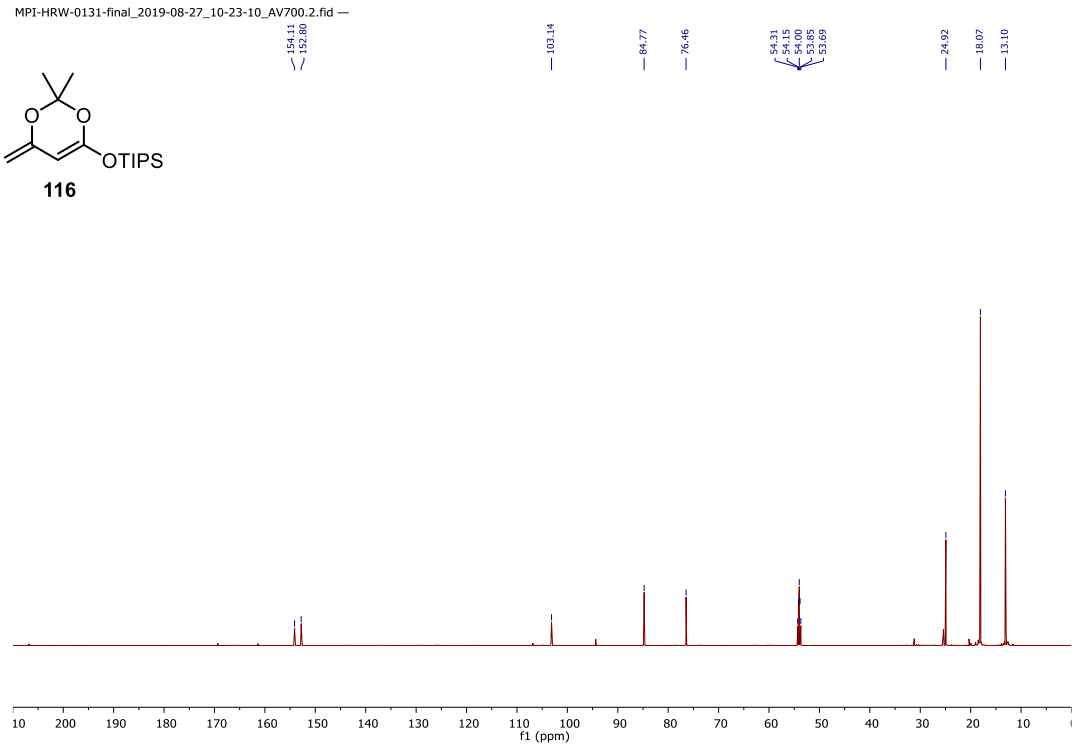

^{13}C NMR spectrum of compound **116** (176 MHz, in CD_2Cl_2)

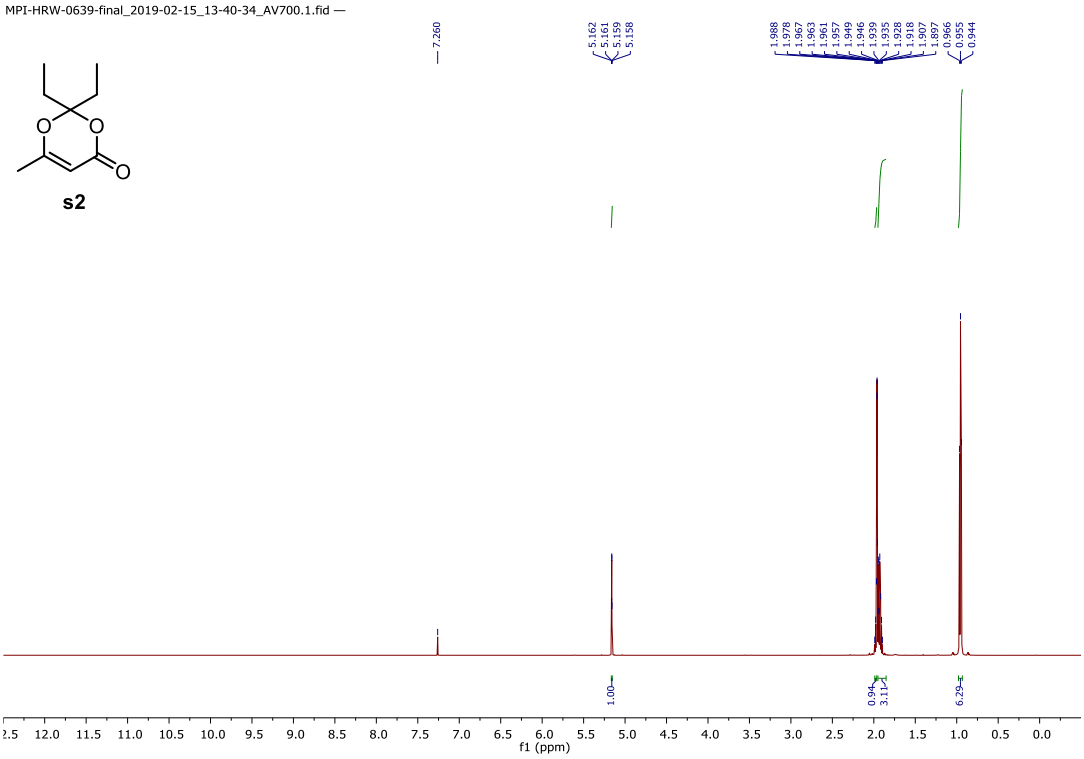

^{1}H NMR spectrum of compound **s2** (700 MHz, in $CDCl_3$)

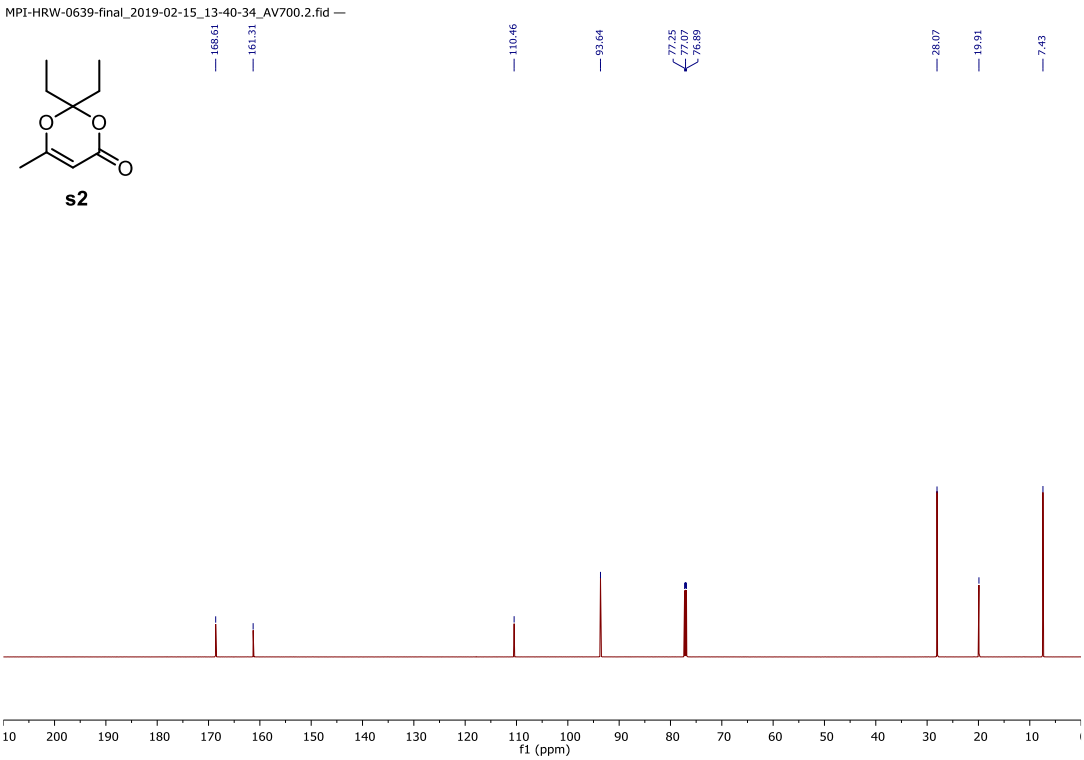

^{13}C NMR spectrum of compound **s2** (176 MHz, in $CDCl_3$)

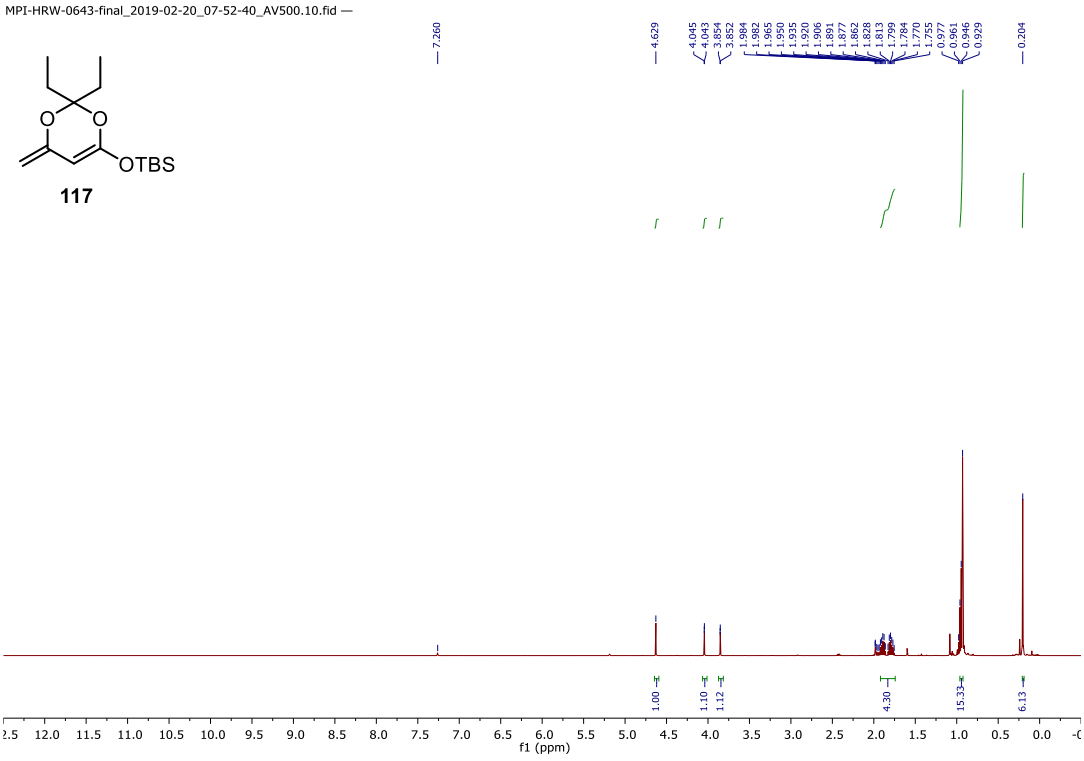

^{1}H NMR spectrum of compound **117** (500 MHz, in $CDCl_3$)

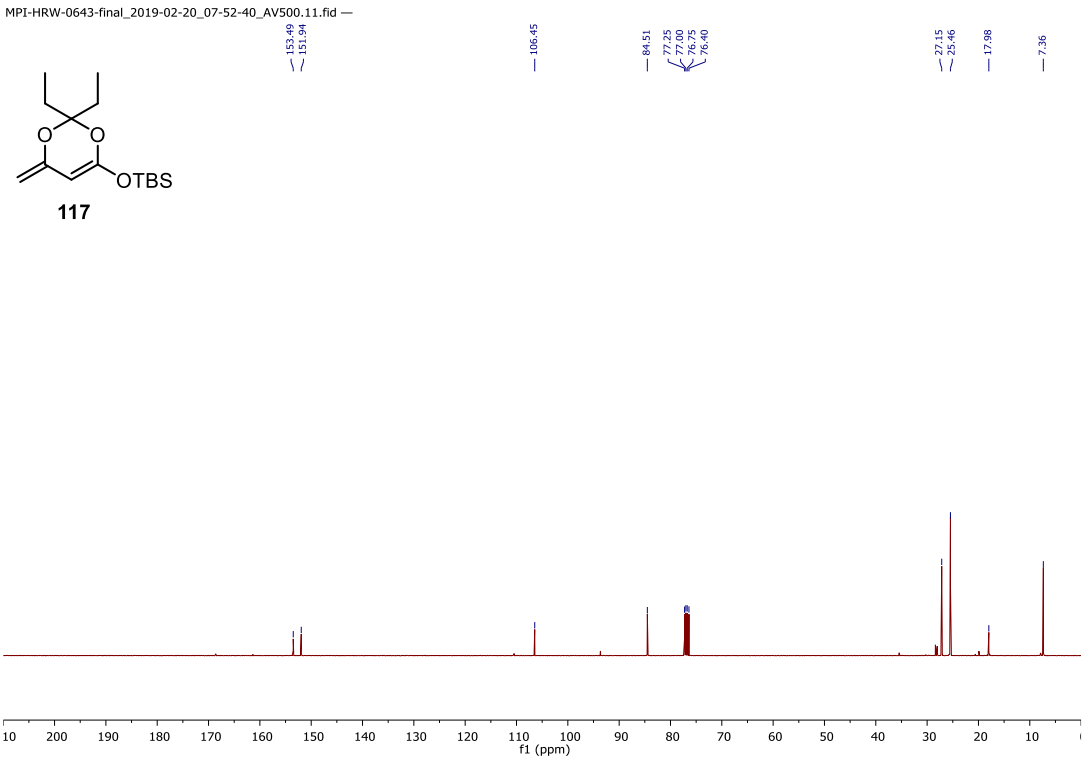

^{13}C NMR spectrum of compound **117** (126 MHz, in $CDCl_3$)

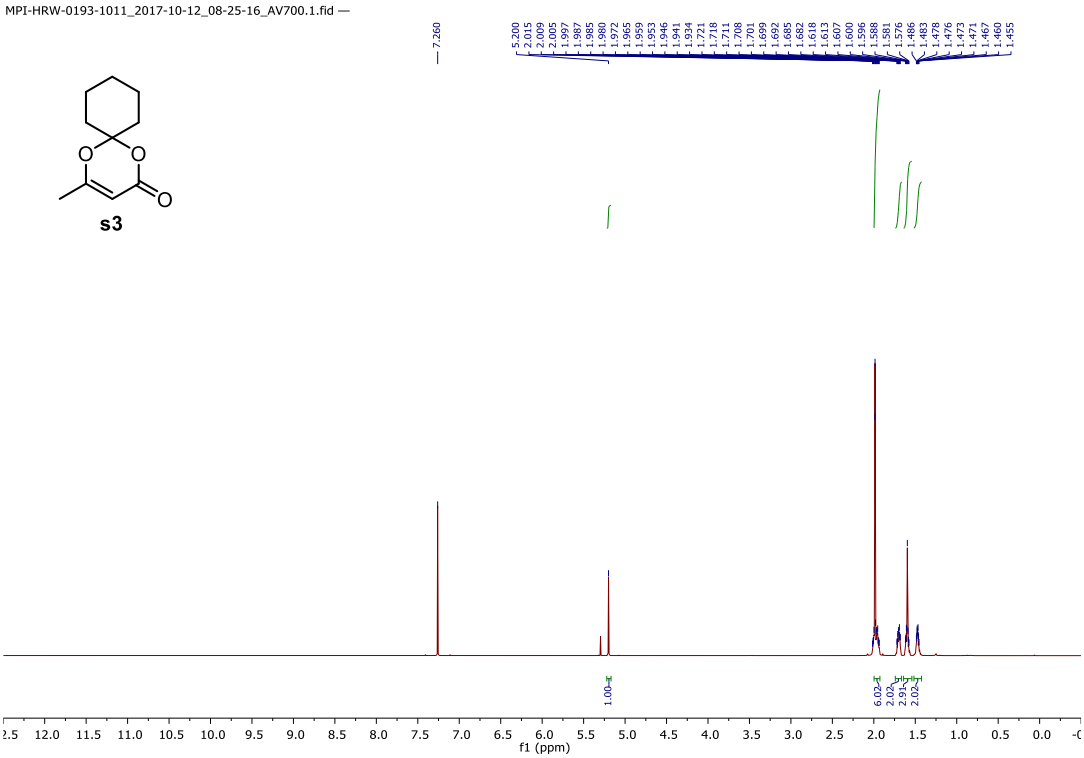

^{1}H NMR spectrum of compound **s3** (400 MHz, in $CDCl_3$)

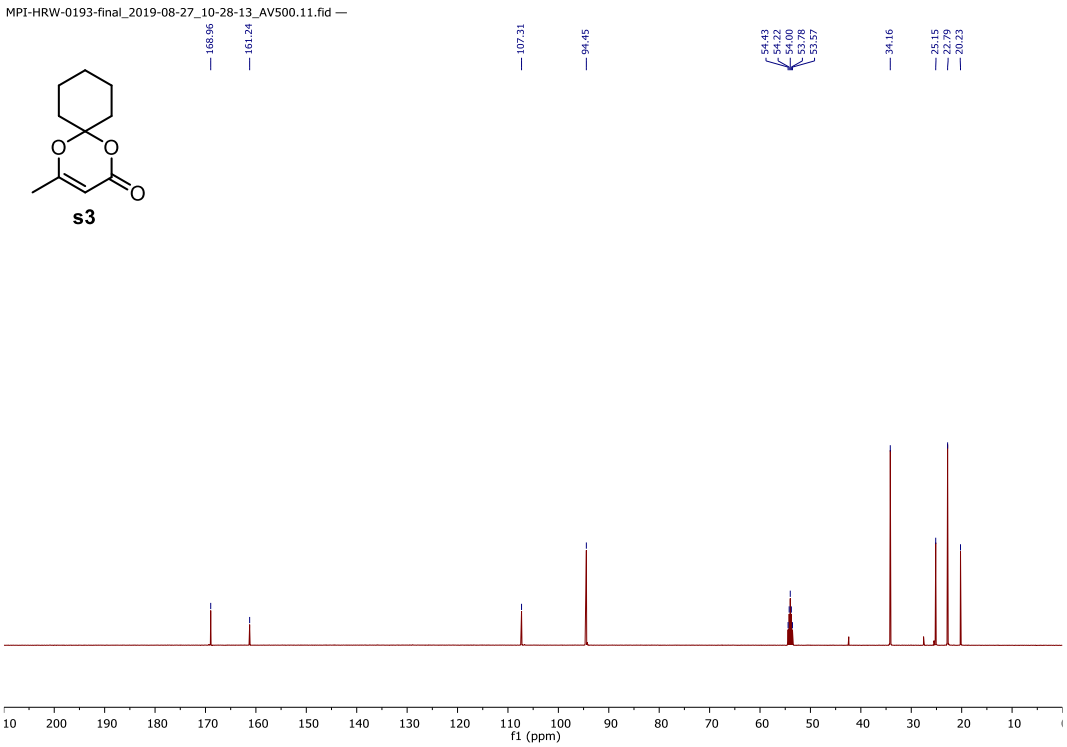

^{13}C NMR spectrum of compound **s3** (126 MHz, in CD_2Cl_2)

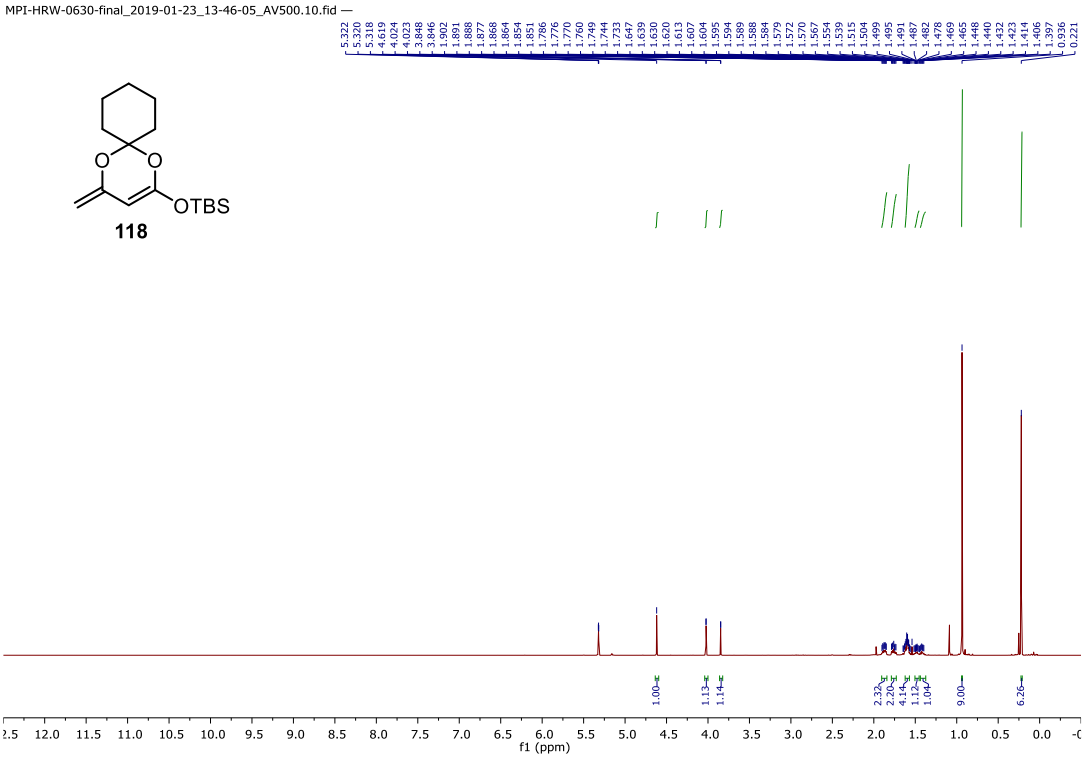

^{1}H NMR spectrum of compound **118** (500 MHz, in CD_2Cl_2)

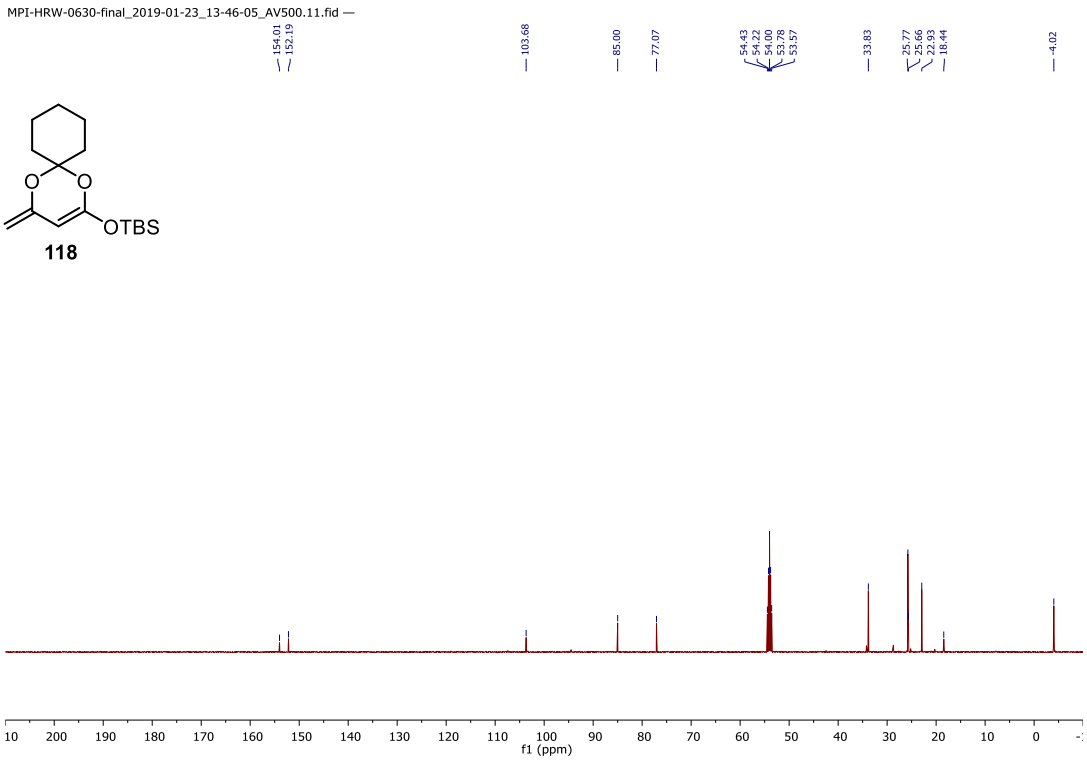

^{13}C NMR spectrum of compound **118** (176 MHz, in CD_2Cl_2)

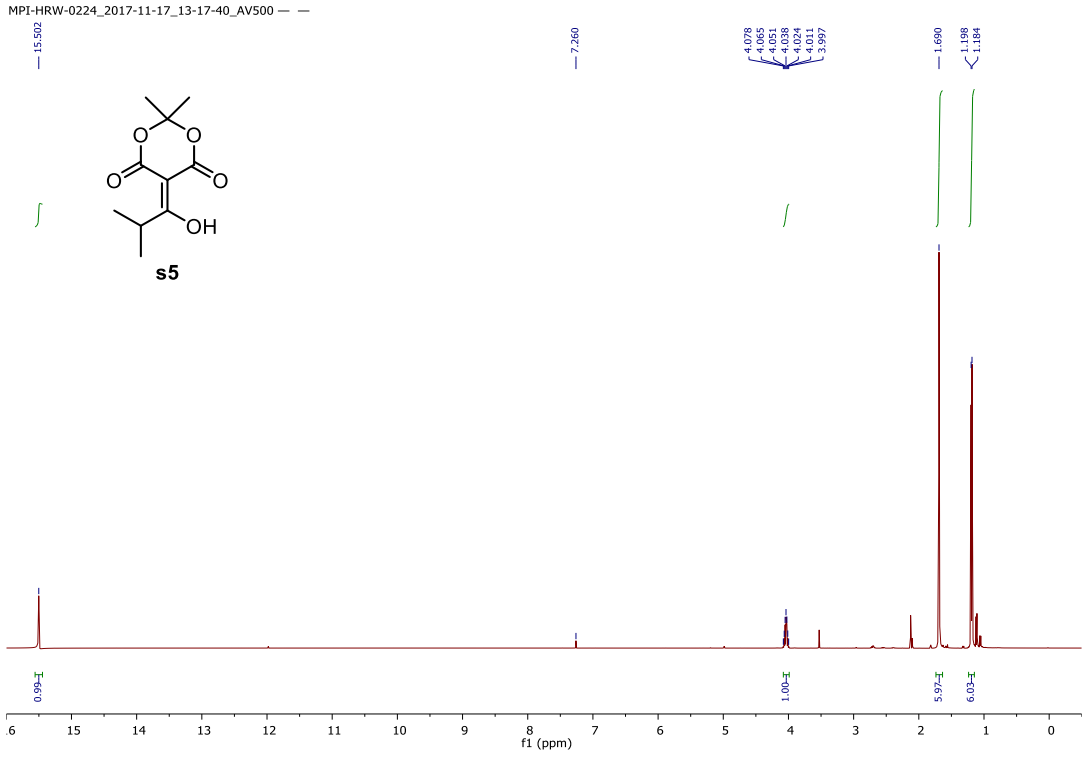

^{1}H NMR spectrum of compound **s5** (500 MHz, in $CDCl_3$)

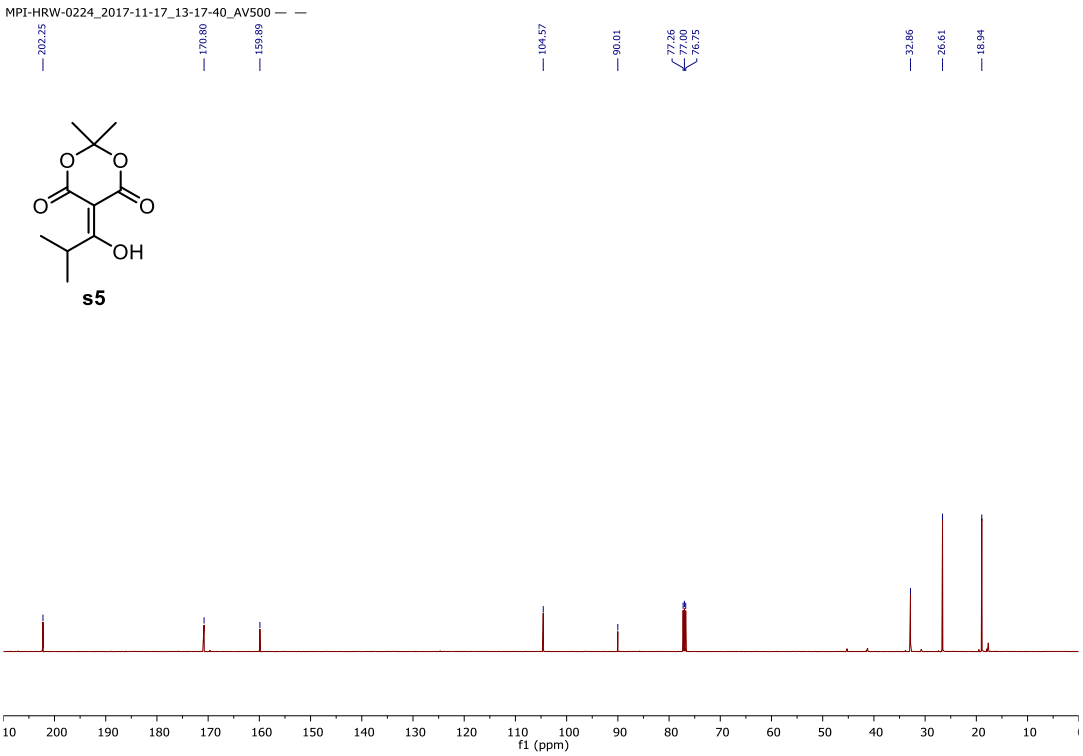

^{13}C NMR spectrum of compound **s5** (126 MHz, in $CDCl_3$)

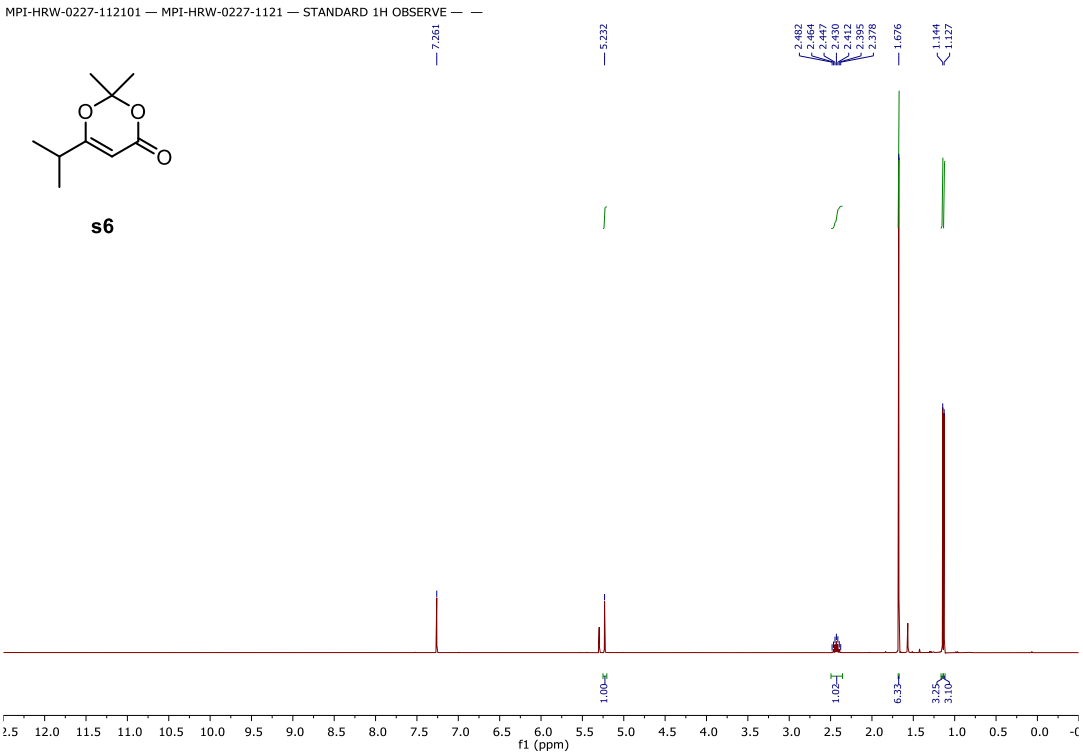

^{1}H NMR spectrum of compound **s6** (400 MHz, in $CDCl_3$)

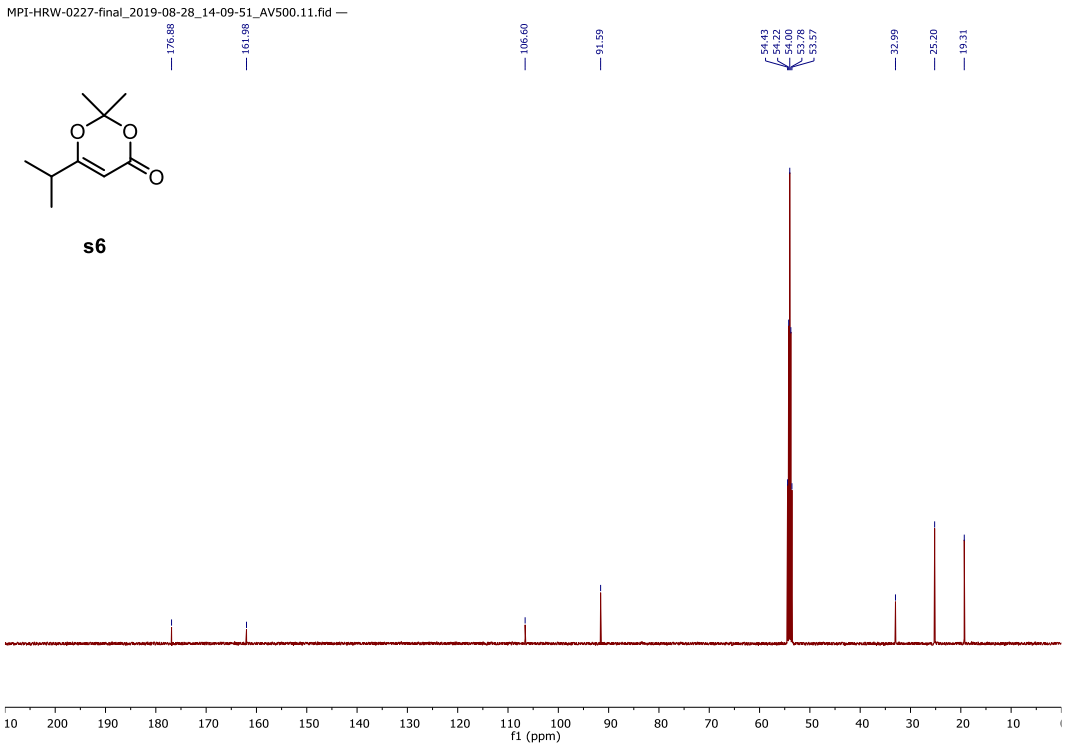

^{13}C NMR spectrum of compound **s6** (126 MHz, in CD_2Cl_2)

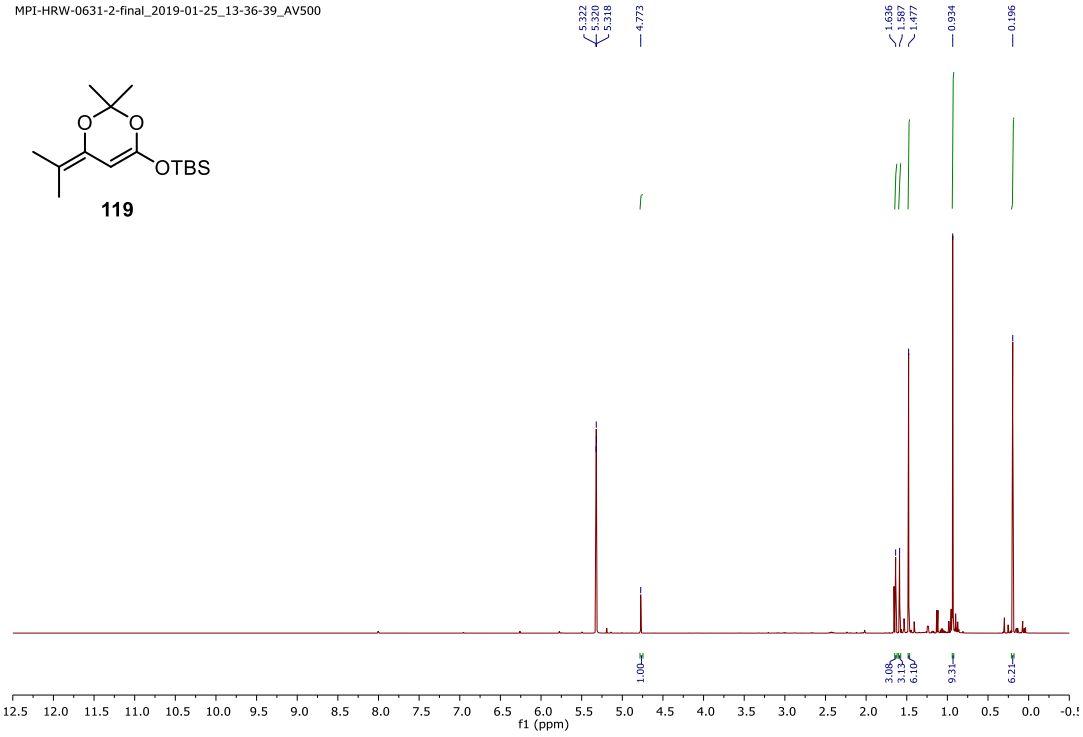

^{1}H NMR spectrum of compound **119** (500 MHz, in CD_2Cl_2)

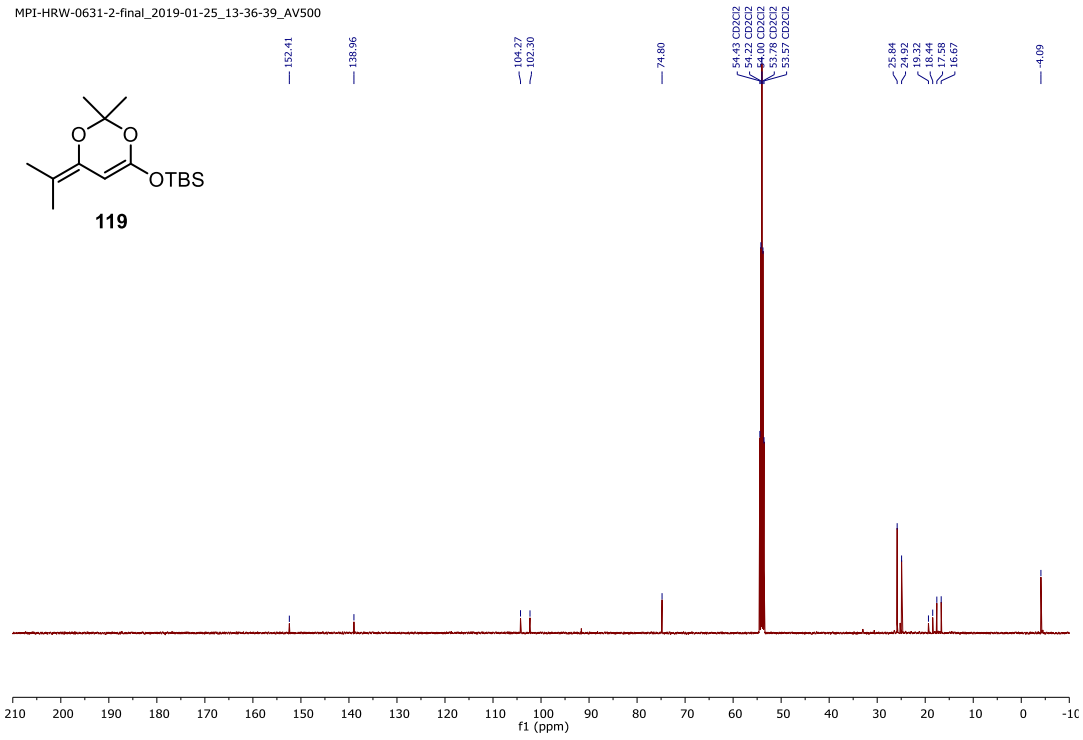

^{13}C NMR spectrum of compound **119** (126 MHz, in CD_2Cl_2)

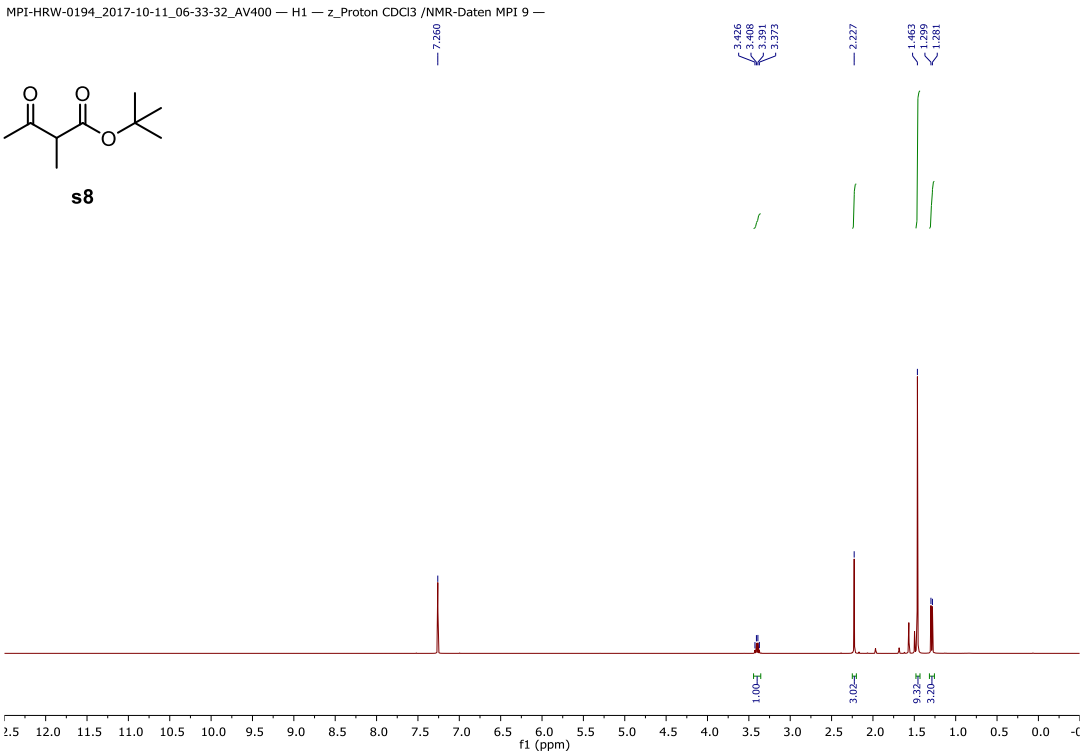

^{1}H NMR spectrum of compound **s8** (400 MHz, in $CDCl_3$)

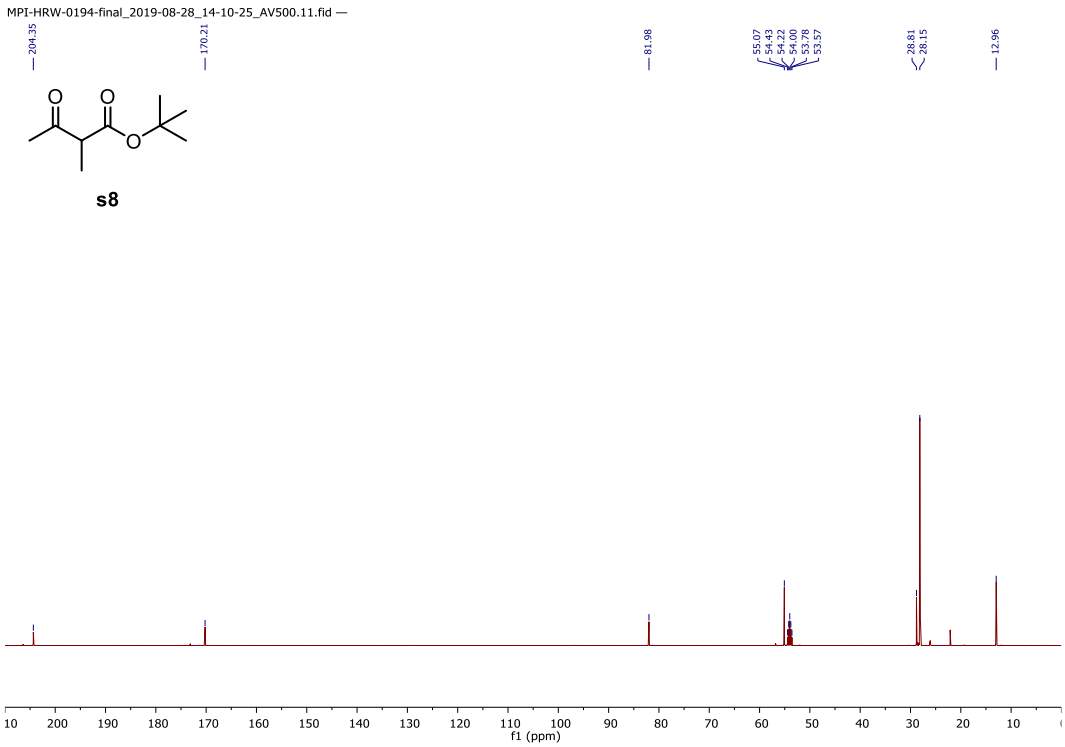

^{13}C NMR spectrum of compound **s8** (126 MHz, in CD_2Cl_2)

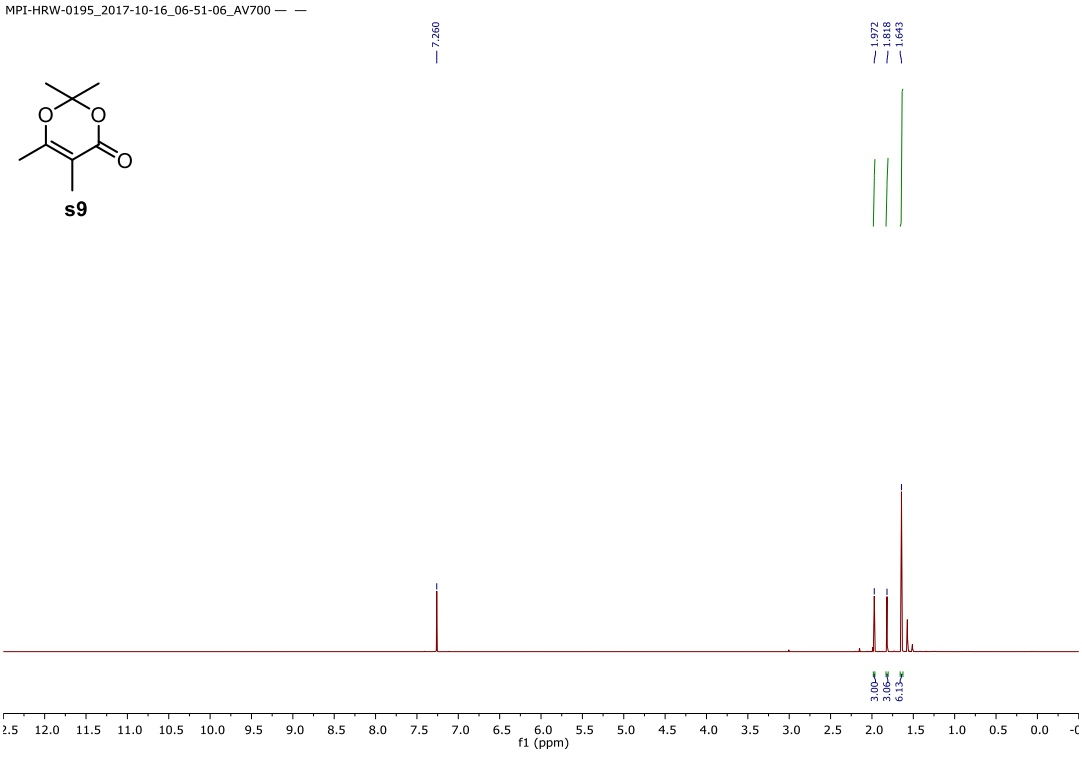

^{1}H NMR spectrum of compound **s9** (700 MHz, in $CDCl_3$)

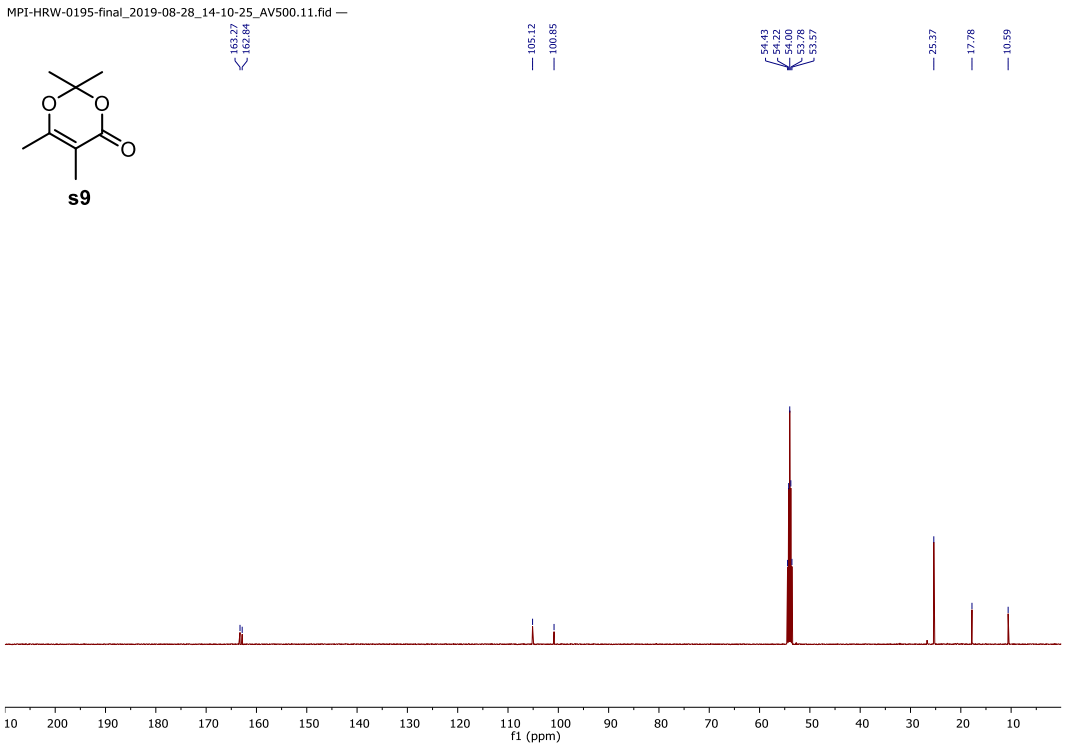

^{13}C NMR spectrum of compound **s9** (126 MHz, in CD_2Cl_2)

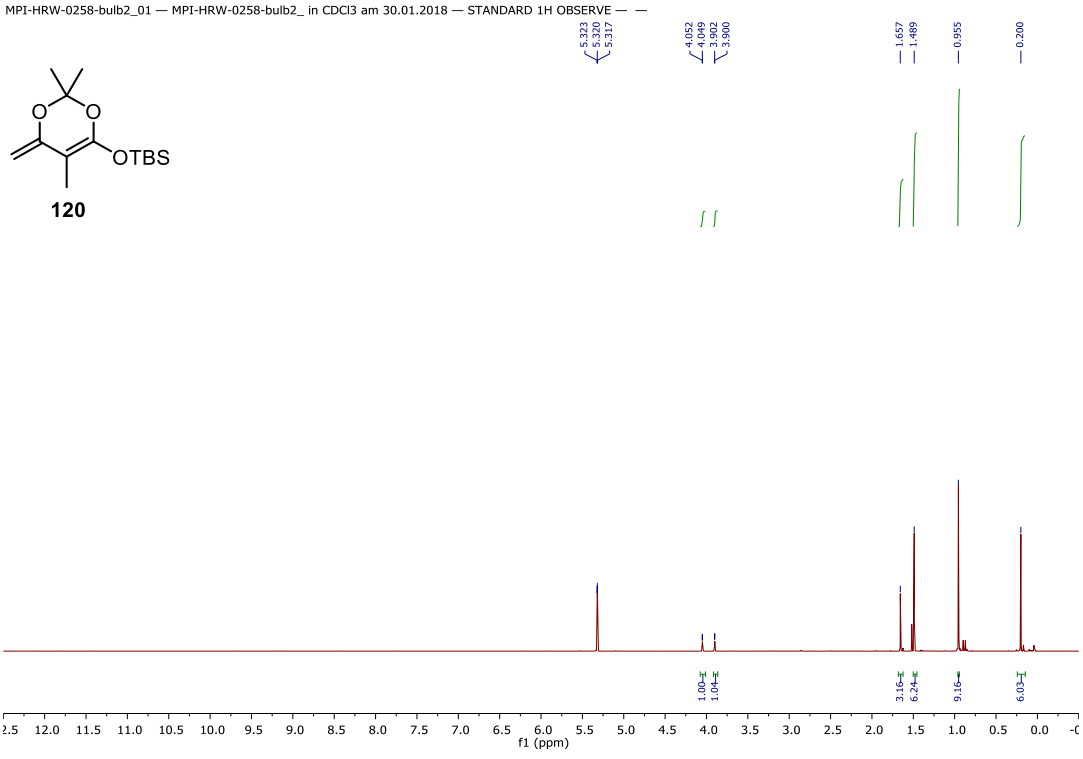

^{1}H NMR spectrum of compound **120** (400 MHz, in $CDCl_3$)

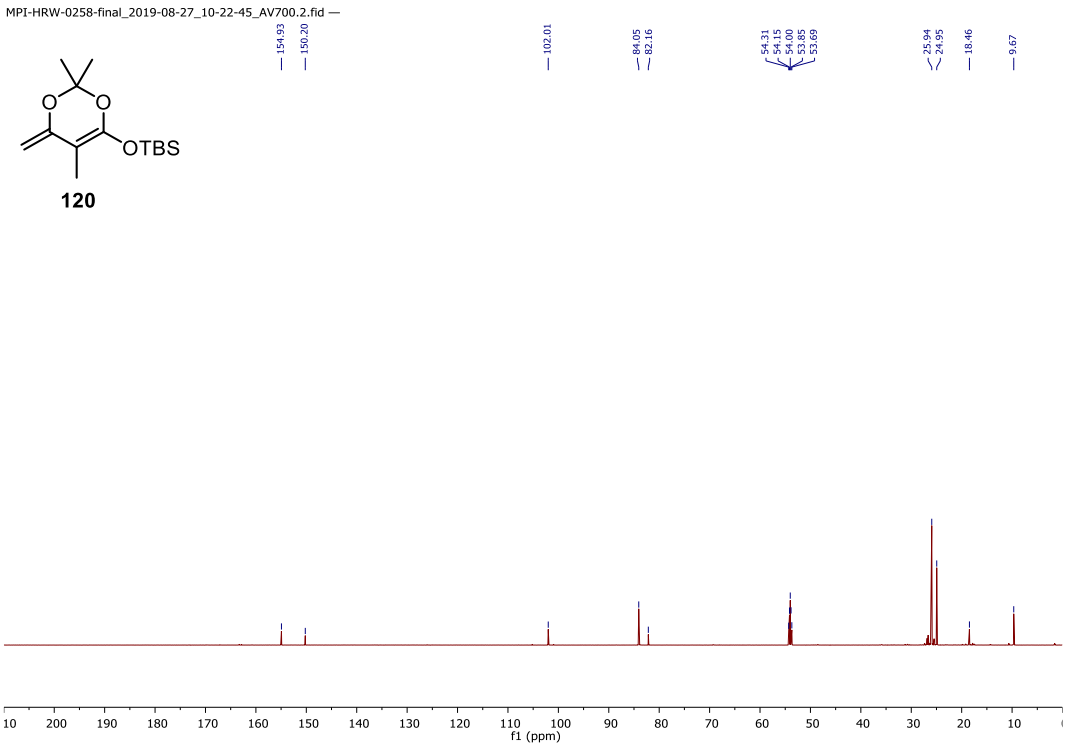

^{13}C NMR spectrum of compound **120** (176 MHz, in CD_2Cl_2)

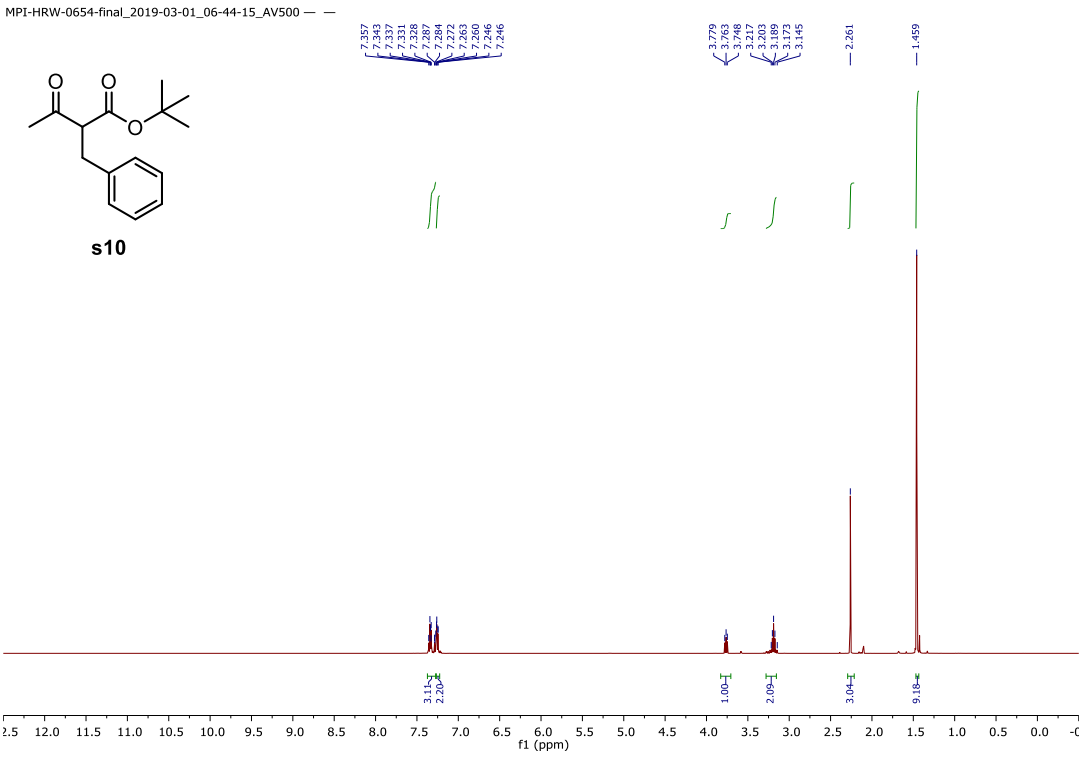

^{1}H NMR spectrum of compound **s10** (500 MHz, in $CDCl_3$)

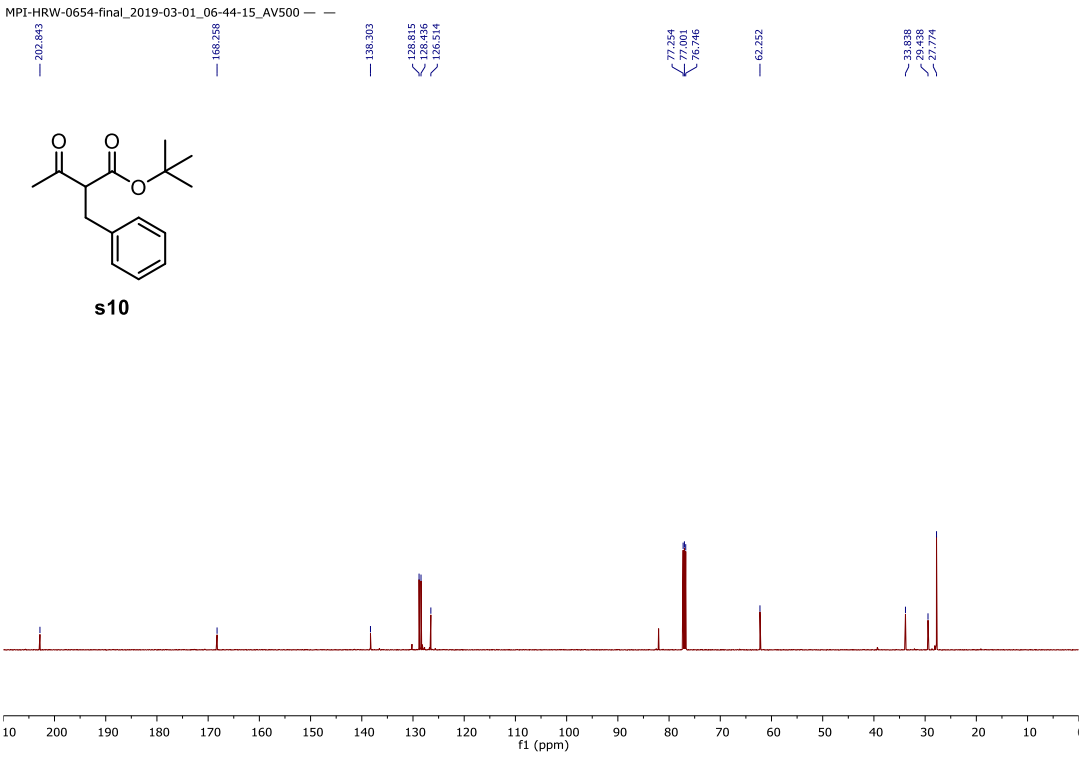

^{13}C NMR spectrum of compound **s10** (126 MHz, in $CDCl_3$)

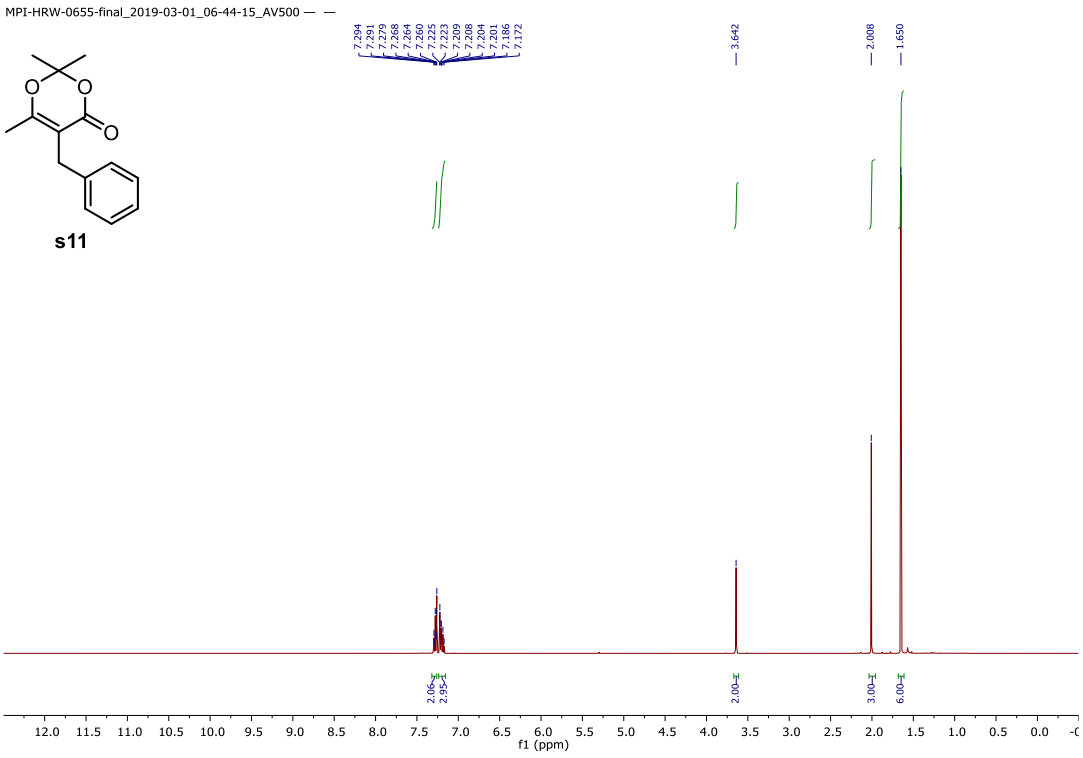

^{1}H NMR spectrum of compound **s11** (500 MHz, in $CDCl_3$)

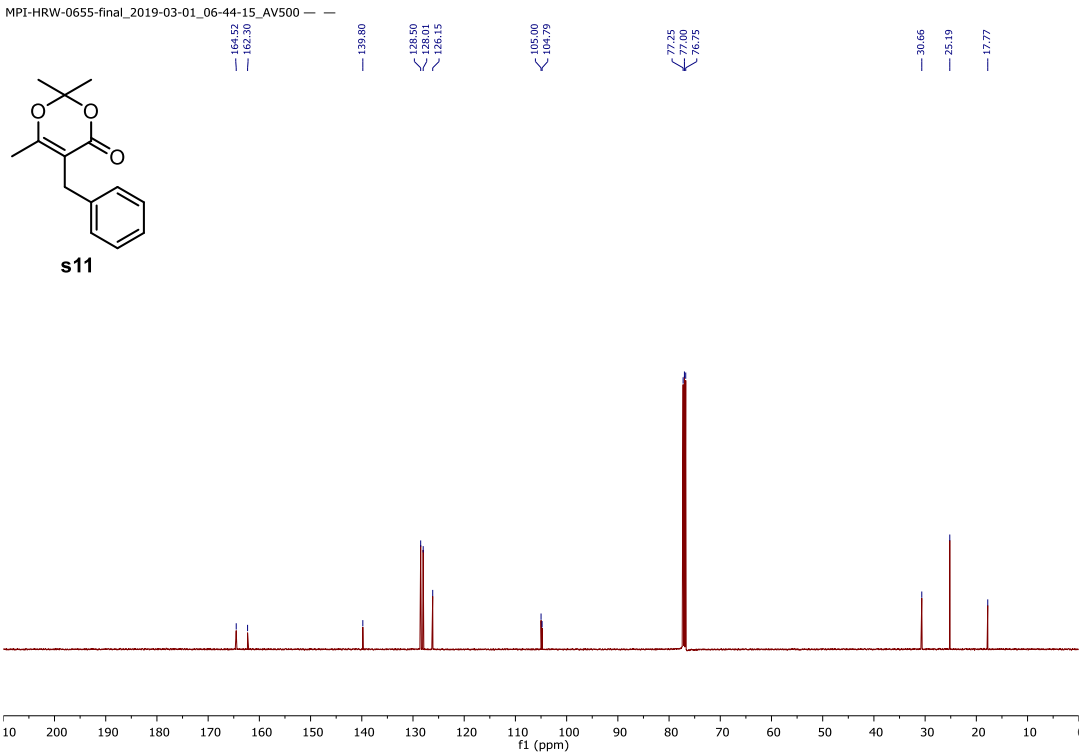

^{13}C NMR spectrum of compound **s11** (126 MHz, in $CDCl_3$)

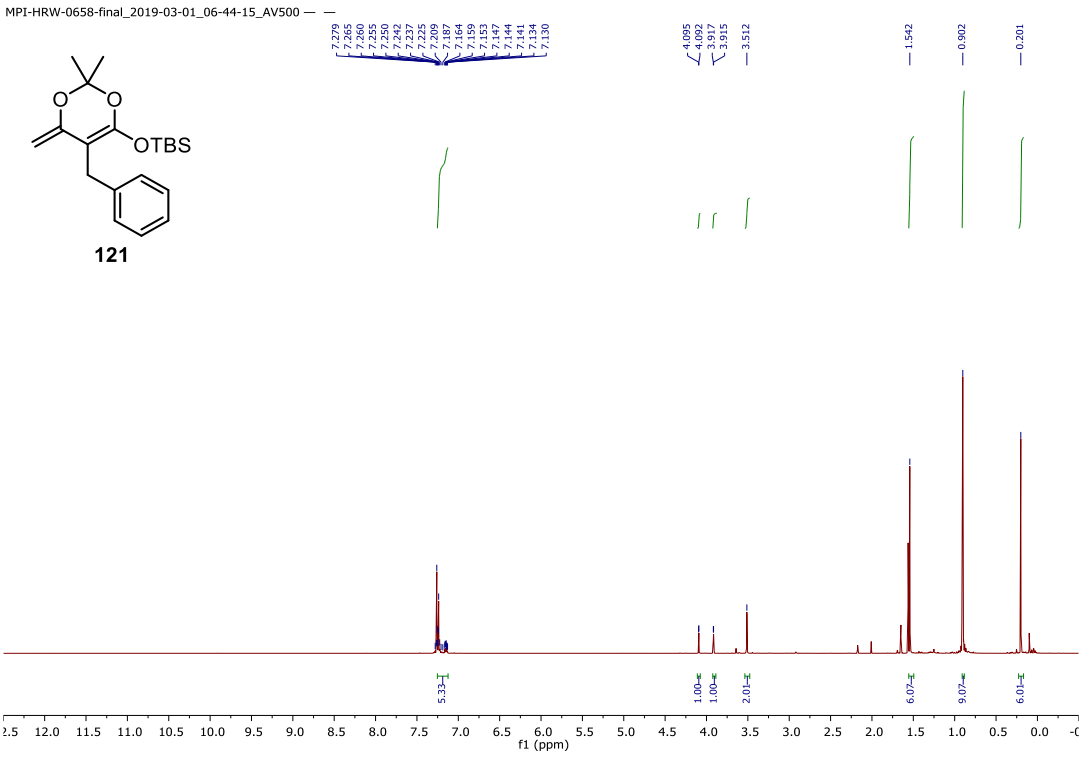

^{1}H NMR spectrum of compound **121** (500 MHz, in $CDCl_3$)

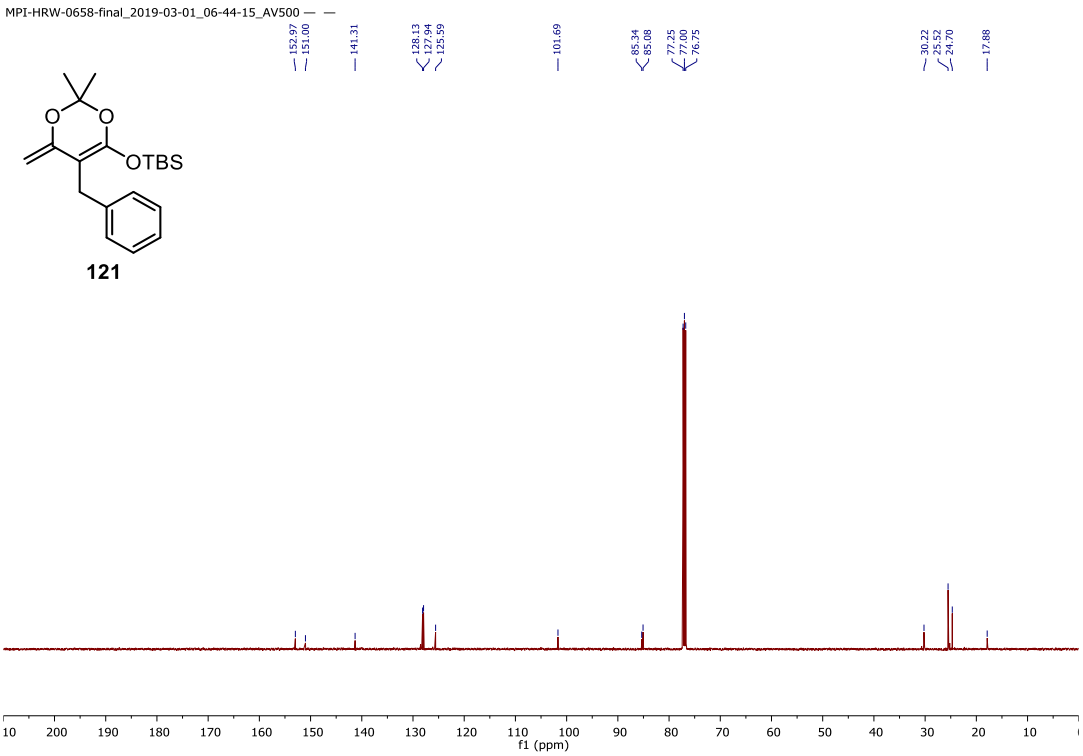

^{13}C NMR spectrum of compound **121** (126 MHz, in $CDCl_3$)

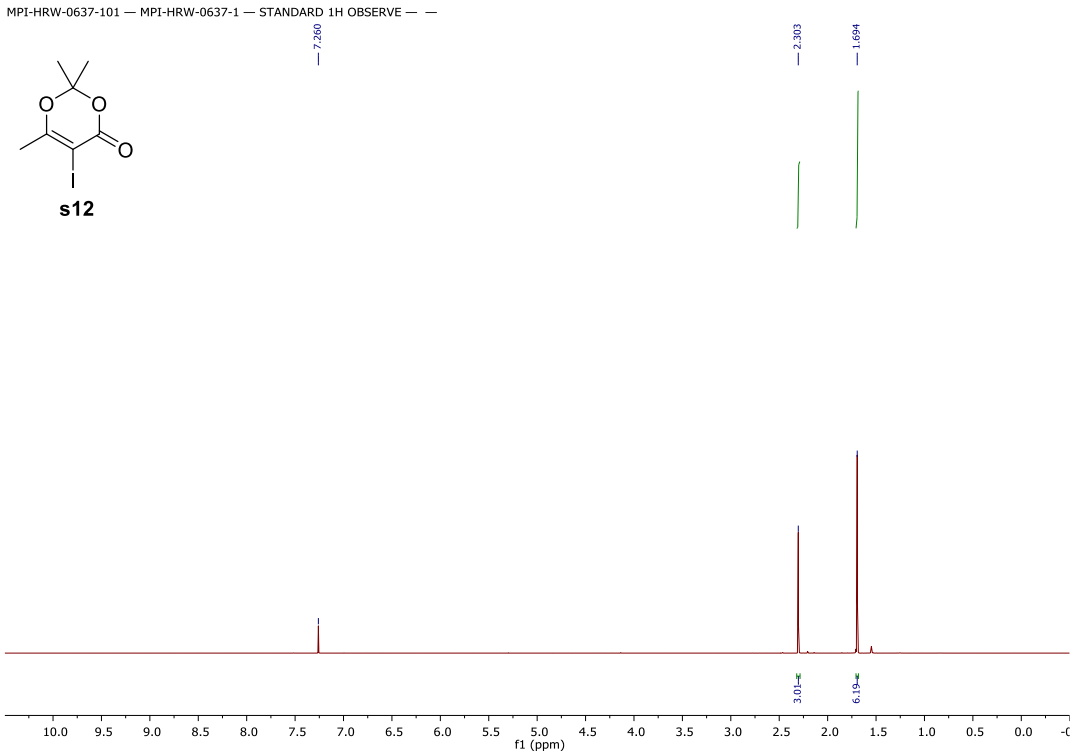

^{1}H NMR spectrum of compound **s12** (400 MHz, in $CDCl_3$)

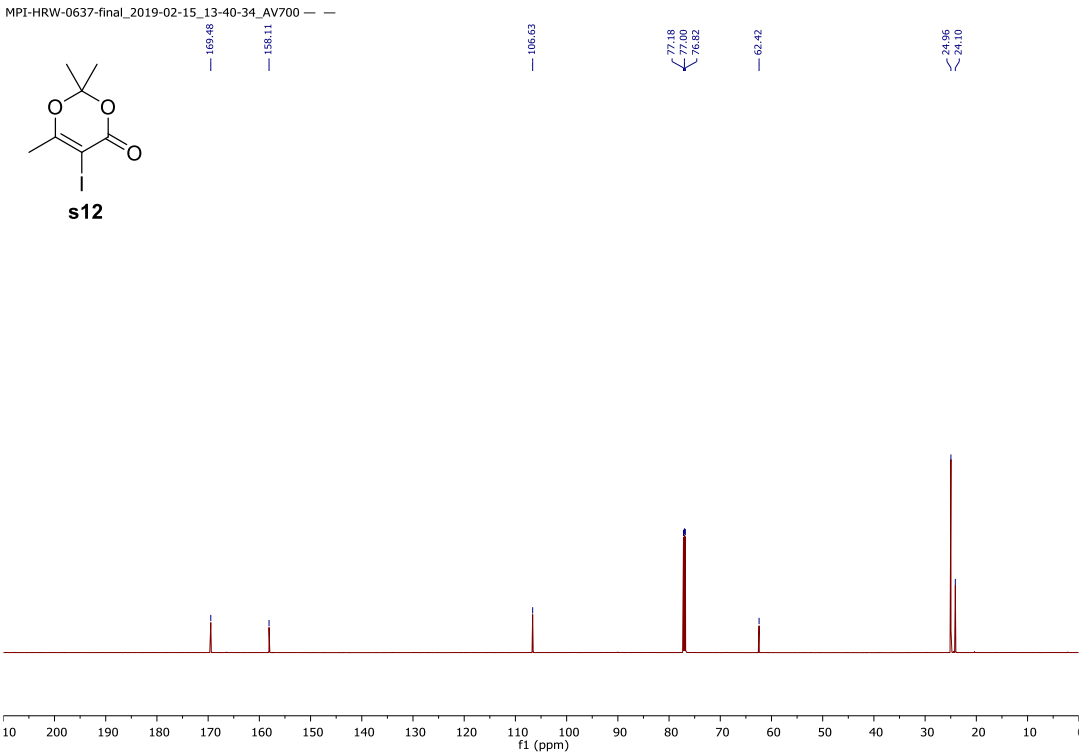

^{13}C NMR spectrum of compound **s12** (176 MHz, in $CDCl_3$)

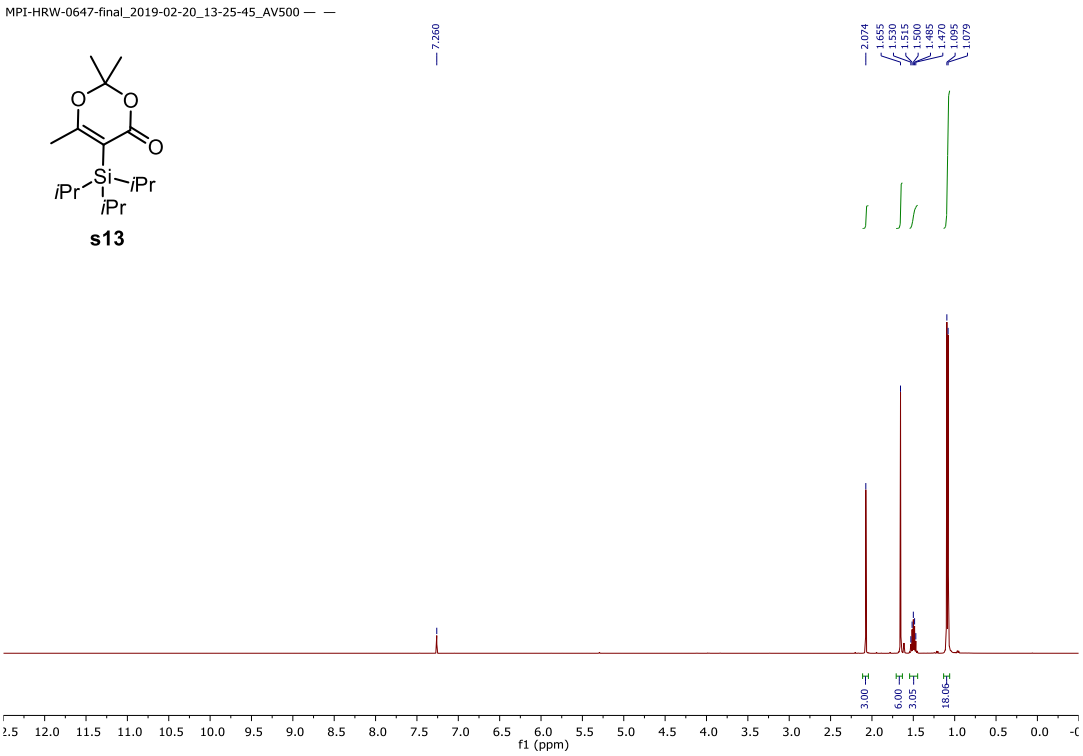

^{1}H NMR spectrum of compound **s13** (500 MHz, in $CDCl_3$)

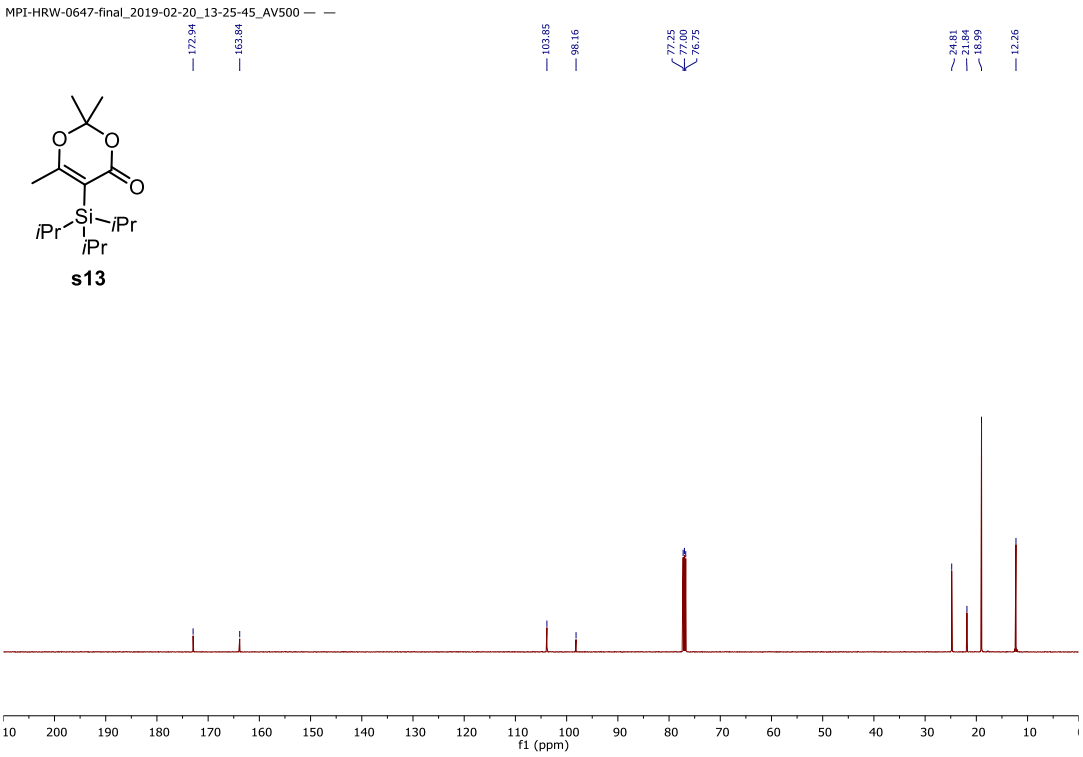

^{13}C NMR spectrum of compound **s13** (126 MHz, in $CDCl_3$)

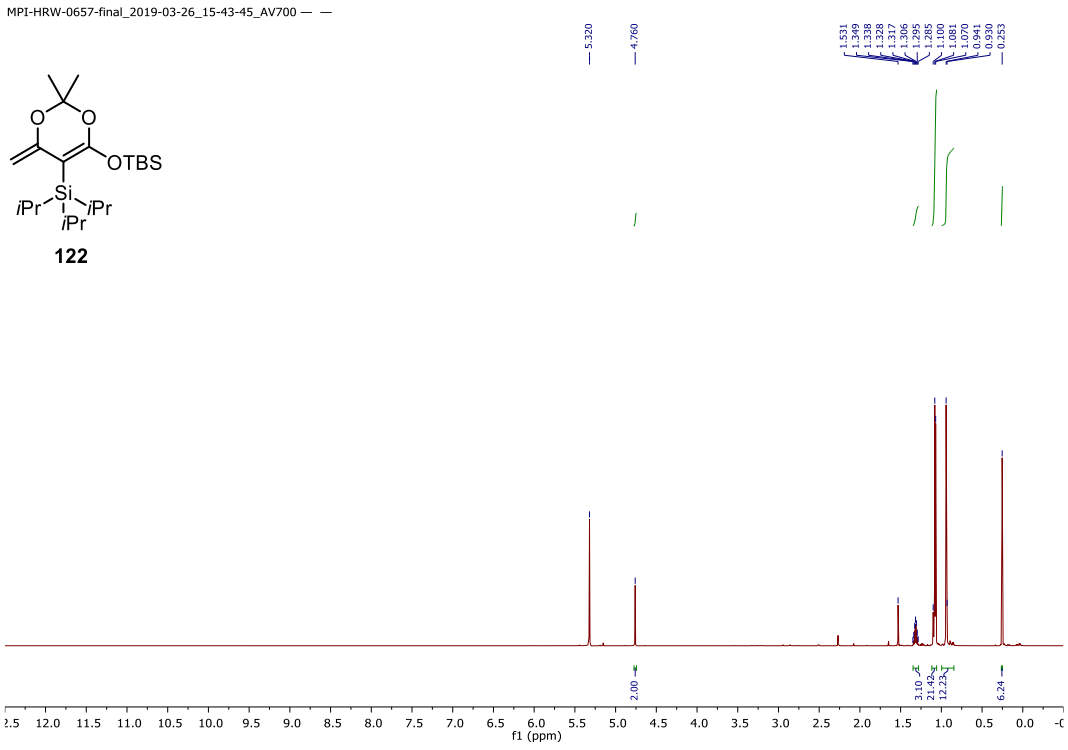

^{1}H NMR spectrum of compound **122** (700 MHz, in CD_2Cl_2)

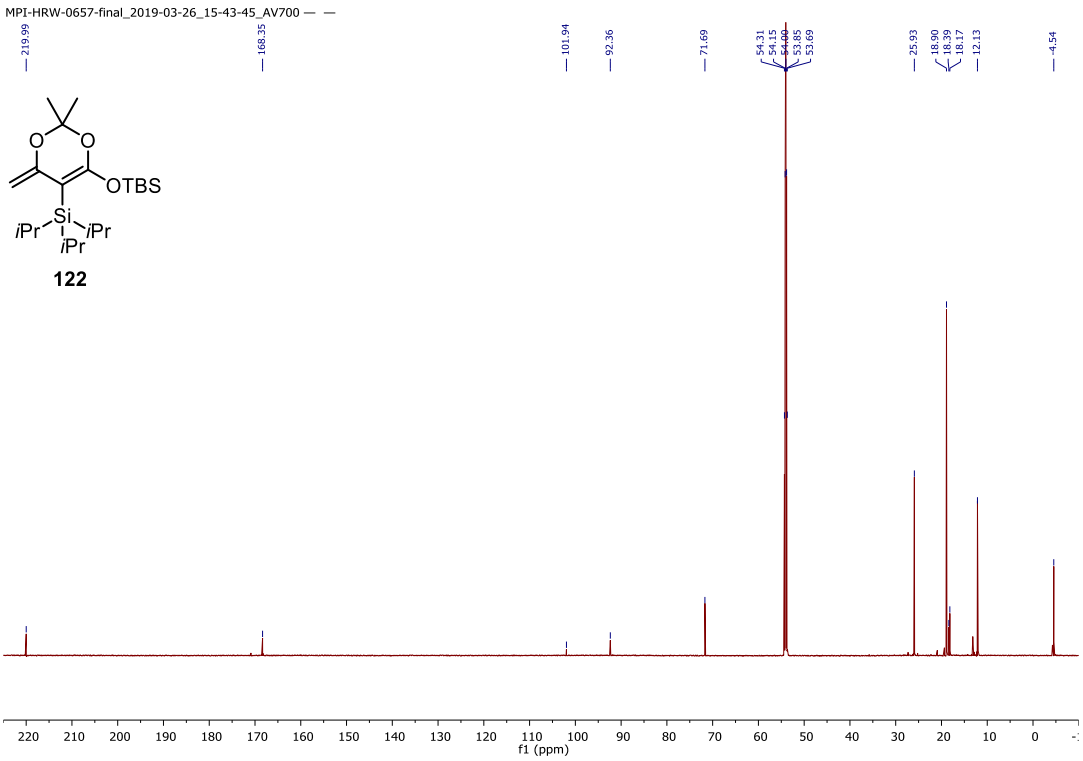

^{13}C NMR spectrum of compound **122** (176 MHz, in CD_2Cl_2)

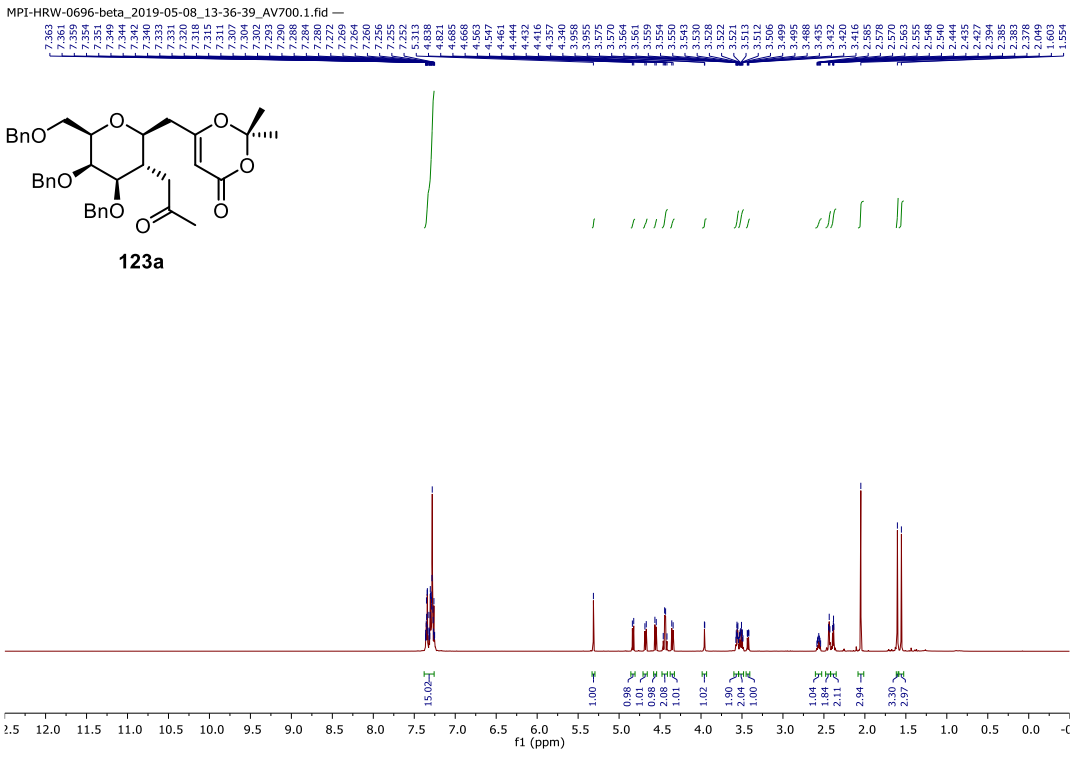

^{1}H NMR spectrum of compound **123a** (700 MHz, in $CDCl_3$)

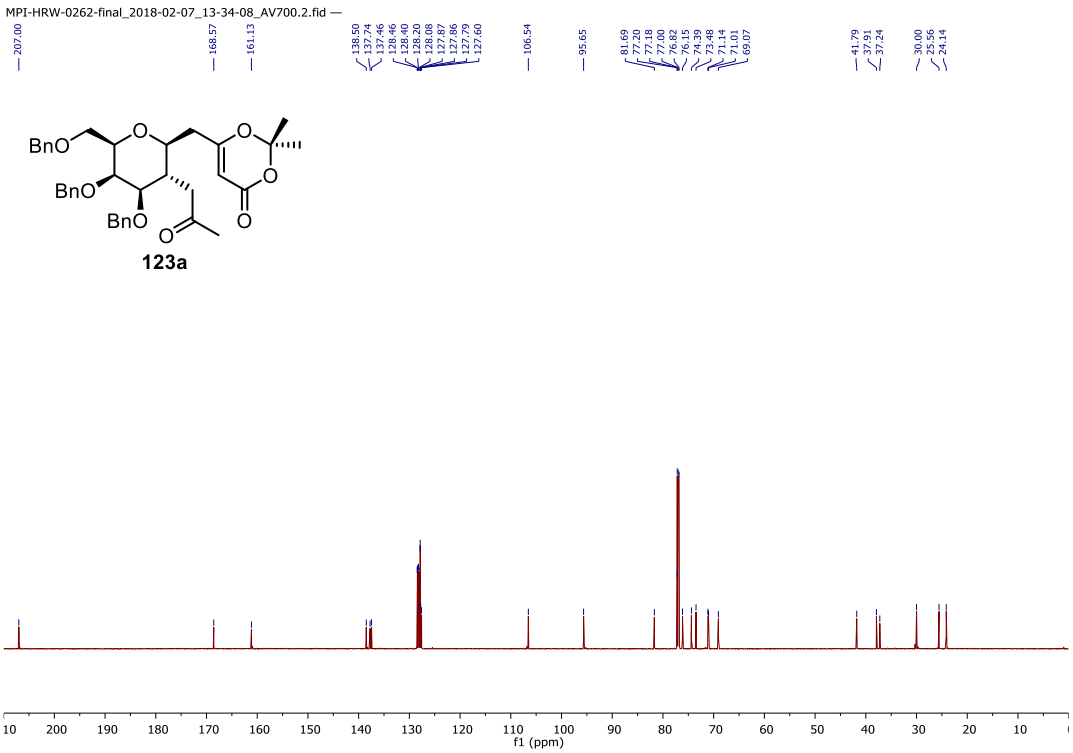

^{13}C NMR spectrum of compound **123a** (176 MHz, in $CDCl_3$)

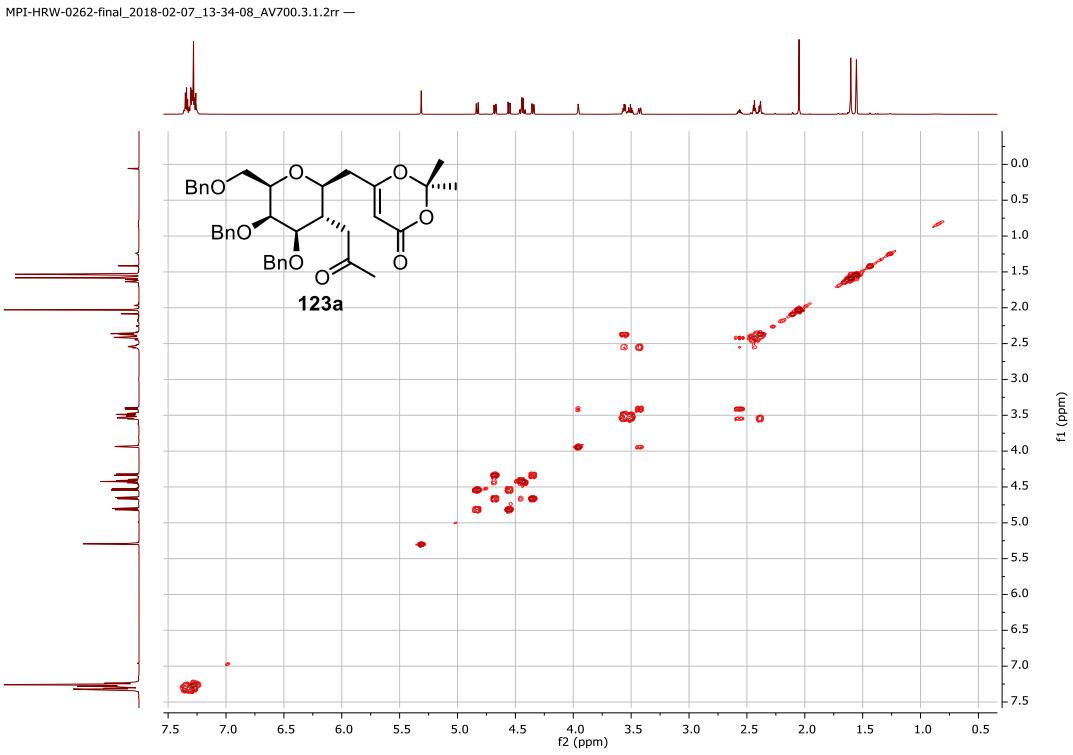

COSY spectrum of compound **123a**

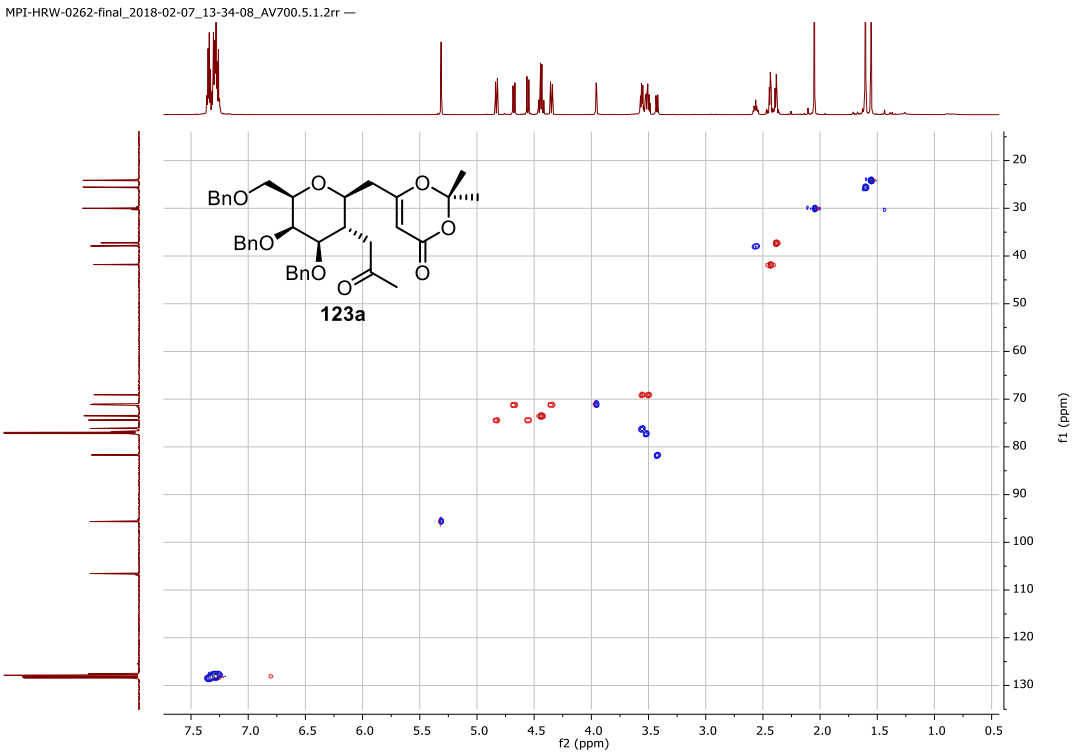

HSQC spectrum of compound **123a**

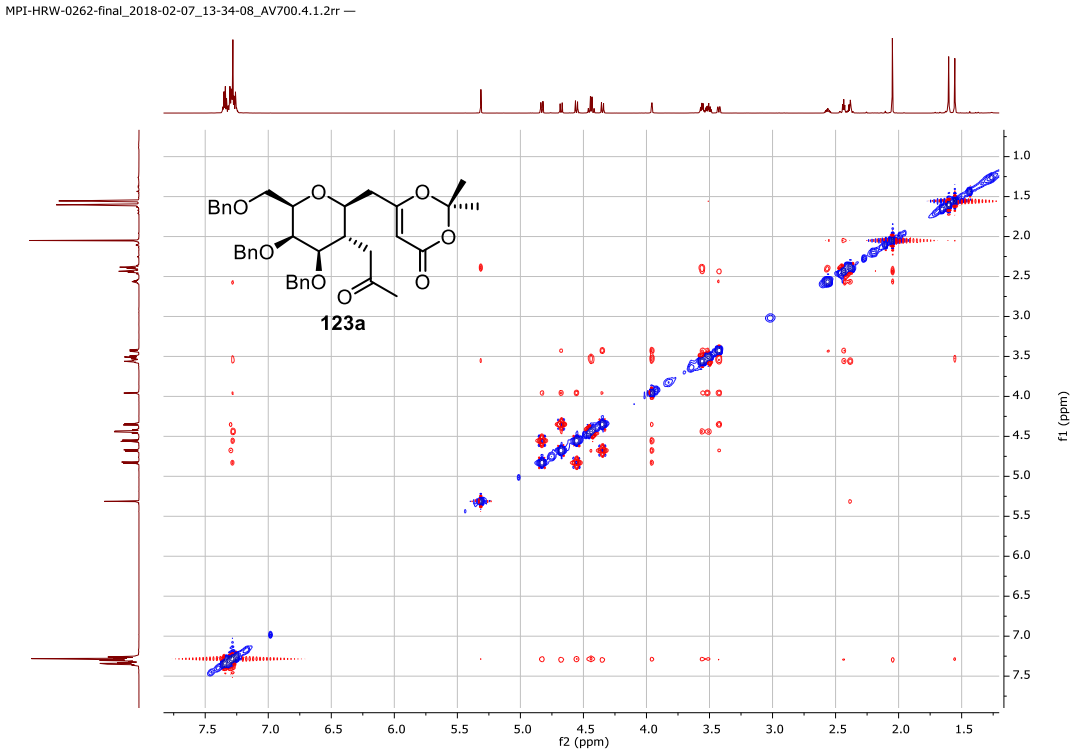

NOESY spectrum of compound **123a**

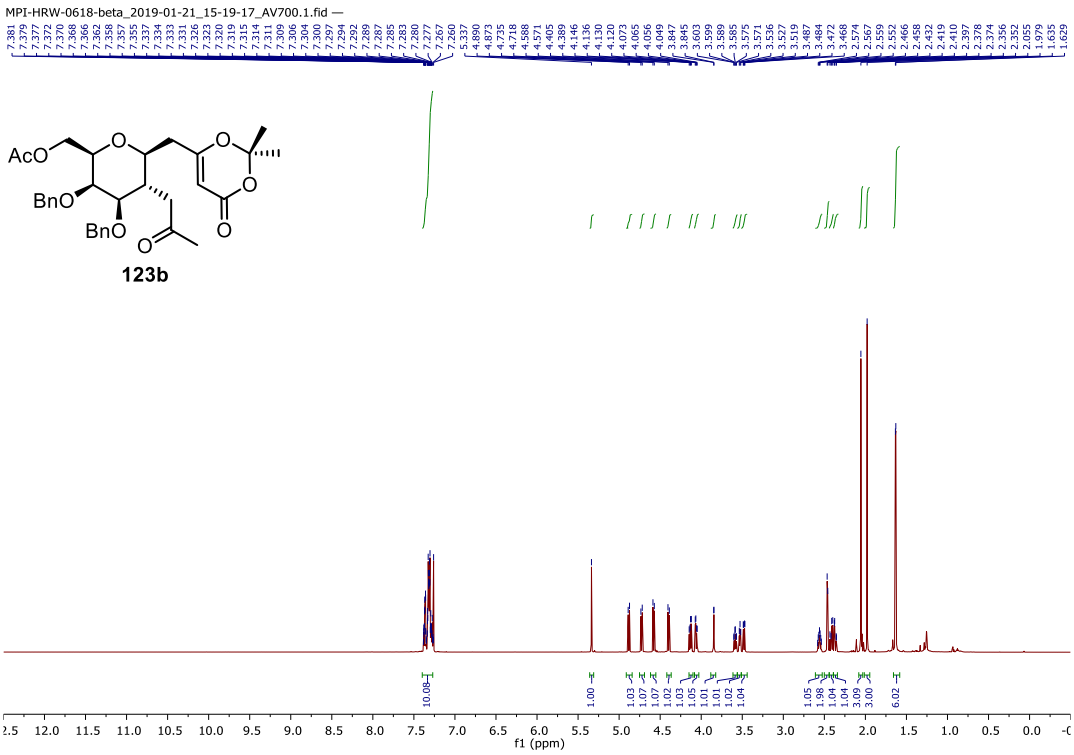

^{1}H NMR spectrum of compound **123b** (700 MHz, in $CDCl_3$)

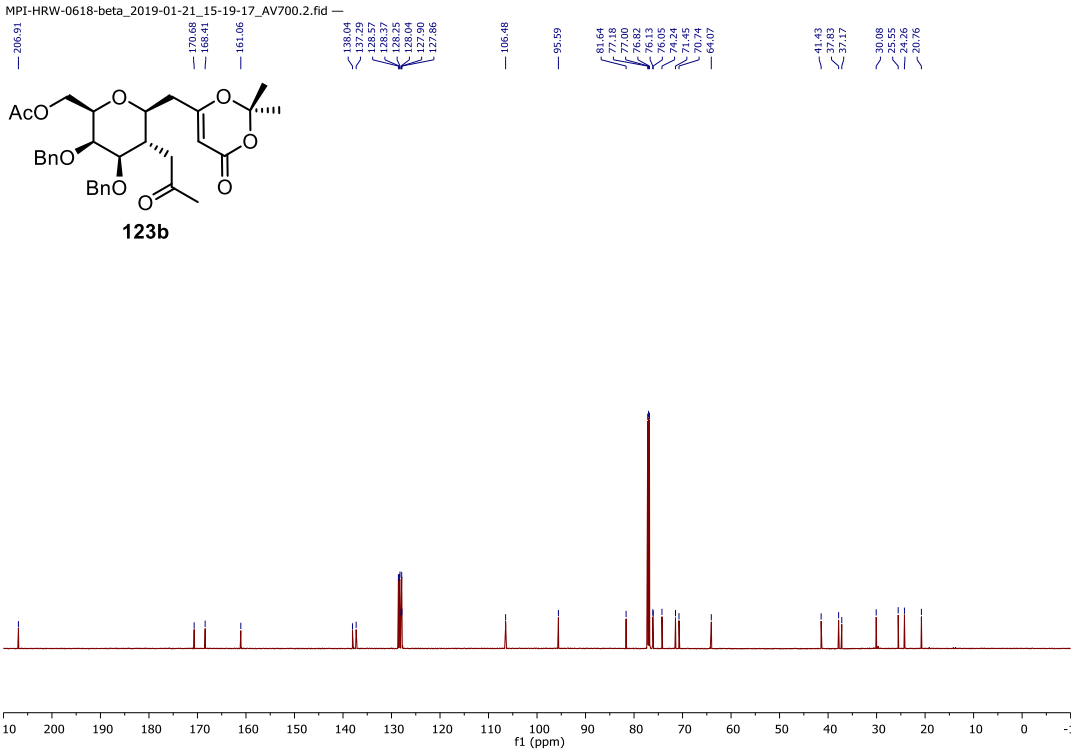

^{13}C NMR spectrum of compound **123b** (176 MHz, in $CDCl_3$)

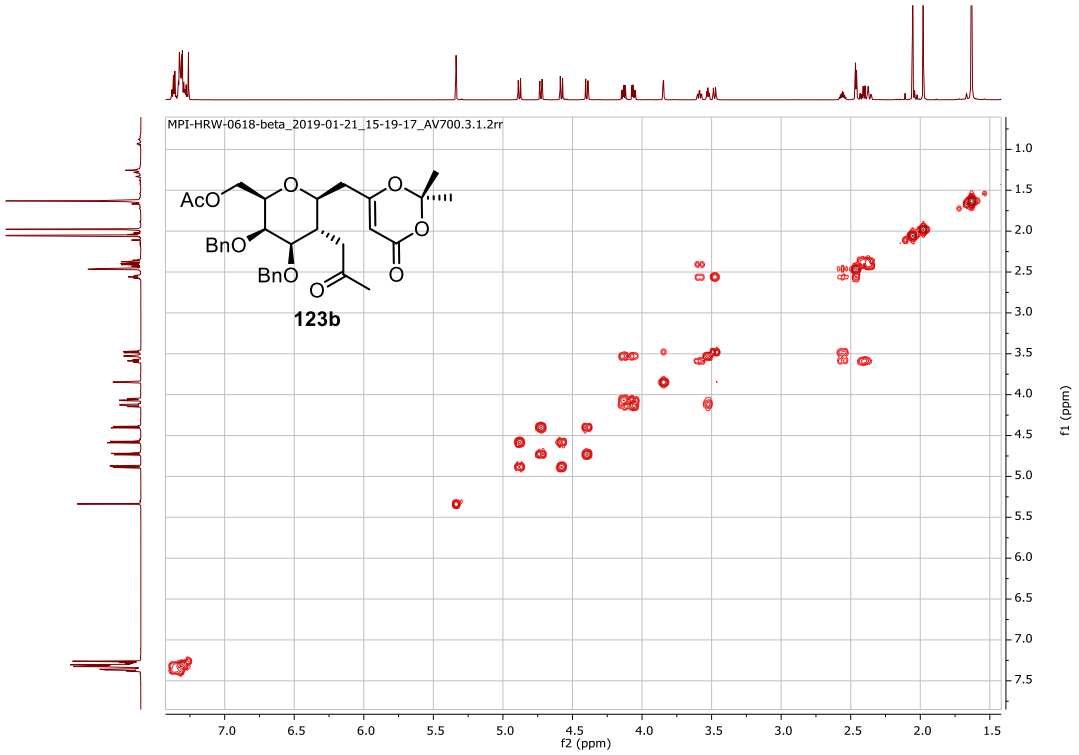

COSY spectrum of compound **123b**

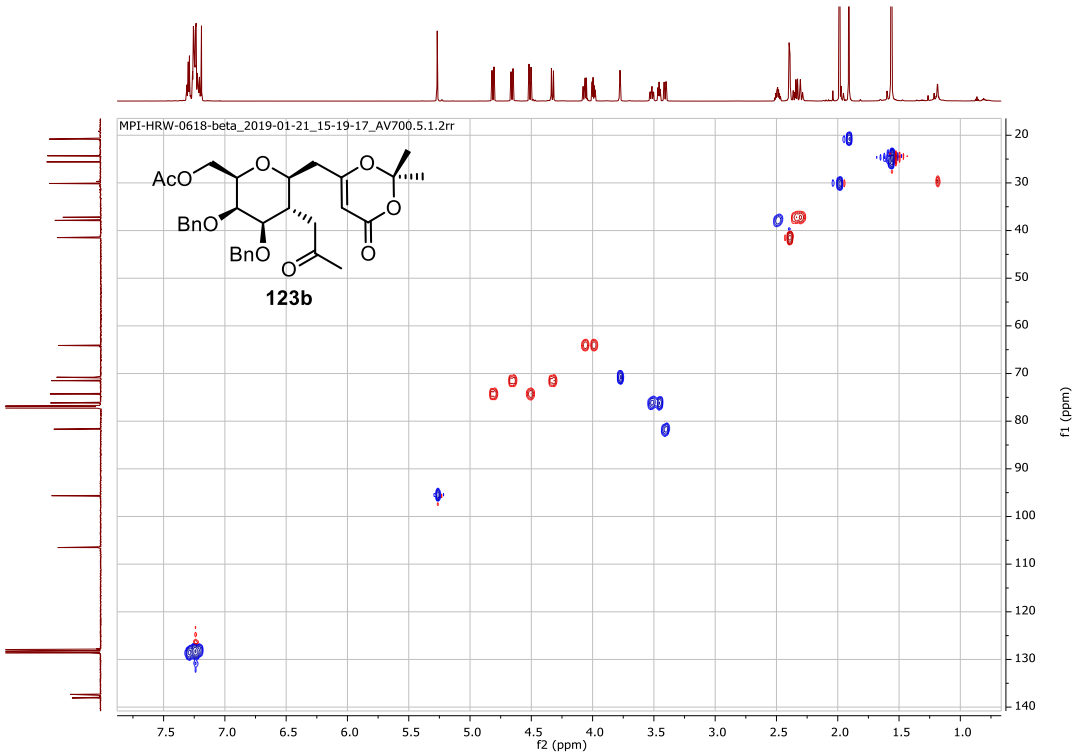

HSQC spectrum of compound **123b**

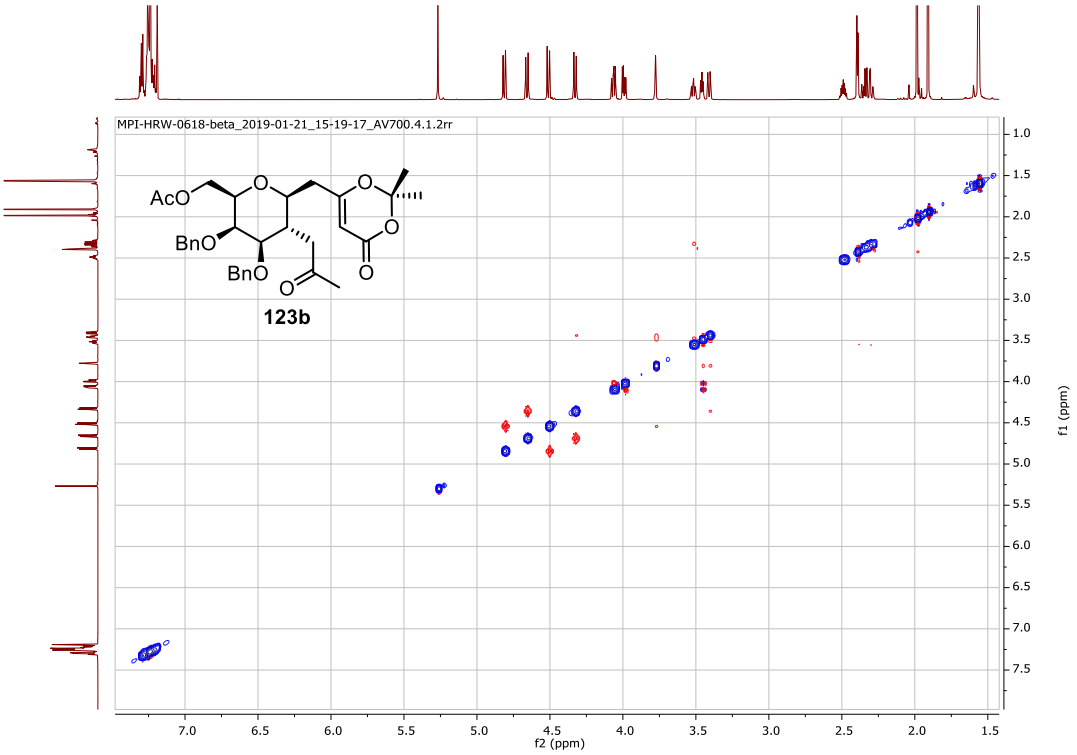

NOESY spectrum of compound **123b**

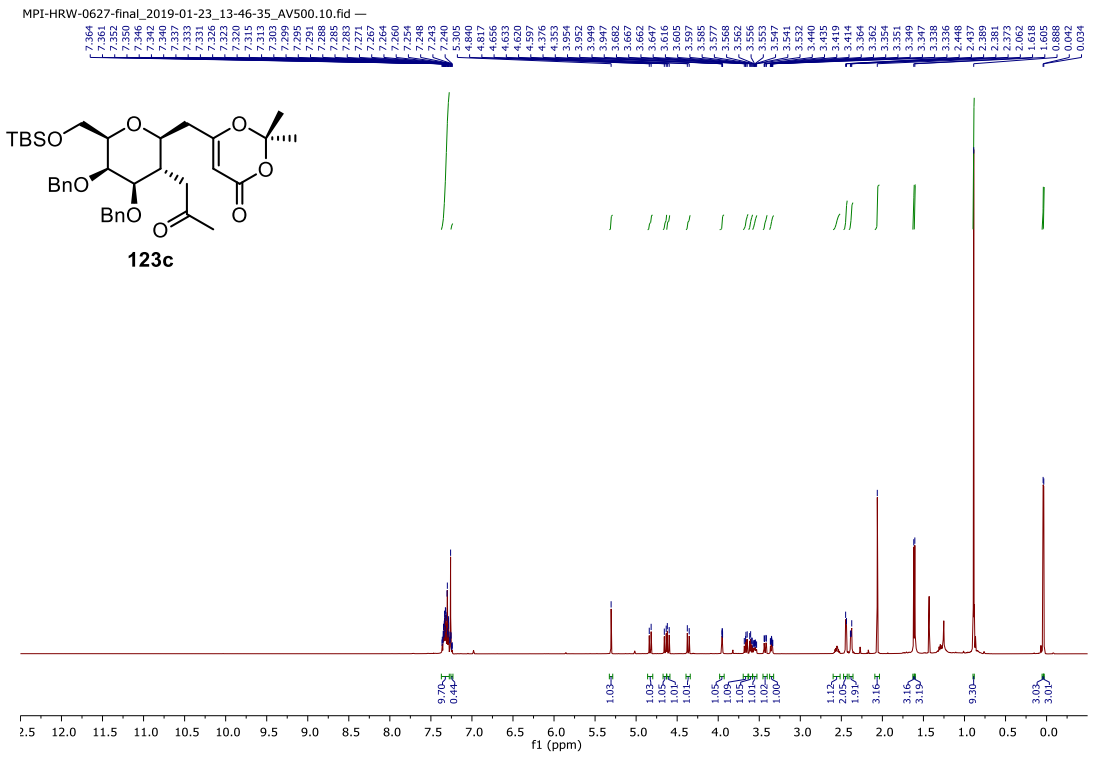

^{1}H NMR spectrum of compound **123c** (500 MHz, in $CDCl_3$)

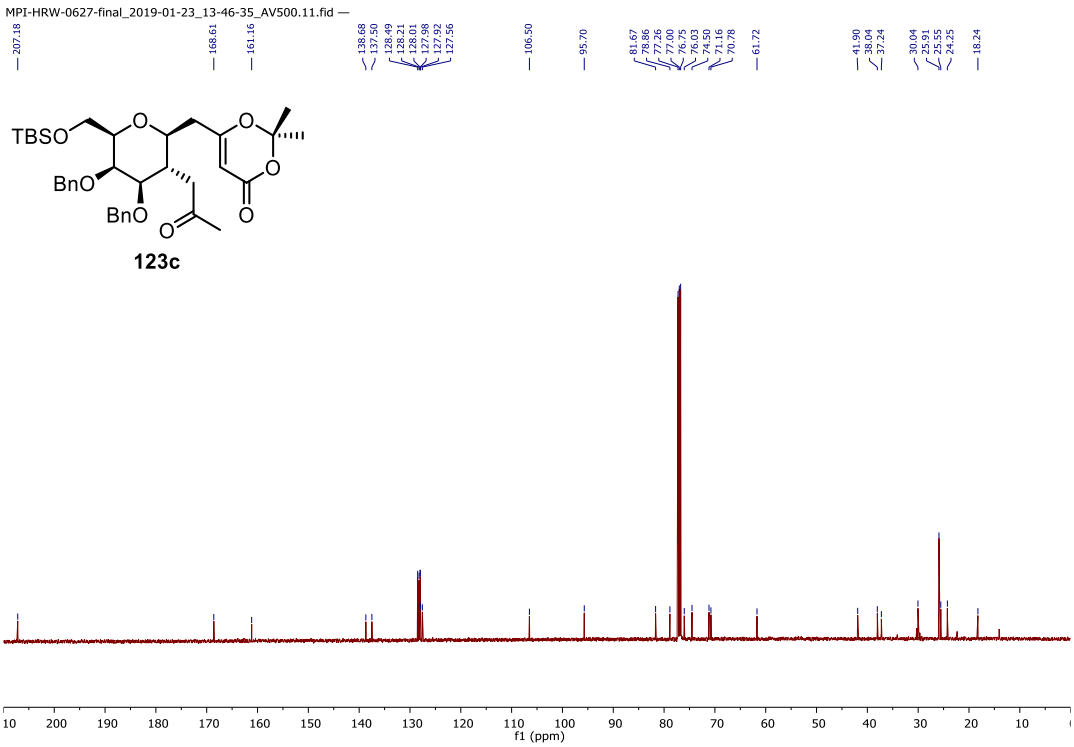

^{13}C NMR spectrum of compound **123c** (126 MHz, in $CDCl_3$)

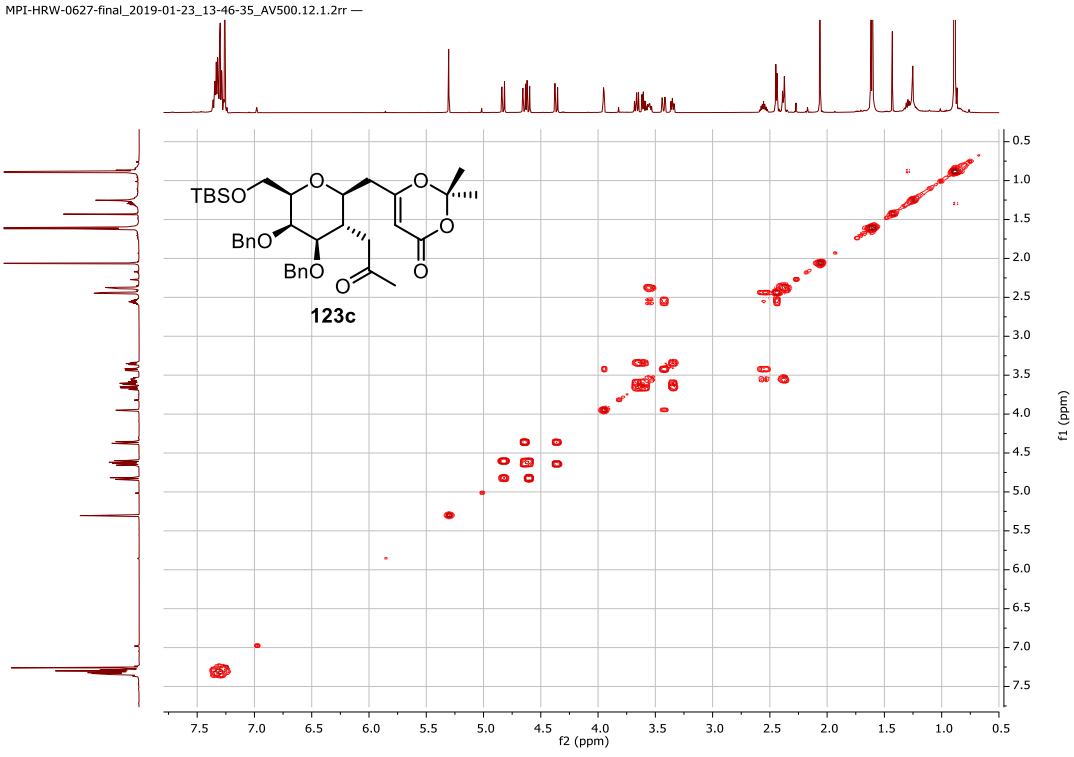

COSY spectrum of compound **123c**

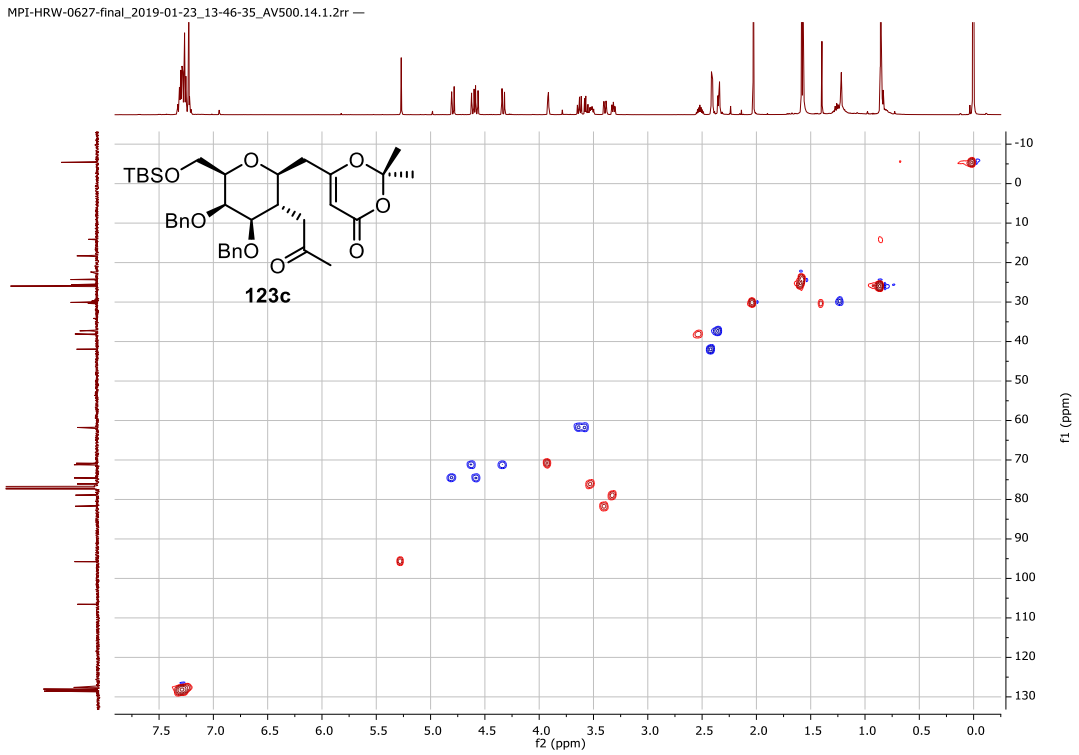

HSQC spectrum of compound **123c**

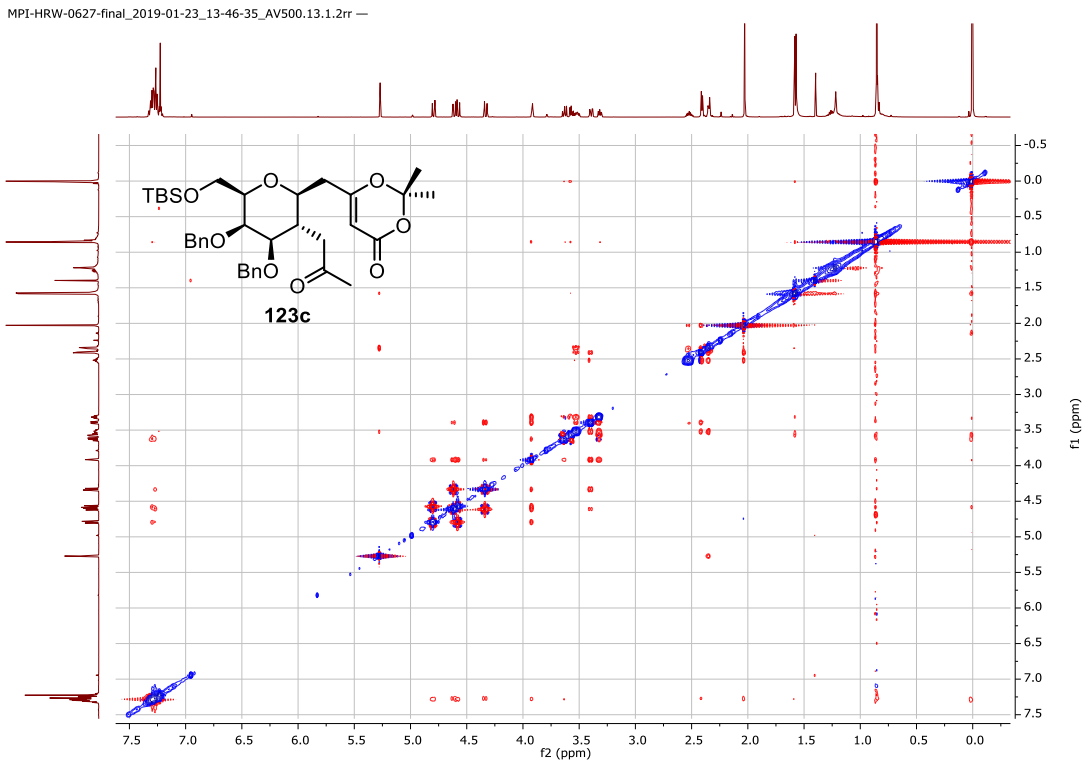

NOESY spectrum of compound **123c**

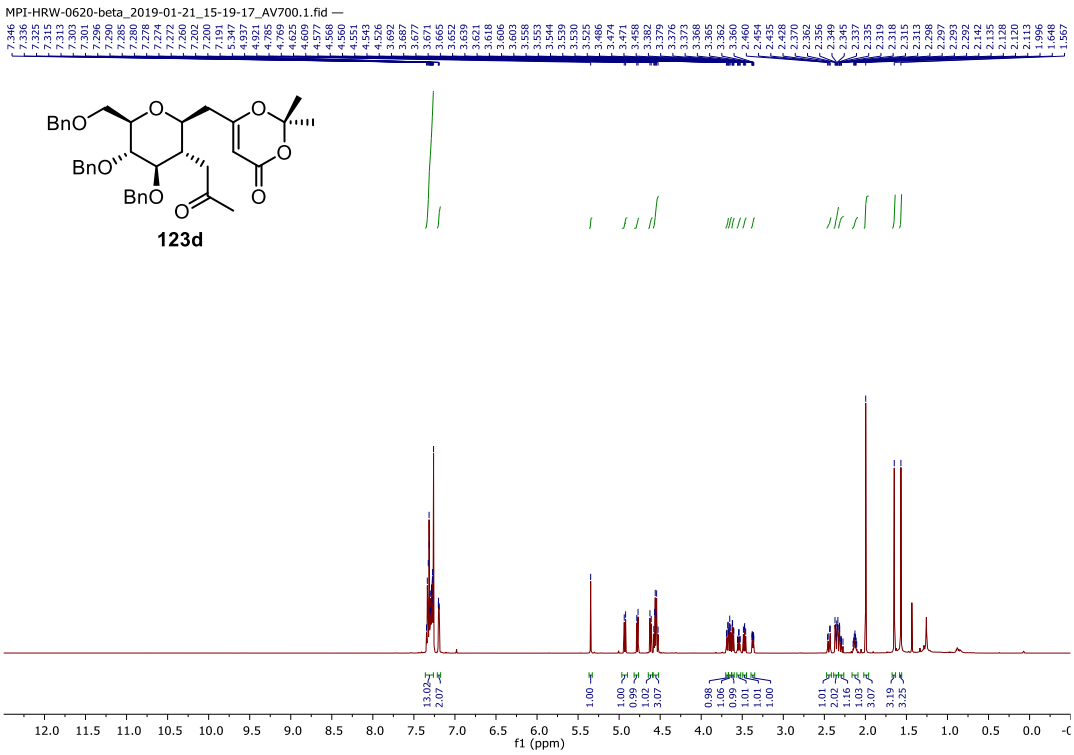

^{1}H NMR spectrum of compound **123d** (700 MHz, in $CDCl_3$)

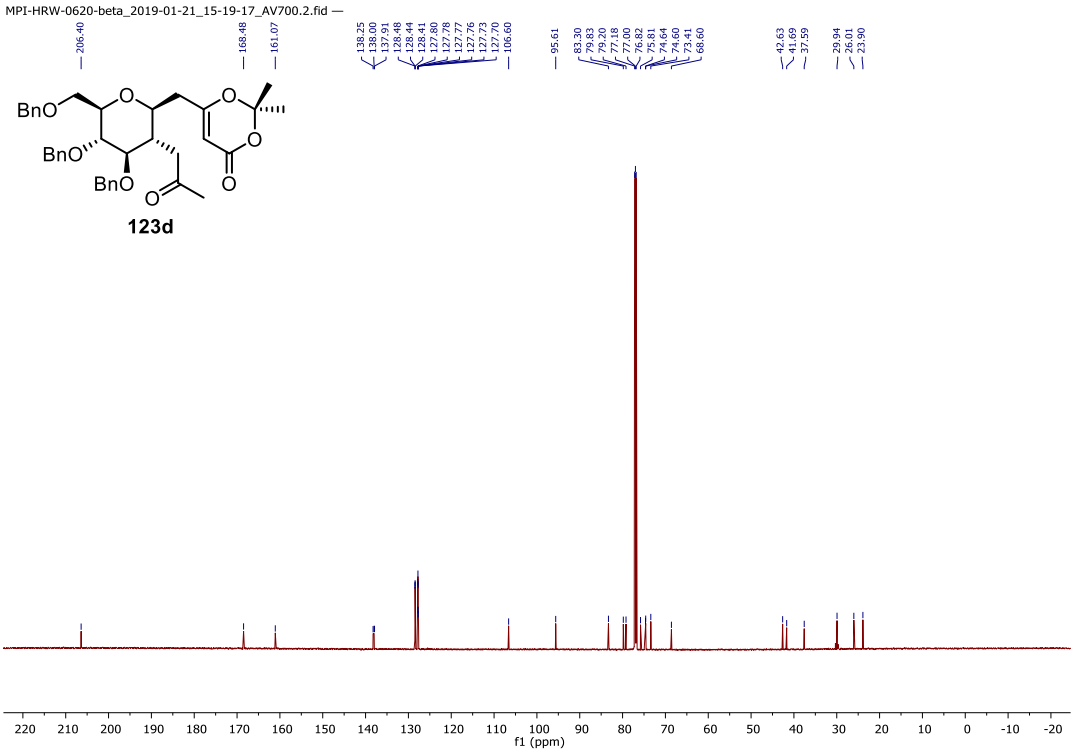

^{13}C NMR spectrum of compound **123d** (176 MHz, in $CDCl_3$)

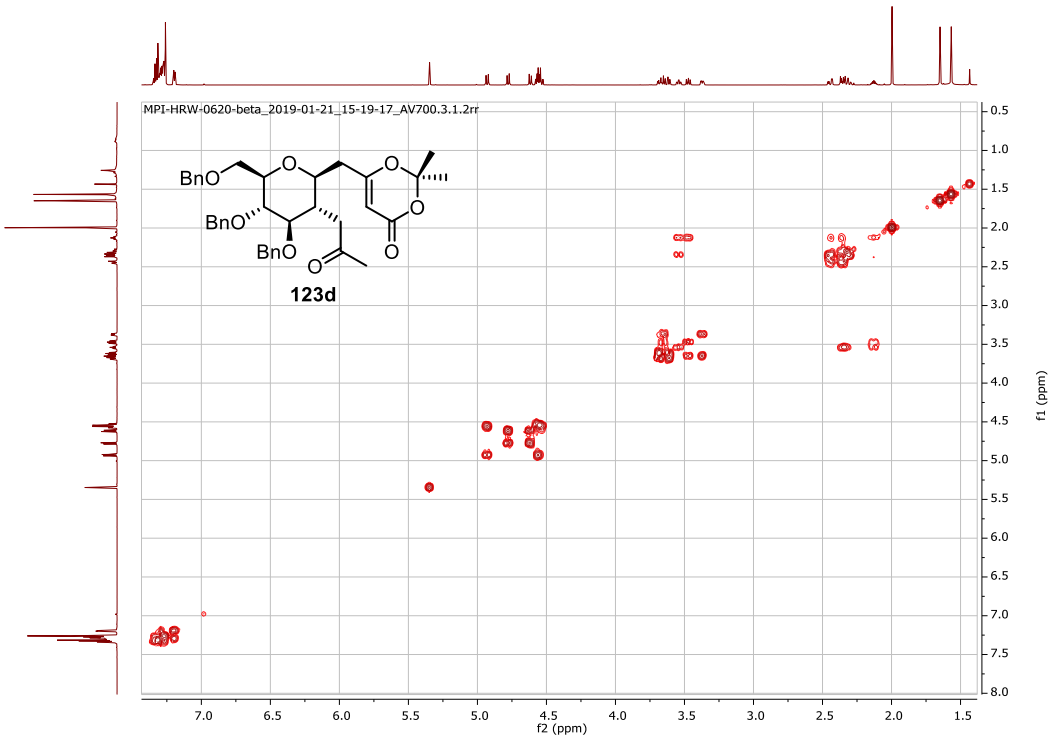

COSY spectrum of compound **123d**

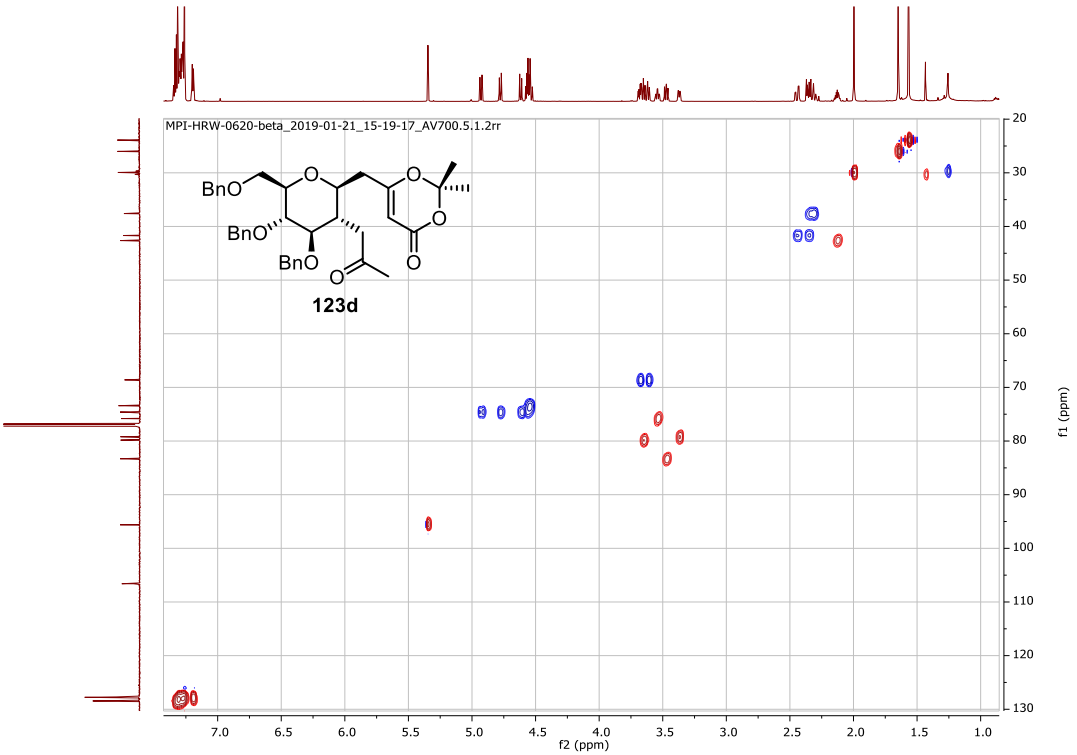

HSQC spectrum of compound **123d**

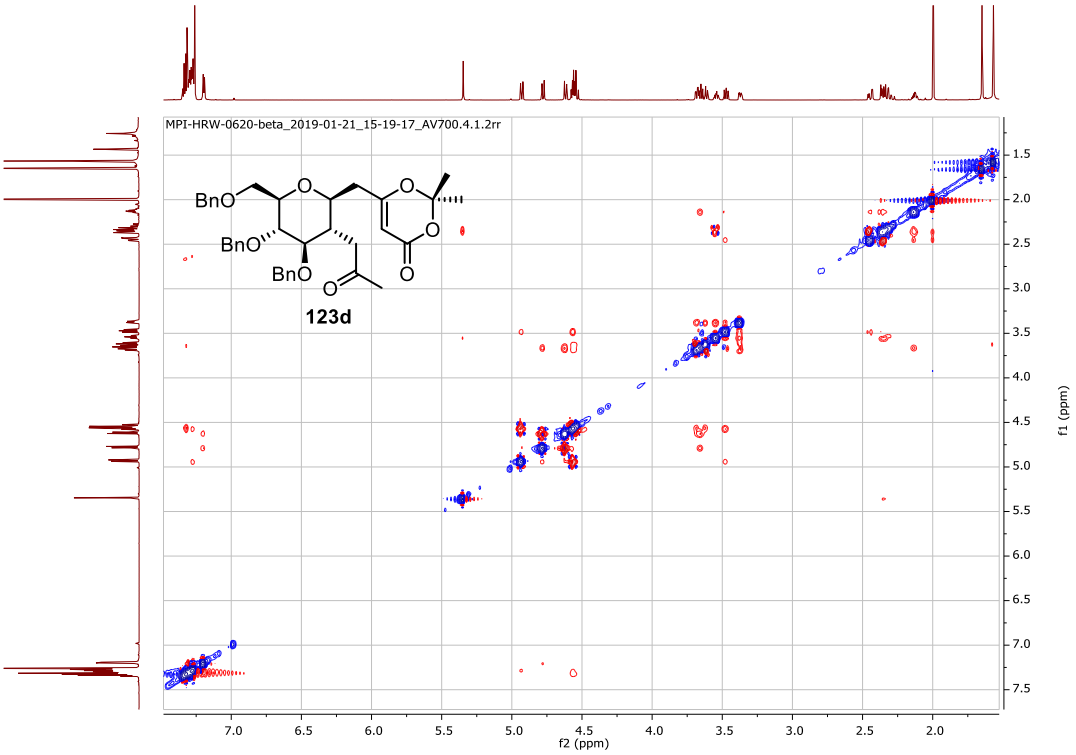

NOESY spectrum of compound **123d**

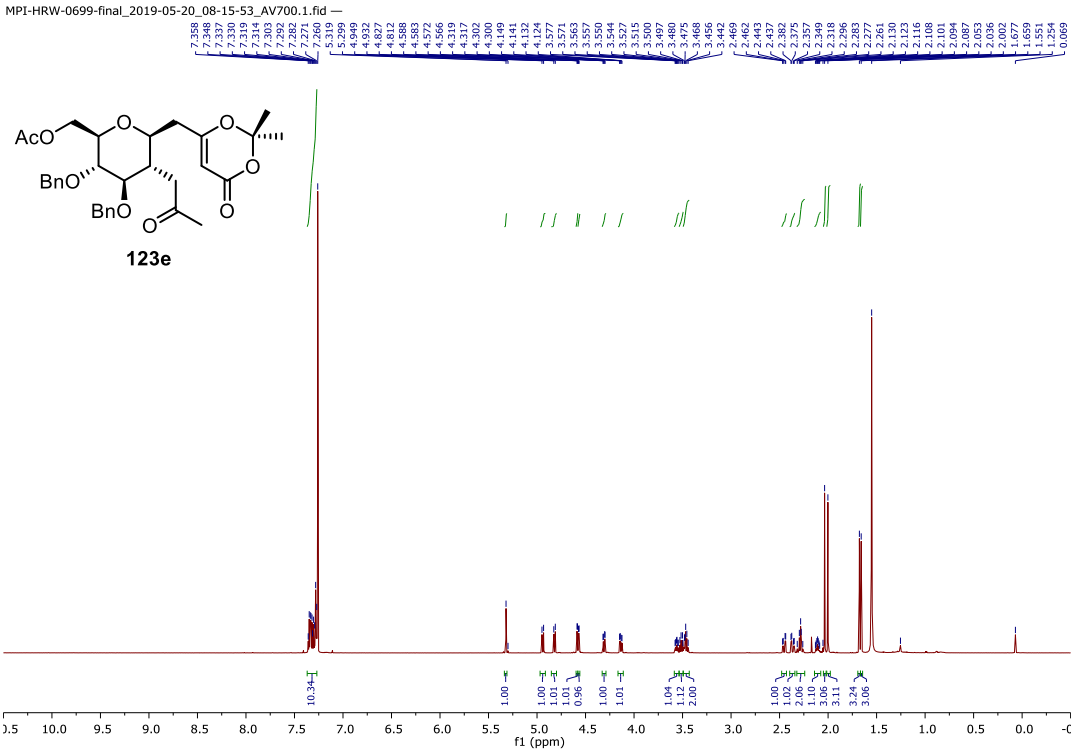

^{1}H NMR spectrum of compound **123e** (700 MHz, in $CDCl_3$)

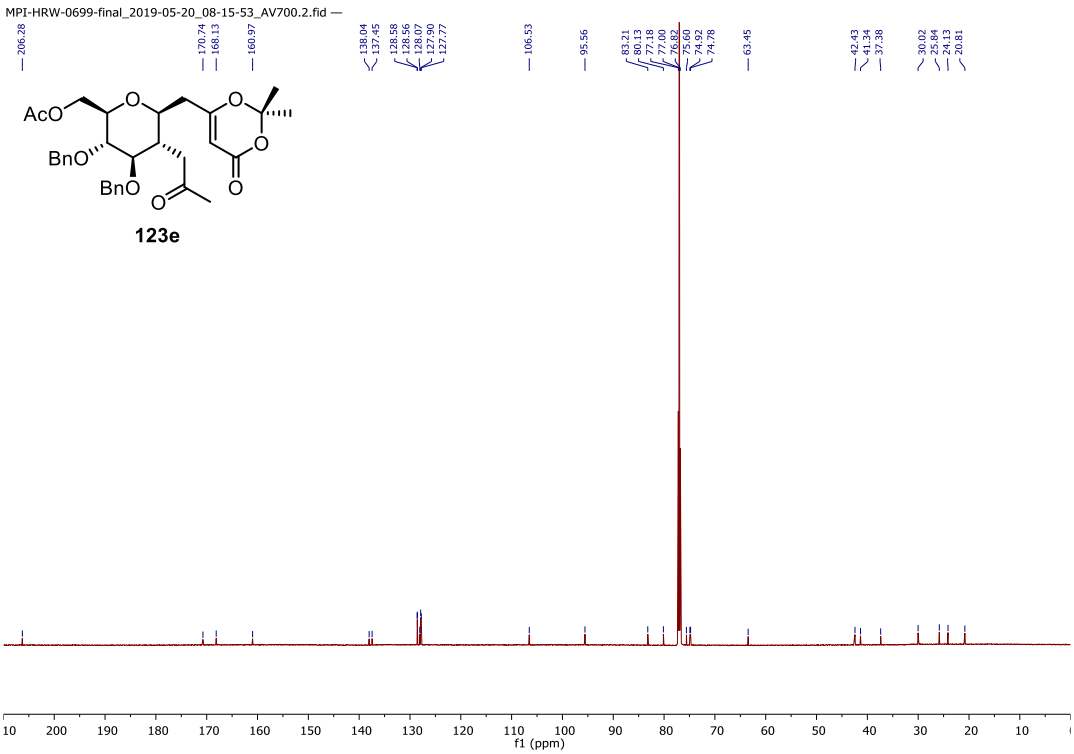

^{13}C NMR spectrum of compound **123e** (176 MHz, in $CDCl_3$)

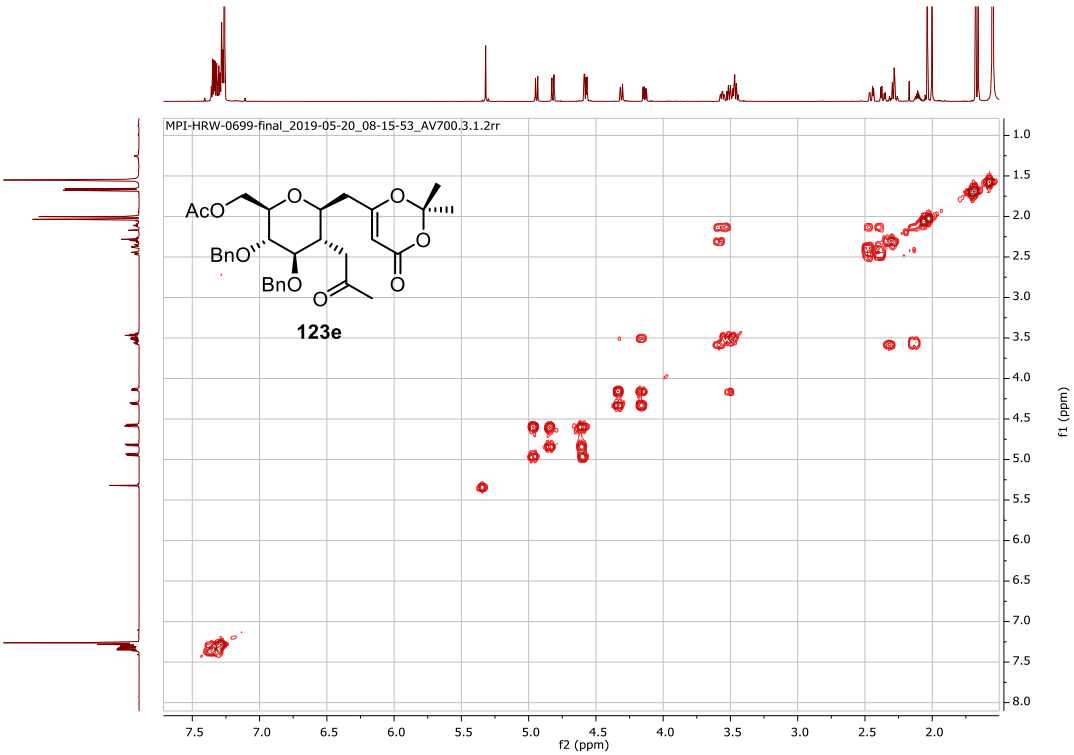

COSY spectrum of compound **123e**

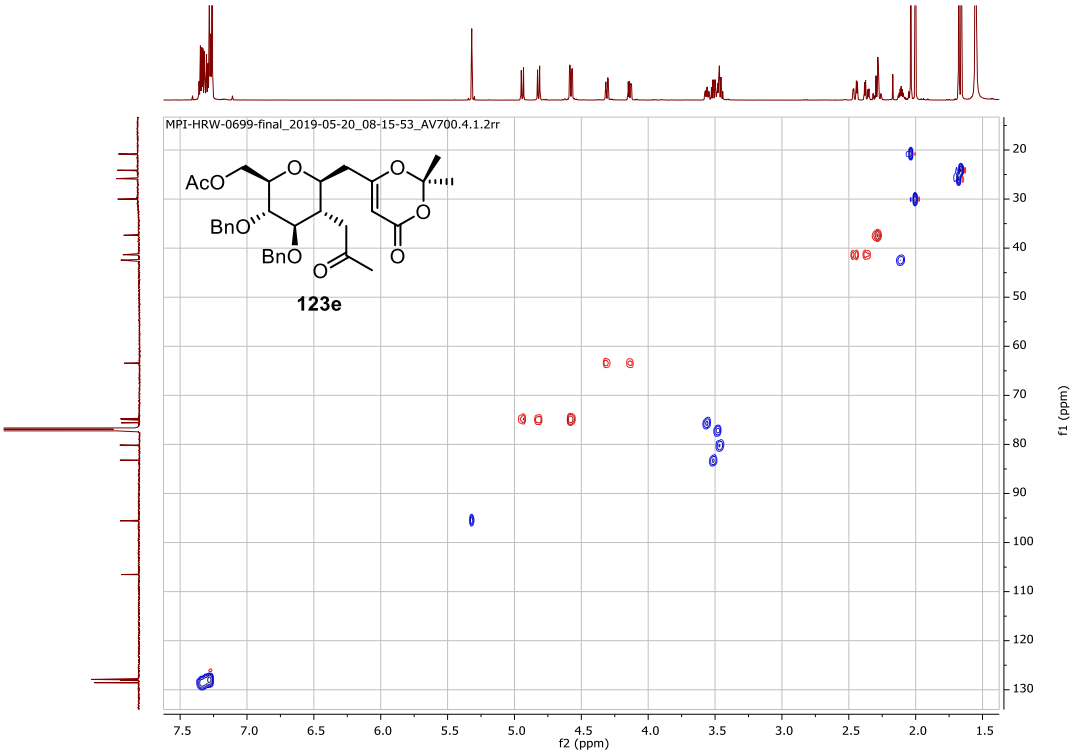

HSQC spectrum of compound **123e**

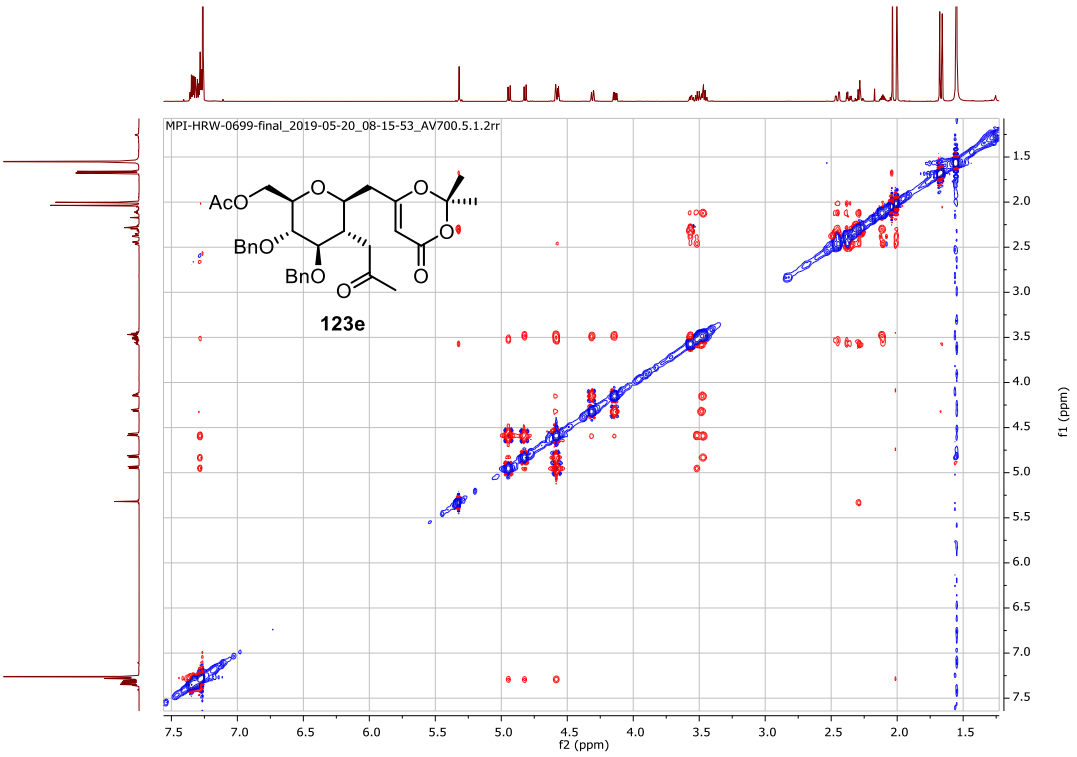

NOESY spectrum of compound **123e**

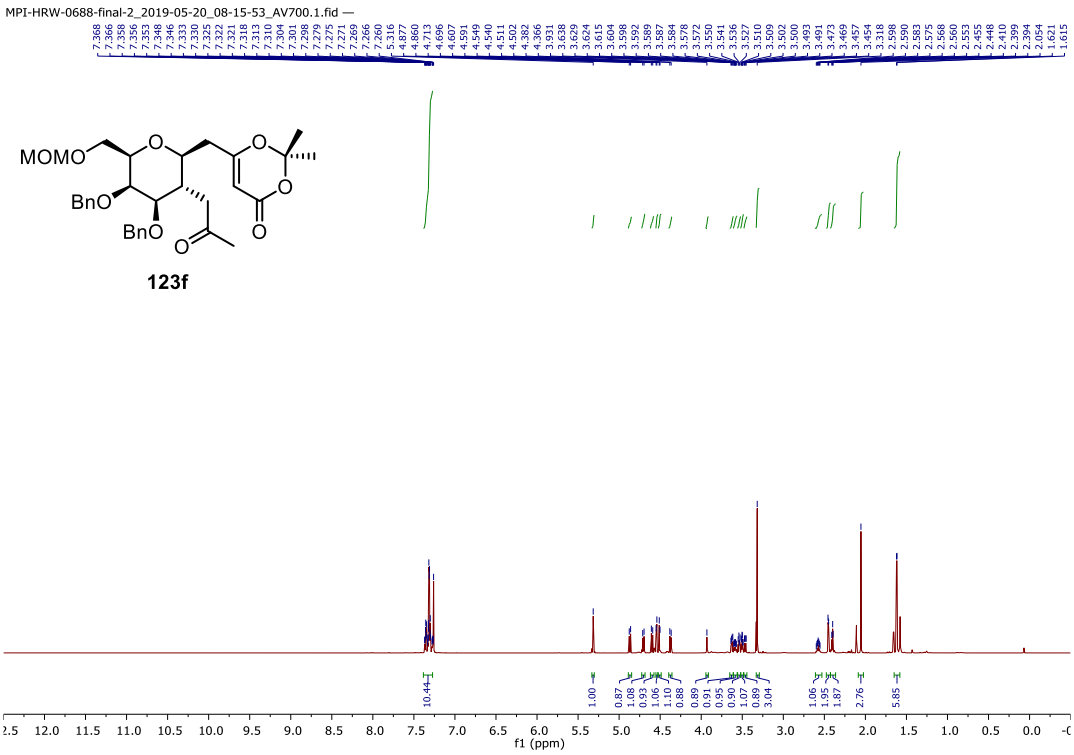

^{1}H NMR spectrum of compound **123f** (700 MHz, in $CDCl_3$)

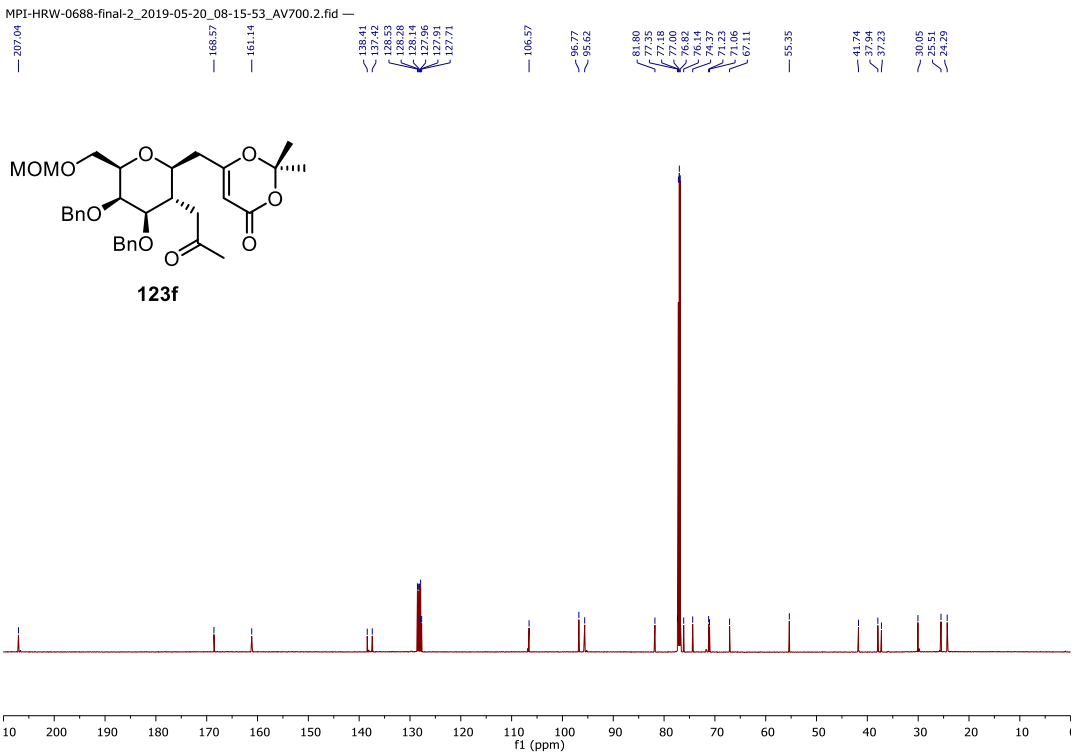

^{13}C NMR spectrum of compound **123f** (176 MHz, in $CDCl_3$)

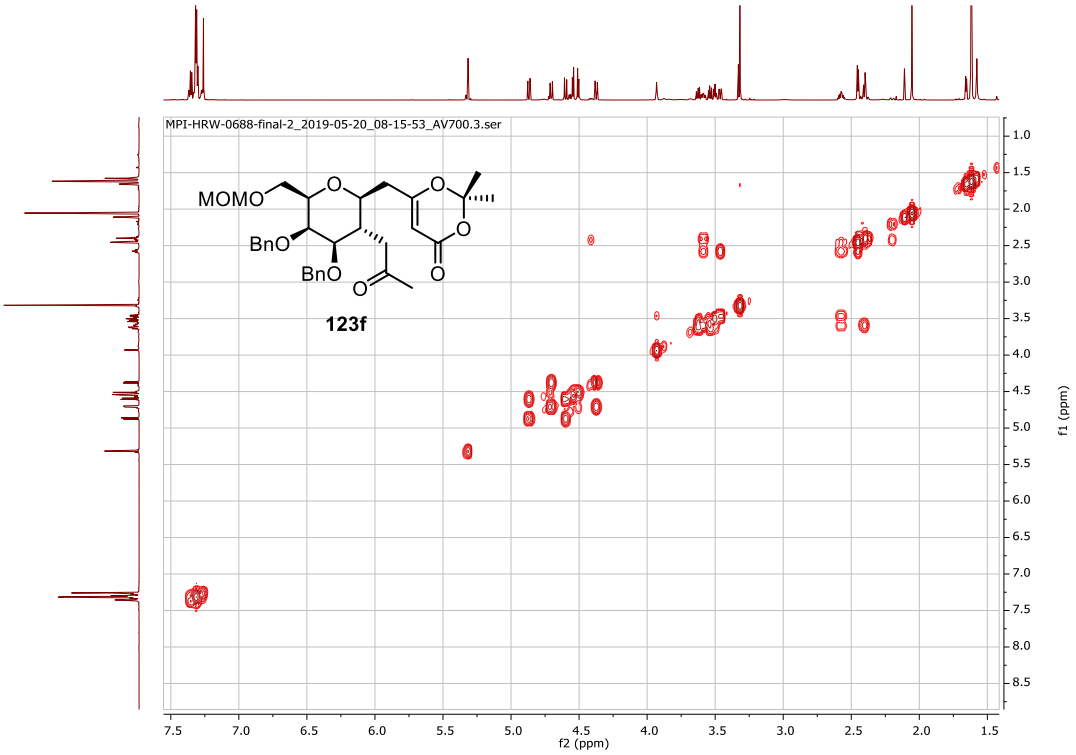

COSY spectrum of compound **123f**

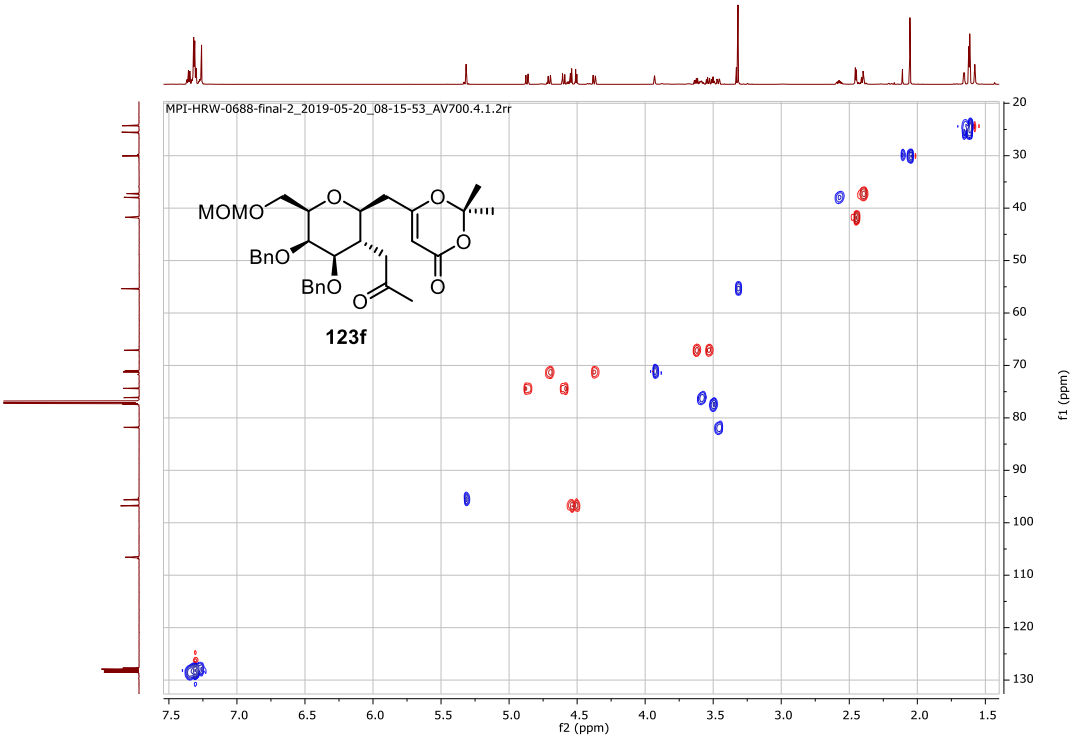

HSQC spectrum of compound **123f**

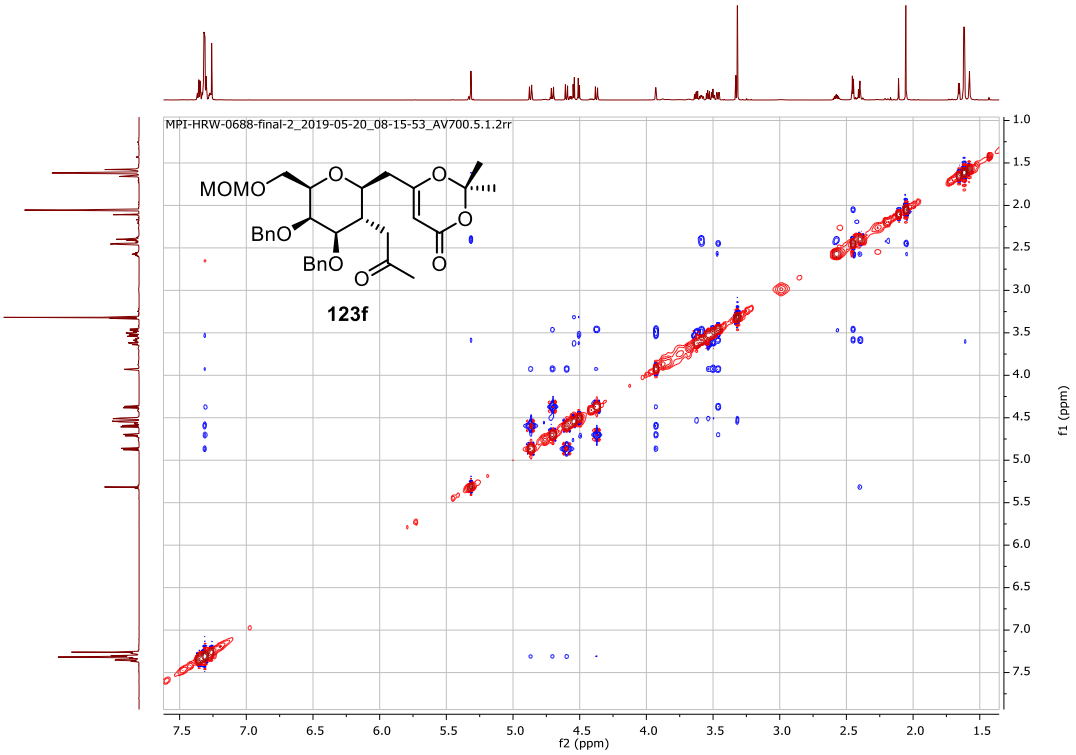

NOESY spectrum of compound **123f**

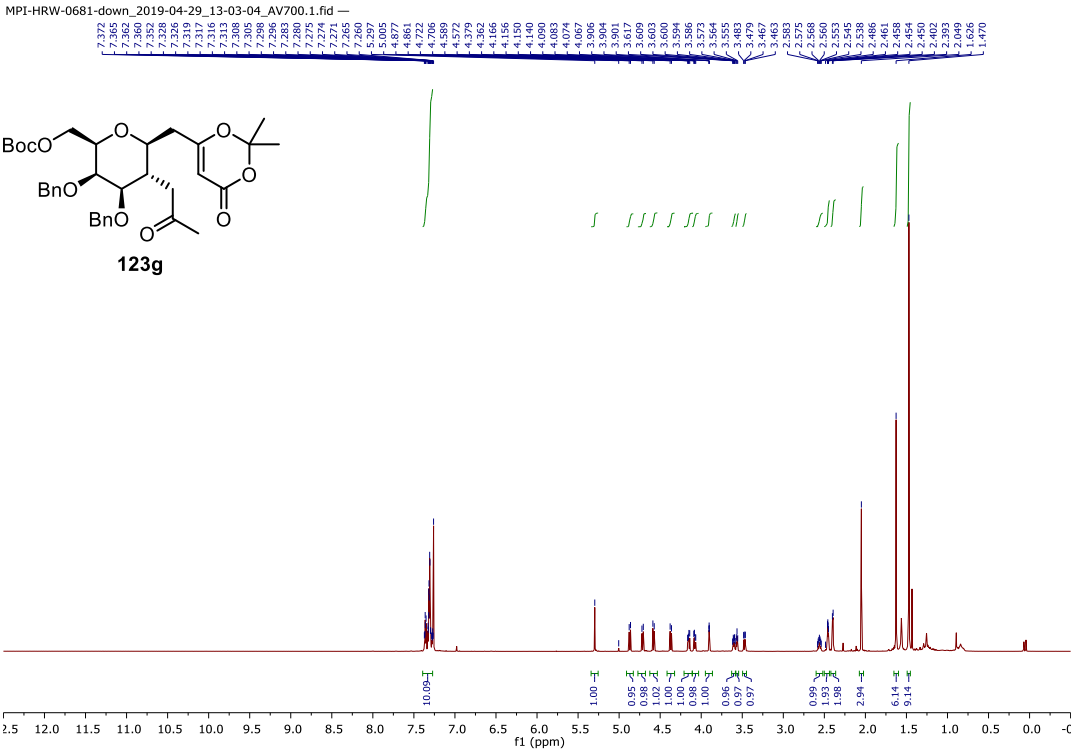

^{1}H NMR spectrum of compound **123g** (700 MHz, in $CDCl_3$)

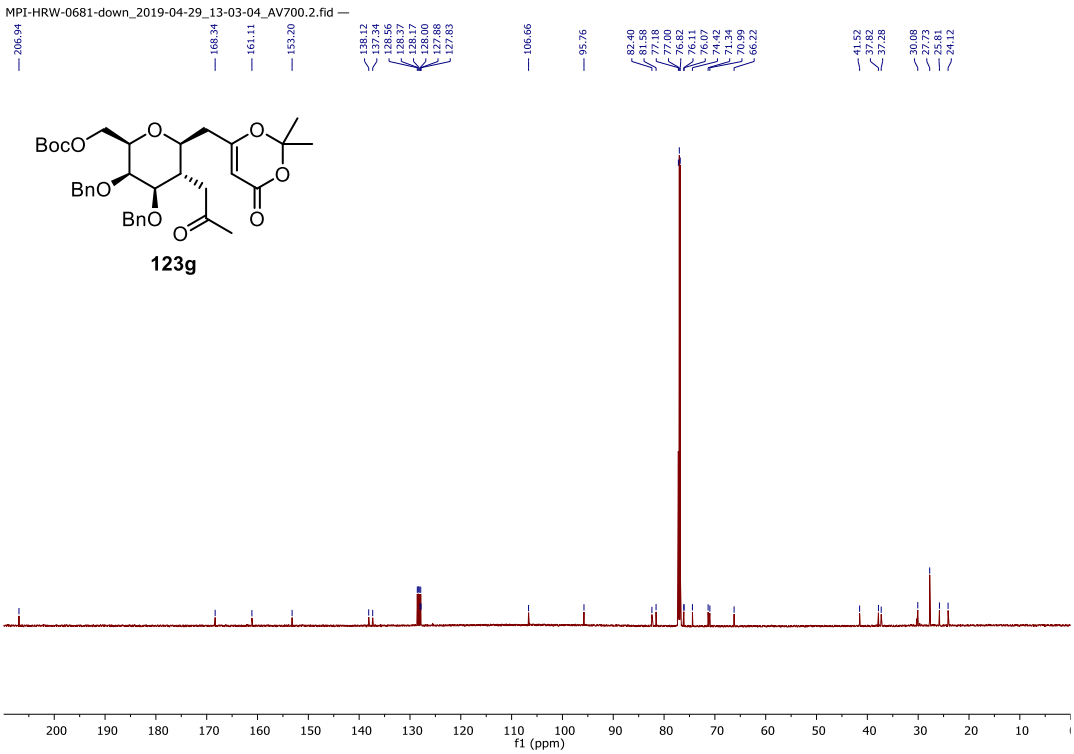

^{13}C NMR spectrum of compound **123g** (176 MHz, in $CDCl_3$)

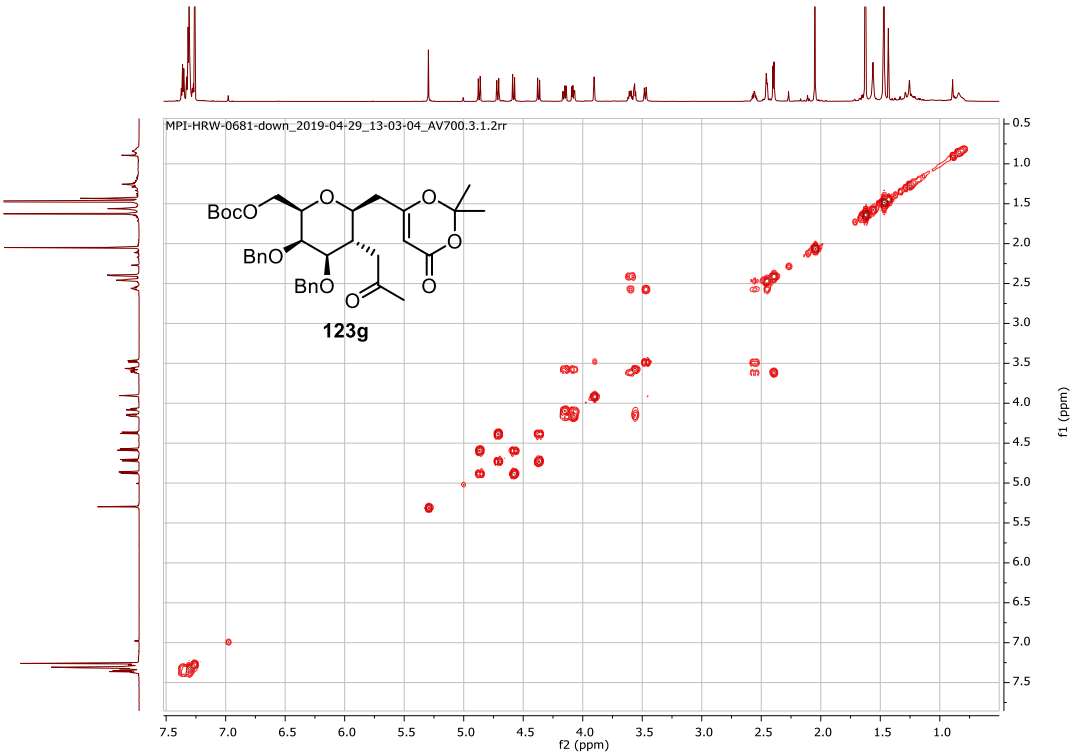

COSY spectrum of compound **123g**

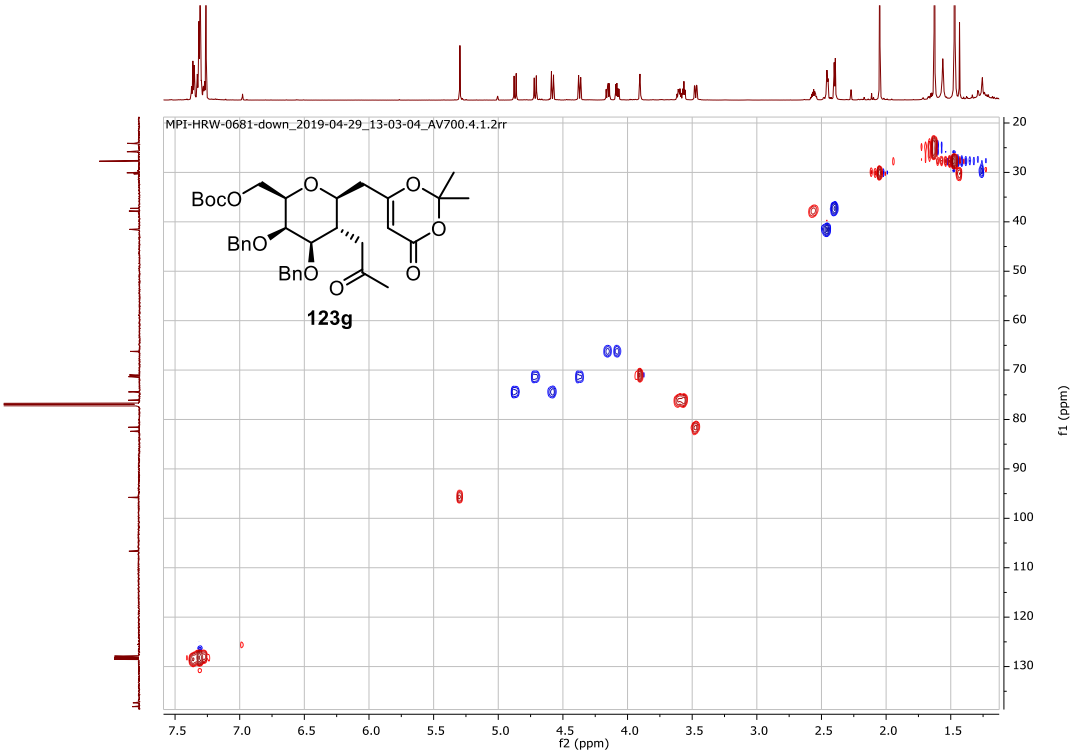

HSQC spectrum of compound **123g**

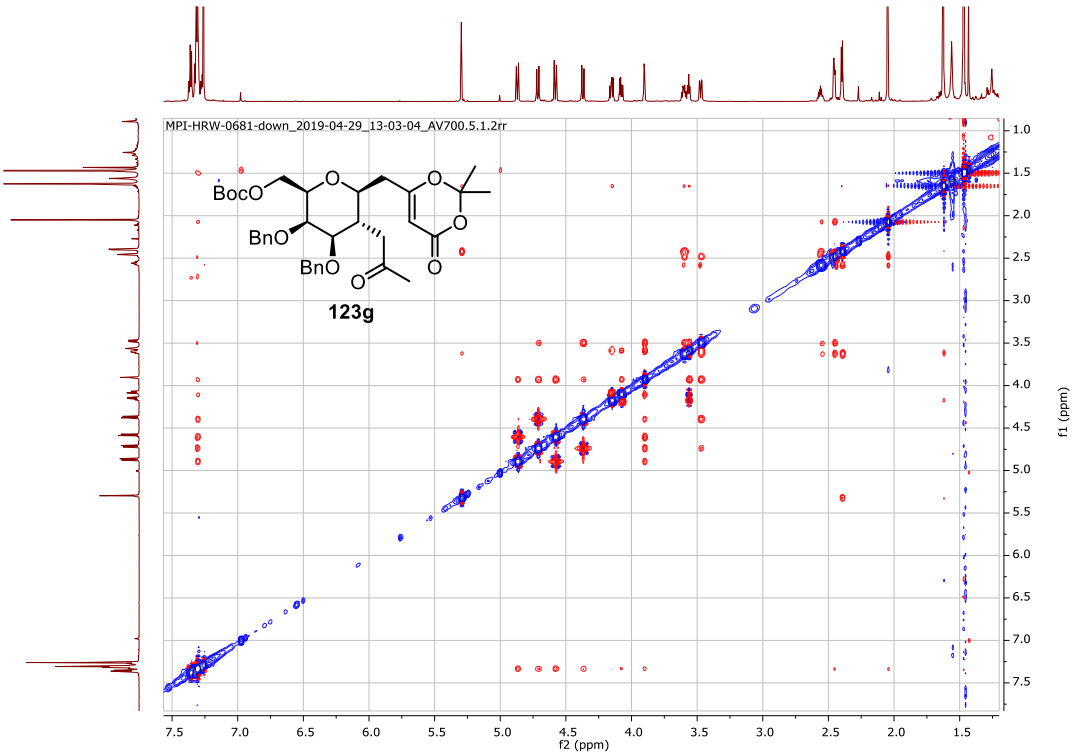

NOESY spectrum of compound **123g**

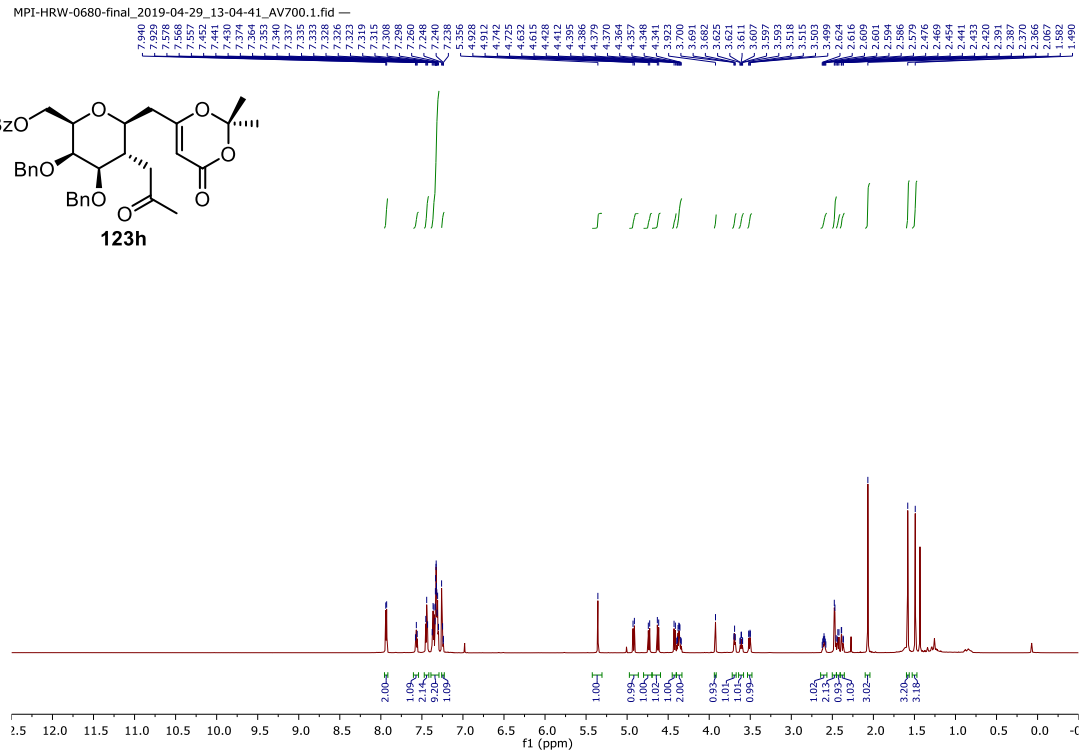

^{1}H NMR spectrum of compound **123h** (700 MHz, in $CDCl_3$)

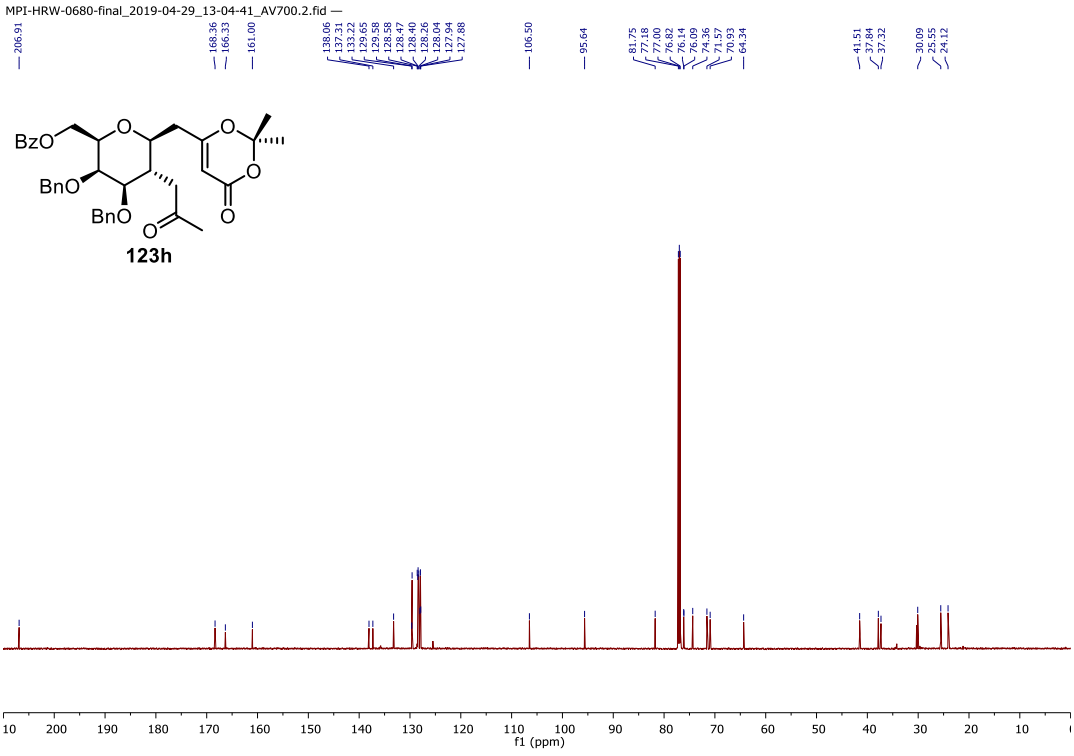

^{13}C NMR spectrum of compound **123h** (176 MHz, in $CDCl_3$)

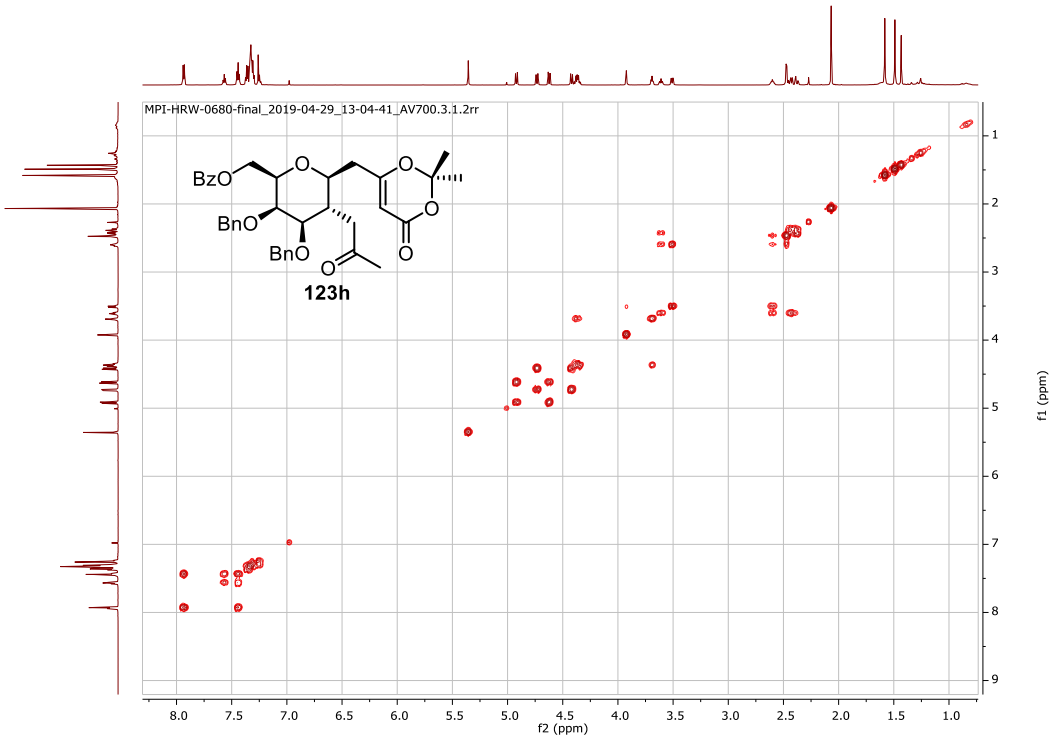

COSY spectrum of compound **123h**

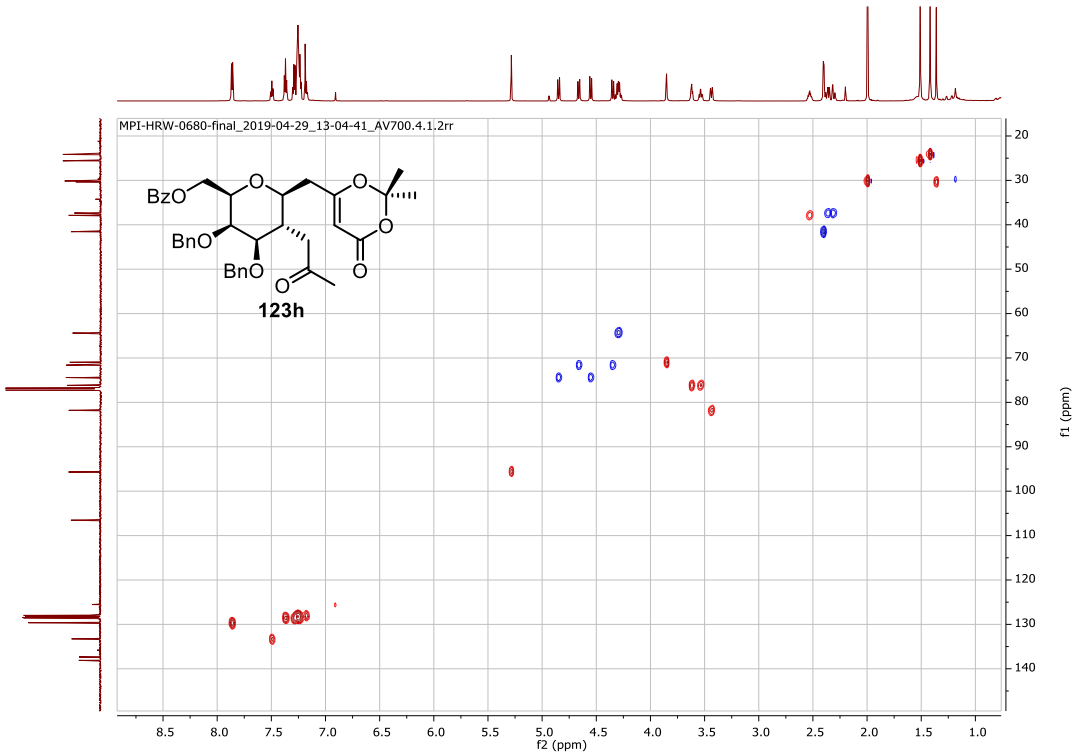

HSQC spectrum of compound **123h**

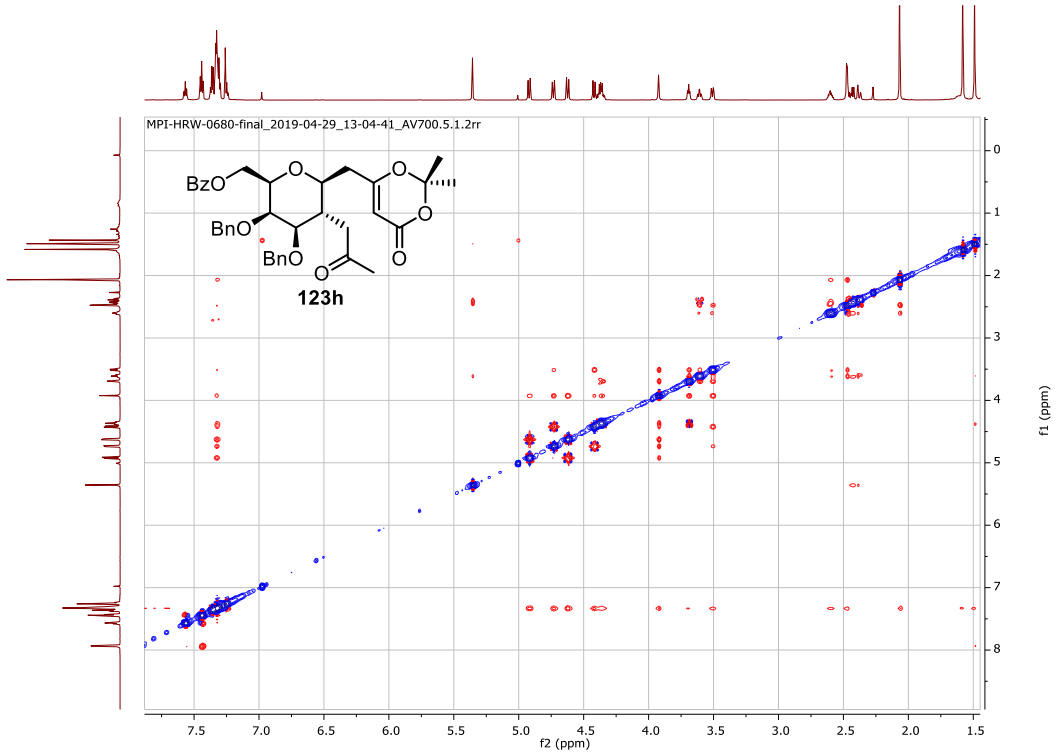

NOESY spectrum of compound **123h**

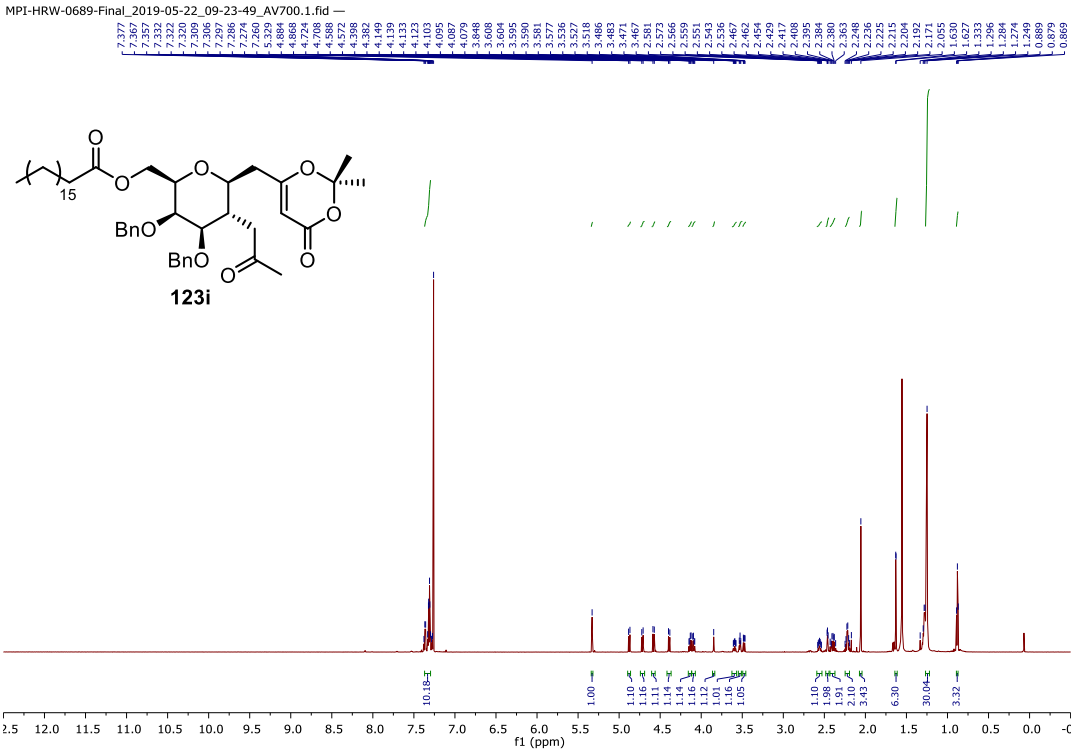

^{1}H NMR spectrum of compound **123i** (700 MHz, in $CDCl_3$)

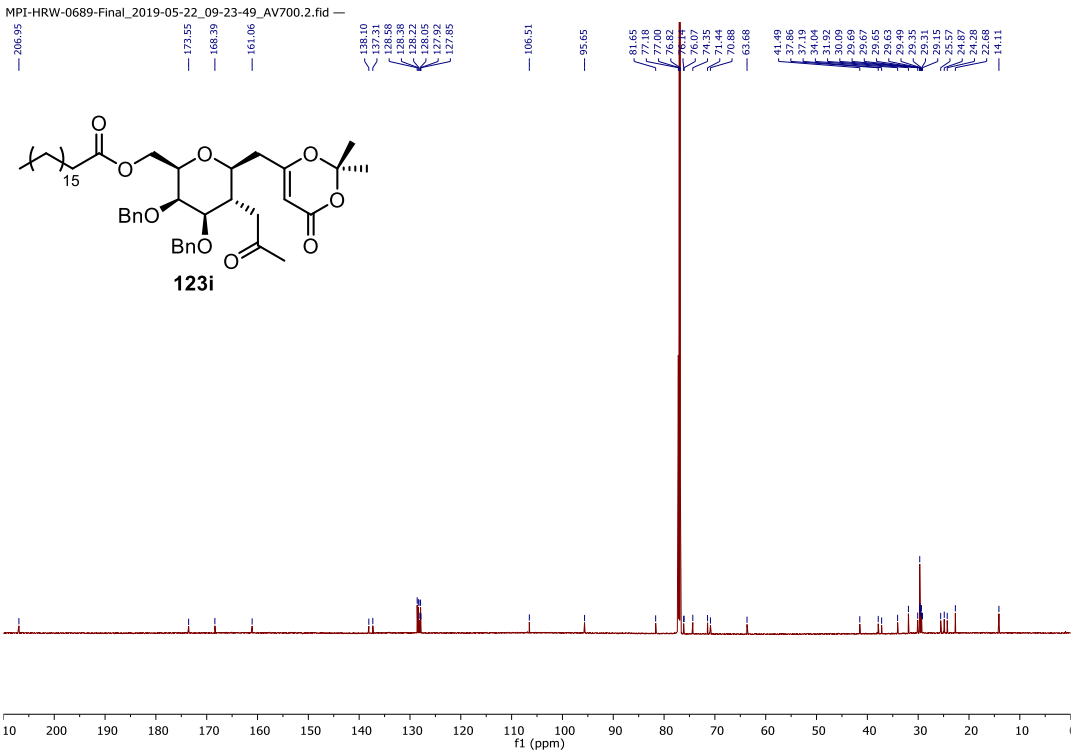

^{13}C NMR spectrum of compound **123i** (176 MHz, in $CDCl_3$)

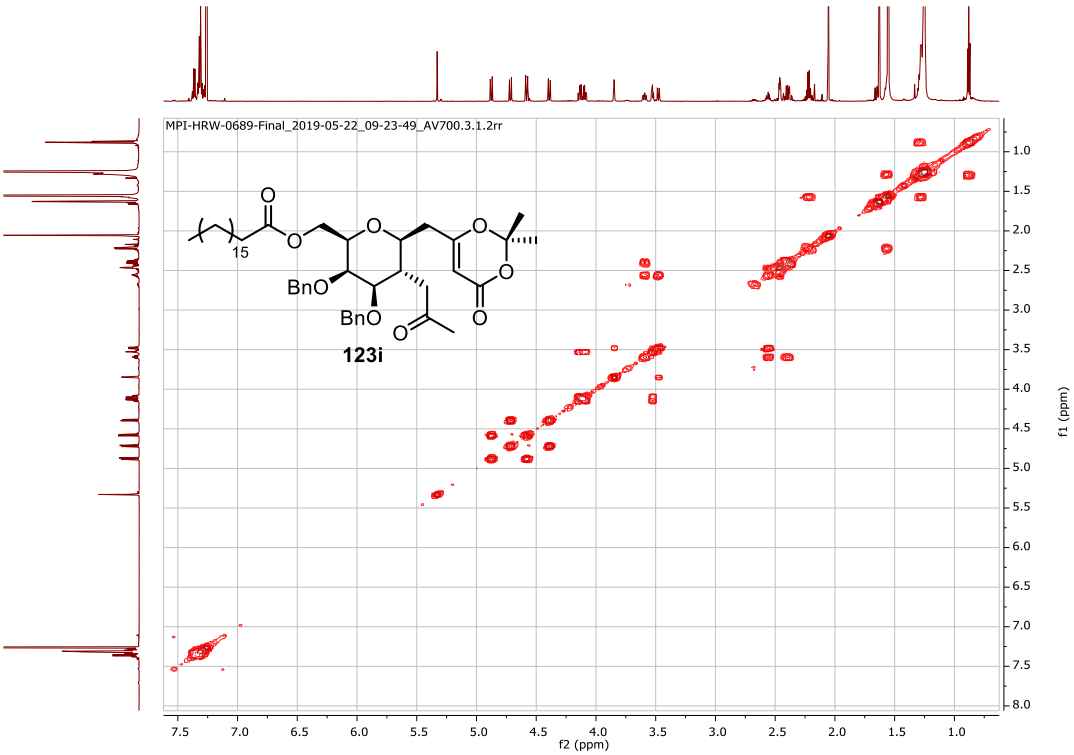

COSY spectrum of compound **123i**

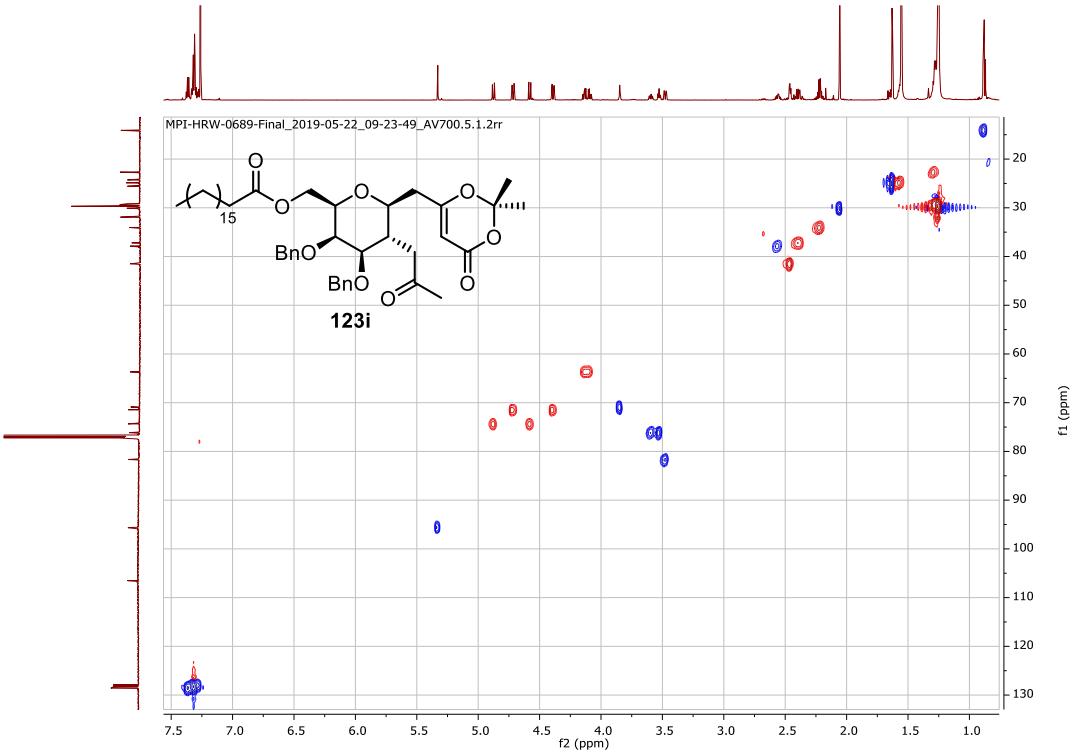

HSQC spectrum of compound **123i**

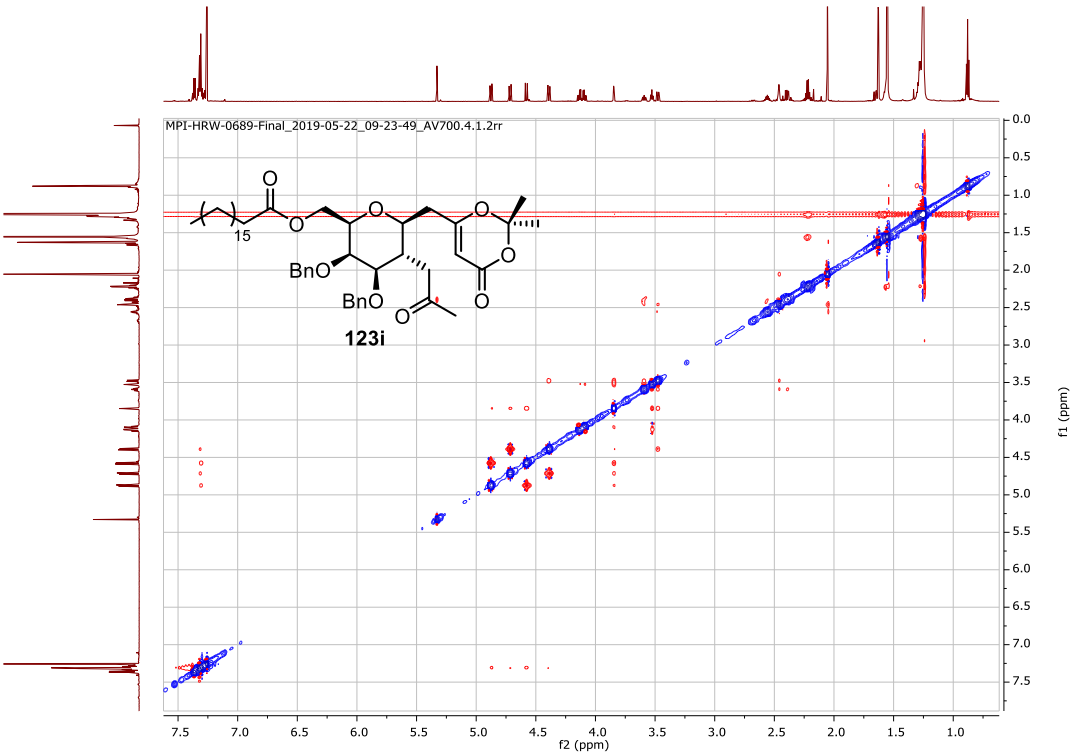

NOESY spectrum of compound **123i**

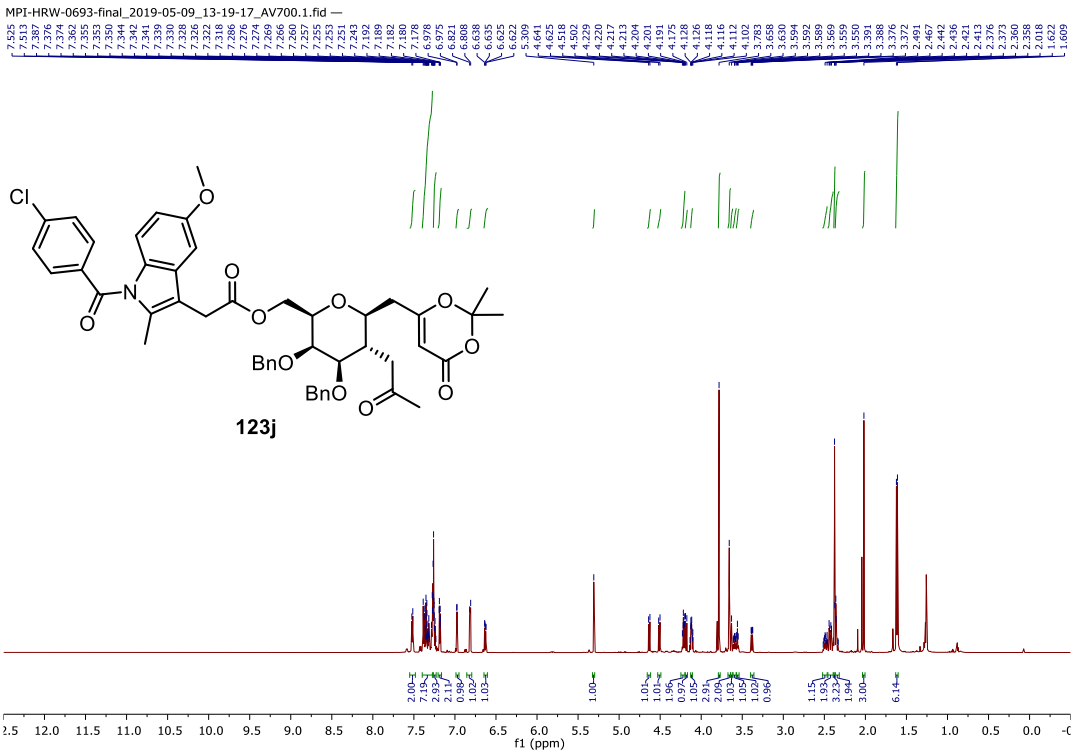

^{1}H NMR spectrum of compound **123j** (700 MHz, in $CDCl_3$)

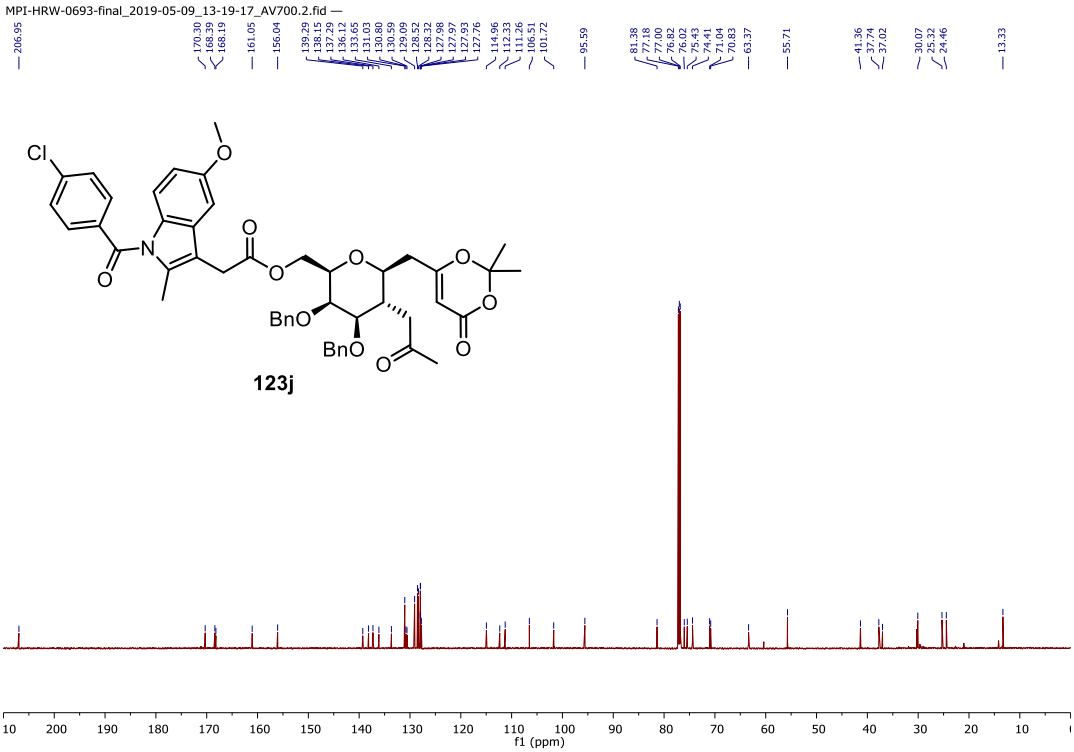

^{13}C NMR spectrum of compound **123j** (176 MHz, in $CDCl_3$)

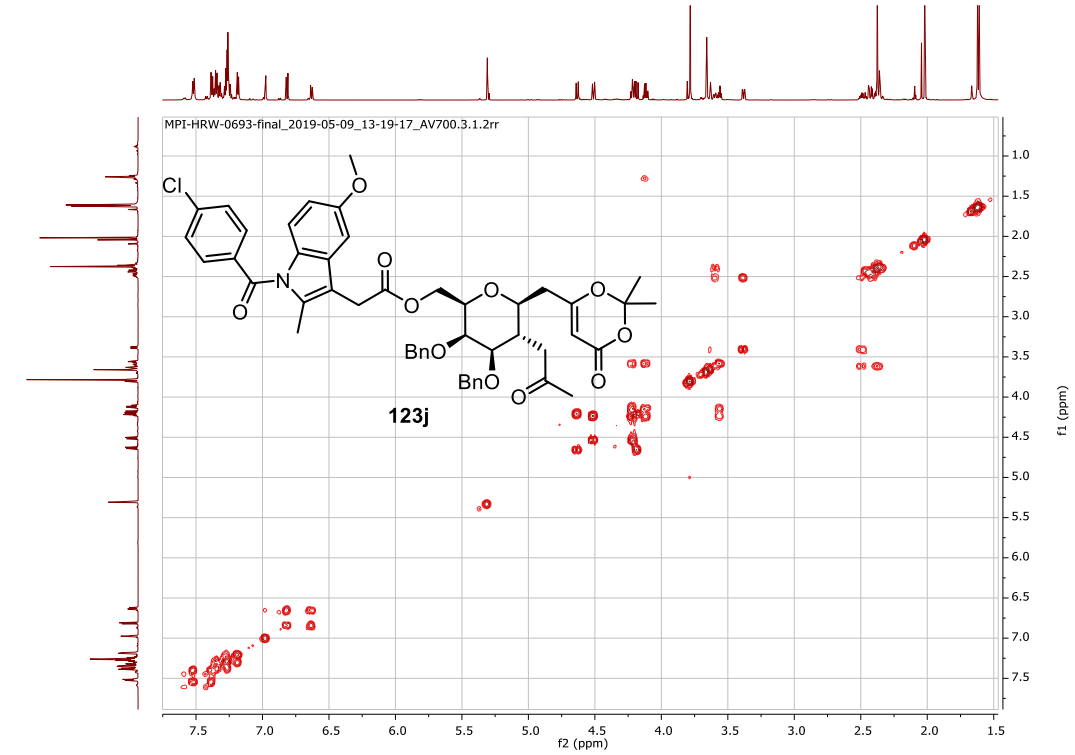

COSY spectrum of compound **123j**

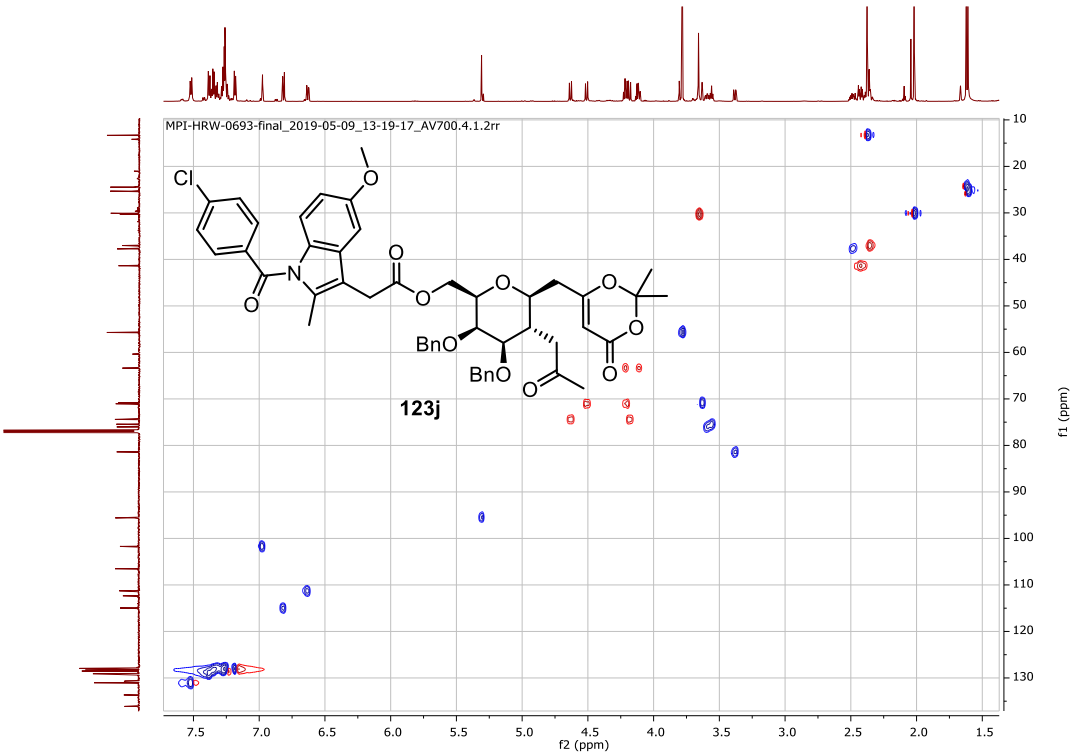

HSQC spectrum of compound **123j**

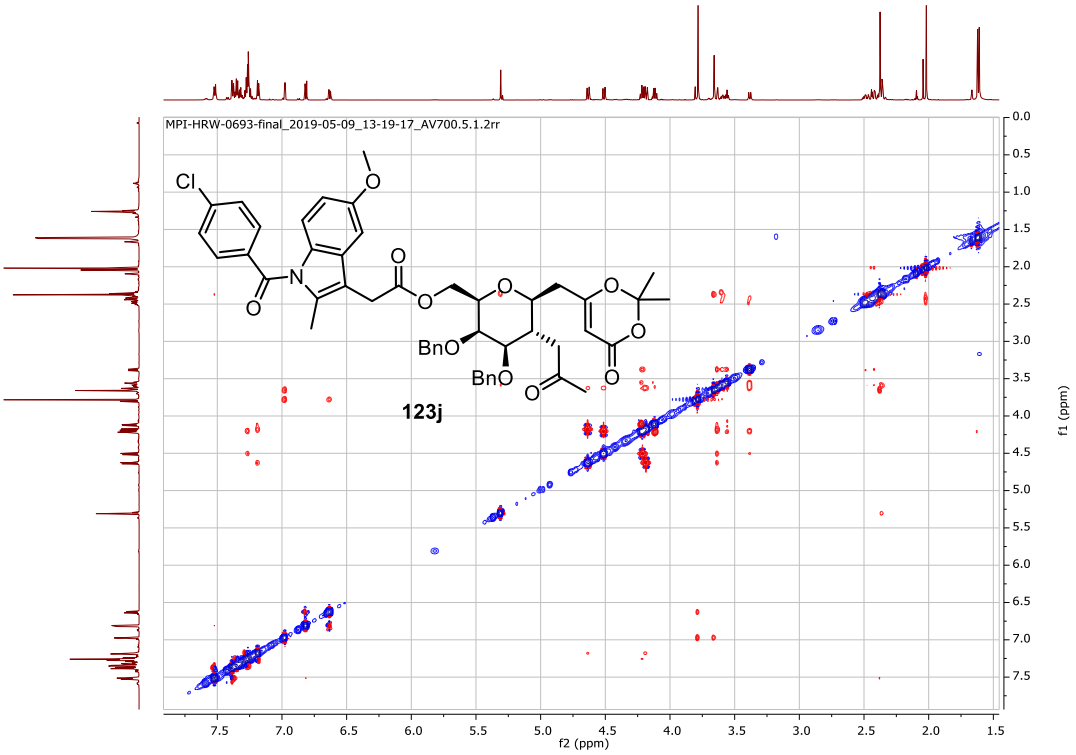

NOESY spectrum of compound **123j**

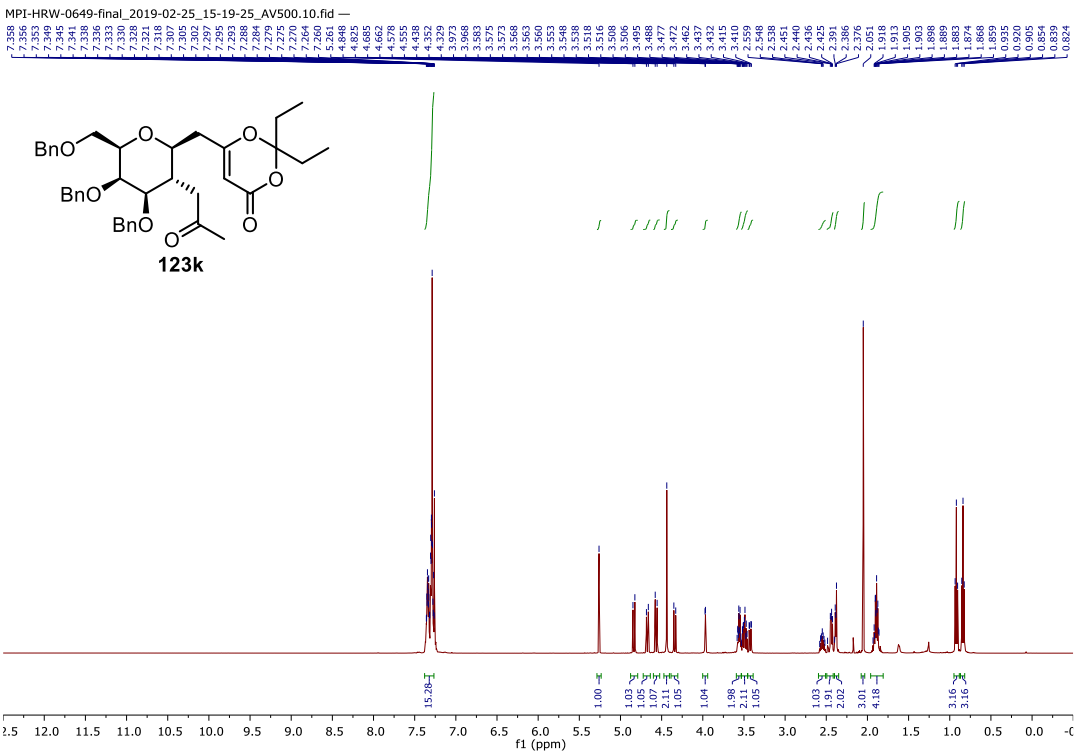

^{1}H NMR spectrum of compound **123k** (500 MHz, in $CDCl_3$)

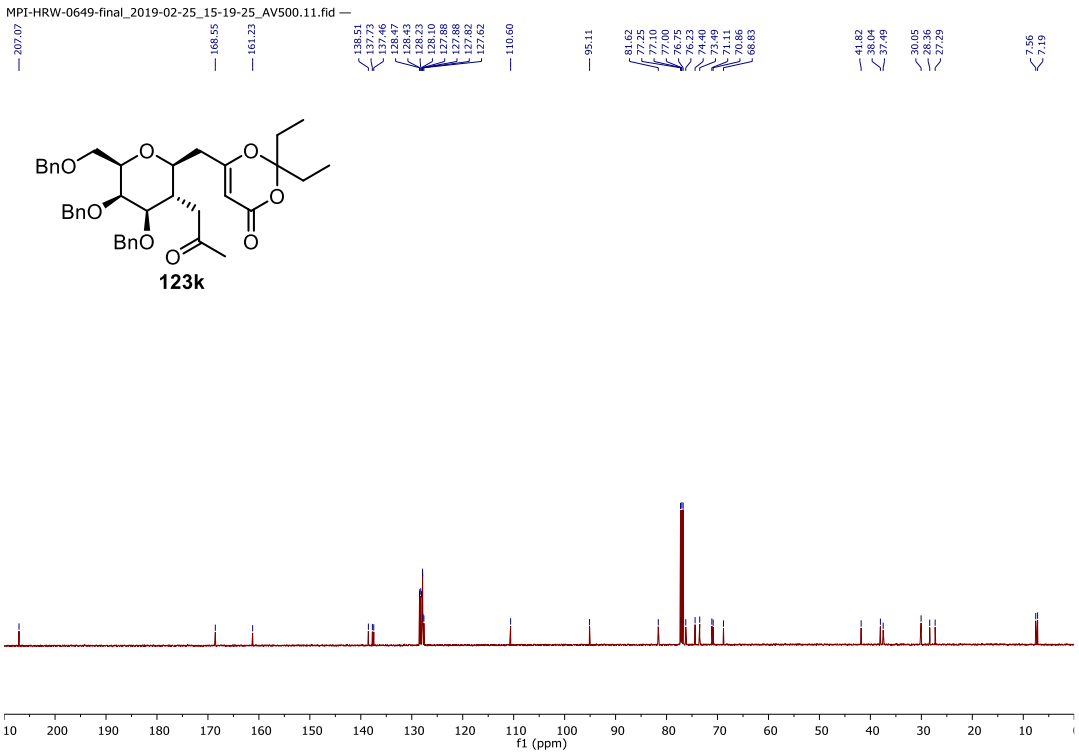

^{13}C NMR spectrum of compound **123k** (126 MHz, in $CDCl_3$)

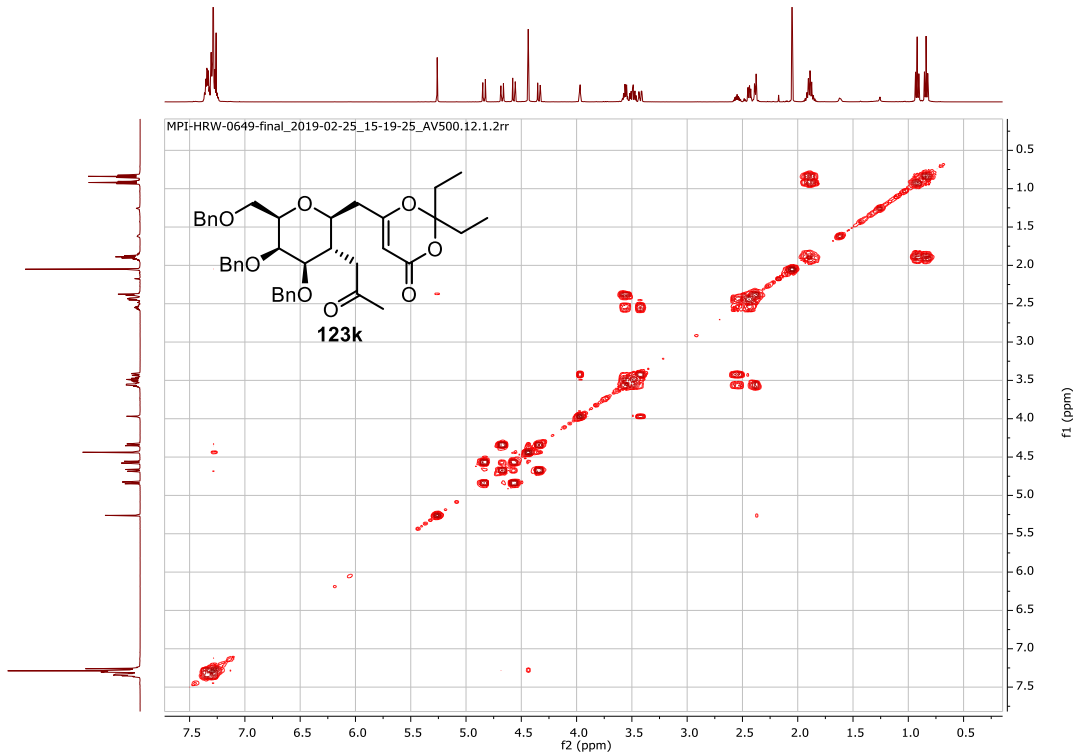

NOSY spectrum of compound **123k**

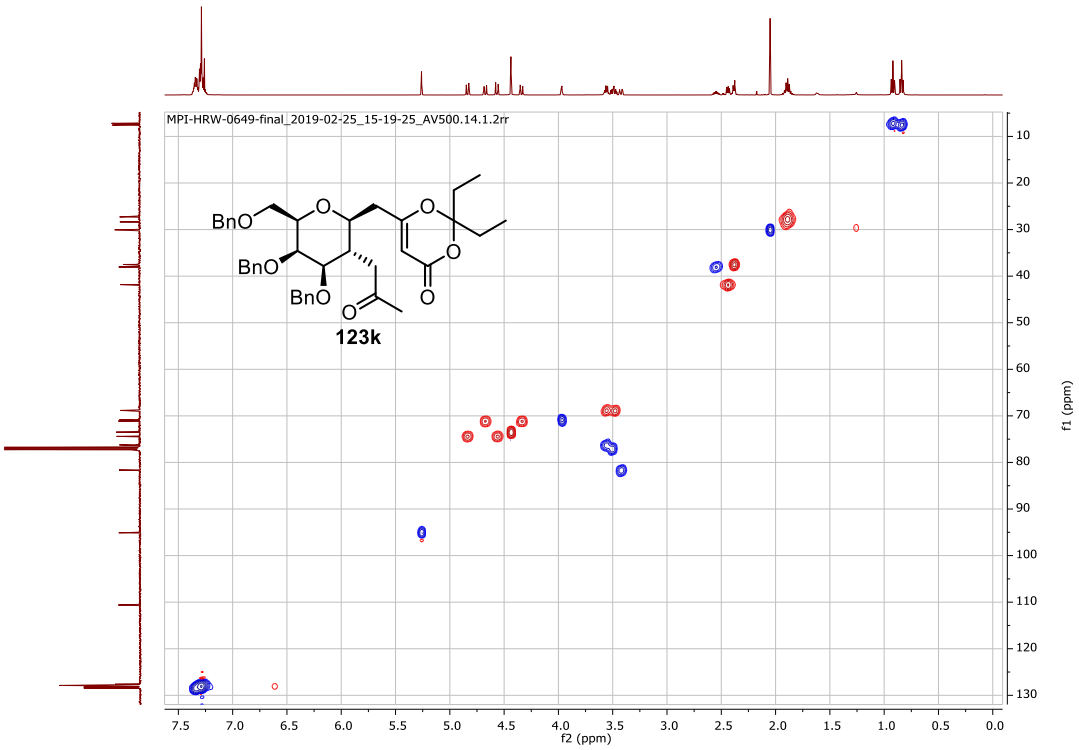

HSQC spectrum of compound **123k**

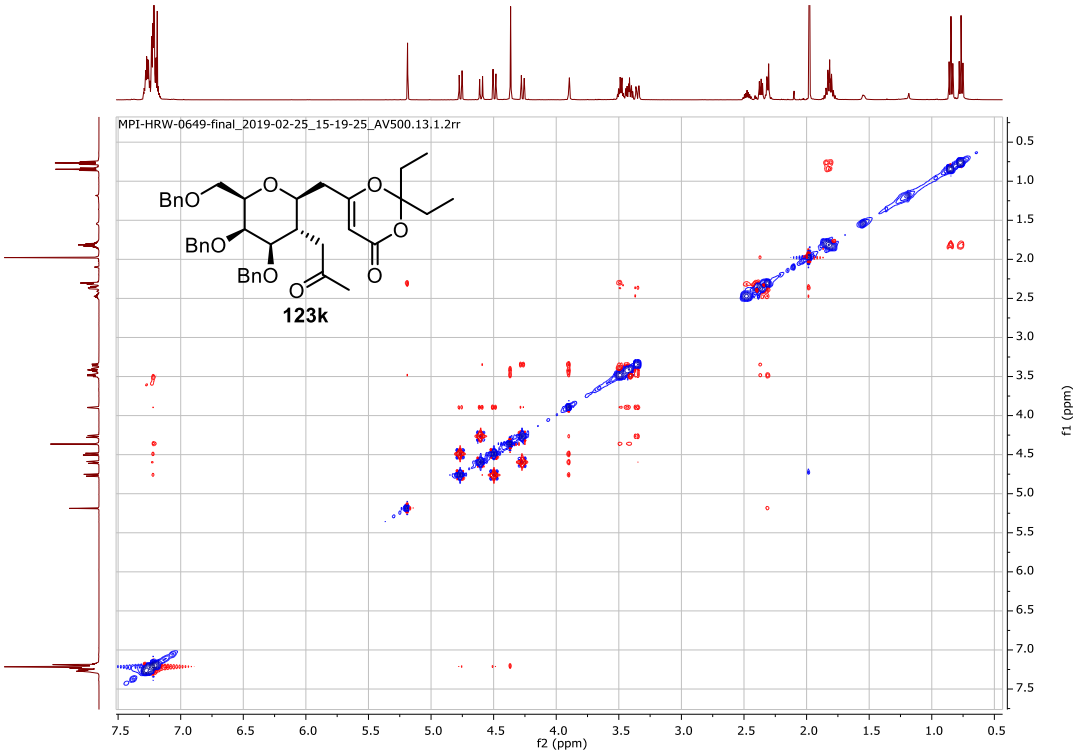

NOESY spectrum of compound **123k**

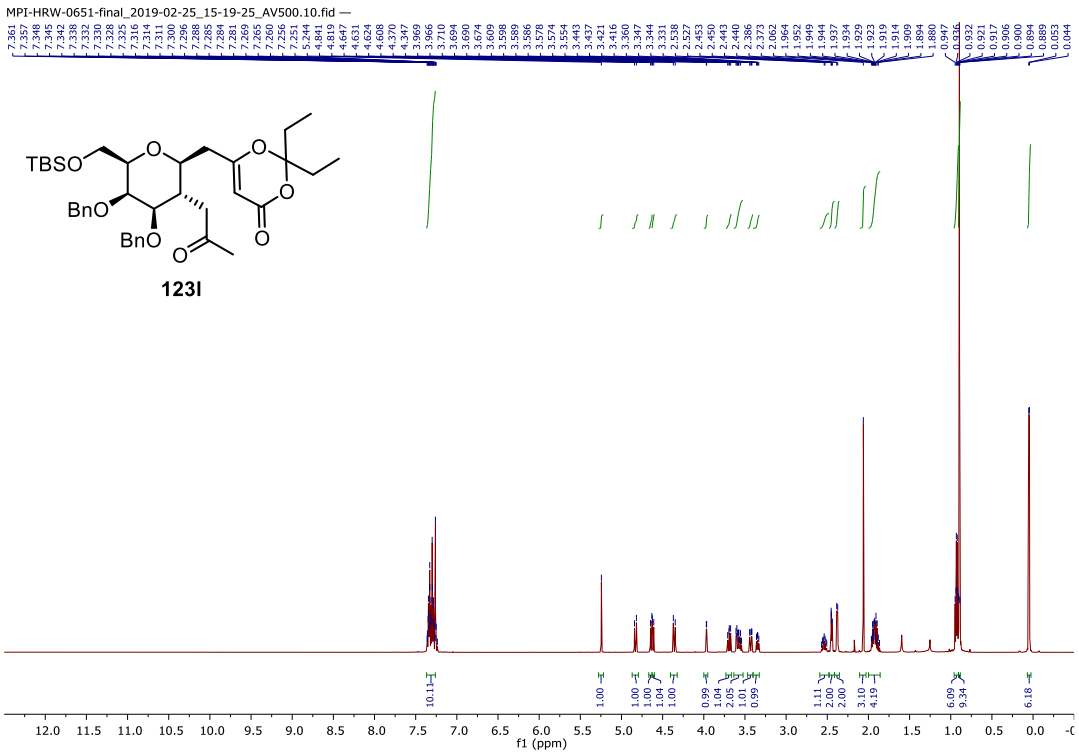

^{1}H NMR spectrum of compound **123l** (500 MHz, in $CDCl_3$)

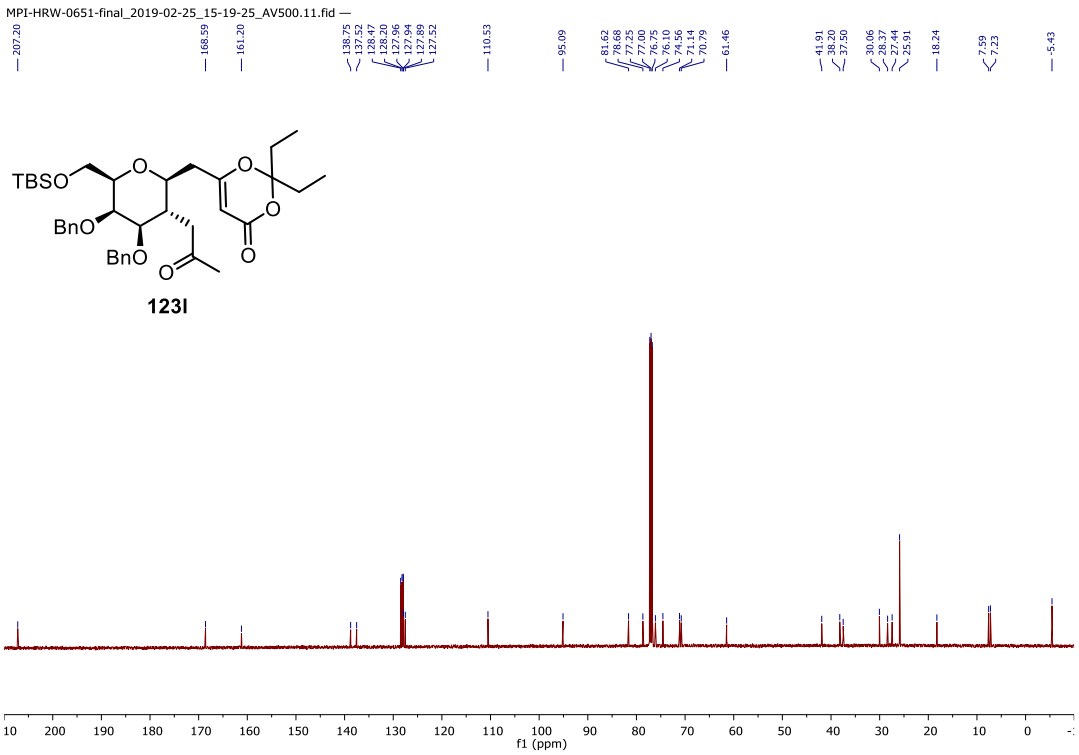

^{13}C NMR spectrum of compound **123l** (126 MHz, in $CDCl_3$)

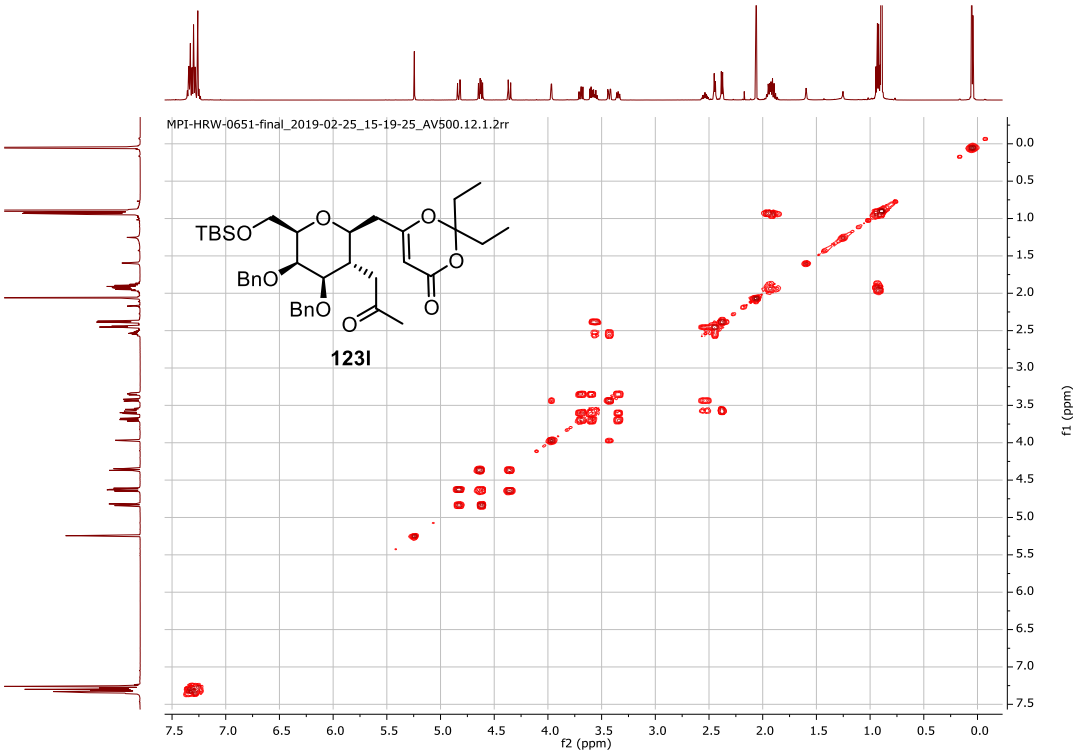

COSY spectrum of compound **123l**

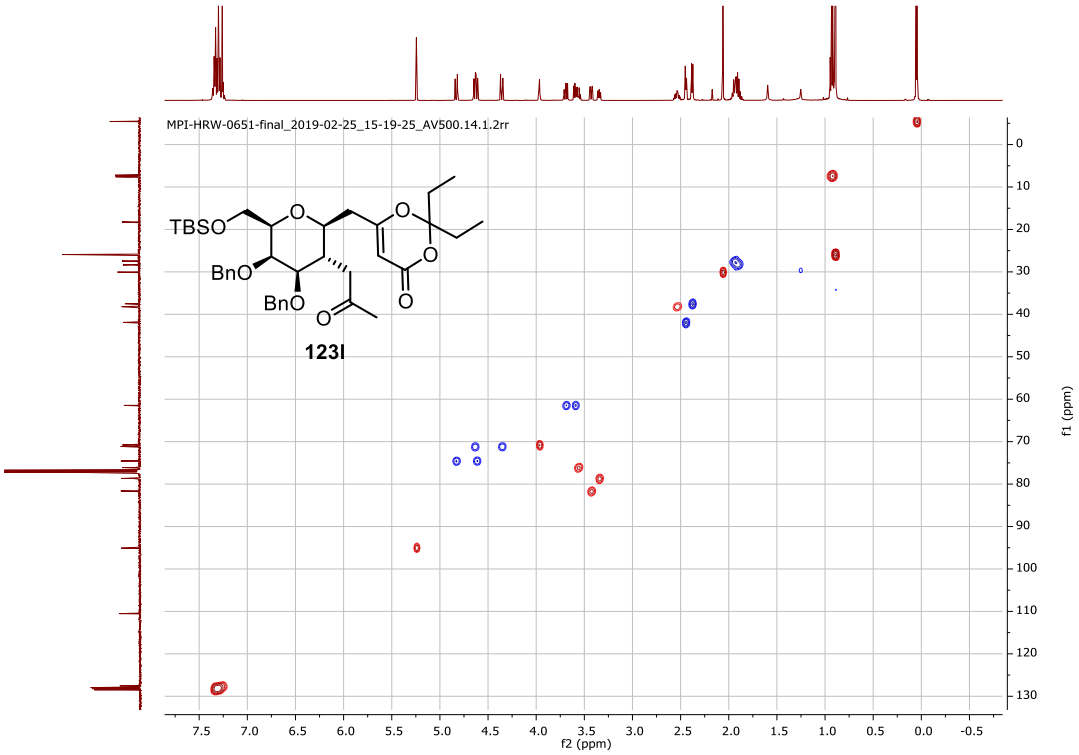

HSQC spectrum of compound **123l**

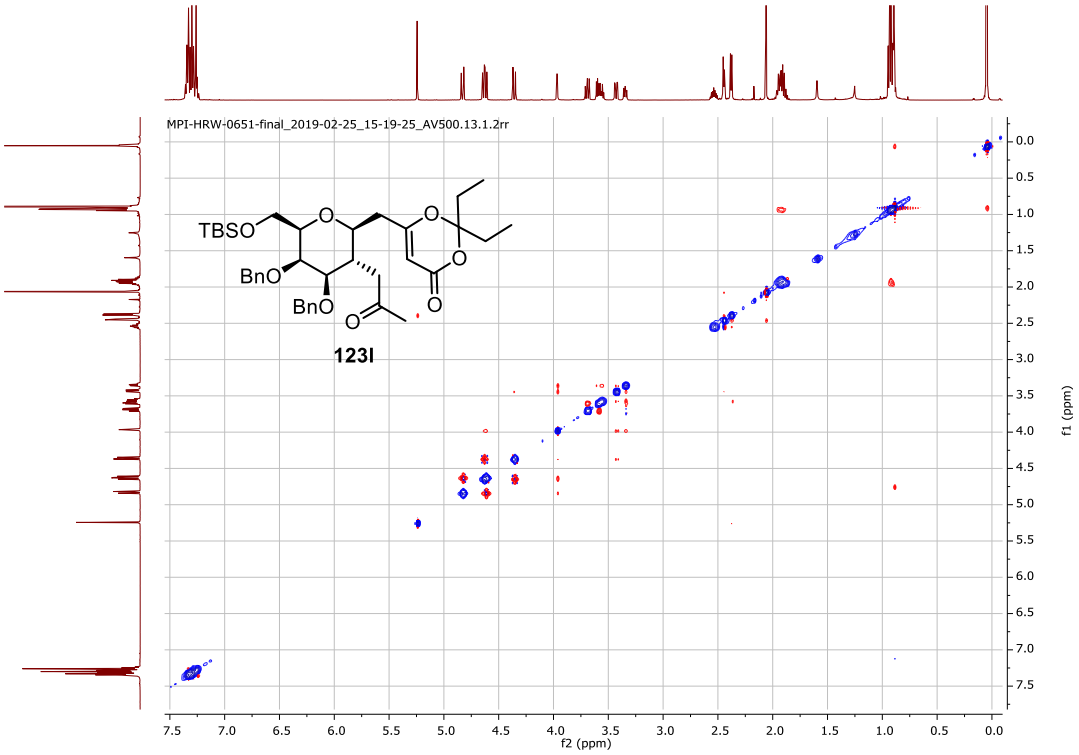

NOESY spectrum of compound **123l**

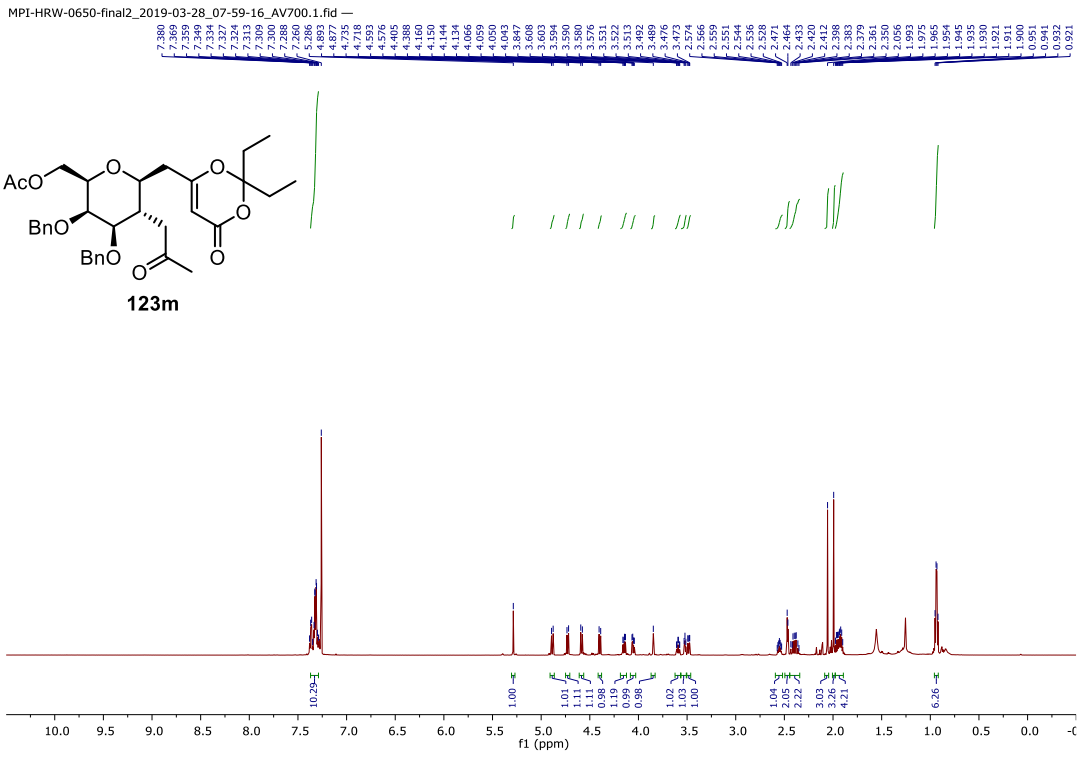

^{1}H NMR spectrum of compound **123m** (700 MHz, in $CDCl_3$)

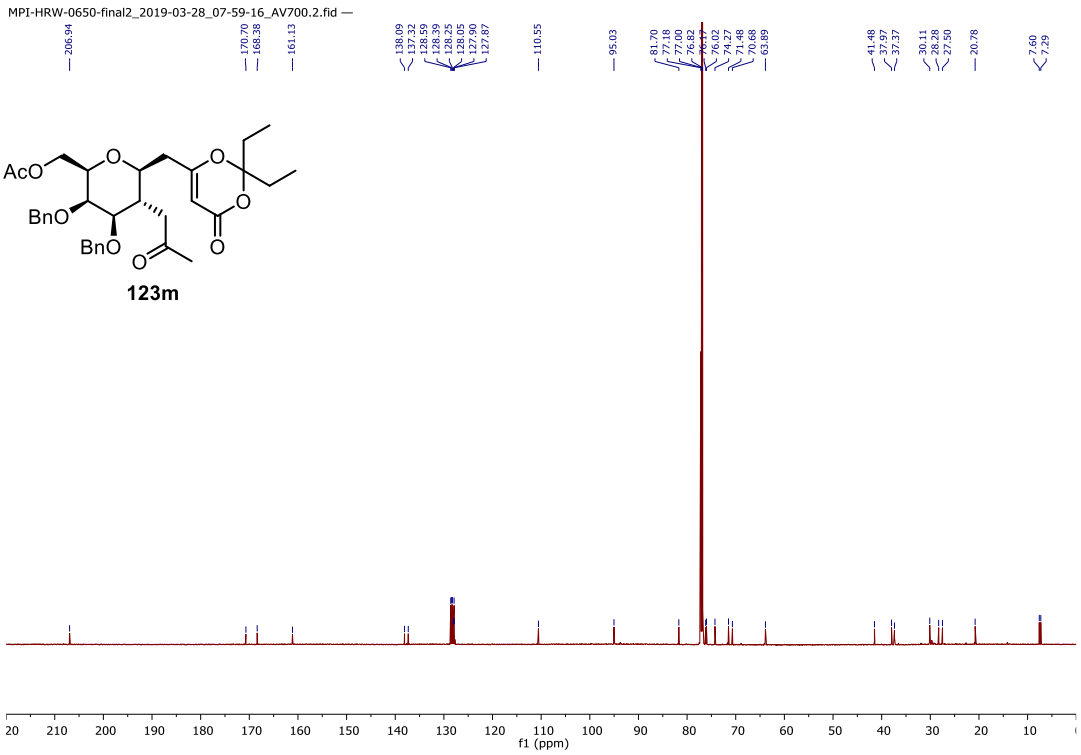

^{13}C NMR spectrum of compound **123m** (176 MHz, in $CDCl_3$)

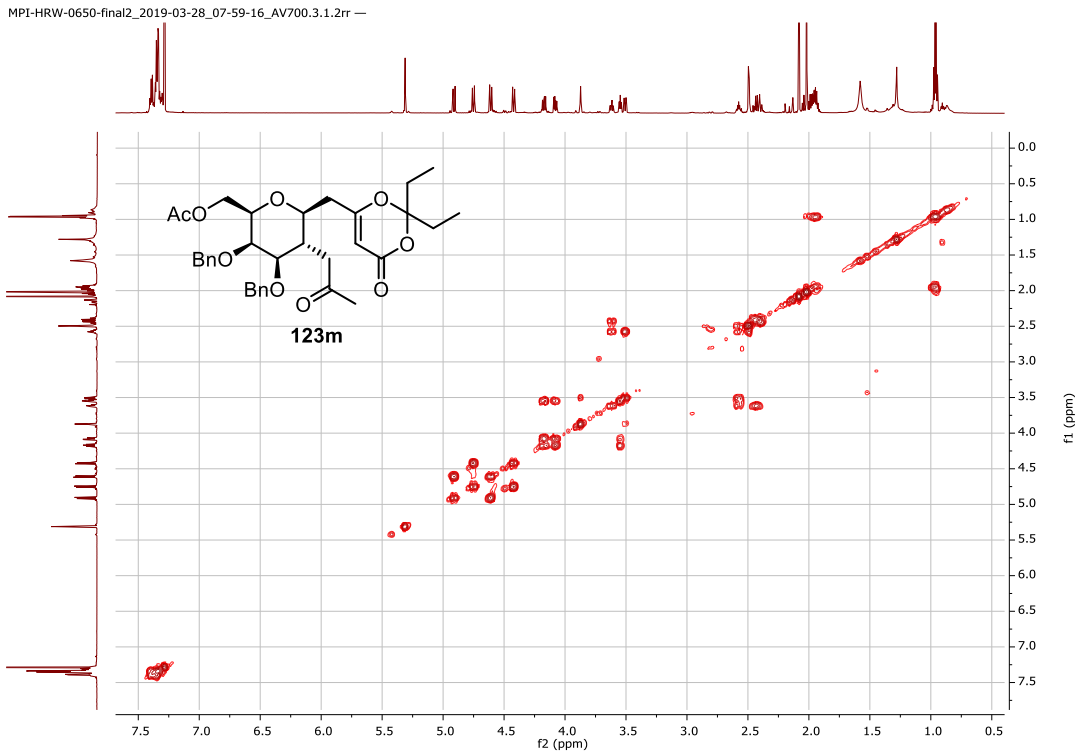

COSY spectrum of compound **123m**

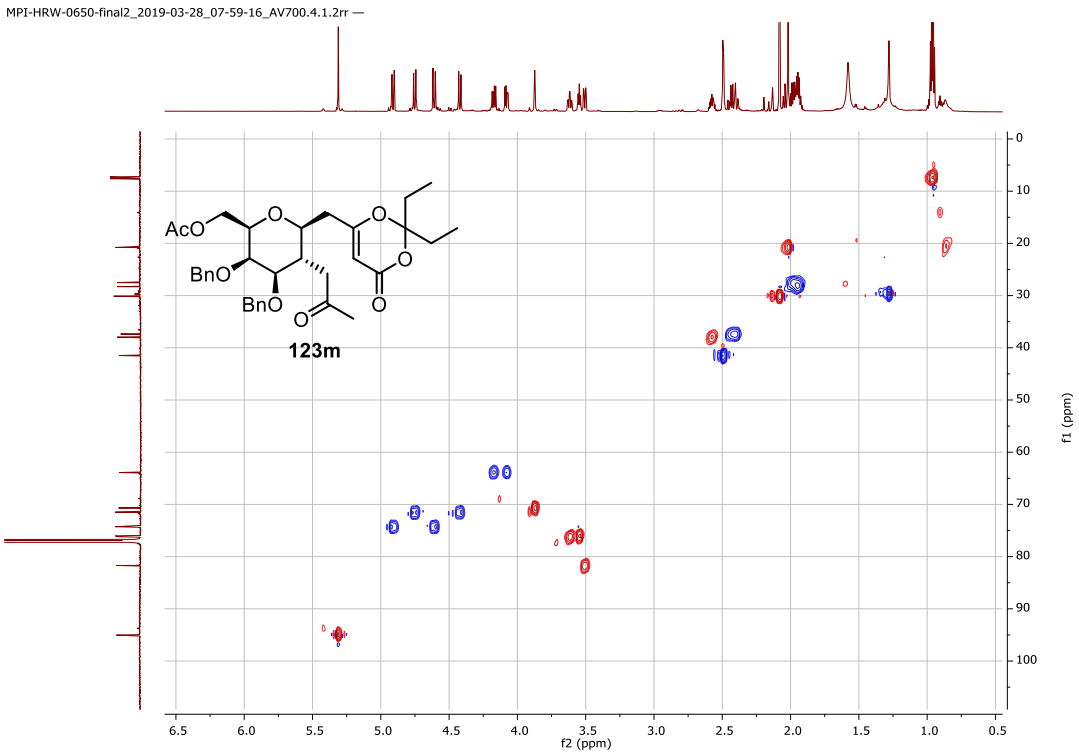

HSQC spectrum of compound **123m**

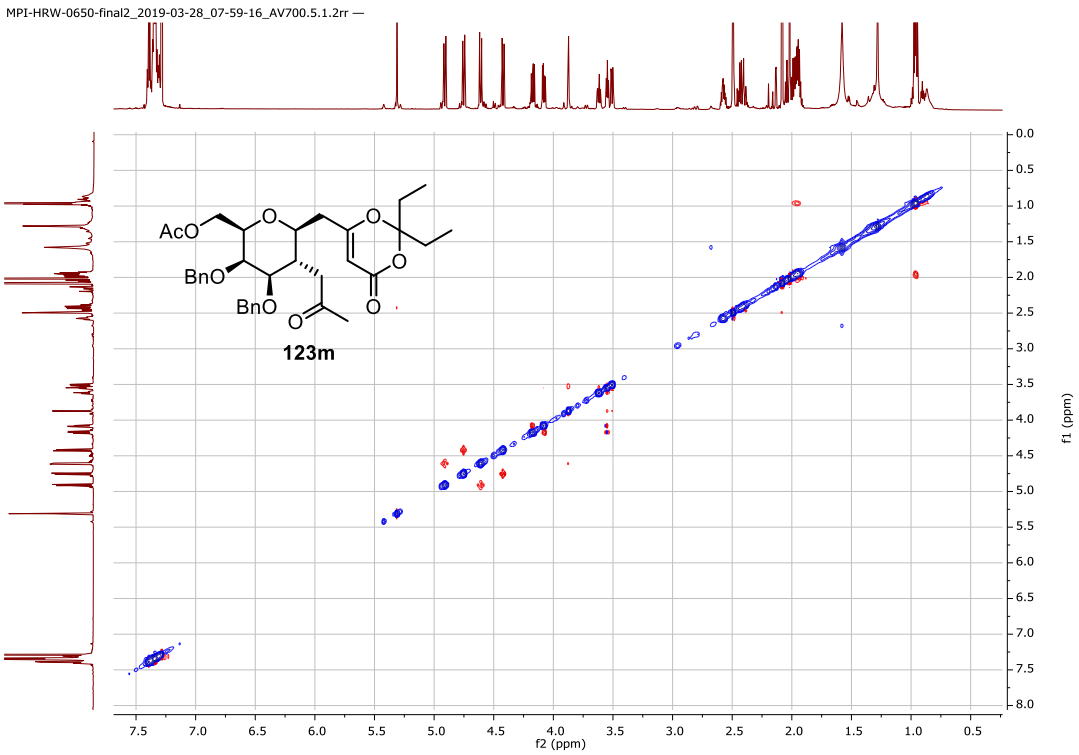

NOESY spectrum of compound **123m**

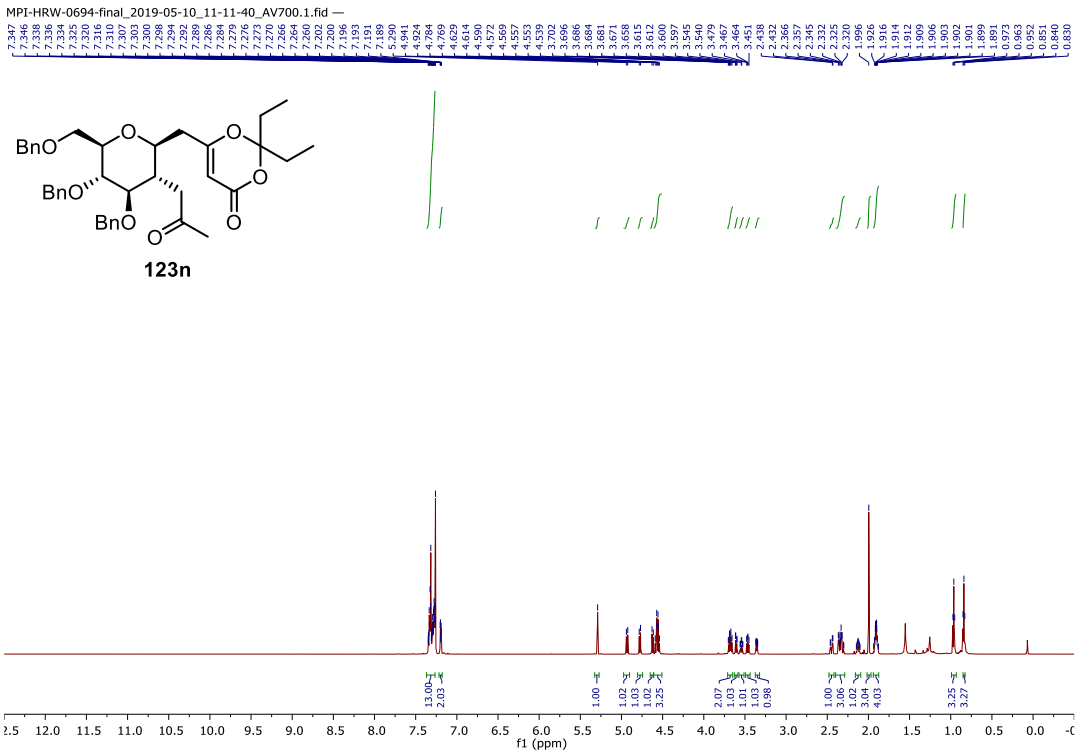

^{1}H NMR spectrum of compound **123n** (700 MHz, in $CDCl_3$)

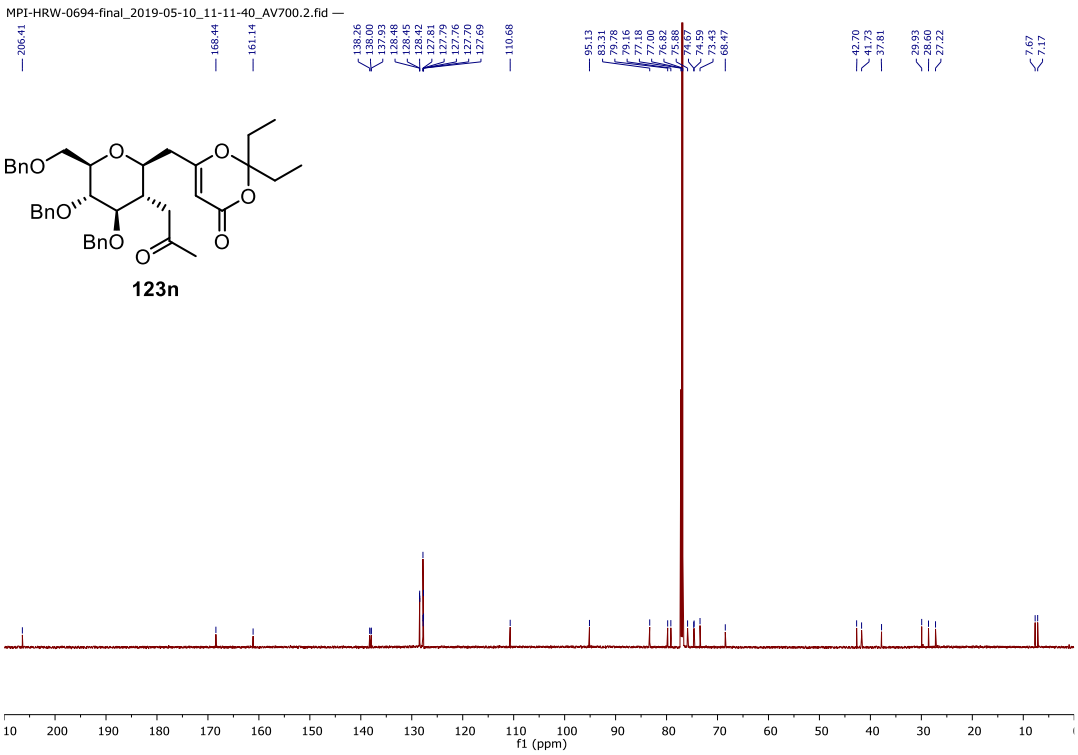

^{13}C NMR spectrum of compound **123n** (176 MHz, in $CDCl_3$)

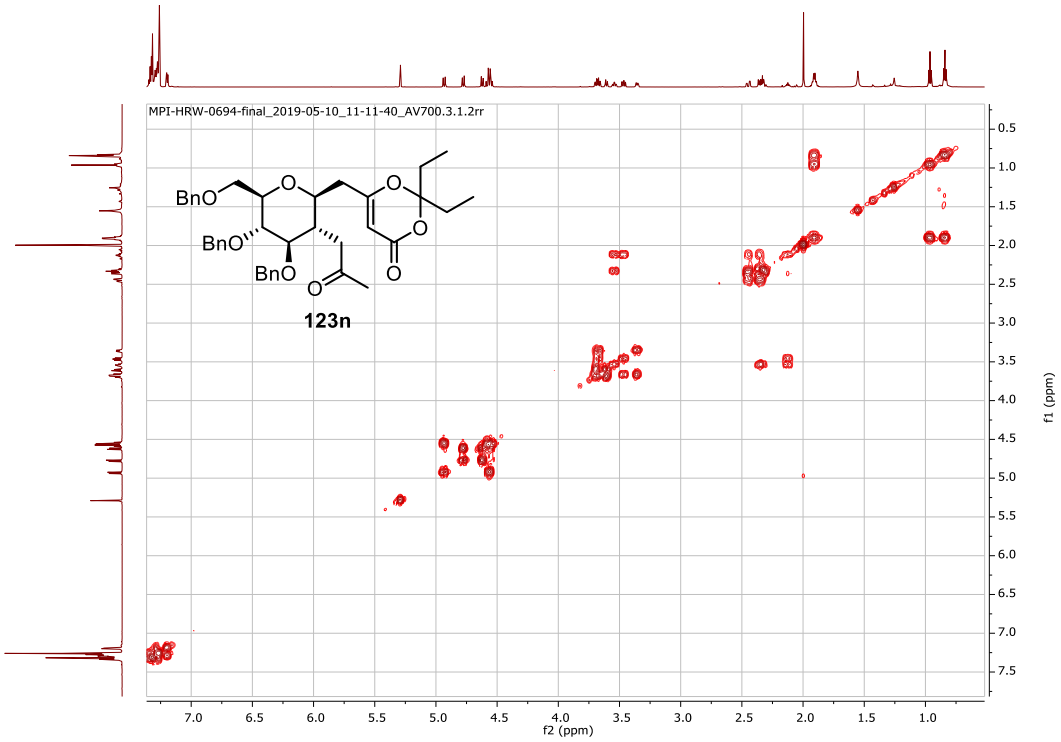

COSY spectrum of compound **123n**

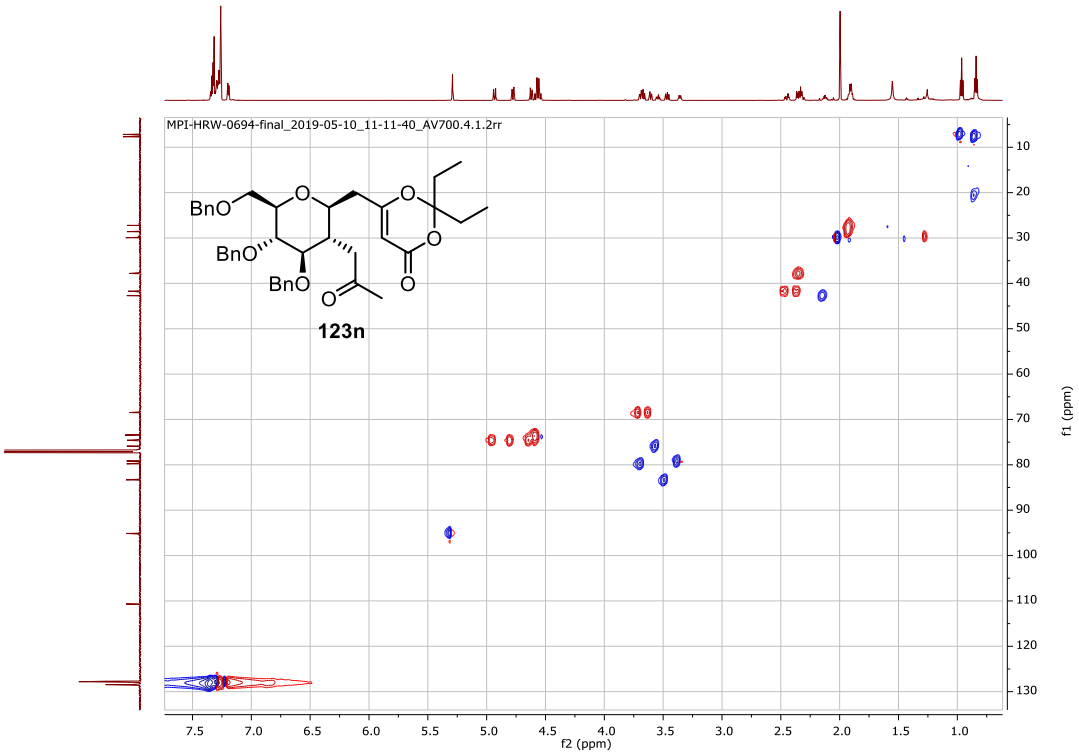

HSQC spectrum of compound **123n**

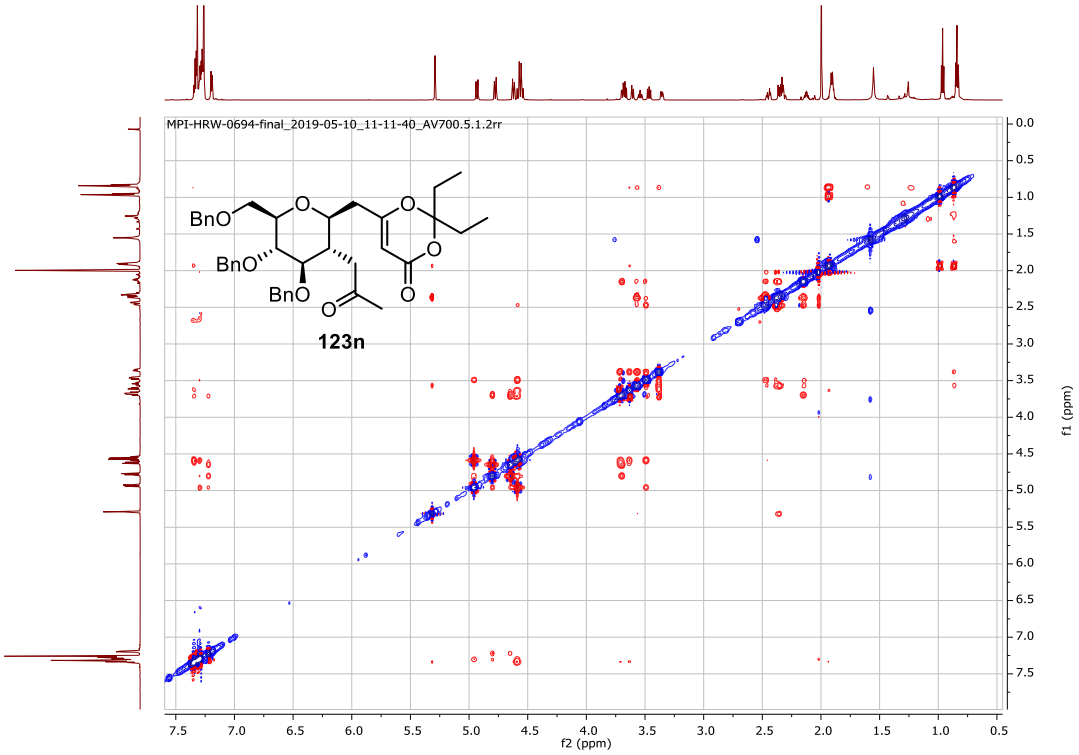

NOESY spectrum of compound **123n**

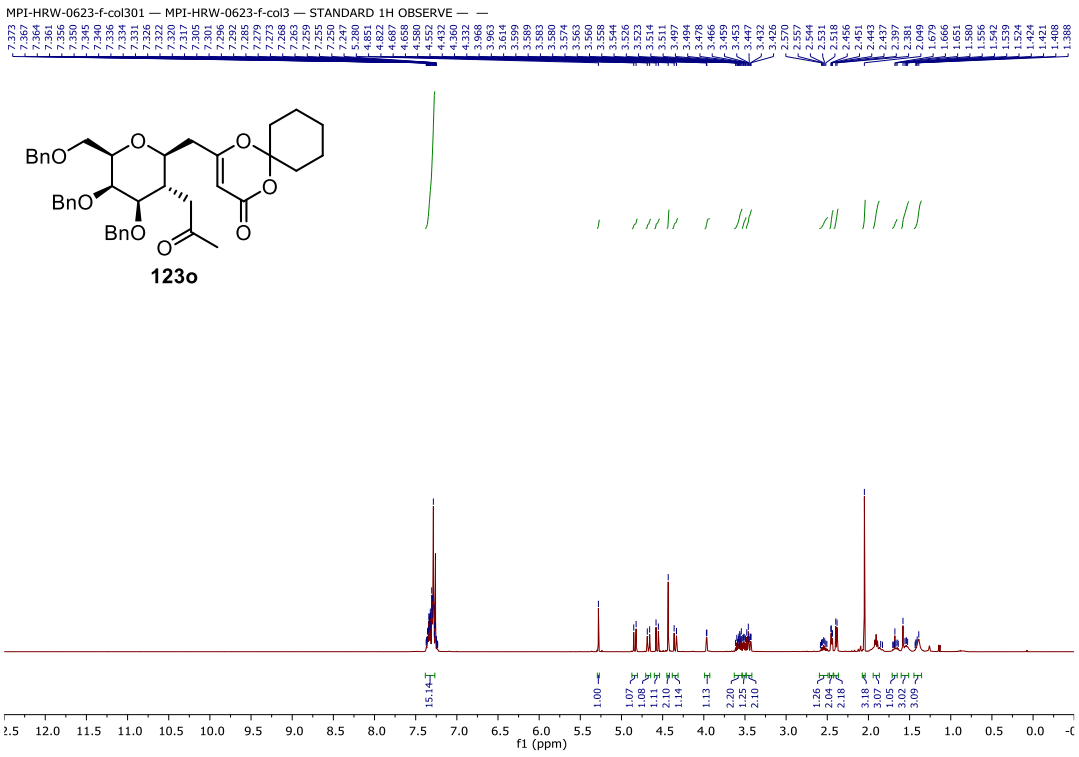

^{1}H NMR spectrum of compound **123o** (500 MHz, in $CDCl_3$)

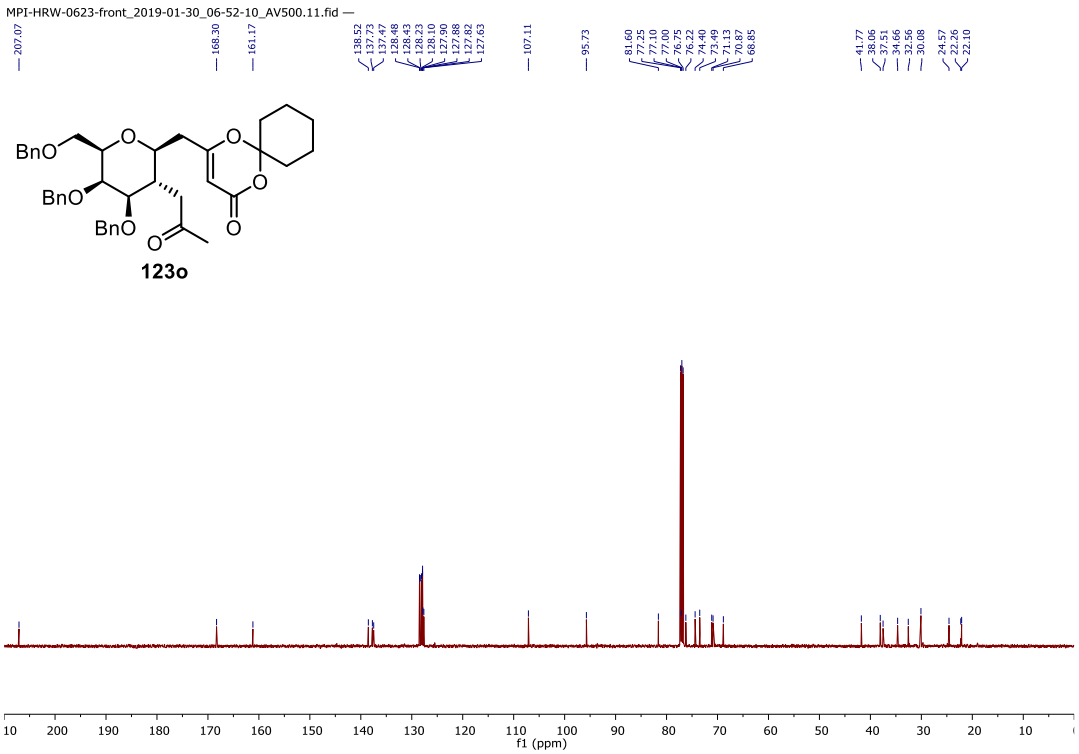

^{13}C NMR spectrum of compound **123o** (126 MHz, in $CDCl_3$)

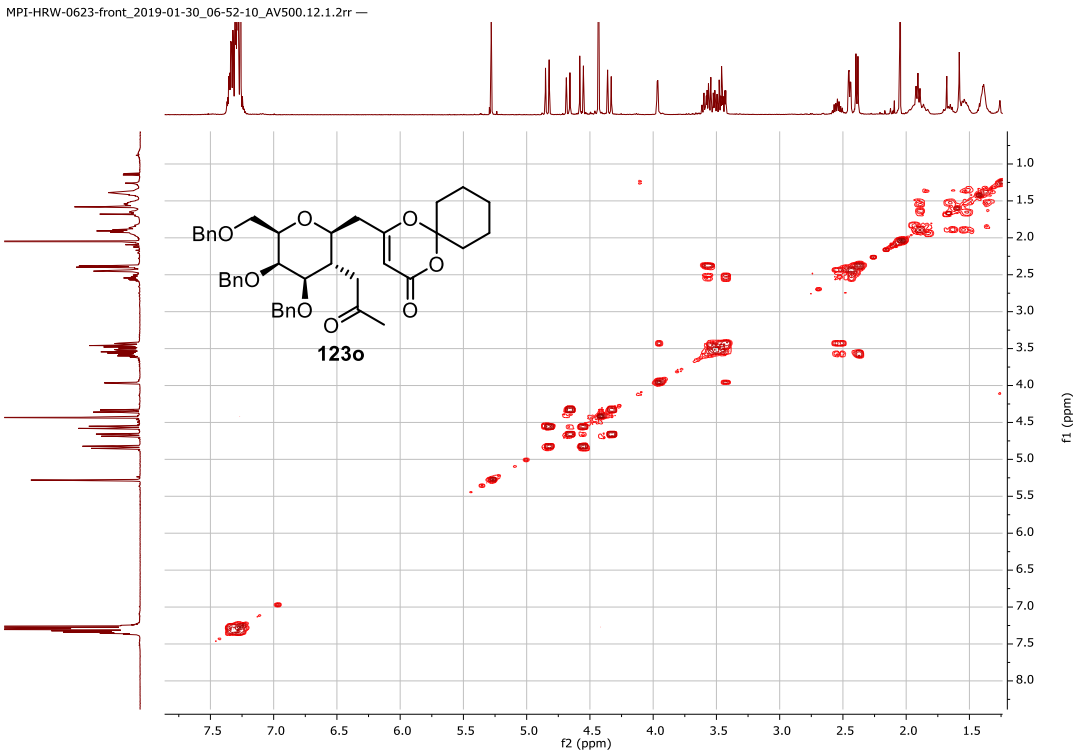

COSY spectrum of compound **123o**

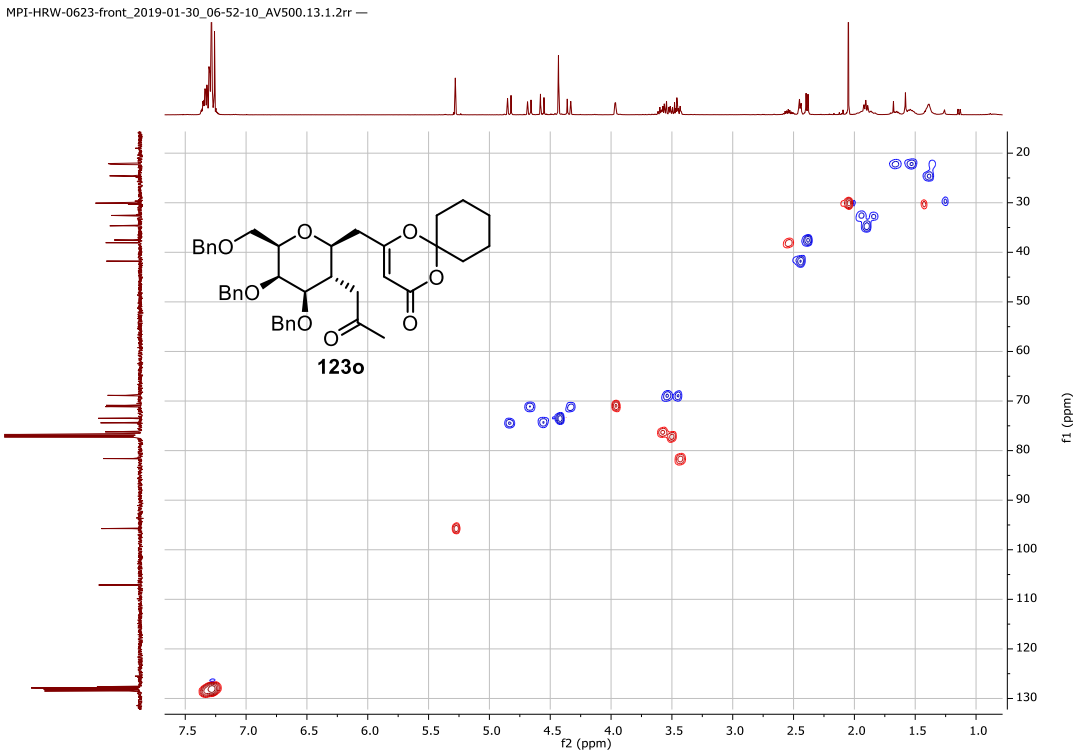

HSQC spectrum of compound **123o**

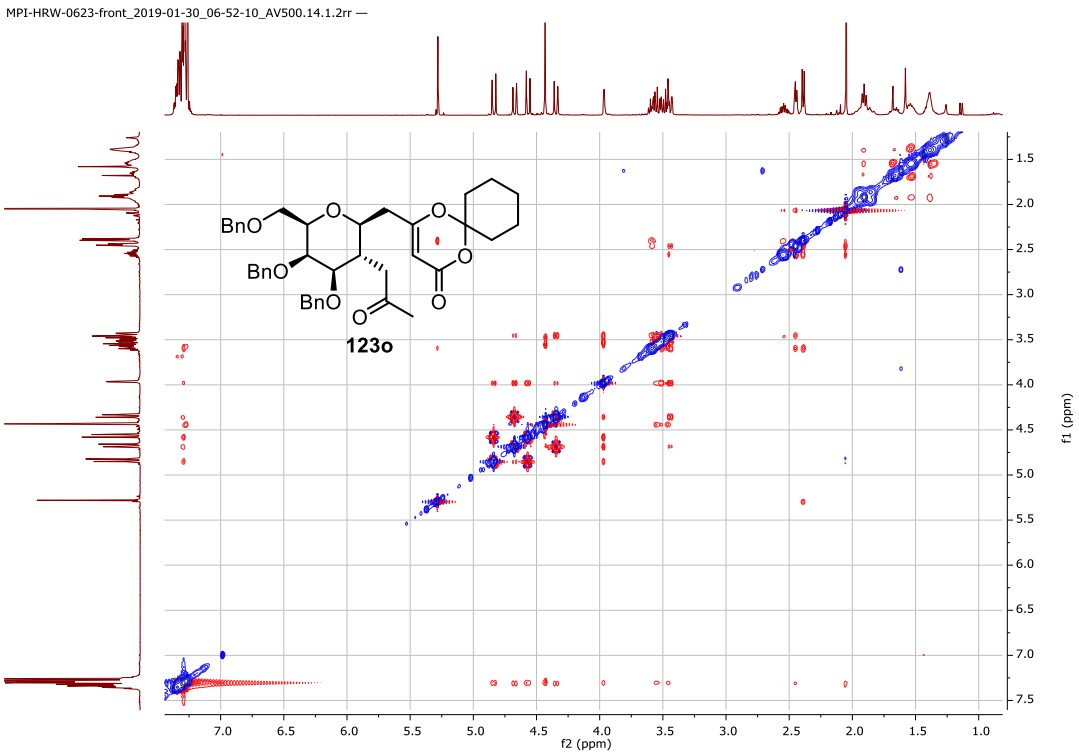

NOESY spectrum of compound **123o**

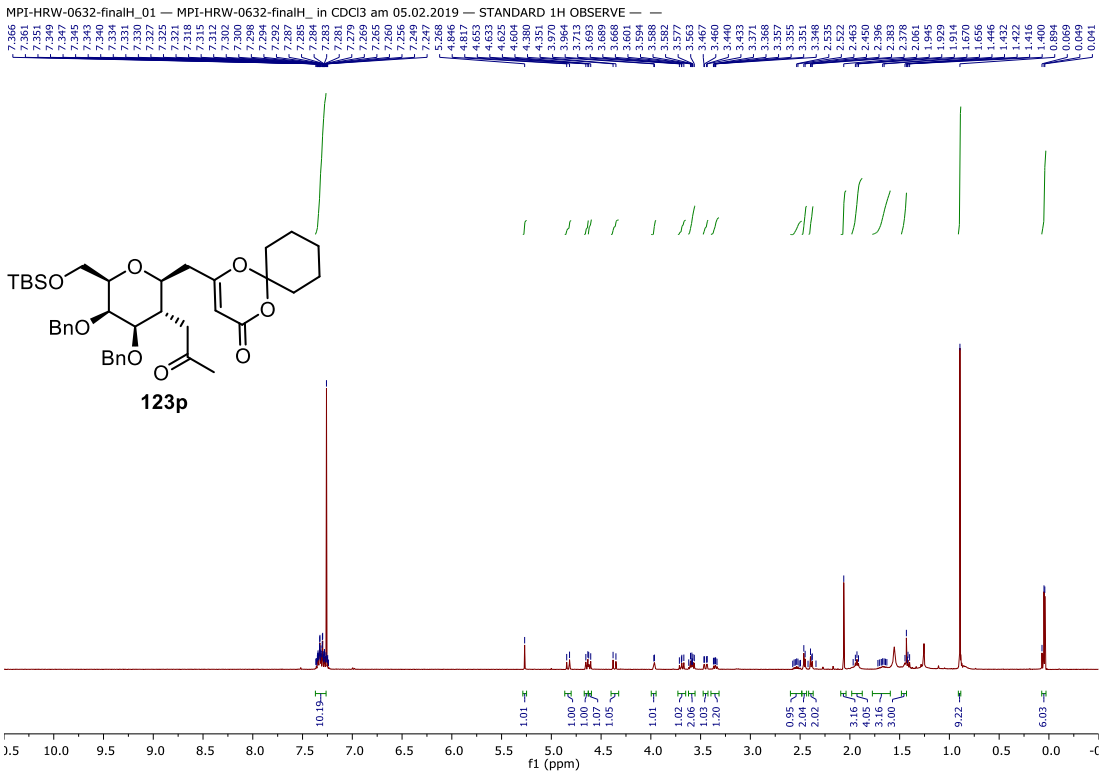

^{1}H NMR spectrum of compound **123p** (400 MHz, in $CDCl_3$)

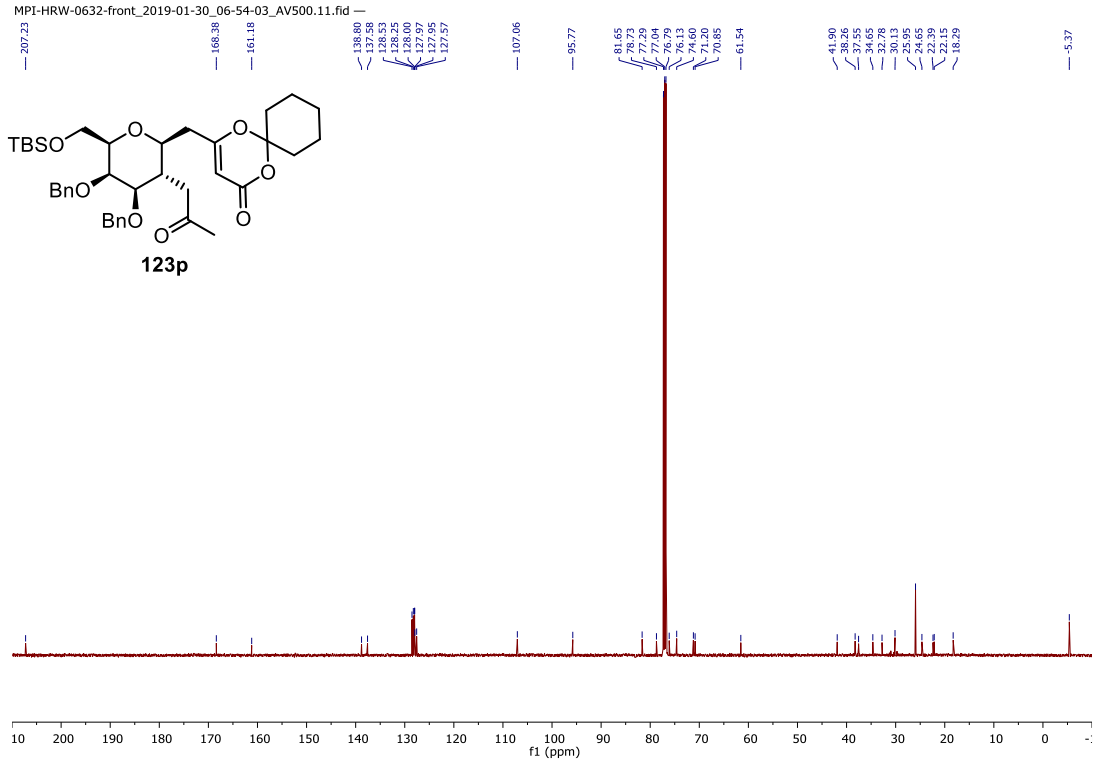

^{13}C NMR spectrum of compound **123p** (126 MHz, in $CDCl_3$)

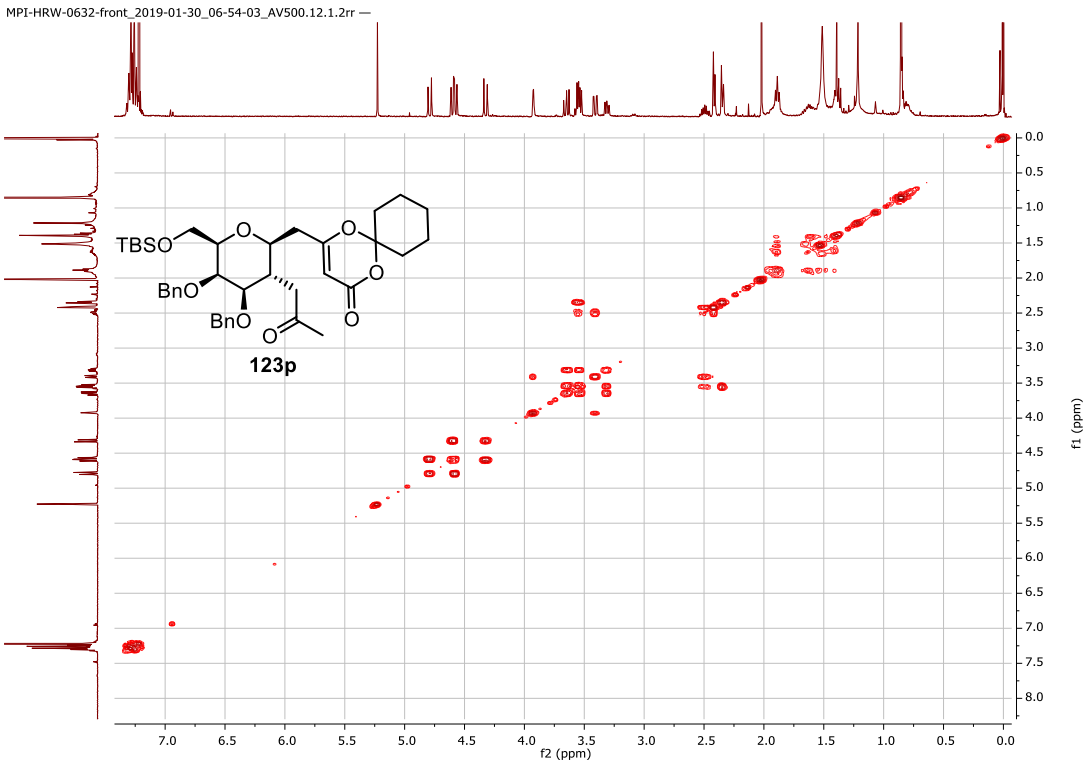

COSY spectrum of compound **123p**

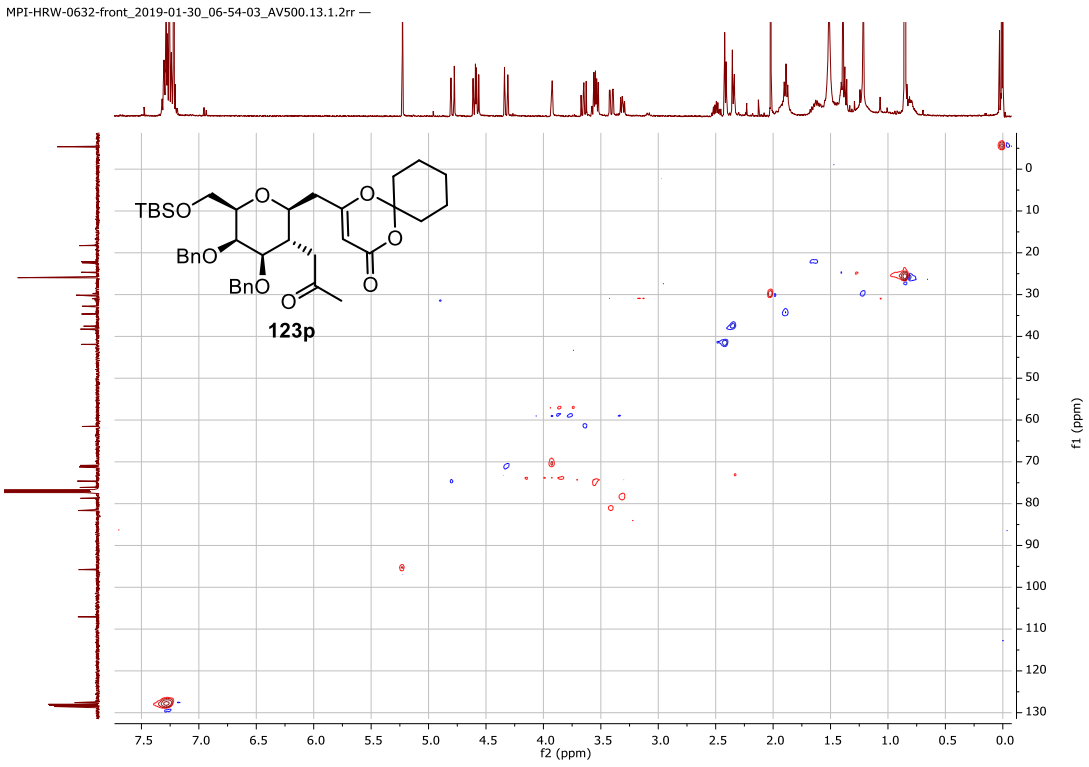

HSQC spectrum of compound **123p**

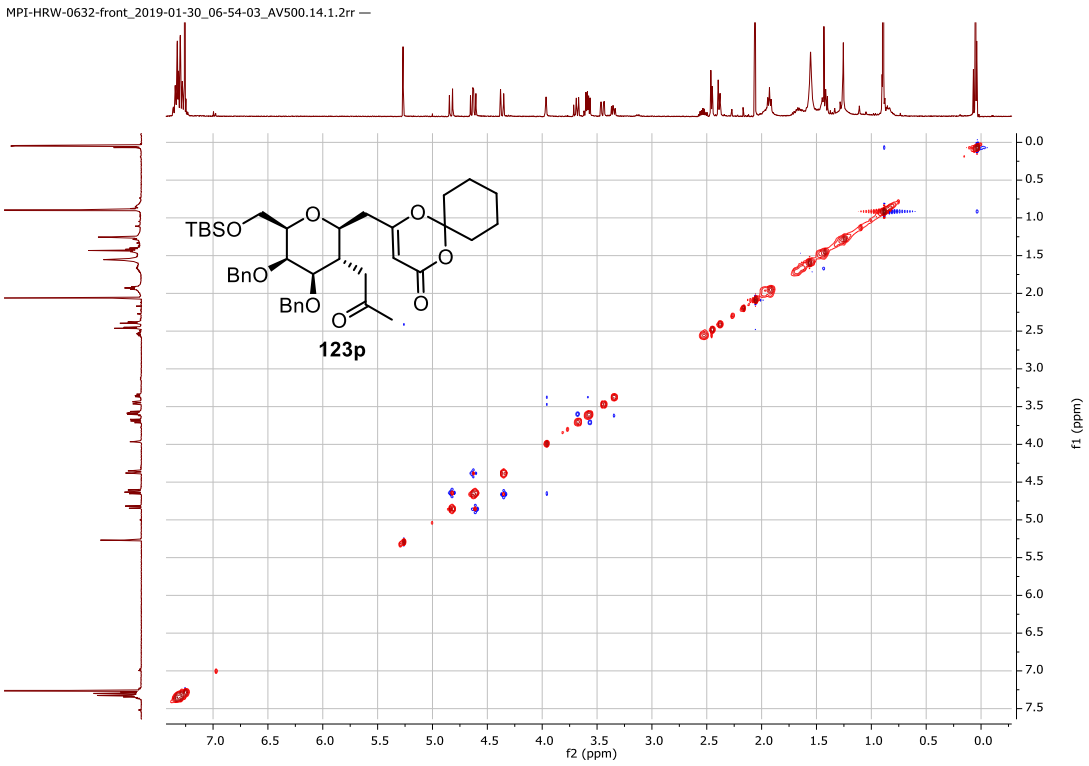

NOESY spectrum of compound **123p**

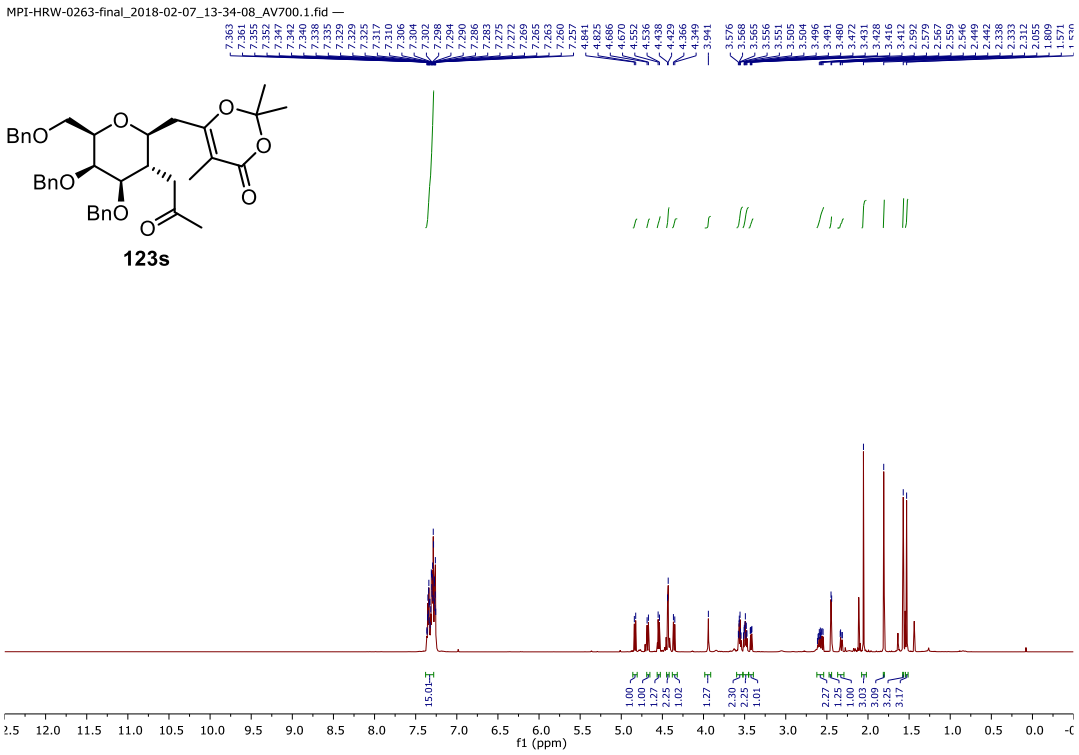

^{1}H NMR spectrum of compound **123s** (700 MHz, in $CDCl_3$)

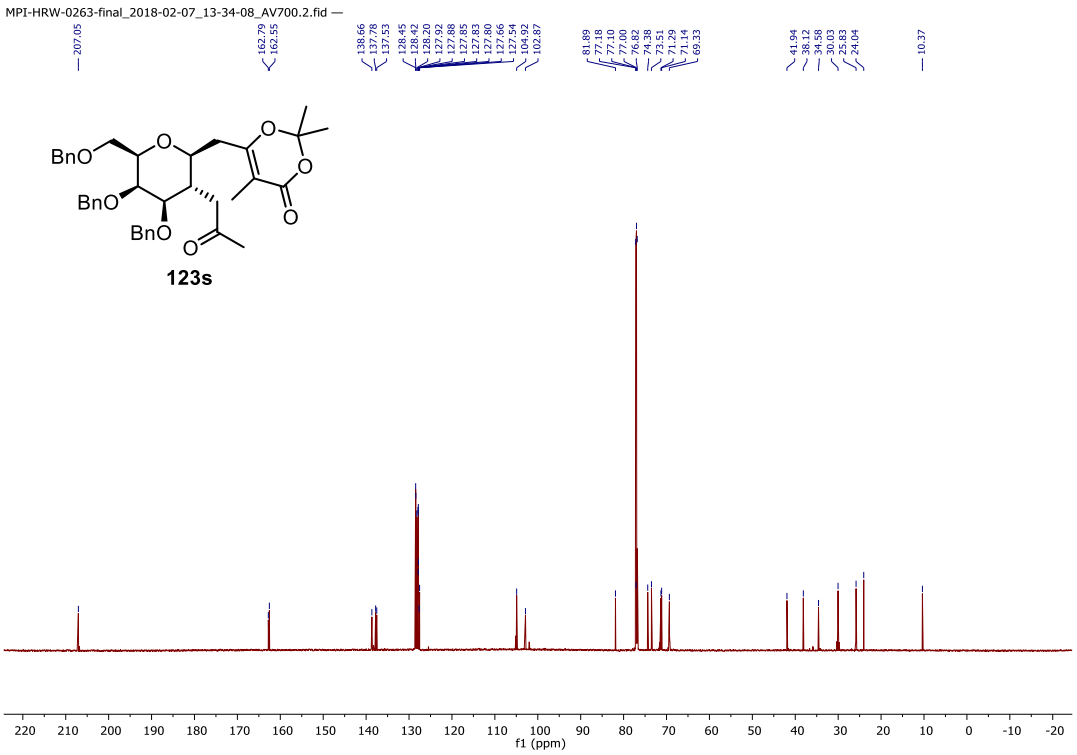

^{13}C NMR spectrum of compound **123s** (176 MHz, in $CDCl_3$)

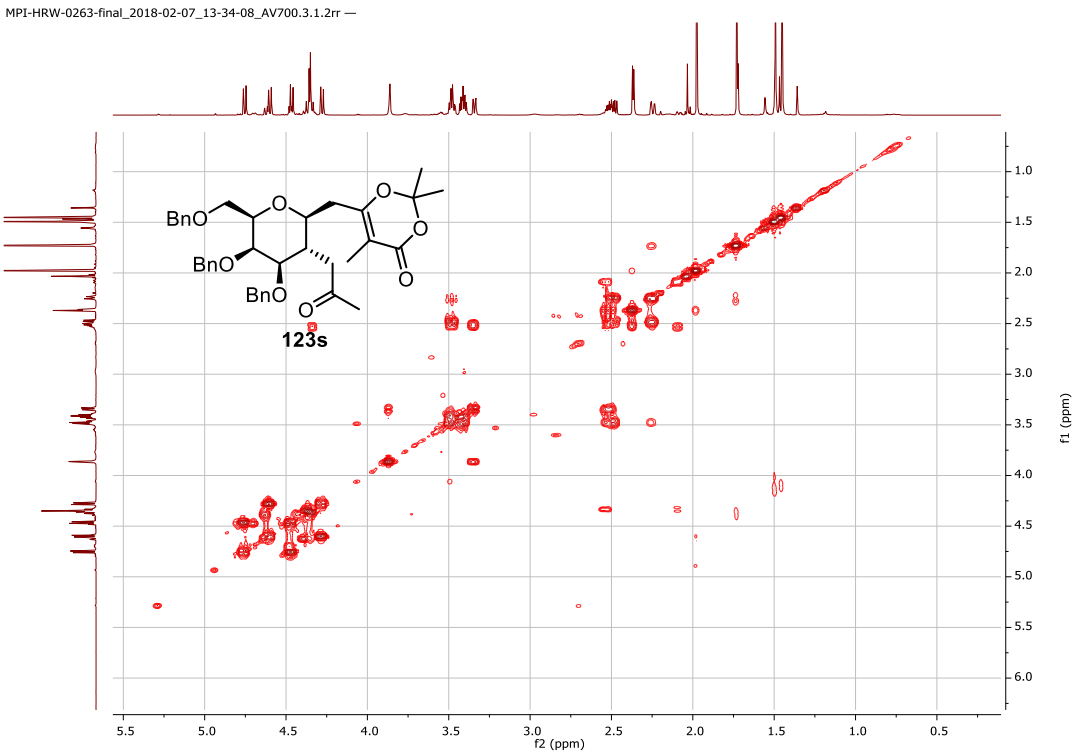

COSY spectrum of compound **123s**

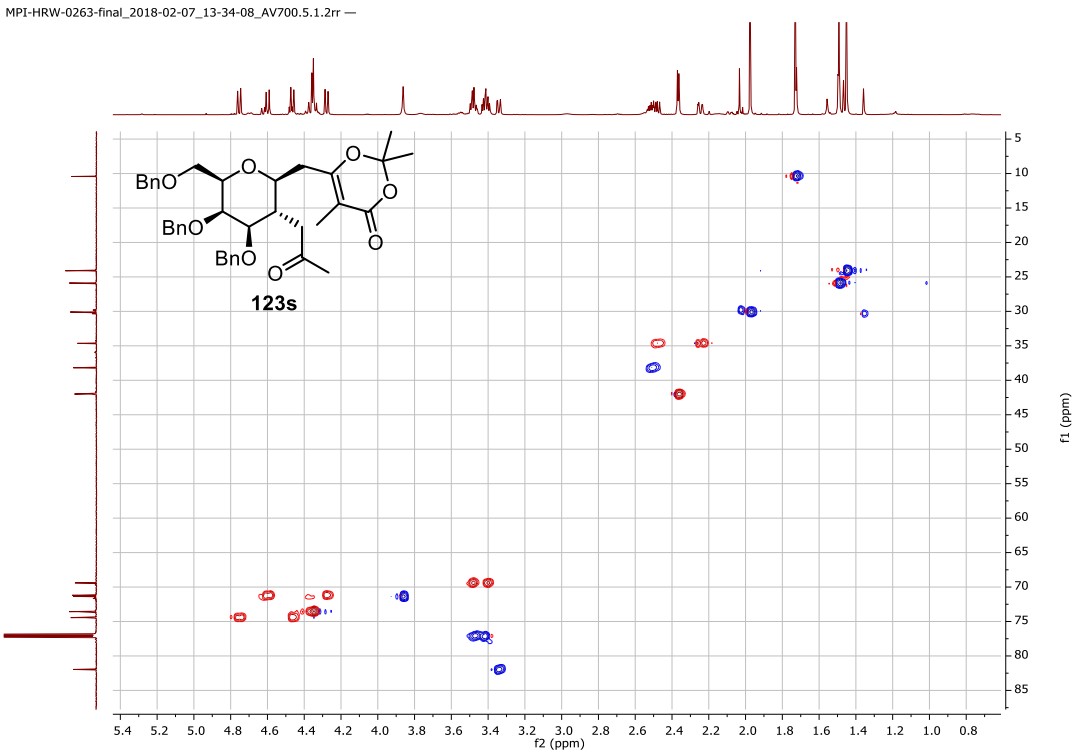

HSQC spectrum of compound **123s**

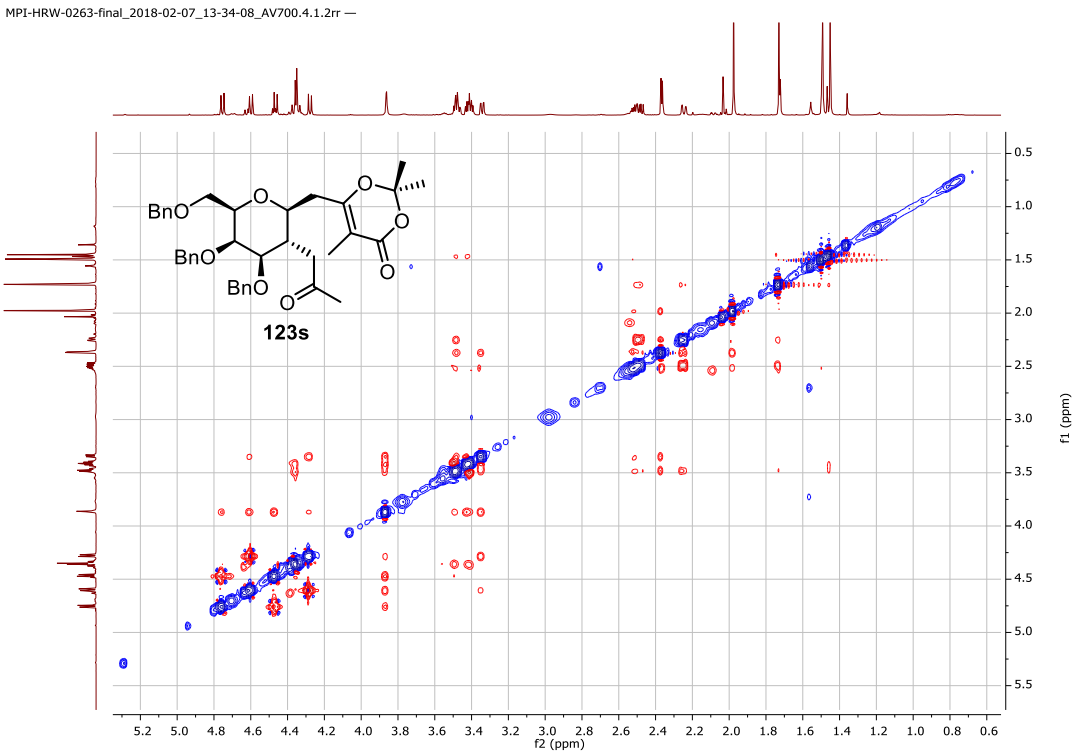

NOESY spectrum of compound **123s**

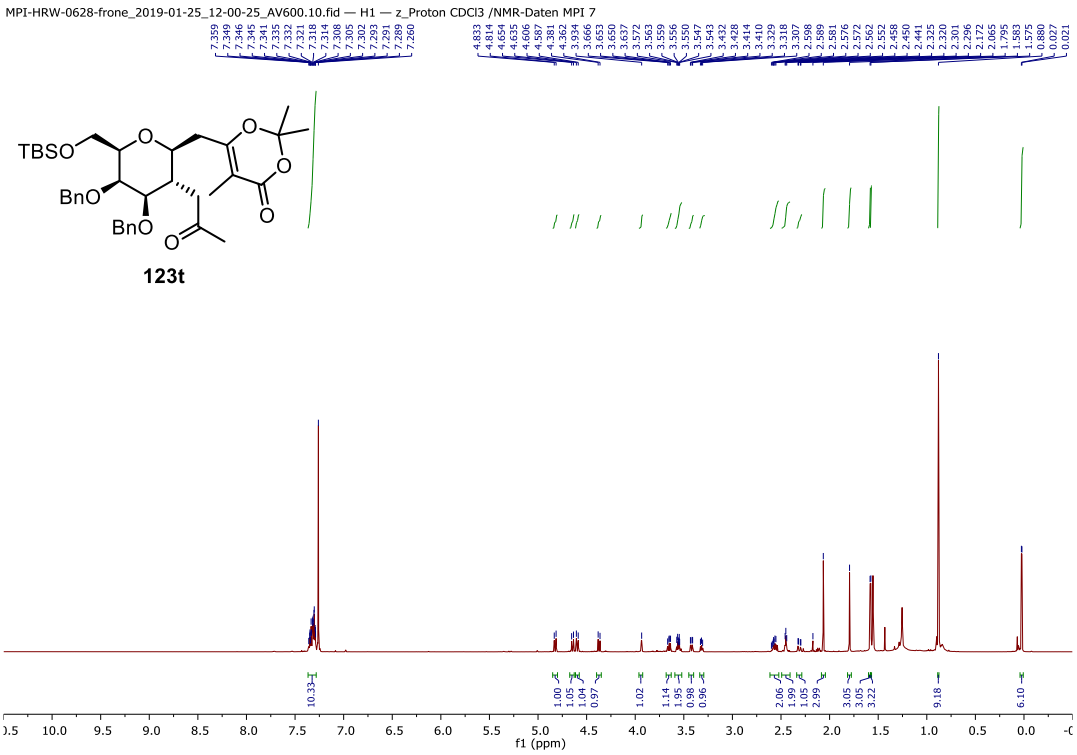

^{1}H NMR spectrum of compound **123t** (600 MHz, in $CDCl_3$)

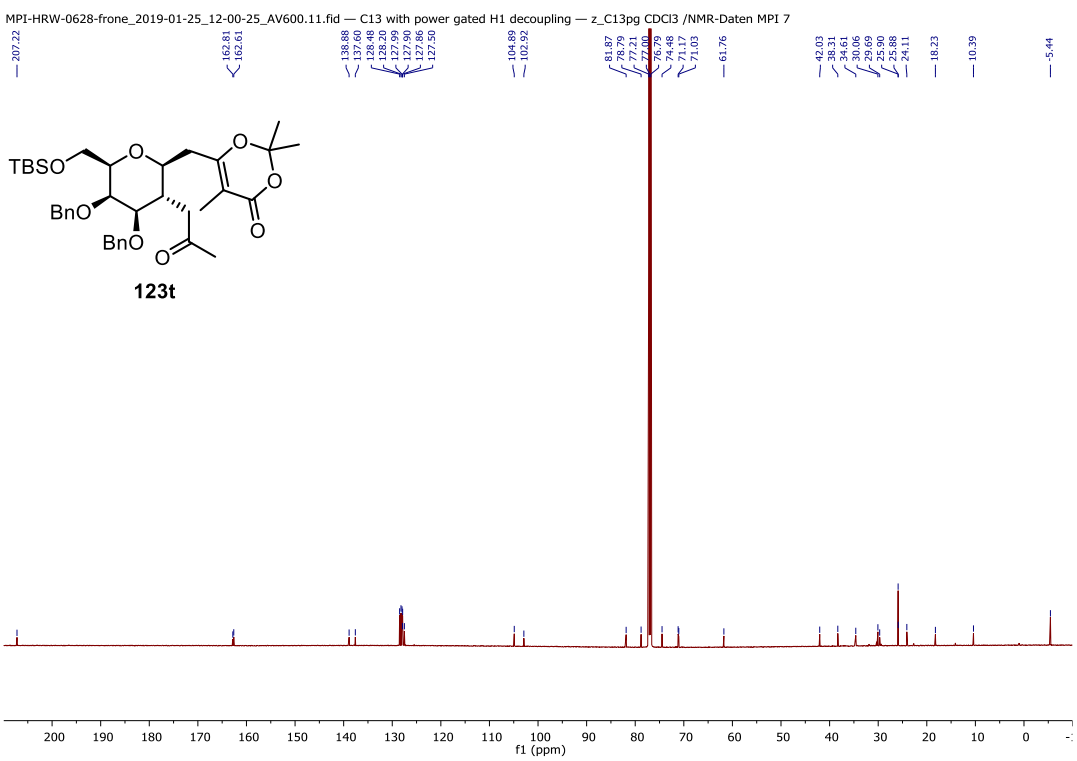

^{13}C NMR spectrum of compound **123t** (151 MHz, in $CDCl_3$)

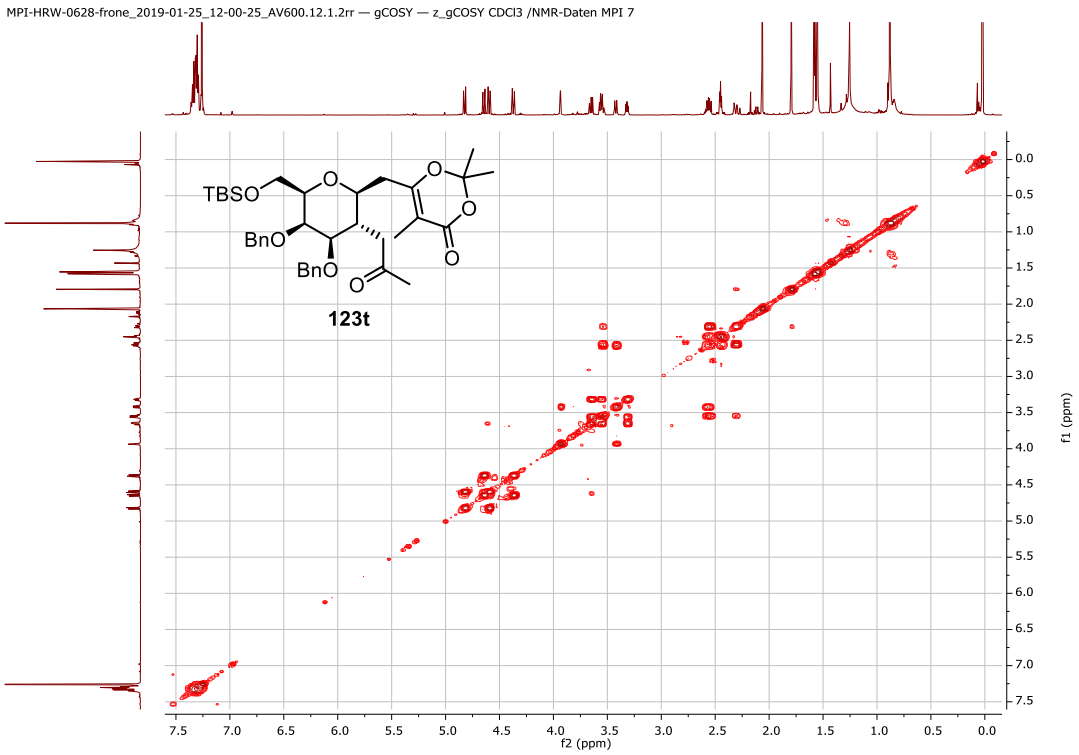

COSY spectrum of compound **123t**

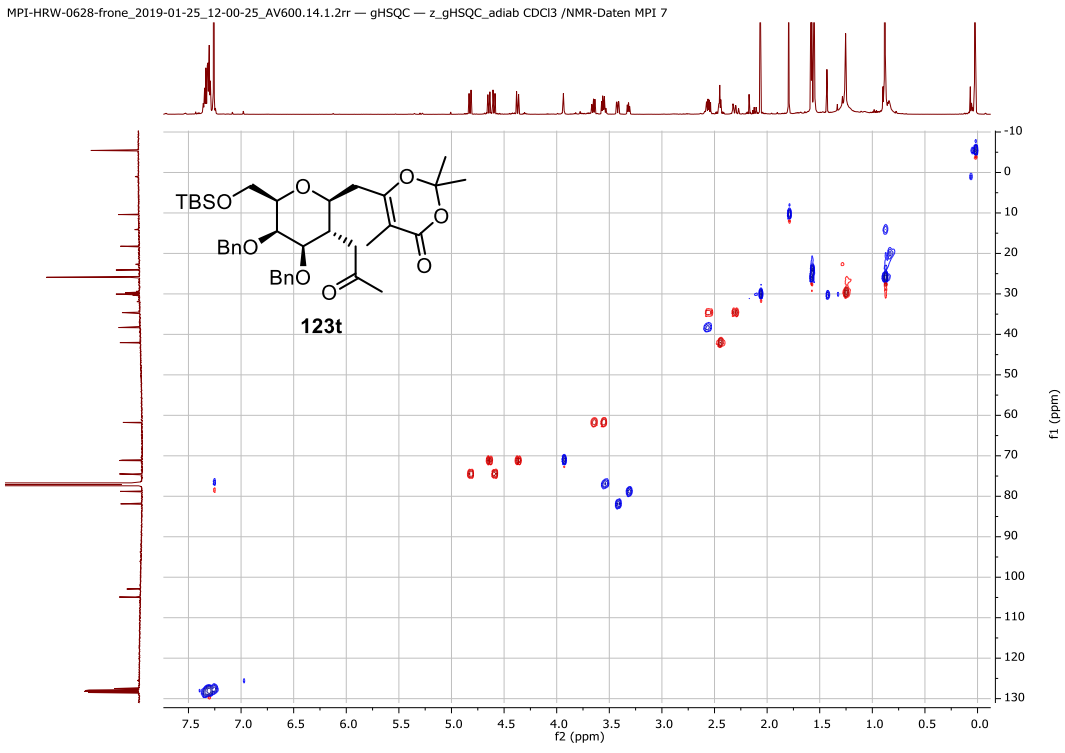

HSQC spectrum of compound **123t**

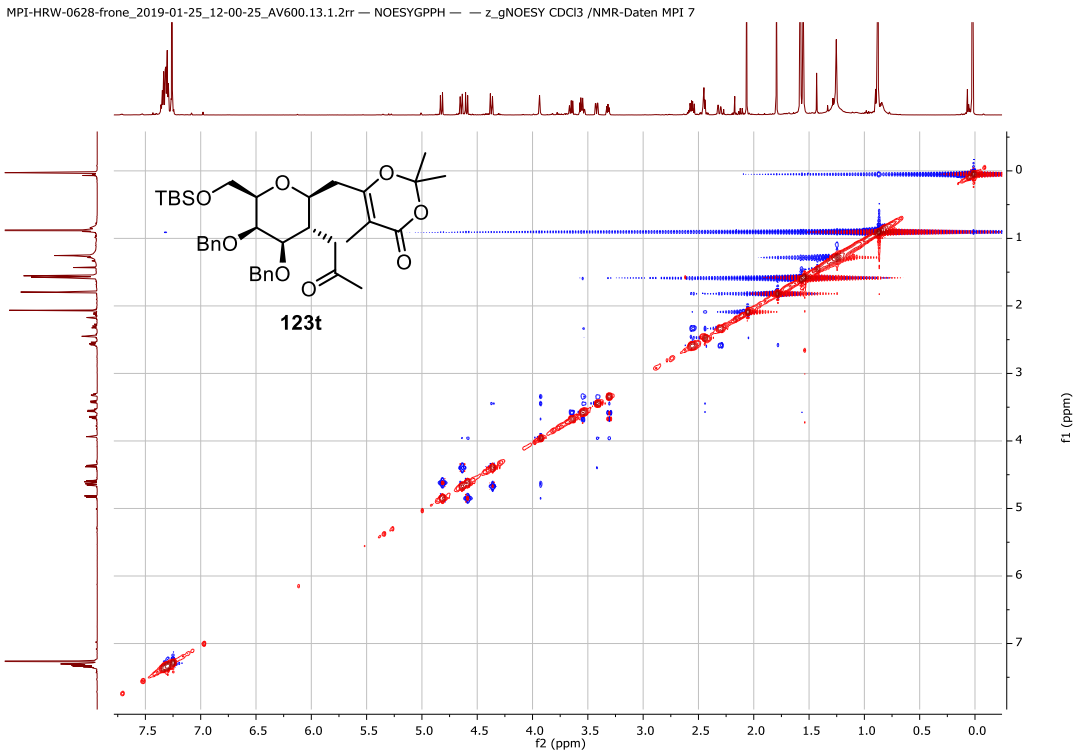

NOESY spectrum of compound **123t**

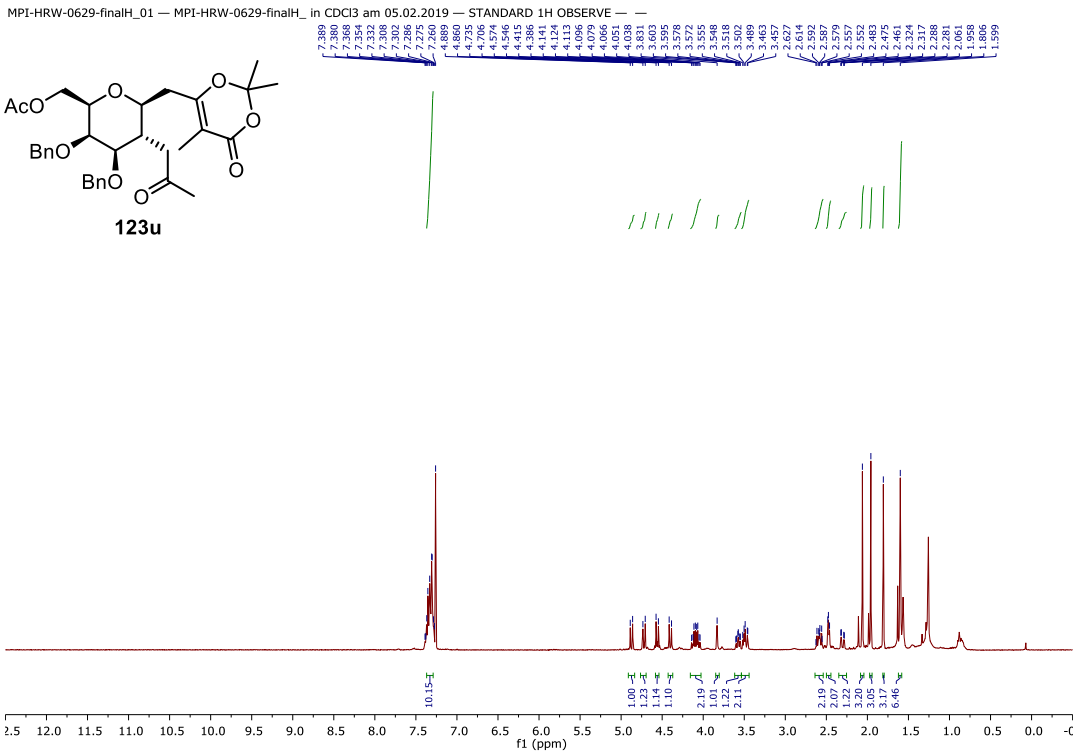

^{1}H NMR spectrum of compound **123u** (400 MHz, in $CDCl_3$)

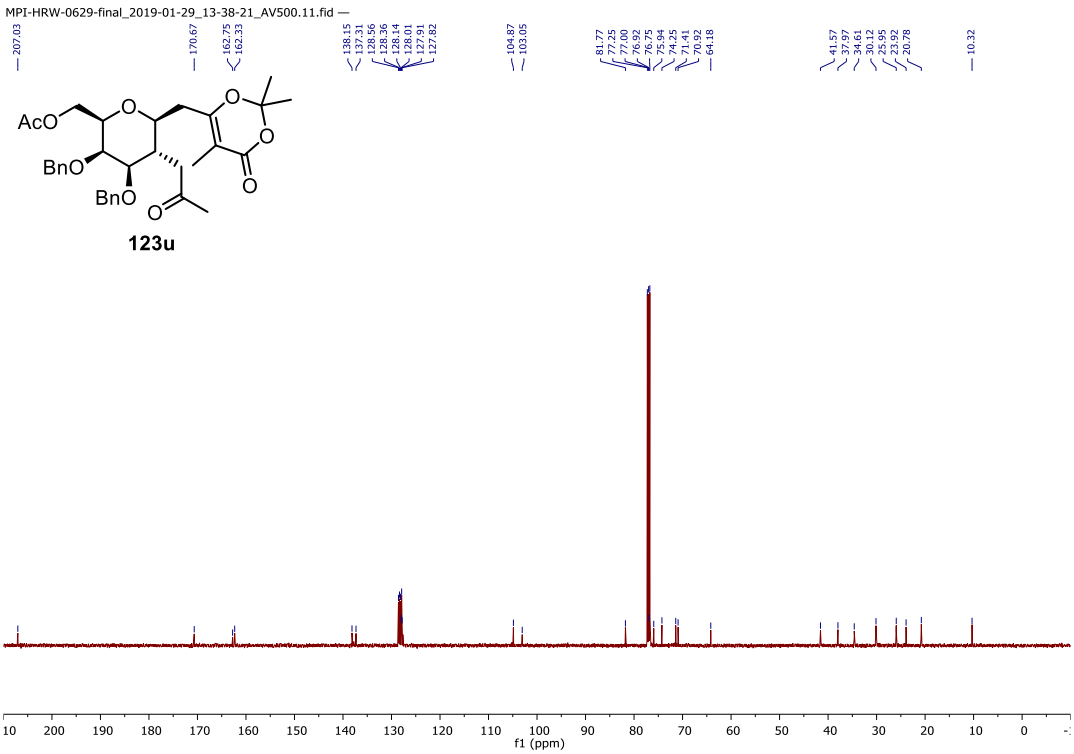

^{13}C NMR spectrum of compound **123u** (126 MHz, in $CDCl_3$)

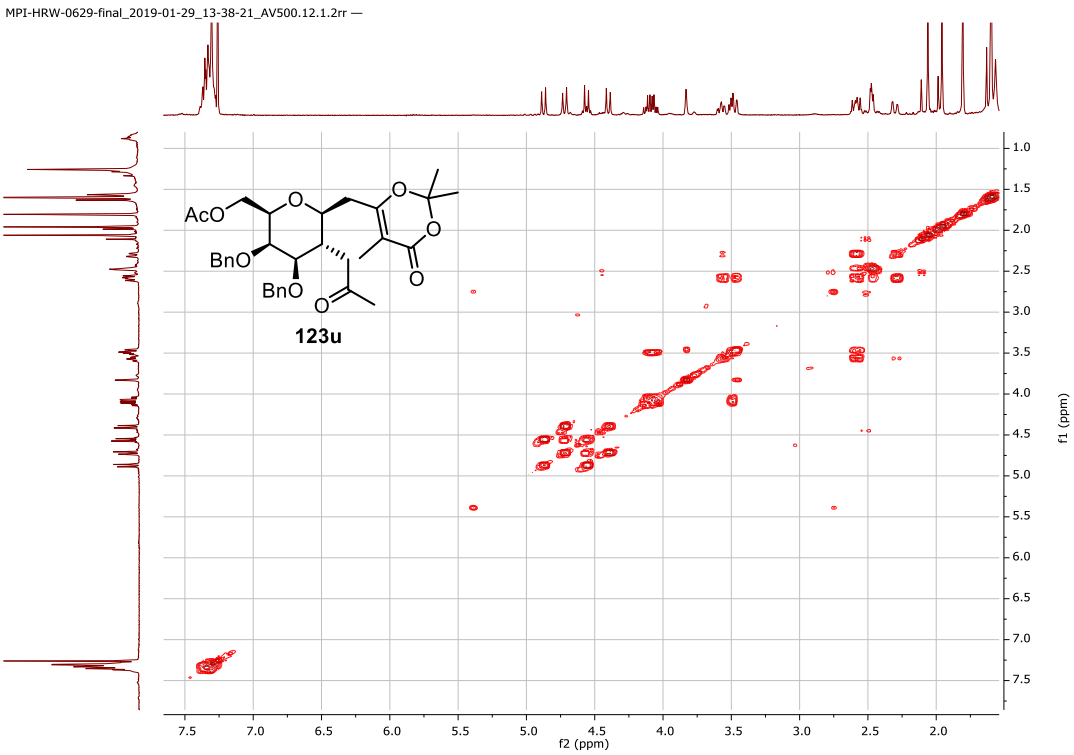

COSY spectrum of compound **123u**

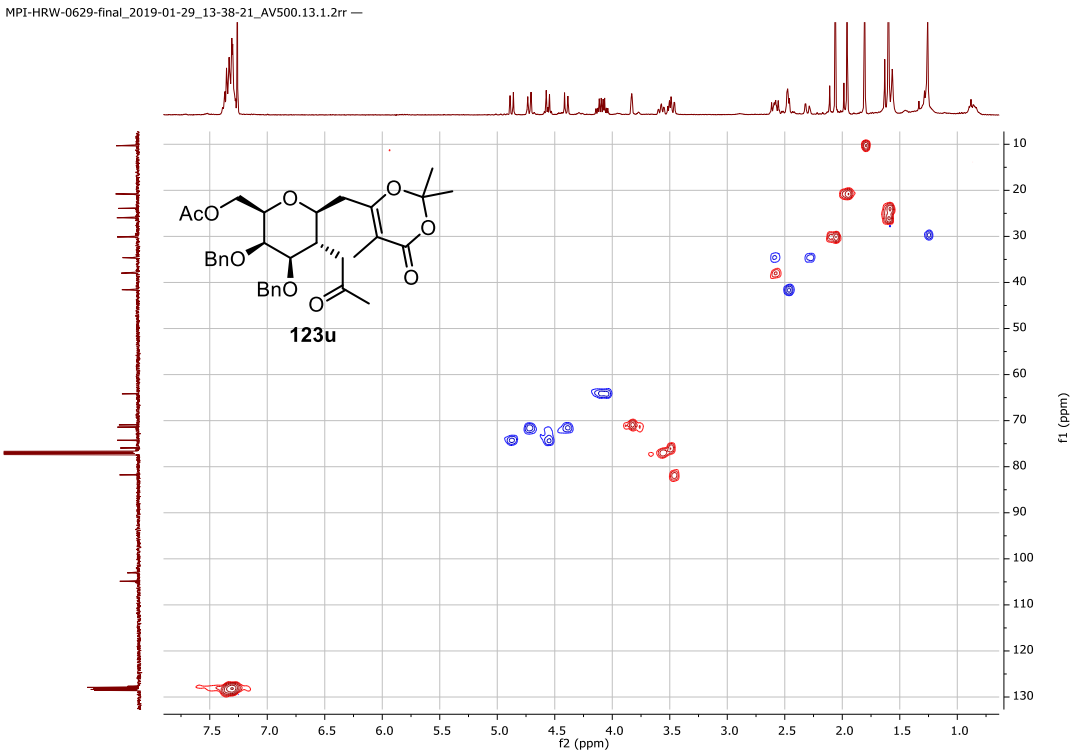

HSQC spectrum of compound **123u**

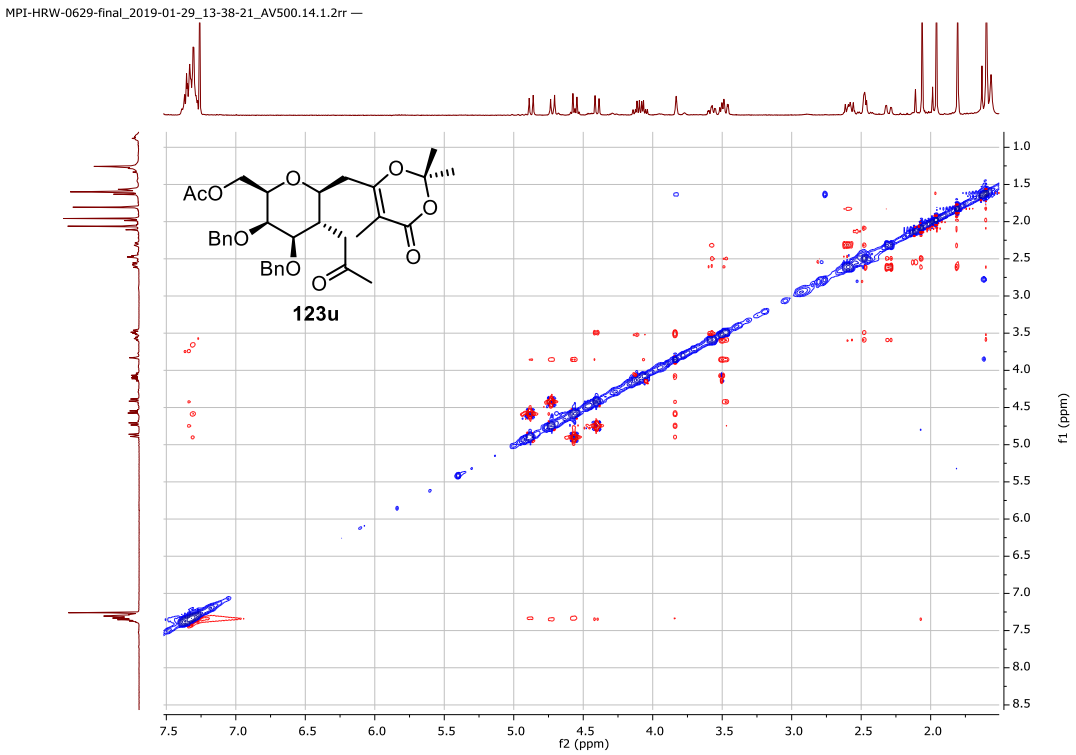

NOESY spectrum of compound **123u**

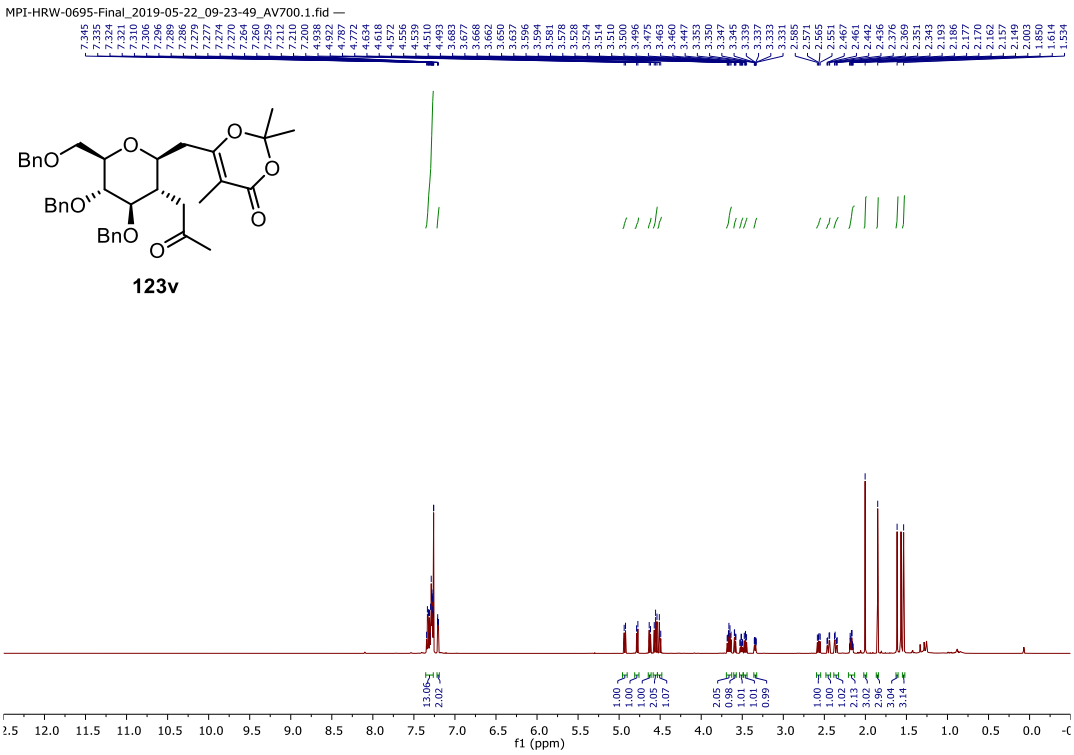

^{1}H NMR spectrum of compound **123v** (700 MHz, in $CDCl_3$)

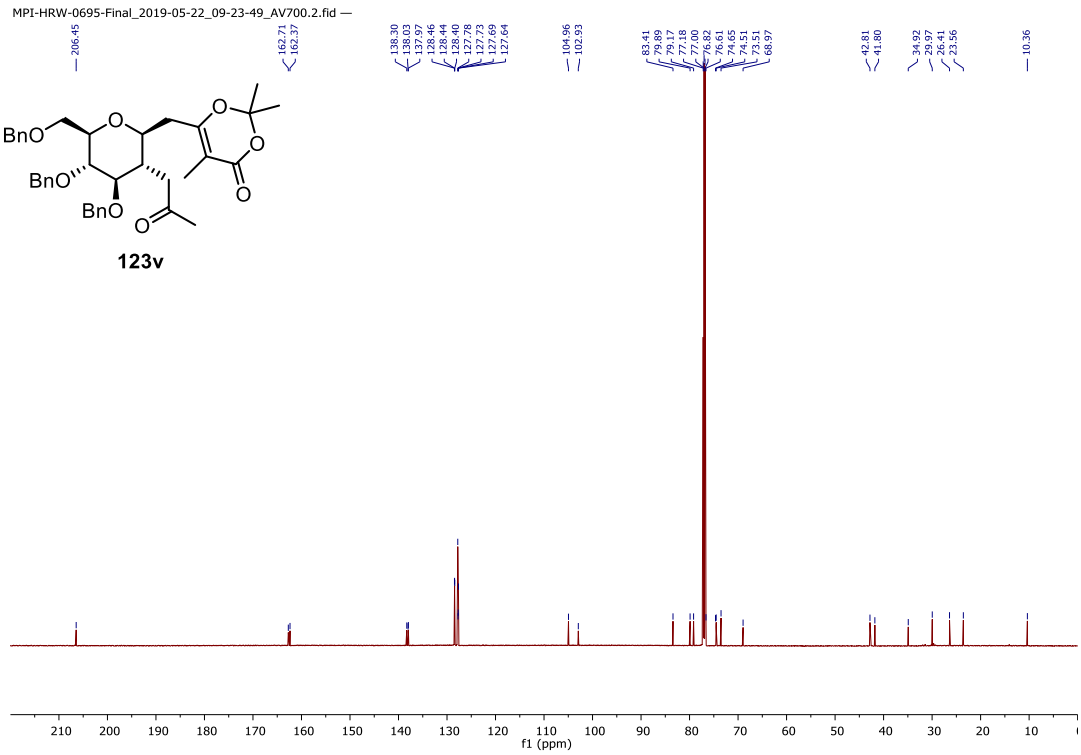

^{13}C NMR spectrum of compound **123v** (176 MHz, in $CDCl_3$)

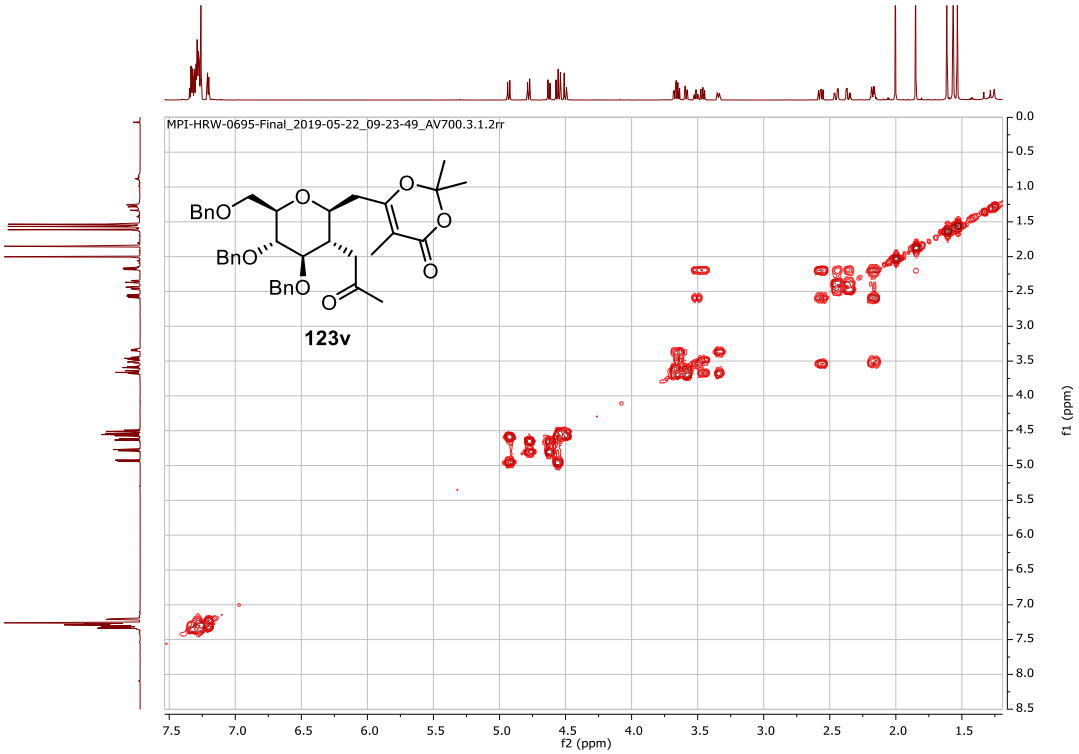

COSY spectrum of compound **123v**

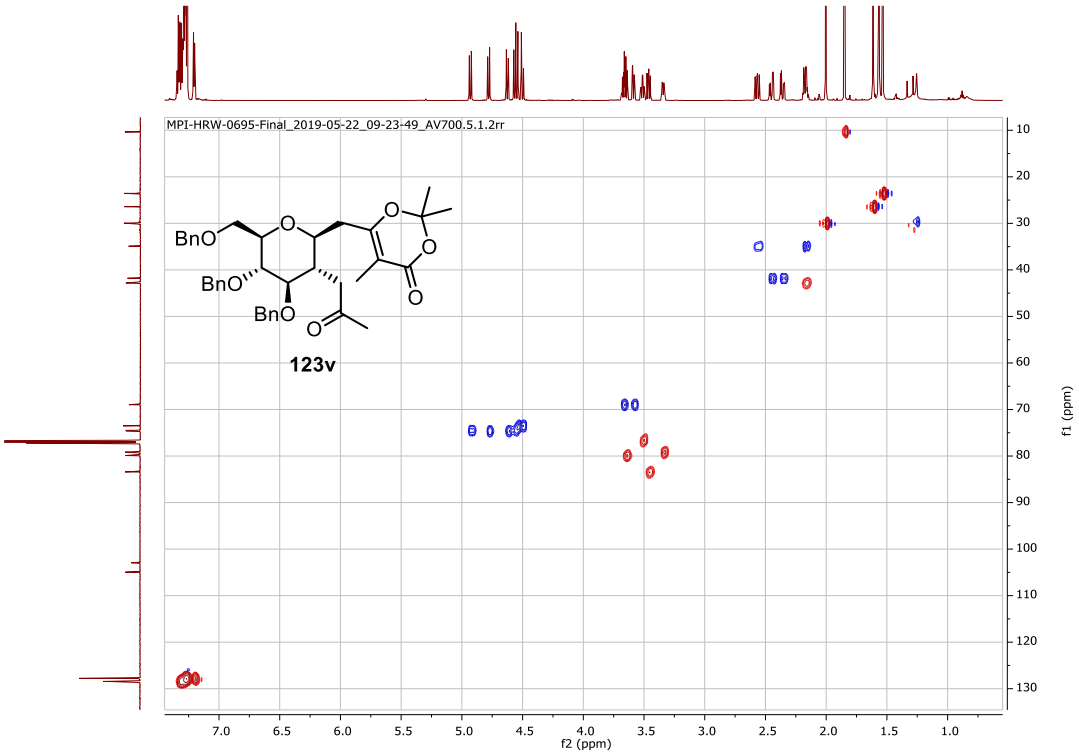

HSQC spectrum of compound **123v**

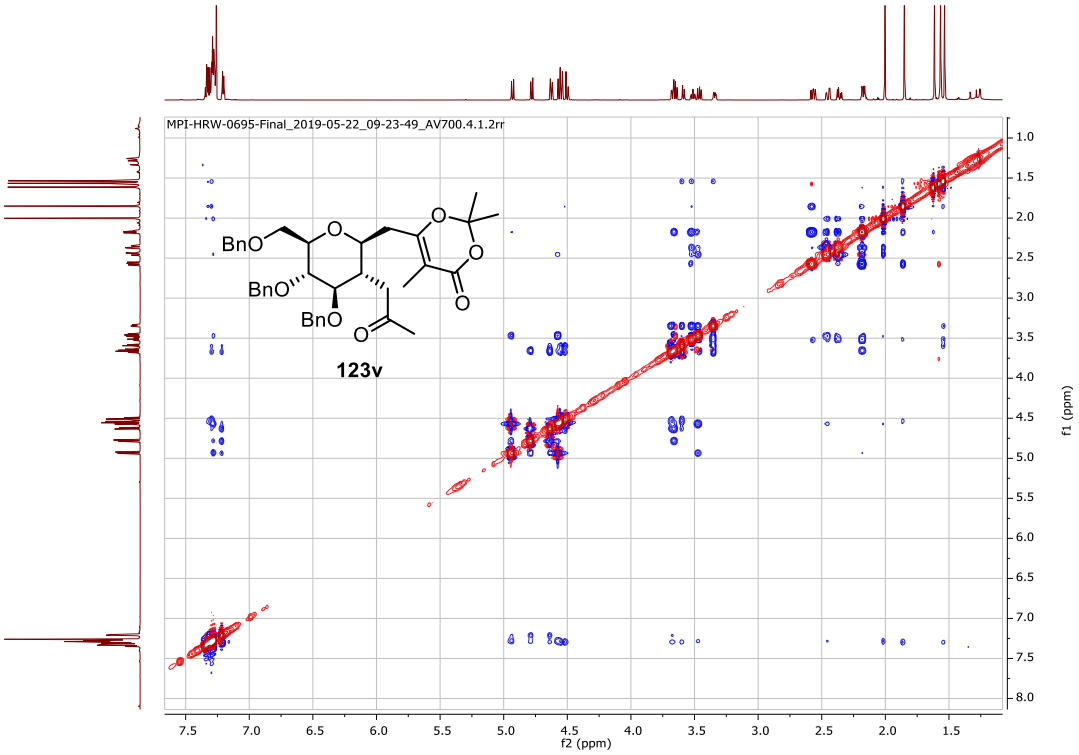

NOESY spectrum of compound **123v**

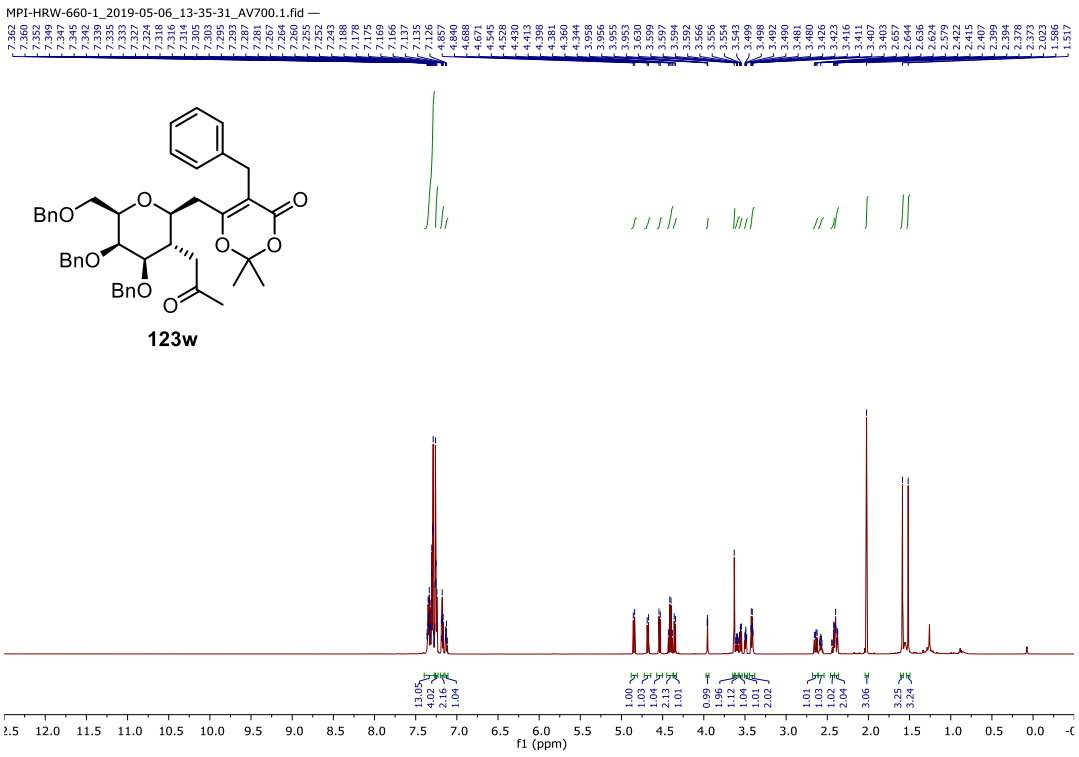

^{1}H NMR spectrum of compound **123w** (700 MHz, in $CDCl_3$)

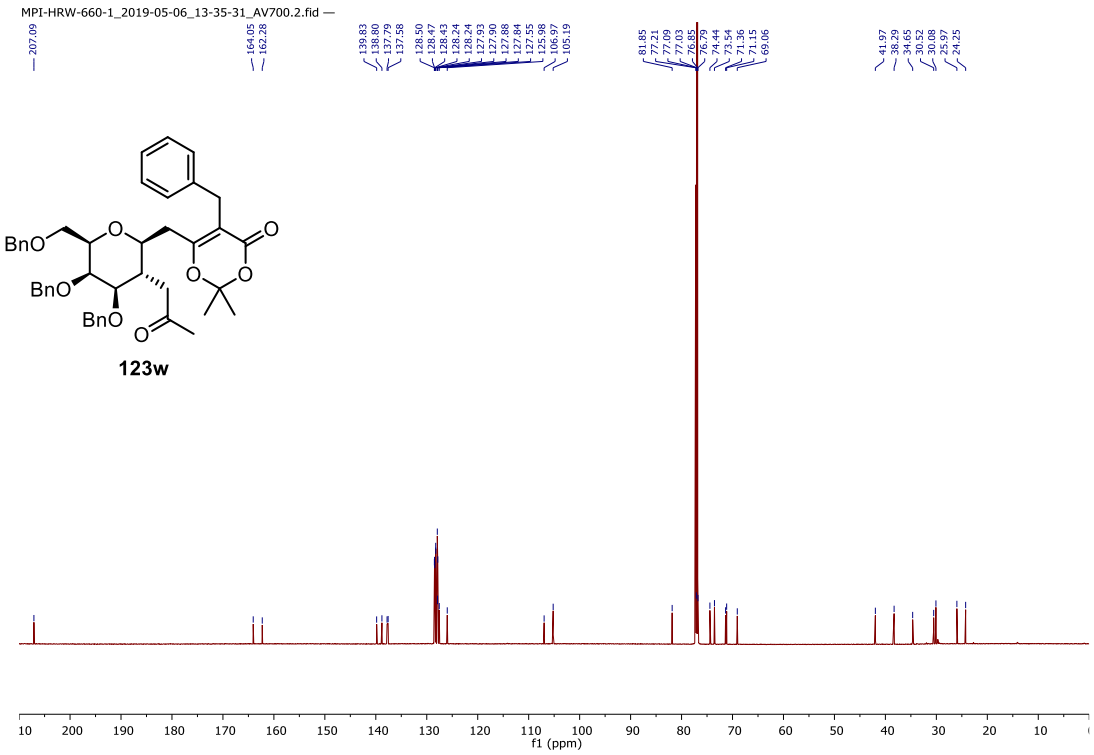

^{13}C NMR spectrum of compound **123w** (176 MHz, in $CDCl_3$)

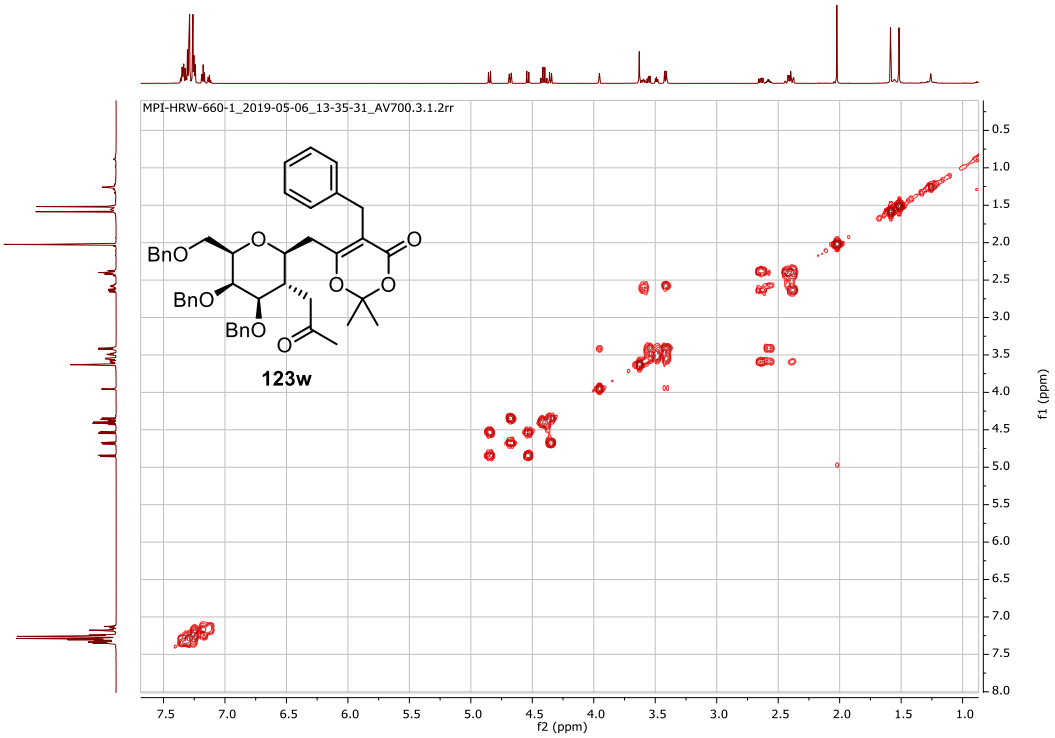

COSY spectrum of compound **123w**

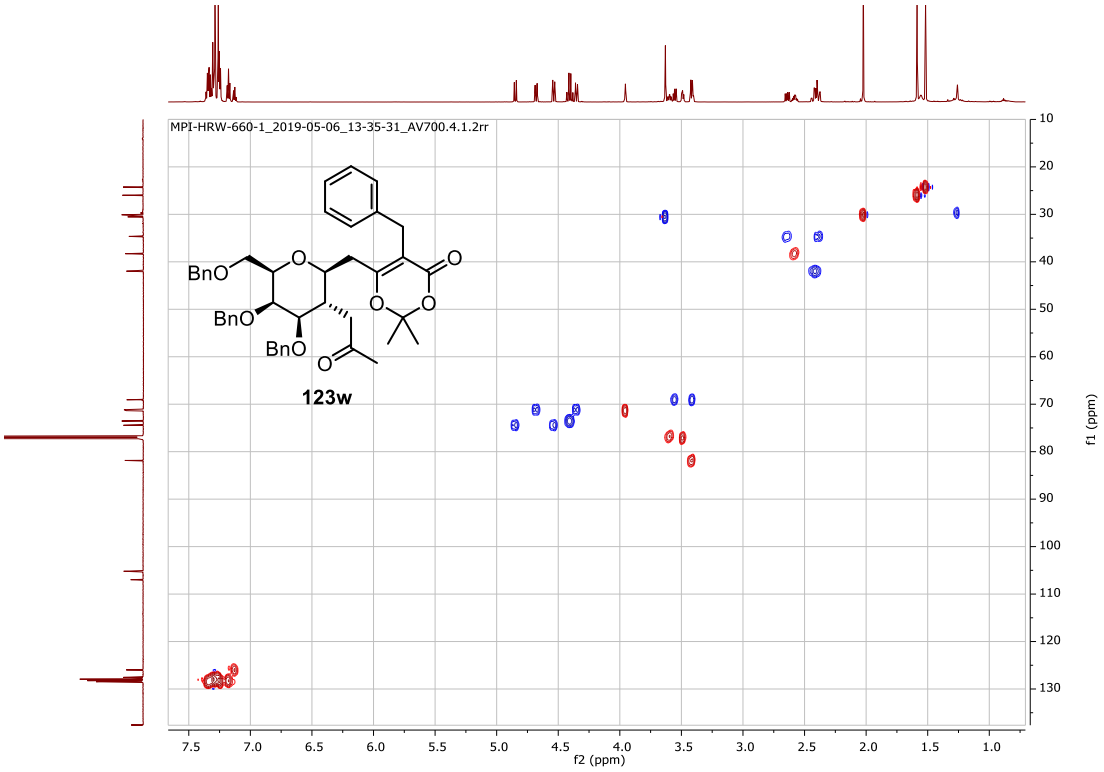

HSQC spectrum of compound **123w**

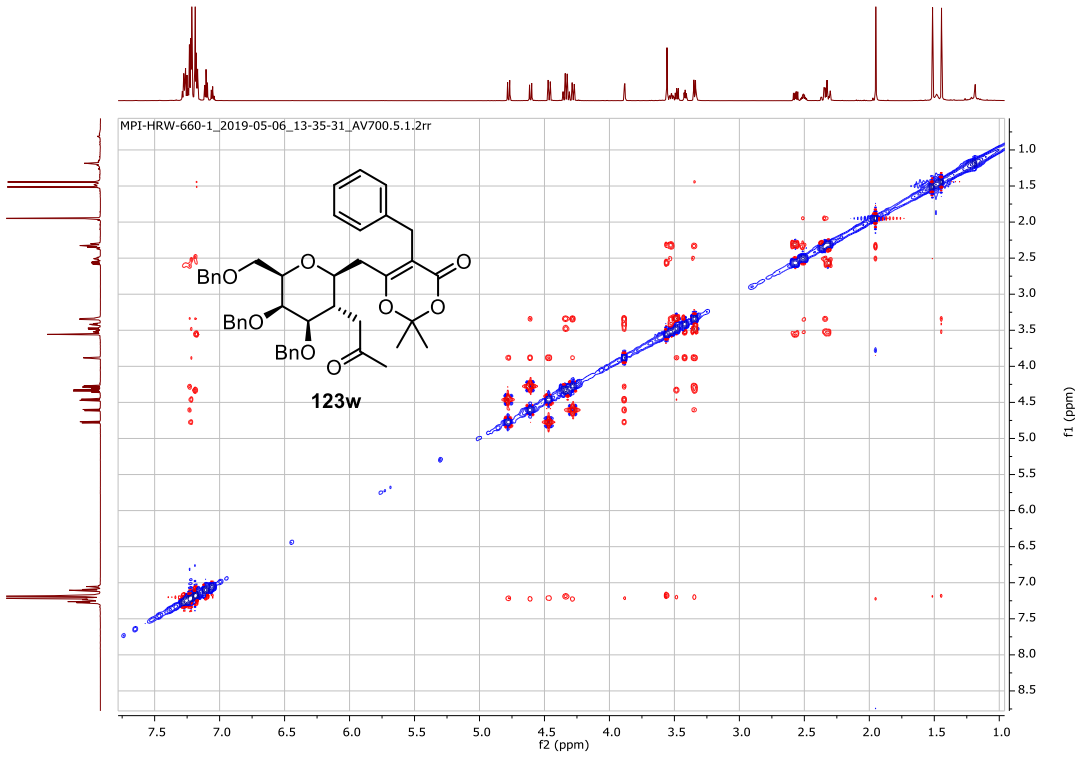

NOESY spectrum of compound **123w**

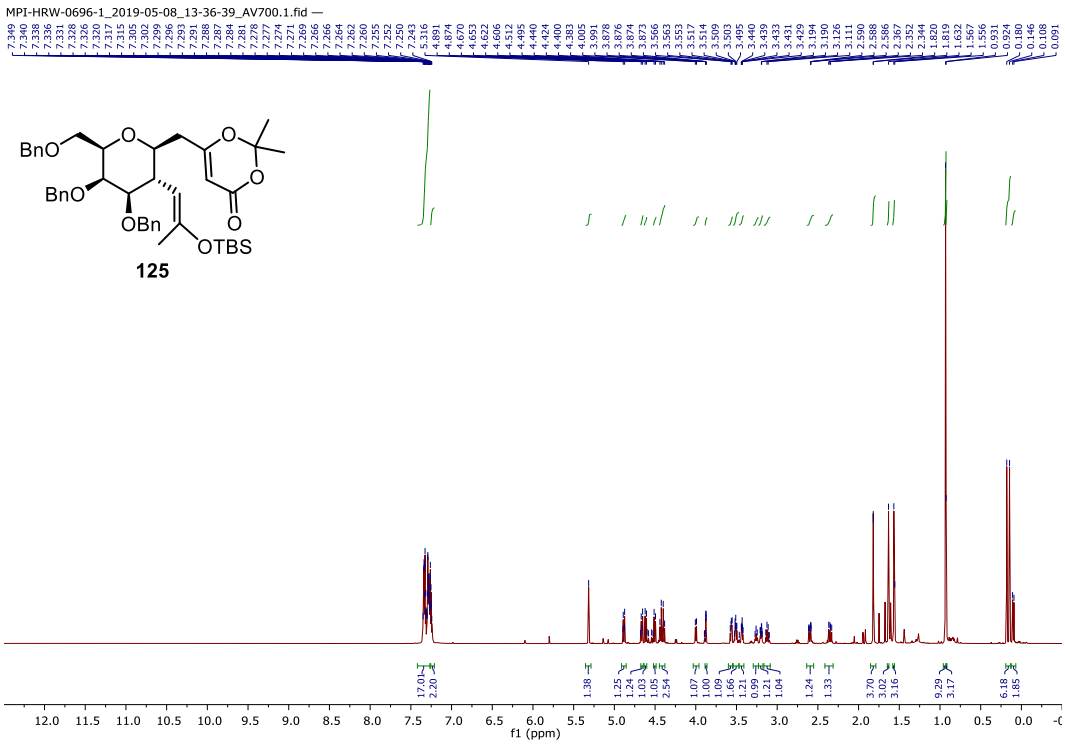

^{1}H NMR spectrum of compound **125** (700 MHz, in $CDCl_3$)

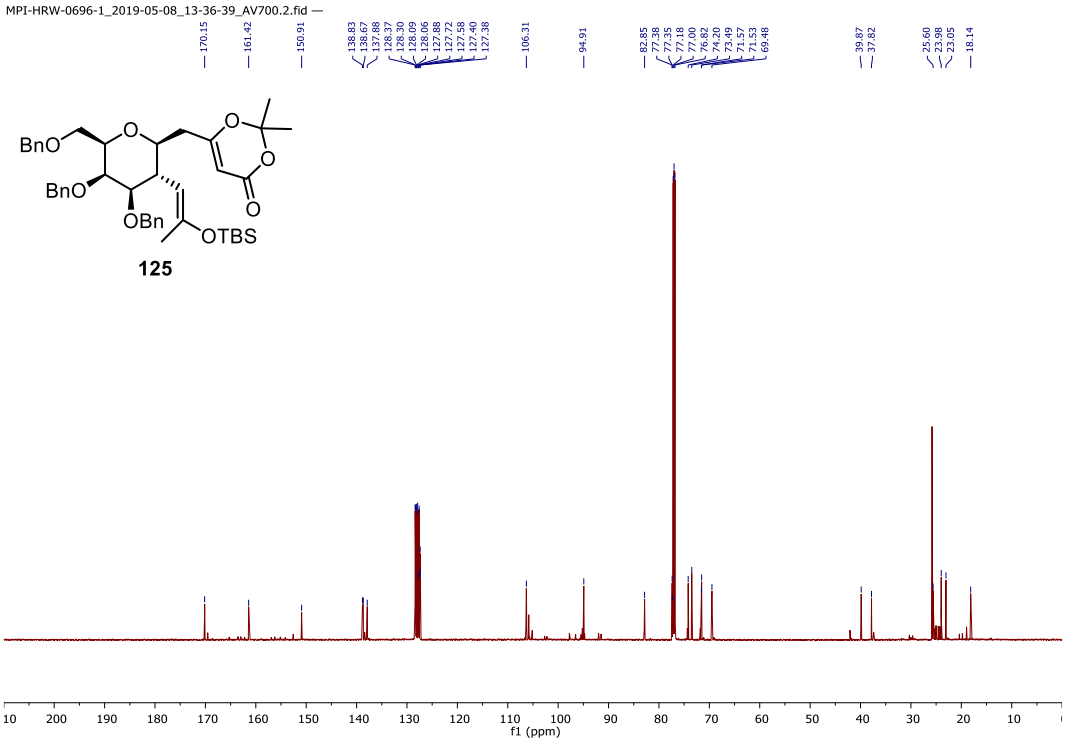

^{13}C NMR spectrum of compound **125** (176 MHz, in $CDCl_3$)

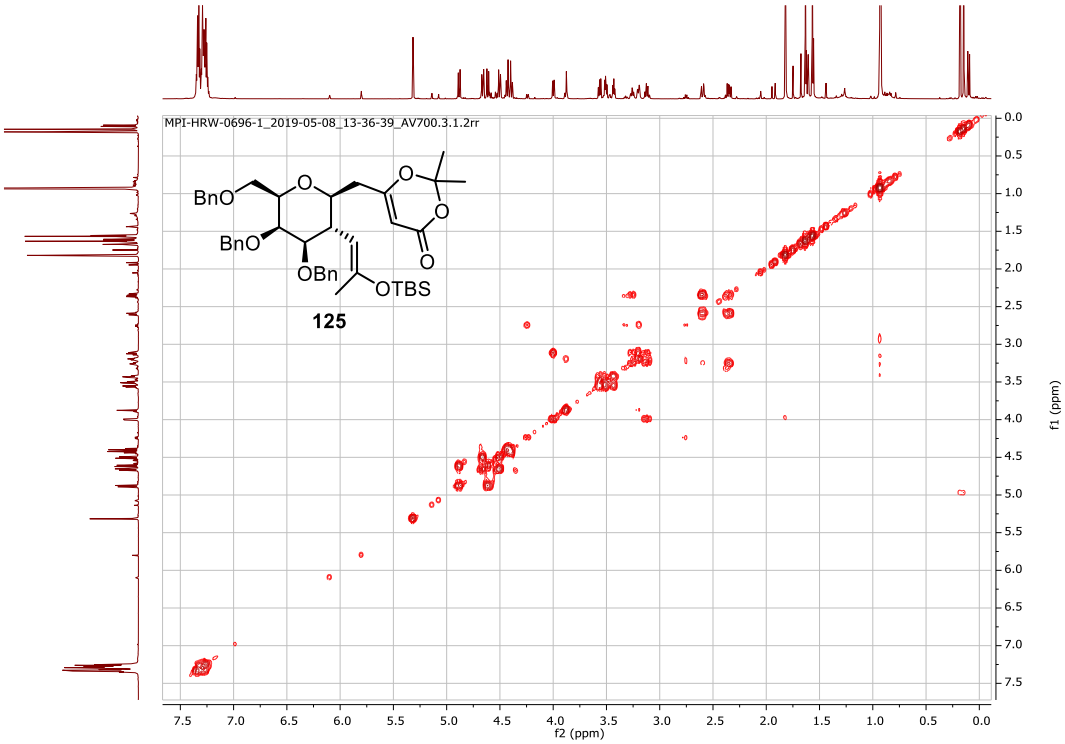

COSY spectrum of compound **125**

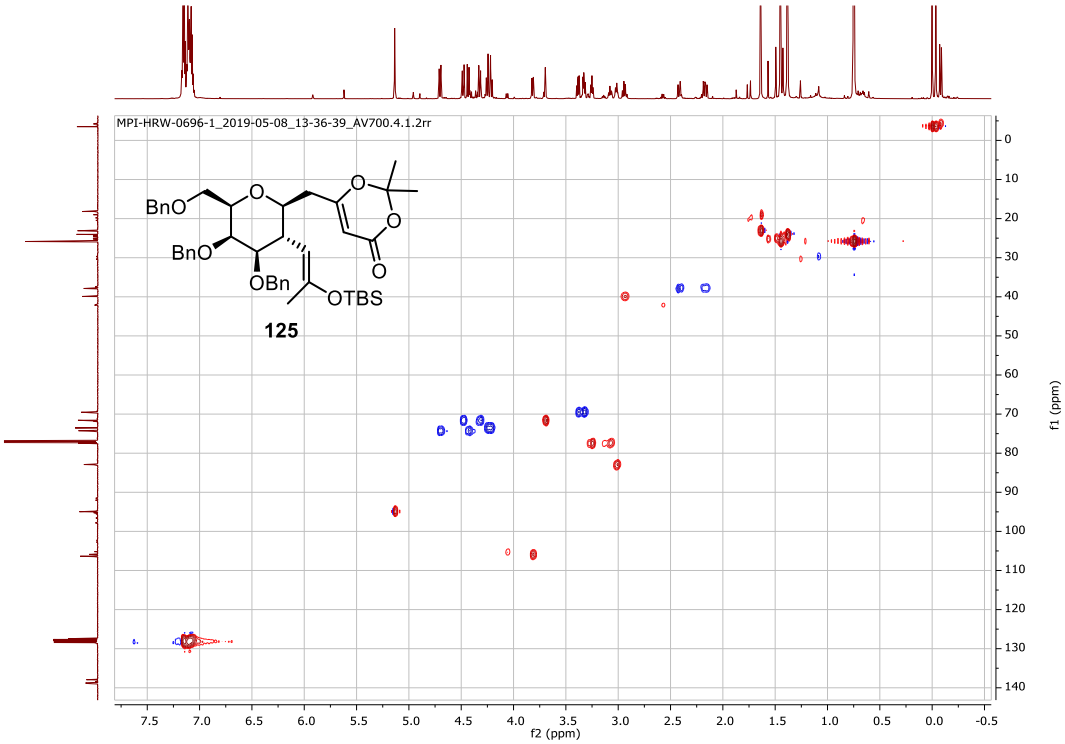

HSQC spectrum of compound **125**

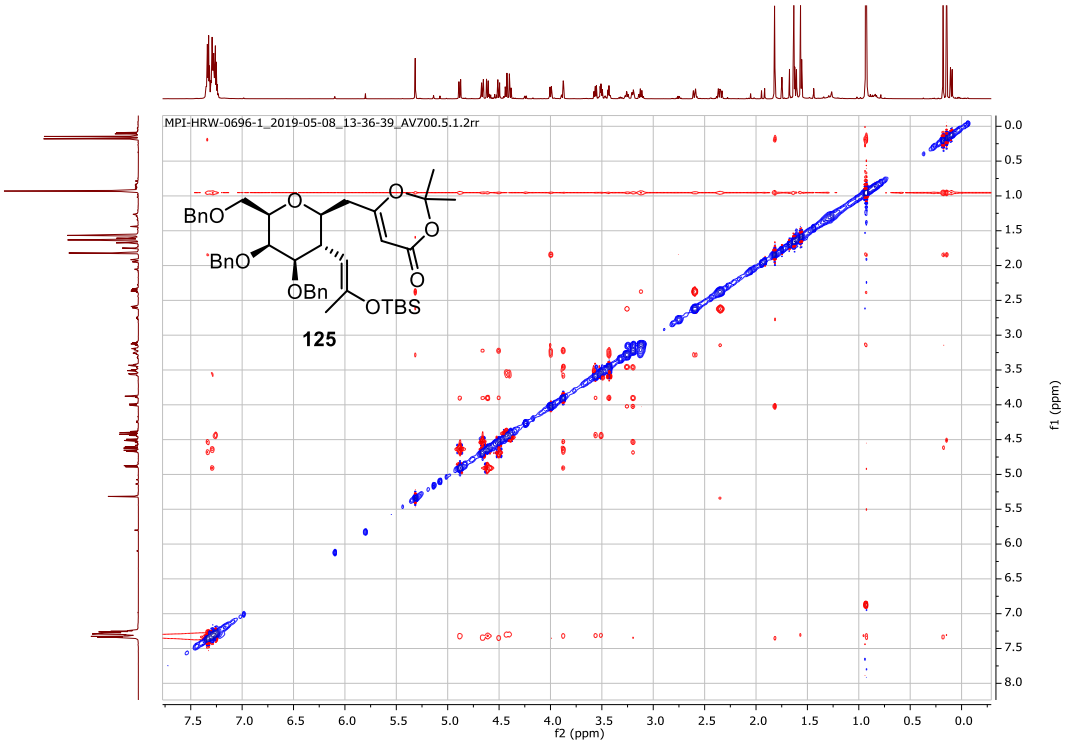

NOESY spectrum of compound **125**

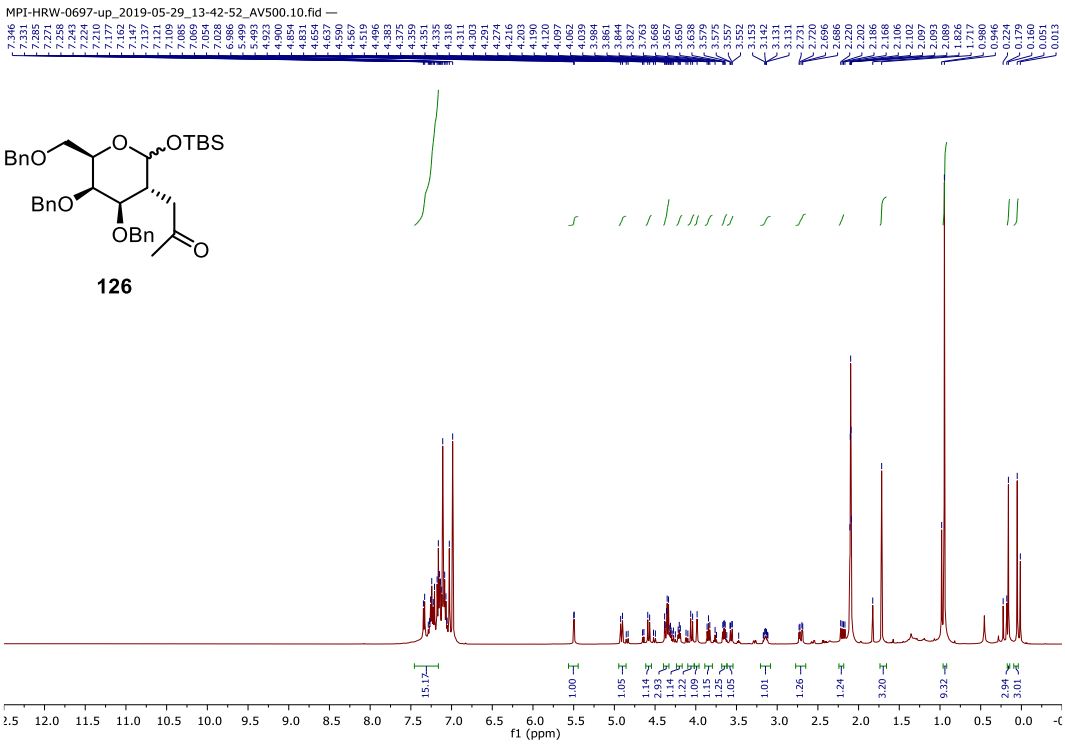

^{1}H NMR spectrum of compound **126** (500 MHz, in toluene-d_8)

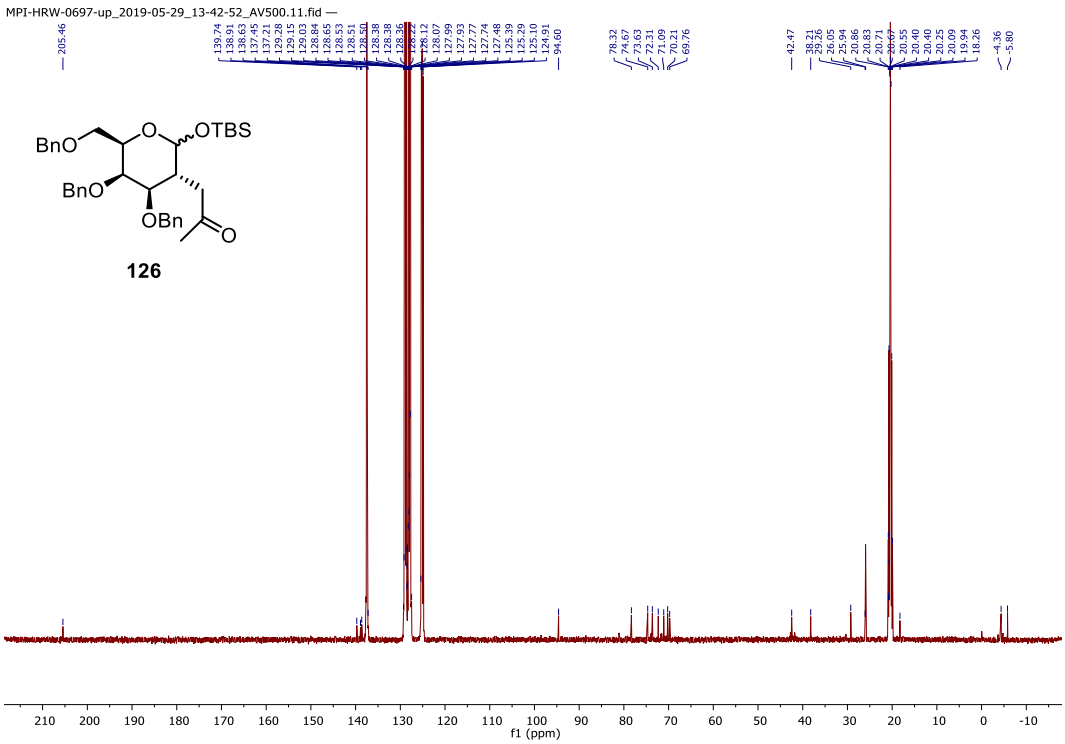

^{13}C NMR spectrum of compound **126** (126 MHz, in toluene-d_8)

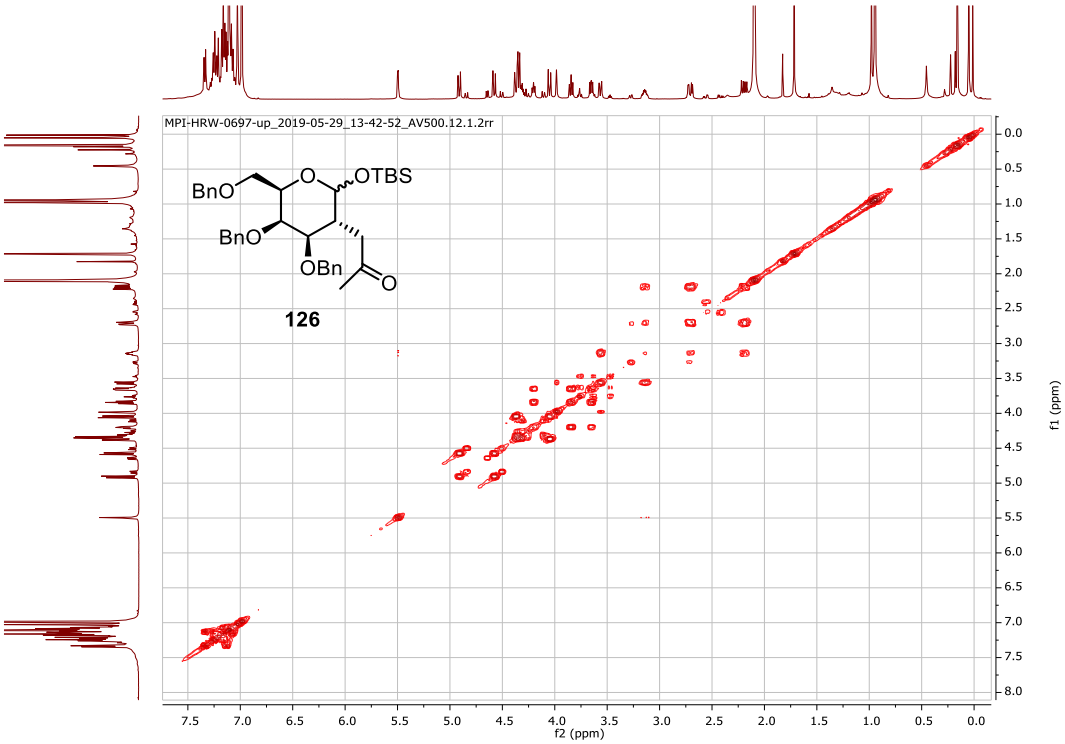

COSY spectrum of compound **126**

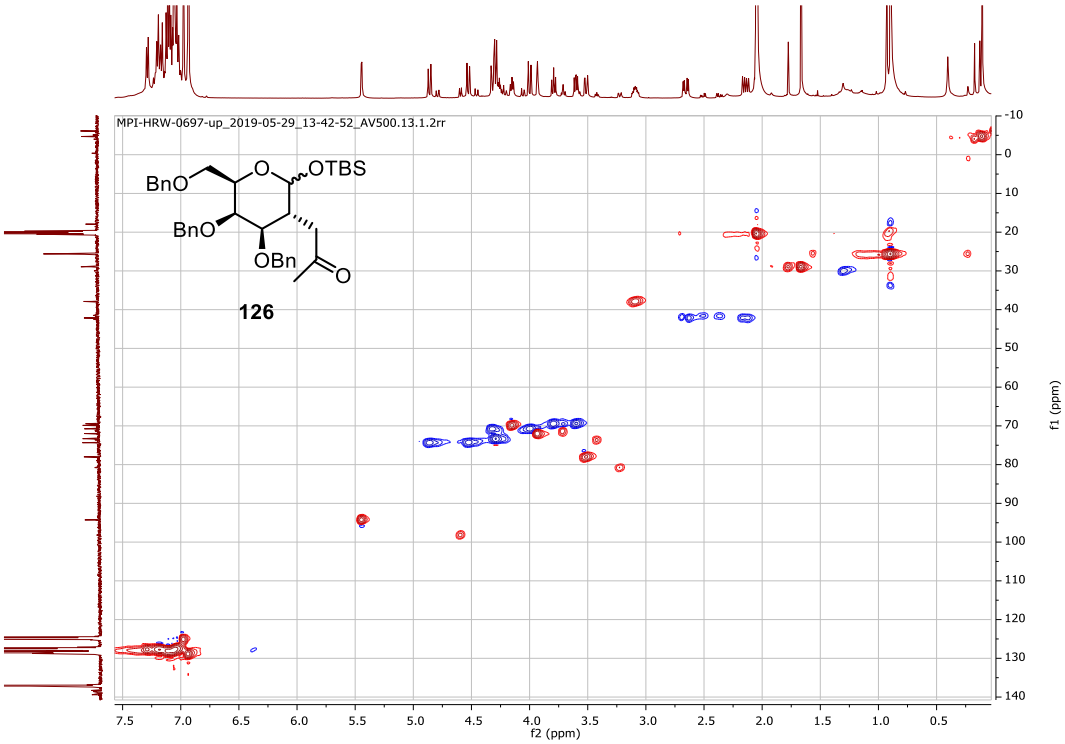

HSQC spectrum of compound **126**

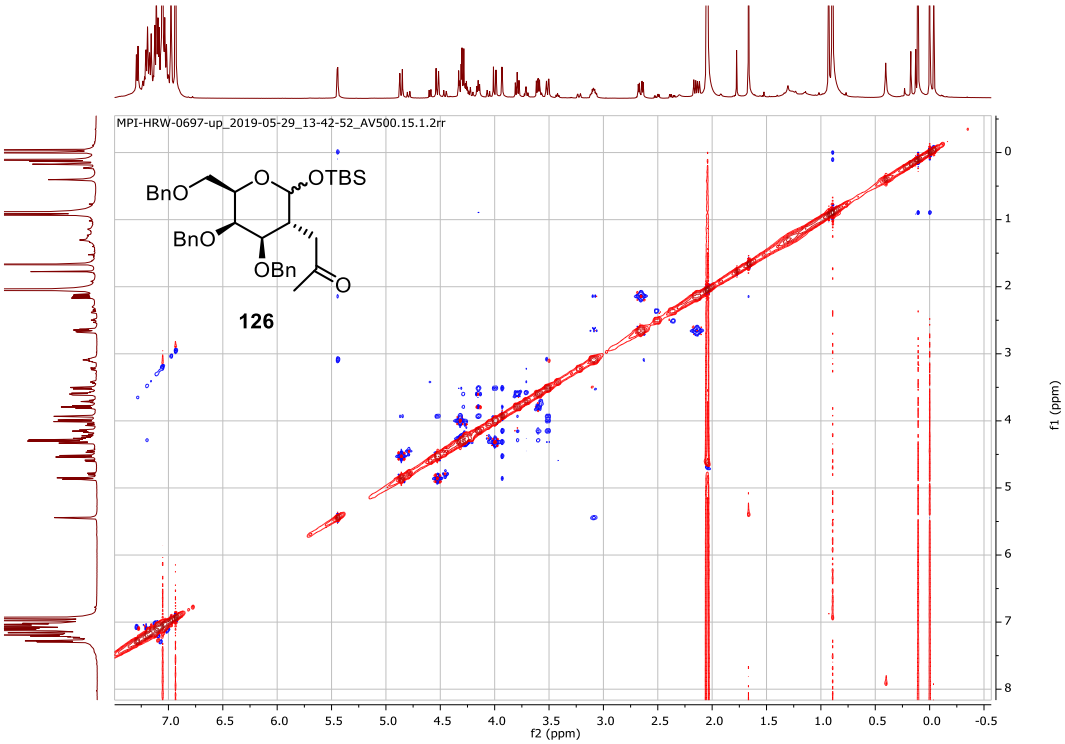

NOESY spectrum of compound **126**

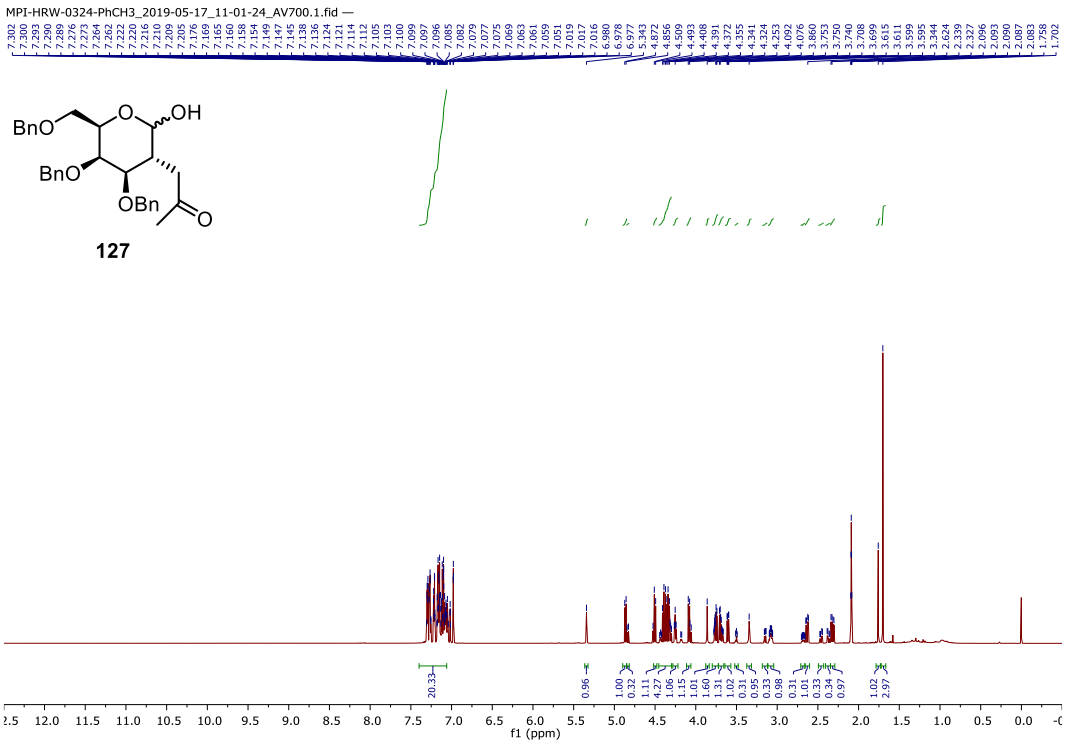

^{1}H NMR spectrum of compound **127** (700 MHz, in toluene-d_8)

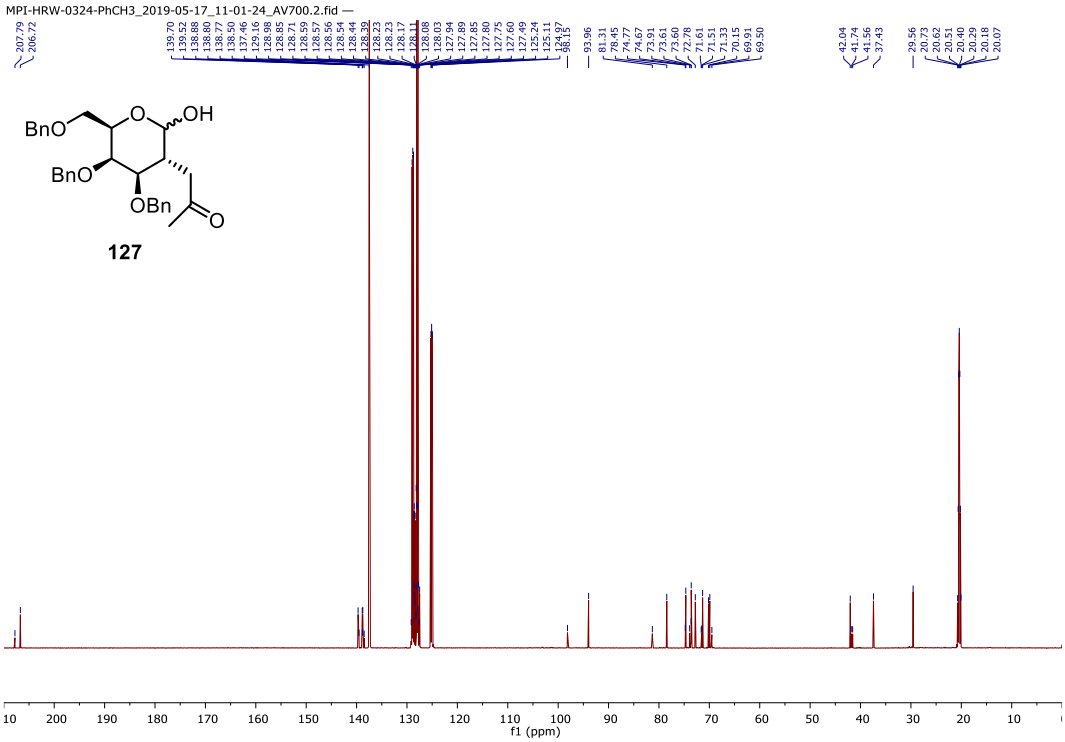

^{13}C NMR spectrum of compound **127** (126 MHz, in toluene-d_8)

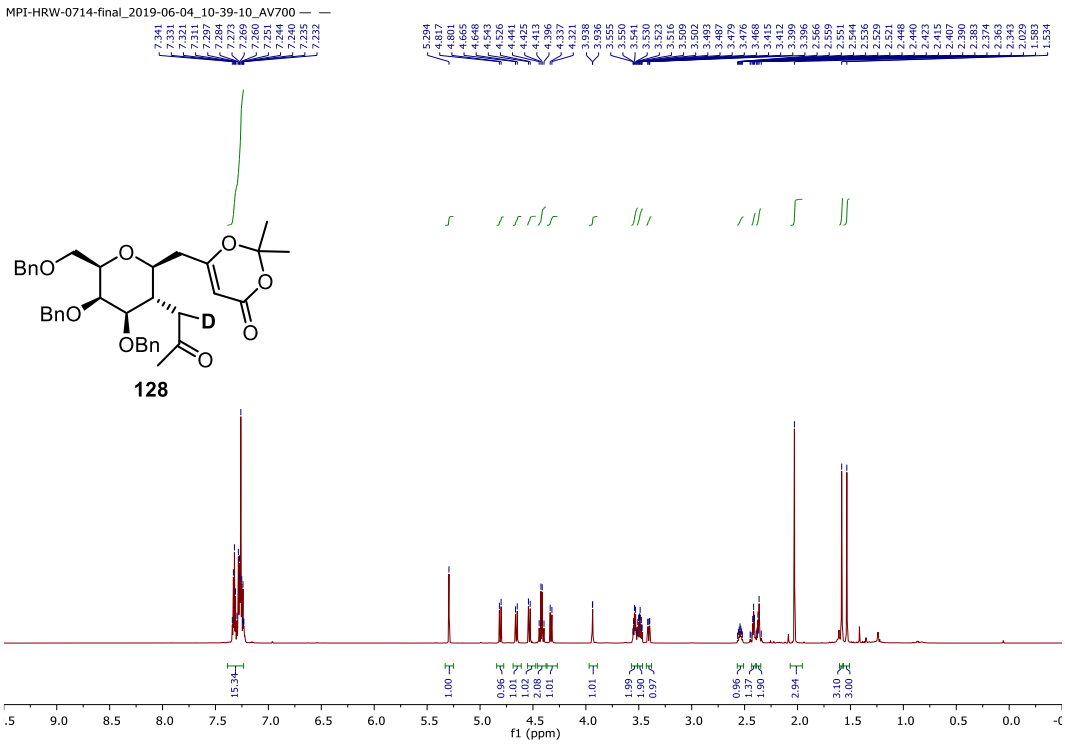

^{1}H NMR spectrum of compound **128** (700 MHz, in $CDCl_3$)

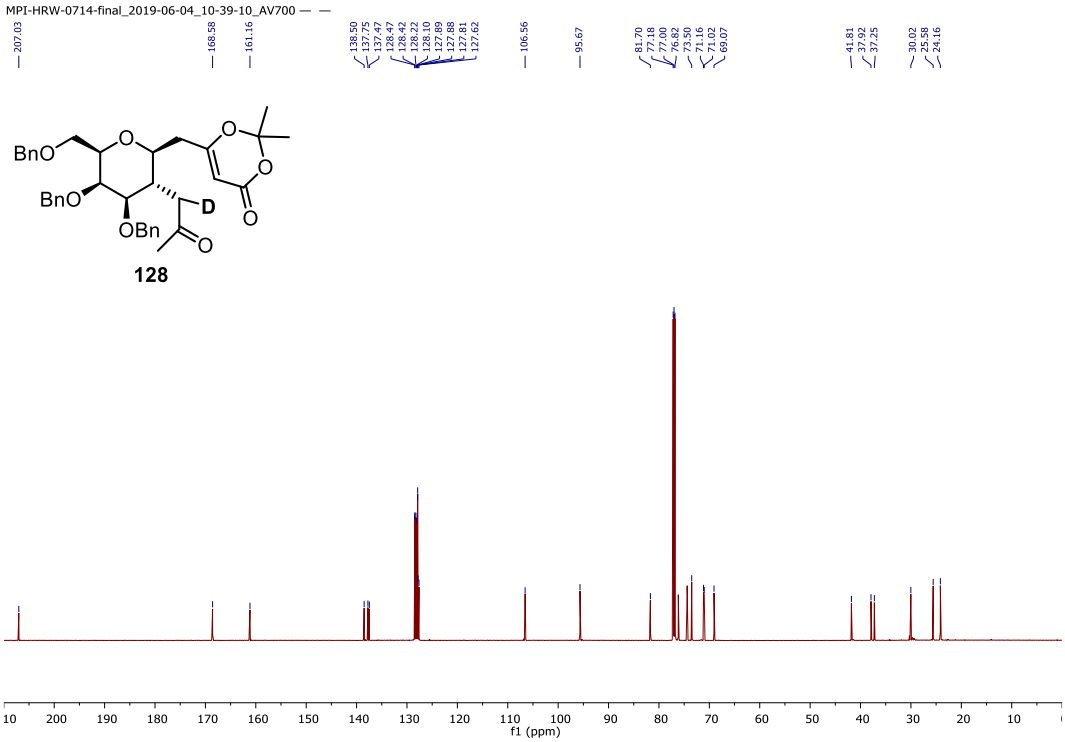

^{13}C NMR spectrum of compound **128** (176 MHz, in $CDCl_3$)

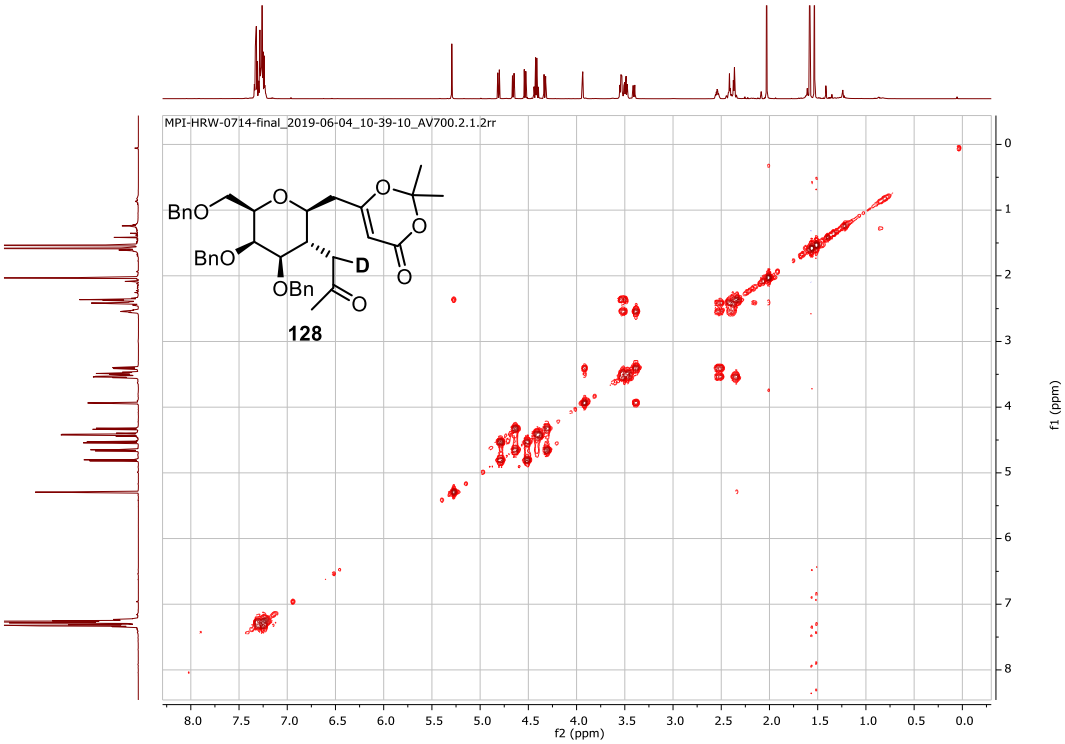

COSY spectrum of compound **128**

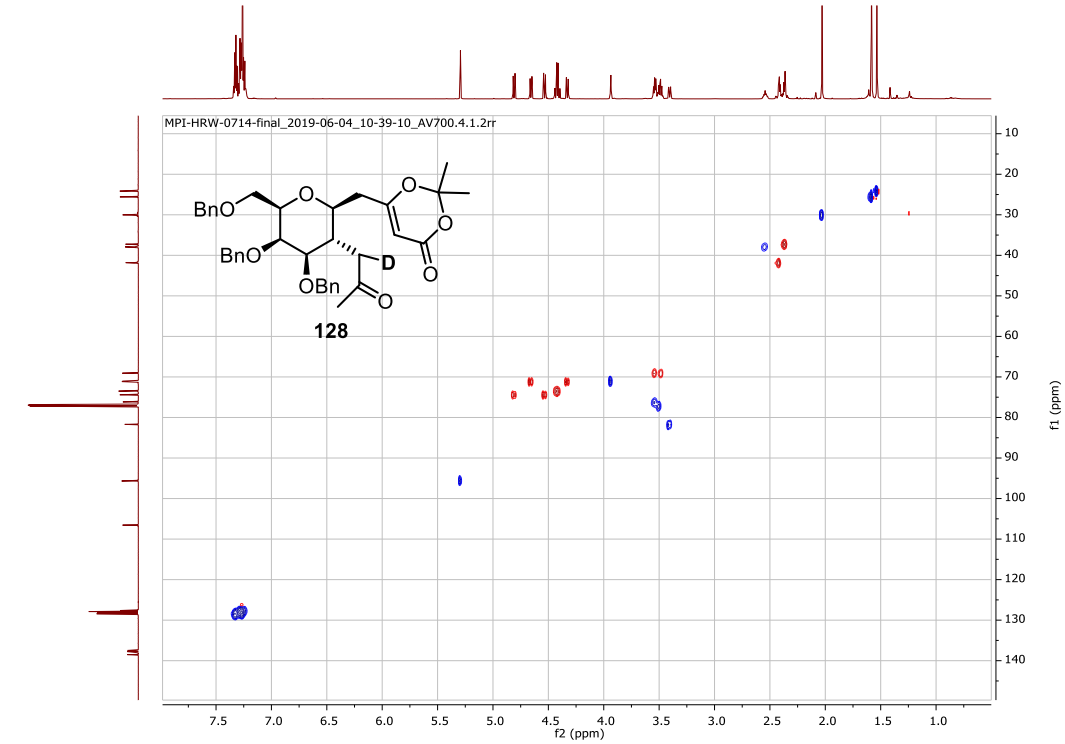

HSQC spectrum of compound **128**

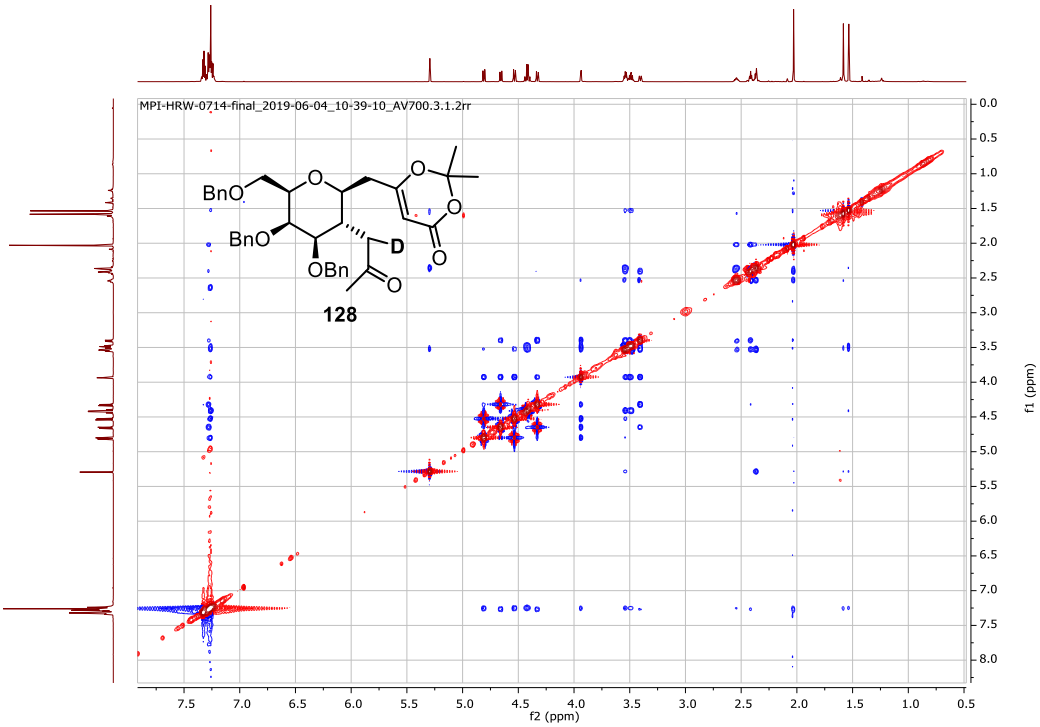

NOESY spectrum of compound **128**

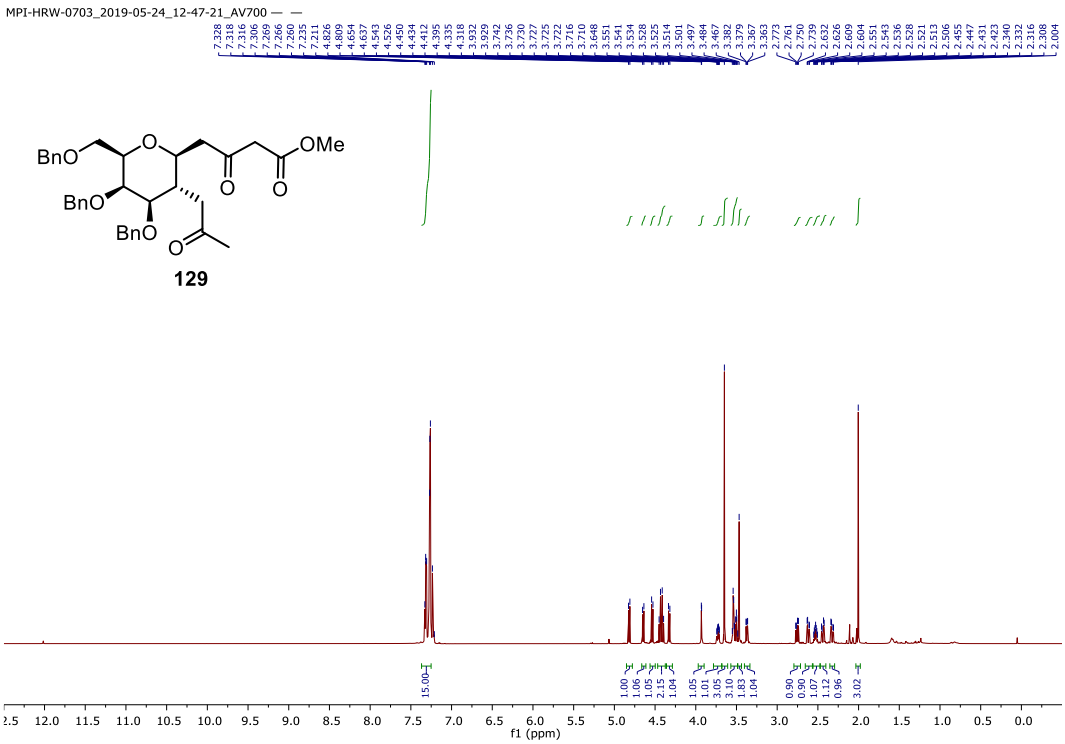

^{1}H NMR spectrum of compound **129** (700 MHz, in $CDCl_3$)

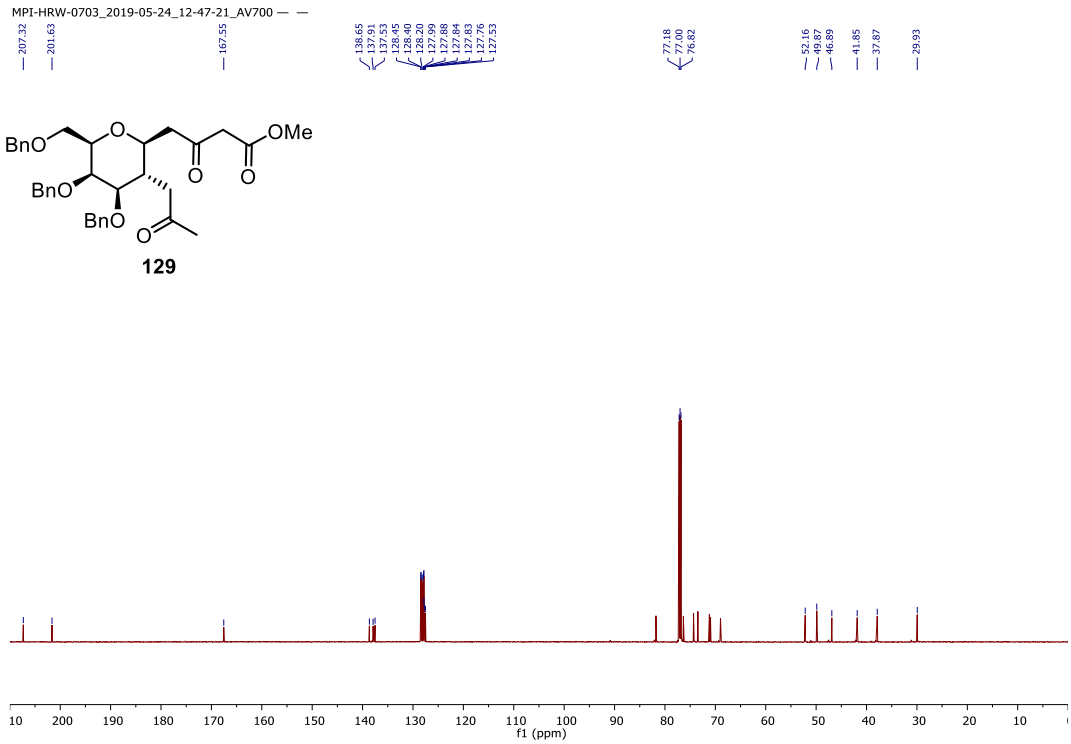

^{13}C NMR spectrum of compound **129** (176 MHz, in $CDCl_3$)

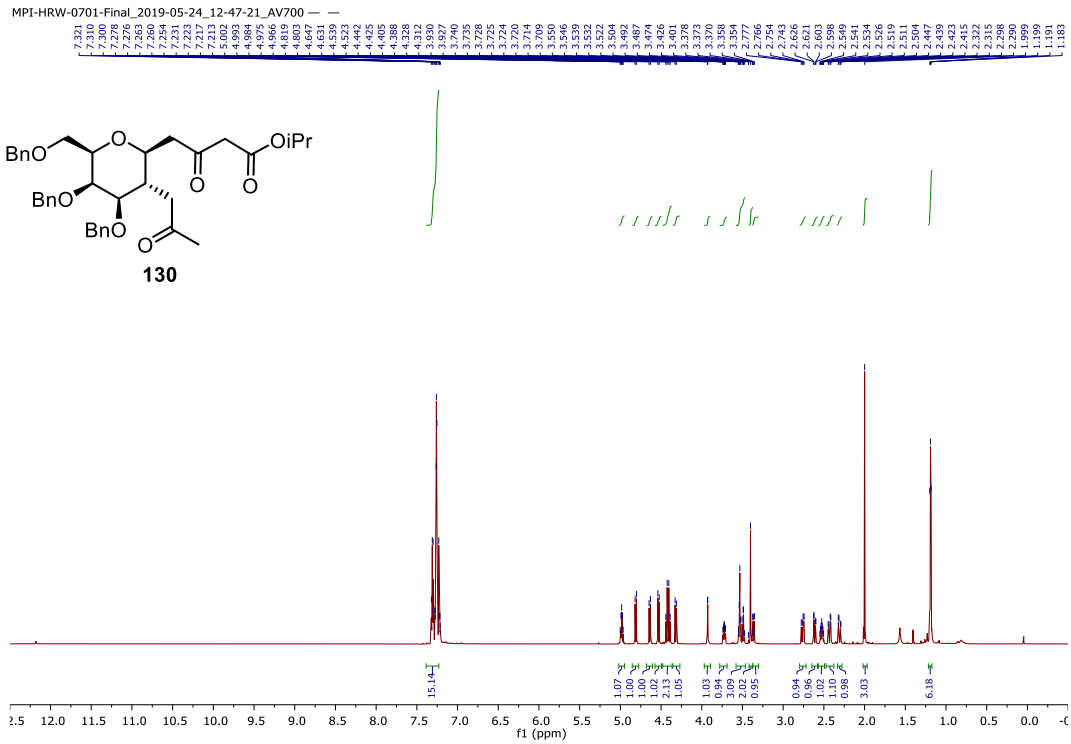

^{1}H NMR spectrum of compound **130** (700 MHz, in $CDCl_3$)

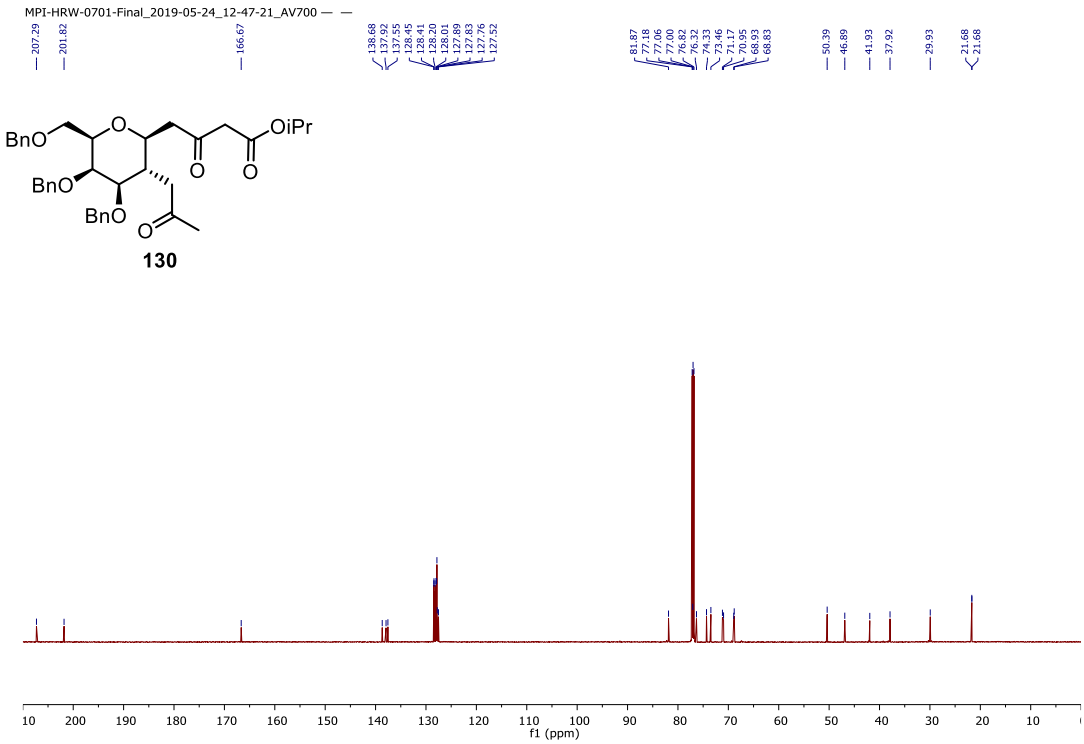

^{13}C NMR spectrum of compound **130** (176 MHz, in $CDCl_3$)

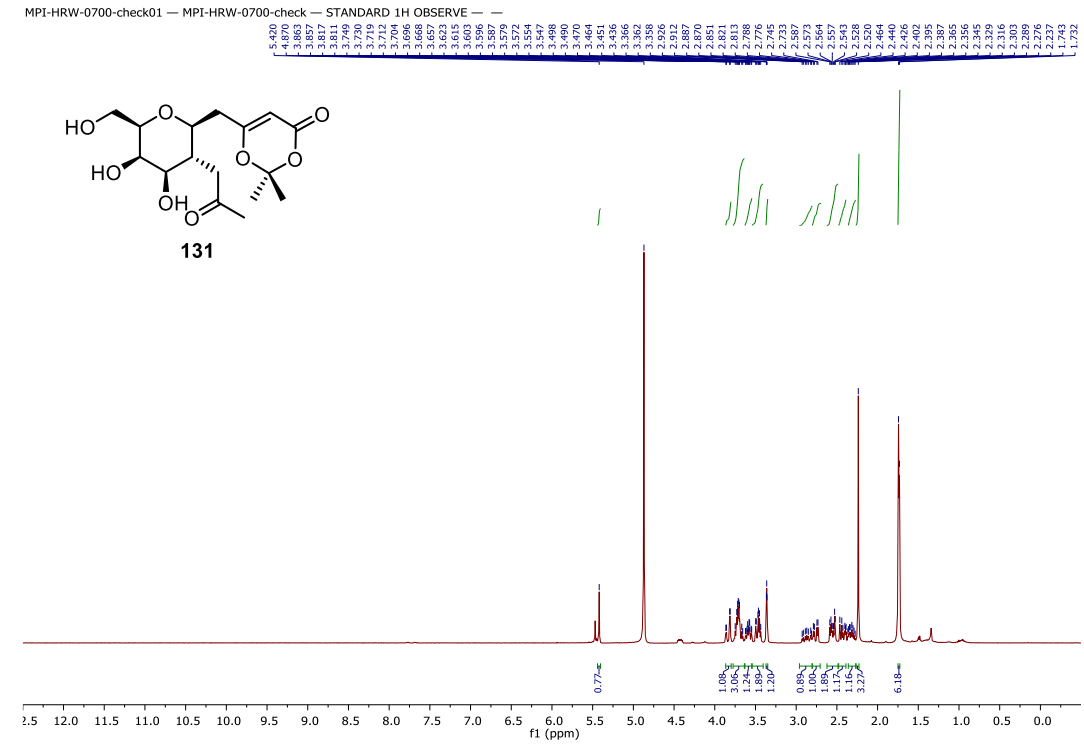

^{1}H NMR spectrum of compound **131** (400 MHz, in CD_3OD)

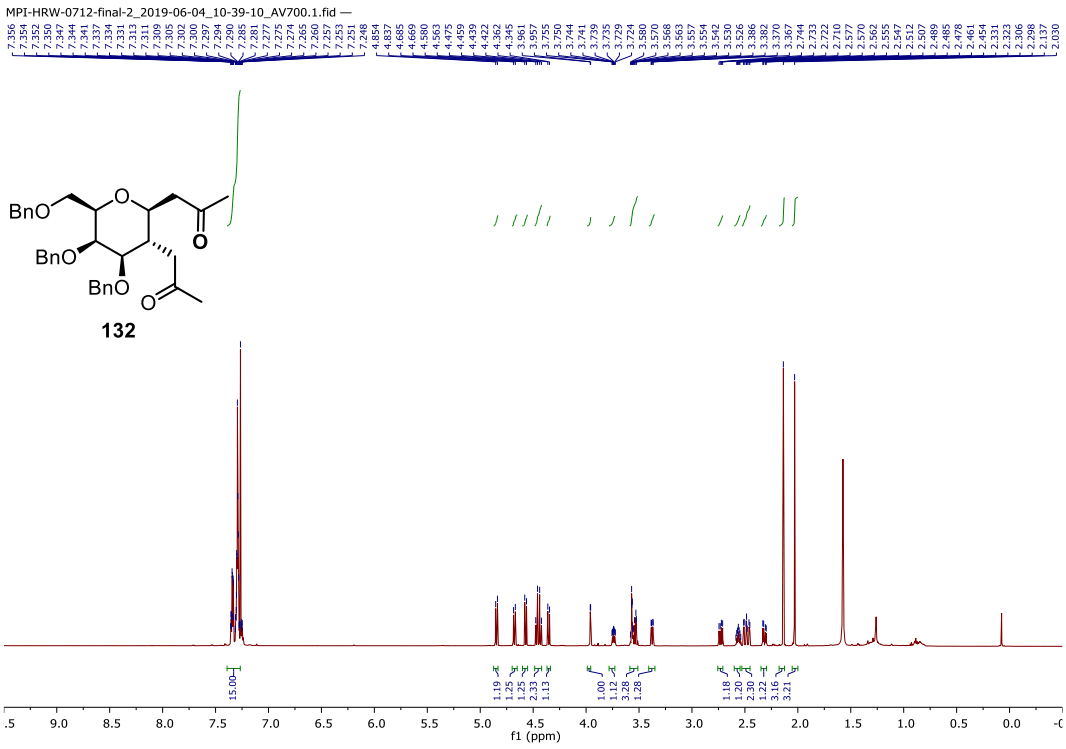

^{1}H NMR spectrum of compound **131** (700 MHz, in $CDCl_3$)

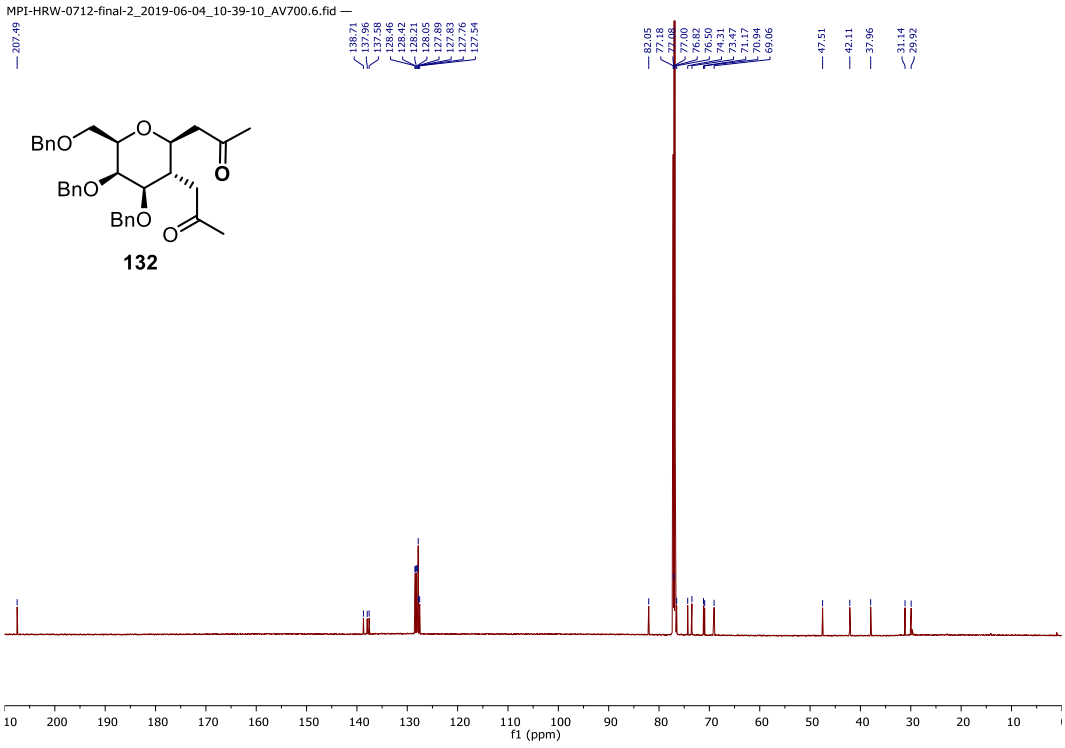

^{13}C NMR spectrum of compound **131** (176 MHz, in $CDCl_3$)

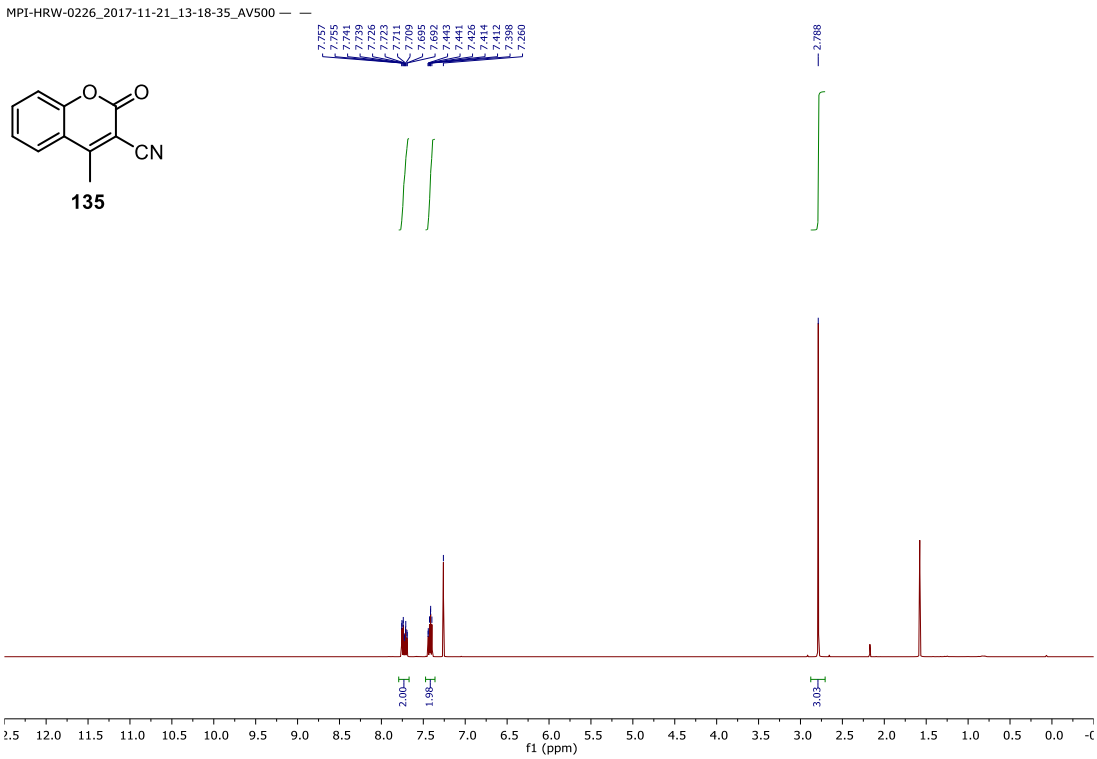

^{1}H NMR spectrum of compound **135** (500 MHz, in $CDCl_3$)

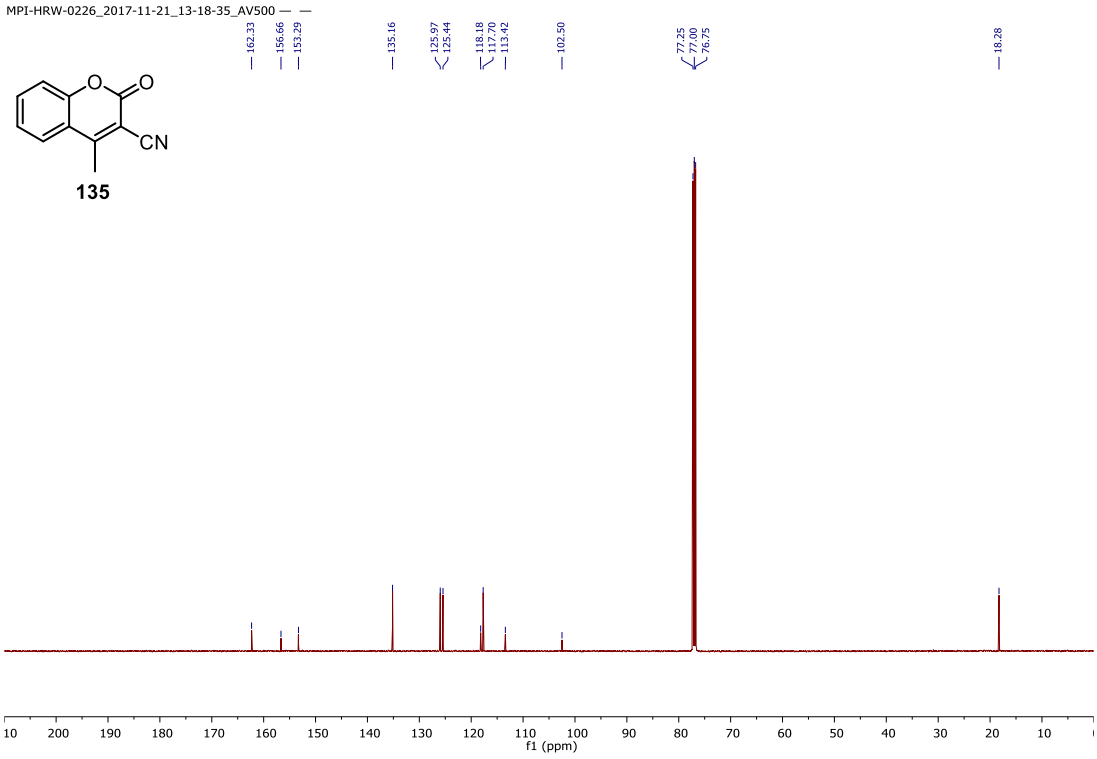

^{13}C NMR spectrum of compound **135** (126 MHz, in $CDCl_3$)

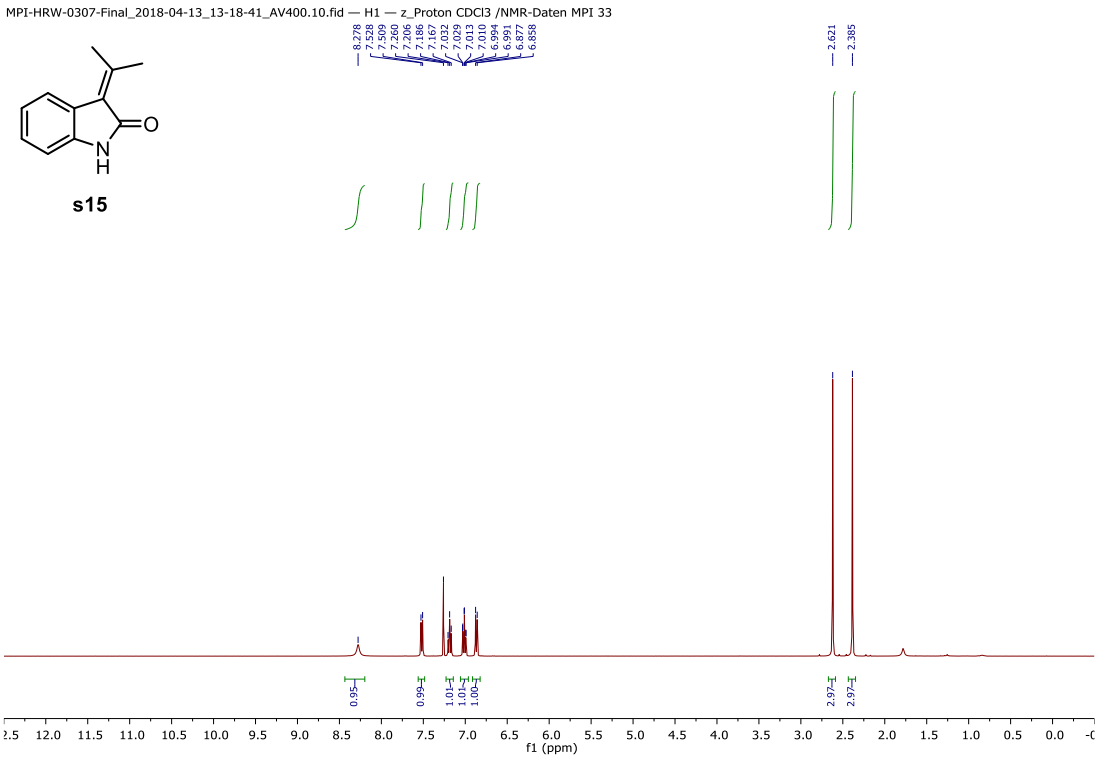

^{1}H NMR spectrum of compound **s15** (400 MHz, in $CDCl_3$)

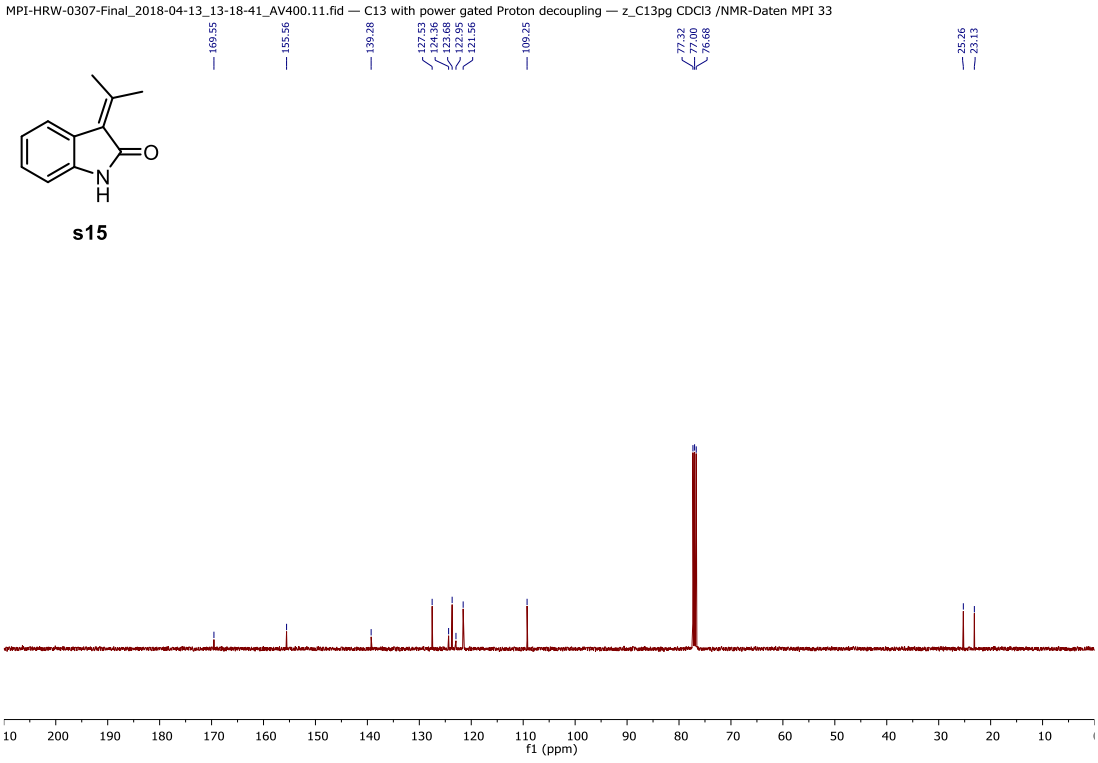

^{13}C NMR spectrum of compound **s15** (101 MHz, in $CDCl_3$)

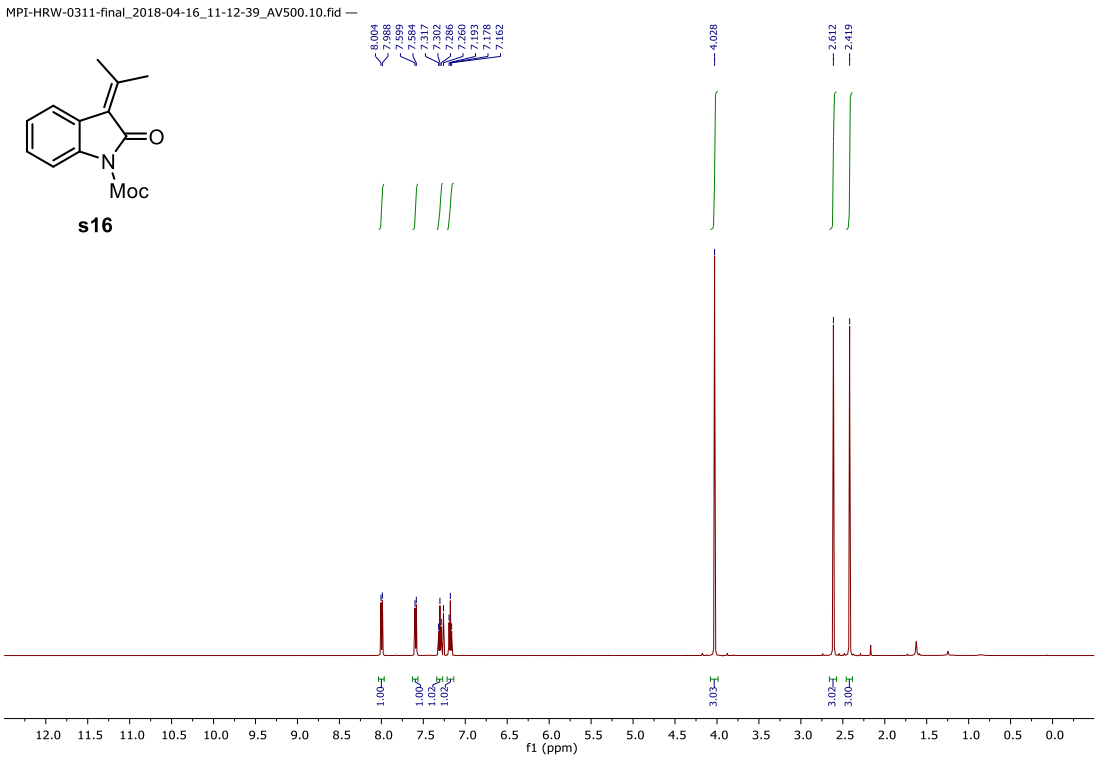

^{1}H NMR spectrum of compound **s16** (400 MHz, in $CDCl_3$)

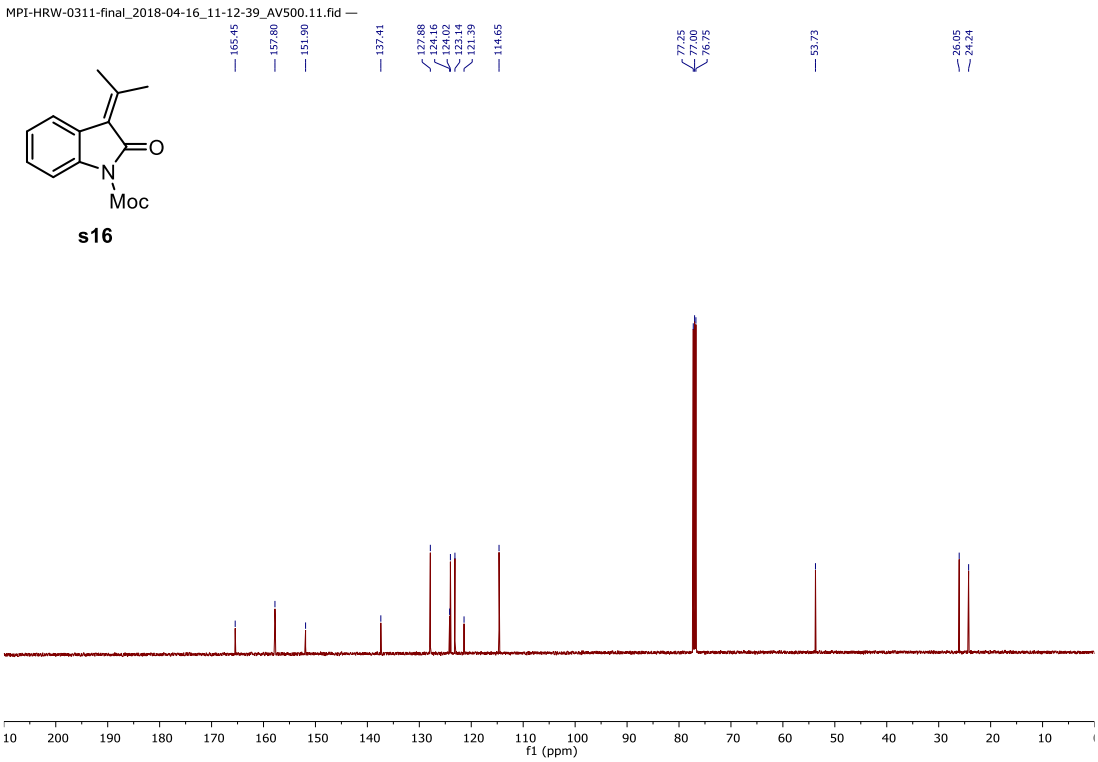

^{13}C NMR spectrum of compound **s16** (126 MHz, in $CDCl_3$)

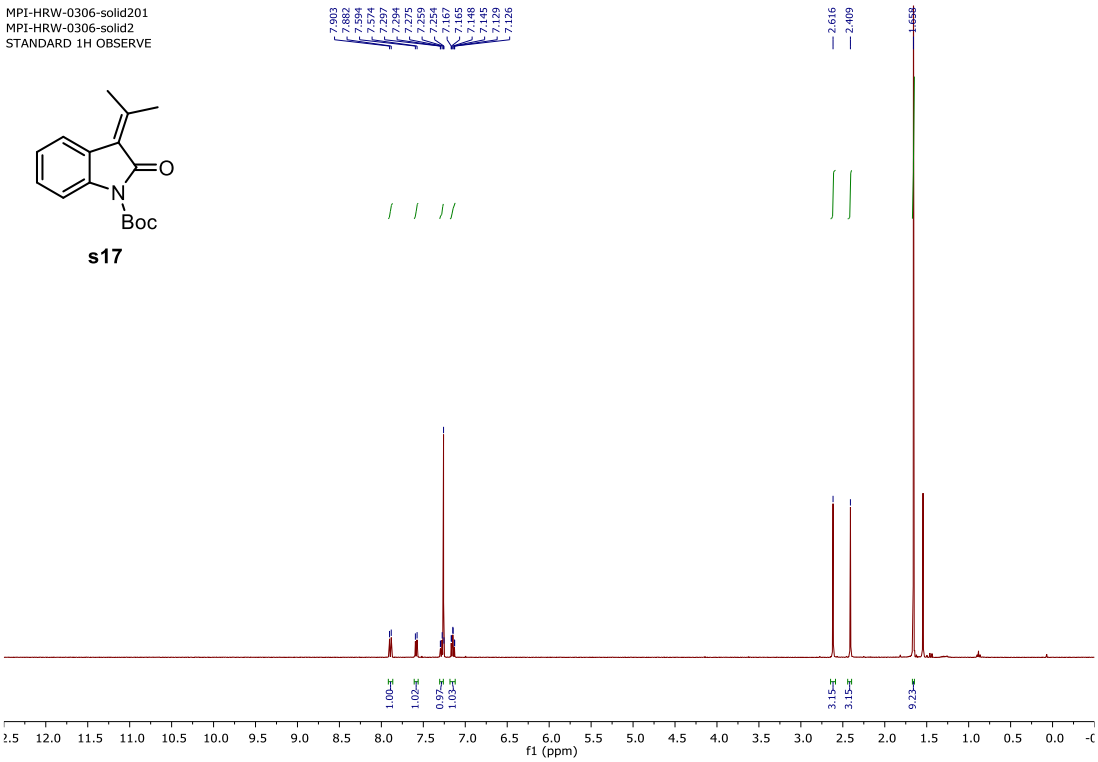

^{1}H NMR spectrum of compound **s17** (400 MHz, in $CDCl_3$)

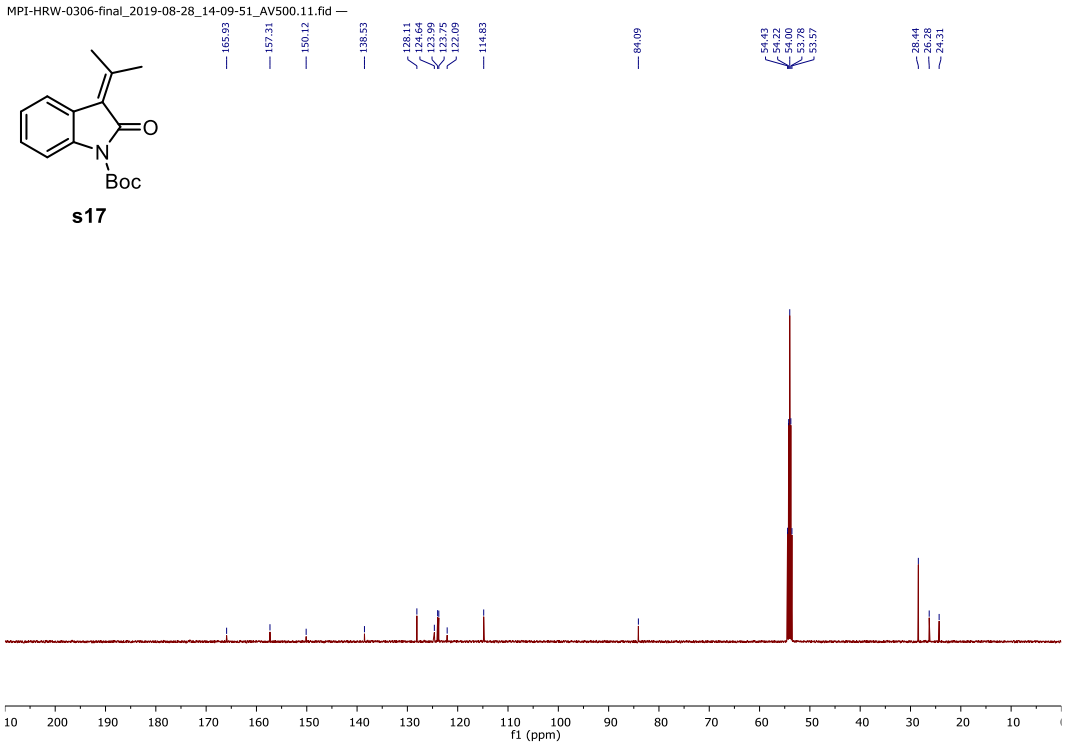

^{13}C NMR spectrum of compound **s17** (126 MHz, in CD_2Cl_2)

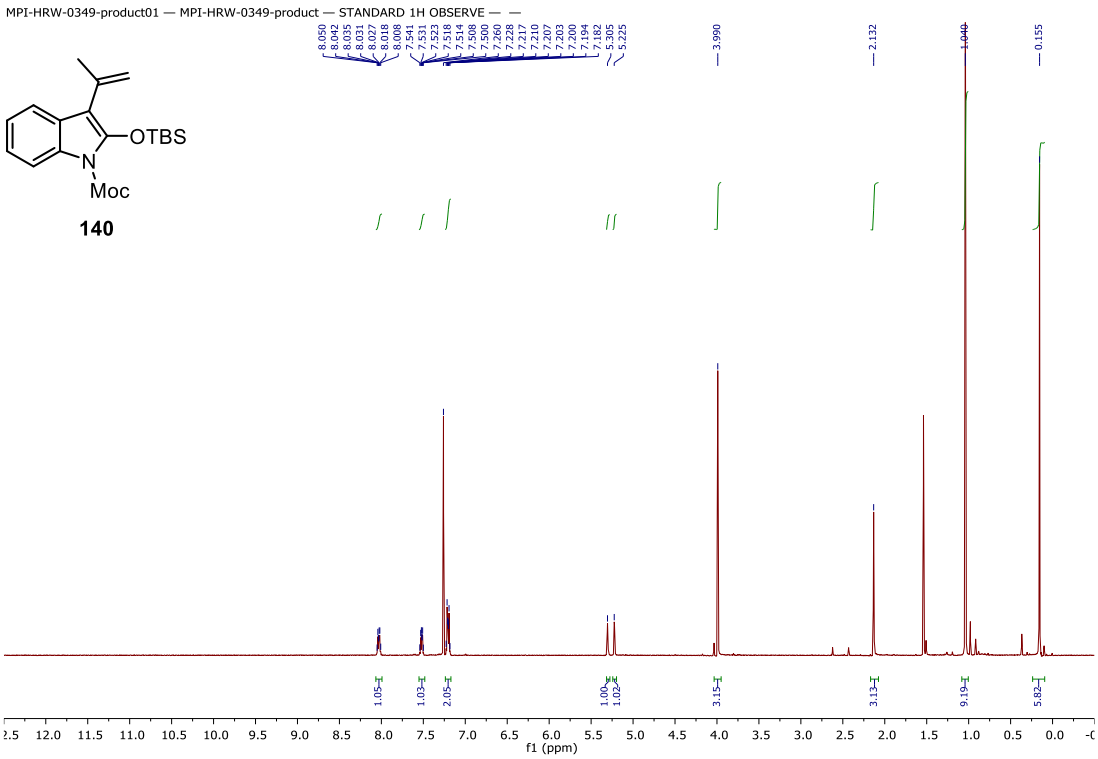

^{1}H NMR spectrum of compound **140** (400 MHz, in $CDCl_3$)

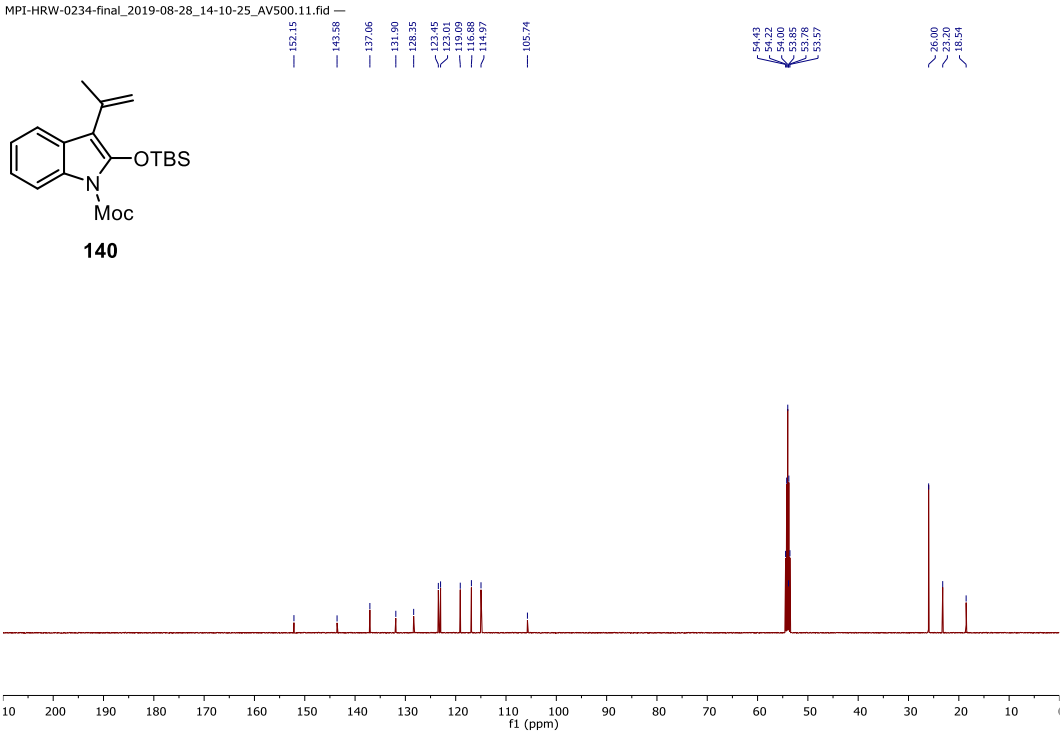

^{13}C NMR spectrum of compound **140** (126 MHz, in CD_2Cl_2)

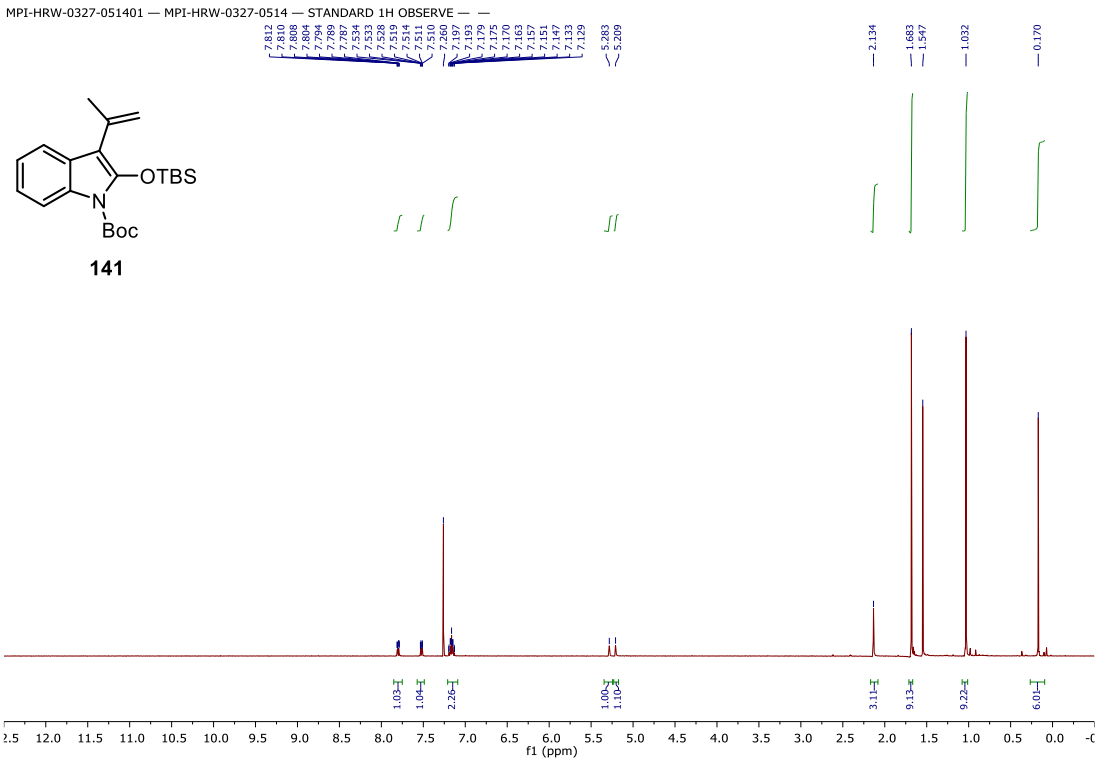

^{1}H NMR spectrum of compound **141** (400 MHz, in $CDCl_3$)

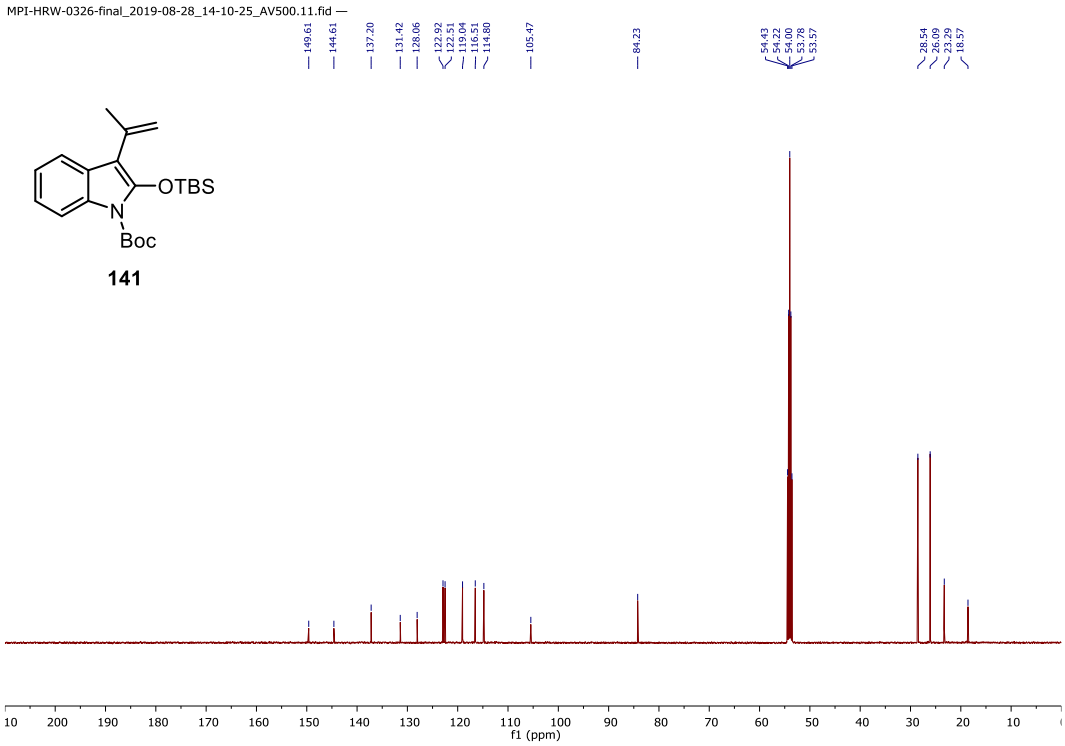

^{13}C NMR spectrum of compound **141** (126 MHz, in CD_2Cl_2)

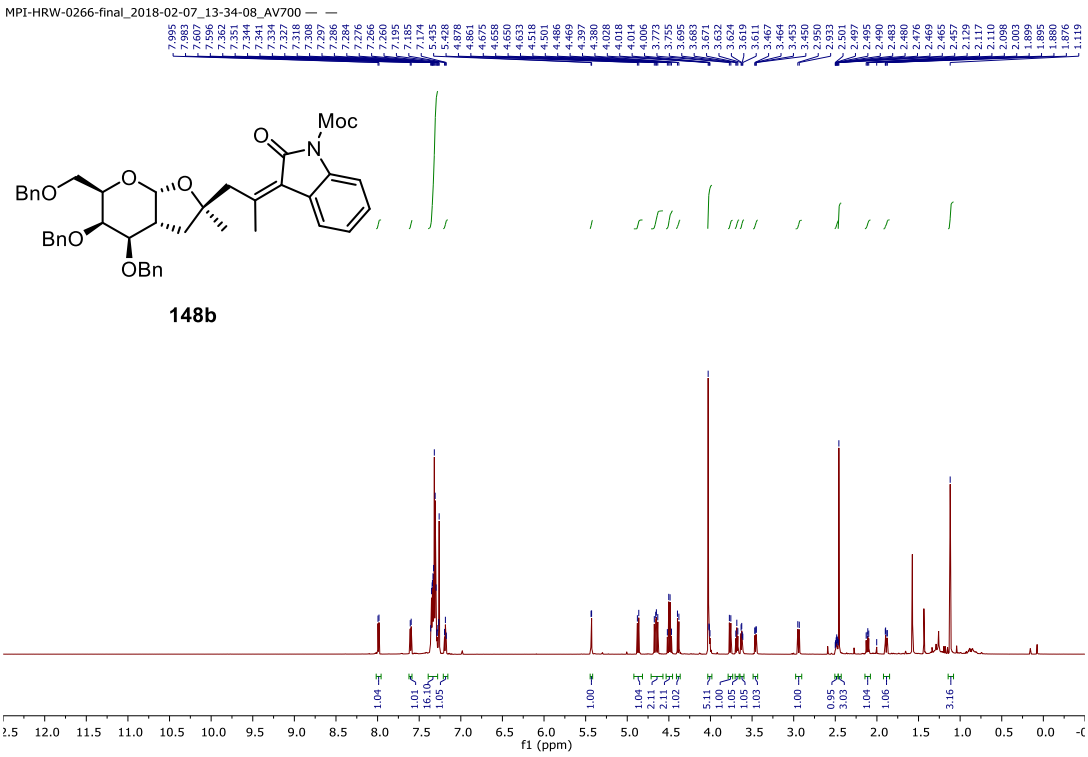

^{1}H NMR spectrum of compound **148b** (700 MHz, in $CDCl_3$)

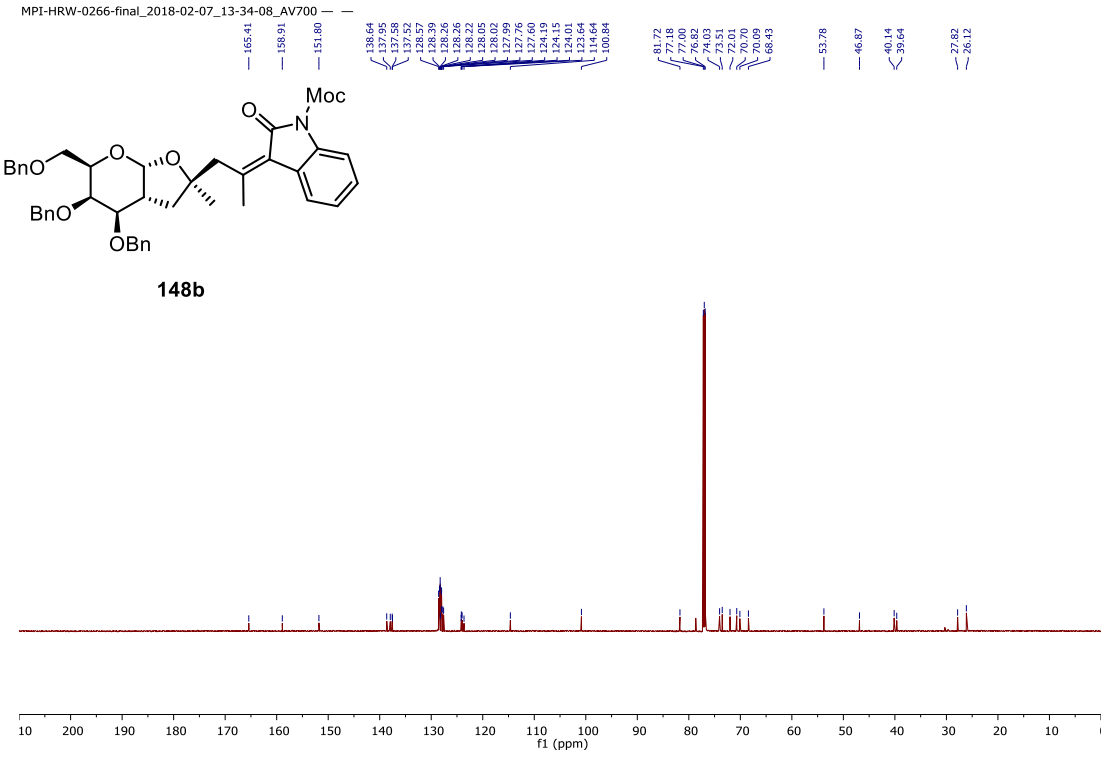

^{13}C NMR spectrum of compound **148b** (176 MHz, in $CDCl_3$)

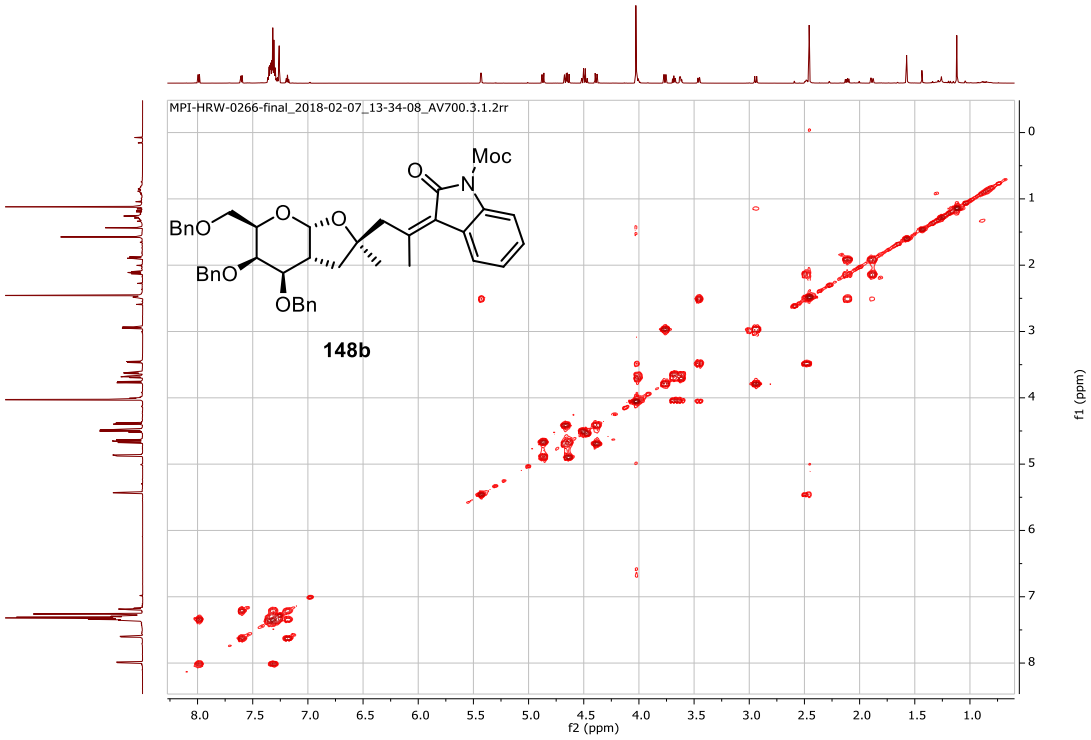

COSY spectrum of compound **148b**

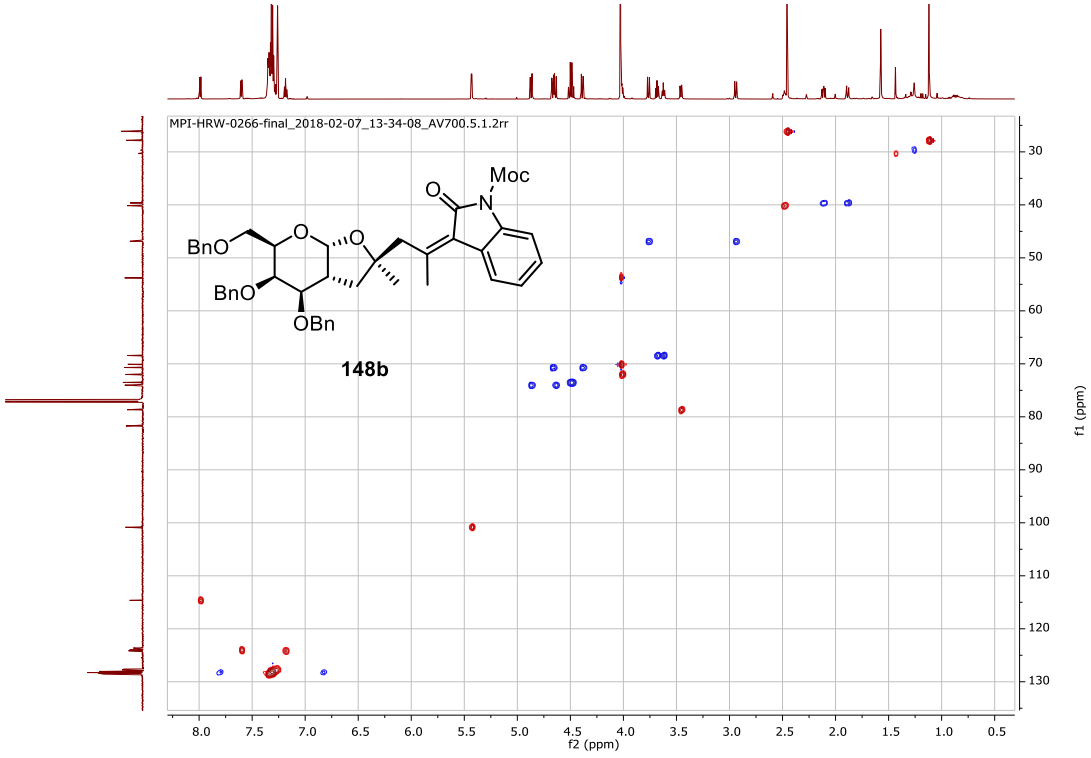

HSQC spectrum of compound **148b**

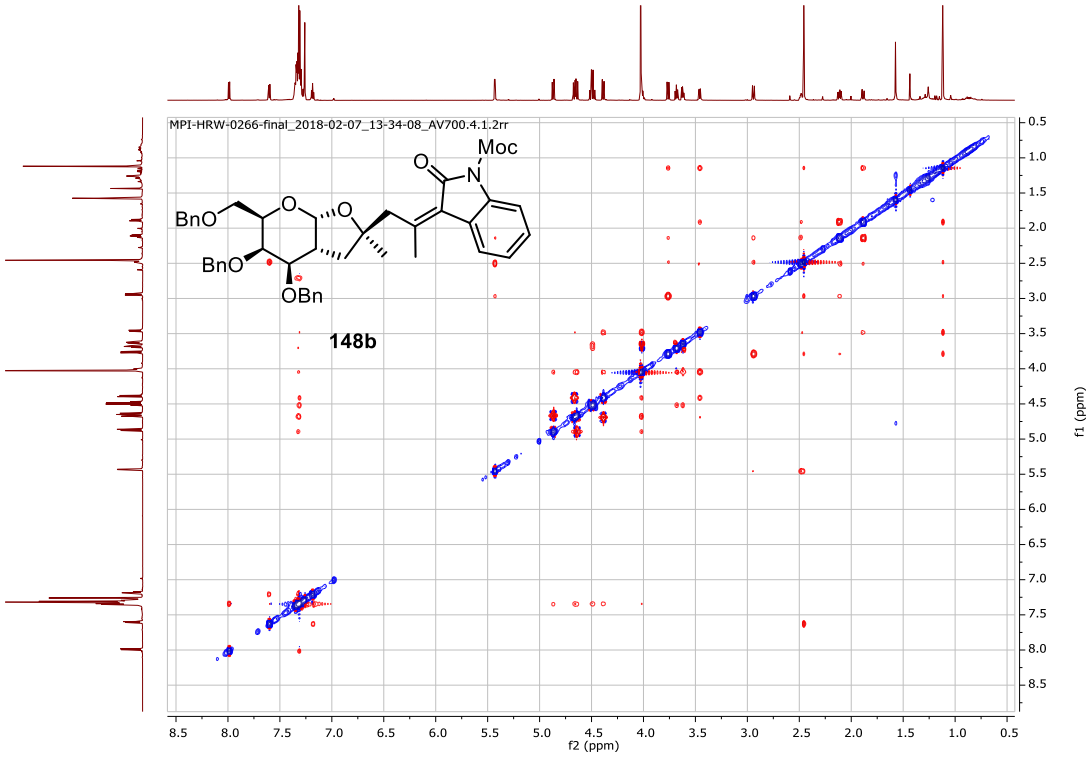

NOESY spectrum of compound **148b**

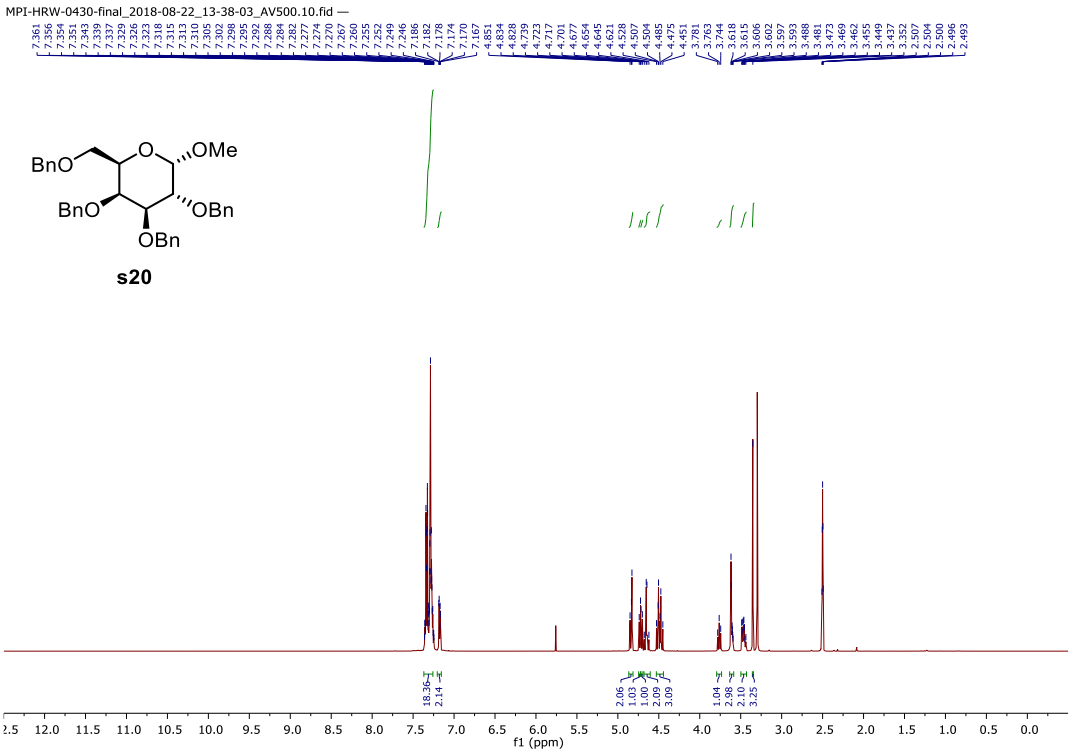

^{1}H NMR spectrum of compound **s20** (500 MHz, in DMSO–d_6)

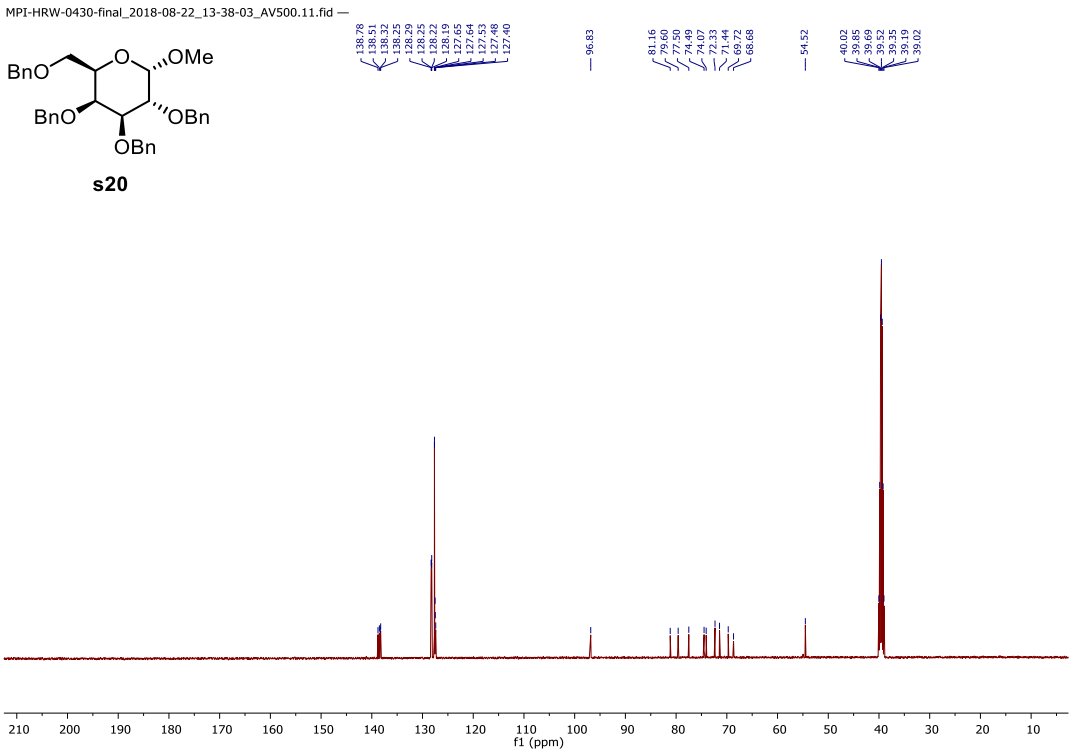

^{13}C NMR spectrum of compound **s20** (126 MHz, in DMSO–d_6)

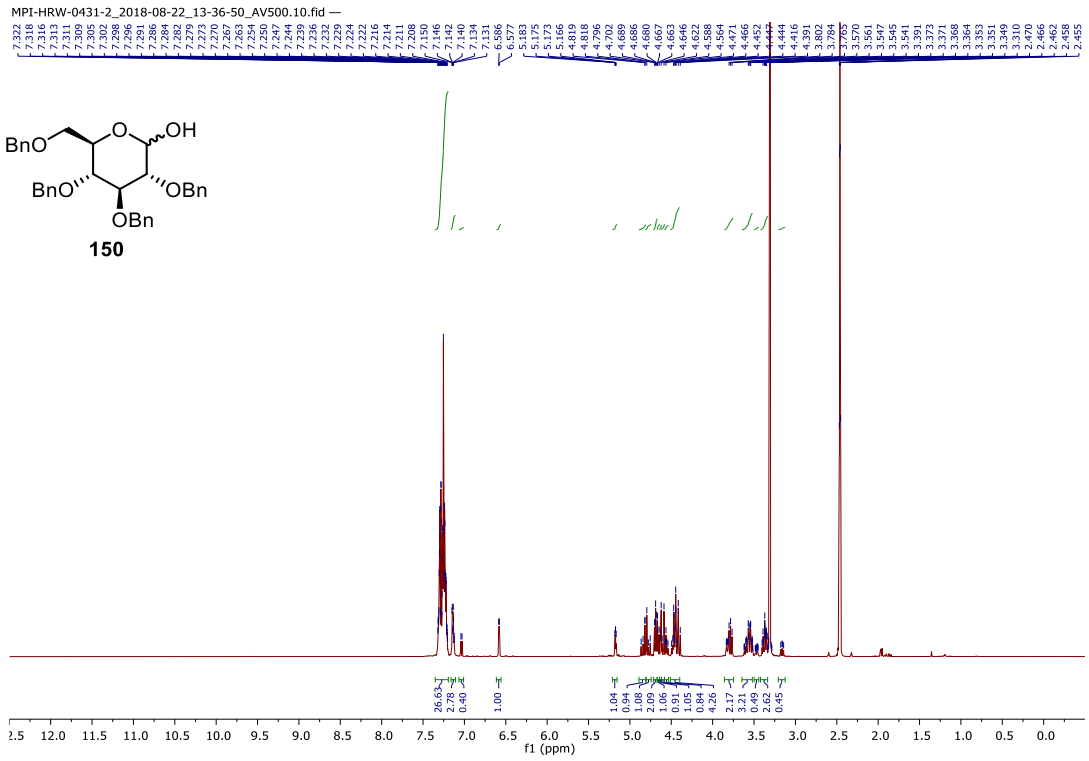

^{1}H NMR spectrum of compound **150** (500 MHz, in CD_3OD)

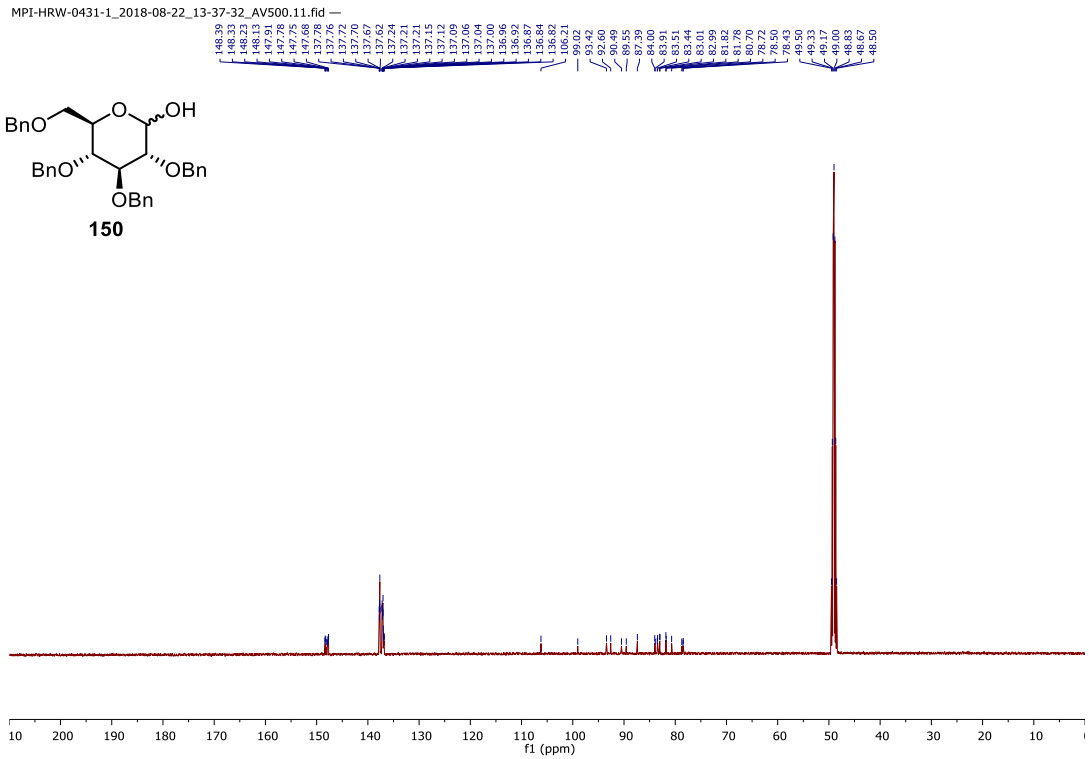

^{13}C NMR spectrum of compound **150** (126 MHz, in CD_3OD)

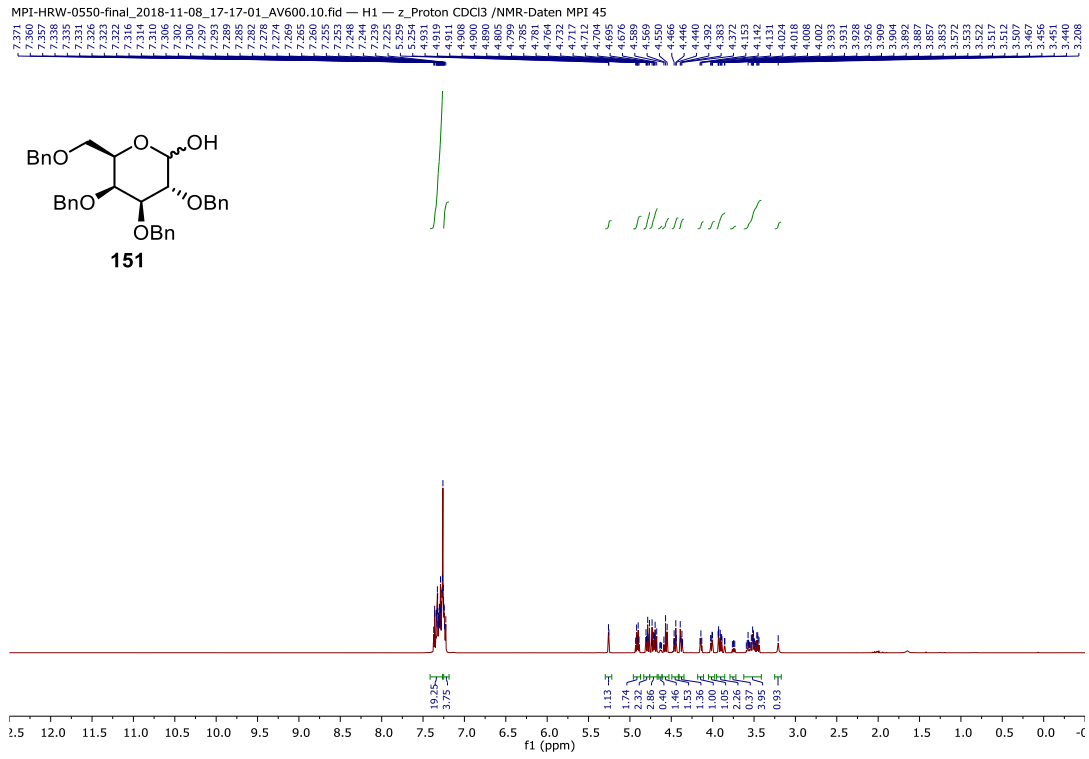

^{1}H NMR spectrum of compound **151** (600 MHz, in $CDCl_3$)

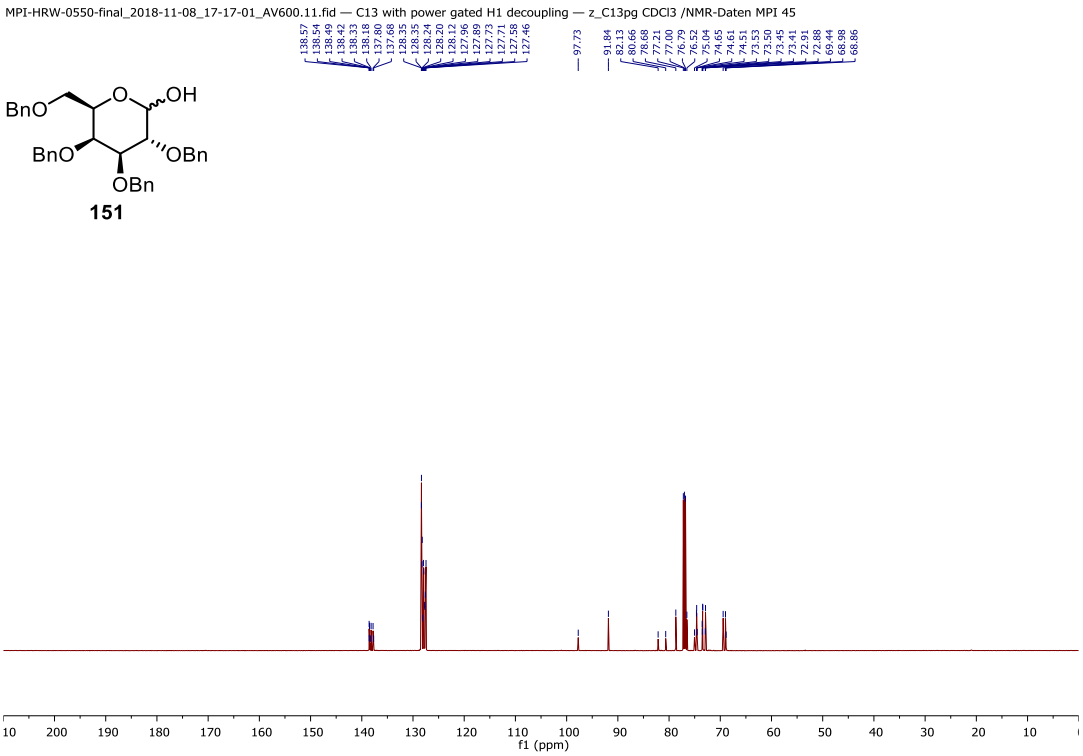

^{13}C NMR spectrum of compound **151** (151 MHz, in $CDCl_3$)

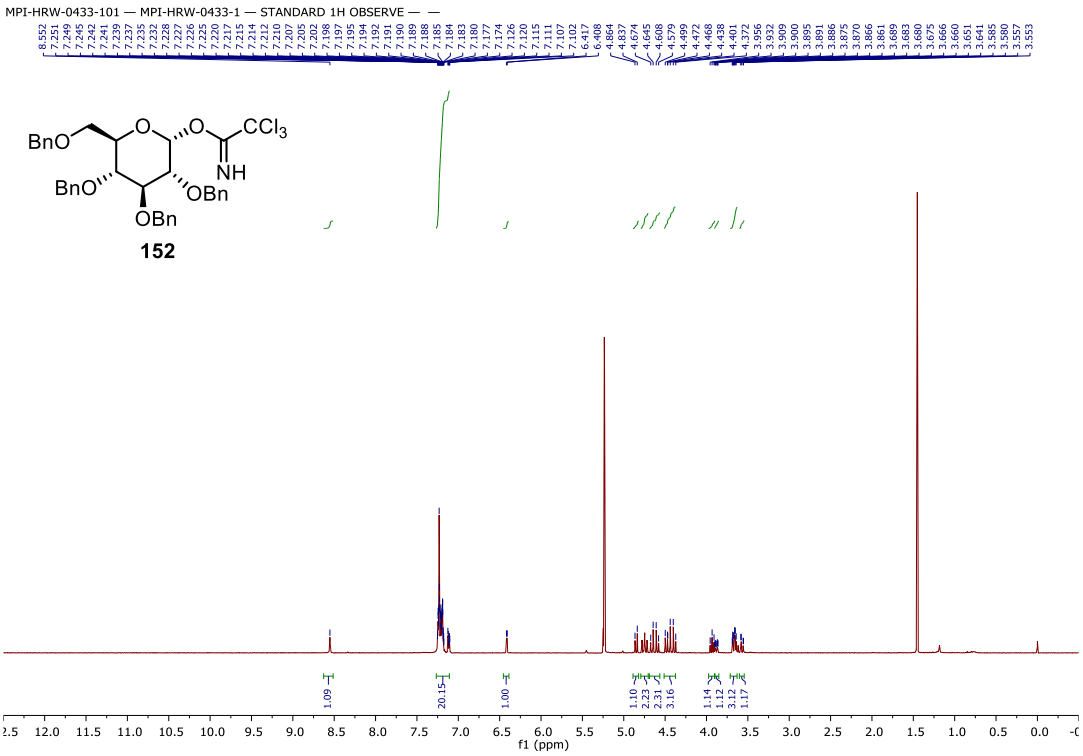

^{1}H NMR spectrum of compound **152** (400 MHz, in CD_2Cl_2)

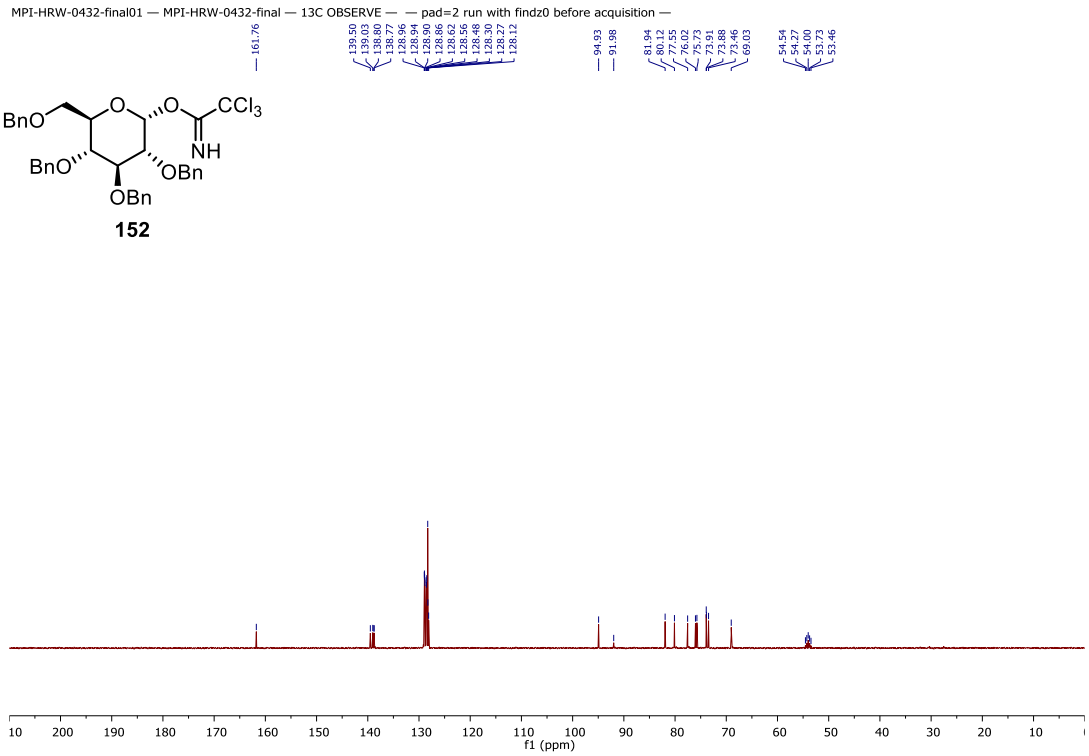

152

^{13}C NMR spectrum of compound **152** (101 MHz, in CD_2Cl_2)

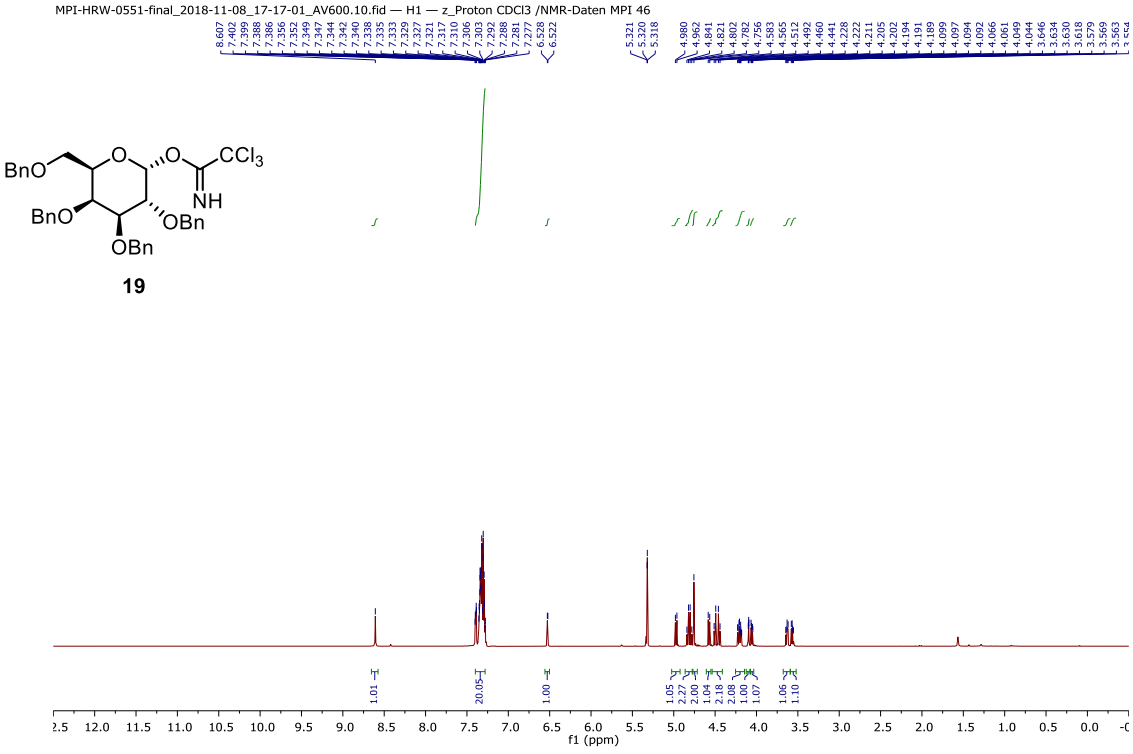

19

^{1}H NMR spectrum of compound **19** (600 MHz, in CD_2Cl_2)

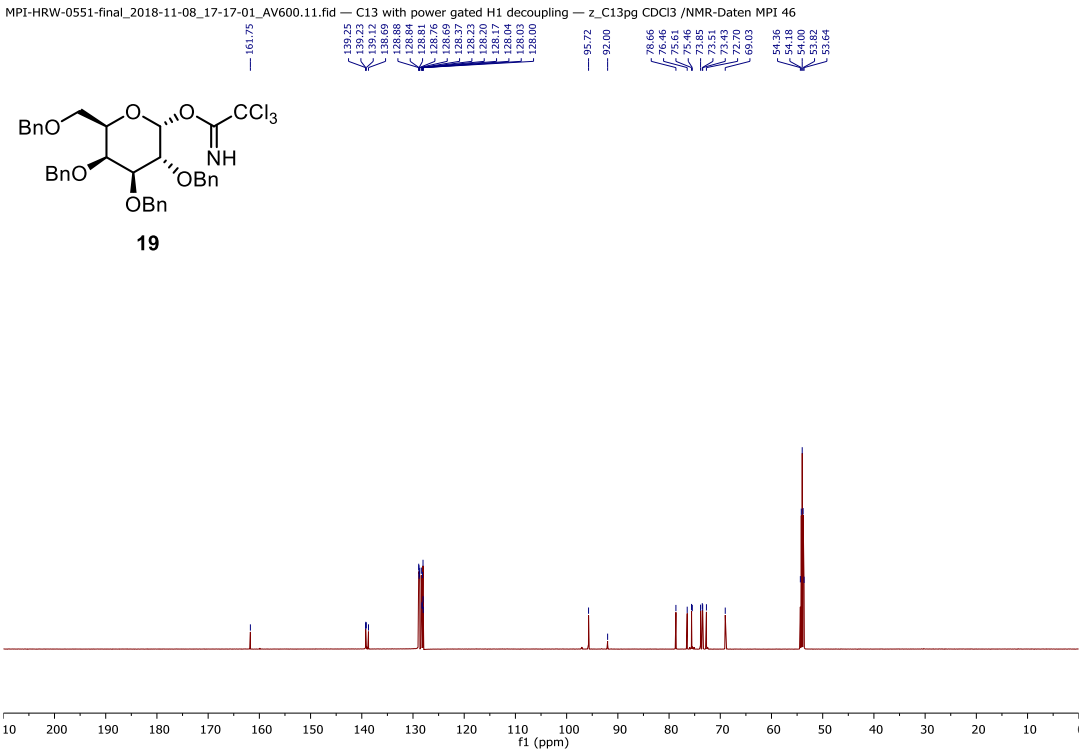

^{13}C NMR spectrum of compound **19** (151 MHz, in CD_2Cl_2)

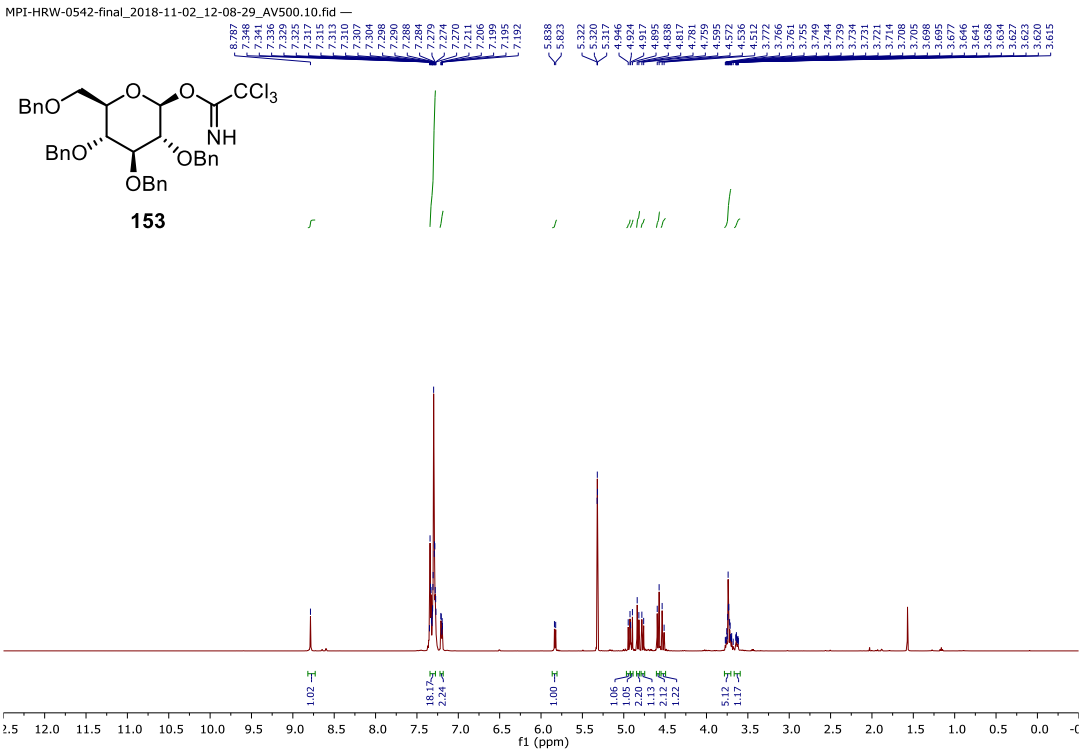

^{1}H NMR spectrum of compound **153** (500 MHz, in CD_2Cl_2)

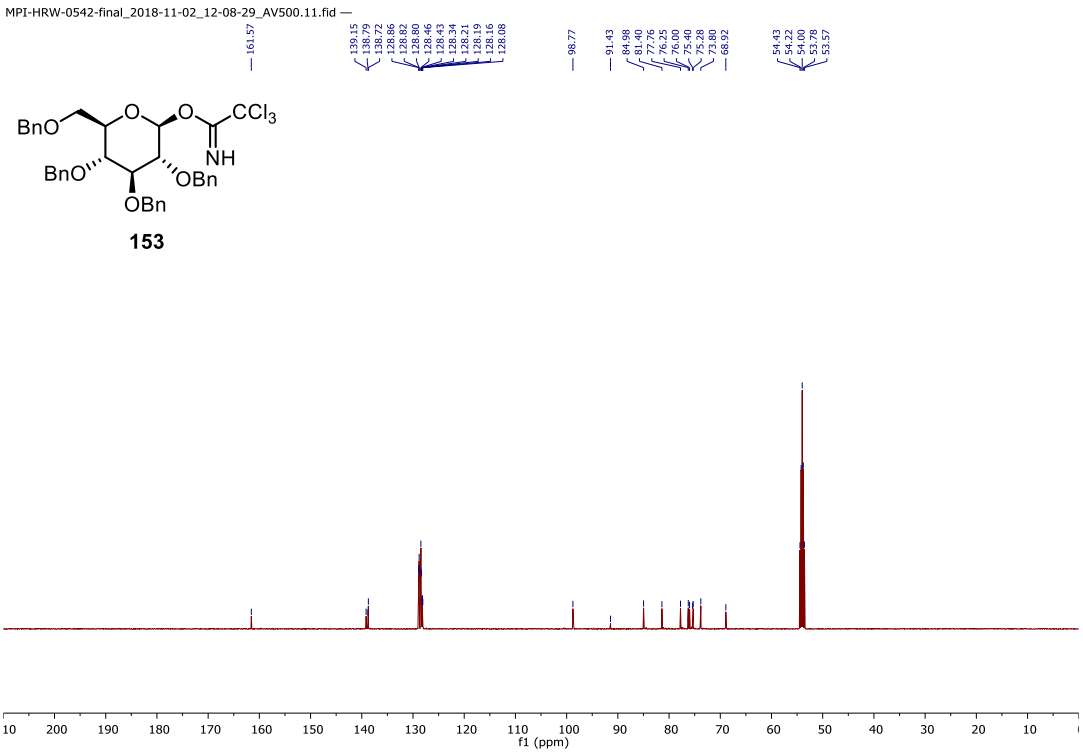

^{13}C NMR spectrum of compound **153** (126 MHz, in CD_2Cl_2)

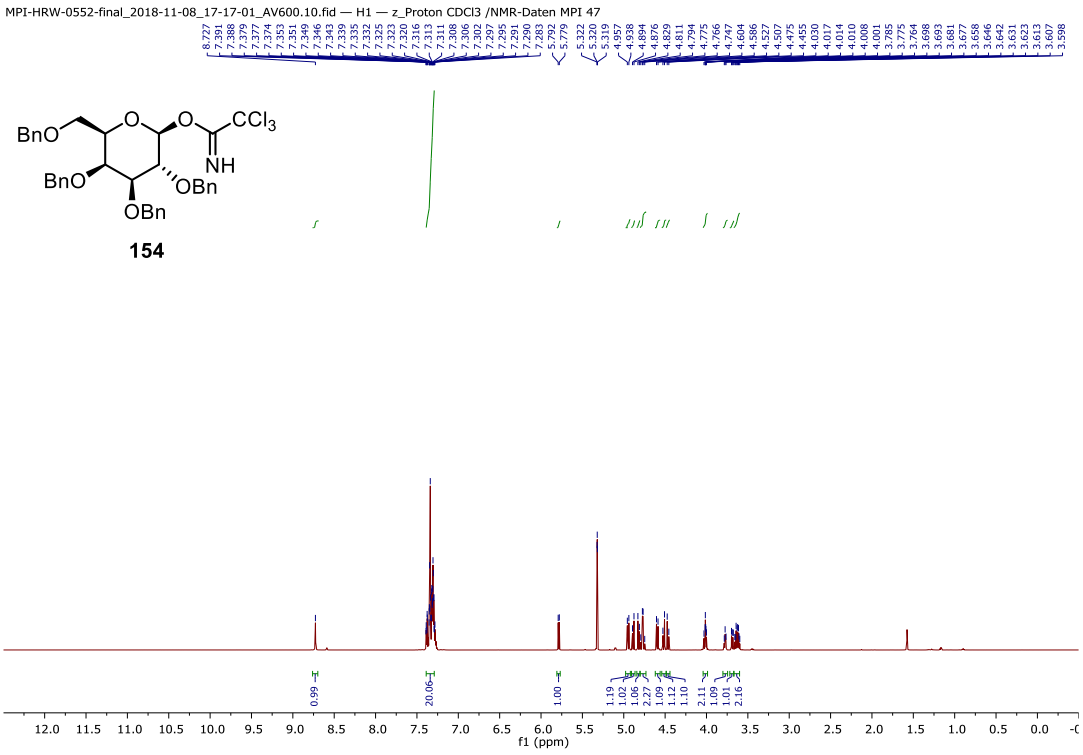

^{1}H NMR spectrum of compound **154** (600 MHz, in CD_2Cl_2)

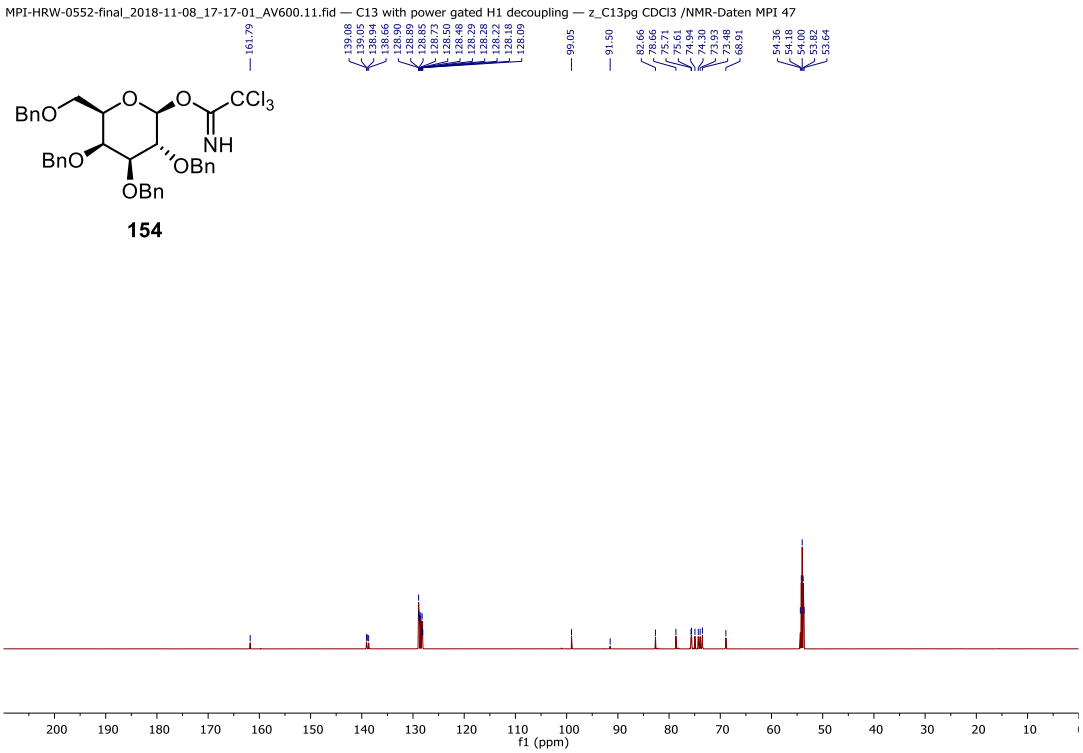

^{13}C NMR spectrum of compound **154** (151 MHz, in CD_2Cl_2)

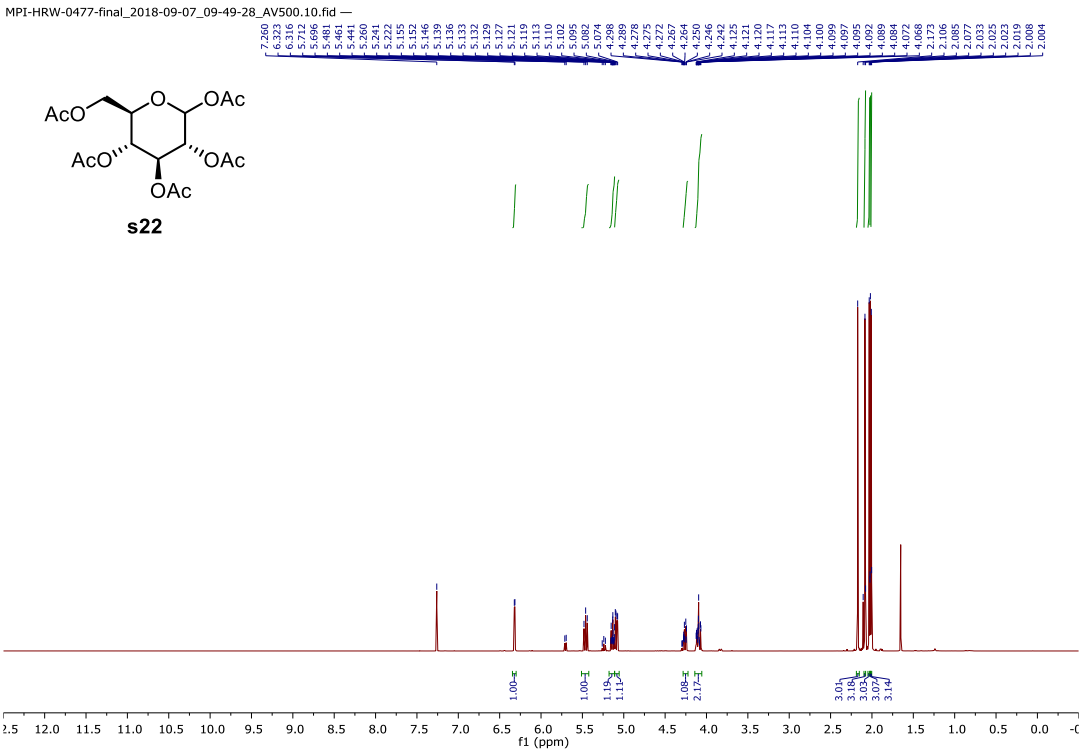

^{1}H NMR spectrum of compound **s22** (600 MHz, in $CDCl_3$)

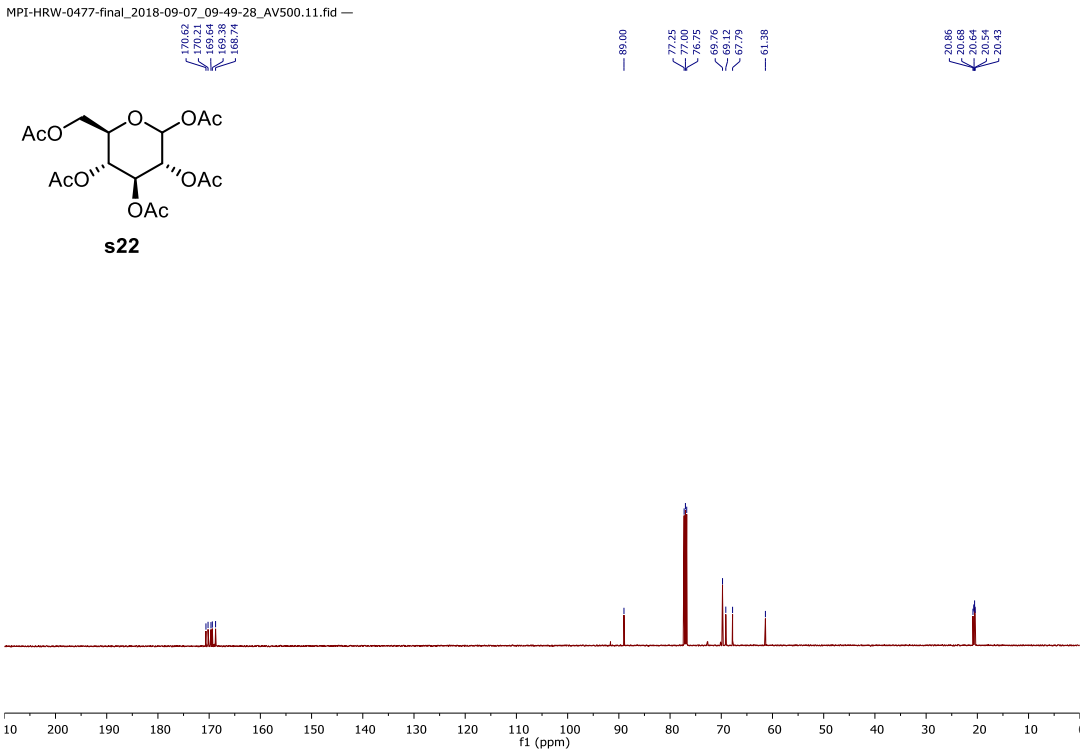

^{13}C NMR spectrum of compound **s22** (151 MHz, in $CDCl_3$)

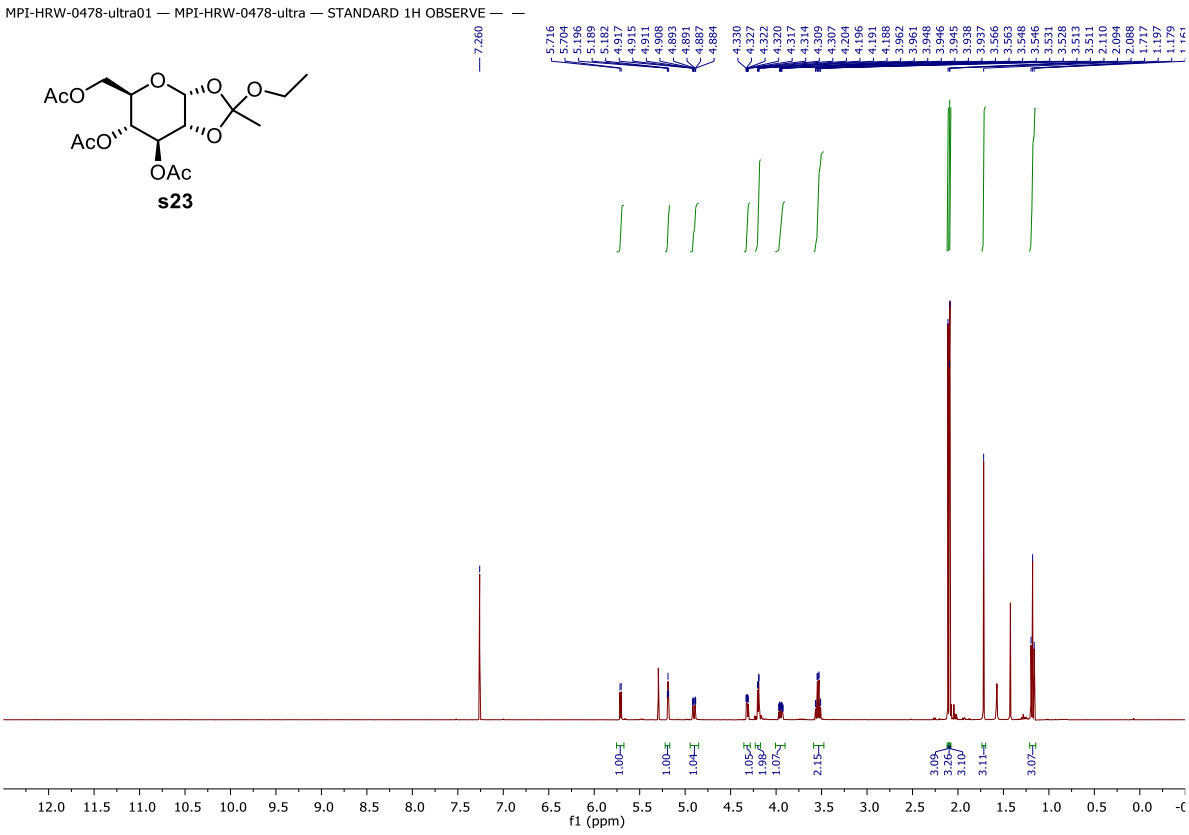

^{1}H NMR spectrum of compound **s23** (400 MHz, in $CDCl_3$)

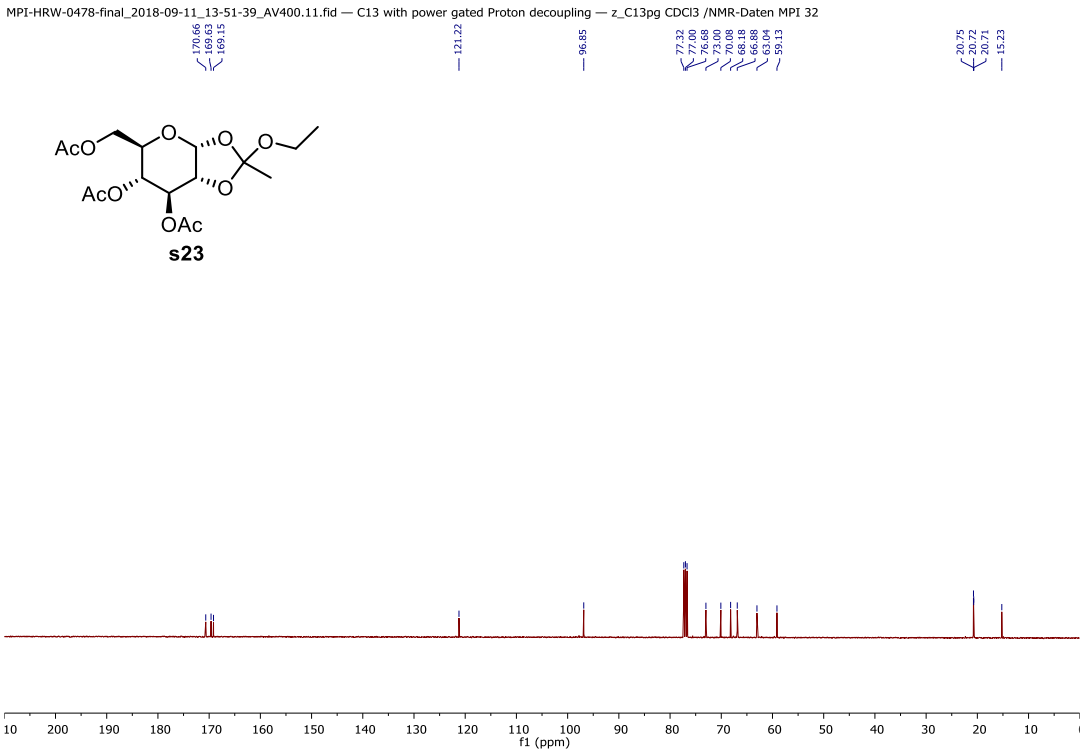

^{13}C NMR spectrum of compound **s23** (101 MHz, in $CDCl_3$)

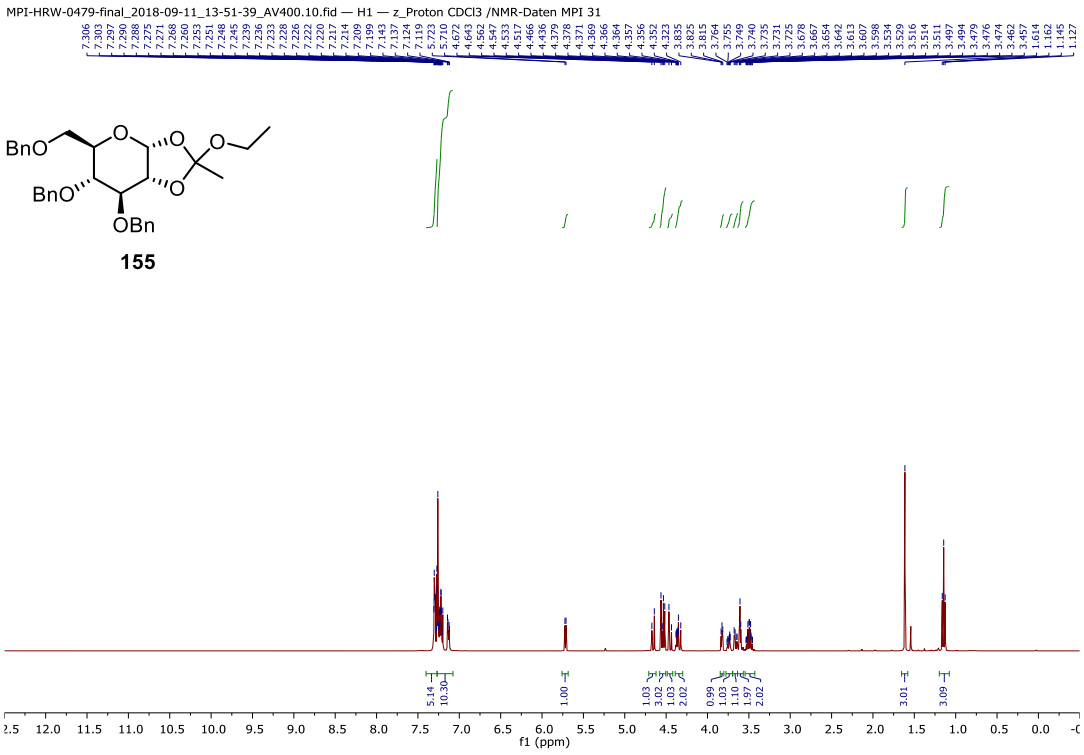

^{1}H NMR spectrum of compound **155** (400 MHz, in $CDCl_3$)

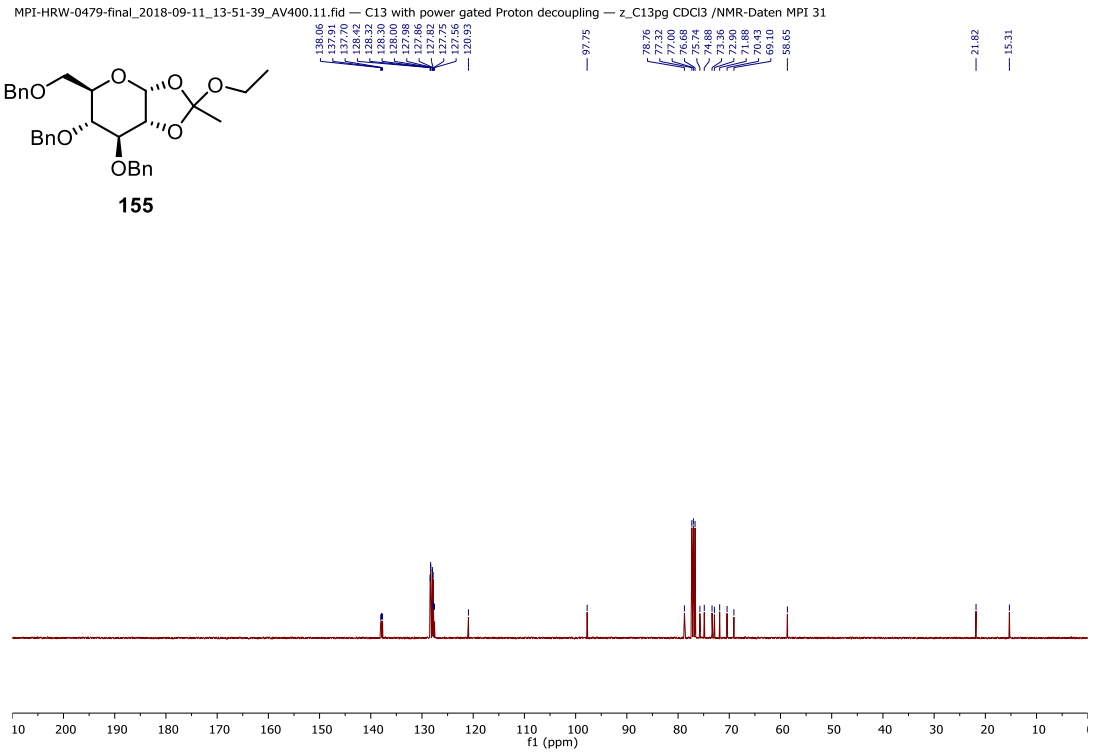

^{13}C NMR spectrum of compound **155** (101 MHz, in $CDCl_3$)

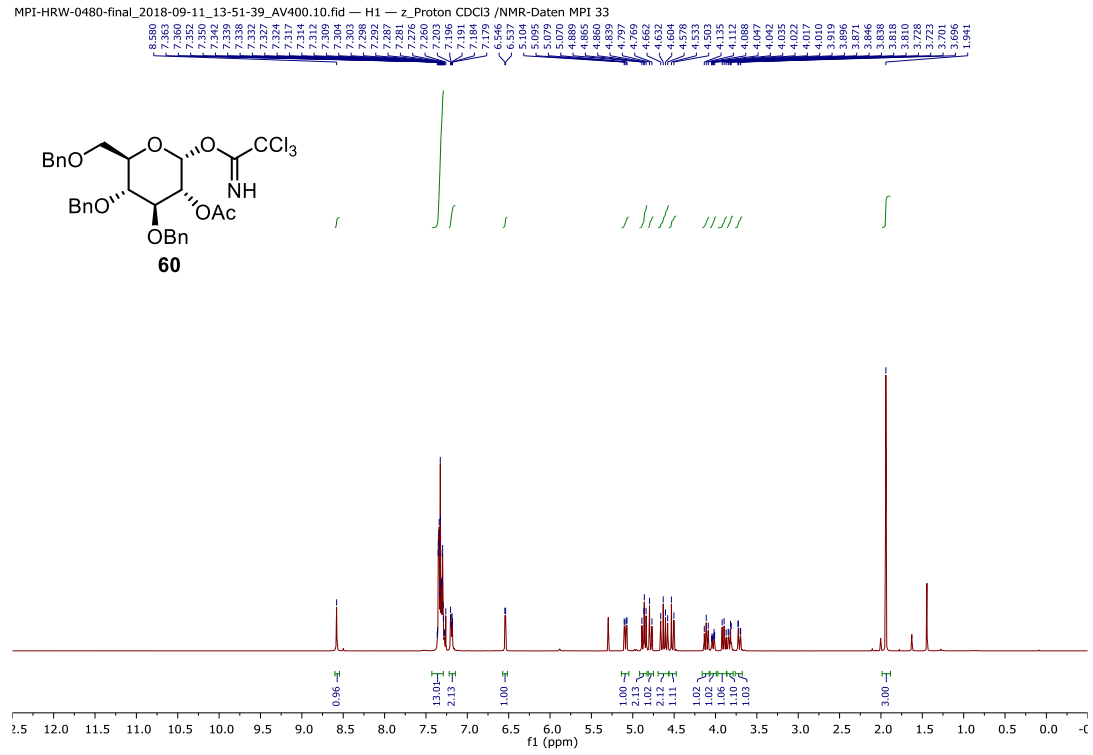

^{1}H NMR spectrum of compound **60** (400 MHz, in $CDCl_3$)

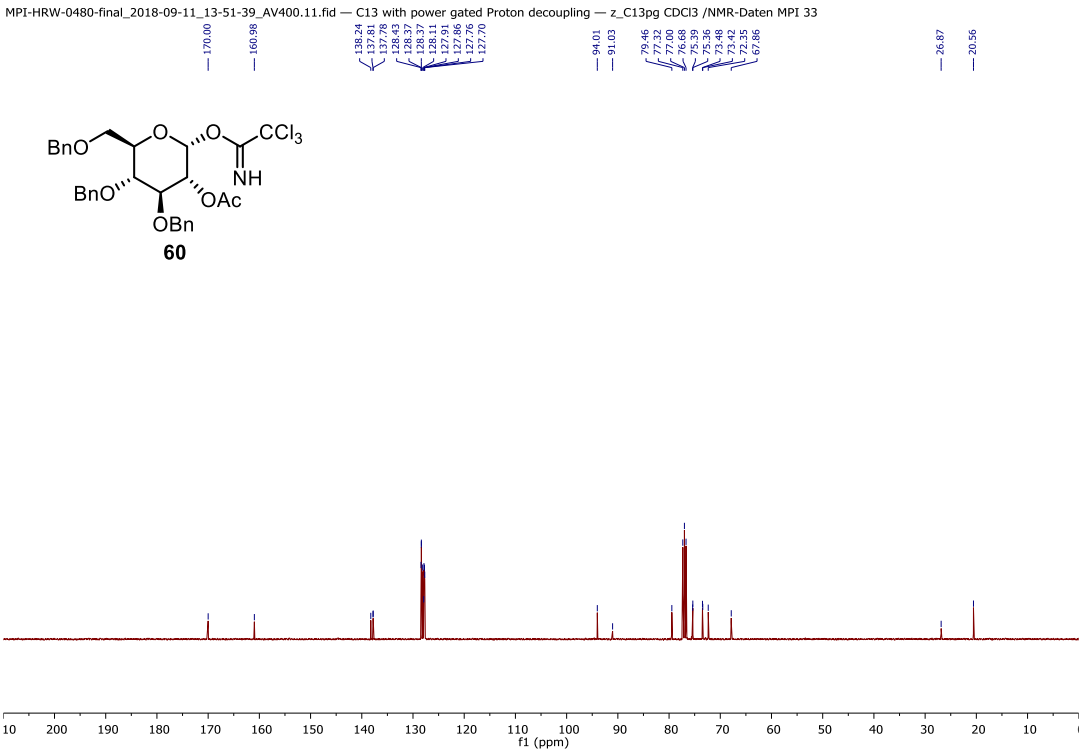

^{13}C NMR spectrum of compound **60** (101 MHz, in $CDCl_3$)

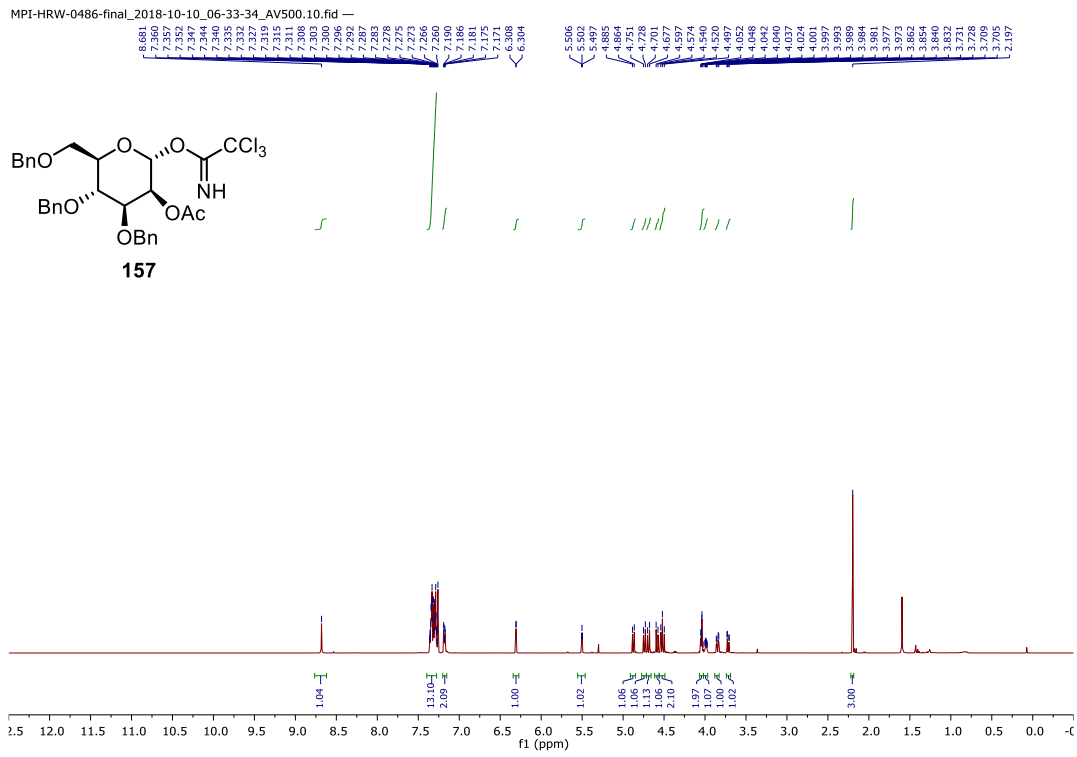

^{1}H NMR spectrum of compound **157** (500 MHz, in $CDCl_3$)

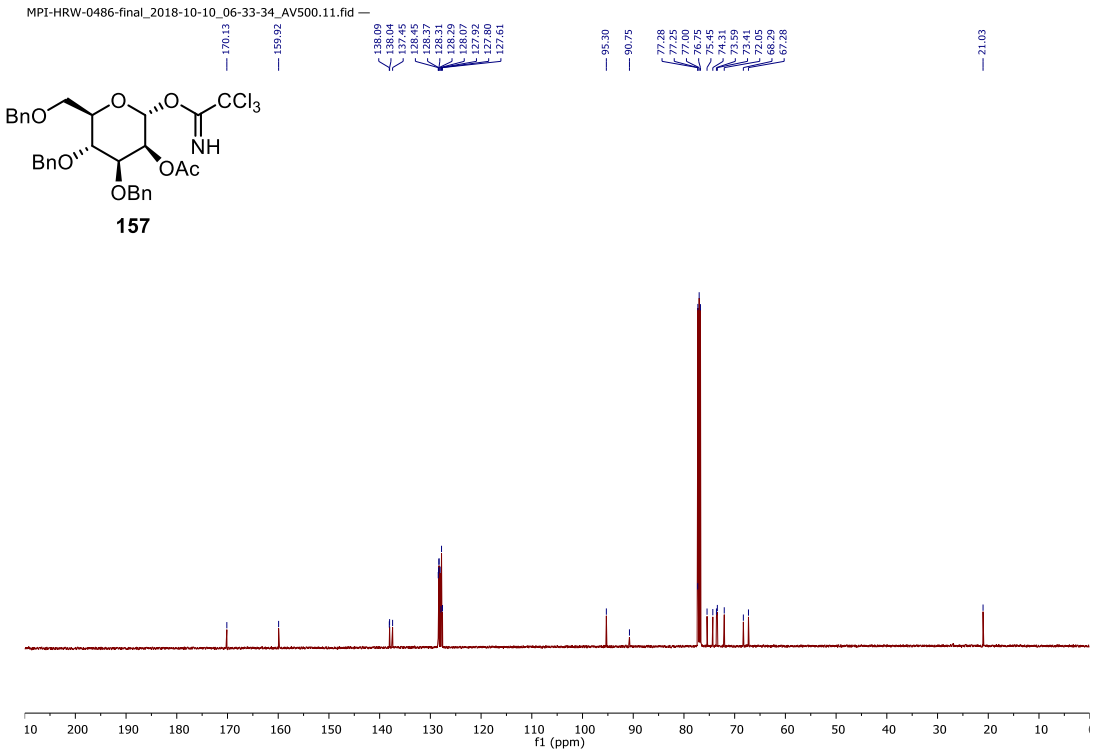

^{13}C NMR spectrum of compound **157** (126 MHz, in $CDCl_3$)

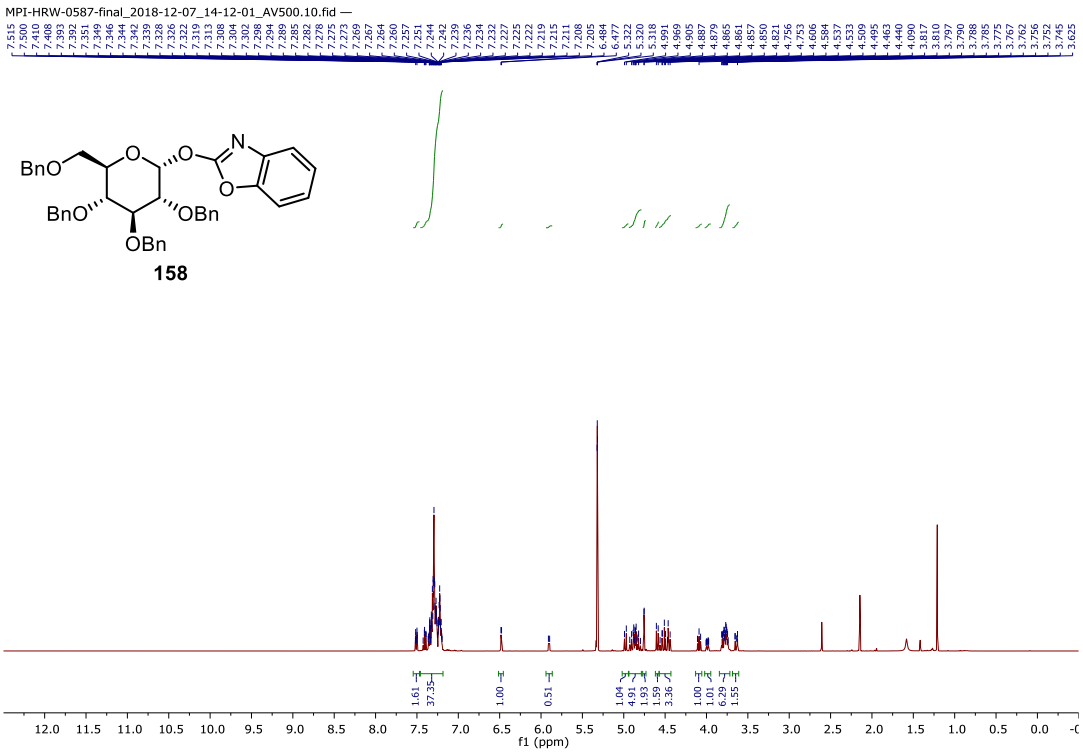

^{1}H NMR spectrum of compound **158** (500 MHz, in CD_2Cl_2)

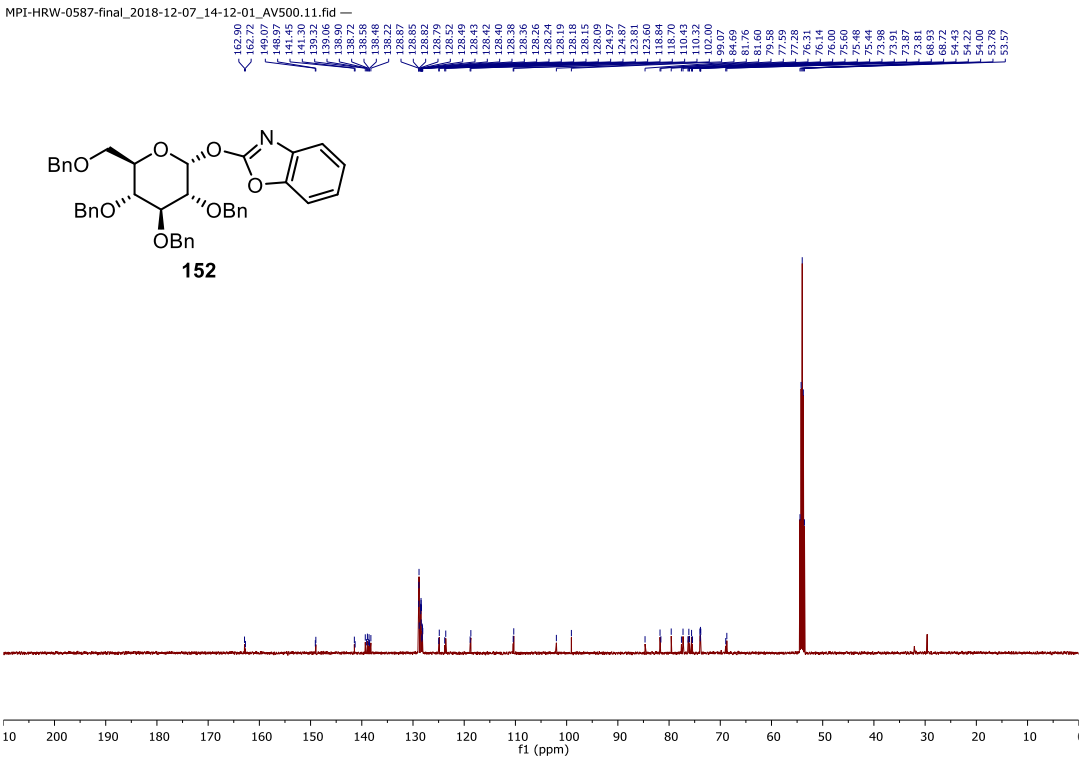

^{13}C NMR spectrum of compound **158** (126 MHz, in CD_2Cl_2)

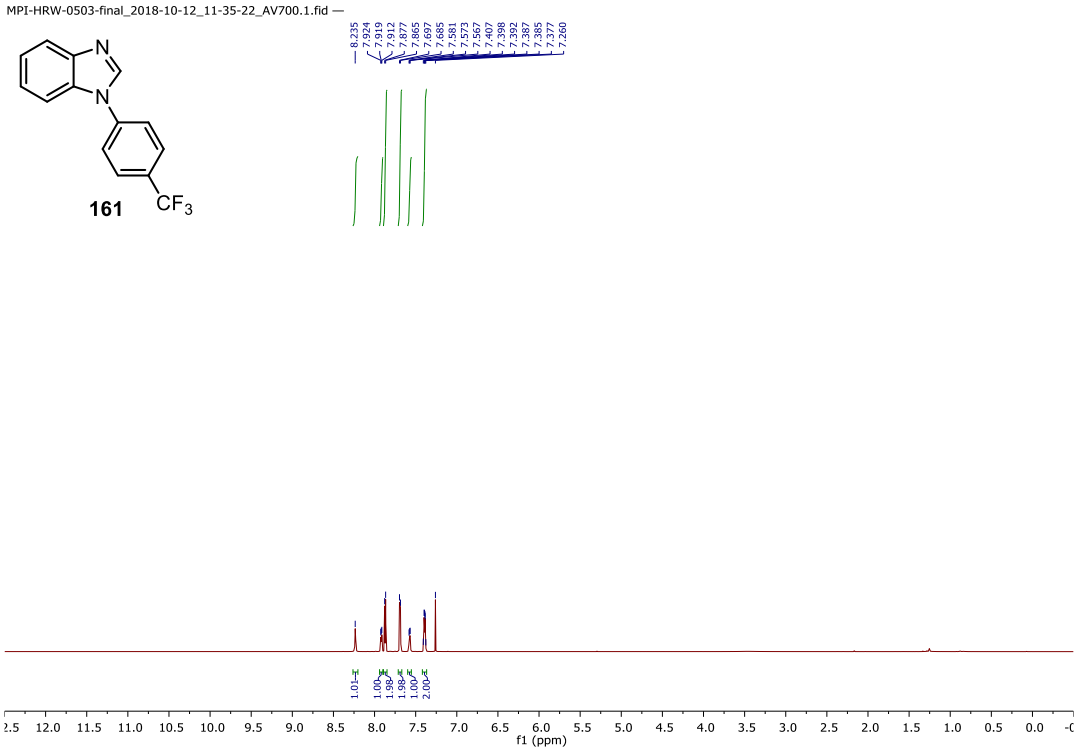

^{1}H NMR spectrum of compound **161** (700 MHz, in $CDCl_3$)

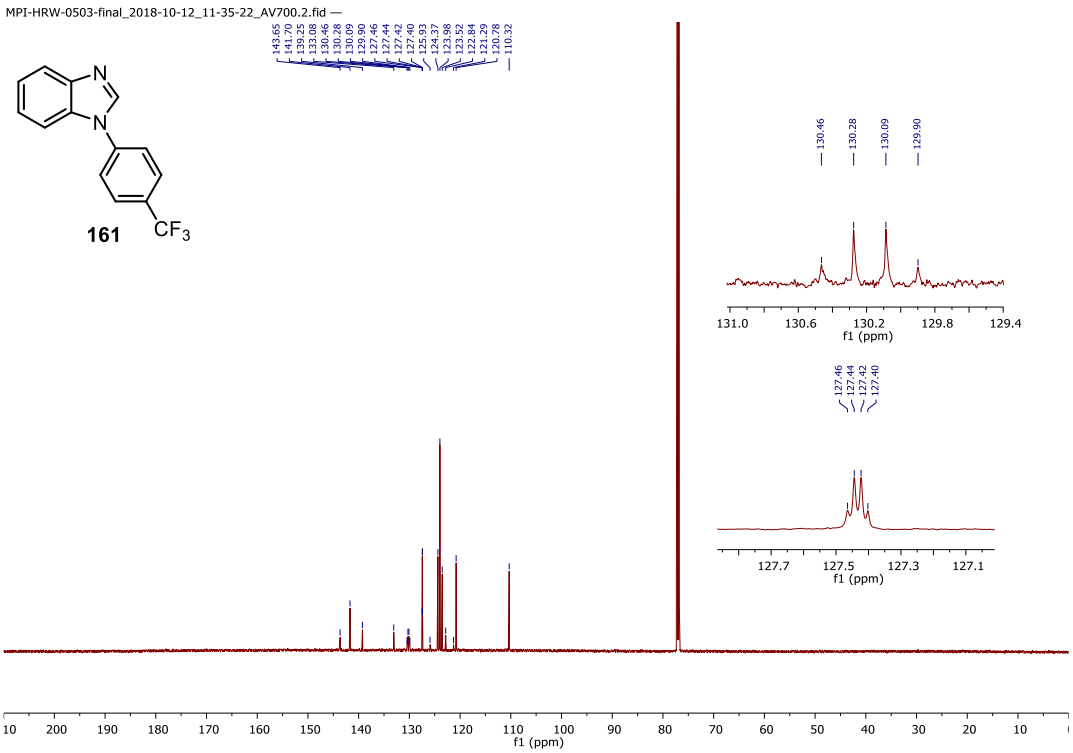

^{13}C NMR spectrum of compound **161** (176 MHz, in $CDCl_3$)

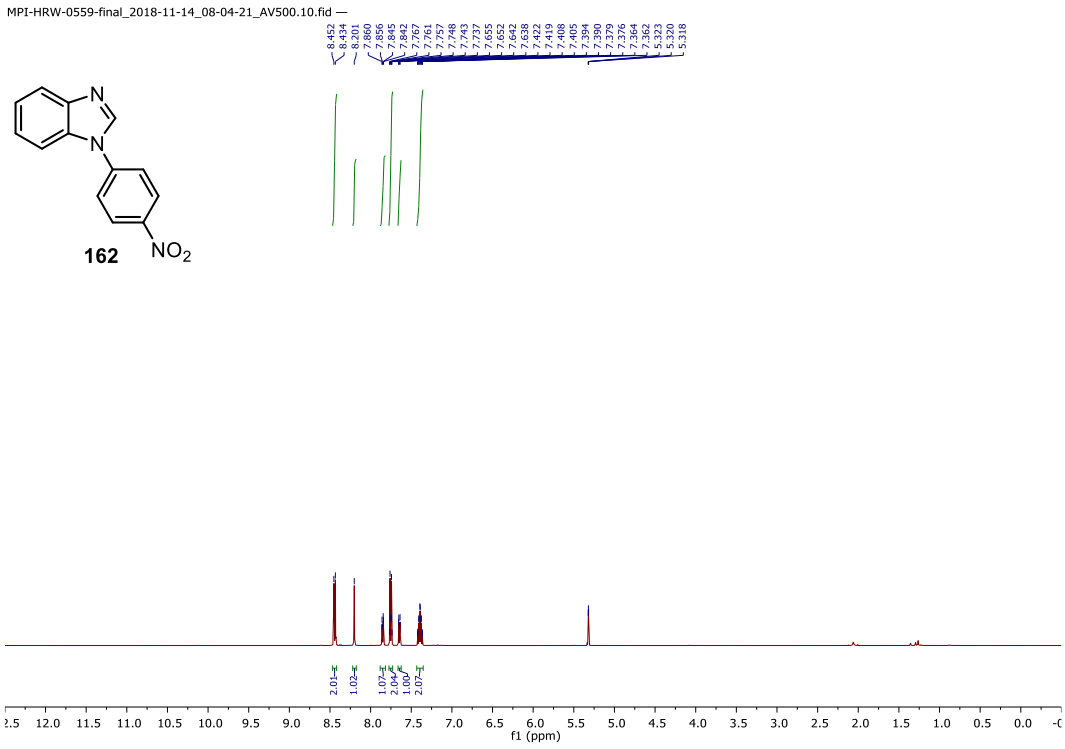

^{1}H NMR spectrum of compound **162** (500 MHz, in CD_2Cl_2)

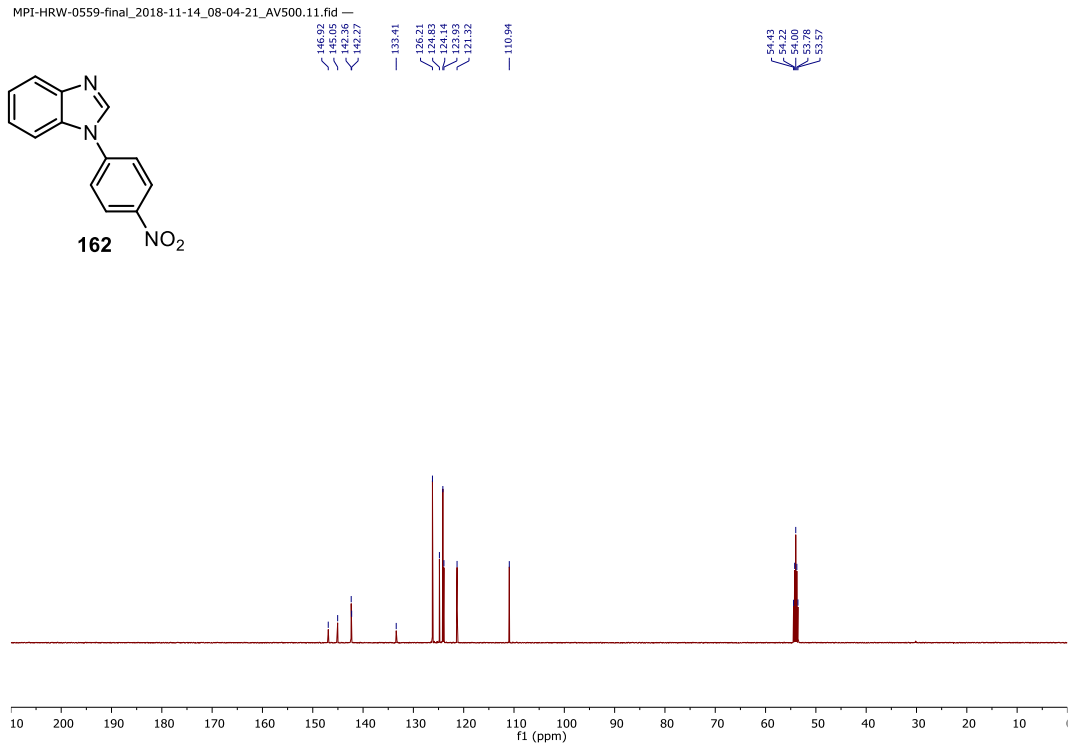

^{13}C NMR spectrum of compound **162** (126 MHz, in CD_2Cl_2)

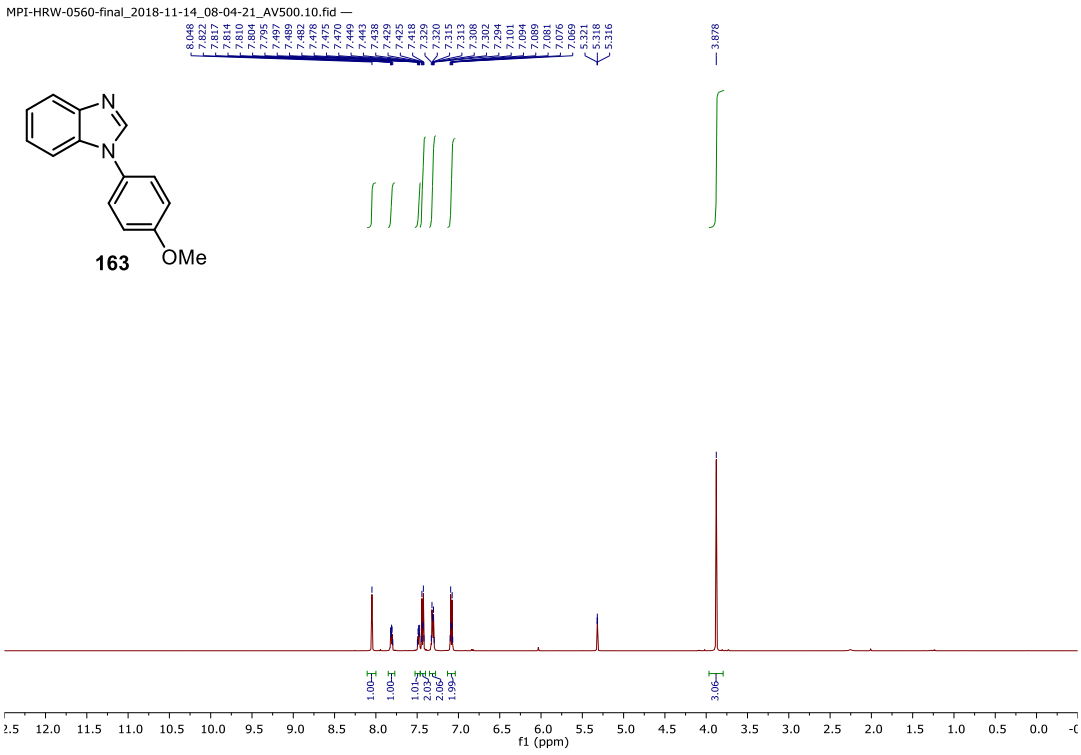

^{1}H NMR spectrum of compound **163** (500 MHz, in CD_2Cl_2)

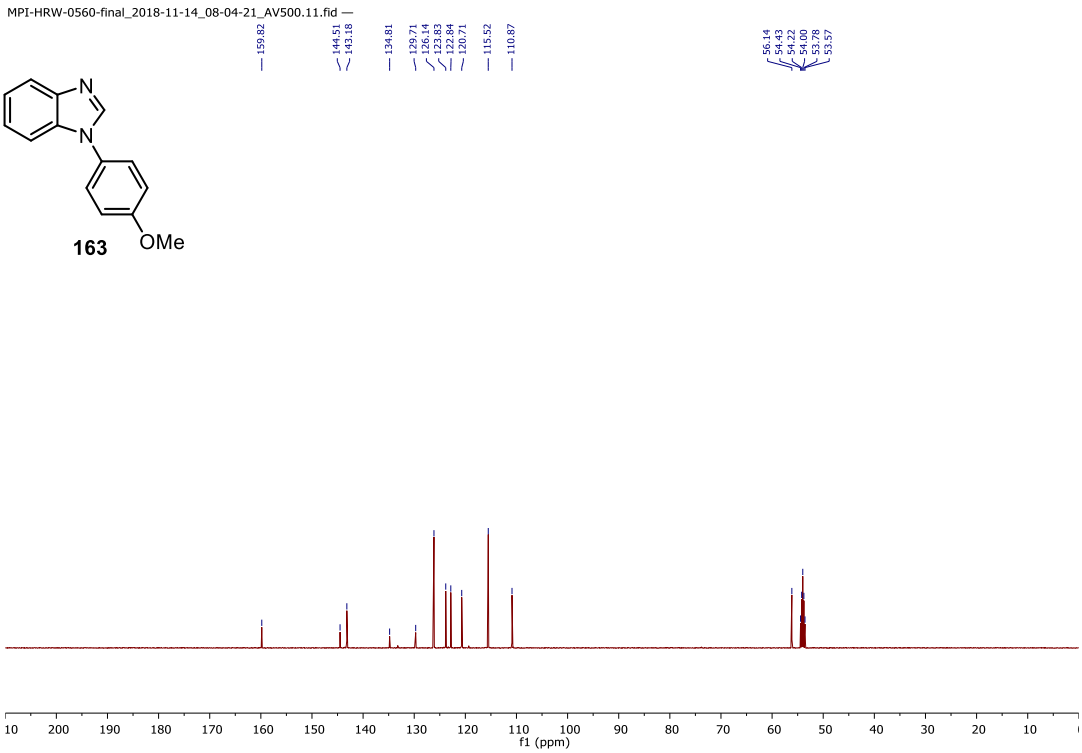

^{13}C NMR spectrum of compound **163** (126 MHz, in CD_2Cl_2)

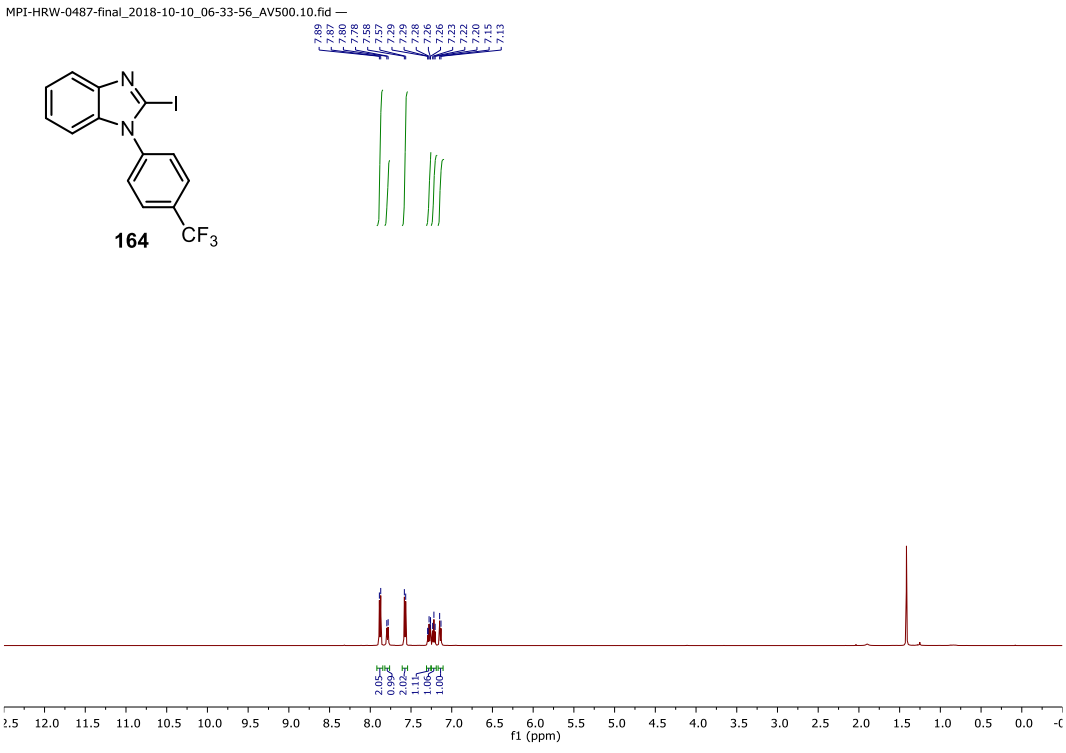

^{1}H NMR spectrum of compound **164** (500 MHz, in $CDCl_3$)

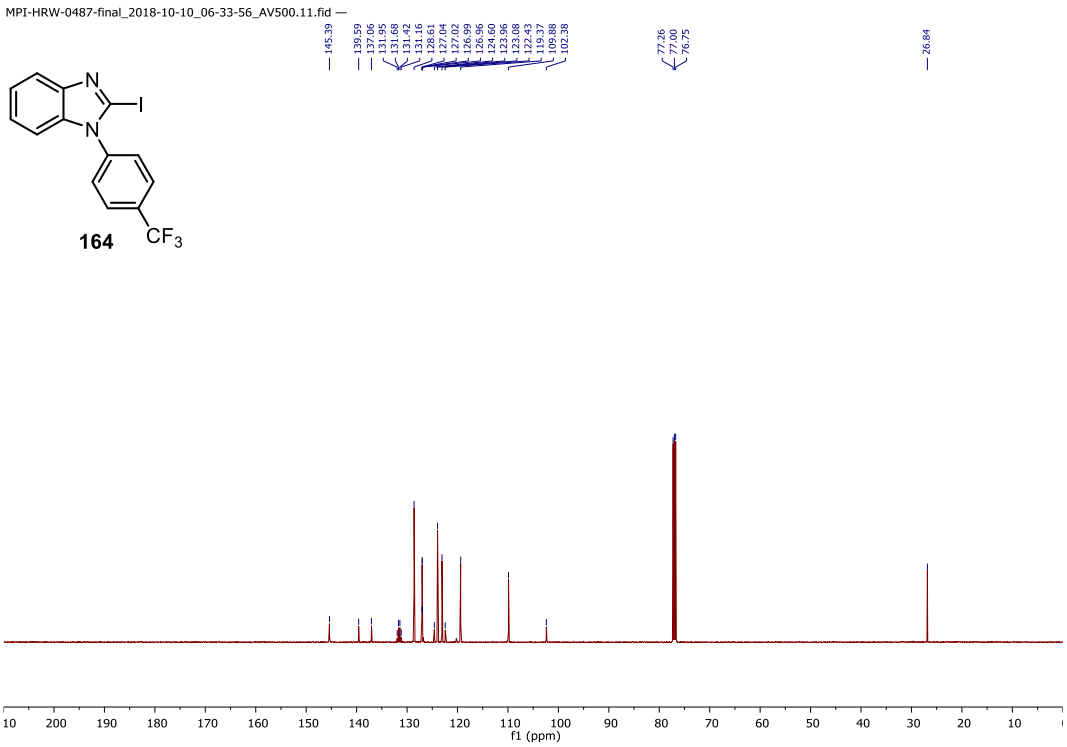

^{13}C NMR spectrum of compound **164** (126 MHz, in $CDCl_3$)

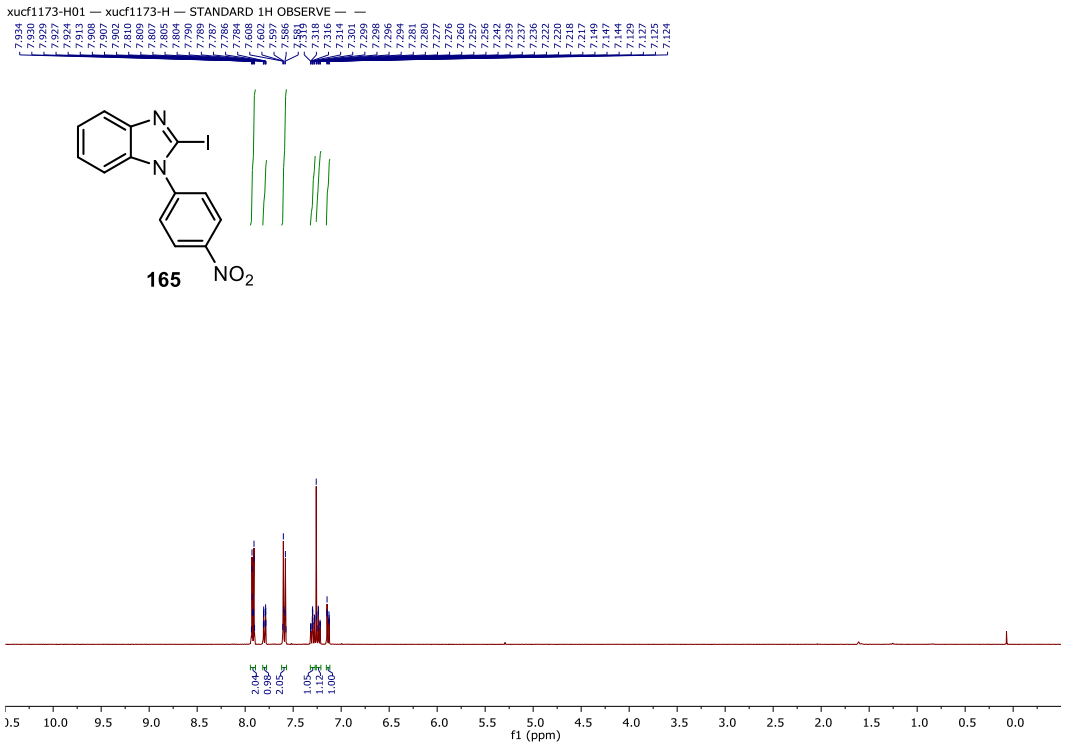

^{1}H NMR spectrum of compound **165** (400 MHz, in $CDCl_3$)

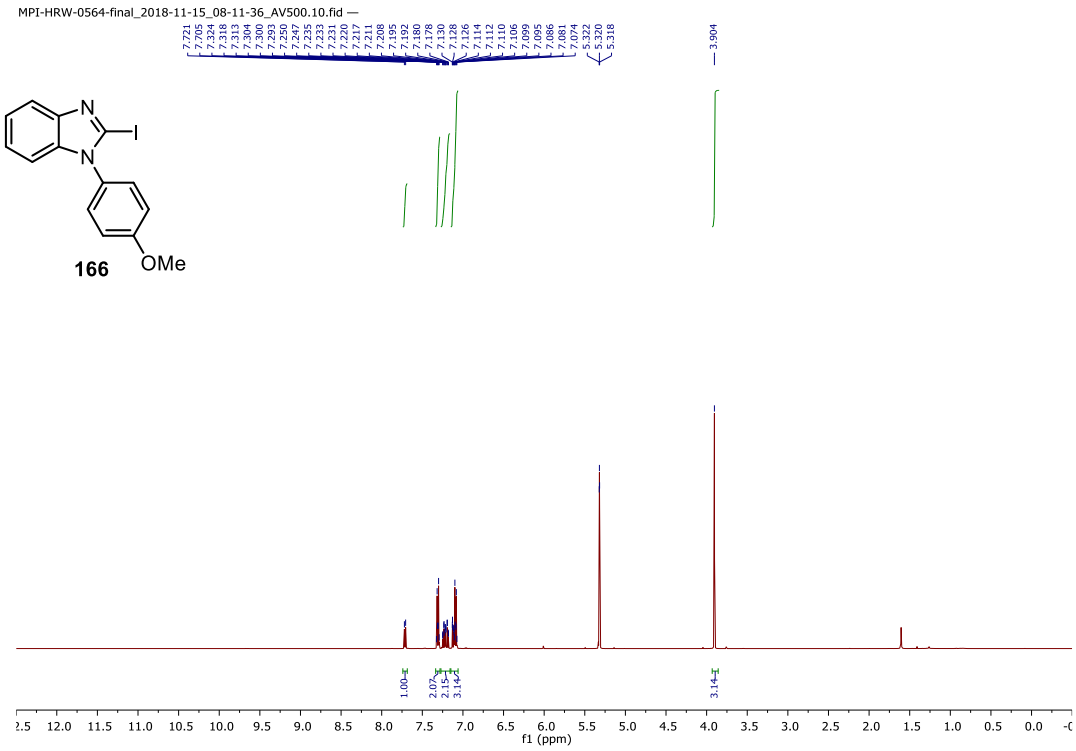

^{1}H NMR spectrum of compound **166** (500 MHz, in CD_2Cl_2)

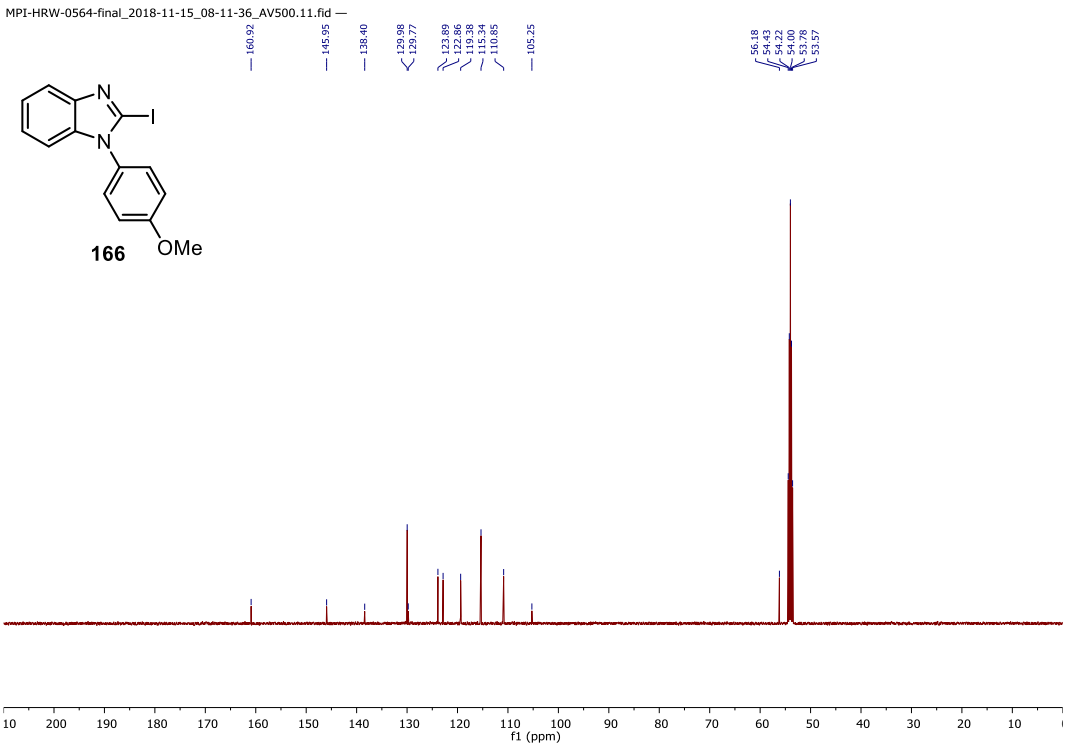

^{13}C NMR spectrum of compound **166** (126 MHz, in CD_2Cl_2)

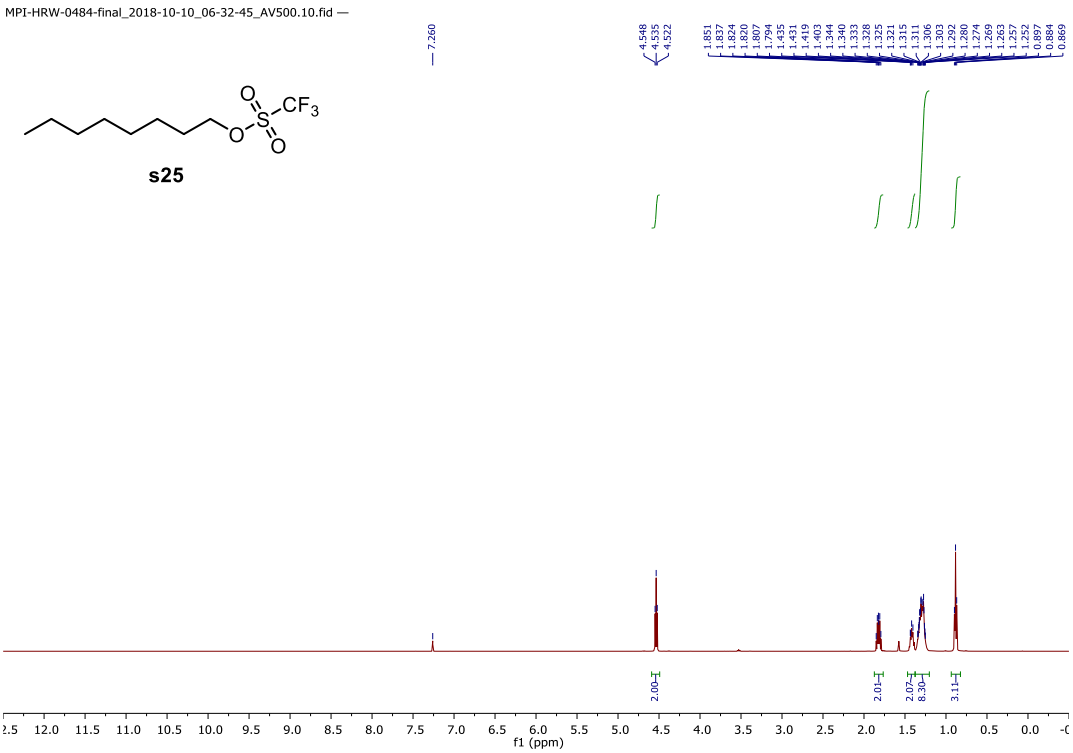

^{1}H NMR spectrum of compound **s25** (500 MHz, in $CDCl_3$)

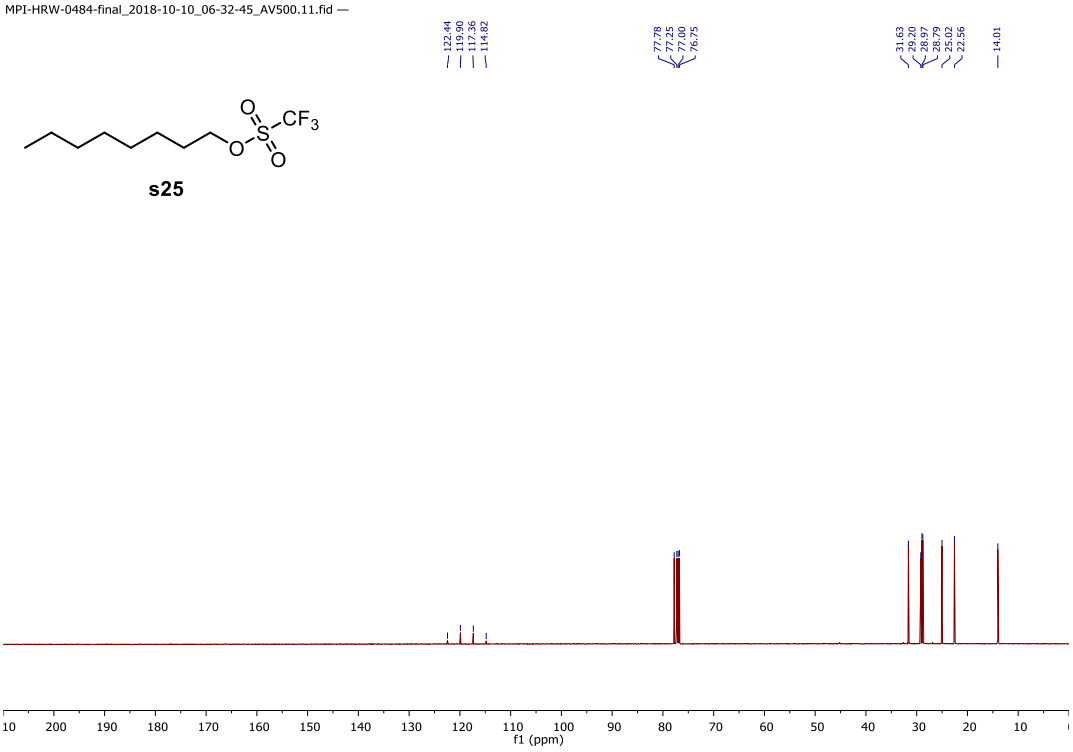

^{13}C NMR spectrum of compound **s25** (126 MHz, in $CDCl_3$)

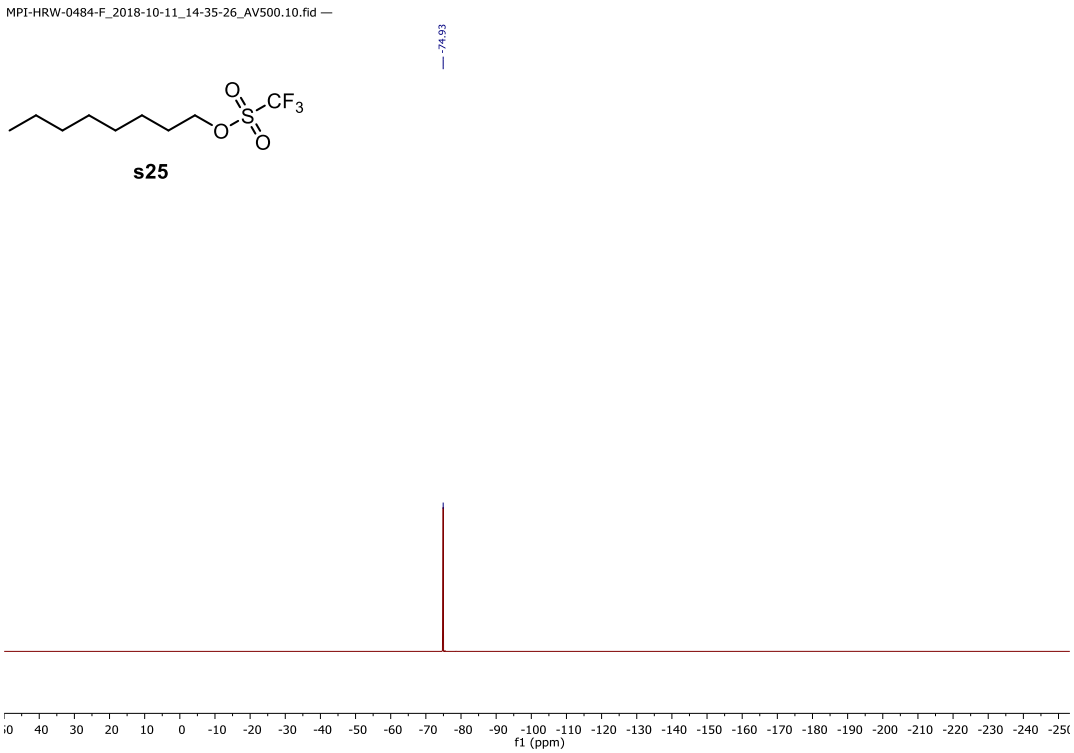

^{19}F NMR spectrum of compound **s25** (470 MHz, in $CDCl_3$)

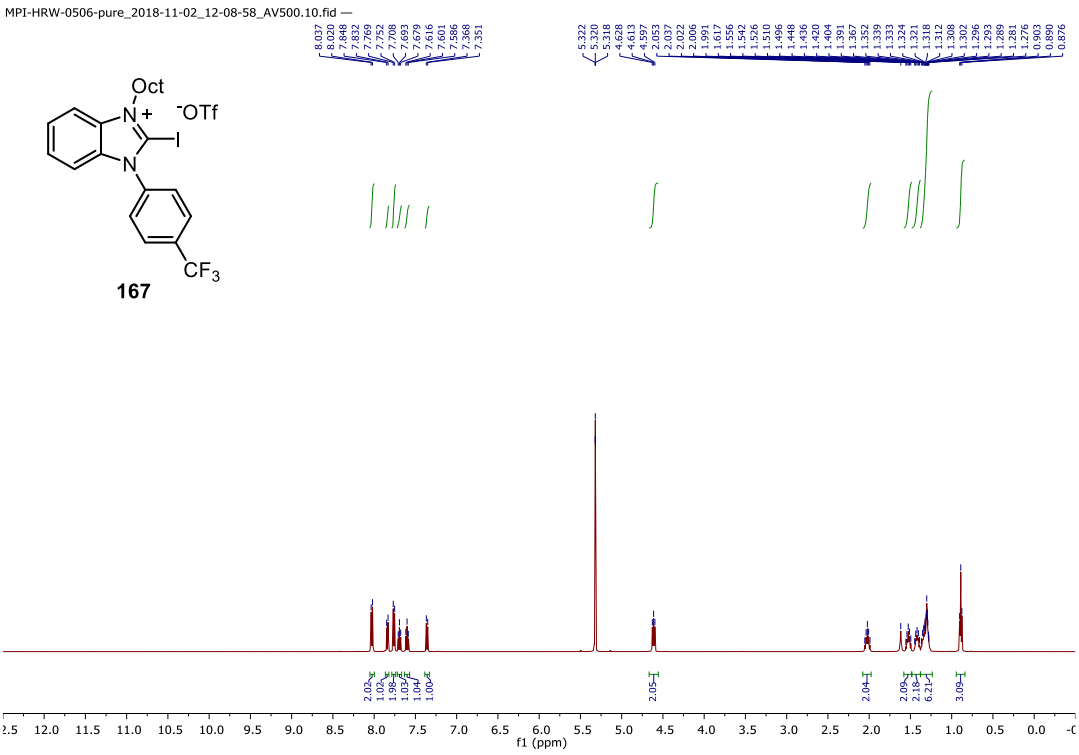

^{1}H NMR spectrum of compound **167** (500 MHz, in CD_2Cl_2)

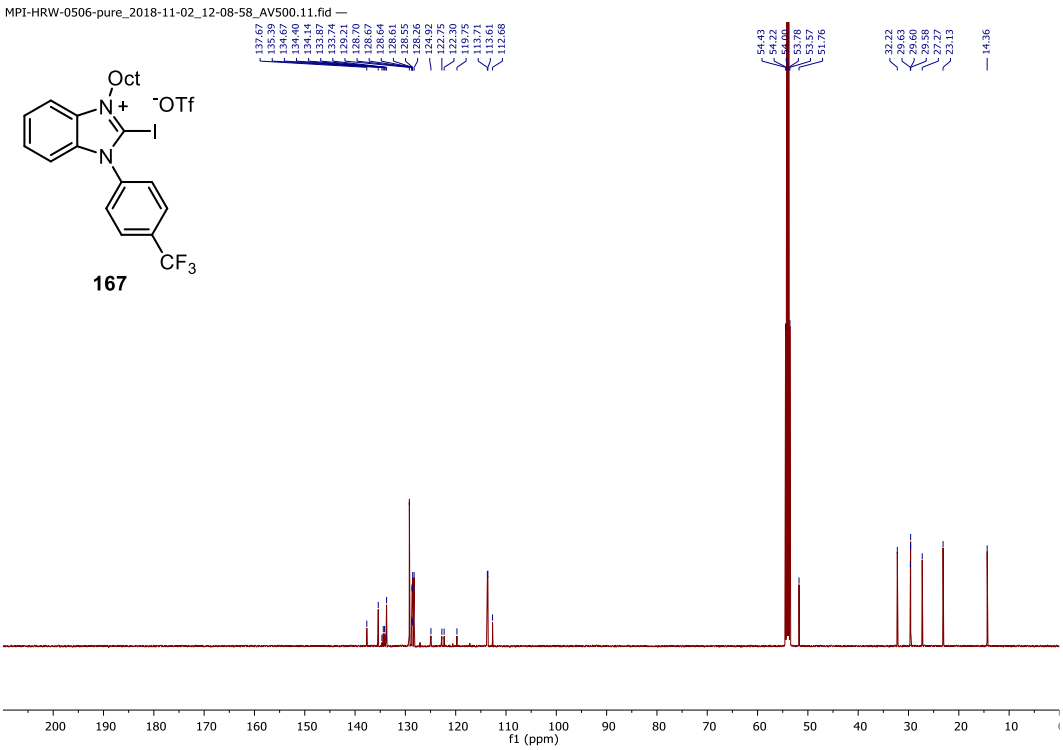

^{13}C NMR spectrum of compound **167** (126 MHz, in CD_2Cl_2)

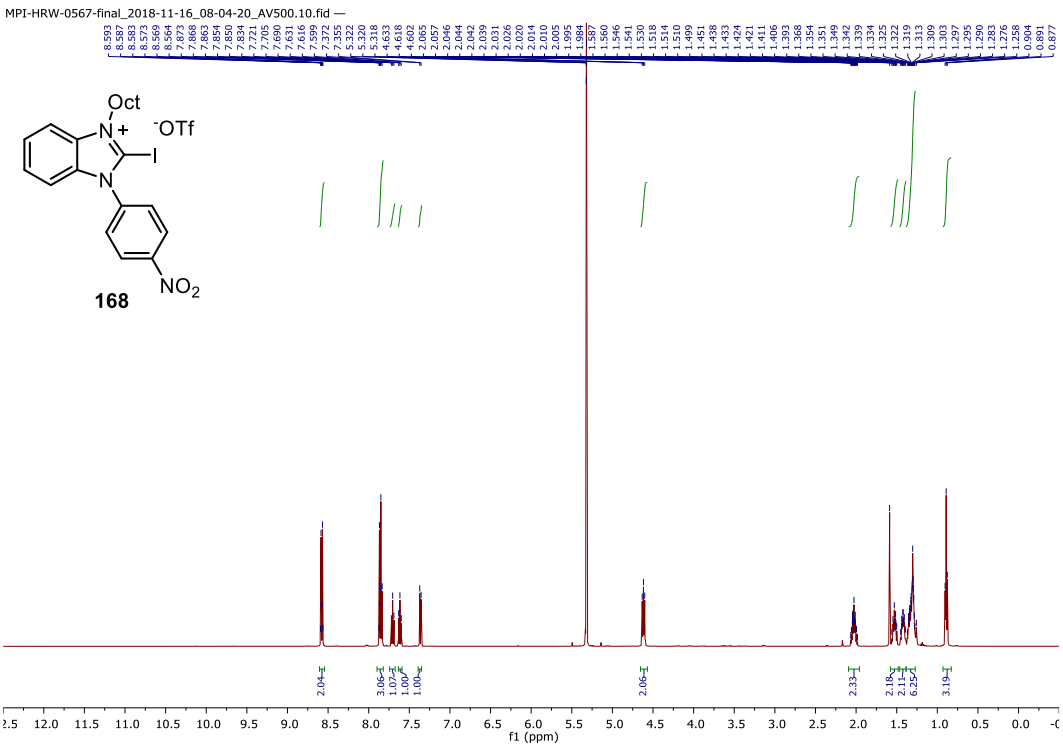

^{1}H NMR spectrum of compound **168** (500 MHz, in CD_2Cl_2)

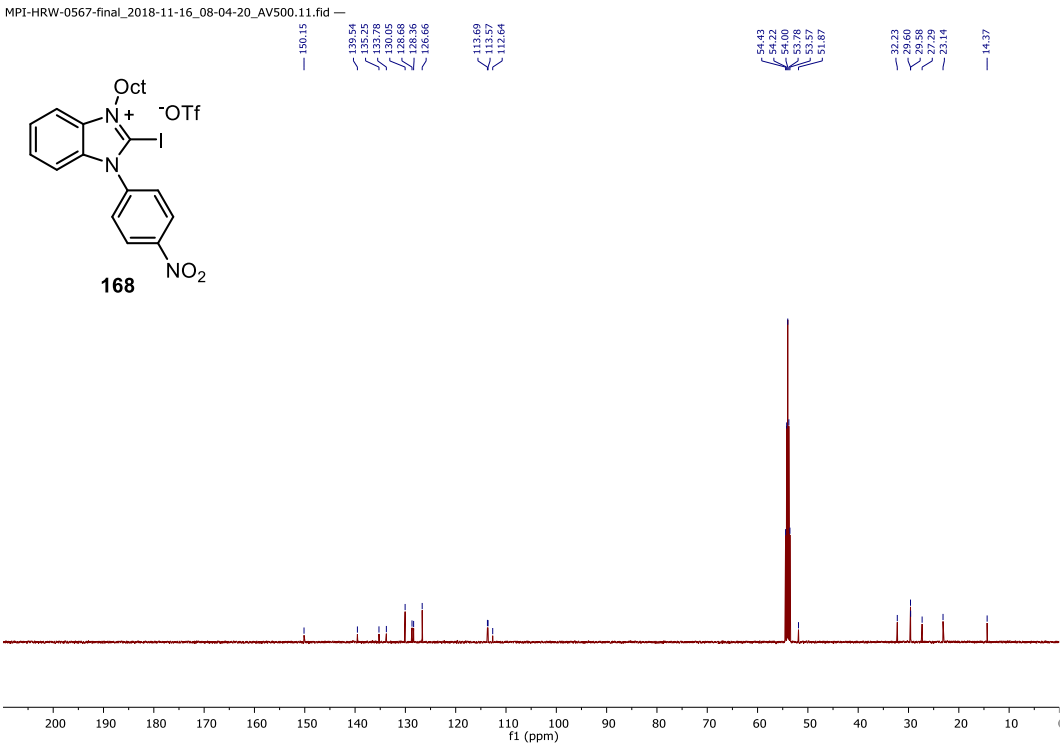

^{13}C NMR spectrum of compound **168** (126 MHz, in CD_2Cl_2)

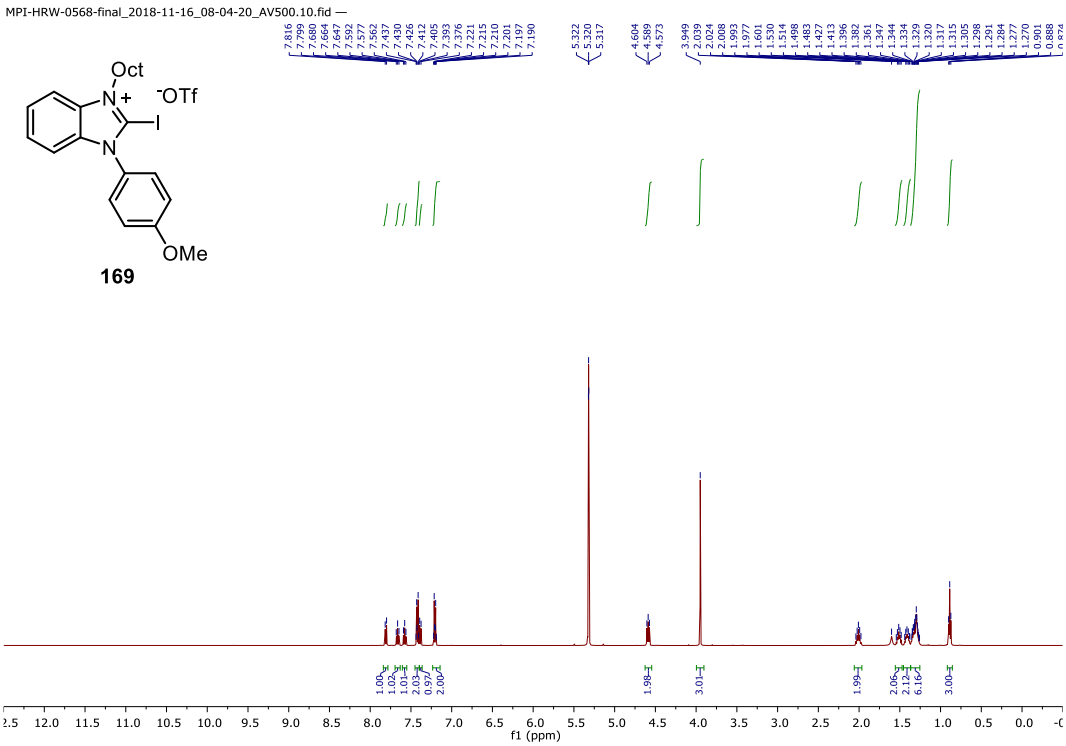

^{1}H NMR spectrum of compound **169** (500 MHz, in CD_2Cl_2)

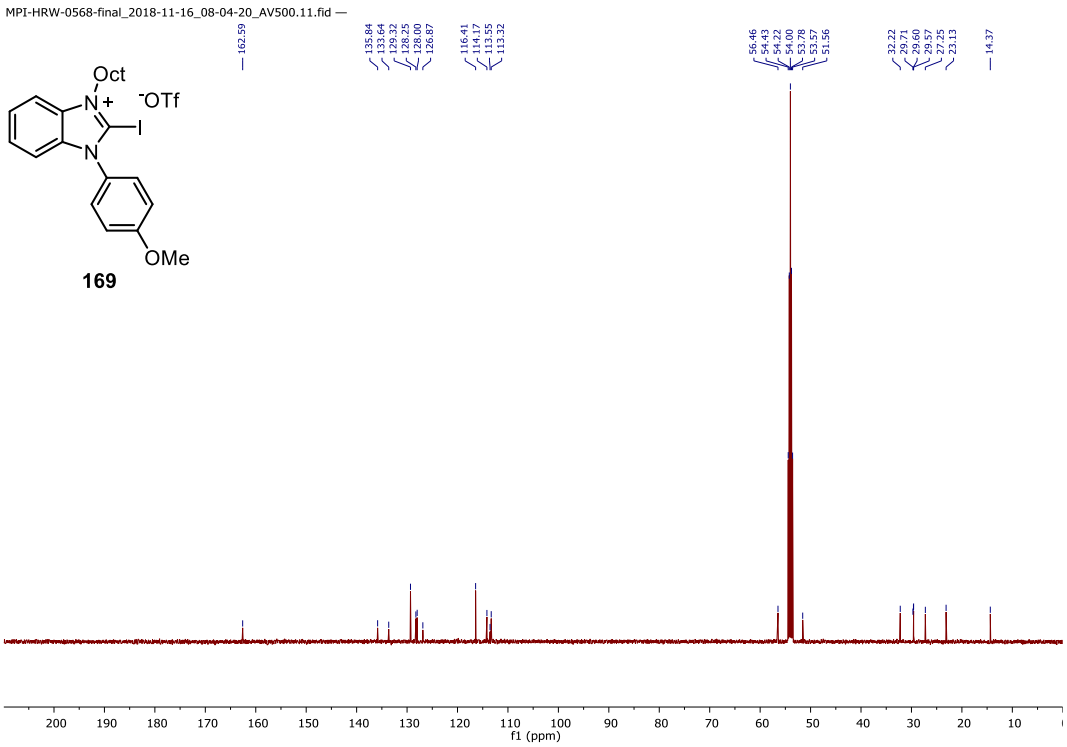

^{13}C NMR spectrum of compound **169** (126 MHz, in CD_2Cl_2)

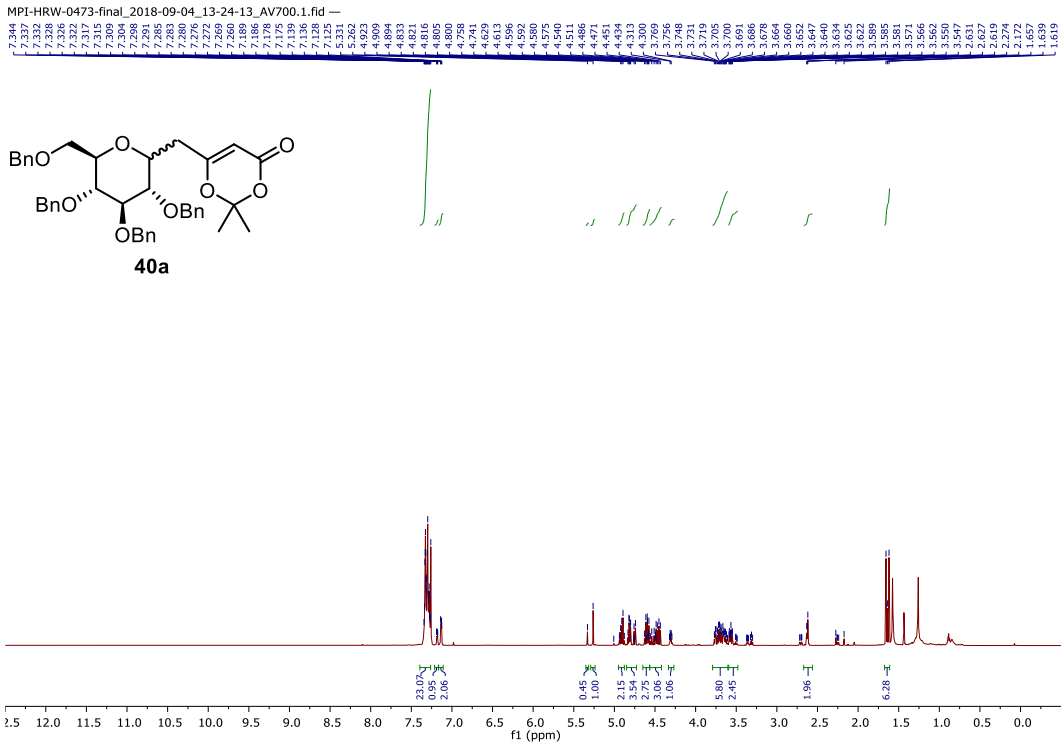

^{1}H NMR spectrum of compound **40a** (700 MHz, in $CDCl_3$)

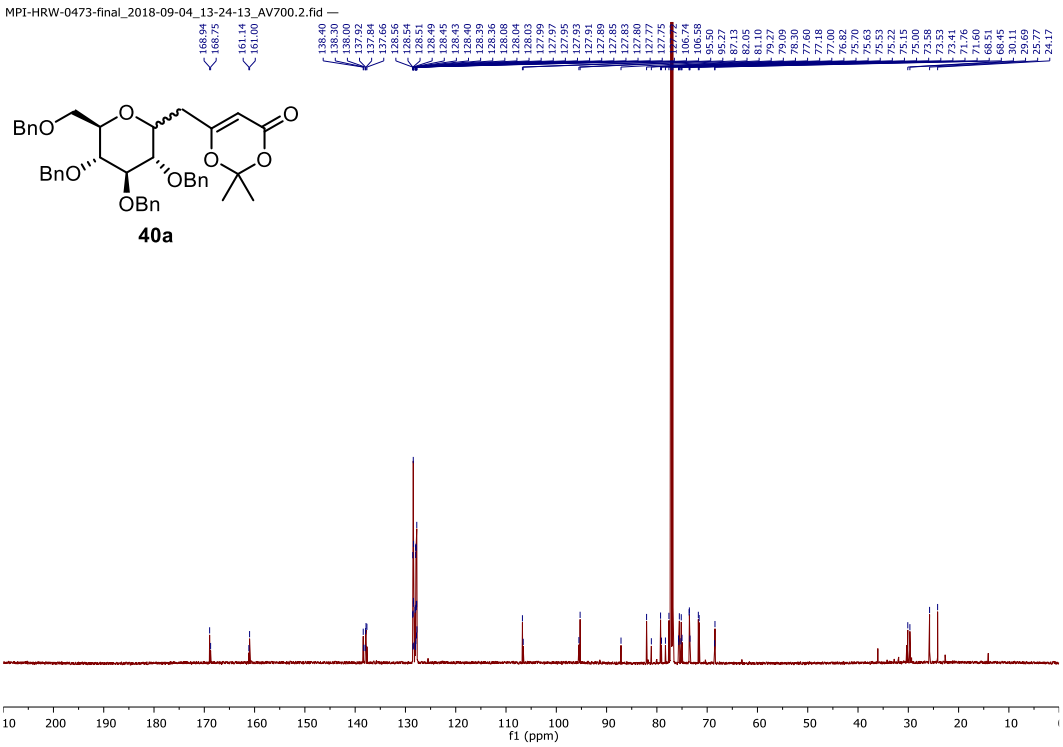

^{13}C NMR spectrum of compound **169** (176 MHz, in $CDCl_3$)

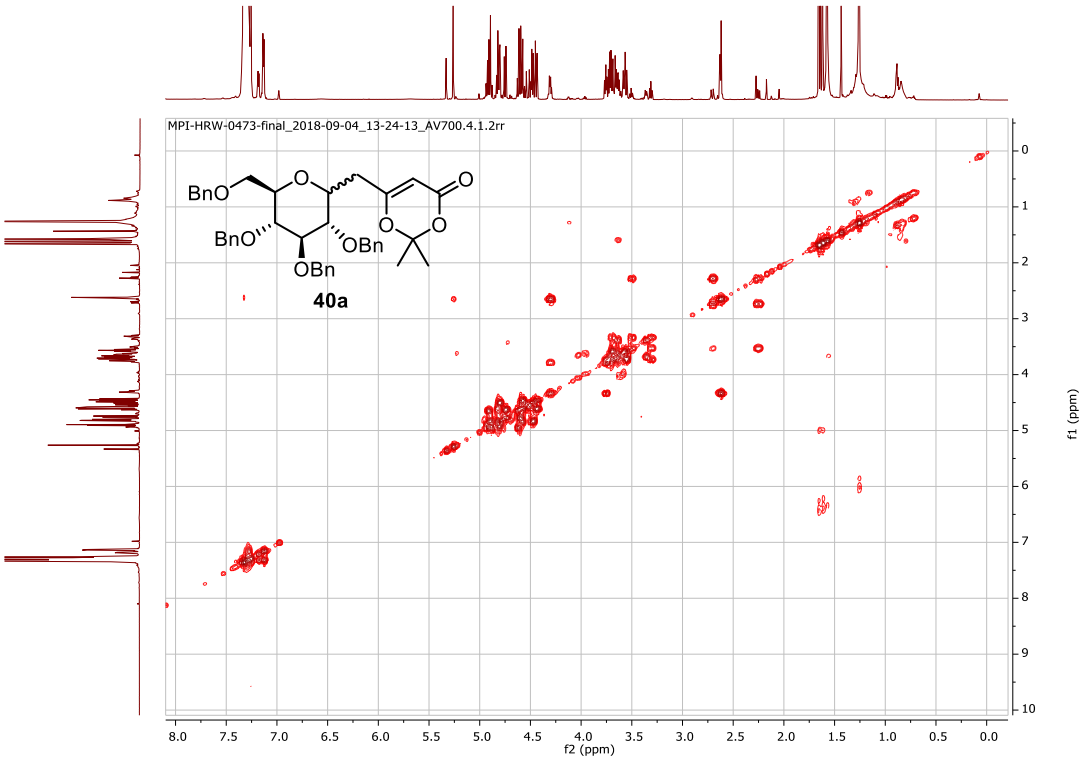

COSY spectrum of compound **40a**

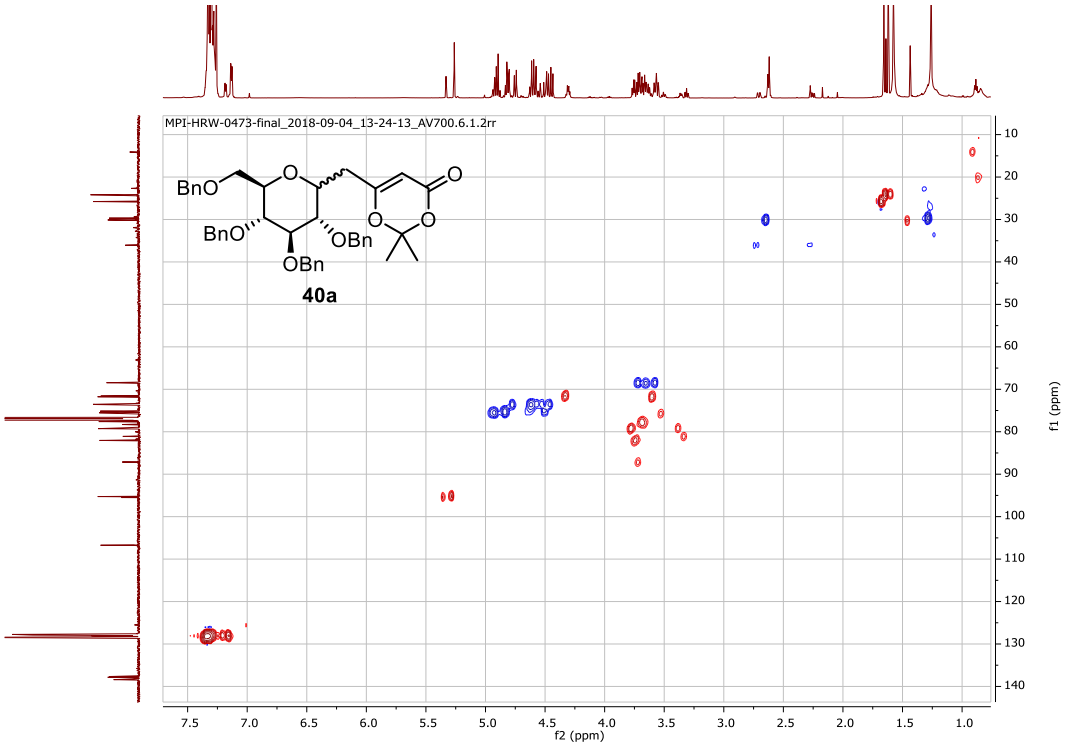

HSQC spectrum of compound **40a**

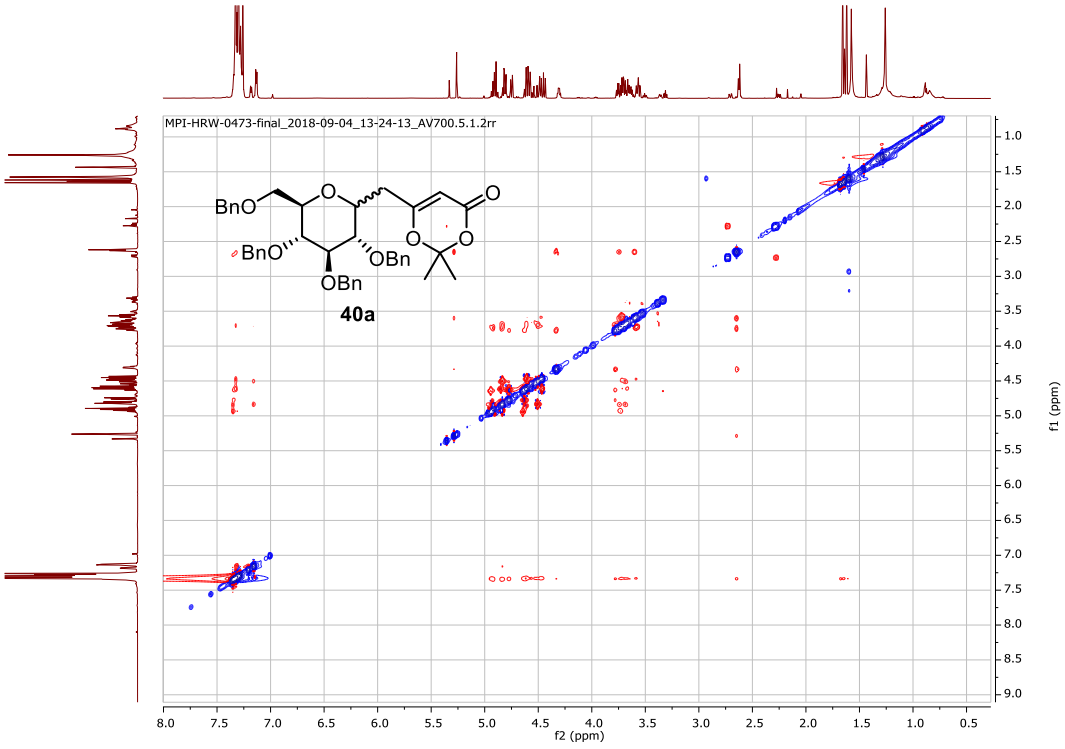

NOESY spectrum of compound **40a**

11.3 List of thesis compound number to Enso experiment number

Compound number	Enso experiment number	Compound number	Enso experiment number
70	MPI_WUHUEI_0007	**98**	MPI_WUHUEI_0050
71	MPI_WUHUEI_0010	**99**	MPI_WUHUEI_0053
72	MPI_WUHUEI_0049	**6**	MPI_WUHUEI_0054
73	MPI_WUHUEI_0019	**100**	MPI_WUHUEI_0315
74	MPI_WUHUEI_0022	**101**	MPI_WUHUEI_0318
77	MPI_WUHUEI_0052	**103**	MPI_WUHUEI_0662
78	MPI_WUHUEI_0429	**104**	MPI_WUHUEI_0664
87	MPI_WUHUEI_0058	**106**	MPI_WUHUEI_0672
88	MPI_WUHUEI_0059	**107**	MPI_WUHUEI_0686
89	MPI_WUHUEI_0061	**108**	MPI_WUHUEI_0354
90a	MPI_WUHUEI_0082	**109**	MPI_WUHUEI_0667
90b	MPI_WUHUEI_0085	**110**	MPI_WUHUEI_0668
90c	MPI_WUHUEI_0084	**111**	MPI_WUHUEI_0678
90d	MPI_WUHUEI_0086	**112**	MPI_WUHUEI_0679
90e	MPI_WUHUEI_0087	**113**	MPI_WUHUEI_0692
90f	MPI_WUHUEI_0090	**116**	MPI_WUHUEI_0131
90g	MPI_WUHUEI_0091	**s2**	MPI_WUHUEI_0639
90h	MPI_WUHUEI_0092	**117**	MPI_WUHUEI_0643
92	MPI_WUHUEI_0003	**s3**	MPI_WUHUEI_0193
93	MPI_WUHUEI_0008	**118**	MPI_WUHUEI_0621
95	MPI_WUHUEI_0011	**s5**	MPI_WUHUEI_0224
97	MPI_WUHUEI_0025	**s6**	MPI_WUHUEI_0227

Compound number	Enso experiment number	Compound number	Enso experiment number
119	MPI_WUHUEI_0622	**123n**	MPI_WUHUEI_0695
s8	MPI_WUHUEI_0194	**123o**	MPI_WUHUEI_0660
s9	MPI_WUHUEI_0202	**123q**	MPI_WUHUEI_0649
120	MPI_WUHUEI_0258	**123r**	MPI_WUHUEI_0651
s10	MPI_WUHUEI_0654	**123s**	MPI_WUHUEI_0650
s11	MPI_WUHUEI_0655	**123t**	MPI_WUHUEI_0694
121	MPI_WUHUEI_0658	**123u**	MPI_WUHUEI_0623
s12	MPI_WUHUEI_0637	**123v**	MPI_WUHUEI_0632
s13	MPI_WUHUEI_0647	**125**	MPI_WUHUEI_0696
122	MPI_WUHUEI_0657	**126**	MPI_WUHUEI_0697
123a	MPI_WUHUEI_0262	**127**	MPI_WUHUEI_0324
123b	MPI_WUHUEI_0627	**128**	MPI_WUHUEI_0714
123c	MPI_WUHUEI_0618	**129**	MPI_WUHUEI_0703
123d	MPI_WUHUEI_0620	**130**	MPI_WUHUEI_0711
123e	MPI_WUHUEI_0699	**131**	MPI_WUHUEI_0700
123f	MPI_WUHUEI_0688	**132**	MPI_WUHUEI_0712
123g	MPI_WUHUEI_0681	**135**	MPI_WUHUEI_0226
123h	MPI_WUHUEI_0680	**s15**	MPI_WUHUEI_0228
123i	MPI_WUHUEI_0689	**s16**	MPI_WUHUEI_0230
123j	MPI_WUHUEI_0693	**s17**	MPI_WUHUEI_0306
123k	MPI_WUHUEI_0263	**140**	MPI_WUHUEI_0349
123l	MPI_WUHUEI_0628	**141**	MPI_WUHUEI_0326
123m	MPI_WUHUEI_0629	**148b**	MPI_WUHUEI_0266

Compound number	Enso experiment number	Compound number	Enso experiment number
s20	MPI_WUHUEI_0430	**158**	MPI_WUHUEI_0587
150	MPI_WUHUEI_0431	**161**	MPI_WUHUEI_0503
151	MPI_WUHUEI_0541	**162**	MPI_WUHUEI_0559
152	MPI_WUHUEI_0432	**163**	MPI_WUHUEI_0560
19	MPI_WUHUEI_0551	**164**	MPI_WUHUEI_0487
153	MPI_WUHUEI_0542	**165**	MPI_WUHUEI_0566
154	MPI_WUHUEI_0552	**166**	MPI_WUHUEI_0564
s22	MPI_WUHUEI_0477	**s25**	MPI_WUHUEI_0484
s23	MPI_WUHUEI_0478	**167**	MPI_WUHUEI_0506
155	MPI_WUHUEI_0479	**168**	MPI_WUHUEI_0567
60	MPI_WUHUEI_0480	**169**	MPI_WUHUEI_0568
157	MPI_WUHUEI_0486	**40a**	MPI_WUHUEI_0473

11.4 Acknowledgment

Though this dissertation is an individual work, I could never reach my goal without the help, support and efforts from a number of people. I would like to thank Dr. Charles C. J. Loh who enables me to research on such a challenge topic. The research will never be achieved without his guidance and supervision. I would like to express my sincere gratitude to Prof. Dr. Herbert Waldmann for the opportunity to be in his department and perform research under his generous assistance and infrastructural support. He always gave me supportive suggestions and encouragements whenever I encountered struggling situation. Furthermore, I am very grateful to Prof. Dr. Carsten Strohmann for accepting the invitation to be the second examiner of my PhD.

Furthermore, I would like especially address my appreciation to Chunfa for his intensive discussions and supportive help through my whole PhD period. I am grateful to meet such good friends, Aylin and Zhwan, for the accompany during the most difficult situations and all the nice time spend together outside the lab. I would also like to thank Caitlin and Gregor for the effort to correct my thesis in such a short time. I am grateful to Sasikala who was always ready for help. I would like to thank Bhaskara-Rao for the pleasant working atmosphere in the lab. In addition, I am grateful to my bachelor student, Adrian, for his effort to perform numerous tough experiments.

I would like to thank all these people: Frau Rose, Petra, Chun-ngai, Sarah, Vicky, Okan, Mahesh, Carl, Jessica, Joseph Hoock, Adrian, Hacer, Marc, Stefan, Michael Grigalunas, Annina, Andreas, Jana, Jose, Tim, Svetlana, Michael Winzker, Stephanie, Elisabeth, Joseph Openy, Georg, Lisa, Jie, Sumer, Rehan, Eleana, Tabea, Saad, Romain, Jens, Fabian, Julian from the department of chemical biology in MPI Dortmund for the supportive working atmosphere and the help during my PhD study.

Additionally, I would like to thank the NMR team for the measurements of all the synthesized compounds and I am especially thankful to Bernhard Griewel for the effort to perform the *in situ* NMR monitoring. I would also like to thank the HRMS team for the evaluation of all the submitted compounds and particularly thankful to Christiane Heitbrink for the endeavor to measure numerous compounds in a short time. I am grateful to the COMAS team for the biological compound screening and data analysis

For the financial support, I thank the Verband der Chemischen Industrie for a Liebig PhD scholarship in the first two years and Max-Planck Society for the third-year funding.

Further, I am sincere thankful to Christa and Lucia for all the helps and supportive discussion during various stages of my PhD. I would like to thank Gudi who guided me through the Germany culture and the warm welcome when I first arrived to Dortmund. I am grateful to Ivy for all her helps in the beginning of my PhD.

In addition, my sincere thank goes to Walter for the tremendous help and strong support during the hard times in my PhD. Without you, I would never go so far to this stage to obtain my PhD. I would like to also thank Irene and Alexander for their warm welcome and supportive suggestions. I am grateful to Willy who joined my life and always brings joy to cheer me up during the bad times.

此外我想特別感謝思涵及岑臻在這段期間持續的鼓勵及關心，讓我能有動力持續堅持下去。同時還有在多特蒙德所認識的朋友們: 彥君，晏溱，冠旬，千瑋，子禎，郁萱，仁堯，晏浦，總是給予最即時的關心，以及頻繁的聚會，讓我能夠在繁忙的博士生涯中，享受異鄉的溫暖。最後，我想要感謝愛我的家人，謝謝你們的支持以及信任，讓我可以隻身前往德國攻讀博士學位，謝謝你們總是在我灰心氣餒的時候，安慰我並成為我的避風港，如果沒有你們的支持與鼓勵，我想我沒有辦法走到這裡，因此我想把這份殊榮致獻給你們。

11.5 Eidesstattliche Versicherung (Affidavit)

Name, Vorname
(Surname, first name)

Matrikel-Nr.
(Enrolment number)

Belehrung:

Wer vorsätzlich gegen eine die Täuschung über Prüfungsleistungen betreffende Regelung einer Hochschulprüfungsordnung verstößt, handelt ordnungswidrig. Die Ordnungswidrigkeit kann mit einer Geldbuße von bis zu 50.000,00 € geahndet werden. Zuständige Verwaltungsbehörde für die Verfolgung und Ahndung von Ordnungswidrigkeiten ist der Kanzler/die Kanzlerin der Technischen Universität Dortmund. Im Falle eines mehrfachen oder sonstigen schwerwiegenden Täuschungsversuches kann der Prüfling zudem exmatrikuliert werden, § 63 Abs. 5 Hochschulgesetz NRW.

Die Abgabe einer falschen Versicherung an Eides statt ist strafbar.

Wer vorsätzlich eine falsche Versicherung an Eides statt abgibt, kann mit einer Freiheitsstrafe bis zu drei Jahren oder mit Geldstrafe bestraft werden, § 156 StGB. Die fahrlässige Abgabe einer falschen Versicherung an Eides statt kann mit einer Freiheitsstrafe bis zu einem Jahr oder Geldstrafe bestraft werden, § 161 StGB.

Die oben stehende Belehrung habe ich zur Kenntnis genommen:

Official notification:

Any person who intentionally breaches any regulation of university examination regulations relating to deception in examination performance is acting improperly. This offence can be punished with a fine of up to EUR 50,000.00. The competent administrative authority for the pursuit and prosecution of offences of this type is the chancellor of the TU Dortmund University. In the case of multiple or other serious attempts at deception, the candidate can also be unenrolled, Section 63, paragraph 5 of the Universities Act of North Rhine-Westphalia.

The submission of a false affidavit is punishable.

Any person who intentionally submits a false affidavit can be punished with a prison sentence of up to three years or a fine, Section 156 of the Criminal Code. The negligent submission of a false affidavit can be punished with a prison sentence of up to one year or a fine, Section 161 of the Criminal Code.

I have taken note of the above official notification.

Ort, Datum
(Place, date)

Unterschrift
(Signature)

Titel der Dissertation:
(Title of the thesis):

Ich versichere hiermit an Eides statt, dass ich die vorliegende Dissertation mit dem Titel selbstständig und ohne unzulässige fremde Hilfe angefertigt habe. Ich habe keine anderen als die angegebenen Quellen und Hilfsmittel benutzt sowie wörtliche und sinngemäße Zitate kenntlich gemacht.
Die Arbeit hat in gegenwärtiger oder in einer anderen Fassung weder der TU Dortmund noch einer anderen Hochschule im Zusammenhang mit einer staatlichen oder akademischen Prüfung vorgelegen.

I hereby swear that I have completed the present dissertation independently and without inadmissible external support. I have not used any sources or tools other than those indicated and have identified literal and analogous quotations.

The thesis in its current version or another version has not been presented to the TU Dortmund University or another university in connection with a state or academic examination.*

*Please be aware that solely the German version of the affidavit ("Eidesstattliche Versicherung") for the PhD thesis is the official and legally binding version.

Ort, Datum
(Place, date)

Unterschrift
(Signature)